# Octahedral Chiral-at-Metal Iridium and Rhodium Complexes as Versatile Asymmetric Catalysts

Dissertation

zur Erlangung
des Doktorgrades der Naturwissenschaften
(Dr. rer. nat.)

Dem Fachbereich Chemie
der Philipps-Universität Marburg
vorgelegt von

Xiaodong Shen, M.Sc.
Nanjing, Jiangsu, P. R. China,

Marburg/Lahn 2016

Die vorliegende Dissertation entstand in der Zeit von September 2012 bis Februar 2016 am Fachb ereich Chemie der Philipps-Universität Marburg in der Arbeitsgruppe und unter der Betreuung von Herrn Prof. Dr. Eric Meggers.
Vom Fachbereich Chemie der Philipps-Universität Marburg (Hochschulkennziffr: 1180) als Dissertation am 15.04.2016 angenommen.

Erstgutachter: Prof. Dr. Eric Meggers
Zweitgutachter: Prof. Dr. Armin Geyer
weitere Mitglieder Prüfungskommission: Prof. Dr. Bernard Roling

Tag der mündlichen Prüfung: 10.05.16

*This thesis is dedicated to my beloved family...*

# Acknowledgements

First and foremost, I would like to begin by thanking my advisor, Prof. Eric Meggers for the continuous support of my Ph.D. study and research. His enduring enthusiasm for chemistry has really been invaluable and admirable, and his conscientious scholarly attitude is respectable. With his patient guidance and encouragement, I have learned how to solve the scientific problems in an efficient way and how to be more successful for research career. I am deeply grateful for the opportunity he offered to me, and all the experiences working with him are valuable fortune for my future career. I wish him all the best in his future endeavors. I would also like to thank my master supervisor Prof. Qi Shen, who led me into the amazing world of organometallic chemistry; I wish her a happy retired life.

I would also like to thank all of the other members of the Meggers group. First of all, I would like to express my gratitude to Dr Lilu Zhang, thank you for your encouragement and kind help. Secretaries Ina Pinnschmidt, Andrea Tschirch, they are always patient and kindness. Dr Zhijie Lin, Dr Yonggang Xiang, Dr Chen Fu, Haohua Huo, and Chuanyong Wang, they gave me a lot help in work and life, and I will miss these good times. And I also need to thank Wei Zuo, Jiajia Ma, Yu Zheng, Dr. Xiao Zhang, Jie Qin, Xiaoqiang Huang, Melanie Helms, Jens Henker, Cornelia Ritter, Yu Su, Bo Zhang, Thomas Cruchter, Thomas Mietke, Elisabeth Martin, Rajathees Rajaratnam, Markus Dörr, Timo Völker, Dr. Vladimir Larionov, Tom Breiding, Peter Göbel, Manuel Streib, Anja Kastl, Marianne Wenzel, and Kathrin Wähler for providing an exciting and supportive work environment. I also would like to thank the facilities directors in chemistry department, Dr. Klaus Harms in the X-ray crystallography department, Dr. Xiulan Xie of the NMR facility, and Dr. Uwe Linne of MS facility. Without their help, it would be more difficult in my research. I'd like to express my best wishes for them.

It is fortunate that I have met so many nice people in Marburg, Dr Zhiliang You, Dr Min Chen, Qian Zhang, Yuting Ye, Min Chen, Han Zhou, Xiaojuan Liu, Xinle Zou, Tu Wei and some others. We had a lot of fun and shared so much happy memory together, I am truly thankful to all of them.

Last but not the least, there are really not enough words to describe my gratitude to my beloved wife, Wenfeng Lyu, thank you for your unconditional love and support. To my beloved parents, Liqing Shen and Yumei Su, thank you for always concerning my life and supporting my career. To them, I would like to say, there is nothing that I would ever rather do than spend time with any one of you, thank you for believing in me and I will do my best for my whole life.

# Publications

*Part of this work has been already published:*

- Asymmetric photoredox transition-metal catalysis activated by visible light
  Haohua Huo, **Xiaodong Shen**, Chuanyong Wang, Lilu Zhang, Philipp Röse, Liang-An Chen, Klaus Harms, Michael Marsch, Gerhard Hilt, Eric Meggers
  *Nature,* **2014**, *515*, 100 – 103.
- Octahedral Chiral-at-Metal Iridium Catalysts: Versatile Chiral Lewis Acids for Asymmetric Conjugate Additions
  **Xiaodong Shen**, Haohua Huo, Chuanyong Wang, Bo Zhang, Klaus Harms, and Eric Meggers
  *Chem. Eur. J.,* **2015**, *21*, 9720 – 9726.
- Asymmetric Lewis acid catalysis directed by octahedral rhodium centrochirality
  Chuanyong Wang, Liang-An Chen, Haohua Huo, **Xiaodong Shen**, Klaus Harms, Lei Gong, Eric Meggers
  *Chem. Sci.*, **2015**, *6*, 1094 – 1100.
- Asymmetric Radical–Radical Cross-Coupling through Visible-Light-Activated Iridium Catalysis
  Chuanyong Wang, Jie Qin, **Xiaodong Shen**, Radostan Riedel, Klaus Harms, Eric Meggers
  *Angew. Chem. Int. Edit.,* **2016**, 55, 685 – 688.
- Visible-Light-Activated Enantioselective Perfluoroalkylation with a Chiral Iridium Photoredox Catalyst
  Haohua Huo, Xiaoqiang Huang, **Xiaodong Shen**, Klaus Harms, Eric Meggers
  *Synlett*, **2016**, *27*, 749 – 753.
- Bis-Cyclometalated Rhodium Catalyst Superior Over Iridium Congeners for Enantioselective Radical Amination Activated by Visible Light
  **Xiaodong Shen**, Klaus Harms, Michael Marsch, Eric Meggers
  *Chem. Eur. J.,* **2016**, DOI: 10.1002/chem.201601572.
- Expanding the Family of Bis-Cyclometalated Chiral-at-Metal Rhodium(III) Complexes for Asymmetric Catalysis
  Jiajia Ma, **Xiaodong Shen**, Klaus Harms, and Eric Meggers
  *Dalton Trans.,* **2016**, DOI: 10.1039/c6dt01063f.

# Abstract

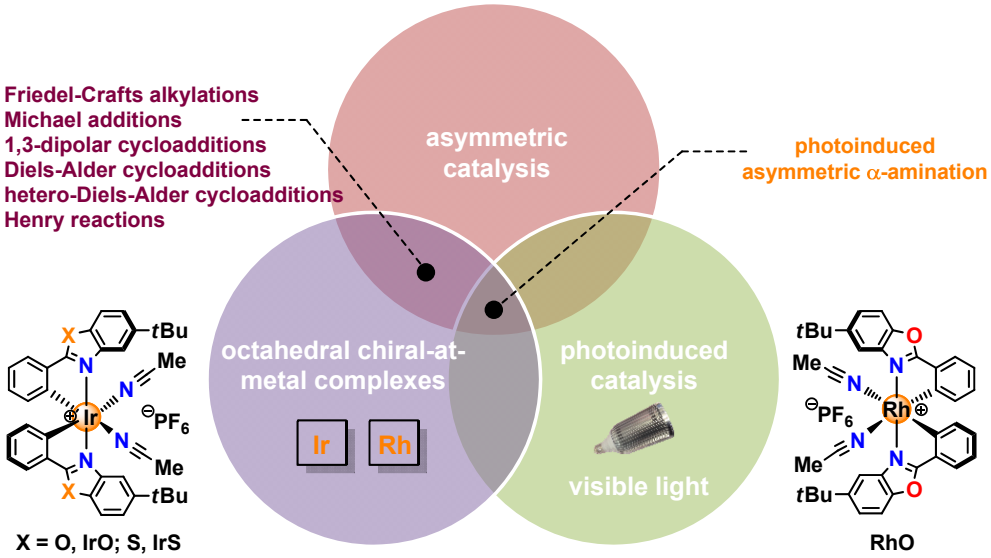


Over the past several years, our group has been interested in designing and synthesizing different novel octahedral chiral-at-metal complexes and their application in asymmetric catalysis, including visible-light-induced asymmetric catalysis.

This thesis mainly includes two parts: one is the versatile asymmetric catalysis by octahedral chiral-at-metal iridium complexes, and the other one is the visible-light-promoted asymmetric α-amination by octahedral chiral-at-metal rhodium complex.

In the first part of this thesis, octahedral chiral-at-metal iridium complexes **IrS** and **IrO** are used as highly effective chiral Lewis acid catalysts for a variety of asymmetric reactions, including Friedel-Crafts alkylations, Michael additions with CH-acidic compounds, 1,3-dipolar cycloadditions, Diels Alder cycloadditions, hetero Diels Alder cycloadditions and Henry reactions.

In the second part of the thesis, a very efficient photoactivated enantioselective radical amination of 2-acyl imidazoles catalyzed by an octahedral chiral-at-metal rhodium complex **RhO** is introduced. Rhodium complex here serves a dual function, namely as a chiral Lewis acid to catalyze asymmetric enolate chemistry and furthermore as a light-activated smart initiator of a radical chain process.

# Abstract (Deutsch)

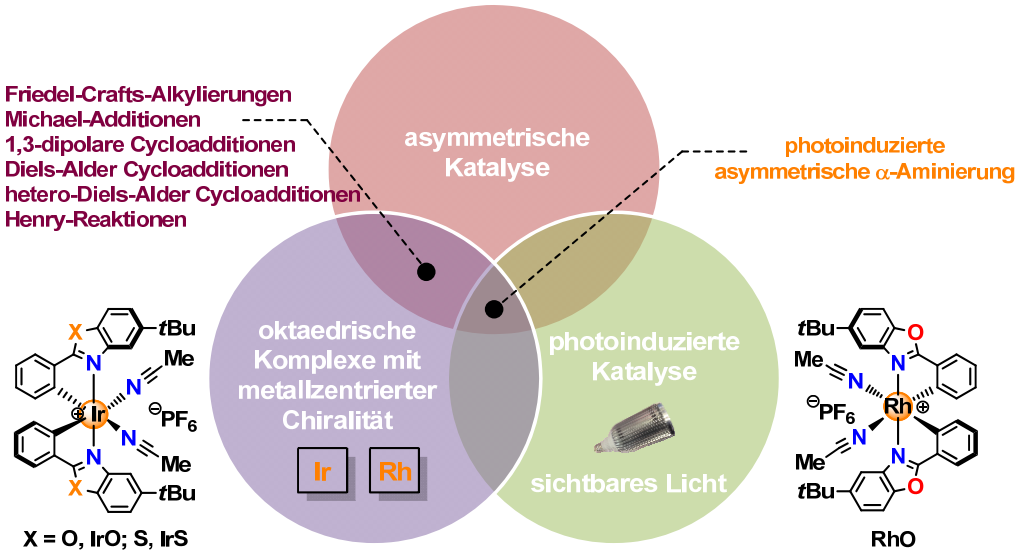



In den letzten Jahren war unsere Arbeitsgruppe daran interessiert, verschiedene neue oktaedrische Komplexe mit metallzentrierter Chiralität zu entwickeln und sie in der asymmetrischen Katalyse einzusetzen. Der Fokus lag dabei vor allem auf der durch sichtbares Licht induzierten asymmetrischen Katalyse.

Diese Arbeit beinhaltet hauptsächlich zwei Teile: der erste Teil handelt von der vielseitigen asymmetrischen Katalyse durch oktaedrische Iridium-Komplexe mit metallzentrierter Chiralität, der zweite Teil handelt von der durch sichtbares Licht geförderten asymmetrischen α-Aminierung durch oktaedrische Rhodium-Komplexe mit metallzentrierter Chiralität.

Im ersten Teil der Arbeit werden die oktaedrischen Iridium-Komplexe **IrS** and **IrO** mit metallzentrierter Chiralität als hocheffektive chirale Lewis-Säure-Katalysatoren für eine Vielzahl von asymmetrischen Reaktionen, wie Friedel-Crafts-Alkylierungen, Michael-Additionen mit CH-aciden Verbindungen, 1,3-dipolare Cycloadditionen, Diels-Alder Cycloadditionen, hetero-Diels-Alder Cycloadditionen und Henry-Reaktionen, eingesetzt.

Im zweiten Teil der Arbeit wird eine sehr effiziente photoaktivierte enantioselektive radikalische Aminierung von 2-Acylimidazolen vorgestellt, die durch einen oktaedrischen Rhodium-Komplex **RhO** mit metallzentrierter Chiralität katalysiert wird. Der Katalysator besitzt die Doppelfunktion als chirale Lewis-Säure die asymmetrische Enolat-Chemie zu katalysieren und darüber hinaus als lichtaktivierter smarter Initiator eines Radikalketten-Prozesses.

# Table of Contents

# Chapter 1. Theoretical Part

## 1.1 Introduction

The field of asymmetric catalysis has grown rapidly and plays an important role in drug discovery and for the synthesis of pharmaceuticals.[1] One of the most interesting and important research areas of current asymmetric catalytic chemistry is asymmetric catalysis by transition-metal complexes.[2] The outermost *d* orbitals of the transition metal ions are incompletely filled with electrons so they can both lend electrons to or take electrons from other molecules. By taking advantage of their outmost *d* orbitals, transition metal complexes can activate substrates and accelerate reactions by means of coordination, ligand exchange insertion, elimination, and so on.[3] The selectivity, activity and stability of chiral transition metal complexes can be tuned by modification of their ligands.

Visible-light-induced photoredox catalysis has sparked much excitement in recent years because visible light which is considered an inexpensive, abundant, and environmentally benign form of energy offers a sustainable, convenient and very mild method to initiate the transfer of single electron.[4] However, the cooperation of such photoredox chemistry with asymmetric catalysis poses significant challenges due to the high reactivities and limited life times of radical ion and radical intermediates which is indicated by the still limited number of catalytic asymmetric photoredox systems.[5]

This chapter will focus on introduction of chiral transition metal complexes and their application for asymmetric catalysis and visible-light-promoted asymmetric catalysis.

## 1.2 Asymmetric Catalysis by Chiral Only-at-Metal Complexes

Chiral metal complexes are one of the important research objects in current organometallic chemistry.[6] This research interest is mainly driven by the potential application of chiral metal complexes in the field of catalysis[2], matericals science[7], and life science[8]. Traditionally, chirality is established in metal complexes with chiral ligands,[9] the chiral information is then located in the coordination sphere of the metal ion. A less well studied of chirality in chiral metal complexes is where the metal center itself is chiral, relying on achiral ligands in the coordination sphere (chiral only-at-metal complex). In this perspective, chiral only-at-metal complexes, including tetrahedaral chiral only-at-metal complexes,[10] half-sandwich chiral only-at-metal complexes,[11] and octahedral chiral only-at-metal complexes,[12] and their application in asymmetric catalysis would be introduced.

### 1.2.1 Tetrahedral chiral only–at–metal complexes

Similar with chiral carbon, tetrahedral metal complexes bearing four different ligands are also chiral (tetrahedral chiral-at-metal complexes) (Figure 1). However, most of tetrahedral chiral-at-metal complexes are not configurationally stable,[13] and their application in asymmetric catalysis is rarely investigated. There are only few reports about using tetrahedaron chiral-at-metal for catalysis.

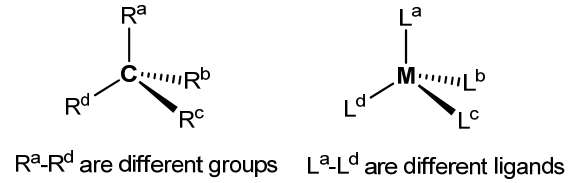


**Figure 1** Chiral carbon center and organometallic analog.

In 2008, the Hoveyda group reported a class of novel tetrahedral chiral-at-metal compplexes that initiate alkene metalthesis with very high efficiency and enantioselectivity (Scheme 1).[14] These new catalysts have a stereogenic metal center with four different monodentate ligands. In the presence of 1 mol% molybdenum complex **Mo(1)**, generated in *situ*, triene is transformed to a relatively natural product (+)-quebrachamine in 84% yield with 96% ee. In 2012, they reported the first examples of catalytic enantioselective ring opening/cross-metathesis (EROCM) reactions by tetrahedral chiral-at-metal Mo complexes (Scheme 2).[15] In the presence of 0.07−1.0 mol% chiral-at-metal molybdenum complex **Mo(2)**, the desired products are formed in up to 90% yield and >99:1 enantiomeric ratio (er) with the disubstituted enol ether generated in >90% *Z* selectivity. These findings outline a promosing direction for the development of tetrahedral chiral-at-metal complexes.

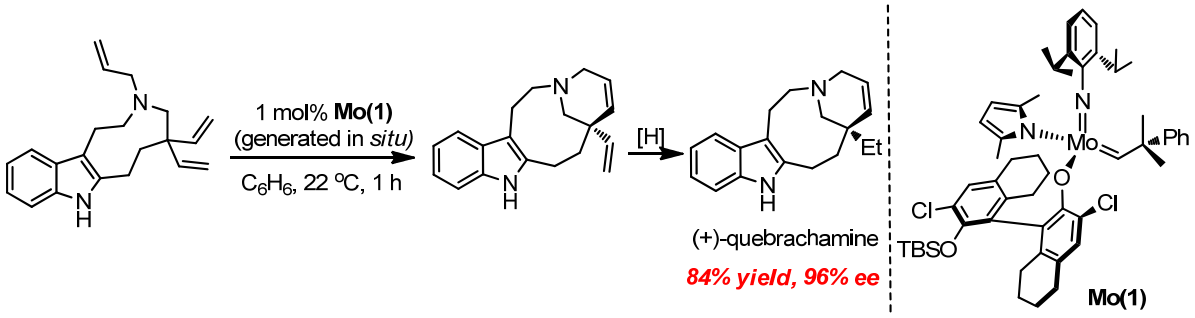


**Scheme 1** Efficient and Highly Enantioselective Synthesis of (+)-Quebrachamine

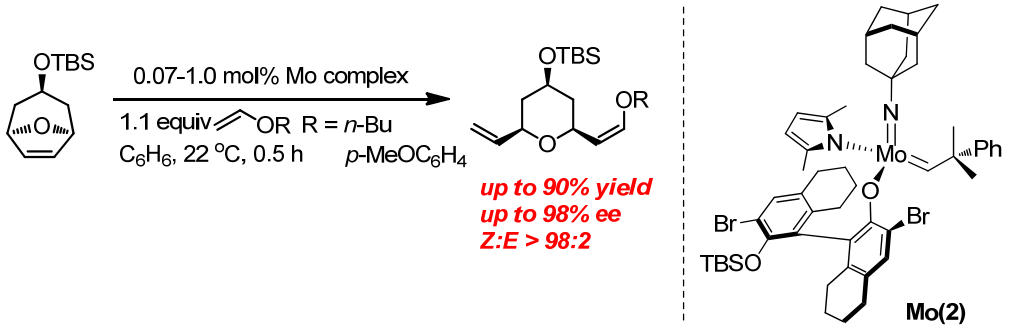


**Scheme 2** Highly Efficient, *Z*- and Enantioselective ROCM Reactions with Chiral-at-Mo Complex

### 1.2.2 Half-sandwich chiral only–at–metal complexes

Compare to tetrahedral chiral-at-metal complexes, half-sandwich chiral-at-metal complexes are somewhat more stable. [6] This class of complexes is common and many examples are known (some representative half-sandwich chiral-at-metal complexes, see Figure 2).[11]

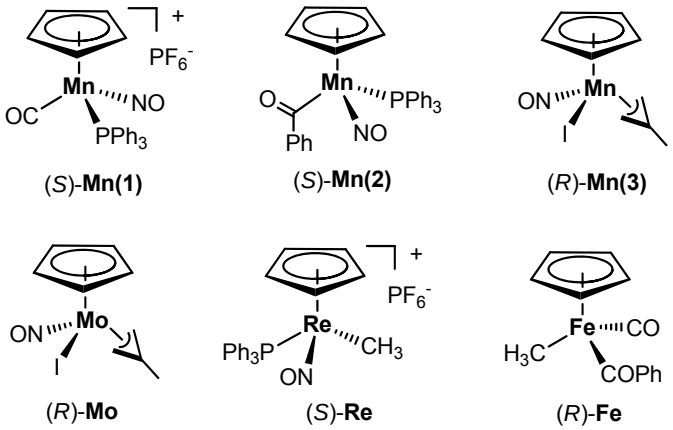


**Figure 2** Some representative half-sandwich chiral-at-metal complexes.

However, the report of asymmetric catalysis by these half-sandwich chiral-at-metal complexes is also rare because most of these chiral complexes are not confugurationally stable in solution.[16] The metal-ligand bond is so week that could break easily, leading to isomerizaiton progress. In 2006, the Gladysz group reported one example of half-sandwich chiral-at-metal complex (*S*)-**Re(2)** for enantioselective cycloadditions involving allenes and imines (Scheme 3).[17] In the presence of 20 mol% (*S*)-**Re(2)**, the [3+2] cycloaddition products were obtained in 90–93% yield with moderate enantioselectivity (51–60% ee). By using the same catalyst (*S*)-**Re(2)** (10 mol% catalyst loading), the products of intramolecular Morita-Baylis-Hillman reaction were isolated in 88–99% yield with 38–74% ee (Scheme 4).[18] Although the enantioselectivity was not high, these findings indeed encouraged us to explore more numerous and stable chiral-at-metal complexes.

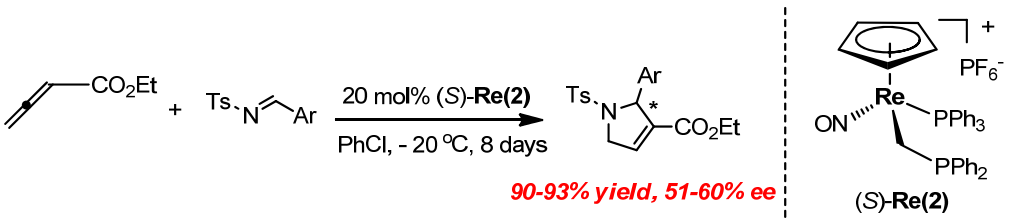


**Scheme 3** Asymmetric [3+2] Cycloadditions by (*S*)-**Re(2)**

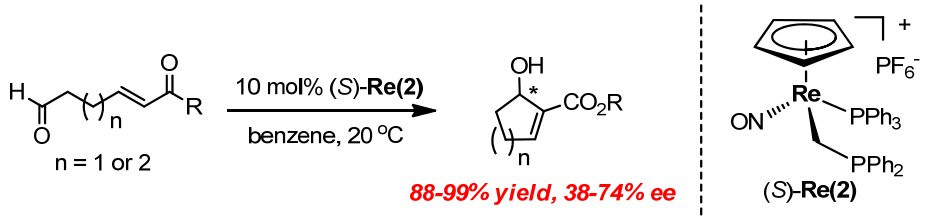


**Scheme 4** Asymmetric intramolecular Morita-Baylis-Hillman Reaction by (*S*)-**Re(2)**

### 1.2.3 Octahedral chiral only–at–metal complexes

In 1893, Werner's coordination theory that octahedral coordination complexes are capable of possessing metal-centered optical activity was proposed. In 1911, Alfred Werner reported the resolution of enantiomers of the octahedral chiral-at-metal cobalt complexs $[Co(en)_2X(NH_3)]^{2+}$ (X = Cl or Br, en = ethylenediamine) into their individual mirror-imaged Λ- and Δ-enanotiomers (Figure 3).[19] These studies represented a powerful evidence to validate Werner's coordinary theory. However, the coordination chemistry of the octahedral chiral-at-metal complexes is more complicate than those of the tetrahedral chiral-at-metal complexes or half-sandwich chiral-at-metal complexes mentioned before. In the next 100 years, there are a few reports about synthesizing enantiopure octahedral chiral-at-metal complexes because the synthesis of enantiopure octahedral chiral-at-metal complexes is full of challenge, and their application for asymmetric catalysis is even fewer.[20]

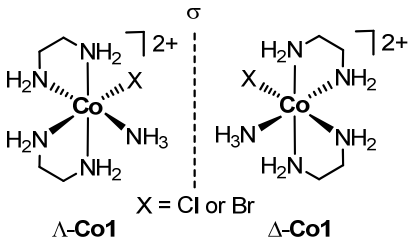


**Figure 3** The resolution of enantiomers of the octahedral chiral-at-metal cobalt complexs.

In 2001, the Soai group reported the highly enantioselective asymmetric autocatalysis induced by chiral octahedral cobalt complexes (Scheme 5).[21] In the presence of 2.4 mol% Δ-**Co(2)**, the enantiomer excess of the corresponding product pyrimidyl alkanol can reached 94%. It is postulated that enantioselective addition occurs at the interface between the crystal of Δ-**Co(2)** and the solvent (the solubility of Δ-**Co(2)** is poor in toluene). The potassium ion within the cobalt salt might as a Lewis acid affords the product with low enantioselectivity. And then, chirality amplification occurs in the subsequent asymmetric autocatalysis progeress.[22] So, strictly speaking, Δ-**Co(2)** here is not a true catalyst but acts as an initiator in this progress.[23]

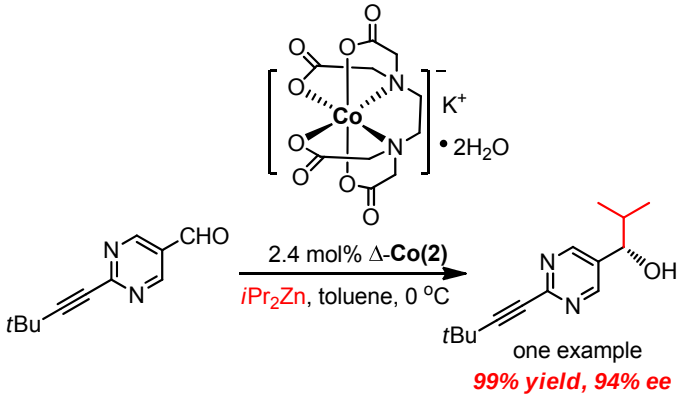


**Scheme 5** Enantioselective Addition of Diisopropylzinc to Aldehyde in the Presence of Chiral Octahedral Cobalt Complex **Co(2)**

Some other examples of asymmetric catalysis by octahedral chiral only-at-metal complexes are shown in Scheme 6. By using these chiral-at-metal complexes as catalyts, the products include sulfoxides (up to 18% ee),[24] alcohols (up to 26% ee)[25], and Michael addition products (up to 33% ee)[26] were obtained with good yield but poor enantioselectivity.

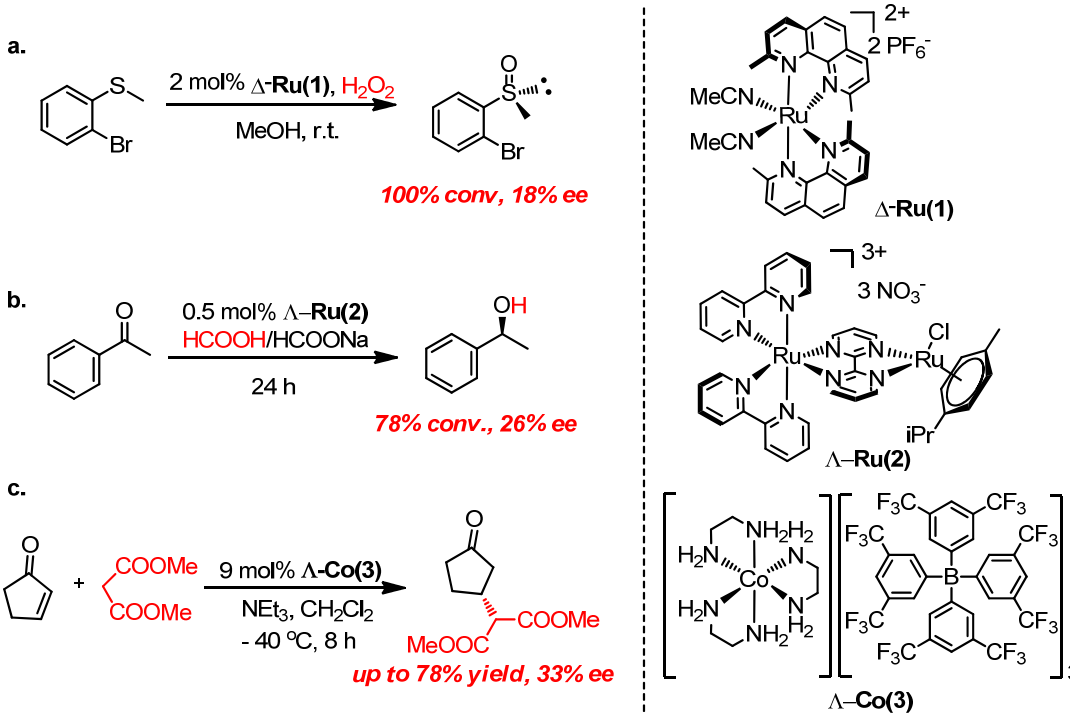


**Scheme 6** Asymmetric Catalysis by Different Chiral-at-Metal Complexes

From 2013, the Meggers group made a great contribution in this area and reported a series of novel work about asymmetric catalysis by octahedral chiral only-at-metal complexes. His work can be divided by two parts: one is inert octahedral chiral only-at-metal complexs as chiral templates for asymmetric catalysis, in which the transition metal serves as a structural center, whereas catalysis is mediated through the organic ligand sphere;[2e] another is octahedral chiral only–at–metal reactive transition metal catalysis, in which the metal center activates a substrate by metal coordination and at the same time comprises the configurationally stable sole element of chirality, thus entirely relying on achiral ligands in the coordination sphere.

*1) Octahedral metal-templated organocatalysis*

In 2013, the Meggers group reported the asymmetric conjugate reduction of nitroalkenes with a Hantzsch ester as the reducing agent by octahedral chiral only-at-metal hydrogen bonding catalysts (Scheme 7).[27] The disired products were obtained in excellent yields (89−96% yield) with excellent enantioselectivities (93−99% ee) in the presence of just 0.1 mol% Λ-**IrO(1)**. The amidopyrazole moiety of Λ-**IrO(1)** searves as a hydrogen-bond donor to nitro group and the OH group is in a proper position to accept a hydrogen bond from NH group of the Hantzsch ester. Afterwards, the Meggers

group extended the research on chiral-at-metal hydrogen bonding catalysts to the enantioselective Friedel Craft alkylation of indoles (Scheme 7).[28] The products with a quaternary all-carbon-substituted stereocenter were also obtained in impressive yields (72−97% yield) with excellent enantioselectivities (92−98% ee) by using 0.5 mol% Λ-**IrO(2)** as a hydrogen bonding catalyst. These researches revealed the potential of octahedral metal complexes as chiral scaffolds for the design of high-performance asymmetric catalysts.

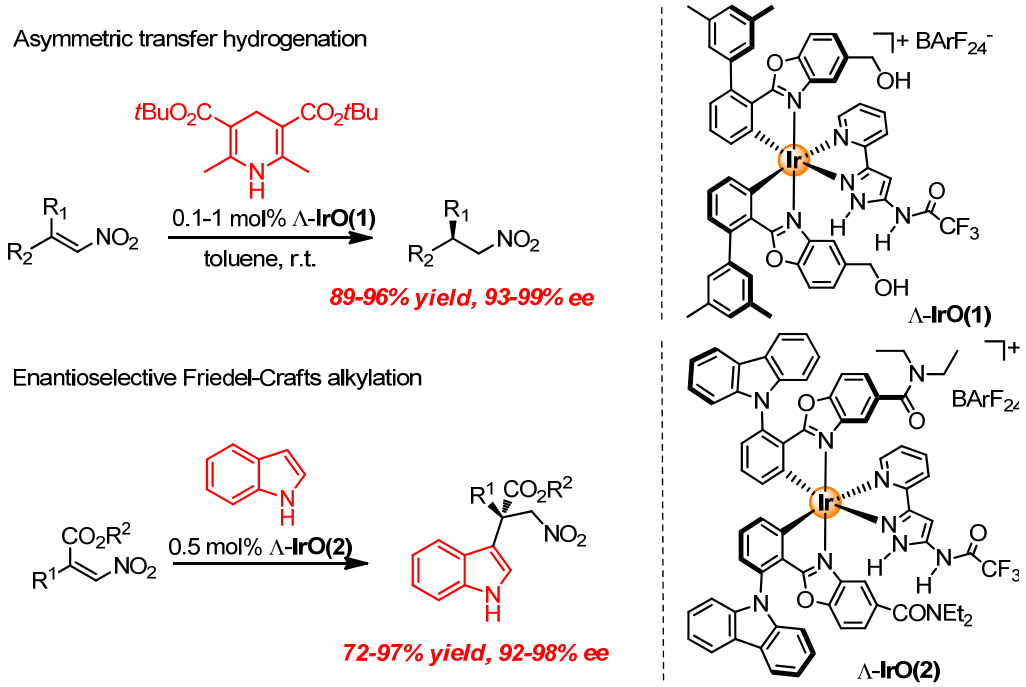


**Scheme 7** Asymmetric Catalysis by Chiral only-at-Metal Hydrogen Bonding Catalysts

On the basis of chiral only-at-metal hydrogen bonding catalysts, the Meggers group developed a new kind of catalyst—chiral only-at-metal brønsted base catalyst in 2014 (Scheme 8). This kind of catalyst can be synthesized easily from hydrogen bonding catalyst by adding base and shaking vigorously for several times. Highly effective asymmetric sulfa-Michael addition (by Λ-**IrO(3)**)[29] and aza-Henry addition (by Λ-**IrO(4)**)[29,30] catalyzed by octahedral chiral-at-metal brønsted base catalysts (catalyst loadings down to 0.02 and 0.25 mol%, respectively) afford the desired products in excellent yields (86−96% and 90−97% yield, respectively) with excellent enantioselectivities (91−97% and 90−98% ee, respectively).

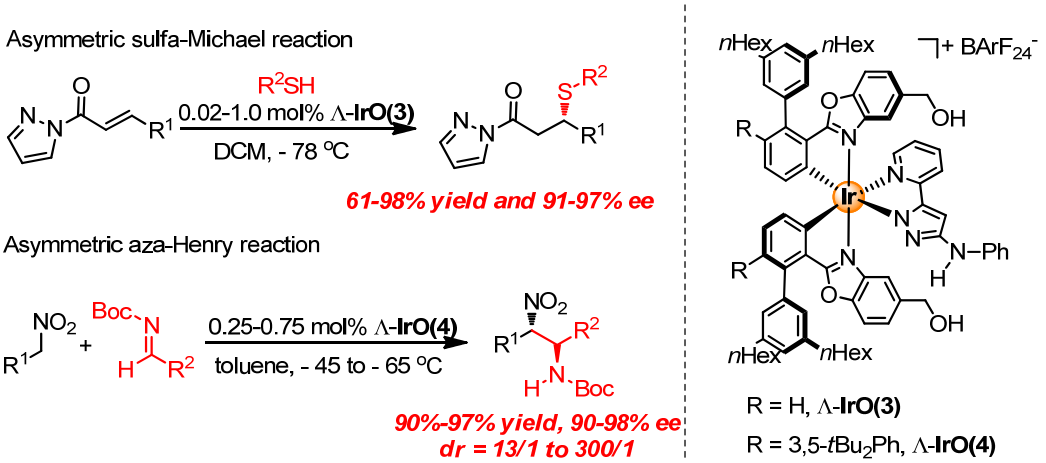


**Scheme 8** Asymmetric Catalysis by Chiral-at-Metal Brønsted Base/H-Bonding Dual Activation Catalysts

The Meggers group also presented an asymmetric enamine catalyst build from an octahedral chiral-at-metal complex (Scheme 9). This iridium complex Λ-**IrO(5)** can convert the aldehyde into a nucleophilic enamine, and activate the azodicarboxylate electrophile through hydrogen bonding with one OH-group at the same time. The desired product *N*-(benzyloxycarbonylamino) oxazolidinones were obtained in very high yields (73−96% yield) with excellent enantioselectivities (87−97% ee). With respect to catalyst loading in asymmetric organocatalysis, Λ-**IrO(5)** is one of the most efficient catalyst for the enantioselective α-amination of aldehydes to date.[31]

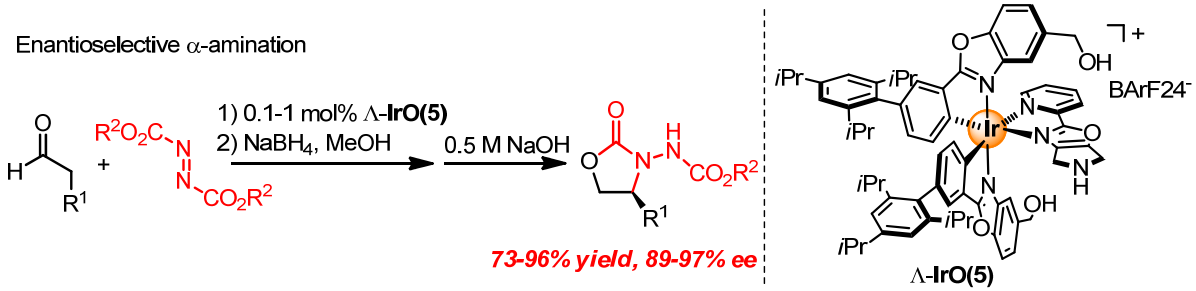


**Scheme 9** Asymmetric Catalysis by Chiral-at-Metal Enamine/H-Bonding Dual Activation Catalysts

*2) Octahedral chiral only–at–metal reactive transition metal catalysis*

In addition, the Meggers group developed a novel concept about the catalysis of octahedral chiral only-at-metal iridium(III) complex, in which the metal center activate one of substrates by coordinaion and at the same time serving as the sole source of chirality (Scheme 10).[32] This complex Λ-**IrO** turns out to be a highly effective asymmetric Lewis catalyst for the enantioselective Friedel−Crafts addition of indoles to α,β-unsaturated 2-acyl imidazoles in high yields (75%−99%) with excellent enantioselectivities (90−98% ee) at low catalyst loadings (0.25−2 mol%) (Scheme 10). And, the octahedral chiral only-at-metal rhodium complex Λ or Δ-**RhO** was also reported to be a catalyst for asymmetric Michael additions (electrophile activation) and asymmetric α-aminations (nucleophile activation) in very high yields (83%−99% and 64−95% yield, respectively) with excellent enantioselectivities (85−99% and 90−97% ee, respectively) in 2015 (Scheme 10).[33]

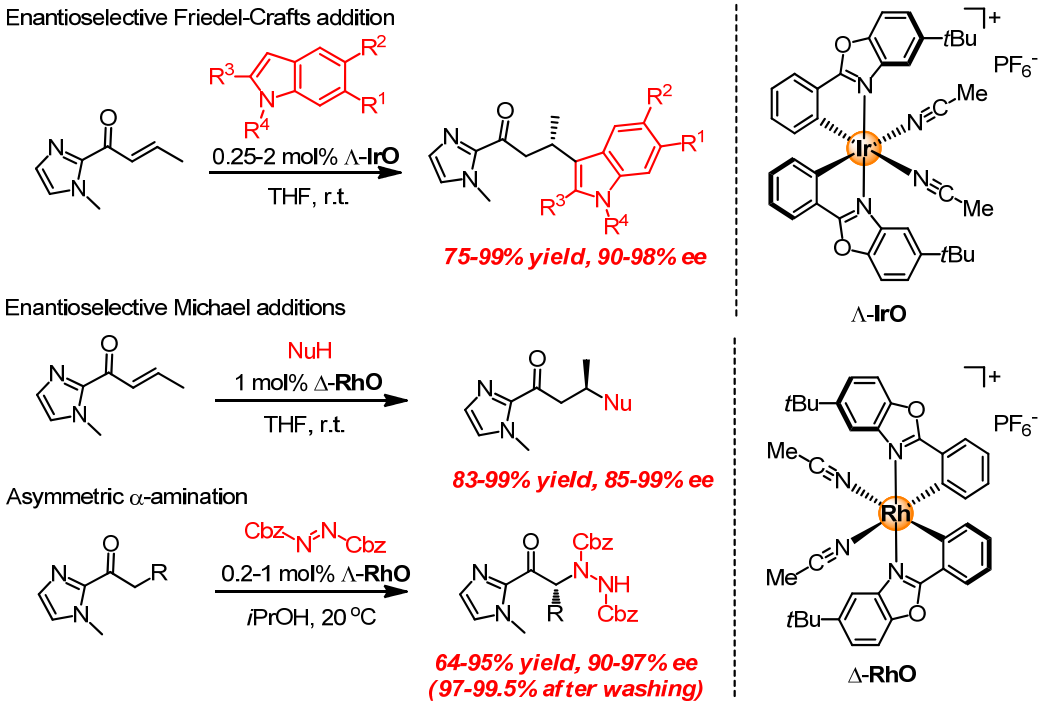


**Scheme 10** Asymmetric Catalysis by Octahedral Chiral-at-Metal Lewis Acid Catalysts

The octahedral chiral-at-metal complexes here serve as versatile catalysts for some asymmetric reactions strongly encourage us to explore more application for the asymmetric organic transformations. Shortly after, the Meggers group demonstrated that these octahedral chiral-at-metal complexes could be used for photo-induced asymmetric catalysis (see Section 1.3.2).

## 1.3 Visible-Light-Induced Asymmetric Catalysis by Metal Complexes

Visible-light-induced organic transformation has been received increasing attention in the recent years, more and more reports appeared in last five years (Figure 4). The organic molecules normally only absorb energy photons which are in the UV region. However, the UV is not a good applicable light source, specialized and expensive equipment for UV needs to be involved; the high energy of UV photons might cause considerable unproductive decomposition reactions. Visible light has its advantages compared to the UV: it is abundant in the solar radiation (44%, see Figure 5), standard LED or household lamb could be used as light source. In a typical visible-light-induced reaction, the visible light is absorbed by photosensitizer which then triggers an energy or electron transfer process. Photoactivated sensitizer are metal complexes or organic dyes, in the following, we only focus on metal complexes used as photosensitizers.[4]

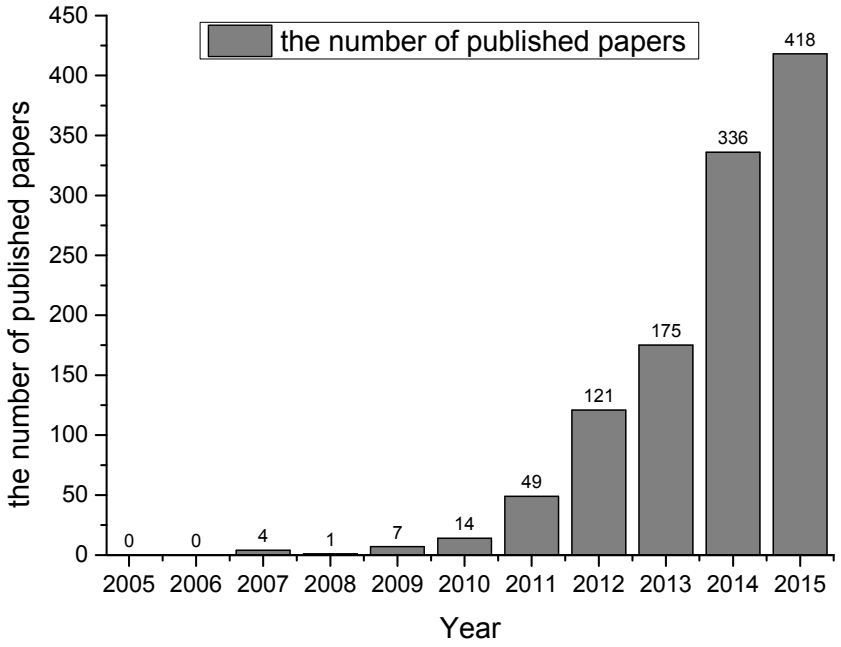


**Figure 4** The growing numbers of published papers about "photoredox catalysis" in recent 10 years. (The results are searched from the *Web of Science*, and the key word is "photoredox catalysis")

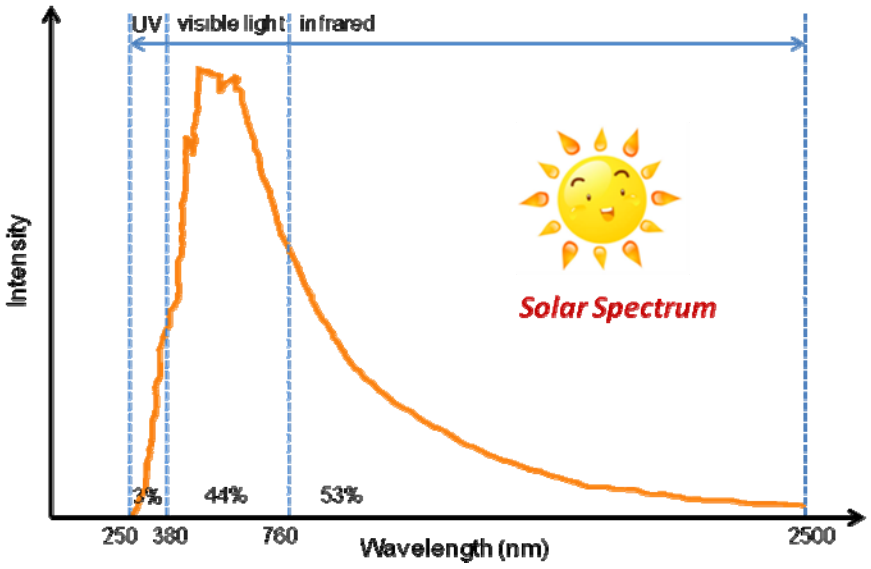


**Figure 5** Solar spectrum.

The common classic transition metal photosensitizers are ruthenium or iridium complexes, such as $Ru(bpy)_3^{2+}$, $Ir(ppy)_3$, $Ir(ppy)_2(dtbbpy)^+$, and $Ir[dF(CF_3)ppy]_2(dtbbpy)^+$ (Figure 6).[4] The excited state of photosensitizer has the remarkable property of being both more oxidizing and more reducing than ground state of photocatalyst.

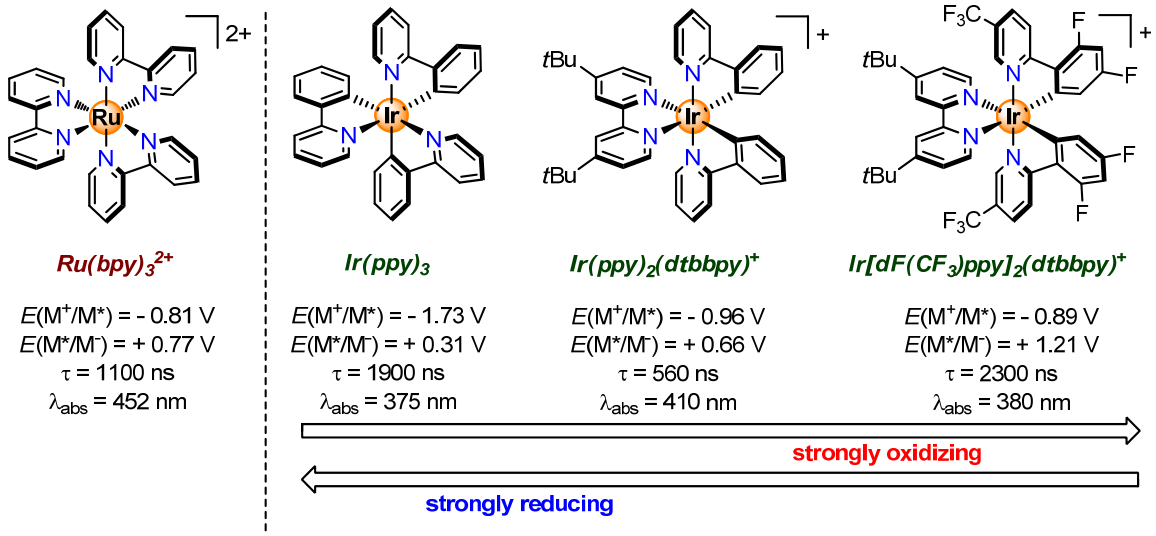


**Figure 6** Popular classic transition metal photocatalysts.

This property could be explained by their molecular orbital diagram, as depicted in Figure 7. The Ru(II) and Ir(III) cations are $d^6$ center (for $Ru^{2+}$: $4d^6$; for $Ir^{3+}$: $5d^6$). Under the irradiation of visible light and upon absorption of one photon, an electron in one of the photosensitizer's metal-centered $t_{2g}$ orbitals is excited to a ligand-centered π* obital, the higher energy electron which is in π* obital maybe expelled from π* obital when the photosensitizer serves as a reductant. If the lower energy vacant in the $t_{2g}$ orbital accepts an electron, then the photosensitizer acts as an oxidant.

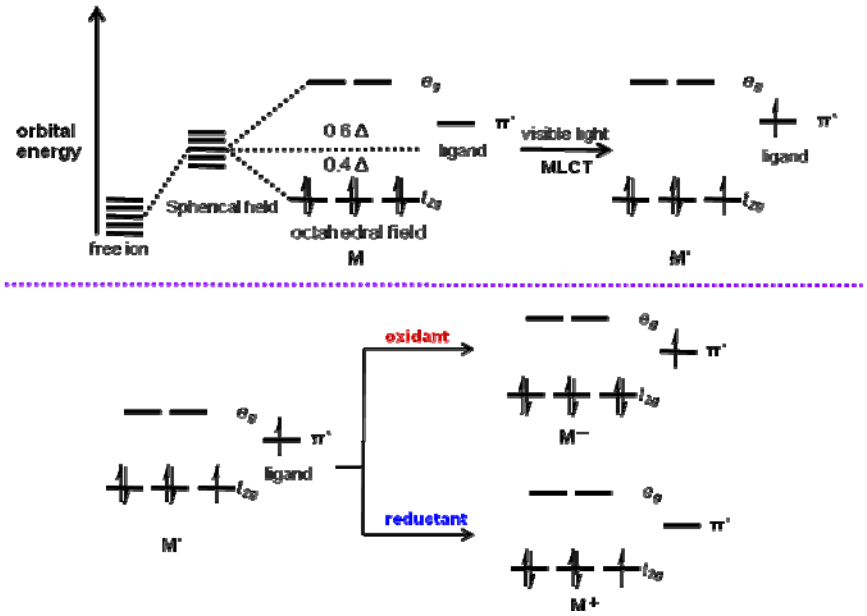


**Figure 7** Simplified molecular orbital diagram.

As a result of this unique property of the photoexcited Ru(II)* or Ir(III)*, redox transformation of Ru(II)* or Ir(III)* could proceed either by oxidative or by reductive quenching cycle (Figure 8a). In the oxidative quenching cycle, the PS* serves as a reductant, gives an electron to the electron acceptor. $PS^+$ is a strong oxidant and may accept an electron from the electron donor, and return to the groud state PS; alternatively, in the reductive quenching cycle, the PS* acts as an oxidant, accepts an

elelctron from the electron donor to form a good reductant $PS^-$. $PS^-$ may donate an electron to the electron acceptor and returned to the groud state PS. In addition, PS* can transfer energy to a suitable substrate directly (Figure 8b). The resulting excited substrate with high energy performs quite differently with its groud state.

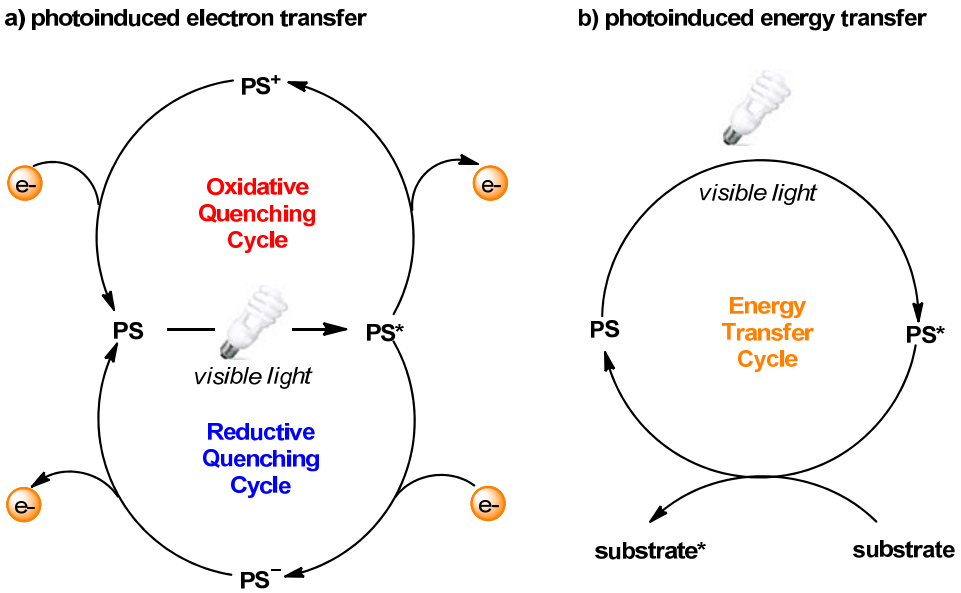


**Figure 8** Induction of chemical processes by visible light activated photosensitizers.

### 1.3.1 Visible-light-induced asymmetric catalysis by a dual-catalysis system

As mentioned before, organic catalysis activated by visible light has experienced a renaissance in the last several years. The asymmetric organic transformations that are activated by visible light are still in its infancy.[5] The combination of organocatalysis or transition-metal catalysis and photosensitizer as dual-catalysis system is the main strategy. We will firstly summarize and discuss some recently progress in visible-light-induced asymmetric catalysis by a dual-catalysis system.

*1) Chiral amine/photosensitizer dual-catalysis system*

In 2008, the MacMillan group reported the first asymmetric alkylation of aldehydes by visible light (Scheme 11).[34] His strategy is to combine the photosensitizer and an imidazodinone organocatalyst to form a dual-catalysis system. By using this strategy, the enantioenriched α-alkylated aldehydes (63−93% yields and 88−99% ee)[34], α-trifluoromethylation of aldehydes (61−89% yield and 90−99% ee)[35] and α-benzylation of aldehydes (72−91% yield and 87−93% ee)[36] can be generated (Scheme 11). The mechanisms of these reactions are quite similar. The proposed mechanism is shown in Figure 9 (the imidazolone **3** is taken for example). The imidazolidinone catalyst reacts with aldehyde to generate π-rich enamine **I**. Then, the electrophilic alkyl radical rapidly undergoes coupling with this π-rich enamine to form intermediate **II**. Intermediate **II** was oxidized to intermediate **III** by the excited

photosensitizers via single-electron transfer (SET) progress. Hydrolysis of intermediate **III** gives the α-alkyl aldehyde product and reconstitutes the imidazolidinone catalyst.

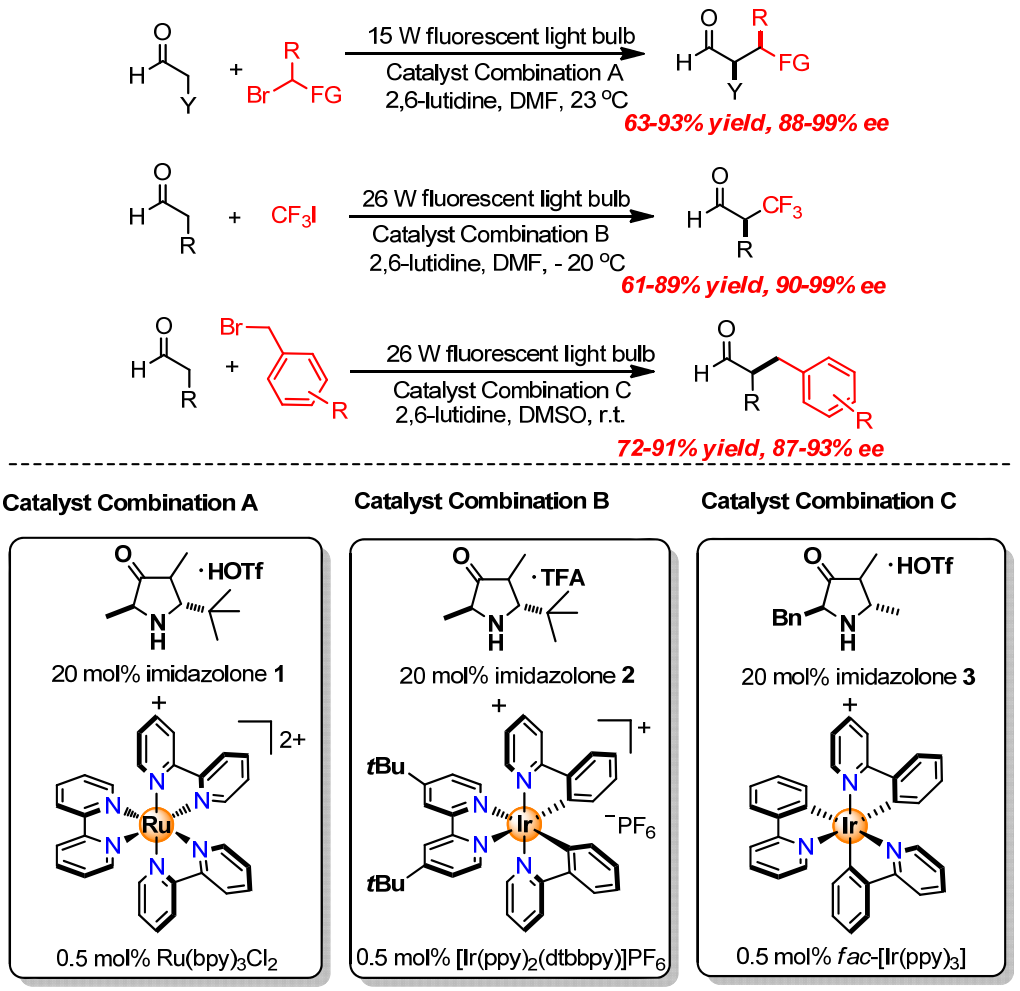


**Scheme 11** Enantioselective α-Alkylation of Aldehydes via Asymmetric Photoredox Catalysis

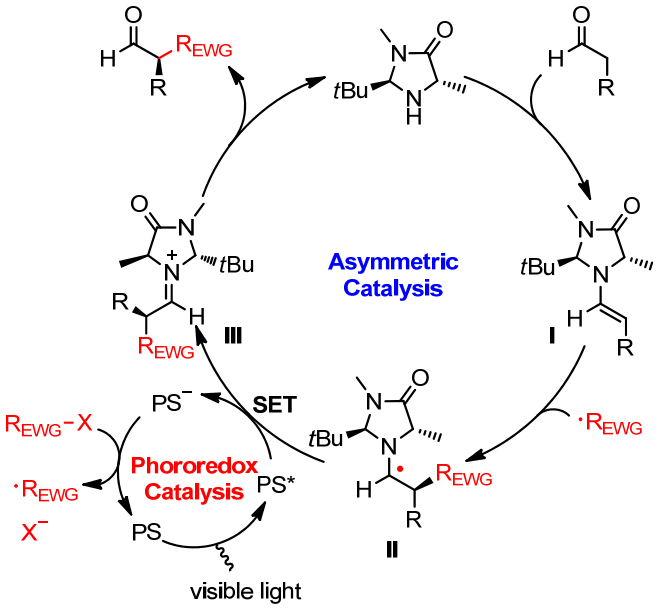


**Figure 9** Putative mechanism for visible-light-induced enantioselective α-alkylation of aldehydes.

In 2014, the Luo group merged chiral primary amine catalysis and photoredox catalysis for the asymmetric α-photoalkylation of β-ketocarbonyls by merging (Scheme 12).[37] The catalyst system enables the creation of all-carbon stereocenters with excellent enantioselectivities (up to 99% ee) and encompass a broad range of substrates including the elusive 1,3-diketones and β-keto amides for the first time in an asymmetric alkylation reaction. This reaction was suggested to proceed with photoredox catalysis (an EDA reaction pathway may also coexist but should be minor in this case) involving phenacyl radical addition as the key C-C forming step and a hydrogen bond in the transition state contributes to the high asymmetric induction.

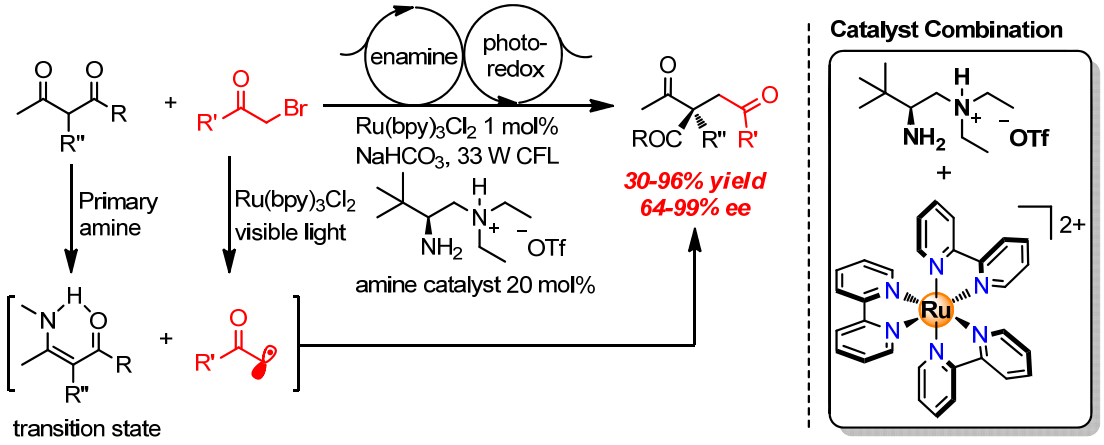


**Scheme 12** α-Photoalkylation of β-Ketocarbonyls

*2) Chiral N-heterocyclic carbene/photosensitizer dual-catalysis system*

In 2012, the Rovis group reported the catalytic asymmetric α-acylation of tertiary amines with aldehydes facilitated by the combination of chiral N-heterocyclic carbine and photoredox catalyst (Scheme 13).[38] The nuclephile intermediate **I** is formed by interaction of an NHC and an aldhyde, it reacts with iminium **II** which is generated from single-electron oxidation of a tertiary amine followed by hydrogen atom abstraction to give intermediate **III**. Elimination of NHC from **III** would give the product amino ketone (up to 94% yield and 92% ee).

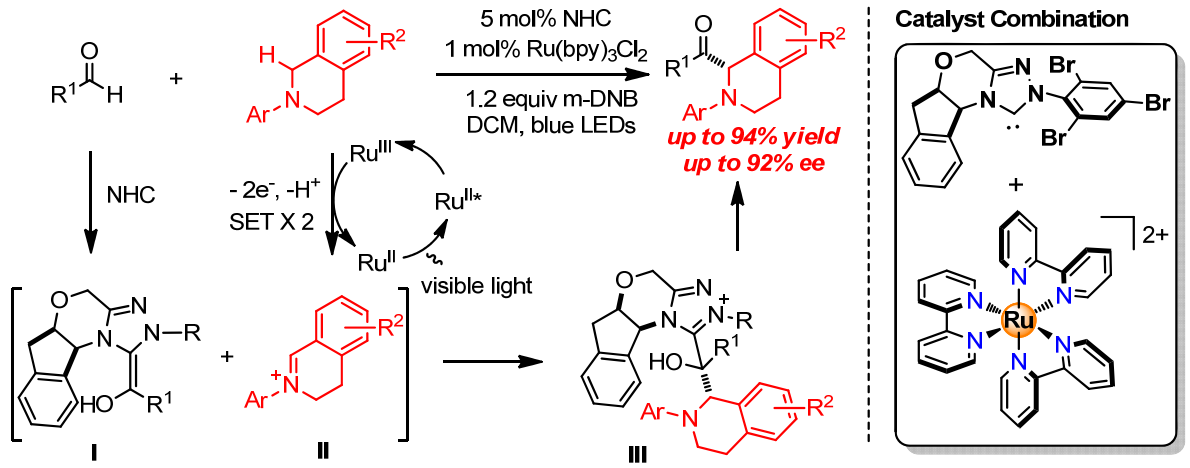


**Scheme 13** Asymmetric α-Acylation of Tertiary Amines with Aldehydes

*3) Chiral brønsted acid/photosensitizer dual-catalysis system*

In 2013, the Knowles group reported the first enantioselective catalytic protocol for the reductive coupling of ketones and hydrazones (45−96% yields and 77−94% ee) (Scheme 14).[39] The aza-pinacol cyclizations proceed through ketyl radical intermediates formed by a concerted proton-coupled electron transfer (PCET) event jointly mediated by a chiral BINOL phosphoric acid and the photoredox catalyst $Ir(ppy)_2(dtbpy)PF_6$. The concept of PCET is interesting because it allows reducing functional groups at significant lower oxidation potentials and provides new opportunities for the further development of catalytic asymmetric radical chemistry by using chial brønsted acid.

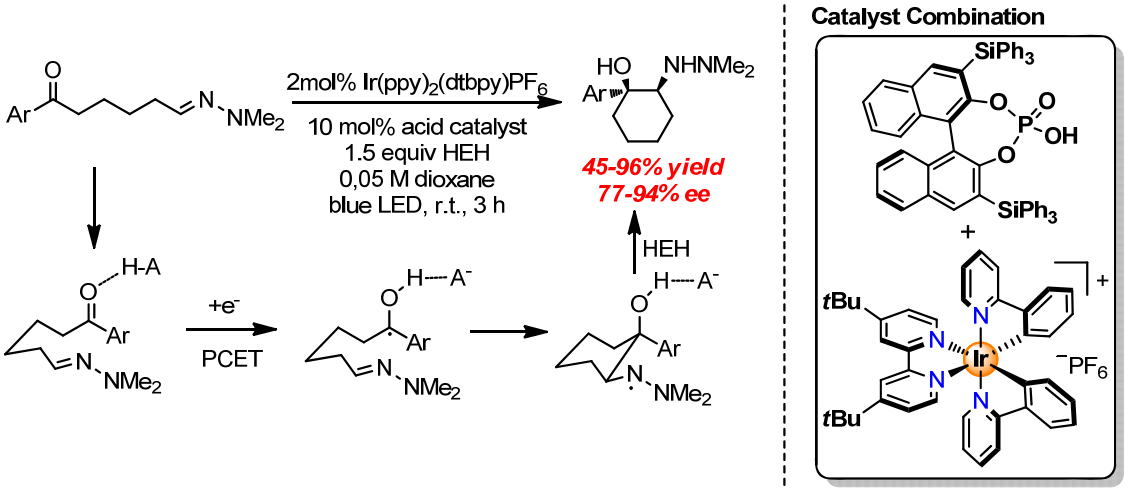


**Scheme 14** Asymmetric Aza-Pinacol Cyclization by Merged Photoredox Catalysis and Chiral Brønsted Acid Catalysis

*4) Chiral Lewis acid/photosensitizer dual-catalysis system*

In 2014, the Yoon group reported a dual-catalysis approach to enantioselective [2+2] photo-cycloadditions by visible light (Scheme 15).[40]

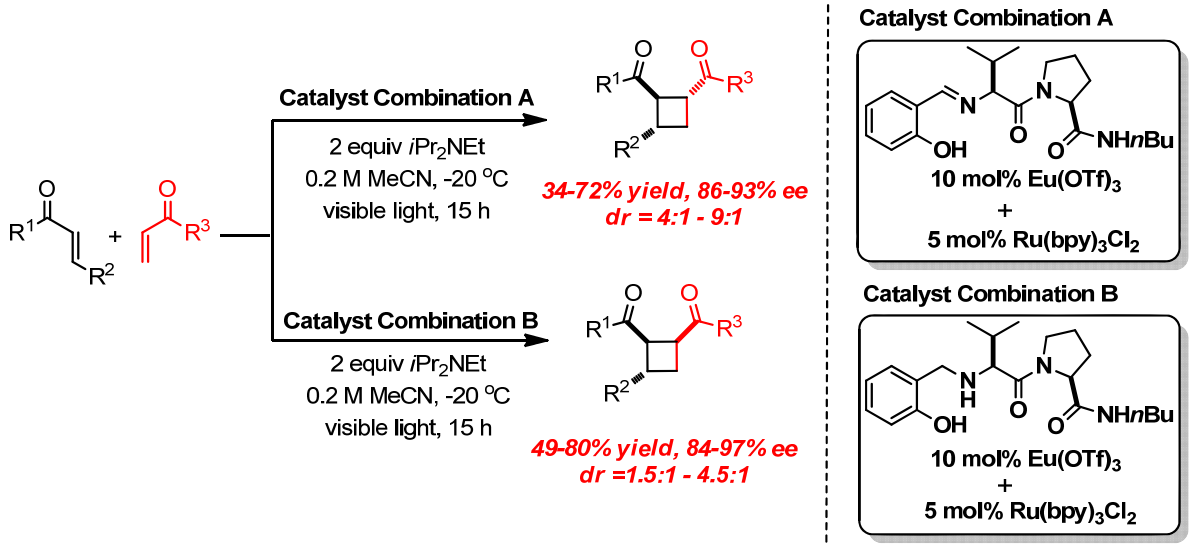


**Scheme 15** A Dual-Catalysis Approach to Enantioselective [2+2] Photocycloadditions Using Visible Light

This dual-catalysis system consists of a visible light activated photoredox catalyst $Ru(bpy)_3Cl_2$ and a chiral Lewis acid co-catalyst. The Lewis acid co-catalyst composed of 10 mol% $Eu(OTf)_3$ and 20 mol% chiral Shiff base afforded 1,2-*trans* cycloadduct in 34−72% yields and 86−93% ee with moderate diastereoselectivities (*dr* = 4/1 to 9/1). Interestingly, the chiral ligand can control both the relative and absolute stereochemistry of the [2+2] photocycloaddition products. Modified the chiral Shiff base to the corresponding reduced secondary amine led to a switch in diastereoselectivity from 1,2-*trans* to 1,2-*cis* cyclobutanes in 49−80% yields and 84−97% ee with moderate diastereoselectivities (*dr* = 1.5/1 to 4.5/1).

The proposed mechanism is shown in Figure 10. The crucial step in this cycloaddition is that $[Ru(bpy)_3]^+$ transfers a single electron to a Lewis acid- activated aryl enones. The hereby generated intermediate radical anions can subsequently react with other Michael acceptors to form cyclobutane containing ketyl radical. The formed cyclobutane containing ketyl radicals loose an electron to give the intermediate that Lewis acid coordinated product. After ligand exchange, the product cyclebutane is formed and a new catalytic cycle is regenerated.

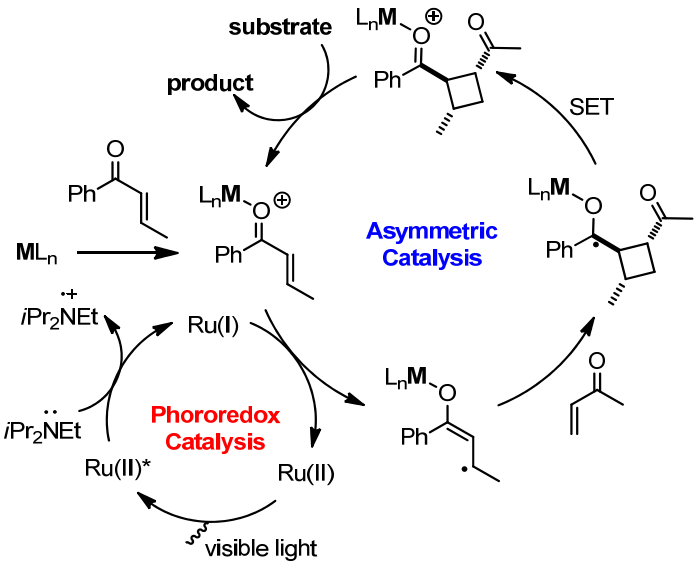


**Figure 10** Plausible mechanism for enantioselective [2+2] photocycloadditions.

*5) Chiral Nickel catalyst/photosensitizer dual-catalysis system*

MacMillan and Fu recently reported enantioselective decarboxylative $C_{sp}^3$-$C_{sp}^2$ cross-coupling reaction of α-amino acids with aryl halides via the merger of photoredox and nickel catalysis (Scheme 16).[41] Decarboxylation of an α-amino acid by photocatalyst-mediated oxidation would give a prochiral α-amino radical **I**. Meanwhile, oxidative addition of an aryl halide to Ni complex would generate a Ni(II)-aryl complex **II**, which would react with α-amino radical **I** to give intermedidate **III**. The resulting intermediate **III** would then undergo reductive elimination to afford the enantioenriched benzylic aminbe product (up to 84% yield and 92% ee).

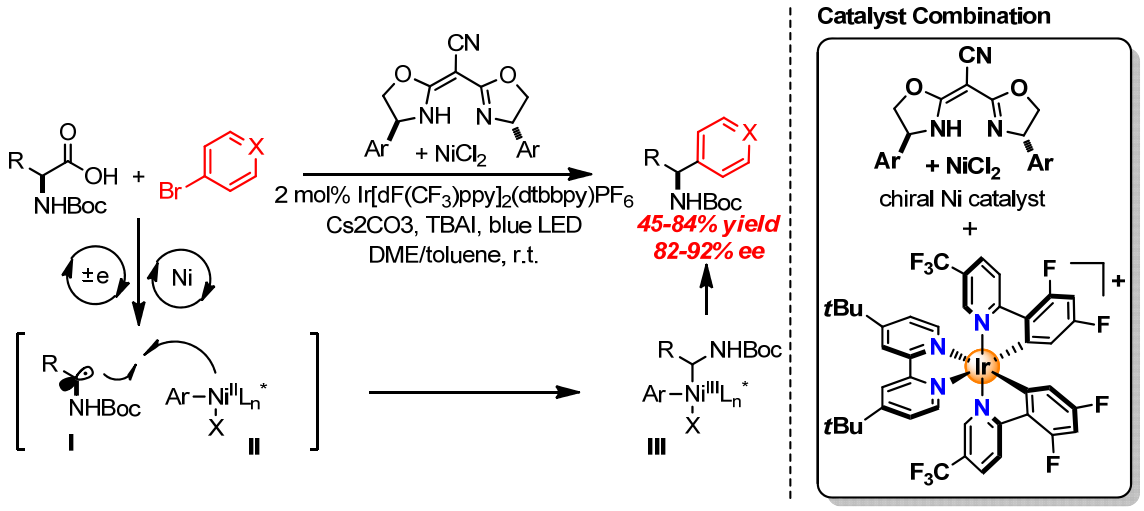


**Scheme 16** Photoinduced Enatioselective Decarboxylative Arylation

## 1.3.2 Visible-light-induced asymmetric catalysis by a "2-in-1" chiral metal complex

*1.3.2.1 Visible-light-induced asymmetric catalysis by a "2-in-1" chiral iridium complex*

In contrast to asymmetric photoredox reactions catalyzed by a dual-catalysis system, the Meggers group has demonstrated visible-light-induced asymmetric catalysis could be realized by single chiral iridium complex since 2014. "2-in-1" chiral iridium complex combines photoredox sensitization and asymmetric induction in a single chiral iridium complex to offer new opportunities for the 'green' synthesis of non-racemic chiral molecules. I would like to introduce this part of works by two parts: one is visible-light-induced asymmetric catalysis by oxidative quenching cycle; another is visible-light-induced asymmetric catalysis by reductive quenching cycle.

*1) Photoinduced asymmetric catalysis by oxidative quenching cycle*

Meggers group reported iridium-catalyzed photoinduced enantioselective alkylation of acyl imidazole with benzyl bromide, affording the α-alkylation products in quantitative yield with a superior enantioselectivity of 99% ee (Scheme 17) in 2014.[42]

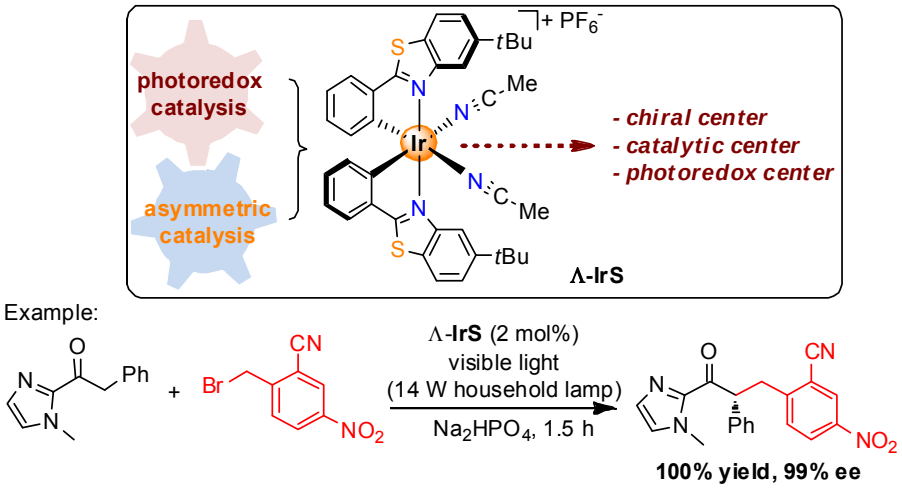


**Scheme 17** Photoinduced Enantioselective Alkylation of Acyl Imidazole with Benzyl Bromide

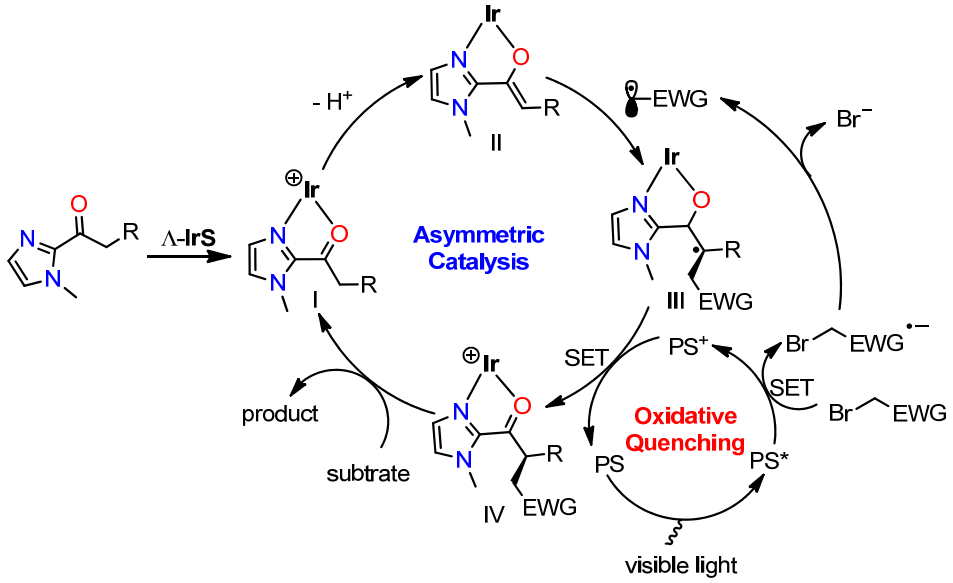


**Figure 11** Plausible mechanism for a combined photoredox and asymmetric catalysis.

A proposed mechanism is shown in Figure 11. The catalysis is initiated by the coordination of 2-acyl imidazoles to the iridium catalyst in a bidentate fashion (intermediate **I**), followed by the formation of iridium enolate complex upon deprotonation (intermediate **II**). The photo-reductively generated benzyl radical then reacted with intermediate **II** to form an iridium-coordinated ketyl radical (intermediate **III**). Intermediate **III** is oxidated to a ketone via single electron transfer. After ligand exchange, intermediate **I** is formed again, followed by a new catalytic cycle. **IrS** and **IrS**-enolate complex (intermediate **II**) here not only serve as a chiral Lewis acids but also serve as photoredox catalysts. Compared to **IrS**, **IrS**-enolate complex (intermediate **II**) has a significantly decreased oxidation potential (Figure 12). In other word, **IrS**-enolate complex is a much strong reducing agent in the groud state (the estimated excited state redox potential of **IrS**-enolate complex is –1.74 V versus Ag/AgCl and it is comparable to that of *fac*-Ir(ppy)$_3$).

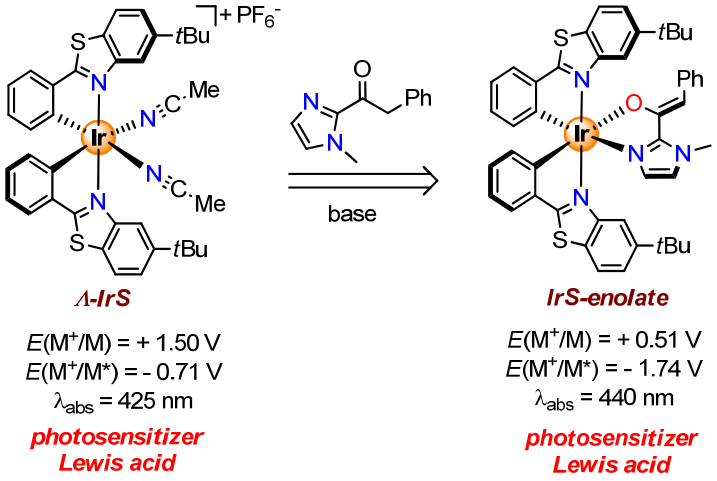


**Figure 12** The properties of **IrS** and **IrS**-enolate.

In 2015, the Meggers group reported firstly an enantioselective, catalytic trichloromethylation through visible light activated photoredox catalysis with a chiral iridium complex **IrS** (Scheme 18).[43] Some

products are formed with 99% ee and even higher. The report of the asymmetric introduction of the trichloromethyl group are limited, although trichloromethyl groups are present in natural products and very useful in the pharmacological research,[44] therefore the method they presented were extremely useful. The proposed mechanism is shown in Figure 13. The key step is the addition of a reductively gernerated electrophilic trichloromethyl radical to the nucleophilic double bond of iridium-enolate complex provides an iridium coordinated ketyl radical (intermediate **III**). A determined quantum yield of 5 (more than 1) indicates that the trichloromethyl radical is also formed by direct single electron transfer from intermediate **III** to $BrCCl_3$ (chain mechanism).

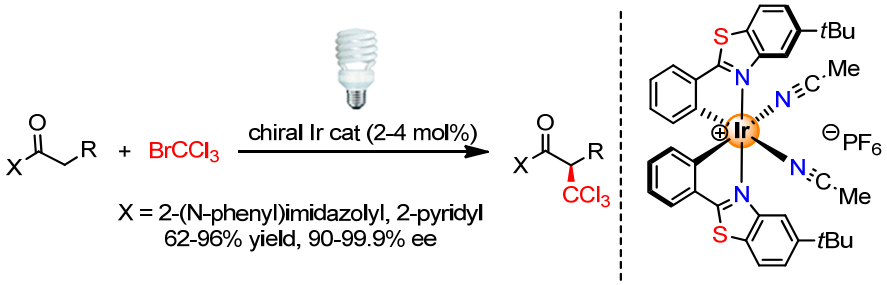


**Scheme 18** The Catalytic Enantioselective α-Trichloromethylation Activated by Visible Light

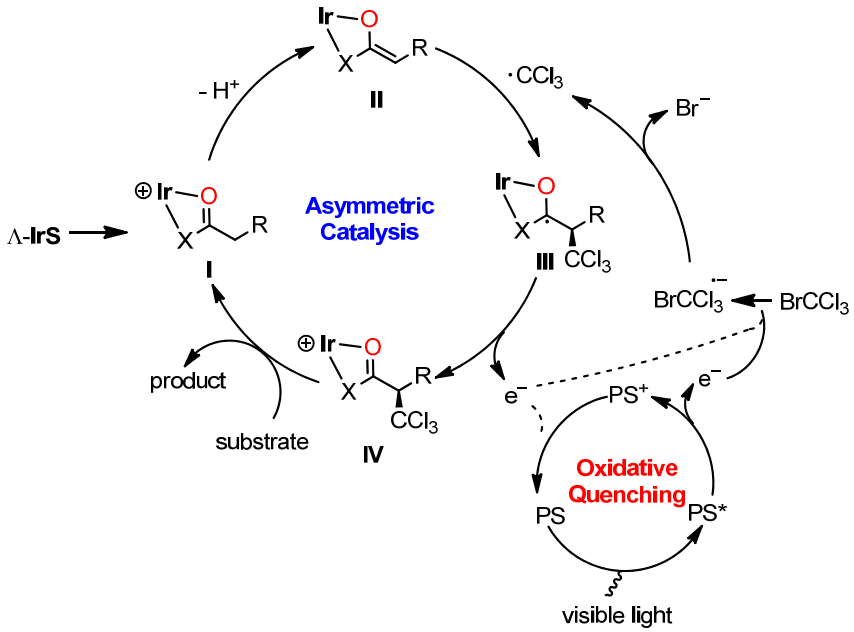


**Figure 13** Putative mechanism for the visible-light-activated enantioselective trichloromethylation.

Meggers group continued to develop the related enantioselective perfluroalkylations. In 2016, the dual function chiral Lewis acid/photoredox catalyst concept (a chiral iridium catalyst) for developping a photoactivated enantioselective perfluoroalkylation of 2-acyl imidazoles was further advanced (Scheme 19).[45] The products with high enantioselectivities (up to >99.5% ee) are observed. The proposed mechnism of perfluoroalkylation is very similar with trichloromethylation's. The key step is the addition of a reductively gernerated electron-deficient perfluoroalkyl radical to the nucleophilic double bond of iridium-enolate complex.

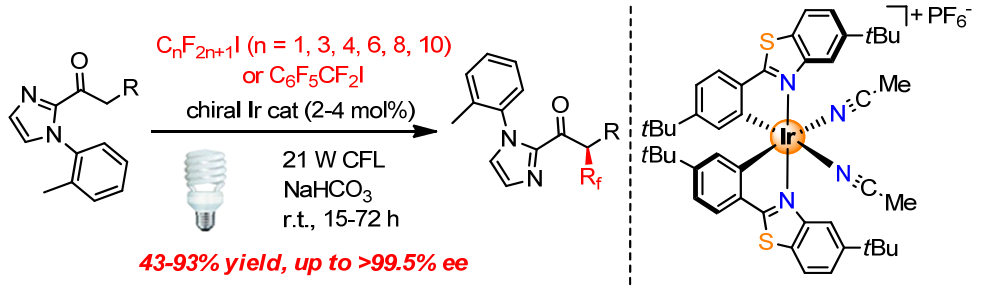


**Scheme 19** The Visible-Light-Induced Enantioselective Perfluoroalkylation

*2) Photoinduced asymmetric catalysis by reductive quenching cycle*

In 2015, the Meggers and coworkers reported the simple chiral iridium complex catalyzes the visible light acitivated asymmetric aerobic α-aminoakylation of 2-acyl imidazoles to provide aminoalkylated products in 61−93% yields with high enantiomeric excess (90−98% ee) (Scheme 20).[46] The iridium complex here has also a dual function of being photosensitized oxidation and asymmetric alkylation. The plausible mechanism is displayed in Figure 14. The catalytic cycle is initiated by the coordination of substrate (2-acyl imidazole) to the iridium complex **IrO** (intermediate **A**), followed by deprotonation to form **IrO**-enolate imtermediate **B**. Intermediate **B** reacts with iminiun ion which is generated by an iridium-photosensitized oxidation of α-silylamine to provide the iridium-coordinated product **C**. After ligand exchange, intermediate **A** is formed again, followed by a new catalytic cycle. Compared with previous work, the photoexcited iridium complex **IrO**(III)* here functions as oxidant, accepting an electron from α-silylamine to form a reductant **IrO**(II). **IrO**(II) can be oxidized to ground state **IrO**(III) by oxgen easily.

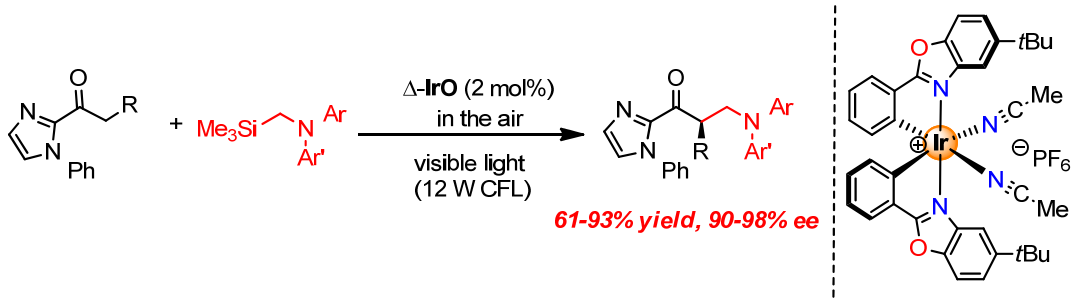


**Scheme 20** The Asymmetric Aerobic α-Aminoakylation of 2-Acyl Imidazoles by Visible Light

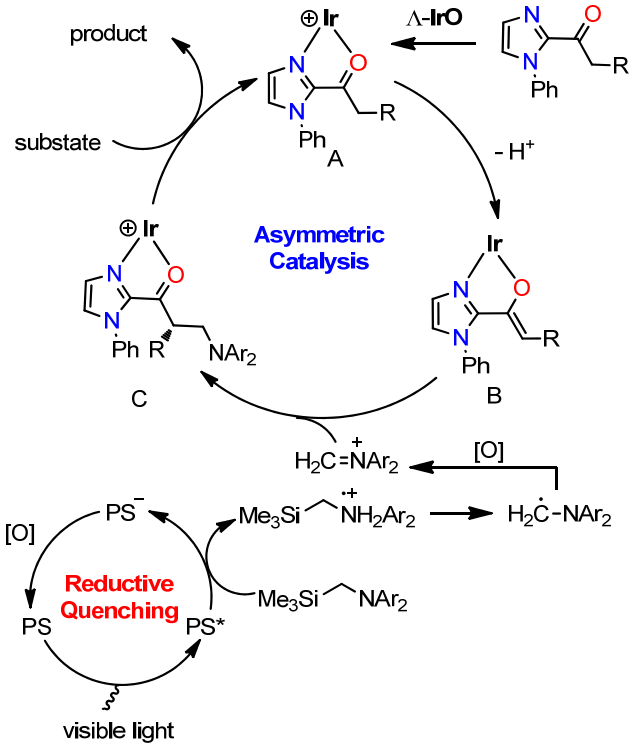


**Figure 14** Putative mechanism for asymmetric aerobic α-aminoakylation.

At the same time, the Meggers group reported a unique catalytic asymmetric process in which a visible light driven single electron transfer reaction between a donor substrate and a catalyst-activated acceptor substrate is followed by a stereocontroled radical-radical recombination (Scheme 21).[47] With the iridium complex as a dual function catalyst, 1,2-amino alcohols were obtained from trifluoromrthyl ketones and tertiary amines in high enantioselectivities (up to 99% ee). The plausible mechanism is shown in Figure 15. The catalytic cycle is initiated by the coordination of substrate (2-acyl imidazole) to the iridium complex **IrS** to form intermediate **I**. The intermediate **I** is activated by visible light to form photoactivated intermediate **II**. And then a single electron transfer from tertiary amine to intermediate **II** to generate an iridium-coordinated ketyl radical **III** and an amino radical cation. After a proton transfer and a radical-radical cross-coupling between the electron-deficient intermediate **IV** and the electron-rich α-aminoalkyl radical, the intermediate **V** (product coordinates the iridium complex) is generated. Finally, the product is replaced by new substate. A quantum yield of 0.09 (<< 1) is in agreement with the expected closed catalytic cycle and no chain progress is possible (At least one photon is needed for each asymmetric C-C bond formation.).

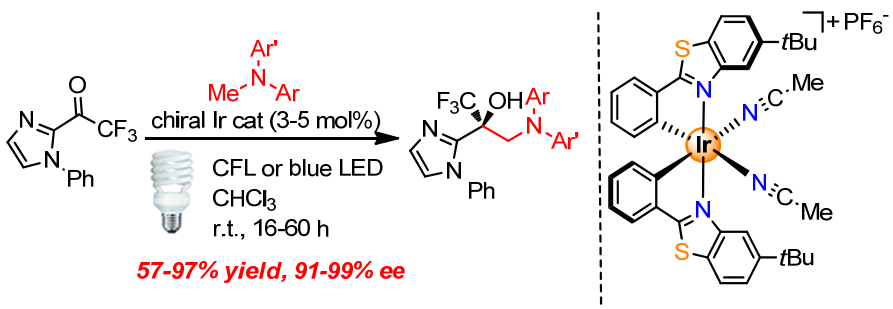


**Scheme 21** Visible-Light-Induced Asymmetric C-C Bond Formation

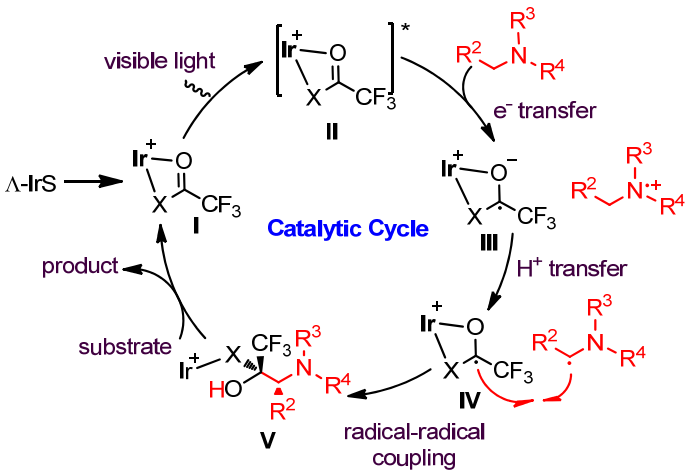


**Figure 15** Putative mechanism for the visible-light-activated asymmetric radical–radical cross-coupling process.

*1.3.2.2 Visible-light-induced asymmetric catalysis by other "2-in-1" chiral metal complexes*

The Meggers group explored "2-in-1" chiral rhodium catalyst in addition to the "2-in-1" chiral iridium complexes. In 2015, they reported the chiral-at-rhodium complex catalyzes the visible light activitated asymmetric cross-coupling with oxygen as the oxidant to afford the products in 35−81% yield with 79−97% ee (Scheme 22).[48] This work is the first example for an asymmetric photoredox reaction catalyzed by a chiral rhodium complex. Rhodium complex here does not only serve as a catalyst for the enatioselective enolate chemistry, but also acts as a photosensitizer. The proposed mechanism involves a rhodium coordination of the substrate followed by deprotonation (Figure 16). The intermediate rhodium enolate complex then reacts with iminiun ion which is formed by photosensitized oxidation of the corresponding *N*,*N*-diakylaniline.

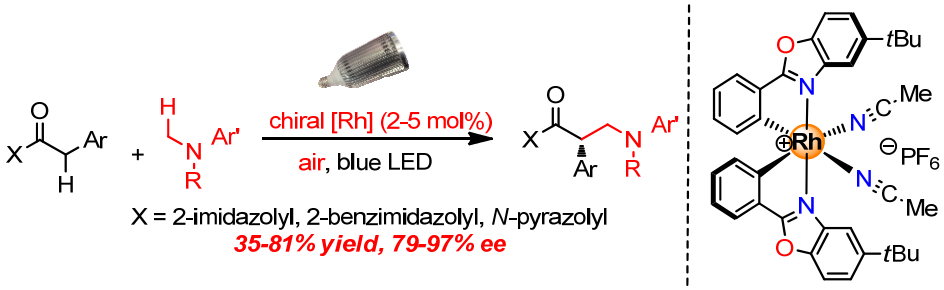


**Scheme 22** Aerobic Asymmetric Dehydrogenative Cross-Coupling

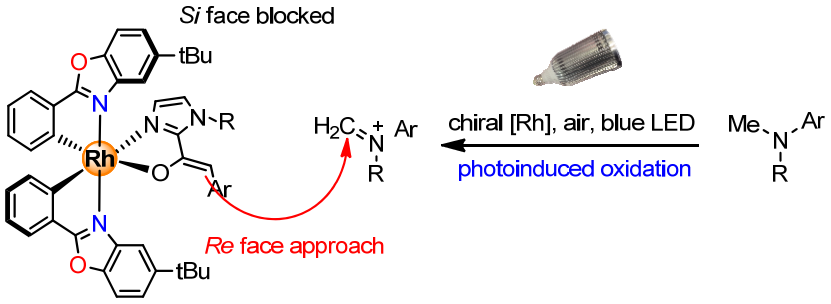


**Figure 16** Putative mechanism for the catalytic asymmetric cross-dehydrogenative couplings.

Shortly thereafter, the Fu group reported asymmetric copper-catalyzed C-N cross-couplings induced by visible light (Scheme 23).[49] The copper catalyst here is formed in *situ* by CuCl, chiral ligand and nuclophiles, acting as both the photocatalyst and the source of asymmetric induction. Irradiation of the cross-coupling partners by a blue light-emitting diode at −40 °C for 16 h in the presence of CuCl, chiral ligand, and a base provides the amines in good yields (73−98%) with excellent enantioselectivities (87−99% ee). An outline of a possible mechanism for this reaction is illustrated in Figure 17. The catalytic cycle is initiated by the formation of the copper-nucleophile complex (**A**). Under the irradiation of visible light, the copper-nucleophile complex (**A**) is activated to an excited-state complex (**B**) which would then enage in SET with alkyl halide (R-X) to form intermediate (**C**) and an alkyl radical. Then, the product amine is formed by the bonding formation between nuleophile and the alkyl radical through an innersphere pathway involving intermediate (**C**).

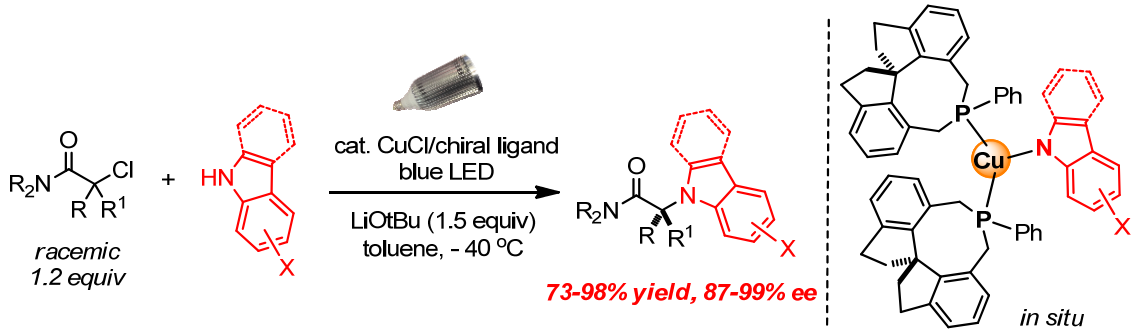


**Scheme 23** Asymmetric Copper-Catalyzed C-N Cross-Couplings Induced by Visible Light

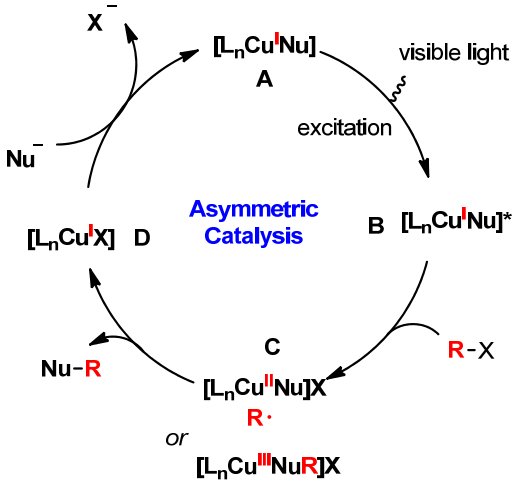


**Figure 17** Outline of a possible pathway for photoimduced copper-catalyzed C-N cross-couplings of alkyl halides.

To sum up, this section elaborated visible-light-induced asymmetric catalysis by a dual-catalysis system or a "2-in-1" chiral metal complex. The report of visible-light-induced asymmetric catalysis catalyzes by a "2-in-1" metal complex is not much, especially catalyzed by a "2-in-1" chiral rhodium complex or other chiral transition metal complexes. This field is growing rapidly and it will play a pivotal role in the 'green' synthesis of non-racemic chiral molecules.

## 1.4 References


1 a.) J. Halpern, B. M. Trost, *Proc. Natl. Acad. Sci. U. S. A.* **2004**, *101*, 5347; b.) K. Mikami, M. Lautens, *New Frontiers in Asymmetric Catalysis*, Wiley, **2007**.

2 a.) T. Hayashi, M. Kumada, *Acc. Chem. Res.* **1982**, *15*, 395−401; b.) G. C. Fu, *Acc. Chem. Res.* **2004**, *37*, 542−547; c.) G. C. Fu, *Acc. Chem. Res.* **2006**, *39*, 853−860; d.) G. L. Hamilton, E. J. Kang, M. Mba, F. D. Toste, *Science* **2007**, *317*, 496−499; e.) L. Gong, L. A. Chen, E. Meggers, *Angew. Chem. Int. Ed.* **2014**, *53*, 10868−10874.

3 Q.-L. Zhou, *Angew. Chem. Int. Ed.* **2016**, DOI: 10.1002/anie.201509164.

4 a.) C. K. Prier, D. A. Rankic, D. W. C. MacMillan, *Chem. Rev.* **2013**, *113*, 5322−5363; b.) D. M. Schultz, T. P. Yoon, *Science* **2014**, *343*, 1239176.

5 E. Meggers, *Chem. Commun.* **2015**, *51*, 3290−3301.

6 E. B. Bauer, *Chem. Soc. Rev.* **2012**, *41*, 3153−3167.

7 a.) B. Kesanli, W. Lin, *Coord. Chem. Rev.* **2003**, *246*, 305−326; b.) L. Ma, C. Abney, W. Lin, *Chem. Soc. Rev.* **2009**, *38*, 1248−1256; c.) J. Crassous*, Chem. Soc. Rev.* **2009**, *38*, 830−845.

8 a.) B. M. Zeglis, V. C. Pierre, J. K. Barton, *Chem. Commun*. **2007**, 4565−4579; b.) F. R. Keene, J. A. Smith, J. G. Collins, *Coord. Chem. Rev*. **2009**, *253*, 2021−2035; c.) E. Meggers, *Chem. Commun.* **2009**, 1001−1010.

9 a.) T. Ohkuma, H. Ooka, T. Ikariya, R. Noyori, *J. Am. Chem. Soc.,* **1995***, 117,* 10417−10418; b.) C.-M. Che, J.-S. Huang, *Coord. Chem. Rev.* **2003**, *242*, 97−113; c.) J. S. Fossey, R. Matsubara, P. Vital, S. Kobayashi, *Org. Biomol. Chem.*, **2005**, 3, 2910−2913; d.) J. S. Fossey, R. Matsubara, H. Kiyohara, S. Kobayashi, *Inorg. Chem.*, **2008**, 47, 781−783.

10 H. Amouri, M. Gruselle, *Chirality in Transition Metal Chemistry*, Wiley, Chichester, UK, **2008**.

11 a.) H. Brunner, *Angew. Chem., Int. Ed. Engl.* **1969**, *368*, 120−126; b.) H. Brunner and H. D. Schindler, *J. Organomet. Chem.* **1970**, *24*, C7−C10; c.) D. Carmona, M. P. Lamata, F. Viguri, R. Rodríguez, L. A. Oro, F. J. Lahoz, A. I. Balana, T. Tejero, P. Merino, *J. Am. Chem. Soc.* **2005**, *127*, 13386−13398.

12 a.) A. von Zelewsky, *Stereochemistry of Coordination Compounds*, Wiley, Chichester, **1996**. b.) B. Kolp, H. Viebrock, A. von Zelewsky, D. Abeln, *Inorg. Chem.* **2001**, *40*, 1196−1198; c.) H. Amouri, R. Thouvenot, M. Gruselle, B. Malézieux, J. Vaissermann, *Organometallics* **2001**, *20*, 1904−1906.

13 D. H. Busch, *J. Chem. Educ.* **1964**, *41*, 77−85.

14 S. J. Malcolmson, S. J. Meek, E. S. Sattely, R. R. Schrock, A. H. Hoveyda, *Nature* **2008**, *456*, 933−937.

15 M. Yu, I. Ibrahem, M. Hasegawa, R. R. Schrock, A. H. Hoveyda, *J. Am. Chem. Soc.* **2012**, *134*, 2788−2799.

16 H. Brunner, *Eur. J. Inorg. Chem*. **2001**, 905−912.

17 A. Scherer, J. A. Gladysz, *Tetrahedron Lett.* **2006**, *47*, 6335−6337.

18 J. Gladysz, F. Seidel, *Synlett* **2007**, *6*, 986−988.

19 A. Werner, *Ber. Dtsch. Chem. Ges.* **1911**, *44*, 1887−1898.

20 E. Meggers, *Eur. J. Inorg. Chem.* **2011**, 2911−2926.

21 I. Sato, K. Kadowaki, Y. Ohgo, K. Soai, H. Ogino, *Chem. Commun.* **2001**, 1022−1023.

22 K. Soai, T. Kawasaki, A. Matsumoto, *Acc. Chem. Res.* **2014**, *47*, 3643−3654.

23 Z.-Y. Cao, W. D. G. Brittain, J. S. Fossey, F. Zhou, *Catal. Sci. Tech.* **2015**, *5*, 3441−3451.

24 M. Chavarot, S. Menage, O. Hamelin, F. Charnay, J. Pecaut, M. Fontecave, *Inorg. Chem.* **2003**, *42*, 4810−4816.

25 O. Hamelin, M. Rimboud, J. Pécaut, M. Fontecave, *Inorg. Chem.* **2007**, *46*, 5354−5360.

26 C. Ganzmann, J. A. Gladysz, *Chem. Eur. J.* **2008**, *14*, 5397−5400.

27 L.-A. Chen, W. Xu, B. Huang, J. Ma, L. Wang, J. W. Xi, K. Harms, L. Gong, E. Meggers, *J. Am. Chem. Soc.* **2013**, *135*, 10598–10601.

28 L.-A. Chen, X. Tang, J. Xi, W. Xu, L. Gong, E. Meggers, *Angew. Chem. Int. Ed.* **2013**, *52*, 14021−14025.

29 J. Ma, X. Ding, Y. Hu, Y. Huang, L. Gong, E. Meggers, *Nat. Commun.* **2014**, *5*, 4531.

30 X. Ding, H. Lin, L. Gong, E. Meggers, *Asian J. Org. Chem.* **2015**, *4*, 434−437.

31 a.) A. Bøgevig, K. Juhl, N. Kumaragurubaran, W. Zhuang, K. A. Jørgensen, *Angew. Chem. Int. Ed.* **2002**, *41*, 1790–1793; b.) B. List, *J. Am. Chem. Soc.* **2002**, *124*, 5656–5657.

32 H. Huo, C. Fu, K. Harms, E. Meggers, *J. Am. Chem. Soc.* **2014**, *136*, 2990–2993.

33 C. Wang, L.-A. Chen, H. Huo, X. Shen, K. Harms, L. Gong, E. Meggers, *Chem. Sci.* **2015**, *6*, 1094–1100.

34 D. A. Nicewicz, D. W. C. MacMillan, *Science* **2008**, *322*, 77−80.

35 D. A. Nagib, M. E. Scott, D. W. C. MacMillan, *J. Am. Chem. Soc.* **2009**, *131*, 10875−10877.

36 H.-W. Shih, M. N. Vander Wal, R. L. Grange, D. W. C. MacMillan, *J. Am. Chem. Soc.* **2010**, *132*, 13600−13603.

37 Y. Zhu, L. Zhang, S. Luo, *J. Am. Chem. Soc.* **2014**, *136*, 14642−14645.

38 D. A. DiRocco, T. Rovis, *J. Am. Chem. Soc.* **2012**, *134*, 8094−8097.

39 L. J. Rono, H. G. Yayla, D. Y. Wang, M. F. Armstrong, R. R. Knowles, *J. Am. Chem. Soc.* **2013**, *135*, 17735−17738.

40 J. Du, K. L. Skubi, D. M. Schultz, T. P. Yoon, *Science* **2014**, *344*, 392−396.

41 Z. Zuo, H. Cong, W. Li, J. Choi, G. C. Fu, D. W. C. MacMillan, *J. Am. Chem. Soc.* **2016**, *138*, 1832−1835.

42 H. Huo, X. Shen, C. Wang, L. Zhang, P. Rose, L. -A. Chen, K. Harms, M. Marsch, G. Hilt, E. Meggers, *Nature* **2014**, *515*, 100−103.

43 H. Huo, C. Wang, K. Harms, E. Meggers, *J. Am. Chem. Soc.* **2015**, *137*, 9551−9554.

44 Natural products containing trichloromethyl groups: a.) W. Hofheinz, W. E. Oberhansli, *Helv.*

*Chim. Acta*. **1977**, *60*, 660−669; b.) M. D. Unson, C. B. Rose, D. J. Faulkner, L. S. Brinen, J. R. Steiner, J. Clardy, *J. Org. Chem.* **1993**, *58*, 6336−6343; c.) J. Orjala, W. H. Gerwick, *J. Nat. Prod.* **1996**, *59*, 427−430; d.) X. Fu, L.-M. Zeng, J.-Y. Su, M. Pais, *J. Nat. Prod.* **1997**, *60*, 695−696; e.) J. B. MacMillan, E. K. Trousdale, T. F. Molinski, *Org. Lett.* **2000**, *2*, 2721−2723.

45 H. Huo, X. Huang, X. Shen, K. Harms, E. Meggers, *Synlett* **2016**, *27*, 749−753.

46 C. Wang, Y. Zheng, H. Huo, P. Rose, L. Zhang, K. Harms, G. Hilt, E. Meggers, *Chem. Eur. J.* **2015**, *21*, 7355−7359.

47 C. Wang, J. Qin, X. Shen, R. Riedel, K. Harms, E. Meggers, *Angew. Chem. Int. Ed.* **2016**, *55*, 685−688.

48 Y. Tan, W. Yuan, L. Gong, E. Meggers, *Angew. Chem. Int. Ed.* **2015**, *53*, 13045−13048.

49 Q. M. Kainz, C. D. Matier, A. Bartoszewicz, S. L. Zultanski, J. C. Peters, G. C. Fu, *Science* **2016**, *351*, 681−684.

# Chapter 2. Aim of the Work

My research work can be divided into the following two main parts:

**1) Explore the generality of chiral Lewis acid catalysts with respect to reaction types and substrates by octahedral chiral-at-metal complexes**

Asymmetric catalysts which draw their chirality exclusively from a chiral metal center are much less investigated although such catalysts might display some attractive features such as structural simplicity (only achiral ligands required) and an effective chirality transfer in the course of the reaction due to direct proximity of the metal-based stereocenter to the metal-coordinating substrate.

Recently, our group introduced octahedral chiral-at-metal iridium(III) and rhodium(III) complexes as a novel class of chiral Lewis acid catalysts. One highly appealing goal in this area of research is the development of chiral Lewis acid catalysts that exhibit a broad generality with respect to reaction types and substrates. In this work, we would like to first design and synthesize different octahedral chiral-at-metal complexes by modifying the ligands in order to find the higher activity and better selectivity transition metal chiral catalysts. And, explore their catalytic behavior in some different kinds of reactions such as Friedel-Crafts alkylations, Michael additions with CH-acidic compounds, a variety of cycloadditions and Henry reactions. In addition, we want to expand the scope of substituted alkenes, in order to make them more general. The mechanism of reactions will be also investigated.

**2) Explore the visible-light-induced enantioselective C-N formation by octahedral chiral-at-metal complex**

Reactions involving single electron transfer (SET) steps have sparked much attention over the last several years. Visible light photosensitization offers a sustainable, convenient and very mild method to initiate the transfer of single electron. However, the cooperation of such photoredox chemistry with asymmetric catalysis poses significant challenges due to the high reactivities and limited lifetimes of radical ion and radical intermediates which is indicated by the still limited number of catalytic asymmetric photoredox systems.

Nitrogen-centered radicals (NCRs) hold much promise as useful synthetic intermediates and they can be generated via single electron transfer (SET) progress by photoredox catalysis under mild

conditions.

Therefore, we would like to explore the possibility of visible-light-induced enantioselective C-N formation via nitrogen-centered radicals by the octahedral chiral-at-metal complexes. If possible, the octahedral chiral-at-metal complexes here would serve a dual function, namely as a chiral Lewis acid to catalyze asymmetric enolate chemistry and furthermore as a photoredox sensitizer. In addition, we will focus on the mechanism study for this reaction, in order to comprehend the progress of visible-light-induced asymmetric catalytic reaction and provide some useful information for exploring other asymmetric photoredox reactions.

# Chapter 3. Results and Discussion

Metal-based asymmetric catalysts are typically constructed from a central metal ion in combination with one or multiple chiral ligands.[1] In contrast, asymmetric catalysts which draw their chirality exclusively from a chiral metal center[2] are much less investigated although such catalysts might display some attractive features such as structural simplicity (only achiral ligands required) and an effective chirality transfer in the course of the reaction due to the direct proximity of the metal-based stereocenter to the metal-coordinating substrate.[3] In this section, a number of octahedral metal complexes were designed and synthesized, and their catalytic activities were carefully studied.

## 3.1 Design of New Catalysts

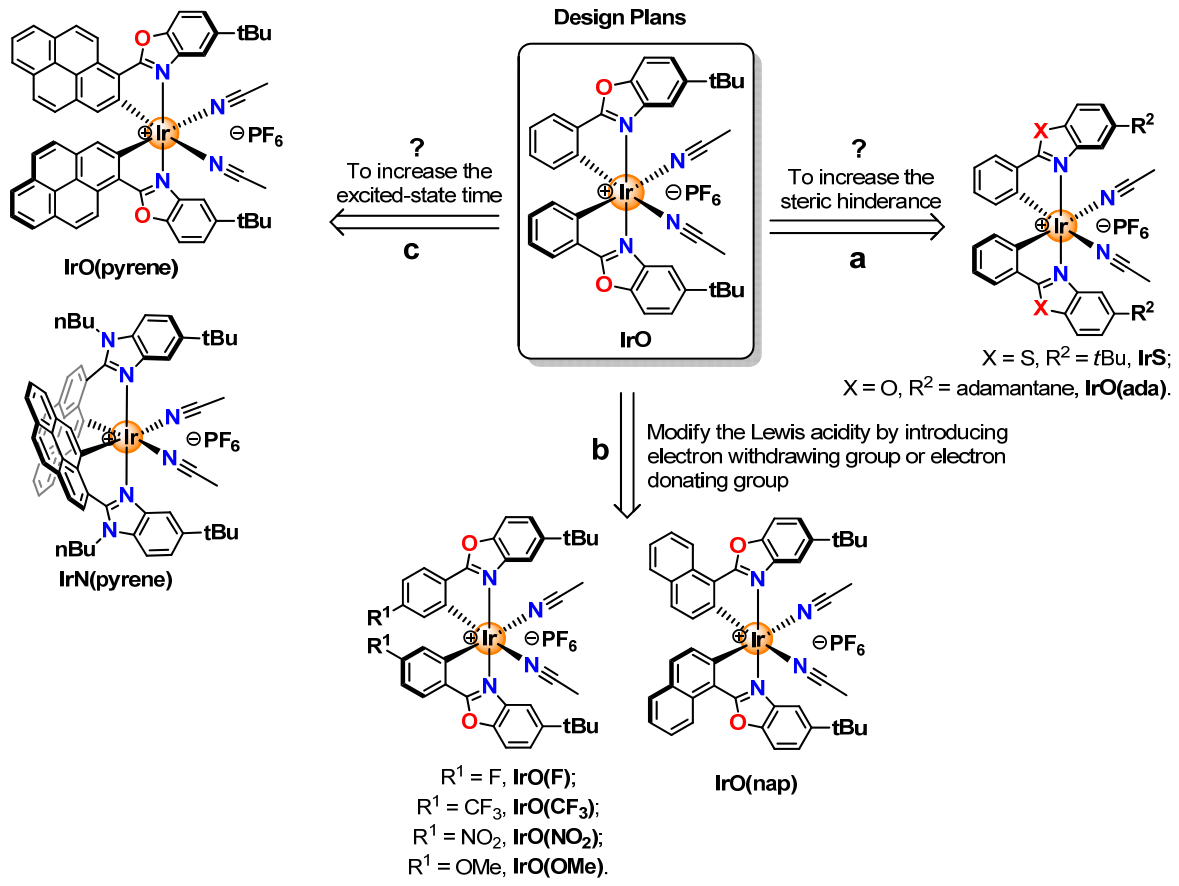


**Figure 18** Design plans of catalysts.

Our group developed an octahedral chiral-at-metal iridium(III) complex **IrO**, in which the metal center served as Lewis acid to activate one of substrates and at the same time serving as the sole source of chirality.[4] We wondered whether it is possible to develop the higher activity and better selectivity transition metal catalysts by modifying the ligands.

Based on **IrO**, the modifications of iridium catalyst are shown in Figure 18:

a) Two iridium complexes with larger steric hinderance around the central metal were designed. One is replacing cyclometalated 2-phenylbenzoxazole by 2-phenylbenzothiazole because the long C-S bonds which might position the two *tert*-butyl groups closer to the two vacant coordination sites (**IrS**); another is replacing *tert*-butyl group of 2-phenylbenzoxazole by adamantyl group which has larger size than *tert*-butyl group (**IrO(ada)**).

b) Five iridium complexes with electron withdrawing group or electron donating group were designed (**IrO(F)**, **IrO($CF_3$)**, **IrO($NO_2$)**, **IrO(OMe)**, **IrO(nap)**). The Lewis acidity of iridium complexes would be different by introducing the different groups to cyclometalated ligand.

c) Two cyclometalated pyrenyl iridium complexes were designed (**IrO(pyrene)** and **IrN(pyrene)**) because they might have longer triplet excited state lifetimes ($\tau_T$) so that they might be more efficient catalysts in photoinduced reactions.

### 3.1.1 Synthesis of chloro-bridged Ir or Rh dimers

The chloro-bridged Ir or Rh dimers with *N,N-trans*-configuration *rac*-**11-13** were synthesized according to a published route with some modifications (Method A), which involves refluxing $IrCl_3 \bullet nH_2O$ or $RhCl_3 \bullet nH_2O$ with 2–2.2 equivalents of cyclometalating ligand in a 3:1 mixture of 2-ethoxyethanol and water at 120–130 °C for 24 hours (Scheme 24).[5]

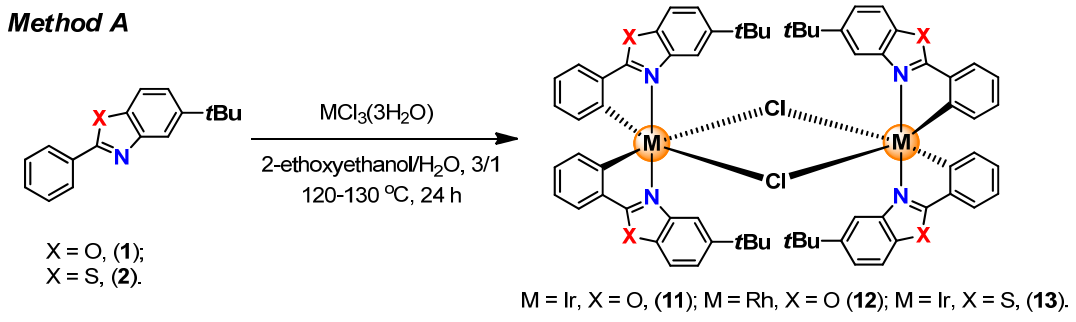


**Scheme 24** The Synthesis of Chloro-Bridged Ir or Rh Dimers with *N,N-trans*-Configuration

However, when there are electron withdrawing groups on the cyclometalating ligands, the *N,N-cis*-Ir-dimers *rac*-**14**, **16**, **18** instead of *N,N-trans*-Ir-dimers were obtained via method A (Scheme 25). The formation of *N,N-cis*-dimer was proved by $^1$HNMR and the crystal structure, and the structure of *N,N-cis*-Ir-dimers *rac*-**18** is shown in Figure 19.

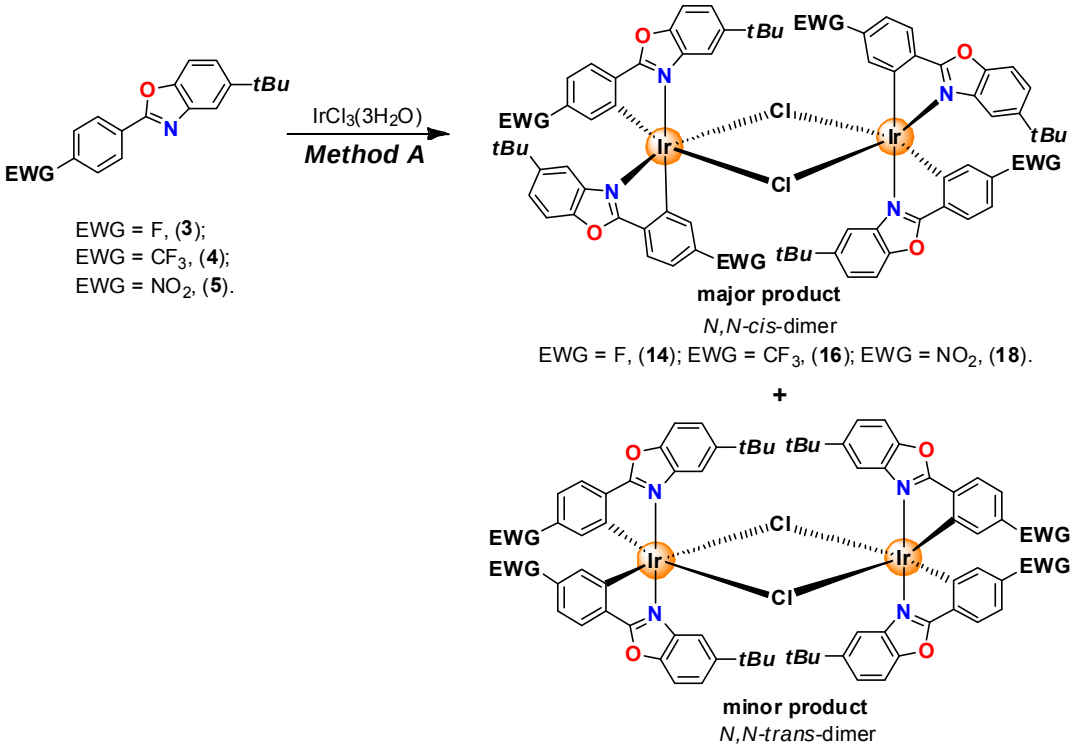


**Scheme 25** The Synthesis of Chloro-Bridged Ir Dimers with *N,N-cis*-Configuration

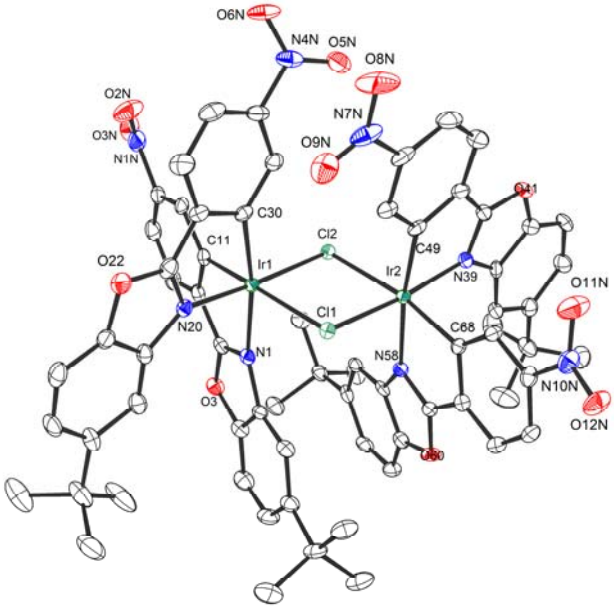


**Figure 19** Crystal structure of *rac*-**18** (*N,N-cis*-configuration). ORTEP drawing with 50% probability thermal ellipsoids. Selected bond lengths (Å) and angles (deg): Ir1−N1 = 2.131(3), Ir1−N20 = 2.040(3), Ir1−C11 = 2.003(4), Ir1−C30 = 2.023(4), Ir1−Cl1 = 2.4811(10), Ir1−Cl2 = 2.3744(10), Ir2−N39 = 2.028(3), Ir2−N58 = 2.161(3), Ir2−C49 = 2.007(4), Ir2−C68 = 2.003(4), Ir2−Cl1 = 2.3718(10), Ir2−Cl2 = 2.4824(3); N20−Ir1−Cl1 = 95.33(10), Cl1−Ir1−Cl2 = 83.80(3), Cl2−Ir1−C11 = 87.49(12), C11−Ir1−N20 = 94.29(15), C30−Ir1−N1 = 171.66(16).

The corresponding *N,N-trans*-Ir-dimers *rac*-**15**, **17**, **19** can be synthesized with Method B by avoiding water and increasing the temperature to 140–150 °C, and other related *N,N-trans*-Ir-dimers *rac*-**20-24** could also be synthesized by this method as shown in Scheme 26.

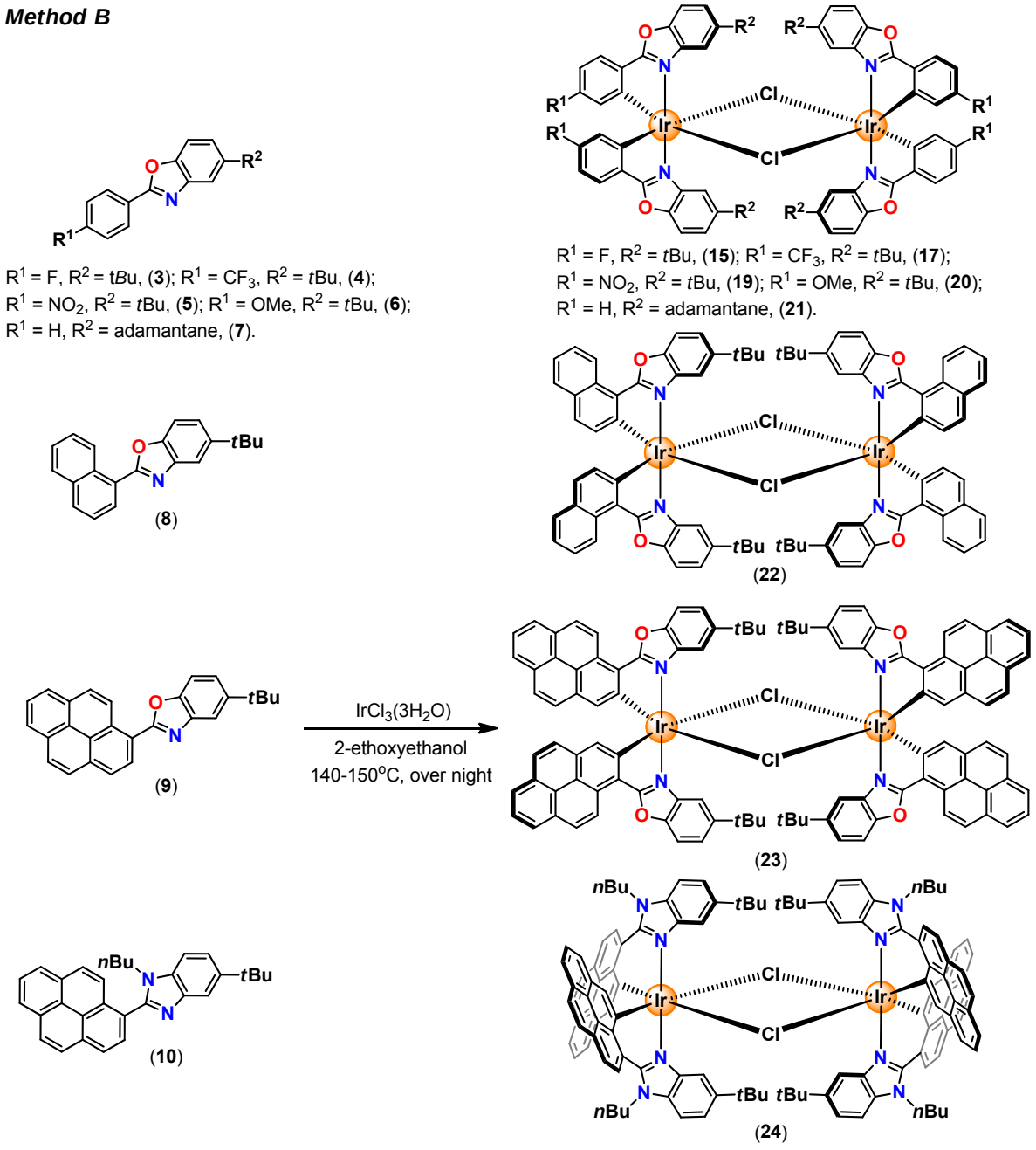


**Scheme 26** The Synthesis of Chloro-Bridged Ir Dimers with *N,N-trans*-Configuration

### 3.1.2 Synthesis of racemic Ir or Rh catalysts

Racemic Ir or Rh catalysts were synthesized according to the literature procedure[6] with some modifications. Heating the corresponding *N,N-trans*-dimer with 2.2–2.5 equivalents of $AgPF_6$ in acetonitrile at 50–70 °C over night afforded desired racemic Ir or Rh catalysts in 80–99% yield (Scheme 27). The crystal structures of catalysts *rac*-**IrO(NO$_2$)**, *rac*-**IrO(ada)**, *rac*-**IrO(nap)**,

*rac*-**IrO(pyrene)** and *rac*-**IrN(pyrene)** were obtained, which are shown in Figure 20-Figure 24, respectively.

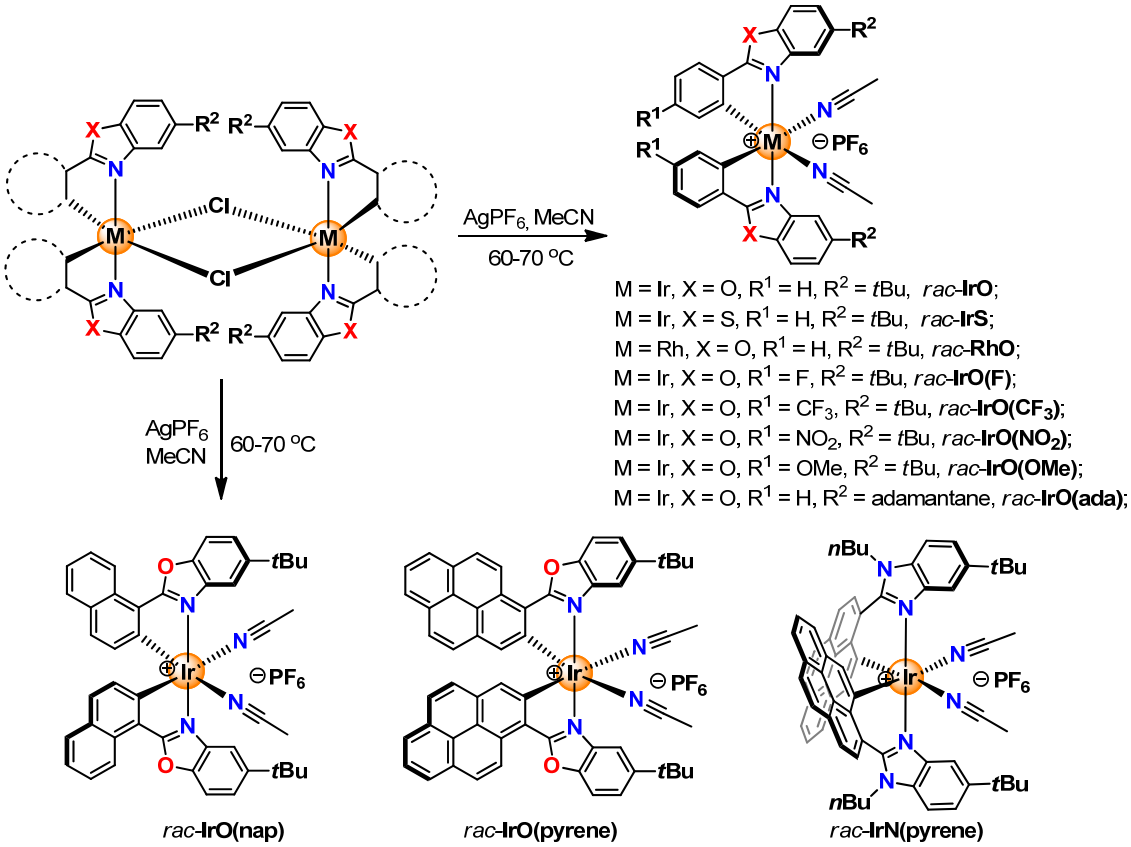


**Scheme 27** The Synthesis of Racemic Ir or Rh Catalysts

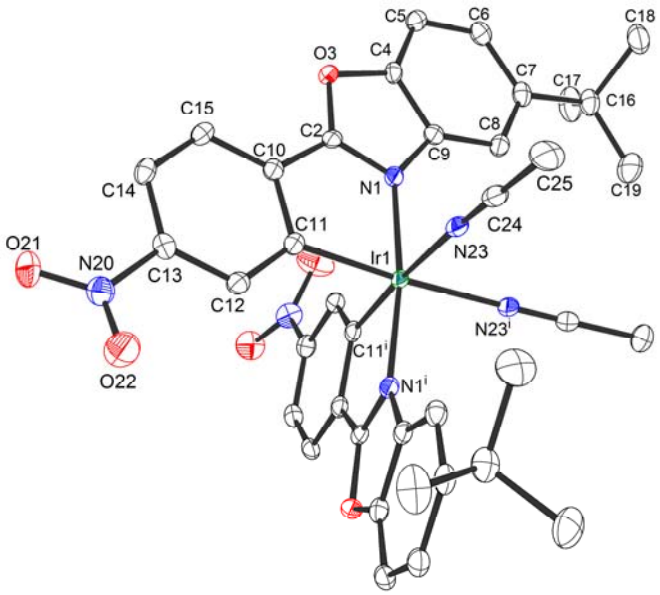


**Figure 20** Crystal structure of *rac*-**IrO(NO$_2$)**. Only Δ-**IrO(NO$_2$)** is shown and the hexafluorophosphate counteranion is omitted for clarity. ORTEP drawing with 50% probability thermal ellipsoids. Selected bond lengths (Å) and angles (deg): Ir1−N1 = 2.0459(16), Ir1−N23 = 2.1095(15), Ir1−C11 = 2.0282(18); N23$^i$−Ir1−N23 = 94.23(10), N23−Ir1−C11 = 90.30(6), C11−Ir1−C11$^i$= 90.86(9), C11$^i$−Ir1−N23$^i$ = 91.30(6), N1−Ir1−N1$^i$ = 171.22(8). Symmetry transformations used to generate equivalent atoms: #1 -x+1, y, -z+1/2.

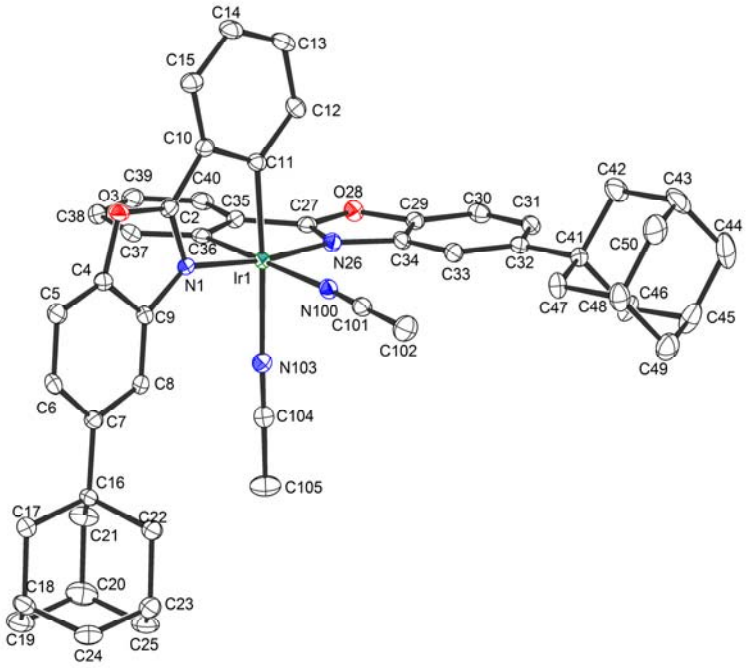


**Figure 21** Crystal structure of *rac*-**IrO(ada)**. Only Λ-**IrO(ada)** is shown and the hexafluorophosphate counteranion is omitted for clarity. ORTEP drawing with 50% probability thermal ellipsoids. Selected bond lengths (Å) and angles (deg): Ir1−N1 = 2.033(2), Ir1−N26 = 2.035(2), Ir1−N100 = 2.113(2), Ir1−N103 = 2.107(2), Ir1−C11 = 2.028(3), Ir1−C26 = 2.023(3); N100−Ir1−C11 = 94.23(10), C11−Ir1−C36 = 87.12(10), C36−Ir1−N103 = 90.98(10), N103−Ir1−N100 = 87.76(9), N1−Ir1−N26 = 171.64(9).

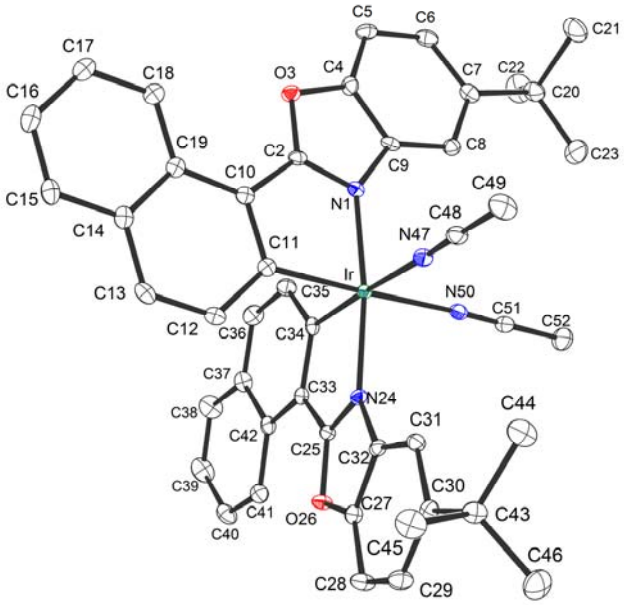


**Figure 22** Crystal structure of *rac*-**IrO(nap)**. Only Δ-**IrO(nap)** is shown and the hexafluorophosphate counteranion is omitted for clarity. ORTEP drawing with 50% probability thermal ellipsoids. Selected bond lengths (Å) and angles (deg): Ir1−N1 = 2.0385(15), Ir1−N24 = 2.0372(15), Ir1−N47 = 2.1172(16), Ir1−N50 = 2.1067(16), Ir1−C11 = 2.0223(18), Ir1−C35 = 2.0209(18); N50−Ir1−N47 = 90.12(6), N47−Ir1−C11 = 93.09(6), C11−Ir1−C34 = 86.56(7), C34−Ir1−C50 = 90.43(6), N1−Ir1−N24 = 172.23(6).

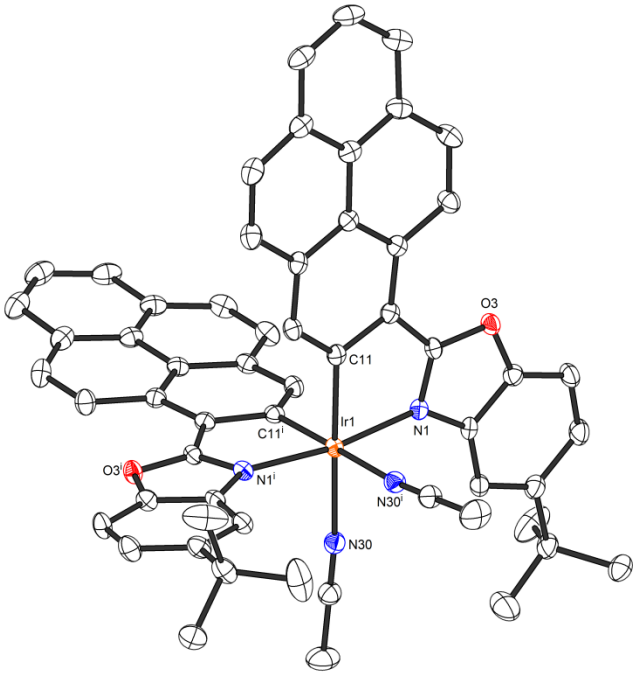


**Figure 23** Crystal structure of *rac*-**IrO(pyrene)**. Only Δ-**IrO(pyrene)** is shown and the hexafluorophosphate counteranion is omitted for clarity. ORTEP drawing with 50% probability thermal ellipsoids. Selected bond lengths (Å) and angles (deg): Ir1−N1 = 2.0470(17), Ir1−N30 = 2.1163(17), Ir1−C11 = 2.0321(19); N30−Ir1−N30$^{i}$ = 91.47(9), N30$^{i}$−Ir1−C11 = 88.86(7), C11−Ir1−C11$^{i}$ = 90.85(10), C11$^{i}$−Ir1−N30 = 88.86(7), N1−Ir1−N1$^{i}$ = 170.77(8). Symmetry transformations used to generate equivalent atoms: #1 –x, y, -z+1/2.

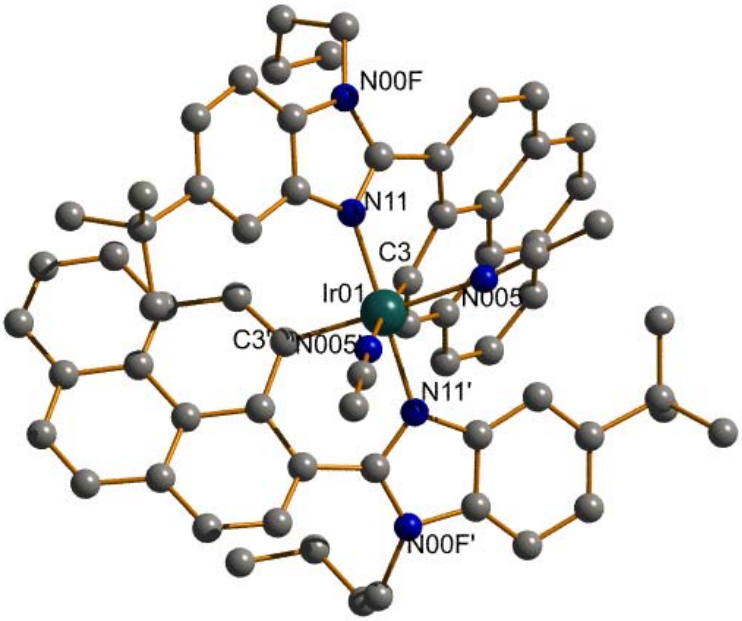


**Figure 24** Crystal structure of *rac*-**IrN(pyrene)**. Only Δ-**IrN(pyrene)** is shown and the hexafluorophosphate counteranion is omitted for clarity. Selected bond lengths (Å) and angles (deg): Ir01−N11 = 2.036(8), Ir01−N005 = 2.136(6), Ir1−C3 = 2.028(5); N005−Ir01−C3 = 90.58(9), C3−Ir01−C3' = 93.79(4), C3'−Ir01−N005' = 90.60(5), N005'−Ir01−N005 = 85.17(1), N11−Ir01−N11' = 178.70(6). Symmetry transformations used to generate equivalent atoms: 1–x, y, -z+3/2. (The quality of this crystal is not good enough.)

### 3.1.3 Synthesis of non-racemic Ir or Rh Lewis acid catalysts

The chiral-at-metal complexes can be synthesized with high enantiomeric purity through a convenient auxiliary-mediated strategy developed in our laborator.[7] The synthesis of Λ-**IrS** and Δ-**IrS** is shown in Scheme 28.

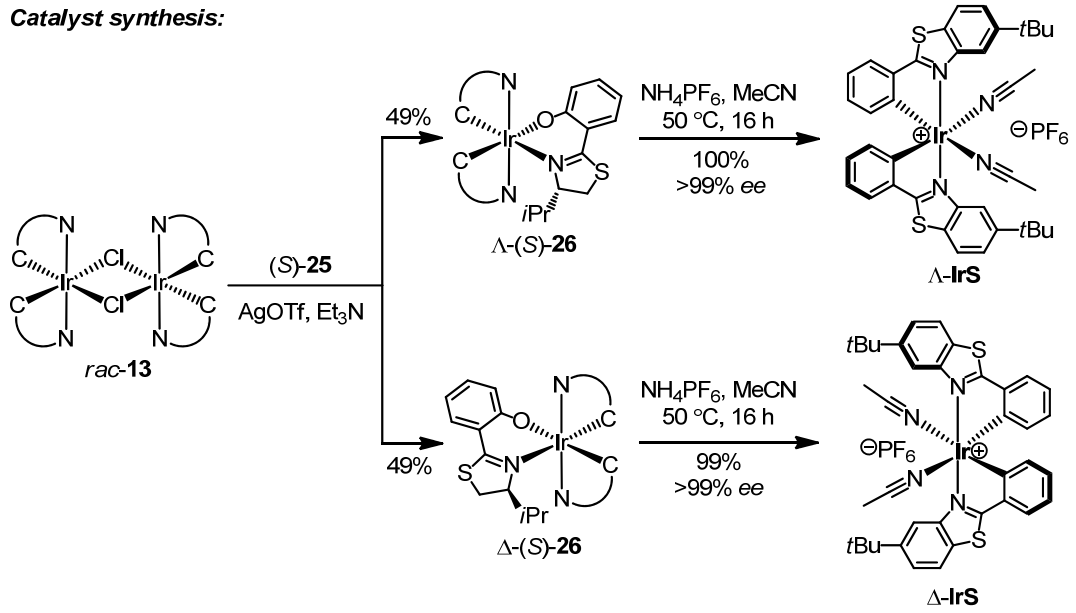


**Scheme 28** Auxiliary-Mediated Synthesis of the Enantiomerically Pure Chiral-at-Metal Iridium(III) Complexes Λ-**IrS** and Δ-**IrS**

Accordingly, the iridium dimer complex *rac*-**13** is reacted with the chiral auxiliary ligand (*S*)-4-isopropyl-2-(2'-hydroxyphenyl)-2-thiazoline ((*S*)-**25**) to afford the iridium(III) complexes Λ-(*S*)-**26** and Δ-(*S*)-**26** as a mixture of diastereomers, which can be resolved easily by standard silica gel chromatography on a gram scale (Figure 25).[12] Upon reaction in acetonitrile in the presence of the weak acid such as $NH_4PF_6$, at slightly elevated temperature (50 °C), these complexes are converted to virtually enantiopure complexes Λ-**IrS** and Δ-**IrS** (each >99% *ee*) by a stereospecific substitution of the (protonated) chiral auxiliary with two acetonitrile ligands under retention of configuration. The confirguration of this new catalyst was proved by X-ray crystal structure, which is shown in Figure 26. The enantiomeric purity of Λ-**IrS** or Δ-**IrS** was verified by HPLC on a chiral stationary phase (Figure 27).

Λ-**IrO(ada)** and Δ-**IrO(ada)** can be synthesized by the same method with some modifications (see Experimental Part for more details). The synthesis of non-racemic **IrO**[11] or chiral **RhO**[8] is followed published procedures.

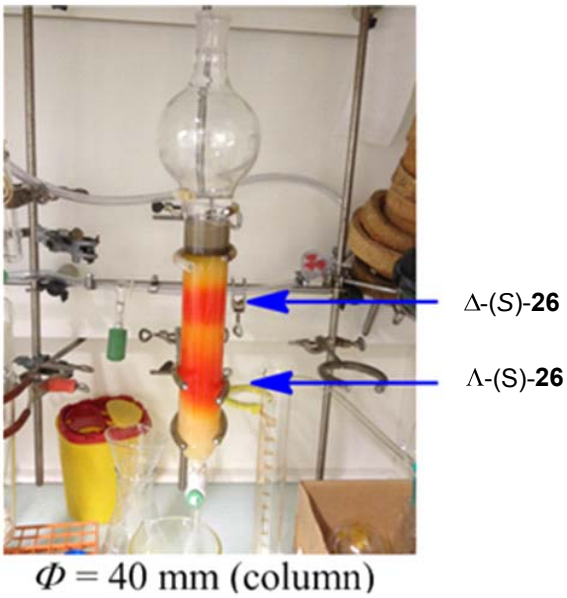


**Figure 25** Two diastereomers could be resolved by standard silica gel chromatography on a gram scale.

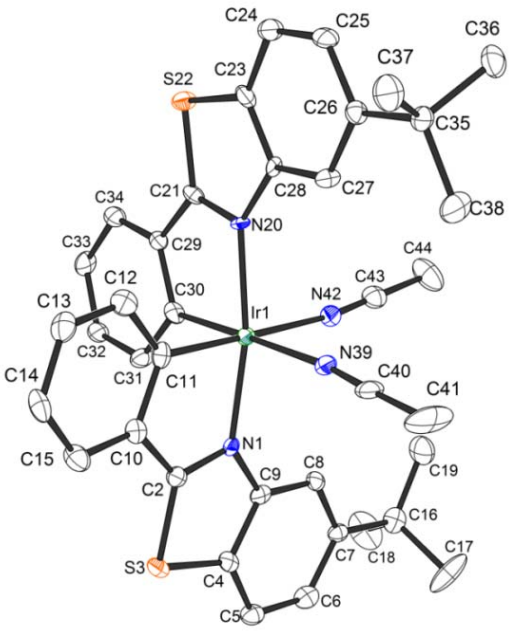


**Figure 26** Crystal structure of Λ-**IrS**. The hexafluorophosphate counteranion is omitted for clarity. ORTEP drawing with 50% probability thermal ellipsoids. Selected bond lengths (Å) and angles (deg): Ir1−N1 = 2.065(6), Ir1–N20 = 2.072(7), Ir1−N39 = 2.119(6), Ir1−N42 = 2.123(7), Ir1−C11 = 2.011(9), Ir1−C30 = 2.012(8); N39−Ir1−N42 = 88.7(3), N42−Ir1−C30 = 92.0(3), C30−Ir1−C11 = 89.5(3), C11−Ir1−N39 = 89.9(3), N1−Ir1−N20 = 169.6(3).

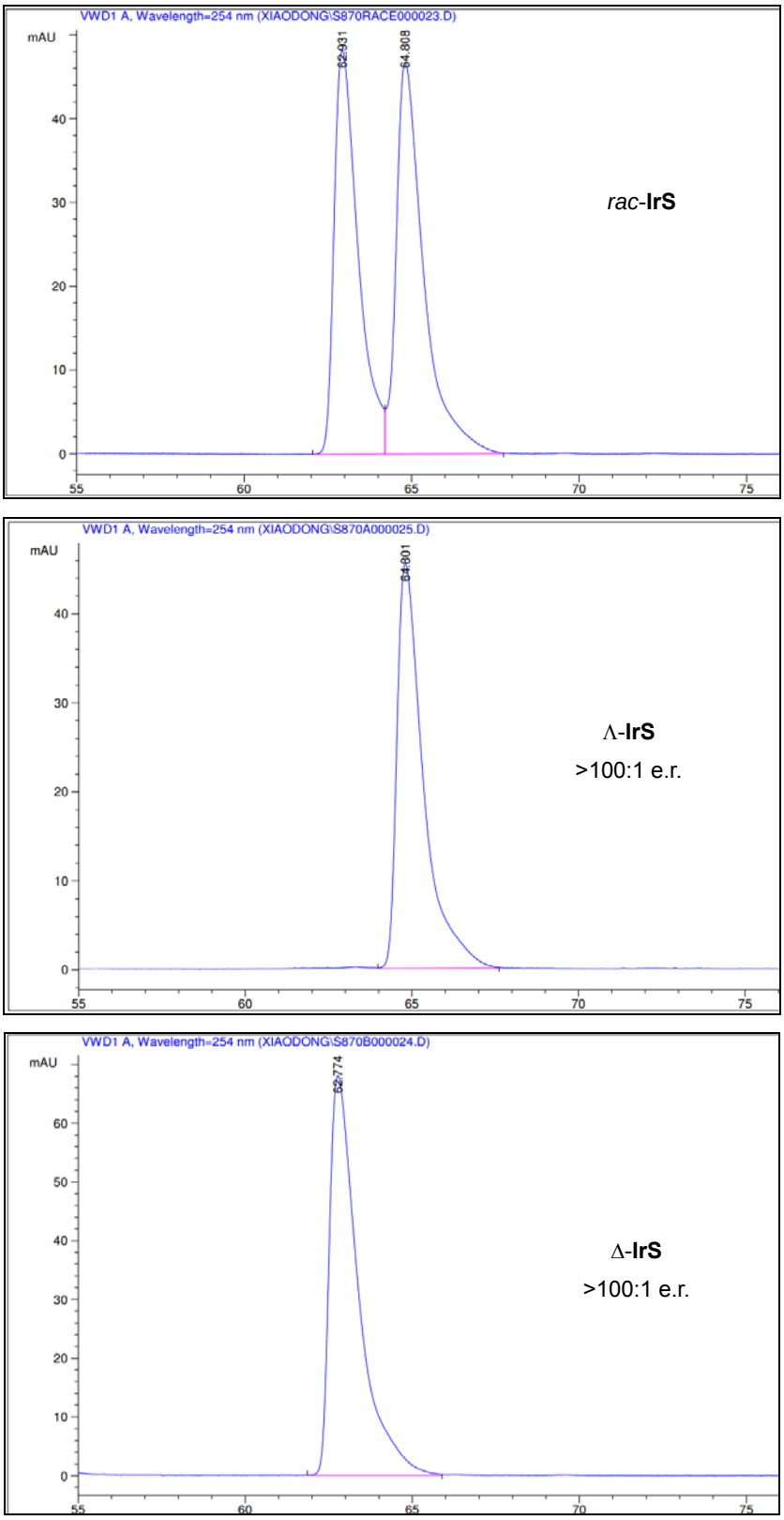


**Figure 27** Enantiomeric purities of the catalysts Λ-**IrS** and Δ-**IrS**.

*HPLC conditions: Daicel Chiralpak IB (250 × 4.6 mm); mobile phase: A = 0.1% TFA, B = MeCN; gradient: 38% to 46% B in 60 min; flow rate: 1.0 mL/min; 254 nm; 20 °C.*

The chiral auxiliary (*S*)-**25** [9] can be synthesized in three steps starting from acid chloride **27** in an overall yield of 57%. Reaction with the chiral amino alcohol (*S*)-**28** affords amide **29** (91%), which is cyclized to the thiazoline **30** with $P_2S_5$ (93%), followed by ether cleavage with $BBr_3$ (67%) (Scheme 29). It is noteworthy that the chiral auxiliary can be recovered after this reaction in high yield (96%) and without any loss of enantiomeric purity (≥99.9% *ee*) (Figure 28).

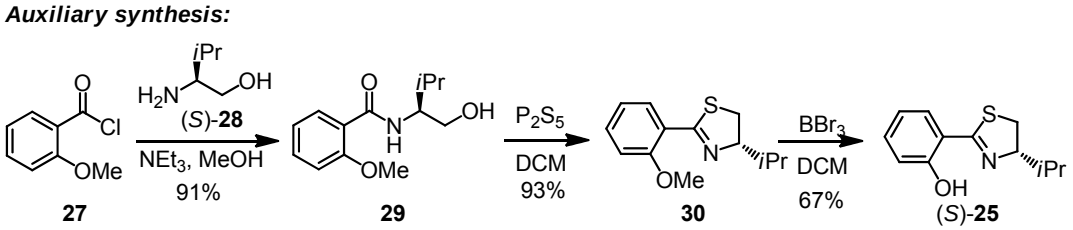


**Scheme 29** The Synthesis of the Chiral Auxiliary (*S*)-**25**

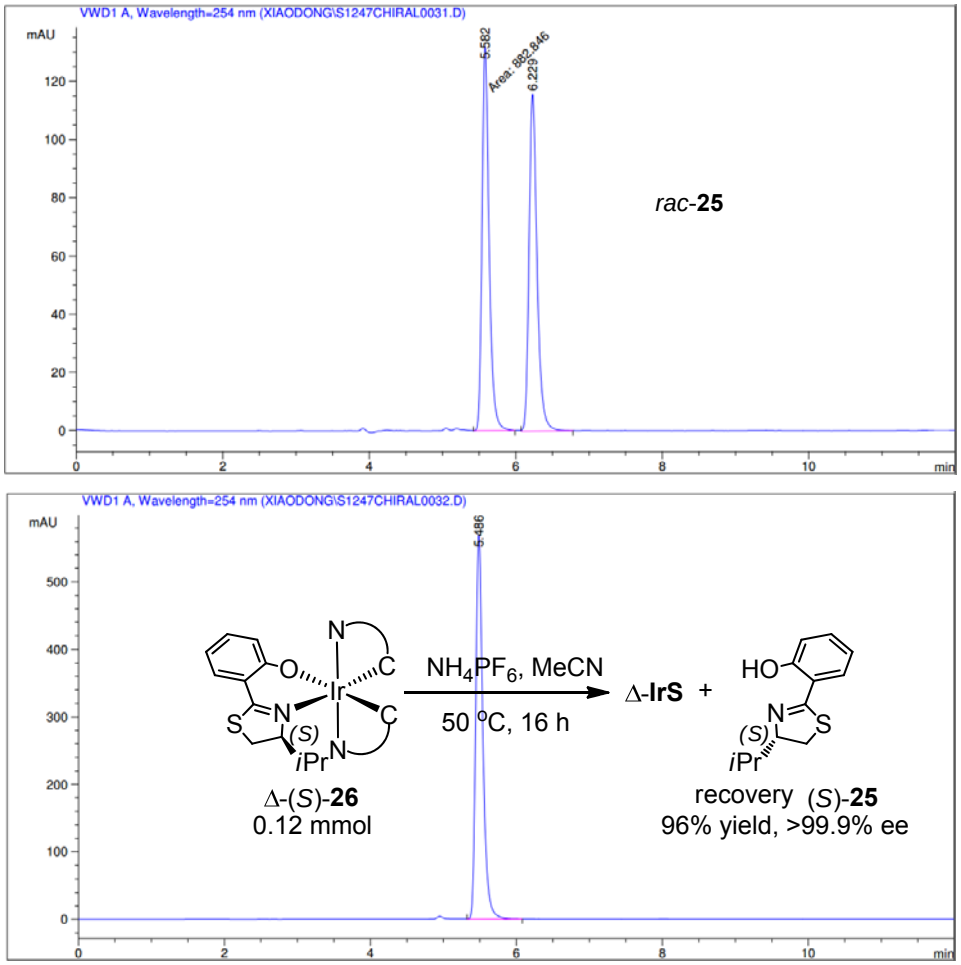


**Figure 28** HPLC traces of recovery of auxiliary.

*HPLC conditions: OD-H (250 × 4.6 mm); mobile phase: hexane/isopropanol = 99: 1; flow rate: 1.0 mL/min; 254 nm; 25 °C.*

All these chiral catalysts are configurationally stable, as they did not show any significant sign of configurational lability or decomposition from $^1$H NMR and HPLC upon storage under $N_2$ in a refrigerator (5 °C) for 3 months.

X-ray diffraction analyses showed that Λ-**IrS** and Λ-configuration of *rac*-**IrO(NO$_2$)**, *rac*-**IrO(ada)**, *rac*-**IrO(nap)**, *rac*-**IrO(pyrene)** are isostructural and all are six-coordinate monomers. The central metal in Λ-**IrS**, *rac*-**IrO(NO$_2$)**, *rac*-**IrO(ada)**, *rac*-**IrO(nap)** and *rac*-**IrO(pyrene)** is ligated by two cyclometalating ligands and two MeCN molecules. The six-coordinate metal can be described as an octahedron with two nitrogen atoms from two cyclometalating ligands repectively occupying the axial sites in an distorted fashion. The average Ir1-N(MeCN) bond lengths (2.121(7) Å for Λ-**IrS**, 2.1095(15) Å for *rac*-**IrO(NO$_2$)**, 2.110(2) Å for *rac*-**IrO(ada)**, 2.1120(16) Å for *rac*-**IrO(nap)**, 2.1163 (17) Å for *rac*-**IrO(pyrene)**) are comparable to the corresponding values found in **IrO** (2.106(9) Å)[11], but shorter than the cooresponding values found in *rac*-**IrN(pyrene)** (2.136(6) Å) or **RhO** (2.148(2) Å for Rh1-N(MeCN)[8].

## 3.2 Investigation for Asymmetric Lewis Acids Catalysis

Many functional groups in organic chemistry are amenable to Lewis acid activation in a straightforward and predictable fashion and chiral Lewis acids are therefore attractive tools for effective asymmetric catalysis.[10] One highly appealing goal in this area of research is the development of chiral Lewis acid catalysts which exhibit a broad generality with respect to reaction types and substrates. **IrO**[11,12] and **RhO**[8] complexes were found to be able to act as efficient chiral Lewis acid catalysts by our group. The octahedral metal center of these complexes is coordinated irreversibly by two cyclometalating bidentate ligands in a propeller-type fashion. Two additional exchange-labile coordinated acetonitriles allow substrates to become activated by two-point binding. These complexes are structurally quite simple and only contain achiral ligands, with metal-centered chirality being the exclusive source of chirality.[2] Importantly, despite the two labile acetonitrile ligands, the catalysts are configurationally inert and retain their relative and absolute configurations throughout the catalysis. In this work, we demonstrate the high versatility of the iridium(III) complexes Λ-**IrO** and Λ-**IrS** as chiral Lewis acid catalysts for a variety of asymmetric reactions with acceptor-substituted alkenes, including Friedel–Crafts alkylations, Michael additions with CH-acidic compounds, and cycloadditions.

### 3.2.1 Asymmetric conjugate additions by chiral-at-metal Lewis acids

As shown in Scheme 30, the catalytic activity of the following six different octahedral Lewis acids complexes on the Michael addition of malonodinitrile was firstly tested. It is found that the performance of these new synthesized catalysts were worse than **IrO**, modifying the ligand by introduction electron withdrawing or electron donating group on the cyclometalated 2-phenylbenzoxazole could not improve the activity of catalyst.

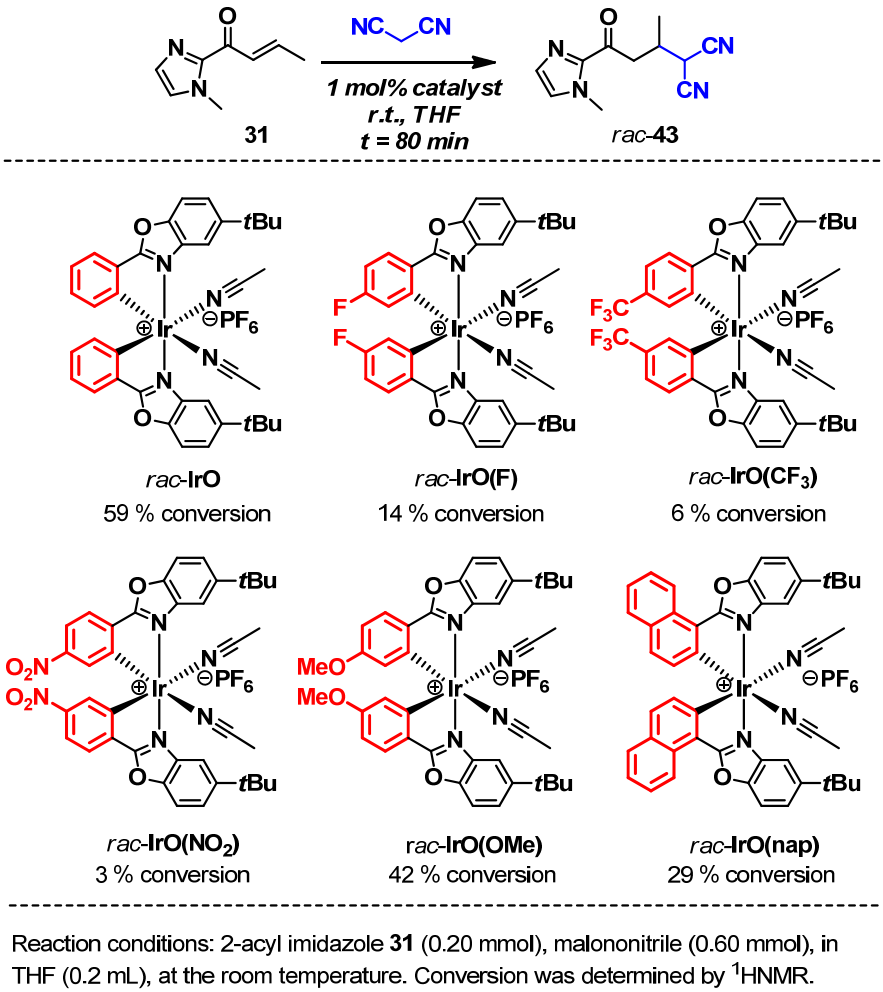


**Scheme 30** Comparison of Different Octahedral Lewis Acid Catalysts for Michael Addition of Malonodinitrile

We then were speculating that the derivative Λ- and Δ-**IrS**,[12] in which the cyclometalated 2-phenylbenzoxazole is replaced by a 2-phenylbenzothiazole, might provide a higher asymmetric induction due to the long C-S bonds which position the two *tert*-butyl groups closer to the two vacant coordination sites. Beside, we thought that the derivative Λ- and Δ-**IrO(ada)**, in which the *tert*-butyl group at the cyclometalated 2-phenylbenzoxazole is replaced by an adamantyl group, would have a bigger steric hinderance due to the bigger size of adamantane. Thus Λ- and Δ-**IrO(ada)** might also provide the better asymmetric induction (see Figure 21). Based on the result and speculation, we focused on catalysts Λ-**IrO**, Λ-**IrS**, and Λ-**IrO(ada)** for further study.

### 3.2.1.1 Asymmetric Friedel-Crafts alkylations

Λ- and Δ-**IrO** could efficiently catalyze the enantioselective Friedel-Crafts addition of indoles to α,β-unsaturated 2-acyl imidazoles.[11] We compared our new catalysts to this reaction at the same conditions.

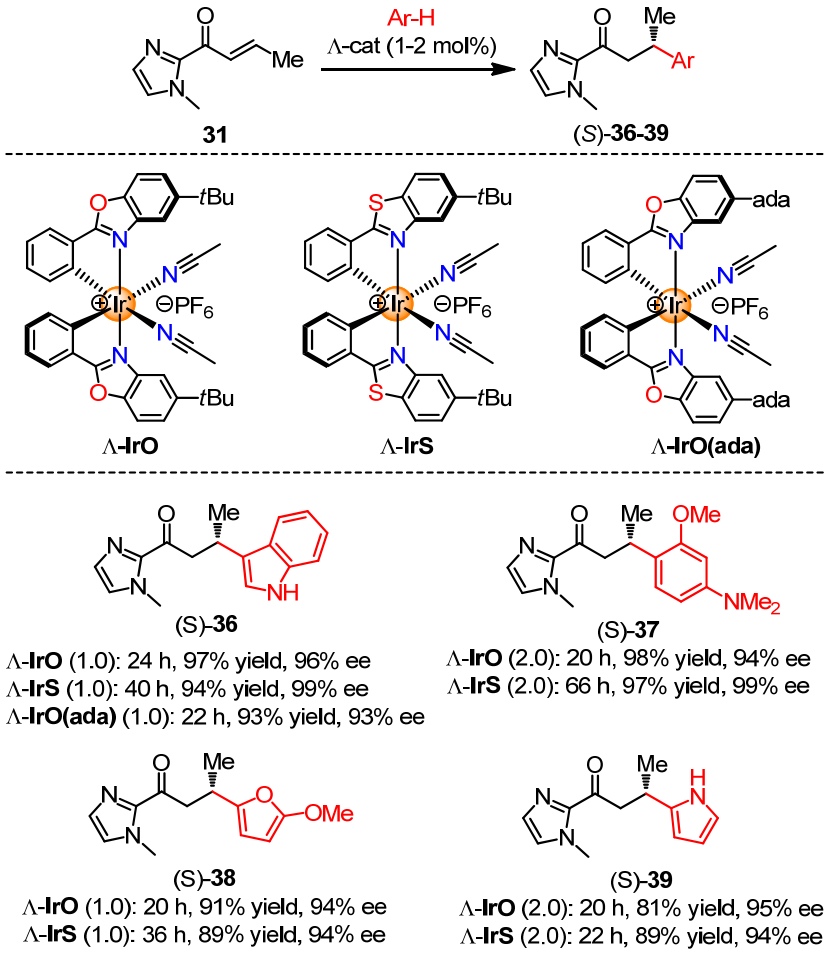


**Figure 29** Chiral octahedral iridium (III) Lewis acid catalysis applied to Friedel-Crafts alkylations with α,β-unsaturated 2-acyl imidazole **31**. *Haohua Huo (PhD student in Meggers Group) did a preliminary exploration by using Λ-**IrO** as catalyst.*

By using Λ-**IrS** (1.0 mol%) as catalyst, the Friedel-Crafts alkylation of indole with 2-acyl imidazole **31** afforded expected alkylation product (*S*)-**36** with 99% *ee* at room temperature compared to 96% *ee* for Λ-**IrO** (as shown in Figure 29).[13,14] However, Λ-**IrO(ada)** failed to give the alkylation product (*S*)-**36** with higher ee (only 93% ee). Then, we focused on comparison of Λ-**IrO** and Λ-**IrS**. The trend holds also for the Friedel-Crafts reaction with 3-dimethylaminoanisole, for which Λ-**IrS** (2.0 mol%) affords (*S*)-**37** in 97% yield and with higher 99% *ee*, compared to 94% *ee* when using Λ-**IrO** (2 mol%) instead. In contrast, for 2-methoxyfuran[14a,14b] and pyrrole[14a,14b,15] the respective Friedel-Crafts products (*S*)-**38** and (*S*)-**39** were obtained with almost equal enantioselectivities (as shown in Figure 29). Overall, compared to Λ-**IrO**, Λ-**IrS** generally requires somewhat elongated reaction time which can be attributed to the larger steric hinderance around the coordination sites.[16] The larger steric hinderance of **IrS** was confirmed by a crystal structure. As shown in Figure 30, a plane through the iridium and two MeCN ligands was drawn. The distance between the quaternary carbon atoms of the *tert*-butyl groups and plane in **IrS** (4.82 Å) is shorter than that in **IrO** (5.10 Å).

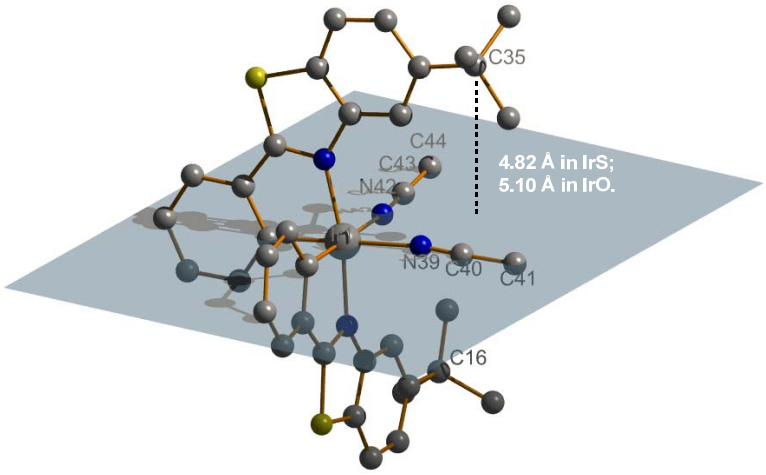


**Figure 30** Distances between the quaternary carbon atoms of the *tert*-butyl groups and the plane which through Iridium and MeCN ligands in **IrS** and **IrO**.

Meantime, the reactions can be accelerated by raising the temperature without affecting much the enantioselectivity (Table 1). For example, increasing the temperature for the reaction **31**→(*S*)-**37** from room temperature to 60 °C leads to full conversion in just 5 hours with only a slightly diminished enantioselectivity of 98% *ee* (Table 1, entry 5).

**Table 1** Friedel-Crafts Alkylation with α,β-Unsaturated 2-Acyl Imidazoles: Effects of Temperature[a]

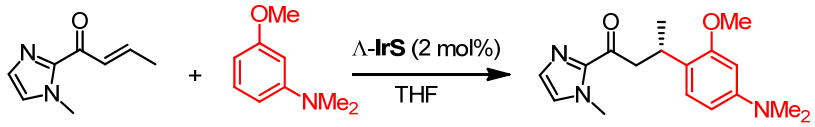


**31** (*S*)-**37**

| entry | substrate | product | cat. loading | temp (°C) | time (h) | yield (%)[b] | *ee* (%)[c] |
|---|---|---|---|---|---|---|---|
| 1 | R = Me (**31**) | (*S*)-**37** | 2.0 mol% | r.t. | 66 | 97 | 99 |
| 2 | R = Me (**31**) | (*S*)-**37** | 2.0 mol% | 30 | 48 | 94 | 99 |
| 3 | R = Me (**31**) | (*S*)-**37** | 2.0 mol% | 40 | 25 | 95 | 99 |
| 4 | R = Me (**31**) | (*S*)-**37** | 2.0 mol% | 50 | <20 | 99 | 98 |
| 5 | R = Me (**31**) | (*S*)-**37** | 2.0 mol% | 60 | 5 | 96 | 98 |

[a] Reaction conditions: 2-acyl imidazole **31** (0.20 mmol), 3-dimethylaminoanisole (0.60 mmol), in THF (0.1 mL). [b] Isolated yields. [c] Enantiomeric excess was determined by HPLC on chiral stationary phase.

Interestingly, this reaction is insensitive to air, and the product (*S*)-**37** was formed in a slight reduced yield (83% yield) with excellent enantioselectivity (99% ee) under the air (Table 2, entry 1). It is also noteworthy that the catalyst loading can be decreased for this reaction to 0.5 mol%, and the (*S*)-**37** was still obtained in excellent yield (96% yield) with excellent enantioselectivity (98% ee) by just prolong the reaction time (Table 2, entry 2). The different acyl imidazole substrates **32**-**34** also provide the

respective Friedel-Crafts alkylation products (*R*)-**40**, (*S*)-**41** and (*S*)-**42** in high yields (81−99% yield) with excellent enantioselectivities (96−99% ee) (Table 2, entries 3-5).

**Table 2** Friedel-Crafts Alkylation with α,β-Unsaturated 2-Acyl Imidazoles: Effects of Catalyst Loading andSubstituents [a]

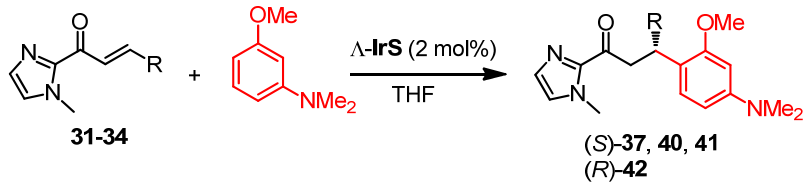


**31-34** (*S*)-**37**, **40**, **41** (*R*)-**42**

| entry | substrate | product | cat. loading | temp (°C) | time (h) | yield (%)[b] | *ee* (%)[c] |
|---|---|---|---|---|---|---|---|
| 1 [d] | R = Me (**31**) | (*S*)-**37** | 2.0 mol% | 40 | 25 | 83 | 99 |
| 2 | R = Me (**31**) | (*S*)-**37** | 0.5 mol% | 60 | 32 | 96 | 98 |
| 3 | R = Ph (**32**) | (*R*)-**40** | 2.0 mol% | 40 | 18 | 99 | 99 |
| 4 | R = $CO_2$Et (**33**) | (*S*)-**41** | 2.0 mol% | 40 | 24 | 95 | 99 |
| 5 | R = *n*Bu (**34**) | (*S*)-**42** | 2.0 mol% | 40 | 48 | 81 | 96 |

[a] Reaction conditions: 2-acyl imidazoles **31-34** (0.20 mmol), 3-dimethylaminoanisole (0.60 mmol), in THF (0.1 mL). [b] Isolated yields. [c] Enantiomeric excess was determined by HPLC on chiral stationary phase. [d] Yield and enantioselectivity for the analogous reaction performed under air.

### 3.2.1.2 Asymmetric Michael additions

Next, we studied our catalysts on the asymmetric Michael additions, the addition of CH-acidic malonodinitrile and 1,3-dicarbonyl compounds to the Michael acceptor **31**.

*1) Asymmetric addition of malononitrile*

By using Λ-**IrO** at a loading of 1.0 mol%, the malonodinitrile addition product (*S*)-**43**[17] was formed in a full conversion with 70% *ee* (Table 3, entry 1). Compared to Λ-**IrO**, Λ-**IrS** afforded the product with much higher enantioselectivity at the same conditions (84% ee, see entry 2). After conditions screening (entries 3-10), by using 1.2 equiv of malononitrile and 1.0 mol% of Λ-**IrS**, the (*S*)-**43** was generated in a yield of 95% with 90% ee at room temperature after 24 hours (entry 5). At the optimized conditions, Λ-**IrO** afforded the product in a yield of 96% with a slightly lower ee (88% ee, see entry 11). Λ-**IrO(ada)** was also tried for this reaction and gave the similar result with Λ-**IrS** (96% yield and 90% ee, see entry 12).

**Table 3** Asymmetric Addition of Malononitrile[a]

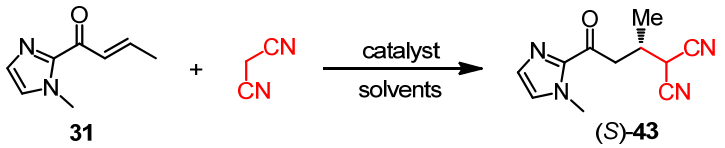


| entry | catalyst[b] | solvent | equiv of malononitrile | concn.[c] | t (h) | conv. (%)[d] | ee (%)[e] |
|---|---|---|---|---|---|---|---|
| 1 | Λ-**IrO** (1.0) | THF | 3 | 1.0 M | 18 | >99 | 70 |
| 2 | Λ-**IrS** (1.0) | THF | 3 | 1.0 M | 14 | >99 | 84 |
| 3[f] | Λ-**IrS** (1.0) | THF | 3 | 1.0 M | 40 | >99 | 84 |
| 4 | Λ-**IrS** (1.0) | THF | 3 | 0.5 M | 40 | >99 | 85 |
| 5 | Λ-**IrS** (1.0) | THF | 1.2 | 0.5 M | 24 | >99 (95)[g] | 90 |
| 6 | Λ-**IrS** (2.0) | THF | 1.2 | 0.5 M | 14 | >99 | 90 |
| 7 | Λ-**IrS** (1.0) | THF | 1.2 | 0.1 M | 30 | n.d. | 80 |
| 8 | Λ-**IrS** (1.0) | $Et_2O$ | 1.2 | 0.5 M | 16 | >99 | 88 |
| 9 | Λ-**IrS** (1.0) | cyclohexane | 1.2 | 0.5 M | 16 | n.d. | 54 |
| 10 | Λ-**IrS** (1.0) | *i*PrOH | 1.2 | 0.5 M | 16 | n.d. | 64 |
| 11 | Λ-**IrO** (1.0) | THF | 1.2 | 0.5 M | 16 | >99 (96)[g] | 88 |
| 12 | Λ-**IrO(ada)** (1.0) | THF | 1.2 | 0.5 M | 14 | >99 (96)[g] | 90 |

[a] Reaction conditions: 2-acyl imidazoles **31** (0.20 mmol), malononitrile (0.24 mmol or 0.60 mmol), in THF, at room temperature. [b] Catalyst loading given in brackets. [c] Concentration of 2-acyl imidazoles **31**. [d] Conversion is determined by $^1$H NMR. [e] Enantiomeric excess was determined by HPLC on chiral stationary phase. [f] The reaction is operated at 5 °C. [g] Isolated yield. *The experiment in entry 1 was investigated by Haohua Huo (PhD student in Meggers group).*

*2) Asymmetric addition of Meldrum's acid*

Then, the asymmetric addition of Meldrum's acid was investigated (Table 4). By using Λ-**IrS** (2.0 mol%) as catalyst, the Micheal addition of Meldrum's acid with 2-acyl imidazole **31** afforded expected product (*S*)-**44** in a yield of 94% with 91% *ee* (entry 3) at room temperature compared to 81% *ee* for Λ-**IrO** (entry 5).

**Table 4** Asymmetric Addition of Meldrum's Acid[a]

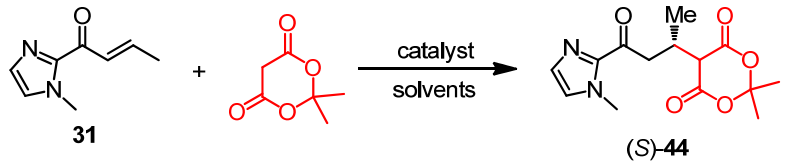


**31** (*S*)-**44**

| entry | catalyst[b] | concn.[c] | T (°C) | t (h) | conv. (%)[d] | ee (%)[e] |
|---|---|---|---|---|---|---|
| 1 | Λ-**IrO** (1.0) | 0.5 M | r.t. | 18 | >99 | 64 |
| 2 | Λ-**IrS** (1.0) | 0.5 M | r.t. | 16 | >99 | 80 |
| 3 | Λ-**IrS** (2.0) | 1.0 M | r.t. | 6 | >99 (94)[f] | 91 |
| 4 | Λ-**IrS** (2.0) | 1.0 M | 5 | 20 | >99 | 92 |
| 5 | Λ-**IrO** (2.0) | 1.0 M | r.t. | 6 | >99 (93)[f] | 81 |

[a] Reaction conditions: 2-acyl imidazoles **31** (0.20 mmol), Meldrum's Acid (0.60 mmol), in THF, at room temperature. [b] Catalyst loading given in brackets. [c] Concentration of 2-acyl imidazole **31**. [d] Conversion is determined by $^1$H NMR. [e] Enantiomeric excess was determined by HPLC on chiral stationary phase. [f] Isolated yield. *The experiment in entry 1 was investigated by Haohua Huo (PhD student in Meggers group).*

*3) Generation of asymmetric quaternary stereocenters with Michael additions*

Λ-**IrO** and Λ-**IrS** are also suitable to catalyze the formation of an all-carbon quaternary stereocenter[18]. In the presence of Λ-**IrS** (2.0 mol%), the reaction of *tert*-butyl 2-oxocyclopentane-1-carboxylate with 2-acyl imidazole **31** afforded (*S*,*S*)-**46** in 85% yield with 96% *ee*, and 1.5:1 *dr* compared to 53% yield with 90% ee for Λ-**IrO** (*dr* = 1.8:1). The related Michael addition of 2,3-dihydro-1-oxo-1*H*-indene-2-carboxylic acid *tert*-butyl ester to 2-acyl imidazole **31** provided (*S*,*S*)-**47** in 93% yield with 97% *ee* and 22:1 *dr* by using Λ-**IrS** (1.0 mol%). Compared to Λ-**IrS**, Λ-**IrO** afforded (*S*,*S*)-**47** with the identical enantioselectivity (97% ee) albeit with lower diastereomeric ratio (*dr* = 10:1). (Figure 31)

Next, a brief substrate scope was investigated by using Λ-**IrS** as catalyst. *tert*-Butyl 5-oxo-6,7-dihydro-5*H*-indeno[5,6-*d*][1,3]dioxole-6-carboxylate reacted with 2-acyl imidazole **31** to afford (*S*,*S*)-**48** in 72% yield with 97% ee and 11:1 *dr*. The related reaction of *tert*-butyl 2-oxocyclopentane-1-carboxylate with different 2-acyl imidazoles **33**, **34**, **45** afforded the product (*S*,*S*)-**49** (81% yield with 96% *ee*, and 15:1 *dr*), (*S*,*S*)-**50** (20% yield with 85% *ee*, and 9:1 *dr*) and (*S*,*S*)-**51** (87% yield with 96% *ee*, and 49:1 *dr*) respectively (Figure 31). The relative configuration of the main diastereomer of (*S*,*S*)-**51** was assigned from a crystal structure (Figure 32).

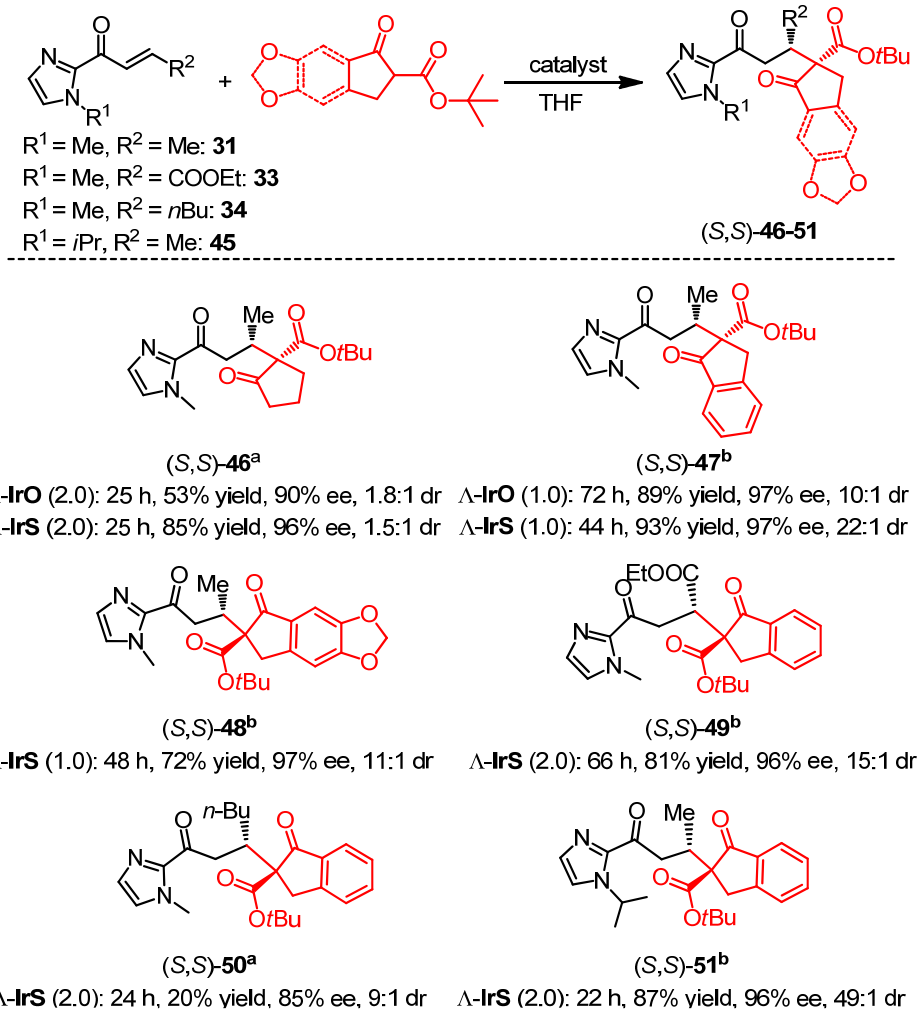


**Figure 31** Generation of asymmetric quaternary stereocenters with Michael additions.

*[a]Reaction conditions: 2-acyl imidazoles (0.20 mmol), 1,3-dicarbonyl compounds (0.40 mmol), in THF, at 40 °C. [b]Reaction conditions: 2-acyl imidazoles (0.20 mmol), 1,3-dicarbonyl compounds (0.40 mmol), in THF, at room temperature. Chuanyong Wang (PhD student in Meggers group) did the conditions screening for* ***46*** *and* ***47****.*

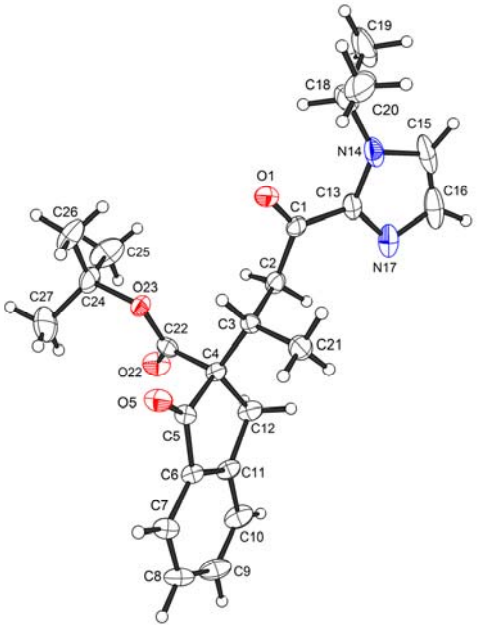


**Figure 32** The crystal structure of (*S*,*S*)-**51**. ORTEP drawing with 50% probability thermal ellipsoids.

### 3.2.1.3 Asymmetric cycloadditions

Asymmetric cycloadditions with α,β-unsaturated 2-acyl imidazoles by using Λ-**IrO** and Λ-**IrS** as catalysts were next investigated (Figure 33). Accordingly, the reaction of **31** with the nitrone catalyzed by 2.0 mol% of Λ-**IrS** provided the 1,3-dipolar cycloaddition product **52** in a yield of 86% with excellent 98% *ee*, while virtually forming just one diastereomer (*endo*:*exo* >100:1).[19,20] The enantioselectivity was significantly lower by using Λ-**IrO** (92% *ee*). In contrast, for the hetero-Diels-Alder reaction between **31** or **35** with 2,3-dihydrofuran under formation of the dihydropyrans **53** and **54**, respectively, Λ-**IrO** (2 mol%) turned out to be the catalyst of choice, providing higher yield with higher diastereo- and enantioselectivities (99% yield, 98% ee and *endo/exo* > 50:1 for **53**; 81 yield, 99% ee and *endo/exo* > 50:1 for **54**) than those of Λ-**IrS** (80% yield, 95% ee and *endo/exo* > 30:1 for **53**; 40% yield, 99% ee and *endo/exo* > 20:1 for **54**).[21,22] At last, the Diels-Alder reaction of **31** with isoprene provided the desired product **55** with excellent enantio- and diastereoselectivities with Λ-**IrO** and Λ-**IrS** (76% yield, 98% ee and *dr* > 99:1 for Λ-**IrO**; 56% yield, 99% ee and *dr* > 99:1 for Λ-**IrS**).[23]

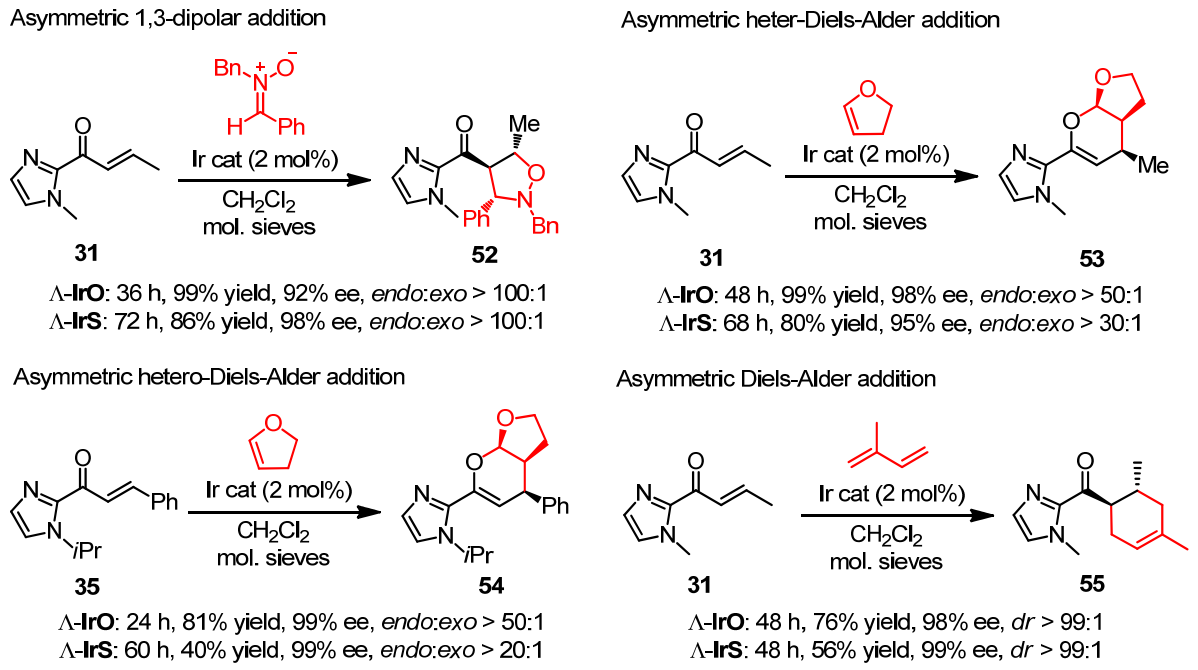


**Figure 33** Chiral octahedral iridium(III) Lewis acid catalysis applied to cycloadditions with α,β-unsaturated 2-acyl imidazoles.

*Haohua Huo (PhD student in Meggers Group) did a preliminary exploration for 1,3-dipolar addition by using Λ-**IrO** as catalyst and Bo Zhang (Master student in Meggers Group) did a preliminary exploration for Diels-Alder addition by using Λ-**IrO** as catalyst.*

In order to determine the absolute and relative configuration of the Diels-Alder product, 2-acyl imidazole **55** was transformed into **56** by treatment with MeOTf (methylation of **55**) and a base (DBU) (Scheme 31). The observed optical rotation of **56** is opposite to that of (1*S*, 6*S*)-**56** in literature,[24,25] and absolute and relative configuration of **55** is 1*R*, 6*R*.

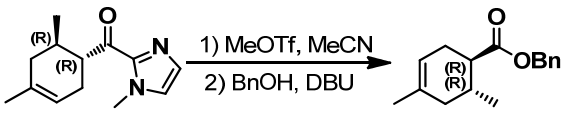


**55** **56**
99% yield, 98% ee

**Optical rotation of (1*R*, 6*R*)-56:**

$[\alpha]_D^{20} = -131.6°$ (*c* 0.7, $CH_2Cl_2$, 98% ee).

Lit.[24] : $[\alpha]_D^{20} = +54°$ (*c* 0.055, $CH_2Cl_2$), (1*S*,6*S*)-**56**.

Lit.[25] : $[\alpha]_D = +171°$ (*c* 1.0, $CH_2Cl_2$, 99% ee), (1*S*,6*S*)-**56**.

**Scheme 31** Assignment of the Absolute and Relative Configuration of the Diels-Alder Product **56**

### 3.2.1.4 Scope of acceptor-substituted alkenes

After revealing that **IrO** and **IrS** catalyse the asymmetric conjugate addition of a wide variety of nucleophiles to α,β-unsaturated 2-acyl imidazoles, the scope with respect to acceptor substituted alkenes was next investigated and the enantioselective Friedel-Crafts alkylation with 3-dimethylaminoanisole was used as model reaction (Figure 34).

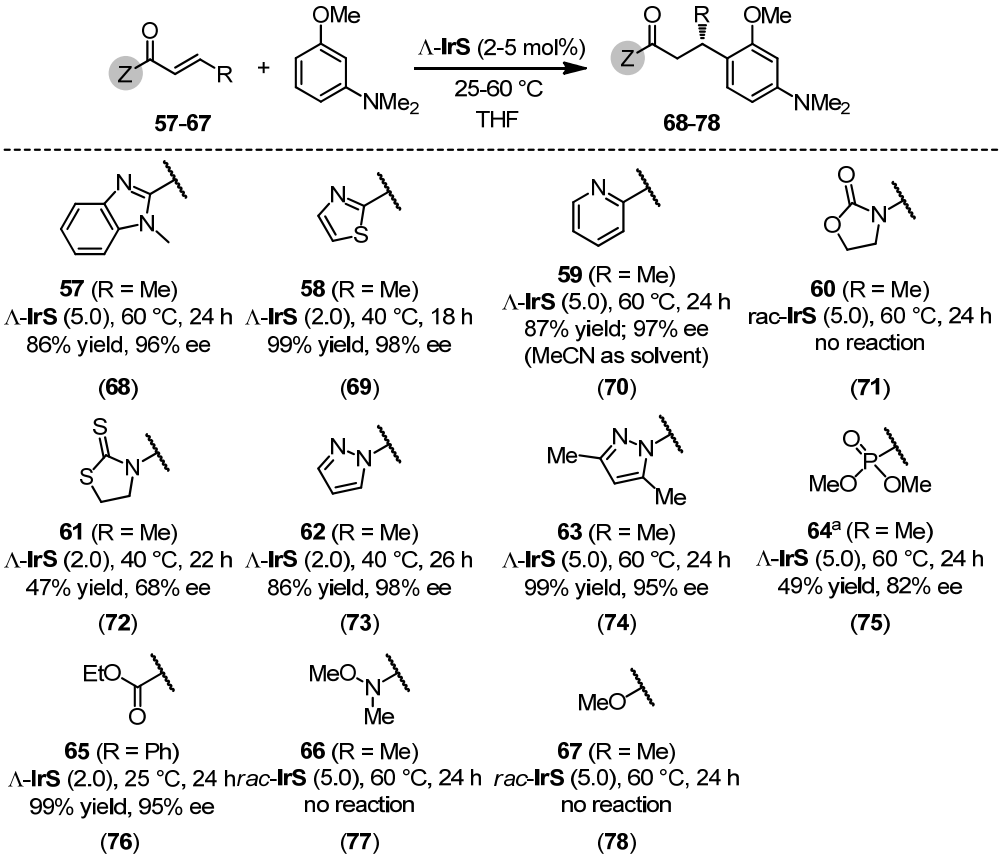


**Figure 34** Substrate scope with respect to electron acceptor substituted alkenes. [a]The yield and ee were determined with the ester derivative.

We were pleased to find that a significant number of the tested acceptor-substituted alkenes **57-67**[14a,14b,26-34] proved to be suitable substrates, providing the expected products in high yields with high enantioselectivities, such as the benzimidazole **57** (86% yield, 96% *ee*),[26] 2-thiazole **58** (99%

yield, 98% *ee*),[27] pyridine **59** (87% yield, 97% *ee*),[28] pyrazoles **62** (86% yield, 98% ee), **63** (99% yield, 95% ee),[31] and α-ketoester **65** (99% yield, 95% ee).[33] Apparently, only substrates that can efficiently coordinate to the iridium catalyst in a bidentate fashion give satisfactory results, whereas the simple α,β-unsaturated carboxylic ester **67** does not afford any product even at higher catalyst loadings of 5 mol% and an elevated temperature of 60 °C. On the other hand, we do not have an explanation for the failing or sluggish conversion of some of the other substrates such as the 2-oxazolidinone **59** (no reaction),[29] 2-thiazolidinethione **61** (47% yield, 68% ee),[30] phosphonate **64** (49% yield, 82% ee),[31] and Weinreb amide **66** (no reaction).[34] However, it is believed that the addition to α,β-unsaturated ketoesters,[33] α,β-unsaturated *N*-acyl pyrazoles,[31] α,β-unsaturated 2-acyl thiazoles[27, 35] and α,β-unsaturated 2-acyl imidazoles[36] are particularly useful substrates since they are easily converted to a variety of different carbonyl compounds.

### 3.2.1.5 Mechanistic considerations

It is plausible that the catalytic cycle starts with the bidentate coordination of the α,β-unsaturated carbonyl compound to the catalyst through the carbonyl and one additional moiety (e.g. imidazole, benzimidazole, pyrazole, pyridine or carboxylic ester) under release of the two labile acetonitrile ligands, thereby leading to the intermediate **A** (**79**, Figure 35). This two-point binding of the substrate increases the electrophilicity of the double bond and promotes a nucleophilic addition to the β-position of the alkene. Figure 36 displays a crystal structure of such an intermediate **A**, namely the substrate **35** coordinated to Λ-**IrO** (Scheme 32). The space filling model of this structure also convincingly illustrates that the prochiral *Si*-face is shielded by one *tert*-butyl group and therefore guides the nucleophilic addition to the *Re*-face. This is consistent with the obtained absolute configuration of the addition products and leads to the intermediate enolate complex **B**, which after protonation, provides the bidentate coordinated substrate (intermediate **C**). The replacement of the coordinated product by a new substrate, followed by a new catalytic cycle, presumably occurs through an intermediate in which the product is monocoordinated and the sixth coordinate site either filled by acetonitrile or the new substrate (intermediate **D**, **80**). Such formed iridium coordinated product was trapped for the conversion **35**→**54**. Figure 37 shows that the cycloaddition product **54** is coordinated to the catalyst through the imidazole moiety and an acetonitrile ligand is filling the remaining coordination sphere (also see Scheme 33).

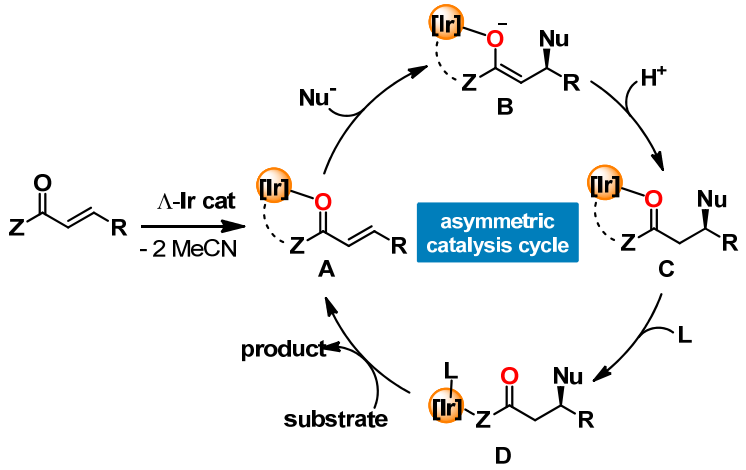


**Figure 35** Plausible mechanistic cycle for the reported asymmetric Lewis acid catalysis.#

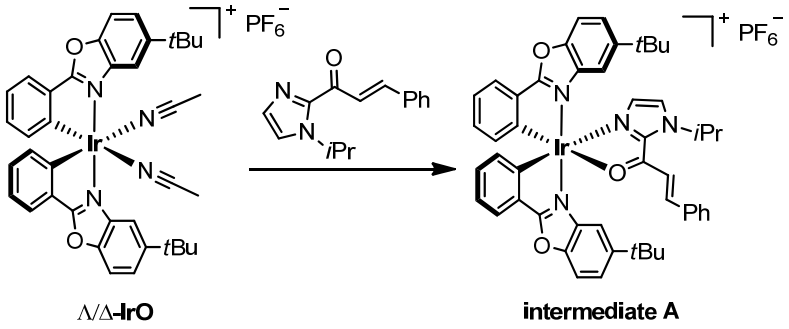


**Scheme 32** Iridium-Coordinated Substrate (Intermediate **A**, **79**)

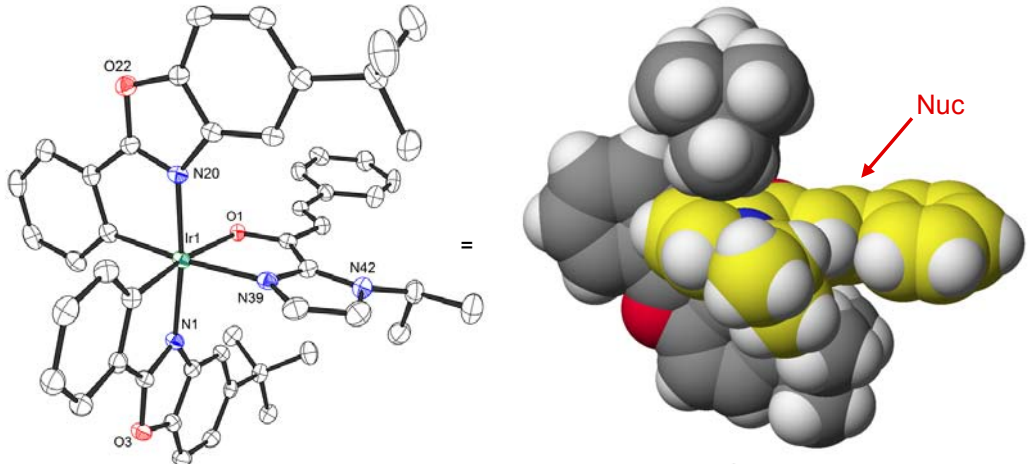


**Figure 36** Crystal structure obtained upon reaction of Λ/Δ-**IrO** with the substrate **35**. See Experimental Part for more details. Only the Λ-enantiomer is shown and the hexafluorophosphate counteranion is omitted for clarity. ORTEP drawing with 50% probability thermal ellipsoids and space filling representation with an adjusted orientation.

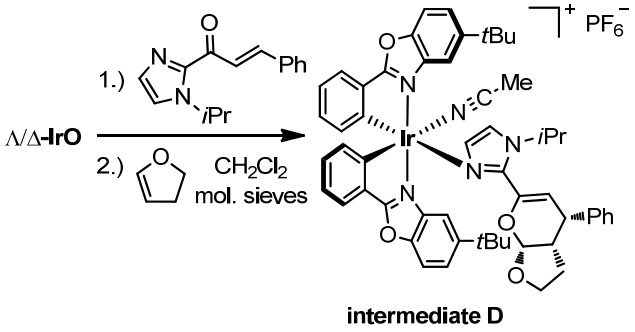


**Scheme 33** Iridium-Coordinated Product (Intermediate **D**, **80**)

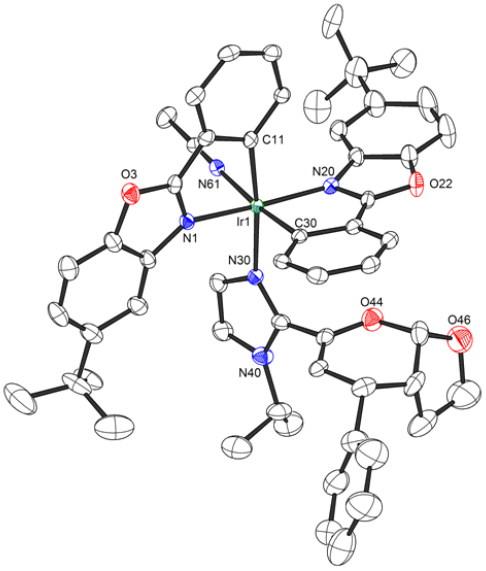


**Figure 37** Crystal structure obtained upon the reaction of racemic Λ/Δ-**IrO** with substrate **35** over night, followed by the addition of 2,3-dihydrofuran. See Experimental Part for more details. Only the Δ-enantiomer is shown and the hexafluorophosphate counteranion is omitted for clarity. ORTEP drawing with 50% probability thermal ellipsoids.

Finally, kinetic experiments (Figure 38, see Experimental Part for more details) performed with the reaction **31**→**37** revealed that the rate of the overall catalysis does not depend on the concentration of the nucleophile 3-dimethylaminoanisole but is directly proportional to the concentration of the α,β-unsaturated 2-acyl imidazole **31**, thus demonstrating that rate determining step cannot be the nucleophilic addition to the iridium-coordinated substrate (conversion **A**→**B** in Figure 35) but instead must be the replacement of iridium-coordinated product with a new substrate molecule (conversion **D**→**A** in Figure 35). This is not unexpected because of the well known kinetic stability of coordinative bonds to iridium(III) in octahedral complexes.

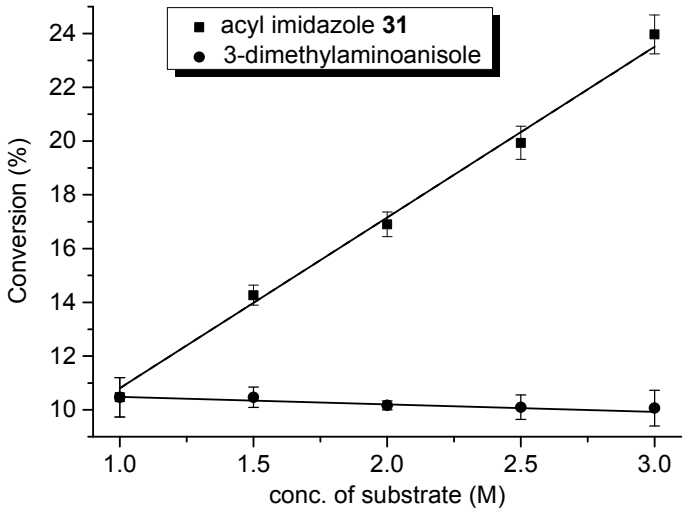


**Figure 38** Kinetic experiments to get insight into the rate determining step. Dependence of the conversion **31→37** as a function of substrate concentrations.

In summary, the reactions discussed here reveal the versatility of the chiral-at-metal iridium(III) catalysts. It is quite remarkable that a single class of chiral Lewis acid catalysts is capable of effectively catalyzing different reaction types, as demonstrated for Friedel-Crafts alkylations (including indole (up to 99% ee), 3-dimethyl-aminoanisole (up to 99% ee), 2-methoxyfuran (up to 94% ee), and pyrrole (up to 95% ee)), Michael additions of CH-acidic compounds (including malonodinitrile (up to 90% ee), and 1,3-dicarbonyl compounds (up to 97% ee)), and a variety of cycloadditions (including 1,3-dipolar cycloaddition (up to 98% ee, *endo: exo* > 100:1), hetero-Diels-Alder reactions (up to 99% ee, *endo: exo* > 50:1), and Diels-Alder reaction (up to 99% ee, *d.r.* >99:1)). A significant variability also exists with respect to the α,β-unsaturated carbonyl substrates as long as they allow a two-point binding to the iridium catalyst. It is convincing that this novel class of chiral-only-at-metal catalysts are of significant practical value as they are accessible in a straightforward fashion, are unproblematic for long term storage, provide excellent yields and asymmetric inductions at low catalyst loadings, can be used at room temperature or slightly elevated temperatures, and do not require a stringent exclusion of air and moisture.

### 3.2.2 Generation of asymmetric quaternary stereocenters with the Henry reaction

The asymmetric Henry reaction, namely the addition of nitroalkane with α-hydrogen to an aldehyde or ketone (form a β-nitro alcohol), is a highly useful C–C bond forming reaction and provides straightforward access to a variety of nitrogen-containing chiral building blocks and scaffolds. To our best of knowledge, there is no report about asymmetric Henry reaction with 2-acyl pyridine due to strong background reaction, and only one report that was dealt with the direct asymmetric Henry reaction with 2-acyl-pyridine *N*-oxides, leading to pyridine-derived tertiary nitroaldols as far. In 2014, Pedro reported the asymmetric addition of nitromethane to 2-acylpyridine *N*-oxides catalyzed by Cu(II)-BOX complexes to give the corresponding tertiary nitroaldols in variable yield (17–96% yield) with moderate to good enatiomeric excesses (48–96% ee).[37] For their study, the high catalyst loading (20 mol%), low temperature (–30 °C) and long time (24–96 h) were necessary. These products can be easily transformed into pyridyl amino alcohols bearing a quaternary stereocenter which are very useful in the pharmaceutical industry, agrochemical industry and asymmetric catalysis.[37] Some representative applications based on pyridyl amino alcohols[38-41] are shown in Figure 39.

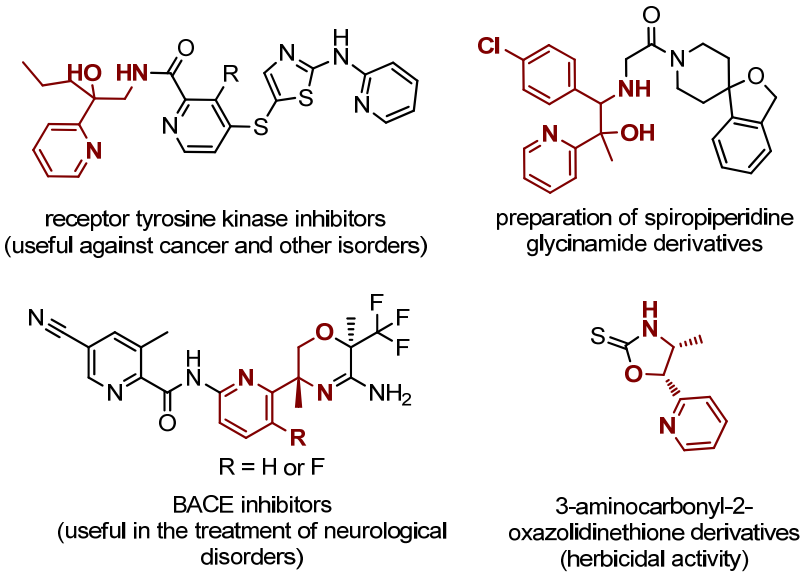


**Figure 39** Representative applications based on pyridyl aminoalcohols.

We present that our Λ-**IrO** and Λ-**IrS** could act as effective asymmetric catalysts (4 mol% catalyst loading) for Henry reaction (up to 98% ee) at room temperature. Based on the reported literature[37], nitromethane was chosen as solvent, in the presence of diisopropylamine (20 mol%) and Λ-**IrS** (4 mol%), the target product tertiary nitroaldol was obtained with modest enantiomeric excess of 76% ee within 50 min at room temperature (Table 5, entry 1). A solvent screening reveals that DCM, THF, toluene and $Et_2O$ provides the product with much better enantioselectivity (entry 4–7). Although reaction offered the best result by using $Et_2O$ as the solvent, by changing base from diisopropylamine to diisopropylethylamine led to a high ee of 91% at room temperature within 17 hours (entry 8), it was found that the product easilier racemize in this solvent at the same time. We therefore decided to use toluene as our solvent for the following study. Control experiment in the absence of base fails to

provide any product (entry 14). By comparison of catalysts Λ-**IrO**, Λ-**IrS**, and Λ-**RhO** in this reaction, it was found that Λ-**IrO** was the best option which afforded the product with the highest enantioselectivity (96% ee) (entry 15–17).

**Table 5** Screening of Solvents, Bases and Catalysts[a]

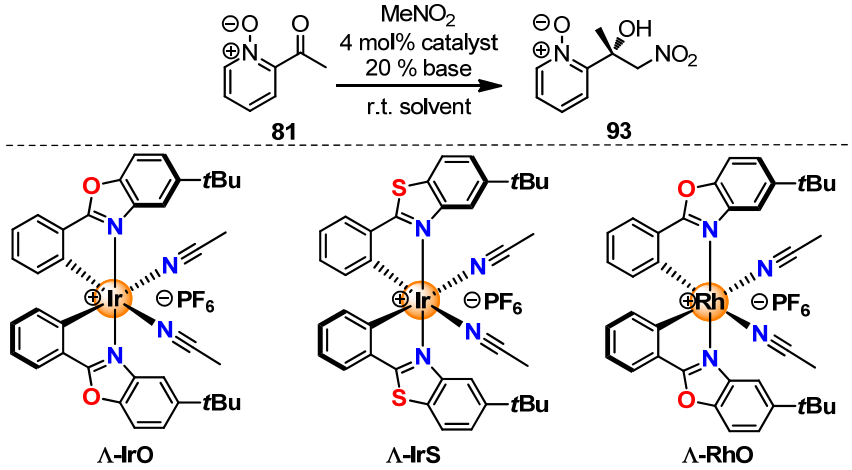


| entry | catalyst | base | solvent | 50 min ("conv."[b]; ee[c]) | 2 h ("conv. "[b]; ee[c]) |
|---|---|---|---|---|---|
| 1 | Λ-**IrS** | $i$Pr$_2$NH | $MeNO_2$ | 75%; 76% ee | n.d. |
| 2 | Λ-**IrS** | $i$Pr$_2$NH | MeOH | 95%; 42% ee | n.d. |
| 3 | Λ-**IrS** | $i$Pr$_2$NH | MeCN | 7%; 11% ee | n.d. |
| 4 | Λ-**IrS** | $i$Pr$_2$NH | $CH_2Cl_2$ | 56%; 87% ee | 74%; 83% ee |
| 5 | Λ-**IrS** | $i$Pr$_2$NH | THF | 59%; 86% ee | 76%; 85% ee |
| 6 | Λ-**IrS** | $i$Pr$_2$NH | toluene | 62%; 87% ee | 78%; 86% ee |
| 7 | Λ-**IrS** | $i$Pr$_2$NH | $Et_2O$ | 80%; 86% | 90%; 83% |
| 8 | Λ-**IrS** | $i$Pr$_2$NEt | $Et_2O$ | 26%; 94% ee | 86% ; 91% ee (17 h) |
| 9 | Λ-**IrS** | $NEt_3$ | $Et_2O$ | 40%; 93% ee | 71% ; 90% ee |
| 10 | Λ-**IrS** | $Et_2NH$ | $Et_2O$ | 33%; 81% ee | n.d. |
| 11 | Λ-**IrS** | DBU | $Et_2O$ | 97%; 0% ee | n.d. |
| 12 | Λ-**IrS** | $NaHCO_3$ | $Et_2O$ | No product | n.d. |
| 13 | Λ-**IrS** | $Na_2HPO_4$ | $Et_2O$ | No product | n.d. |
| 14 | Λ-**IrS** | No base | $Et_2O$ | No product | n.d. |
| 15 | Λ-**IrS** | $i$Pr$_2$NEt | $Et_2O$ | 26%; 94% ee | 86% ; 91% ee (17 h) |
| 16 | Λ-**RhO** | $i$Pr$_2$NEt | $Et_2O$ | 77% ; 96% ee | 91% ; 93% ee |
| 17 | Λ-**IrO** | $i$Pr$_2$NEt | $Et_2O$ | 52% ; 97% ee | 81% ; 96% ee |
| 18 | Λ-**IrO** | $i$Pr$_2$NEt | toluene | 54%; 98% ee (2 h) | 76%; 97% ee (6 h) |

[a]Conditions: **81** (0.05 mmol), base (20 mol%) with catalyst (4.0 mol%) in $MeNO_2$/solvent (v/v= 1:4, 0.4 M for **81**) under nitrogen. [b]"Conv." is determined by HPLC, not real conversion. [c]Ee determined by Chiral HPLC analysis. [d] n.d. = not determined.

Next, the substrate scope of catalyst Λ-**IrO** in Henry reaction was tested (Scheme 34). The effect of substituents on the pyridine ring was first studied. The methyl group at 4, 5, 6 positions of the pyridine ring led to the corresponding products **95**–**97** in moderate yields (59–74% yield) with excellent enantioselectivities (91–98% ee), while the methyl group at 3 position of pyridine ring failed to give any product (**94**) which showed that this reaction was sensitive to the steric hinderance. The methoxyl, ethyl, *n*-propyl or phenyl group at 4 position of pyridine ring also gave the corresponding products **98**–**101** in good yields (72–83% yield) with good enantioselectivities (85–93% ee). However, when the group in 4-position is *tert*-butyl group, the corresponding product **102** has only 52% ee. A substrate scope was also performed under optimized conditions with studied different aliphatic ketones. The high enantiomeric excesses (92–95% ee) of products **103** and **104** were obtained with ethyl or *n*-butyl ketones. Although the yield of these tertiary nitroaldols obtained under these conditions was not high, no other byproducts were formed and all of the unreacted starting material could be recovered.

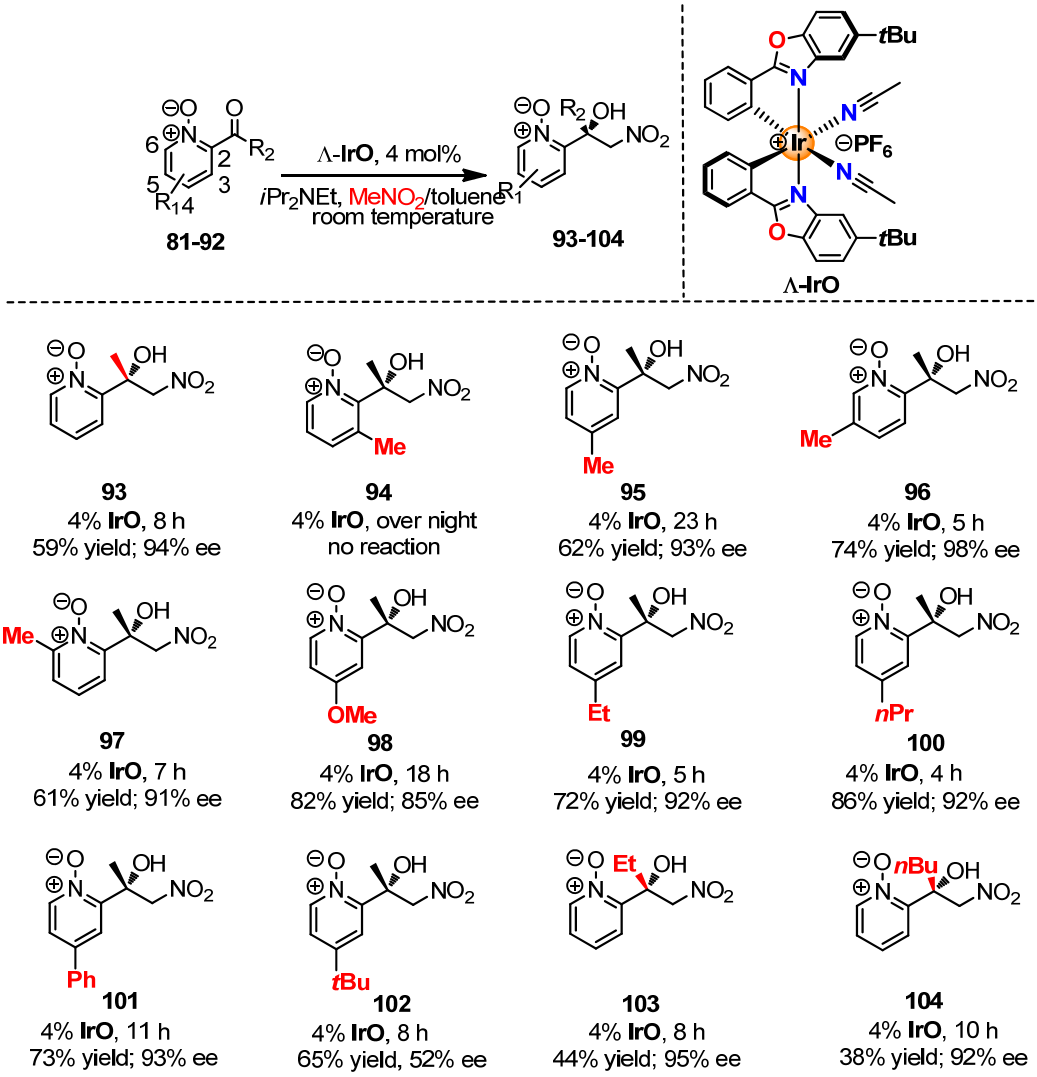


**Scheme 34** Scope of Substrates

It is plausible that the catalytic cycle starts with the bidentate coordination of the 2-acylpyridine *N*-oxides to the catalyst. This two point binding of the substrate increases the electrophilicity of the carbonyl group and promotes a nucleophilic addition to the carbonyl group to form a tertiary nitroaldol. After ligand exchange, the product and regenerated intermediate **I** was formed. (Figure 40)

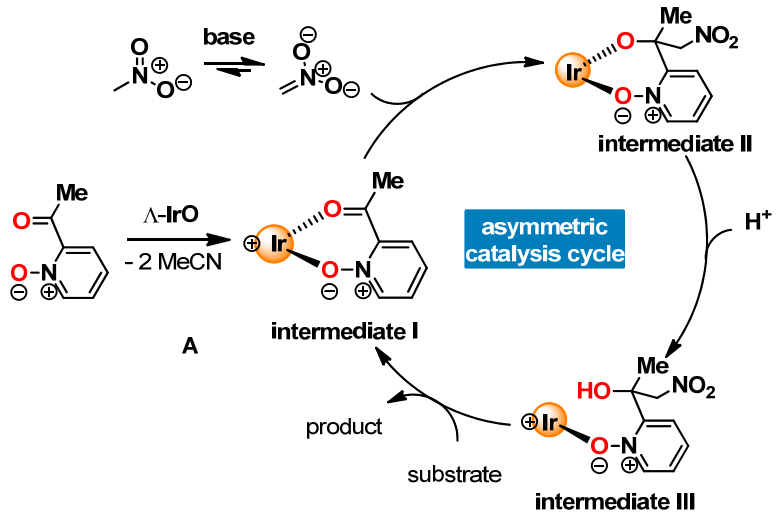


**Figure 40** Proposed mechanism of Henry reaction catalyzed by iridium catalysts.

In summary, a direct asymmetric Henry reaction catalyzed by chiral-at-metal asymmetric catalysts was first reported. Λ-**IrO** could efficient catalyze this reaction to give the corresponding tertiary nitroaldols bearing a quaternary stereocenter that bonded to a pyridine ring in decent yields (up to 86% yield) with excellent enantioselectivities (up to 98% ee). This reaction showed that our chiral-at-metal catalysts are versatile.

## 3.3 Investigation for Asymmetric Photoredox Catalysis

In this section, a surprising finding that a bis-cyclometalated rhodium(III) complex **RhO** serves as a highly effective visible light activated chiral photoredox sensitizer for the enantioselective radical amination of 2-acyl imidazoles would be introduced. After this work, visible-light-induced aerobic dehydrogenative cross-coupling and alkylation of acyl imidazole by cyclometalated pyrene iridium complexes were explored preliminarily.

### 3.3.1 Visible-light-induced enantioselective C-N bond formation

#### 3.3.1.1 Initial experiments of the Visible-Light-Induced C-N Bond Formation

Our group recentnly developed the asymmetric photoredox alkylation of 2-acyl pyridines and 2-acyl imidazoles using iridium complexes which serve a dual function as catalytically active chiral Lewis acids and as visible light triggered photoredox catalysts. [42-44] Consequently, our study was initiated by investigating the reaction of 2-acyl imidazole **105** with the ODN-carbamate **117** in the presence of the

previously disclosed photoredox catalysts Δ-**IrO** (2.0 mol%) or Δ-**IrS** (2.0 mol%) under irradiation with blue LEDs, but failed to provide any C-N bond formation product (Table 6, entries 1 and 2). Even with the optimal substrate **107** (*o*Tol group at imidazole) and longer reaction time (16 h), iridium catalyst *rac*-**IrO** cannot provide acceptable yields as shown for a number of standard solvents (Table 6, entries 3-8).

**Table 6** Initial Experiments of the Visible-Light-Induced C-N Bond Formation by **IrO** or **IrS**[a]

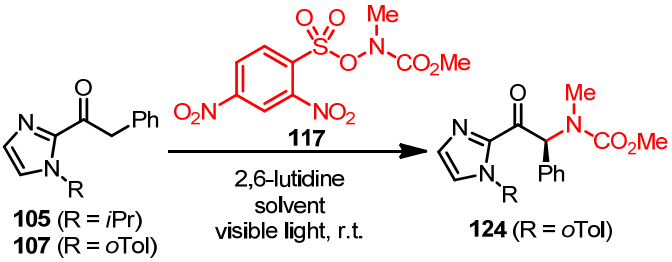


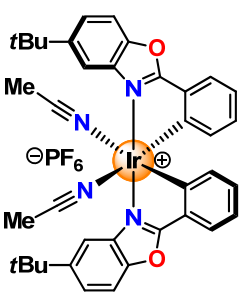

Δ-**IrO**

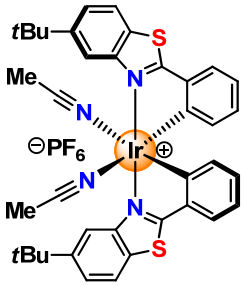

Δ-**IrS**

| entry | catalyst | R | solvent | t (h) | yield (%)[b] |
|---|---|---|---|---|---|
| 1 | Δ-**IrO** (2.0) | *i*Pr | DMSO/MeCN = 1/3 | 12 | 0 |
| 2 | Δ-**IrS** (2.0) | *i*Pr | DMSO/MeCN = 1/3 | 12 | 0 |
| 3 | *rac*-**IrO** (2.0) | *o*Tol | DMSO/MeCN = 1/3 | 16 | <2 |
| 4 | *rac*-**IrO** (2.0) | *o*Tol | DCM | 16 | 26 |
| 5 | *rac*-**IrO** (2.0) | *o*Tol | THF | 16 | 5 |
| 6 | *rac*-**IrO** (2.0) | *o*Tol | Toluene | 16 | 2 |
| 7 | *rac*-**IrO** (2.0) | *o*Tol | $CHCl_3$ | 16 | 9 |
| 8 | *rac*-**IrO** (2.0) | *o*Tol | EtOAc | 16 | 23 |

[a] Conditions: **105** or **107** (0.40 mmol), **117** (0.20 mmol) and 2,6-lutidine (0.34 mmol) with catalyst (2.0 mol%) in solvent (1.0 mL) under nitrogen; 24 W blue LEDs as light source; at room temperature. [b] Yields are determined by $^1$H NMR and based on trimethyl(phenyl)silane as an internal standard.

**Table 7** Preliminary Conditions Screening[a]

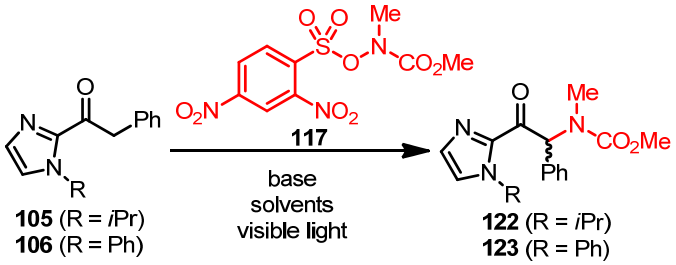


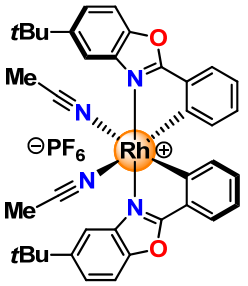

Δ-RhO

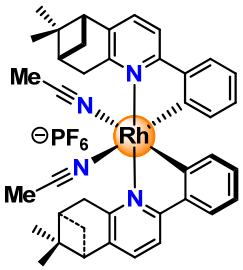

Δ-RhPP

| entry | catalyst[b] | solvents | base | R | t (h) | yield (%)[c] | ee (%)[d] |
|---|---|---|---|---|---|---|---|
| 1 | Δ-**RhO** (2.0) | DMSO/MeCN=1/3 | 2, 6-lutidine | *i*Pr | 12 | 44 | 80 |
| 2 | Δ-**RhO** (2.0) | DMSO/MeCN=1/3 | 2, 6-lutidine | Ph | 2 | 92 | 89 |
| 3 | Δ-**RhO** (2.0) | MeCN | 2, 6-lutidine | Ph | 2 | 40 | 87 |
| 4 | Δ-**RhO** (2.0) | DMSO | 2, 6-lutidine | Ph | 2 | 70 | 84 |
| 5 | Δ-**RhO** (2.0) | DMSO/MeCN=1/1 | 2, 6-lutidine | Ph | 2 | 80 | 89 |
| 6 | Δ-**RhO** (2.0) | NMP/MeCN=1/3 | 2, 6-lutidine | Ph | 2 | 50 | 86 |
| 7 | Δ-**RhO** (2.0) | DMF/MeCN=1/3 | 2, 6-lutidine | Ph | 2 | 63 | 88 |
| 8 | Δ-**RhO** (2.0) | THF | 2, 6-lutidine | Ph | 2 | trace | n.d. |
| 9 | Δ-**RhO** (2.0) | DMSO/MeCN=1/3 | $NaHCO_3$ | Ph | 3 | 75 | 87 |
| 10 | Δ-**RhO** (2.0) | DMSO/MeCN=1/3 | DTBP | Ph | 16 | trace | n.d. |
| 11[e] | Δ-**RhO** (2.0) | DMSO/MeCN=1/3 | 2, 6-lutidine | Ph | 3 | 47 | 89 |
| 12[f] | Δ-**RhO** (2.0) | DMSO/MeCN=1/3 | 2, 6-lutidine | Ph | 2 | 69 | 89 |
| 13[g] | Δ-**RhO** (2.0) | DMSO/MeCN=1/3 | 2, 6-lutidine | Ph | 2 | 81 | 89 |
| 14[h] | Δ-**RhO** (2.0) | DMSO/MeCN=1/3 | 2, 6-lutidine | Ph | 2 | 59 | 86 |
| 15[i] | Δ-**RhO** (2.0) | DMSO/MeCN=1/3 | 2, 6-lutidine | Ph | 2 | 93 | 89 |
| 16 | Δ-**RhPP** (2.0) | DMSO/MeCN=1/3 | 2, 6-lutidine | Ph | 2 | <20 | n.d. |

[a] Conditions: **105-106** (0.20 mmol, 2.0 equiv), **117** (0.10 mmol, 1.0 equiv) and base (0.17 mmol, 1.7 equiv) with catalyst (2.0 mol%) in solvents (0.1 M for **117**) under nitrogen, 24 W blue LEDs. [b] Catalyst loading given in brackets. [c] Isolated yields. [d] Chiral HPLC analysis. n.d. = not determined. [e] The reaction was conducted in the 0 – 10 °C. [f] 1.0 equiv of 2, 6-lutidine was used. [g] 1.0 equiv of **106** was used. [h] 1.0 equiv of **106** (0.10 mmol) and 2.0 equiv of **117** (0.2 mmol) were used in MeCN/DMSO (v/v = 3:1, 1.0 mL). [i] The concentration is 0.2 M for **117**.

However, to our surprise and delight, when we tried the rhodium complex Δ-**RhO**[8,46] (2.0 mol%), the α-aminated 2-acyl imidazole **122** was obtained with 44% yield and with respectable 80% ee (Table 7, entry 1). Replacing the isopropyl substituent of the imidazole moiety with a phenyl (**106**) group improved the yield to 92% with 89% ee (entry 2). A brief solvent screening revealed that mixed solvents (DMSO/MeCN = 1/3) afforded the best result (entries 3-8). The different kinds of bases, ratios of starting materials, and temperatures were also tested but failed to give the better results (entries 9-14). Compared to entry 2, the higher concentration (0.2 M for **117**) afforded a slightly better result (entry 15, 93% yield and 89% ee). Δ-**RhPP** catalyst (it is synthesized by Yu Zheng–PhD student in Meggers group) canld not provide the product with an acceptable yield (entry 16).

**Table 8** Initial Experiments of the Visible-Light-Induced Enantioselective C-N Bond Formation by Rhodium Catalysts[a]

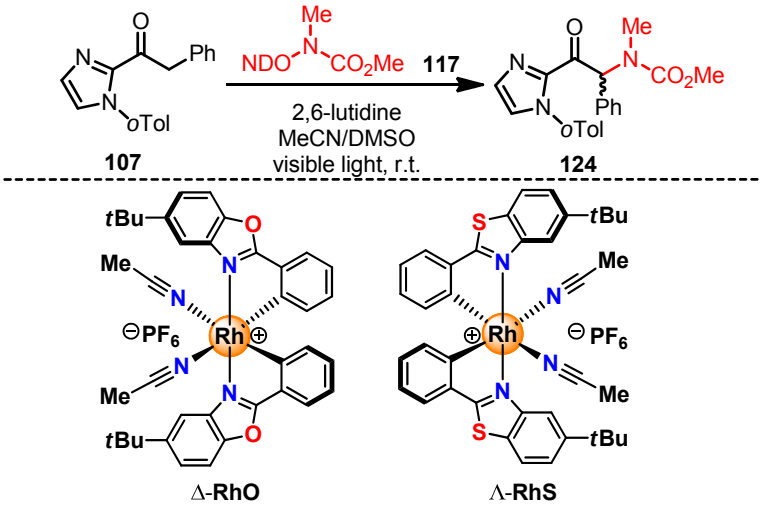


| entry | catalyst[b] | hv[c] | t (h) | product | yield (%)[d] | ee (%)[e] |
|---|---|---|---|---|---|---|
| 1 | Δ-**RhO** (2.0) | blue LEDs | 2 | (*S*)-**124** | 96 | 97 |
| 2 | Δ-**RhO** (2.0) | CFL | 4 | (*S*)-**124** | 94 | 97 |
| 3 | Δ-**RhO** (1.0) | blue LEDs | 6 | (*S*)-**124** | 71 | 97 |
| 4 | Δ-**RhO** (0.5) | blue LEDs | 10 | (*S*)-**124** | 65 | 95 |
| 5 | Δ-**RhO** (2.0) | none | 16 | -- | 0 | n.d. |
| 6 | none | blue LEDs | 16 | -- | 0 | n.d. |
| 7[f] | Δ-**RhO** (2.0) | blue LEDs | 6 | (*S*)-**124** | 38 | 97 |
| 8 | $Sc(OTf)_3$ (2.0) | blue LEDs | 6 | **124** | 8 | n.d. |
| 9 | $Mg(OTf)_2$ (2.0) | blue LEDs | 6 | **124** | 3 | n.d. |
| 10 | Λ-**RhS** (2.0) | blue LEDs | 2 | (*R*)-**124** | 96 | >99.5 |

[a] Conditions: **107** (0.40 mmol), **117** (0.20 mmol) and 2,6-lutidine (0.34 mmol) with catalyst (0.5–2.0 mol%) in MeCN/DMSO (v/v = 3:1, 1.0 mL) under nitrogen. [b] Catalyst loading given in brackets. [c] 24 W blue LEDs or 20 W CFL. [d] Isolated yields. [e] Chiral HPLC analysis. n.d. = not determined. [f] the analogous reaction was run under air.

Replacing the phenyl substituent of the imidazole moiety with an *ortho*-tolyl substituent (**107**) even provided excellent 96% yield with 97% ee (Table 8, entry 1). Intriguingly, a short photolysis time with blue LEDs of just 2 hours is sufficient to achieve full conversion. The reaction can also be activated with a regular compact fluorescent light bulb (CFL), although the reaction time doubles to 4 hours (94% yield and 97% ee, see entry 2). Lower catalyst loadings afford the C-N formation product in somewhat reduced yield but still with high enantioselectivity (95−97% ee, see entries 3 and 4). Importantly, control experiments in the absence of either light (entry 5) or rhodium catalyst (entry 6) fail to provide any product, thereby demonstrating that this catalytic, enantioselective C-N bond formation crucially depends on both the chiral rhodium complex and visible light. In the presence of oxygen, the product **124** can be isolated in a reduced yield (6 h, 38% yield) with excellent selectivity (97% ee) (entry 7). As further control experiments, simple Lewis acids such as $Sc(OTf)_3$ or $Mg(OTf)_2$ are not capable of catalyzing this reaction to a significant degree (entries 8 and 9). At last, the new rhodium catalyst Λ-**RhS**, which was synthesized by Jiajia Ma (PhD student in Meggers group) recently, was also tried in this reaction. It is found that the determined enantioselectivitiy is appreciably higher for the benzothiazole catalyst (**RhS**, > 99.5% ee) over the benzoxazole catalyst (**RhO**, 97% ee) (entry 10). It is consistent and analogous with a comparison of the related benzoxazole and benzothiazole iridium complexes.

### 3.3.1.2 Scope of substates

Scheme 35 displays a substrate scope, revealing that substituents are well tolerated in the aromatic moiety in α-position to the carbonyl group (**125**−**130**; 81−99% yield and 92−98% ee) although a *para*-methoxy group reduces the yield and requires higher catalyst loadings (**131**; 52% yield and 97% ee). Furthermore, a naphthyl moiety affords the C-N formation product in 81% yield with 97% ee (**132**) and more bulky ODN-carbamates **118**–**121** provide excellent results (**133**−**136**; 62−99% yield and 97−98% ee) (for example, the bulky ODN-carbamate with an isobutyl group at the nitrogen (**120**) affording the α-amination product **135** in 99% yield with 98% ee). However, it has to be noted that this reaction only works with aromatic substituents in α-position to the carbonyl group (**137** is failed to be obtained), presumably to lower the p$K_a$ value of the methylene group.

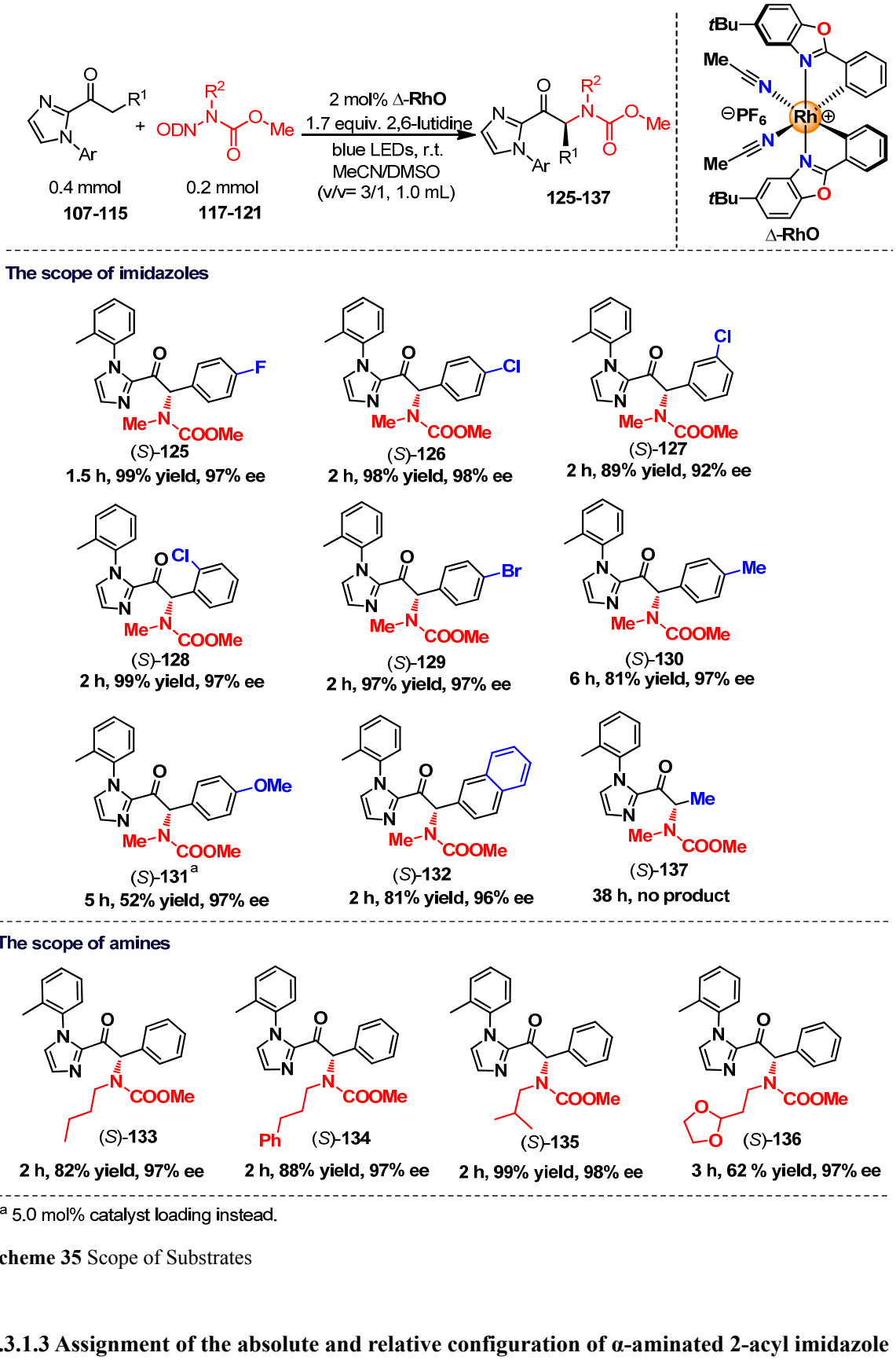


**Scheme 35** Scope of Substrates

### 3.3.1.3 Assignment of the absolute and relative configuration of α-aminated 2-acyl imidazole

In order to figure out the absolute configuration of α-aminated 2-acyl imidazole, the complexation with Δ-**RhO** was used as a handle to determine the absolute configuration of the product **124** (**124** in

Scheme 36 is obtained by using Λ-**RhO** as a catalyst). X-ray analysis of **138**, obtained by successive crystallizations from $CH_2Cl_2$ and *n*-hexane, indicates that α-aminated 2-acyl imidazole is an *R* configuration (Figure 41). In other words, the absolute configuration of α-aminated 2-acyl imidazole **124** is an *S* configuration when Δ-**RhO** is used as a catalyst. The observed absolute configuration is in agreement with the model outlined in Figure 42.

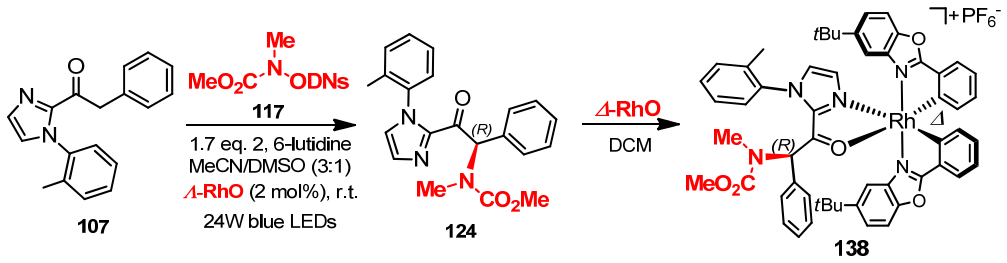


**Scheme 36** Assignment of the Absolute Configuration of α-Aminated 2-Acyl Imidazole **124**

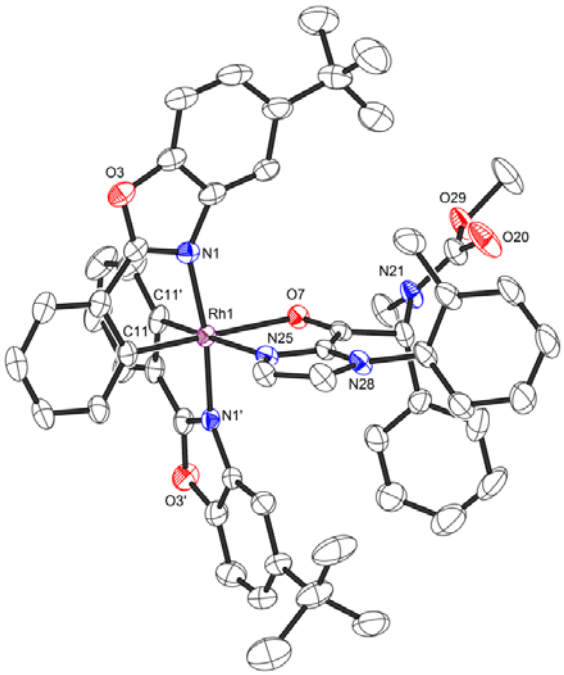


**Figure 41** Crystal structure of **138**. The hexafluorophosphate counteranion is omitted for clarity. ORTEP drawing with 50% probability thermal ellipsoids.

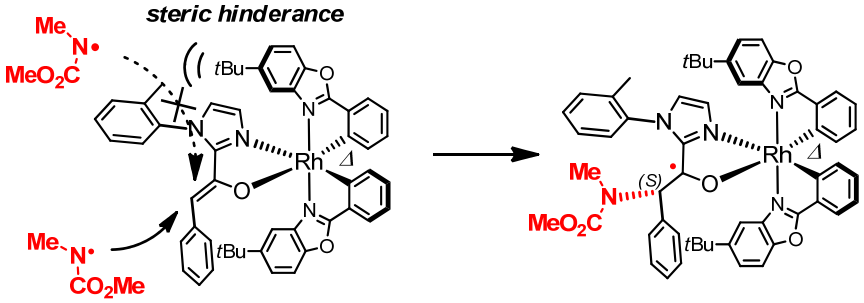


**Figure 42** Stereochemical model of reaction

### 3.3.1.4 Photo reaction in flow

Conducting the photo reaction in flow has many advantages compared to that in batch: a higher surface area to volume to make more efficient to absorb the photons; a more predictable reaction scale-up; more safety, and improved reproducibility.[47,48] Tthe photo reaction **107** with **117** was applied in flow reactor.

A close up photograph of the assembled photo flow reactor is shown in Figure 43. The left picture is Vapourtec's *R*-Series systems (flow system) and the right picture is a simple photo reactor (photo system. 6W blue LEDs; a total of 600 cm the PFA tube is wrapped in figureeights around the glass column). The photo reaction was first conducted on a 0.4 mmol scale (for **107**) in flow. The product was obtained with 96% yield and 98% ee within 30 min. Performing this reaction in flow indeed afforded a much higher reaction rate than that in batch. This photo reaction was then tried on a 4 mmol scale (for **107**), and we obtained a yield of 90% with 97% ee for a reaction time of 3 hours, which demonstrated that this reaction was scalable (on a gram scale) in flow system (Scheme 37).

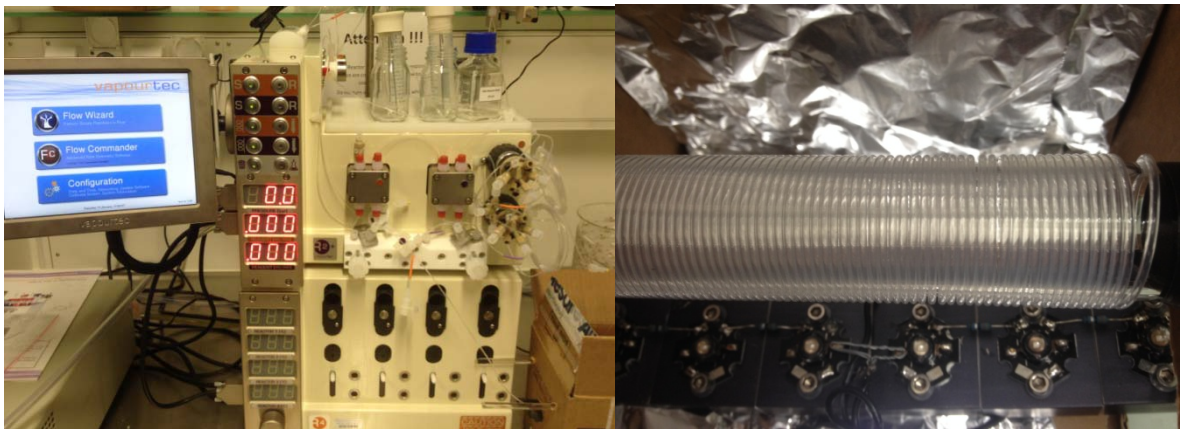


a) flow system b) photo system

**Figure 43** Photo flow reactor.

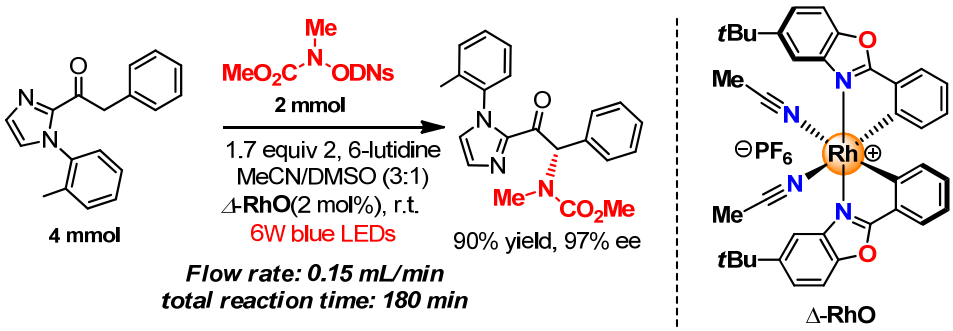


**Scheme 37** Photo Reaction in Flow

*Reaction conditions: 2-acyl imidazole **107** (4.0 mmol), the amine reagent **117** (2.0 mmol), 2, 6-lutidine (3.4 mmol) with catalyst Δ-**RhO** (2.0 mol%) in MeCN/DMSO (v/v = 3:1, 20 mL) were irradiated with blue LEDs (6 W) under nitrogen (see Experimental Part for more details).*

### 3.3.1.5 Mechanism of enantioselective C-N bond formation

MacMillan recently reported a photoinduced enantioselective α-amination of aldehydes using 2,4-dinitrophenylsulfonyloxy (ODN)-*N*- functionalized carbamates catalyzed via chiral secondary amines which was proposed to proceed through the intermediate formation of electron deficient aminyl radicals and their stereocontrolled reactions with chiral enamine intermediates.[49] Combined MacMillan's research with my work, a possible mechanism (**Mechanism A**) is shown in Figure 44.

In MacMillan's system, presumably, photonic excitation of amine yields excited amine*, which readily undergoes single-electron reduction and mesolysis of the weak N−O bond to yield the desired amine-centered radical and ODNs anion. In my system, the control experiments by using simple Lewis acid such as $Sc(OTf)_3$ or $Mg(OTf)_2$ instead of **RhO** are not capable of catalyzing this reaction to significant degrees, which did not support this mechansim (**Mechanism A**) (Table 8, entries 8-9).

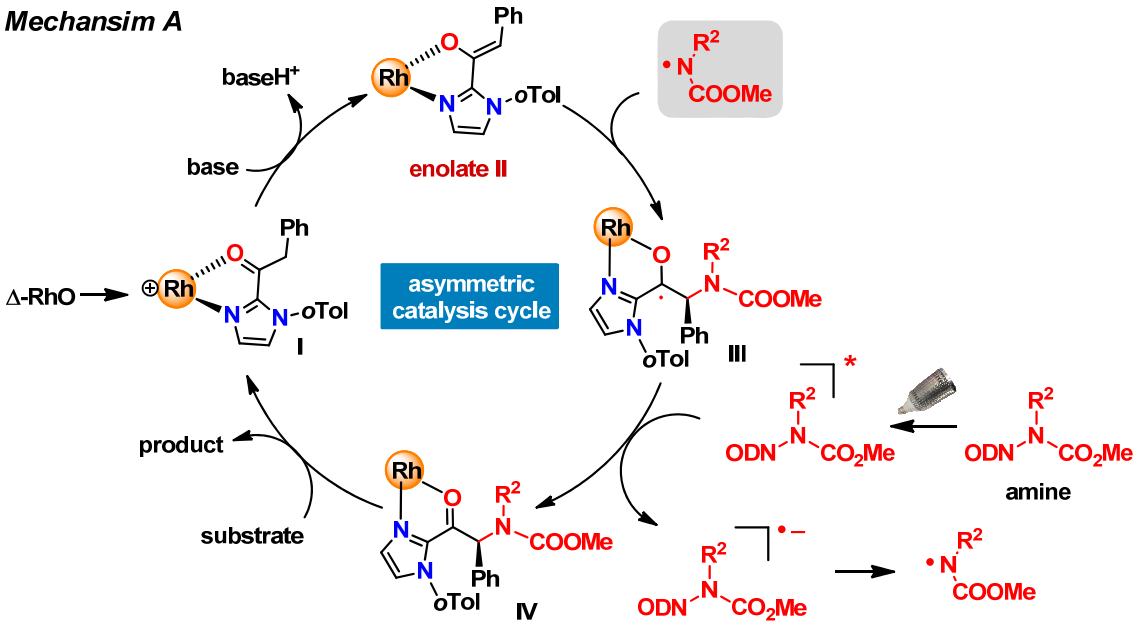


**Figure 44** A possible mechanism for the visible light activated enantioselective rhodium catalysis (initiation via photolabile amine).

Melchiorre recently reported a direct and effective method to install perfluoroalkyl and trifluoromethyl groups within the aromatic ring of a-cyano arylacetates.[50] This reaction is driven by the photochemical activity of *in situ* generated EDA complexes, formed by the aggregation of enolates and perfluoroalkyl iodides. For my system, is it possible that the reaction is driven by EDA complex (enolate as an electron donor and amine as an electron acceptor)? A possible mechanism involved EDA complex is shown in Figure 45 (**Mechanism B**).

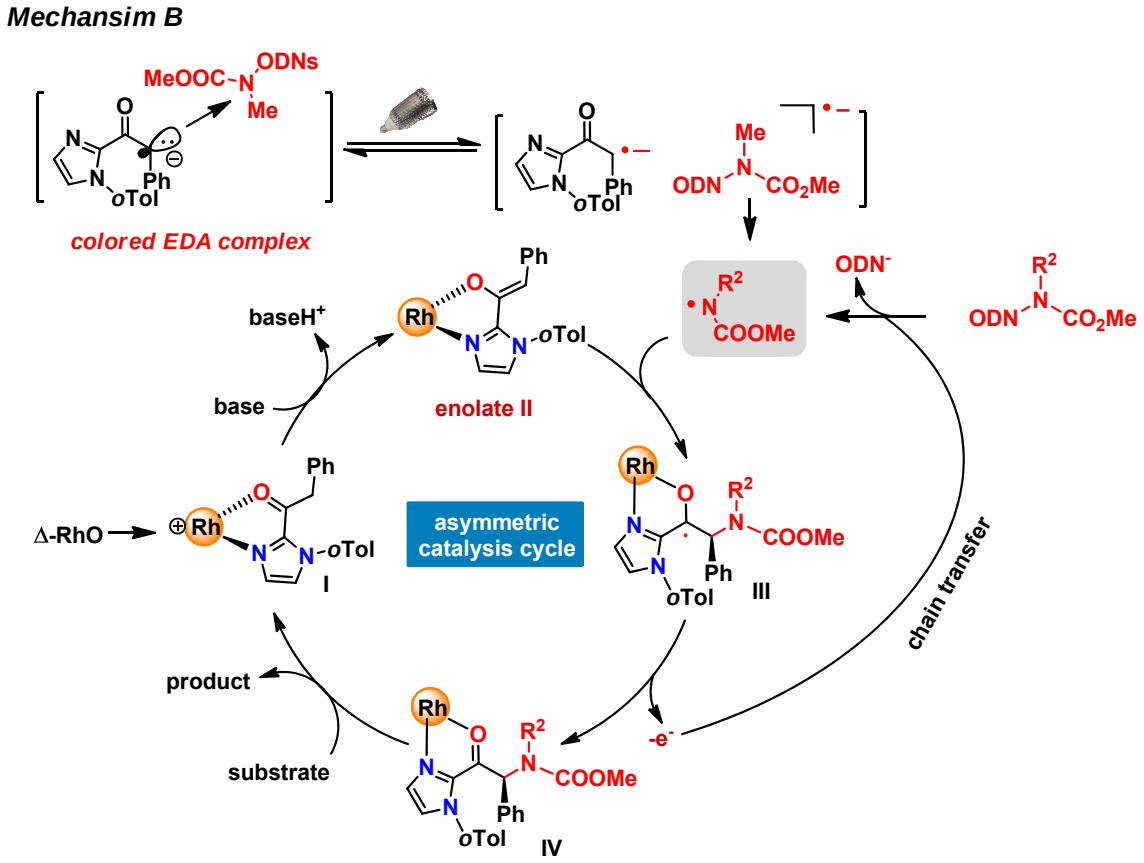


**Figure 45** A possible mechanism for the visible light activated enantioselective rhodium catalysis (initiation via EDA complex).

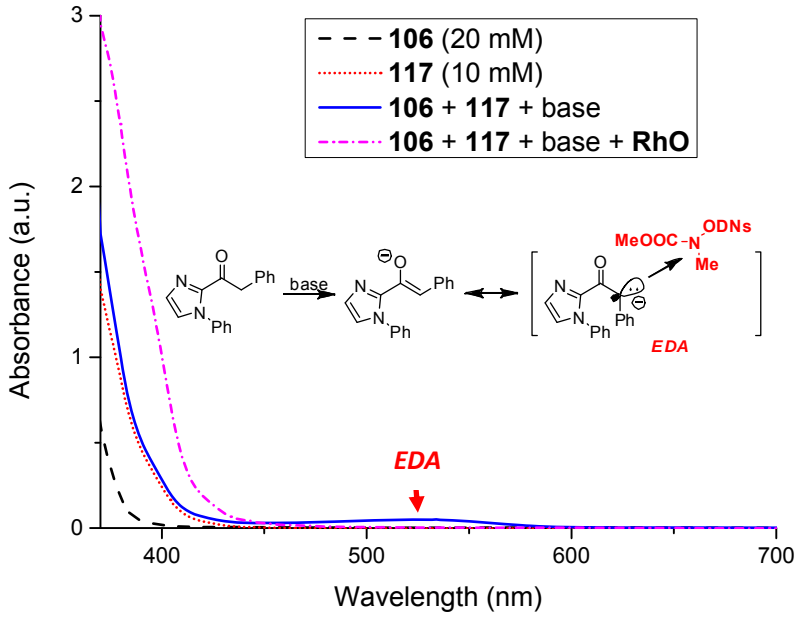


**Figure 46** Optical absorption spectra recorded in MeCN/DMSO (v/v = 3/1) in quartz cuvettes (1 cm path).

Mixed **106** (2.0 equiv), **117** (1.0 equiv) and base (2,6-lutidine, 1.7 equiv) in MeCN/DMSO (v/v = 3/1).

The color of solution changed soon, while its optical absorption spectrum showed a new peak near 520 nm, diagnostic of an EDA complex (enolate as an electron donor and amine as an electron acceptor) (Figure 46). However, this new peak near 520 nm disappeared when *rac*-**RhO** (2 mol%) was added, which indicated that the formation of the EDA complex could be inhibited by rhodium complex. Accordingly, C-N bond formation in my system is not initiated by EDA complex.

We then proposed another mechanism (**Mechanism C**, see Figure 47): The acyl imidazole substrate coordinates to the rhodium catalyst in a bidentate fashion (intermediate **I**) followed by a deprotonation of the α-methylene group which affords a neutral rhodium enolate complex (intermediate **II**). It is believed that this enolate **II** (**139**) has a crucial dual function. Firstly, it serves as an initiator and reinitiator, dubbed "smart initiator" by Studer and Curren,[51] upon photoactivation (**II** + $h\nu \rightarrow$ **II***) by transfering a single electron (**II*** $\rightarrow$ $\mathbf{II}^{+}$ + $e^{-}$) to the ODN-carbamate which then fragments into a sulfonate anion and an aminyl radical. Secondly, enolate **II** contains a very electron rich double bond that reacts with the electrophilic nitrogen-centered radical in a stereocontrolled fashion. This provides a rhodium-coordinated ketyl (intermediate **III**) which is highly reducing and either donates an electron to the photosensitizer redox cycle to regenerate the oxidized photosensitizer ($\mathbf{II}^{+}$ + $e^{-} \rightarrow$ **II**) or directly transfers a single electron to the ODN-carbamate, thereby propagating a chain process.

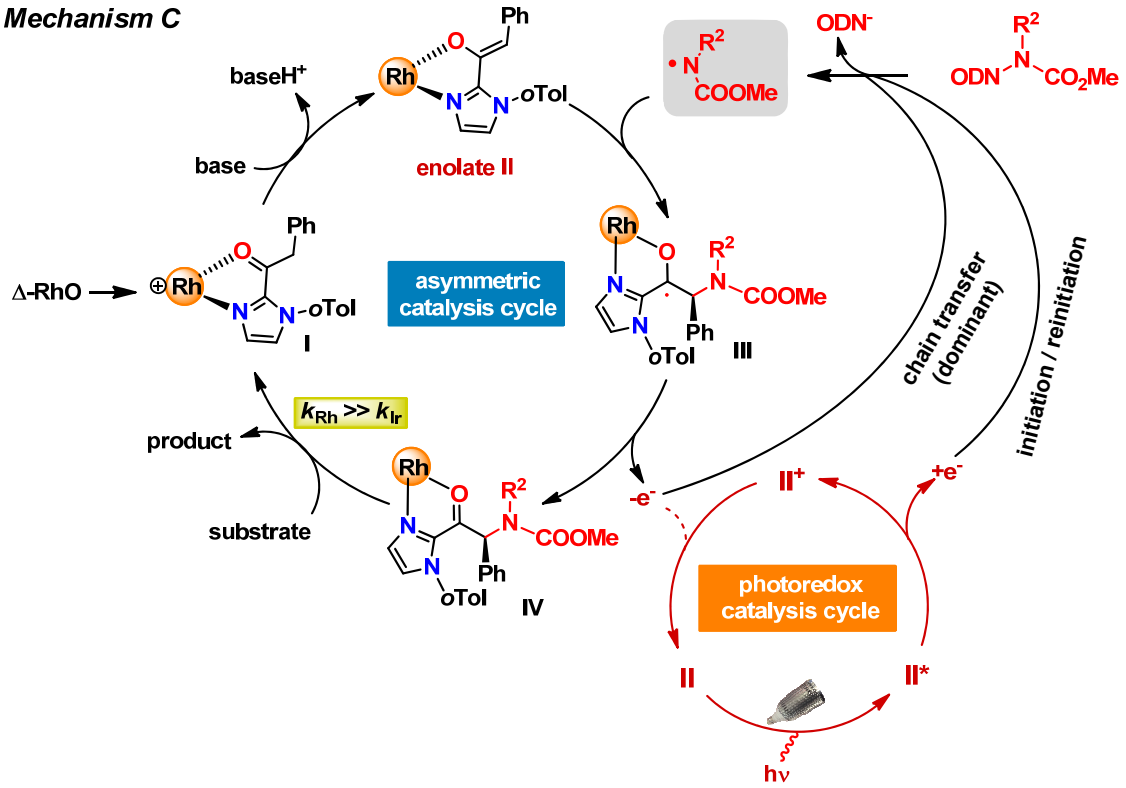


**Figure 47** Putative mechanism for the visible light activated enantioselective rhodium catalysis.

A number of experiments strongly support this mechanism, such as isolation of the intermediate **II**, trapping experiments by TEMPO and *N*-methylindole, "light-dark" experiments, the determination of quantum yield, and kinetic study by NMR (ligand change experiments).

*(1) Crystal structure of the proposed enolate intermediate **II***

The crystal structure of the proposed enolate intermediate **II** was obtained (Figure 48) and its catalytic competence was also confirmed (for the reaction **106** + **117** →**123** catalyzed by intermediate **II**, the product **123** is isolated in a yield of 91% after 2 hours, see Scheme 38).

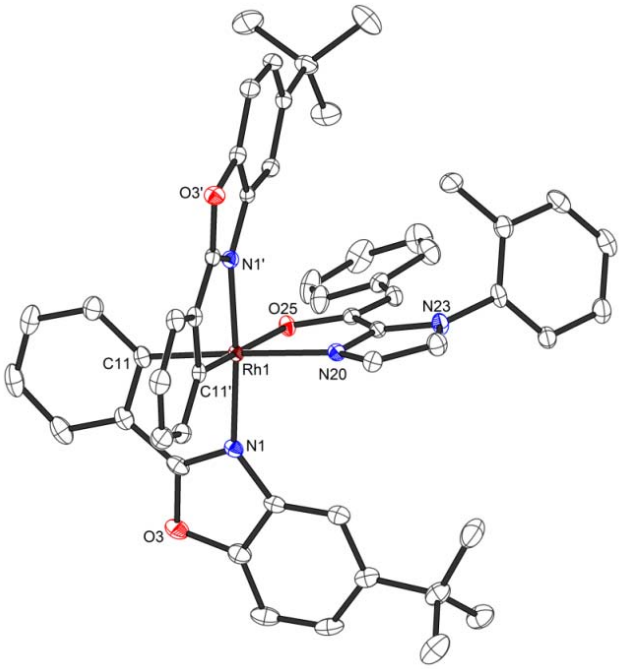


**Figure 48** Crystal structure of the proposed key rhodium enolate intermediate **II** with the deprotonated substrate **107**. ORTEP drawing with 50% probability thermal ellipsoids.

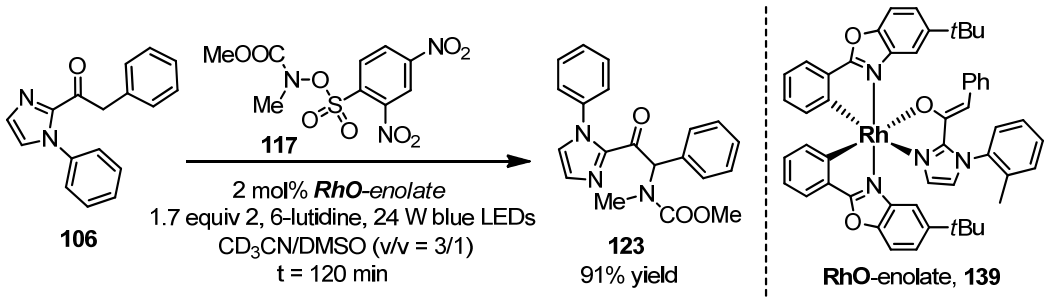


**Scheme 38** Visible-Light-Induced C-N Bond Formation by Intermediate **II**

*(2) Trapping experiments*

The model reaction **107** + **117** →**124** is run by adding 5 equiv of TEMPO, a suppression of product formation below 10% in the presence of TEMPO (as well as a reduced yield in the presence of

oxygen , see Table 8, entry 9) support a radical mechanism (Scheme 39) (see Experimental Part for details).

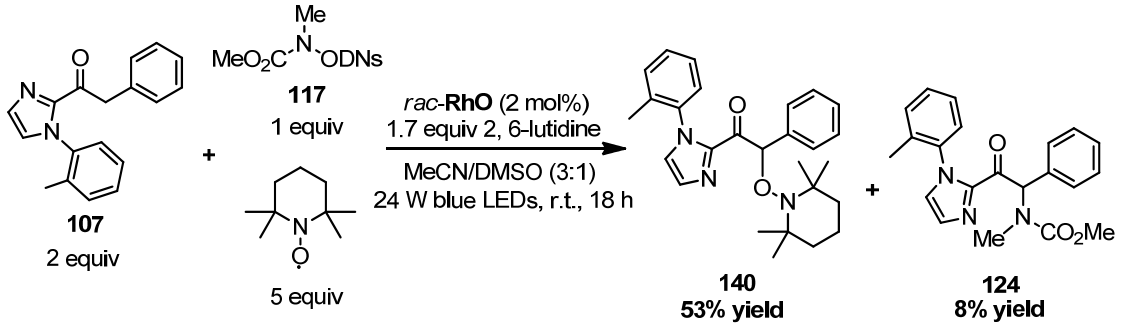


**Scheme 39** Trapping Experiment by TEMPO

**Table 9** Verification of the Formation of Intermediate Nitrogen-Centered Radicals via Trapping Experiments[a]

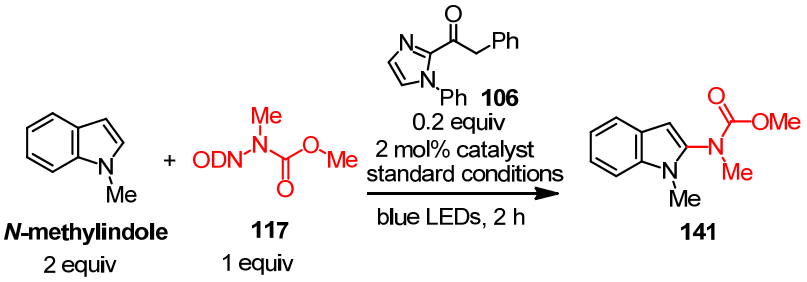


| entry | catalyst | imidazole substrate **106** | yield (%)[b] |
|---|---|---|---|
| 1 | **RhO** (2 mol%) | 20 mol% | 61 |
| 2 | **RhO** (2 mol%) | -- | 6 |
| 3 | no transition metal catalyst | -- | 4 |
| 4 | **IrO** (2 mol%) | 20 mol% | 77 |
| 5 | **IrS** (2 mol%) | 20 mol% | 78 |

[a] Reaction conditions: *N*-methylindole (0.20 mmol), **117** (0.10 mmol), **106** (0.02 mmol or not) and 2,6-lutidine (0.17 mmol) with catalyst (2.0 mol% or not) in MeCN/DMSO (v/v = 3:1, 0.5 mL) were irradiated with blue LEDs (24 W) under nitrogen. [b] Yields are determined by $^1$H NMR and based on trimethyl(phenyl)silane as an internal standard.

Trapping reactions with *N*-methylindole as shown in Table 9 provide further very important insights into the mechanism: a) The observed amination of the 2-position (**141**) is indicative for a radical reaction through intermediate nitrogen-centered radicals. b) **RhO** is an effective catalyst only in the presence of catalytic amounts of 2-acyl imidazole (Table 9, entries 1 and 2), thereby being consistent with our proposal that the intermediate rhodium enolate complex **II** is responsible for the light-activated reductive formation of the nitrogen radical (the role of rhodium enolate **II** as the *in situ* generated photosensitizer is further corroborated by a 30 nm bathochromic wavelength shift of the long wavelength absorbance band compared to *rac*-**RhO**, see Experimental Part). c) In the complete absence of any transition metal catalyst only small amounts of product are formed, thus revealing that

MacMillan's proposed mechanism[49] of a direct activation of the ODN-carbamate could be ignored in our system. d) For **IrO** and **IrS** in the presence of some 2-acyl imidazole, the indole amination product was obtained in high yields upon visible light activation (Table 9, entries 4 and 5). These mean that the incompetence of the established dual function chiral Lewis acid / photoredox catalysts **IrO**[43] and **IrS**[42,44] to catalyze the enantioselective C-N bond formation **107** + **117** → **124** is not related to the photoredox-induced formation of the nitrogen-centered radical intermediate.

*(3)"Light-dark" experiments*

One topic of debate has concerned the extent to which photoredox reactions involve chain process. Studying the reaction progress with alternating periods of irradiation and darkness ("light-dark" experiment) has commonly been used to resolve these processes.[52]

Alternate irradiation (5 min) and dark intervals (60 min) reveal that after a photochemical initiation, the reaction proceeds to some degree in the dark (Figure 49), thereby lending support to a chain mechanism in which the electron transfer from the ketyl intermediate **III** to the ODN-carbamate dominates (apparently, light activation generates small amounts of intermediates or side products which can serve as inefficient initiators of new chain processes during the dark phase).

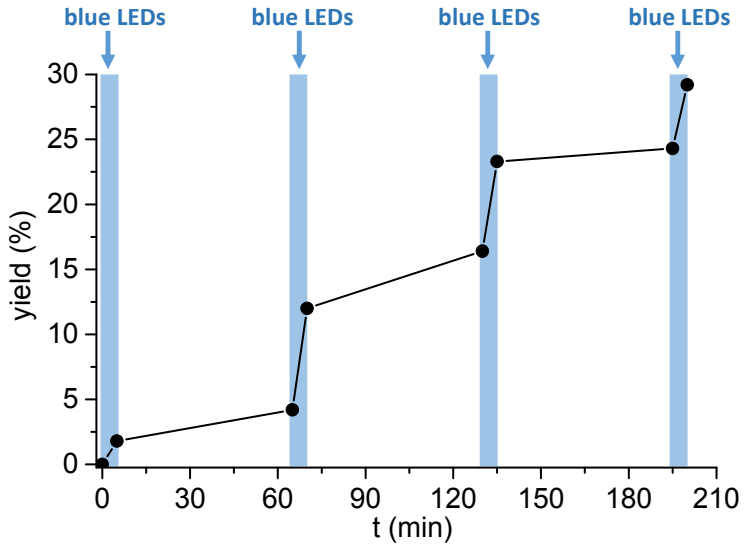


**Figure 49** Light-dark interval reaction **106** + **117** →**123** under standard conditions.

*(4) Measurement of quantam yield*

Melchiorre and Yoon estimated the extent of chain processes in photoredox catalysis through the quantum yield measurements.[53,54] In the quantum yield measurements, the closed catalytic cycle (no chain processes) exhibits a maximum theoretical quantum yield of 1. If the quantum yield is far more than 1 would suggest that the major mechanism for photoredox catalysis is chain mechanism.[52]

The photon flux of light source was measured by standard ferrioxalate actinometry.[55] A 150 W Xenon

lamp (50% of light intensity, 420±5 nm bandpass filter high transmittance) was used as the light source. The moles of products formed were determined by GC measurement (FID detector) using tetradecane as reference standard. A quantum yield (Φ) of 14 (λ = 420 nm) was determined for the model reaction (**106** + **117** →**123**), corroborating a radical chain mechanism as the main pathway (the determination of quantum yield is shown in Experimental Part, see Section 5.5.2.6.). Considering non-productive quenching and energy decay processes of the photoexcited rhodium enolate complex **II**, an even higher chain length can be assumed for this reaction.[53]

*(5) Kinetic study by NMR*

It is intriguing that the here introduced asymmetric photoredox amination works highly efficient with the rhodium catalyst **RhO** but fails to provide significant amounts of the desired C-N bond formation product with the established dual function chiral Lewis acid / photoredox catalysts **IrO** and **IrS**, which have been employed successfully for related enantioselective C-C bond formation reactions[42-44].

From single-crystal structural analysis of the catalysts, we can get some useful information. The average Metal−N(MeCN) bond distances of **IrO**, **IrS**, and **RhO** after subtracting the metal ionic radii (taking into account the differences in metal ionic radii[56]) are 1.426(9), 1.441(7), and 1.483(2) Å, respectively. Compared to Ir−N(MeCN) bond distances, Rh−N(MeCN) bond distance is longer. It indicates that the bond strength of the RhO−N(MeCN) is probably weaker than that of Ir−N(MeCN), and MeCN which coordinated to Rh might be easier replaced by other substrates. In other word, **RhO**-enolate may be formed faster than **IrO/IrS**-enolate.

Therefore, the superiority of **RhO** over its iridium congeners in this reaction can rather be pinpointed to kinetic effects, namely the requirement of a high turnover frequency of the catalysis cycle. Amidyl radicals are known to be highly reactive electrophilic π-type radicals[57] which add to electron rich alkenes much faster than carbon-centered radicals.[58,59] Such electrophilic nitrogen-centered radicals are also highly prone towards reduction.[18] A concomitant short lifetime and fast reaction of the nitrogen-centered radical intermediate with the rhodium enolate **II** require a fast turnover frequency of the catalytic cycle in order to regenerate new rhodium enolate **II** rapidly enough as a reaction partner for the aminyl radical.

In order to confirm our speculation, a series of ligand exchange experiments were conducted (exchange of the acetonitrile ligands against substrate **106**) by proton NMR (Figure 50-52). As shown in Figure 50, mix the **RhO** and substrate **106** in $CD_3CN$/DMSO-6d (v/v = 3/1) without 2,6-lutidine does not afford the rhodium enolate **II**, even does not afford intermediate **I**. However, the rhodium enolate **II** was generated very fast when 2,6-lutidine was added to the solution of *rac*-**RhO** and **106** in $CD_3CN$/DMSO-*6d* (this ligand exchange reaction reached the dynamic equilibrium within 1 min, 77% conv., see Figure 51). The interesting thing is that the formation of iridium enolate (60 min, 2.8% conv.; 960 min, 35% yield, see Figure 52) in the same condition is much slower than the formation of

rhodium enolate **II**. Comparison of initial rates for an exchange of the acetonitrile ligands against substrate in **RhO** *versus* **IrO** demonstrates an increased rate constant for ligand exchange of the rhodium complex by ≥1650-fold (Scheme 40).

On the other hand, the inferior photophysical properties of bis-cyclometalated rhodium over iridium complexes,[60] resulting in a less efficient rhodium photoredox sensitizer, is not relevant for this reaction due to a highly efficient chain propagation as demonstrated by the observed high quantum yield. Thus, the rhodium enolate intermediate **II** serves as a smart initiator[12] which is needed to initiate and from time to time to reinitiate the chain reaction after chain termination.

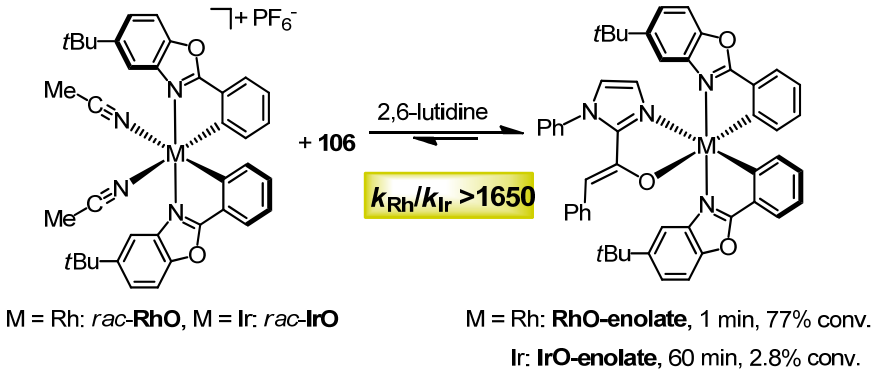


**Scheme 40** Ligand Exchange Kinetics

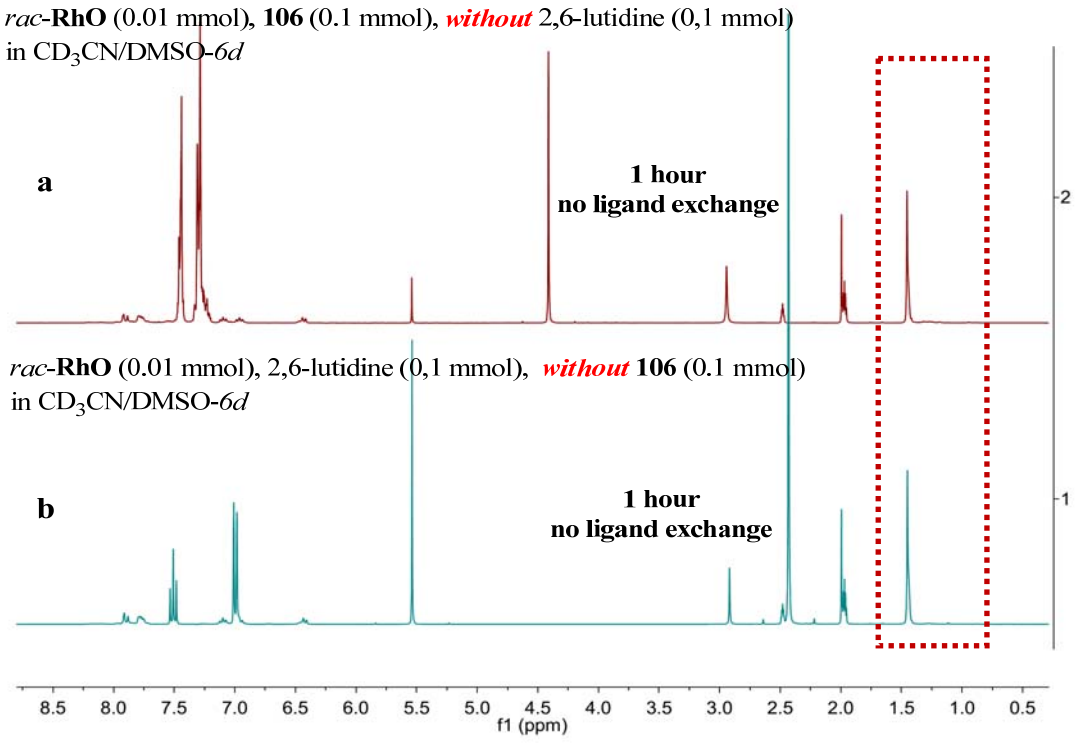


**Figure 50** The background of ligand exchange experiments with *rac*-**RhO**.

*a) To a mixture of rac-**RhO** (8.3 mg) and **106** (26.2 mg) in NMR tube was added $CD_3CN$/DMSO-6d (v/v = 3/1); b) To a solution of rac-**RhO** (8.3 mg) in $CD_3CN$/DMSO-6d (v/v = 3/1) was added 2, 6-lutidine (12 µL).*

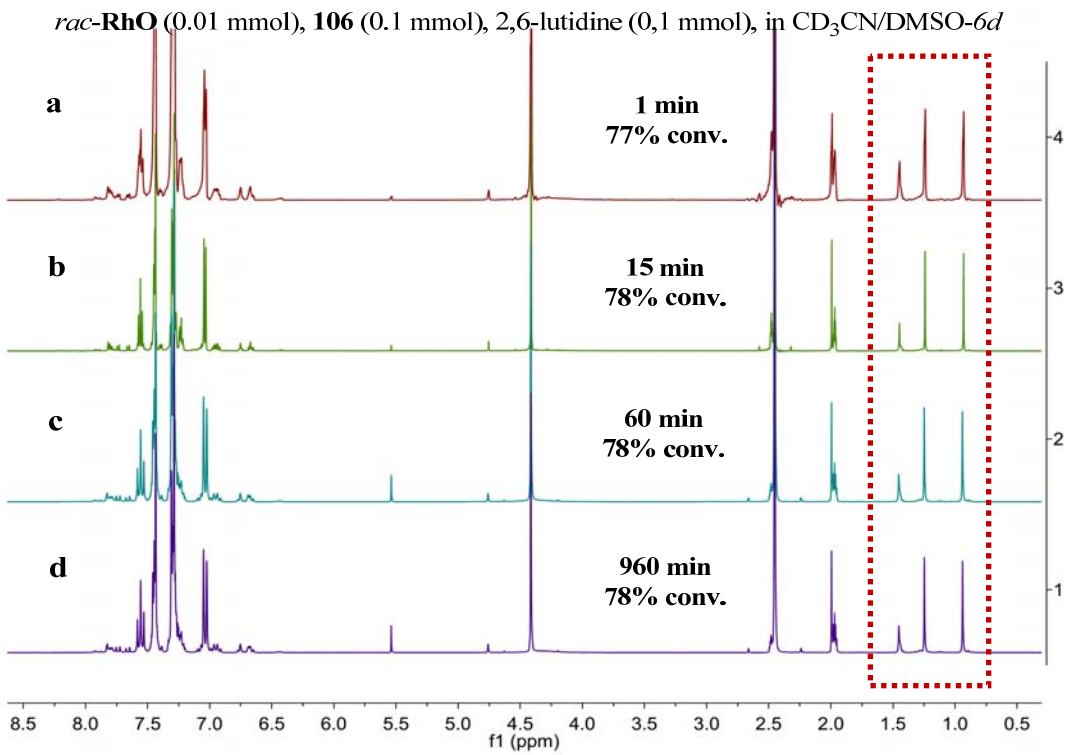


**Figure 51** The ligand exchange experiments with *rac*-**RhO**.

*To a solution of rac-**RhO** (8.3 mg) and **106** (26.2 mg) in 0.6 mL of $CD_3CN$/DMSO-6d (v/v = 3/1) was added the solution of 2, 6-lutidine (12μL) in 0.2 mL of $CD_3CN$/DMSO-6d (v/v = 3/1); Note: when it was tested in 1 minute, don't lock and shim the magnetic field in order to save time.*

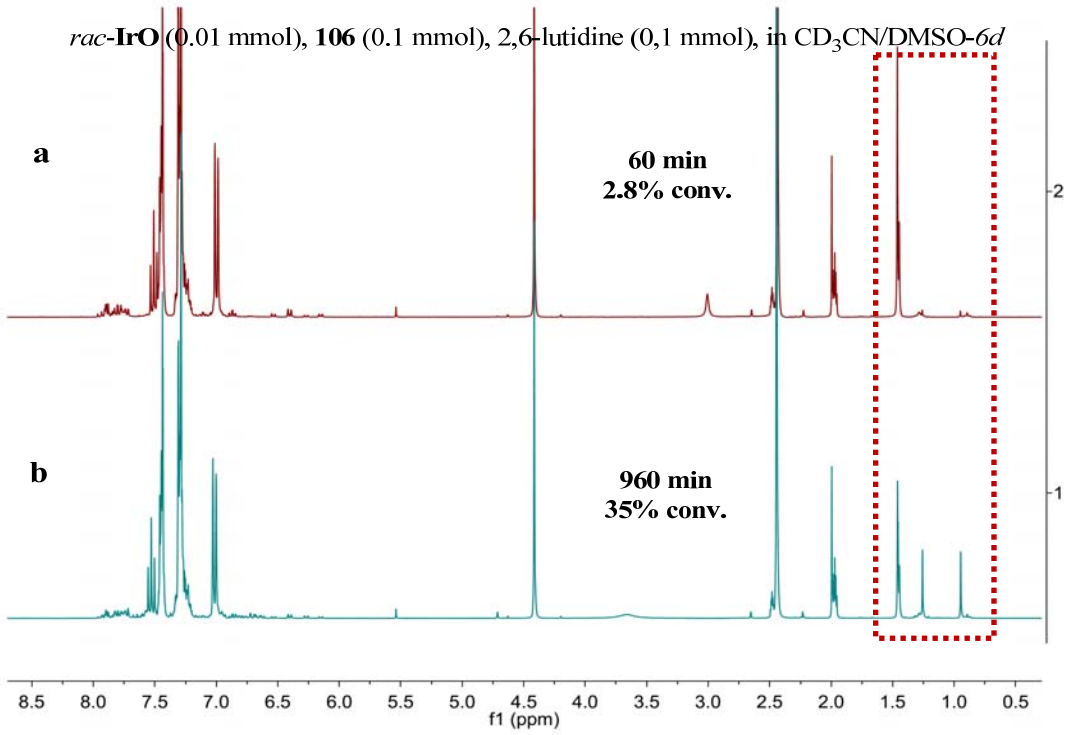


**Figure 52** The ligand exchange experiments with *rac*-**IrO**.

*To a solution of rac-**IrO** (9.2 mg) and **106** (26.2 mg) in 0.6 mL of $CD_3CN$/DMSO-6d (v/v = 3/1) was added the solution of 2, 6-lutidine (12 μL) in 0.2 mL of $CD_3CN$/DMSO-6d (v/v = 3/1).*

In conclusions, a very efficient photoactivated enantioselective radical amination of 2-acyl imidazoles catalyzed by a chiral-at-metal rhodium complex, which serves a dual function, namely as a chiral Lewis acid to catalyze asymmetric enolate chemistry and furthermore as a light-activated smart initiator of a radical chain process was introduced. Intriguingly, under related conditions, previously developed iridium complexes fail to work in this context. This is attributed to much faster ligand exchange kinetics in the rhodium system which is required to match the high reactivity and short lifetime of the intermediate nitrogen-centered radicals. The inferior photosensitization properties of the rhodium system do not play a role here due to an efficient chain mechanism. Thus, this work demonstrates the importance of fine tuned kinetics for radical formation, propagation, and regeneration of key catalytic intermediates in photoredox catalysis.

## 3.3.2 Investigation for other photoredox reactions by *rac*-IrO(pyrene) and *rac*-IrN(pyrene)

Next, other photoreox reactions such as aerobic dehydrogenative cross-coupling, and photoinduced alkylation of acyl imidazole catalyzed by cyclometalated pyrene complexes (*rac*-**IrO(pyrene)** and *rac*-**IrN(pyrene)**) were also explored.

### 3.3.2.1 Aerobic dehydrogenative cross-coupling by visible light

The Pope group found that the cyclometalated pyrene complex of iridium(III) $[Ir(L)_2(bpy)](PF_6)$ (L = 1-butyl-2-(pyren-1-yl)-1*H*-benzo[*d*]imidazole) has much longer triplet excited state lifetimes ($\tau_T$) and shows much larger rate constants compared to $[Ir(ppy)_2(bpy)](PF_6)$.[61] Inspired by Pope's work, the new iridium complexes *rac*-**IrO(pyrene)** and *rac*-**IrN(pyrene)** with the pyrene group were investigated in our system. The visible-light induced aerobic dehydrogenative cross-coupling by cyclometalated pyrene complex of iridium was first tested.

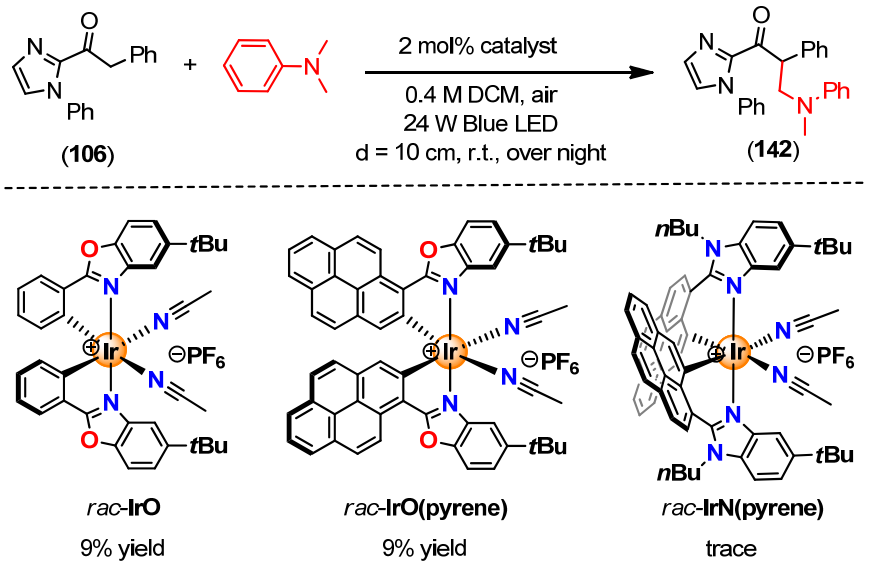


**Scheme 41** Aerobic Dehydrogenative Cross-Coupling by Visible Light

As shown in Scheme 41, by using *rac*-**IrO** or *rac*-**IrO(pyrene)** (2.0 mol%) as catalyst, only 9% yield of the C-C coupling product was isolated. Disappointingly, *rac*-**IrN(pyrene)** afforded only trace product.

### 3.3.2.2 Photoinduced alkylation of acyl imidazole

Photoinduced alkylation of acyl imidazole catalyzed by cyclometalated pyrene complex of iridium was also investigated. As found for the aerobic dehydrogenative cross-coupling, the performance of *rac*-**IrO(pyrene)** was not better than that of *rac*-**IrO**. Meantime, *rac*-**IrN(pyrene)** failed to afford any product in this reaction. The bad performance of *rac*-**IrN(pyrene)** can be explained by the parameters of crystal structure.

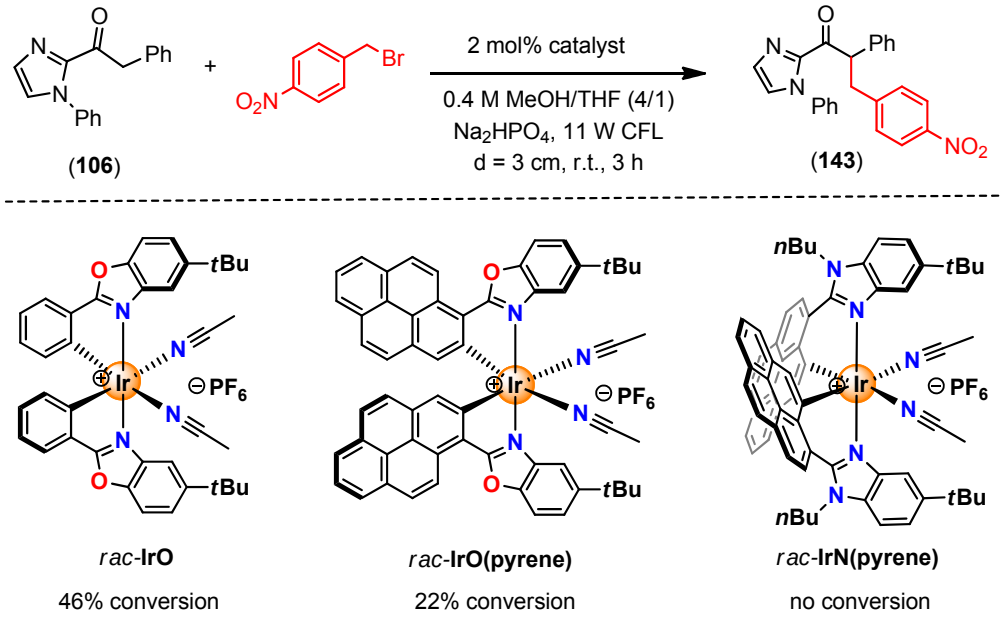


**Scheme 42** Photoinduced Alkylation of Acyl Imidazole

As shown in Figure 53, a plane through the iridium and two MeCN ligands was drawn. The distance between the quaternary carbon atoms of the *tert*-butyl groups and plane in *rac*-**IrN(pyrene)** (4.43 Å) is 0.67 Å shorter than that in *rac*-**IrO** (5.10 Å). It indicates that the steric hinderance around the central iridium ion in *rac*-**IrN(pyrene)** is so larger that it decreased the activity of reactions dramatically.

Although the performance of cyclometalated pyrentyl iridium complexes is not good for aerobic dehydrogenative cross-coupling and photoinduced alkylation of acyl imidazole, it still deserves us to have a further exploration in the future.

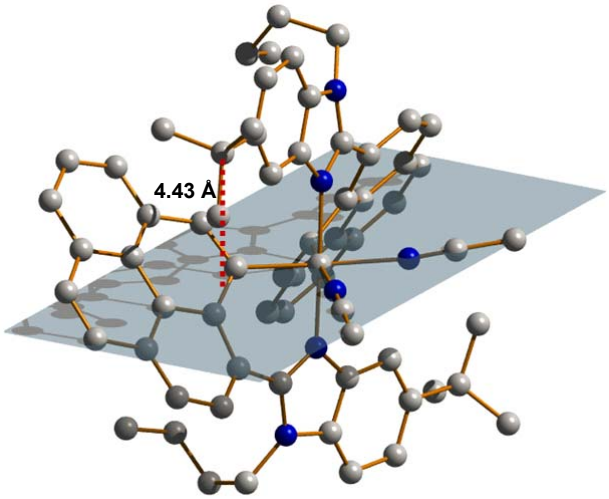


**Figure 53** Distances between the quaternary carbon atoms of the *tert*-butyl groups and the plane which through Iridium and MeCN ligands in *rac*-**IrN(pyrene)**.

## 3.4 References


1 P. J. Walsh, M. C. Kozlowski, *Fundamentals of Asymmetric Catalysis*; University Science Books, Sausalito, California, **2009**.

2 For reviews on different aspects of metal-centered chirality, see: a.) J.-L. Pierre, *Coord. Chem. Rev.* **1998**, *178–180*, 1183–1192; b.) U. Knof, A. von Zelewsky, *Angew. Chem. Int. Ed.* **1999**, *38*, 302–322; c.) P. D. Knight, P. Scott, *Coord. Chem. Rev.* **2003**, *242*, 125–143; d.) H. Amouri, M. Gruselle, *Chirality in Transition Metal Chemistry*, Wiley, Chichester, UK, **2008**; e.) E. Meggers, *Eur. J. Inorg. Chem.* **2011**, 2911–2926; f.) J. Crassous, *Chem. Commun.* **2012**, *48*, 9684–9692; g.) E. C. Constable, *Chem. Soc. Rev.* **2013**, *42*, 1637–1651.

3 For reviews covering chiral-at-metal complexes and their catalytic applications, see: a.) H. Brunner, *Angew. Chem. Int. Ed.* **1999**, *38*, 1194–1208; b.) P. Knight, P. Scott, *Coord. Chem. Rev.* **2003**, *242*, 125–143; c.) C. Ganter, *Chem. Soc. Rev.* **2003**, *32*, 130–138; d.) M. Fontecave, O. Hamelin, S. Ménage, *Top. Organomet. Chem.* **2005**, *15*, 271–288; e.) E. B. Bauer, *Chem. Soc. Rev.* **2012**, *41*, 3153–3167; f.) L. Gong, L.-A. Chen, E. Meggers, *Angew. Chem. Int. Ed.* **2014**, *53*, 10868–10874.

4 H. Huo, C. Fu, K. Harms, E. Meggers, *J. Am. Chem. Soc.* **2014**, *136*, 2990–2993.

5 M. Nonoyama, *Bull. Chem. Soc. Jpn.* **1974**, *47*, 767−768.

6 K. A. McGee, K. R. Mann, *Inorg. Chem.* **2007**, *46*, 7800−7809.

7 M. Helms, Z. Lin, L. Gong, K. Harms, E. Meggers, *Eur. J. Inorg. Chem.* **2013**, 4164–4172.

8 C. Wang, L.-A. Chen, H. Huo, X. Shen, K. Harms, L. Gong, E. Meggers, *Chem. Sci.* **2015**, *6*, 1094–1100.

9 The route of the chiral auxiliary (*S*)-**25** was first developed by the Meggers-Gong group.

10 For reviews and accounts covering different aspects of chiral Lewis acid catalysis, see: a.) K. Narasaka, *Synthesis* **1991**, 1–11; b.) S. Saito, H. Yamamoto, *Chem. Commun.* **1997**, 1585–1592; c.) K. A. Jørgensen, M. Johannsen, S. Yao, H. Audrain, J. Thorhauge, *Acc. Chem. Res.* **1999**, *32*, 605–613; d.) J. S. Johnson, D. A. Evans, *Acc. Chem. Res.* **2000**, *33*, 325–335; e.) G. Desimoni, G. Faita, K. A. Jørgensen, *Chem. Rev.* **2006**, *106*, 3561–3651; f.) S. Kobayashi, C. Ogawa, *Chem. Eur. J.* **2006**, *12*, 5954–5960; g.) S. Kanemasa, M. Hasegawa, F. Ono, *Chem. Record* **2007**, *7*, 137–149; h.) J. Christoffers, G. Koripelly, A. Rosiak, M. Rössle, *Synthesis* **2007**, 1279–1300; i.) M. North, D. L. Usanov, C. Young, *Chem. Rev.* **2008**, *108*, 5146–5226; j.) P. Li, H. Yamamoto, *Top. Organomet. Chem.* **2011**, *37*, 161–183; k.) J. Zhou, Y. Tang, *Top. Organomet. Chem.* **2011**, *36*, 287–312; l.) L. C. Dias, E. C. de Lucca Jr., M. A. B. Ferreira, E. C. Polo, *J. Braz. Chem. Soc.* **2012**, *23*, 2137–2158; m.) H. Yamamoto, *Top. Organomet. Chem.* **2013**, *44*, 315–334.

11 H. Huo, C. Fu, K. Harms, E. Meggers, *J. Am. Chem. Soc.* **2014**, *136*, 2990–2993.

12 H. Huo, X. Shen, C. Wang, L. Zhang, P. Röse, L.-A. Chen, K. Harms, M. Marsch, G. Hilt, E. Meggers, *Nature* **2014**, *515*, 100–103.

13 For chiral octahedral iridium(III) complexes in asymmetric catalysis, see: a.) P. Paredes, J. Díez, M. P. Gamasa, *Organometallics* **2008**, *27*, 2597–2607; b.) C. P. Owens, A. Varela-Álvarez, V. Boyarskikh, D. G. Musaev, H. M. L. Davies, S. B. Blakey, *Chem. Sci.* **2013**, *4*, 2590–2596; c.) D. Carmona, J. Ferrer, N. García, P. Ramírez, F. J. Lahoz, P. García-Orduña, L. A. Oro, *Organometallics* **2013**, *32*, 1609–1619; d.) Y. Kita, K. Yamaji, K. Higashida, K. Sataiah, A. Iimuro, K. Mashima, *Chem. Eur. J.* **2015**, *21*, 1915–1927.

14 For catalytic asymmetric Friedel-Crafts alkylations with α,β-unsaturated 2-acyl imidazoles, see: a.) D. A. Evans, K. R. Fandrick, H.-J. Song, *J. Am. Chem. Soc.* **2005**, *127*, 8942–8943; b.) D. A. Evans, K. R. Fandrick, H.-J. Song, K. A. Scheidt, R. Xu, *J. Am. Chem. Soc.* **2007**, *129*, 10029–10041; c.) A. J. Boersma, B. L. Feringa, G. Roelfes, *Angew. Chem. Int. Ed.* **2009**, *48*, 3346–3348; d.) C. Wang, Y. Li, G. Jia, Y. Liu, S. Lu, C. Li, *Chem. Commun.* **2012**, *48*, 6232–6234; e.) J. Wang, E. Benedetti, L. Bethge, S. Vonhoff, S. Klussmann, J.-J. Vasseur, J. Cossy, M. Smietana, S. Arseniyadis, *Angew. Chem. Int. Ed.* **2013**, *52*, 11546–11549.

15 D. A. Evans, K. R. Fandrick, *Org. Lett.* **2006**, *8*, 2249–2252

16 Comparison with a bis(oxazolinyl)pyridine-scandium(III) triflate catalyst. Reaction with indole: 80% yield and 65% *ee* with 2.5 mol% catalyst at 0 °C (ref. 14a and 14b). Reaction with 3-dimethylaminoanisole (ref. 14b): <20% yield and 22% *ee*. Reaction with 2-methoxyfurane (ref. 14a): 65% yield and 98% *ee* with 2.0 mol% catalyst at –40 °C (ref. 14a). Reaction with pyrrole (ref. 17): 69% yield and 87% *ee* with 5 mol% catalyst at –40 °C.

17 For comparison, a DNA-based copper(II) catalyst (30 mol%) provided for the same malonodinitrile Michael addition product with an enantioselectivity of 36% *ee* at 4 °C. See: Y. Li, C. Wang, G. Jia, S. Lu, C. Li, *Tetrahedron* **2013**, *69*, 6585–6590.

18 For reviews on the asymmetric construction of all-carbon quaternary stereocenters, see: a.) C. J. Douglas, L. E. Overman, *Proc. Nat. Acad. Sci. USA* **2004**, *101*, 5363–5367; b.) J. Christoffers, A. Baro, *Adv. Synth. Catal.* **2005**, *347*, 1473–1482; c.) B. M. Trost, C. Jiang, *Synthesis* **2006**, 369–396; d.) M. Bella, T. Gasperi, *Synthesis* **2009**, 1583–1614; e.) C. Hawner, A. Alexakis, *Chem. Commun.* **2010**, *46*, 7295–7306; f.) J. P. Das, I. Marek, *Chem. Commun.* **2011**, *47*, 4593–4623; g.) R. Dalpozzo, G. Bartoli, G. Bencivenni, *Chem. Soc. Rev.* **2012**, *41*, 7247–7290; h.) K. W. Quasdorf, L. E. Overman, *Nature* **2014**, *516*, 181–191.

19 For comparison, a bis(oxazolinyl)pyridine-cerium(IV) triflate catalyst provided for the same nitrone cycloaddition reaction 99% yield with 97% ee and >99:1 endo:exo with 5 mol% catalyst at 0 °C. See: D. A. Evans, H.-J. Song, K. R. Fandrick, *Org. Lett.* **2006**, *8*, 3351–3354.

20 For related Lewis acid catalyzed asymmetric 1,3-dipolar cycloadditions, see: a.) K. V. Gothelf, K. A. Jørgensen, *J. Org. Chem.* **1994**, *59*, 5687–5691; b.) K. V. Gothelf, I. Thomsen, K. A. Jørgensen, *J. Am. Chem. Soc.* **1996**, *118*, 59–64; c.) S. Kobayashi, M. Kawamura, *J. Am. Chem. Soc.* **1998**, *120*, 5840–5841; d.) S. Kanemasa, Y. Oderaotoshi, J. Tanaka, E. Wada, *J. Am. Chem. Soc.* **1998**, *120*, 12355–12356; e.) C. Palomo, M. Oiarbide, E. Arceo, J. M. García, R. López, A. González, A. Linden, *Angew. Chem. Int. Ed.* **2005**, *44*, 6187–6190; f.) M. P. Sibi, Z. Ma, K. Itoh, N. Prabagaran, C. P. Jasperse, *Org. Lett.* **2005**, *7*, 2349–2352; g.) K. Phomkeona, T. Takemoto, Y. Ishima, K. Shibatomi, S. Iwasa, H. Nishiyama, *Tetrahedron* **2008**, *64*, 1813–1822; h.) S. Barroso, G. Blay, M. C. Muñoz, J. R. Pedro, *Org. Lett.* **2011**, *13*, 402–405; i.) D. Chen, Z. Wang, J. Li, Z. Yang, L. Lin, X. Liu, X. Feng, *Chem. Eur. J.* **2011**, *17*, 5226–5229.

21 For a review on hetero-Diels-Alder reactions of ketones, see: K. A. Jørgensen, *Eur. J. Org. Chem.* **2004**, 2093–2102.

22 For related Lewis acid catalyzed asymmetric hetero-Diels-Alder reactions, see: a.) J. Thorhauge, M. Johannsen, K. A. Jørgensen, *Angew. Chem. Int. Ed.* **1998**, *37*, 2404–2406; b.) D. A. Evans, J. S. Johnson, E. J. Olhava, *J. Am. Chem. Soc.* **2000**, *122*, 1635–1649; c.) H. Audrain, J. Thorhauge, R. G. Hazell, K. A. Jørgensen, *J. Org. Chem.* **2000**, *65*, 4487–4497; d.) Y. Shin, C.-E. Yeom, M. Kim, B. Kim, *Synlett* **2008**, 89–93; e.) Y. Zhu, M. Xie, S. Dong, X. Zhao, L. Lin, X. Liu, X. Feng, *Chem. Eur. J.* **2011**, *17*, 8202–8208; f.) Y. Zhou, Y. Zhu, L. Lin, Y. Zhang, J. Zheng, X. Liu, X. Feng, *Chem. Eur. J.* **2014**, *20*, 16753–16758.

23 For related Lewis acid catalyzed asymmetric Diels-Alder reactions, see: a.) E. J. Corey, N. Imai, H. Y. Zhang, *J. Am. Chem. Soc.* **1991**, *113*, 728–729; b.) D. A. Evans, S. J. Miller, T. Lectka, *J. Am. Chem. Soc.* **1993**, *115*, 6460–6461; c.) K. V. Gothelf, K. A. Jorgensen, *J. Org. Chem.* **1995**, *60*, 6847–6851; d.) D. A. Evans, J. A. Murry, P. von Matt, R. D. Norcross, S. J. Miller, *Angew. Chem. Int. Ed. Engl.* **1995**, *34*, 798–800; e.) A. K. Ghosh, P. Mathivanan, J. Cappiello, *Tetrahedron Lett.* **1996**, *37*, 3815–3818; f.) I. Sagasser, G. Helmchen, *Tetrahedron Lett.* **1998**, *39*, 261–264; g.) S. Otto, G. Boccaletti, J. B. F. N. Engberts, *J. Am. Chem. Soc.* **1998**, *120*, 4238–4239; h.) D. A. Evans,

D. M. Barnes, J. S. Johnson, T. Lectka, P. von Matt, S. J. Miller, J. A. Murry, R. D. Norcross, E. A. Shaughnessy, K. R. Campos, *J. Am. Chem. Soc.* **1999**, *121*, 7582–7594; i.) M. P. Sibi, L. M. Stanley, X. Nie, L. Venkatraman, M. Liu, C. P. Jasperse, *J. Am. Chem. Soc.* **2007**, *129*, 395–405; j.) A. J. Boersma, J. E. Klijn, B. L. Feringa, G. Roelfes, *J. Am. Chem. Soc.* **2008**, *130*, 11783–11790; k.) C. Wang, G. Jia, J. Zhou, Y. Li, Y. Liu, S. Lu, C. Li, *Angew. Chem. Int. Ed.* **2012**, *51*, 9352–9355. l.) A. J. Boersma, B. de Bruin, B. L. Feringa, G. Roelfes, *Chem. Commun.* **2012**, *48*, 2394–2396.

24 D. A. Evans, K. T. Chapman, J. Bisaha, *J. Am. Chem. Soc.* **1988**, *110*, 1238–1256.

25 I. W. Davies, C. H. Senanayake, L. Castonguay, R. D. Larsen, T. R. Verhoeven, P. J. Reider, *Tetrahedron Lett.* **1995**, *36*, 7619–7622.

26 For the conjugate addition to α,β-unsaturated 2-acyl benzimidazoles: M. Yoshida, H. Ohmiya, M. Sawamura, *J. Am. Chem. Soc.* **2012**, *134*, 11896–11899. See also ref. 14b.

27 For the conjugate addition to α,β-unsaturated 2-acyl thiazoles: a.) A. Dondoni, L. Kniezo, M. Martinkova, *J. Chem. Soc., Chem. Commun* **1994**, 1963–1964; b.) A. Dondoni, A. Marra, A. Boscarato, *Chem. Eur. J.* **1999**, *5*, 3562–3572; c.) M. Sani, G. Fossati, F. Huguenot, M. Zanda, *Angew. Chem. Int. Ed.* **2007**, *46*, 3526–3529; d.) P. S. Shankar, M. Sani, G. Terraneo, M. Zanda, *Synlett* **2009**, 1341–1345; e.) P. Kwiatkowski, A. Cholewiak, A. Kasztelan, *Org. Lett.* **2014**, *16*, 5930–5933. See also ref. 14b.

28 For the conjugate addition to α,β-unsaturated 2-acyl pyridines: a.) M. P. Sibi, Y. H. Yang, *Synlett* **2008**, 83–88; b.) P. K. Singh, V. K. Singh, *Org. Lett.* **2008**, *10*, 4121–4124; c.) N. Molleti, N. K. Rana, V. K. Singh, *Org. Lett.* **2012**, *14*, 4322–4325; d.) S. Lin, Y. Wei, F. Liang, *Chem. Commun.* **2012**, *48*, 9879–9881; e.) a.) G. Blay, C. Incerti, M. C. Muñoz, J. R. Pedro, *Eur. J. Org. Chem.* **2013**, 1696–1705; f.) X.-Q. Hao, J.-J. Huang, T. Wang, J. Lv, J.-F. Gong, M.-P. Song, *J. Org. Chem.* **2014**, *79*, 9512–9530.

29 For the conjugate addition to α,β-unsaturated *N*-acyl oxazolidinones: a.) S. Kobayashi, C. Ogawa, M. Kawamura, M. Sugiura, *Synlett* **2001**, 983–985; b.) D. J. Guerin, S. J. Miller, *J. Am. Chem. Soc.* **2002**, *124*, 2134–2136; c.) A. W. Hird, A. H. Hoveyda, *Angew. Chem. Int. Ed.* **2003**, *42*, 1276–1279; d.) Y. Hoashi, T. Okino, Y. Takemoto, *Angew. Chem. Int. Ed.* **2005**, *44*, 4032–4035; e.) C. Palomo, R. Pazos, M. Oiarbide, J. M. García, *Adv. Synth. Catal.* **2006**, *348*, 1161–1164; f.) A. M. M. Abe, S. J. K. Sauerland, A. M. P. Koskinen, *J. Org. Chem.* **2007**, *72*, 5411–5413; g.) L. Fadini, A. Togni, *Tetrahedron: Asymmetry* **2008**, *19*, 2555–2562; h.) M. P. Sibi, Y.-H. Yang, S. Lee, *Org. Lett.* **2008**, *10*, 5349–5352; i.) Y. Liu, B. Sun, B. Wang, M. Wakem, L. Deng, *J. Am. Chem. Soc.* **2009**, *131*, 418–419; j.) S. Murarka, I. Deb, C. Zhang, D. Seidel, *J. Am. Chem. Soc.* **2009**, *131*, 13226–13227; k.) Y. Huang, E. Tokunaga, S. Suzuki, M. Shiro, N. Shibata, *Org. Lett.* **2010**, *12*, 1136–1138; l.) S. Harada, T. Morikawa, A. Nishida, *Org. Lett.* **2013**, *15*, 5314–5317; m.) L.

Wen, L. Yin, Q. Shen, L. Lu, *Acs Catal.* **2013**, *3*, 502–506; n.) Y. Sakaguchi, N. Kurono, K. Yamauchi, T. Ohkuma, *Org. Lett.* **2014**, *16*, 808–811. See also 14b.

30 For the conjugate addition to α,β-unsaturated *N*-acylthiazolidinethiones: D. A. Evans, R. J. Thomson, F. Franco, *J. Am. Chem. Soc.* **2005**, *127*, 10816–10817. See also ref. 14b.

31 For conjugate additions with α,β-unsaturated *N*-acyl pyrazoles, see: a.) C. Kashima, K. Takahashi, I. Fukuchi, K. Fukusaka, *Heterocycles* **1997**, *44*, 289–304; b.) M. P. Sibi, J. J. Shay, M. Liu, C. P. Jasperse, *J. Am. Chem. Soc.* **1998**, *120*, 6615–6616; c.) C. Kashima, K. Fukusaka, K. Takahashi, Y. Yokoyama, *J. Org. Chem.* **1999**, *64*, 1108–1114; d.) K. Itoh, S. Kanemasa, *J. Am. Chem. Soc.* **2002**, *124*, 13394–13395; e.) C. Kashima, Y. Miwa, S. Shibata, H. Nakazono, *J. Heterocycl. Chem.* **2003**, *40*, 681–688; f.) K. Itoh, Y. Oderaotoshi, S. Kanemasa, *Tetrahedron: Asymmetry* **2003**, *14*, 635–639; g.) K. Itoh, M. Hasegawa, J. Tanaka, S. Kanemasa, *Org. Lett.* **2005**, *7*, 979–981; h.) H. Yanagita, K. Kodama, S. Kanemasa, *Tetrahedron Lett.* **2006**, *47*, 9353–9357; i.) K. Ishihara, M. Fushimi, *Org. Lett.* **2006**, *8*, 1921–1924; j.) M. P. Sibi, K. Itoh, *J. Am. Chem. Soc.* **2007**, *129*, 8064–8065; k.) F. Ono, M. Hasegawa, S. Kanemasa, J. Tanaka, *Tetrahedron Lett.* **2008**, *49*, 5105–5107; l.) M. Hasegawa, F. Ono, S. Kanemasa, *Tetrahedron Lett.* **2008**, *49*, 5220–5223; m.) X.-Q. Dong, X. Fang, H.-Y. Tao, X. Zhou, C.-J. Wang, *Chem. Commun.* **2012**, *48*, 7238; n.) X.-Q. Dong, X. Fang, H.-Y. Tao, X. Zhou, C.-J. Wang, *Adv. Synth. Catal.* **2012**, *354*, 1141–1147; o.) J. Zhang, X. Liu, R. Wang, *Chem. Eur. J.* **2014**, *20*, 4911–4915. See also ref. 14b.

32 For the conjugate addition to α,β-unsaturated acyl phosphonates: a.) H. Jiang, M. W. Paixão, D. Monge, K. A. Jørgensen, *J. Am. Chem. Soc.* **2010**, *132*, 2775–2783; b.) D. A. Evans, K. A. Scheidt, K. R. Fandrick, H. W. Lam, J. Wu, *J. Am. Chem. Soc.* **2003**, *125*, 10780–10781; c.) Y. K. Kang, K. H. Suh, D. Y. Kim, *Synlett* **2011**, 1125–1128; d.) N. Takenaka, J. P. Abell, H. Yamamoto, *J. Am. Chem. Soc.* **2007**, *129*, 742–743; e.) P. Bachu, T. Akiyama, *Chem. Commun.* **2010**, *46*, 4112–4114. See also ref. 14b.

33 For the conjugate addition to α,β-unsaturated ketoesters, see for example: a.) K. B. Jensen, J. Thorhauge, R. G. Hazell, K. A. Jørgensen, *Angew. Chem. Int. Ed.* **2001**, *40*, 160–163; b.) K. A. Jørgensen, *Synthesis* **2003**, 1117–1125; c.) M. Rueping, B. J. Nachtsheim, S. A. Moreth, M. Bolte, *Angew. Chem. Int. Ed.* **2008**, *47*, 593–596; d.) S.-L. Zhao, C.-W. Zheng, H.-F. Wang, G. Zhao, *Adv. Synth. Catal.* **2009**, *351*, 2811–2816; e.) Y. Liu, D. Shang, X. Zhou, Y. Zhu, L. Lin, X. Liu, X. Feng, *Org. Lett.* **2010**, *12*, 180–183; f.) J. Lv, X. Li, L. Zhong, S. Luo, J.-P. Cheng, *Org. Lett.* **2010**, *12*, 1096–1099; g.) L. Zhou, L. Lin, W. Wang, J. Ji, X. Liu, X. Feng, *Chem. Commun.* **2010**, *46*, 3601–3603; h.) B. Yang, F. Xie, H. Yu, K. Shen, Z. Ma, W. Zhang, *Tetrahedron* **2011**, *67*, 6197–6201; i.) J. Lv, L. Zhang, Y. Zhou, Z. Nie, S. Luo, J.-P. Cheng, *Angew. Chem. Int. Ed.* **2011**, *50*, 6610–6614; j.) L. Gremaud, A. Alexakis, *Angew. Chem. Int. Ed.* **2012**, *51*, 794–797; k.) L. Liu, H. Ma, Y. Xiao, F. Du, Z. Qin, N. Li, B. Fu, *Chem. Commun.* **2012**, *48*, 9281–9283; l.) J. Duan, F. Cao, X. Wang, C. Ma, *Chem. Commun.* **2013**, *49*, 1124–1126; m.) Y. Zhang, X. Liu, X. Zhao, J.

Zhang, L. Zhou, L. Lin, X. Feng, *Chem. Commun.* **2013**, *49*, 11311–11313; n.) H.-G. Cheng, L.-Q. Lu, T. Wang, Q.-Q. Yang, X.-P. Liu, Y. Li, Q.-H. Deng, J.-R. Chen, W.-J. Xiao, *Angew. Chem. Int. Ed.* **2013**, *52*, 3250–3254; o.) S. Zhang, K. Xu, F. Guo, Y. Hu, Z. Zha, Z. Wang, *Chem. Eur. J.* **2014**, *20*, 979–982; p.) Q. Wang, J. Gong, Y. Liu, Y. Wang, Z. Zhou, *Tetrahedron* **2014**, *70*, 8168–8173; q.) S.-J. Jia, D.-M. Du, *Tetrahedron: Asymmetry* **2014**, *25*, 980–988; r.) J. Wang, B. Wang, P. Cao, J. Liao, *Tetrahedron Lett.* **2014**, *55*, 3450–3453; s.) E. Sánchez-Larios, K. Thai, F. Bilodeau, M. Gravel, *Org. Lett.* **2011**, *13*, 4942–4945; t.) A. Lefranc, L. Gremaud, A. Alexakis, *Org. Lett.* **2014**, *16*, 5242–5245; u.) J. Wang, M. Wang, P. Cao, L. Jiang, G. Chen, J. Liao, *Angew. Chem. Int. Ed.* **2014**, *53*, 6673–6677; v.) Y. Zhang, N. Yang, X. Liu, J. Guo, X. Zhang, L. Lin, C. Hu, X. Feng, *Chem. Commun.* **2015**, *51*, 8432–8435.

34 For conjugate additions to α,β-unsaturated Weinreb amides: a.) R. Shintani, T. Kimura, T. Hayashi, *Chem. Commun.* **2005**, 3213–3214; b.) J. R. de Alaniz, M. S. Kerr, J. L. Moore, T. Rovis, *J. Org. Chem.* **2008**, *73*, 2033–2040; c.) L. Li, J.-Y. Guo, X.-G. Liu, S. Chen, Y. Wang, B. Tan, X.-Y. Liu, *Org. Lett.* **2014**, *16*, 6032–6035.

35 J. Ma, X. Ding, Y. Hu, Y. Huang, L. Gong, E. Meggers, *Nat. Commun.* **2014**, *5*, 4531

36 2-Acyl imidazoles can be converted to a wide variety of carbonyl compounds. See ref. 8b and also: a.) S. Ohta, S. Hayakawa, K. Nishimura, M. Okamoto, *Chem. Pharm. Bull.* **1987**, *35*, 1058–1069; b.) A. Miyashita, Y. Suzuki, I. Nagasaki, C. Ishiguro, K. Iwamoto, T. Higashino, *Chem. Pharm. Bull.* **1997**, *45*, 1254–1258.

37 M. Holmquist, G. Blay, M. C. Muñoz, J. R. Pedro, *Org. Lett.* **2014**, *16*, 1204–1207.

38 A. Marinier, C. Quesnelle, M. Dodier, S. Roy, P. Gill, M. D. Wittman, D. R. Langley, Patent No. WO/2008/079873, July 3, **2008**.

39 C. Bissantz, E. Goetschi, C. Grundschober, R. Masciadri, H. Ratni, M. Rogers-Evans, P. Schnider, Patent No. WO/2008/084005, July 17, **2008**.

40 S. Badiger, M. Chebrolu, K. Hurth, S. Jacquier, R. M. Lueoend, R. Machauer, H. Rueeger, M. Tintelnot-Blomley, S. J. Veenstra, M. Voegtle, Patent No. WO/2012/095469, July 19, **2012**.

41 G. Li, X. Qian, J. Cui, Q. Huang, R. Zhang, H. Guan, *J. Agric. Food. Chem.* **2006**, *54*, 125–129.

42 H. Huo, X. Shen, C. Wang, L. Zhang, P. Röse, L.-A. Chen, K. Harms, M. Marsch, G. Hilt, E. Meggers, *Nature* **2014**, *515*, 100–103.

43 C. Wang, Y. Zheng, H. Huo, P. Röse, L. Zhang, K. Harms, G. Hilt, E. Meggers, *Chem. Eur. J.* **2015**, *21*, 7355–7359.

44 H. Huo, C. Wang, K. Harms, E. Meggers, *J. Am. Chem. Soc.* **2015**, *137*, 9551–9554.

45 C. Wang, Y. Zheng, H. Huo, P. Röse, L. Zhang, K. Harms, G. Hilt, E. Meggers, *Chem. Eur. J.* **2015**, *21*, 7355–7359.

46 Y. Tan, W. Yuan, L. Gong, E. Meggers, *Angew. Chem. Int. Ed.* **2015**, *54*, 13045–13048.

47 R. S. Andrews, J. J. Becker, M. R. Gagne, *Angew. Chem. Int. Ed.* **2012**, *51*, 4140–4143.

48 J. W. Tucker, Y. Zhang, T. F. Jamison, C. R. Stephenson, *Angew. Chem. Int. Ed.* **2012**, *51*, 4144–4147.

49 G. Cecere, C. M. König, J. L. Alleva, D. W. C. MacMillan, *J. Am. Chem. Soc.* **2013**, *135*, 11521–11524.

50 M. Nappi, G. Bergonzini, P. Melchiorre, *Angew. Chem. Int. Edit.* **2014**, *53*, 4921–4925.

51 A. Studer, D. P. Curran, *Angew. Chem. Int. Ed.* **2016**, *55*, 58–102.

52 M. D. Kärkäs, B. S. Matsuura, C. R. J. Stephenson, *Science* **2015**, *349*, 1285–1286.

53 Ł. Woźniak, J. J. Murphy, P. Melchiorre, *J. Am. Chem. Soc.* **2015**, *137*, 5678−5681.

54 M. A. Cismesia, T. P. Yoon, *Chem. Sci.* **2015**, *6*, 5426−5434.

55 S. L. Murov, I. Carmichael, G. L. Hug, Handbook of Photochemistry (Second Edition), New York, **1993**.

56 R. D. Shannon, *Acta Crystallogr., Sect. A: Crytal. Phys. Diffr., Theor. Gen. Crystallogr.* **1976**, 32, 751–767.

57 R. Sutcliffe, D. Griller, J. Lessard, K. U. Ingold, *J. Am. Chem. Soc.* **1981**, *103*, 624–628.

58 J. H. Horner, O. M. Musa, A. Bouvier, M. Newcomb, *J. Am. Chem. Soc.* **1998**, *120*, 7738–7748.

59 Selected review on *N*-centered radicals: S. Z. Zard, *Chem. Soc. Rev.* **2008**, *37*, 1603–1618.

60 Photochemistry and photophysics of rhodium complexes: M. T. Indelli, C. Chiorboli, F. Scandola, *Top. Curr. Chem.* **2007**, *280*, 215–255.

61 A. J. Hallett, N. White, W. Wu, X. Cui, P. N. Horton, S. J. Coles, J. Zhao, S. J. A. Pope, *Chem. Commun.* **2012**, *48*, 10838–10840.

# Chapter 4. Summary and Outlook

In this thesis, a number of octahedral metal complexes containing two bidentate cyclometalating ligands in addition to two labile acetonitrile ligands are designed and synthesized. Among these complexes, the octahedral chiral-at-metal iridium(III) complexes **IrO** and **IrS** are demonstrated to be effective chiral Lewis acid catalysts in a variety of asymmetric catalytic reactions; the octahedral chiral-at-metal rhodium(III) complex **RhO** is proved to be an efficient "2-in-1" catalyst for visible-light-activated enantioselective radical amination of 2-acyl imidazoles.

**1) The synthesis of octahedral metal complexes**

A number of racemic octahedral metal complexes which are tuned by modification of their ligands were synthesized (Scheme 43), in which chiral **IrS** and **IrO(ada)** were synthesized through a convenient auxiliary-mediated strategy developed in our laboratory (Scheme 43), chiral **IrO** or **RhO** were synthesized by published procedures.

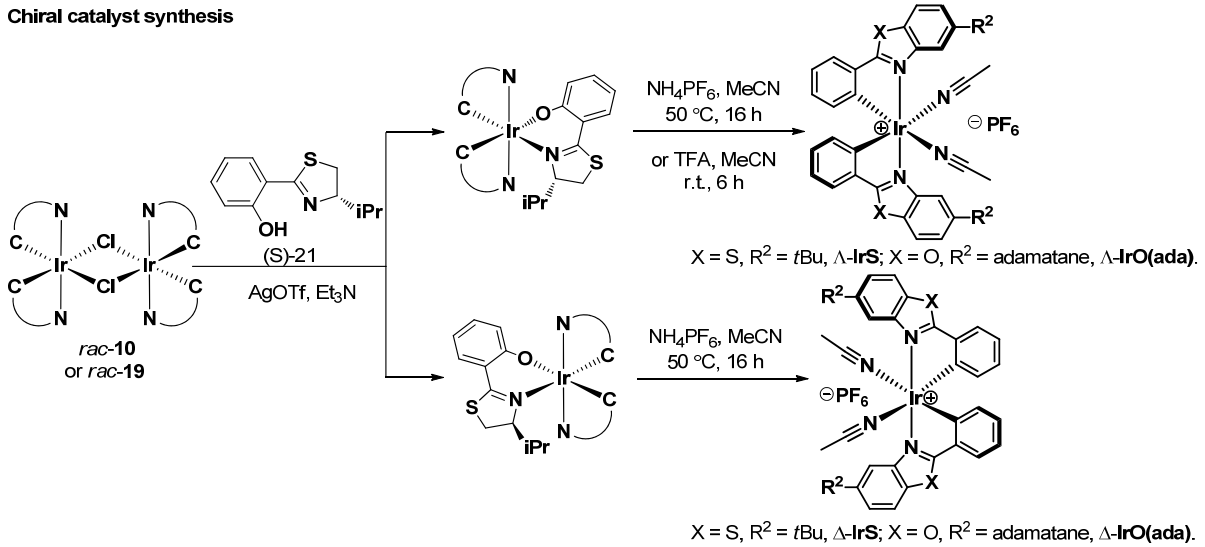


**Scheme 43** The Synthesis of Octahedral Metal Complexes

**2) Asymmetric catalysis by octahedral chiral-at-metal complexes**

We then demonstrated the high versatility of the iridium(III) complexes Λ-**IrO** and Λ-**IrS** as effective chiral Lewis acid catalysts (0.5−5.0 mol% catalyst loading) for a variety of asymmetric reactions with α,β-unsaturated carbonyl compounds, including **Friedel-Crafts alkylations** (up to 99% ee), **Michael additions with CH-acidic compounds** (up to 97% ee), **cycloadditions** (up to 99% ee with high *d.r.*),

and **Henry reactions** (up to 98% ee). (Scheme 44)

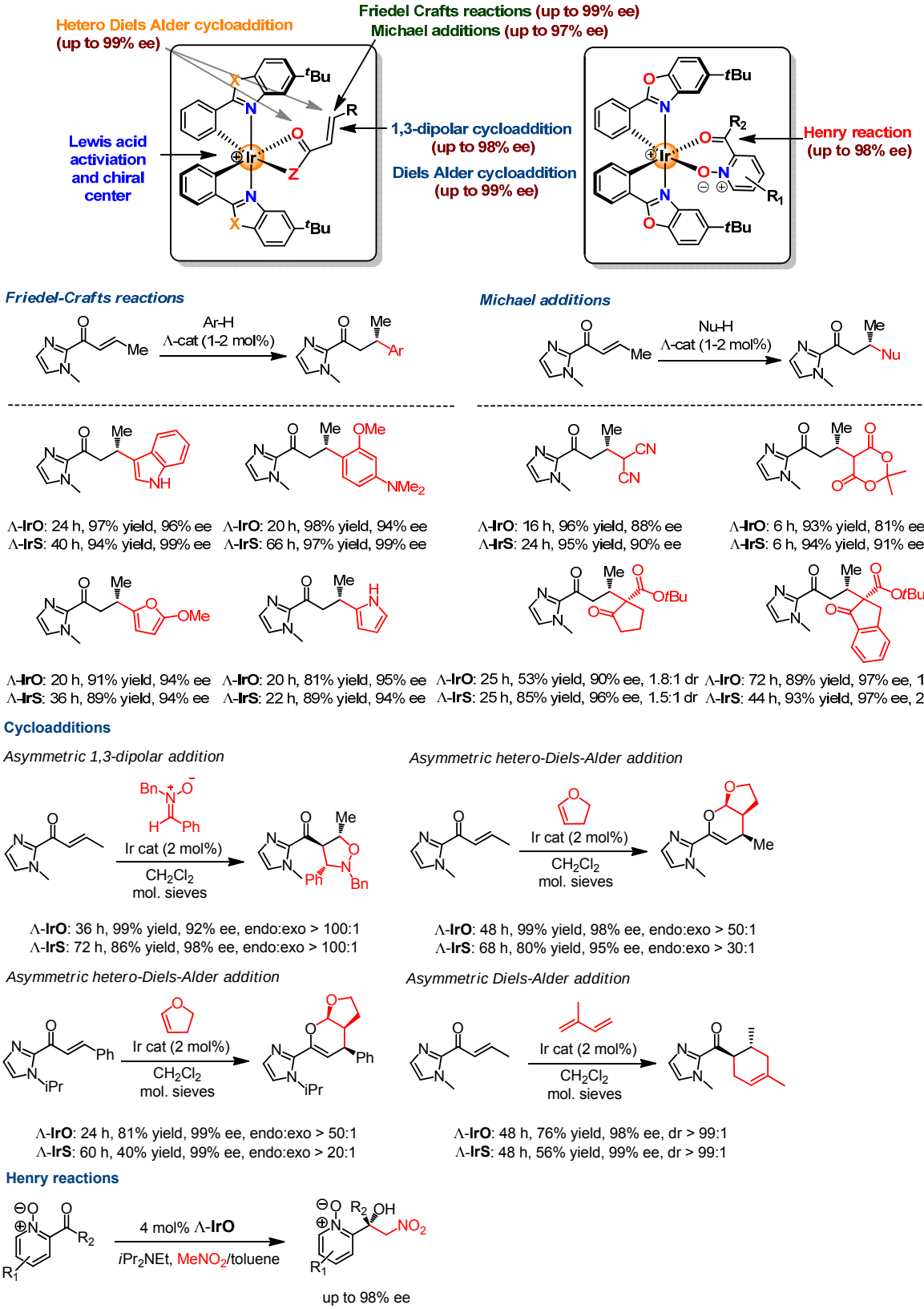


**Scheme 44** Asymmetric Reactions Catalyzed by Λ-**IrO** and Λ-**IrS**#

We studied the scope of acceptor-substituted alkene in addition to 2-acyl imidazoles for the Friedel-Crafts alkylation and found that a significant number of the tested acceptor-substituted alkenes

could be suitable substrates, providing the expected products in high yields with high enantioselectivities, such as the benzimidazole (86% yield, 96% *ee*), 2-thiazole (99% yield, 98% *ee*), pyridine (87% yield, 97% *ee*), pyrazoles (86% yield, 98% ee), (99% yield, 95% ee), and α-ketoester (99% yield, 95% ee).

The mechanism of this Lewis acid catalysis was also studied, some important intermediates were trapped, together with kinetic experiments revealed that the rate of the overall catalysis does not depend on the concentration of the nucleophile but is directly proportional to the concentration of substrate that will coordinate to the iridium catalyst, thus demonstrating that rate determining step must be the replacement of iridium-coordinated product with a new substrate molecule.

### 3) Visible-light-induced enantioselective C-N formation by octahedral chiral-at-metal complex

Finally, it is found the chiral-at-metal rhodium complex **RhO** could catalyze a very efficient photoactivated enantioselective radical amination of 2-acyl imidazoles. Notably, related bis-cyclometalated iridium(III) complexes, which were previously demonstrated to serve as dual function photoredox/chiral Lewis acid catalysts for enantioselective C-C bond formation reactions, are not suitable for the here described enantioselective C-N bond formation chemistry. (Scheme 45)

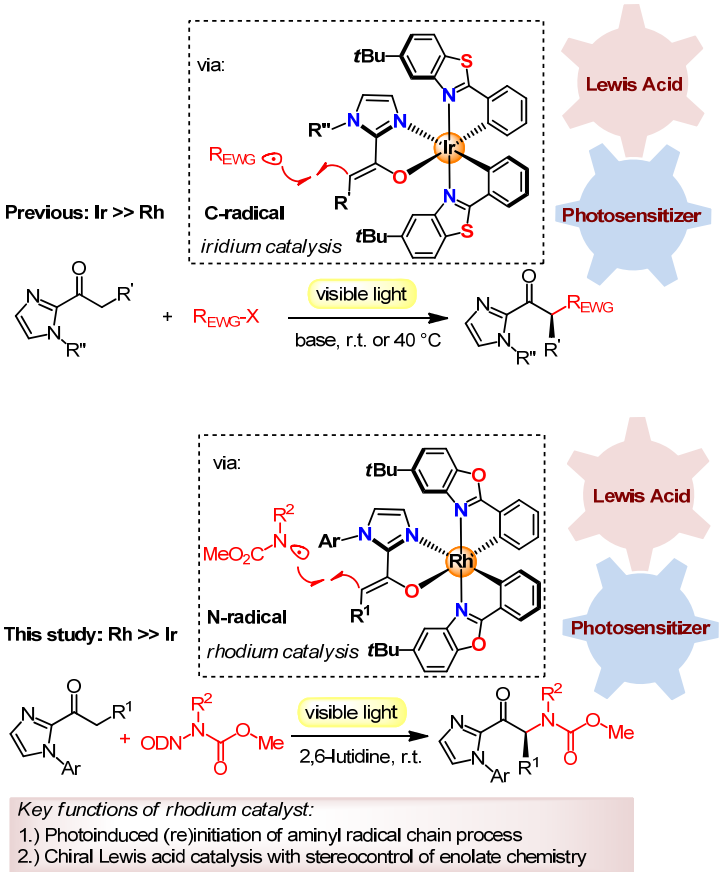


**Scheme 45** Previous Work and This Study Regarding Catalytic Enantioselective Photoredox Chemistry with SingleTransition Metal Complexes

In this reaction, **RhO** serves a dual function, namely as a chiral Lewis acid to catalyze asymmetric enolate chemistry and furthermore as a light-activated smart initiator of a radical chain process. Scheme 46 displays a substrate scope, revealing that substituents are well tolerated in the aromatic moiety in α-position to the carbonyl group (up to 99% yield and 98% ee). However, it has to be noted that this reaction only works with aromatic substituents in α-position to the carbonyl group.

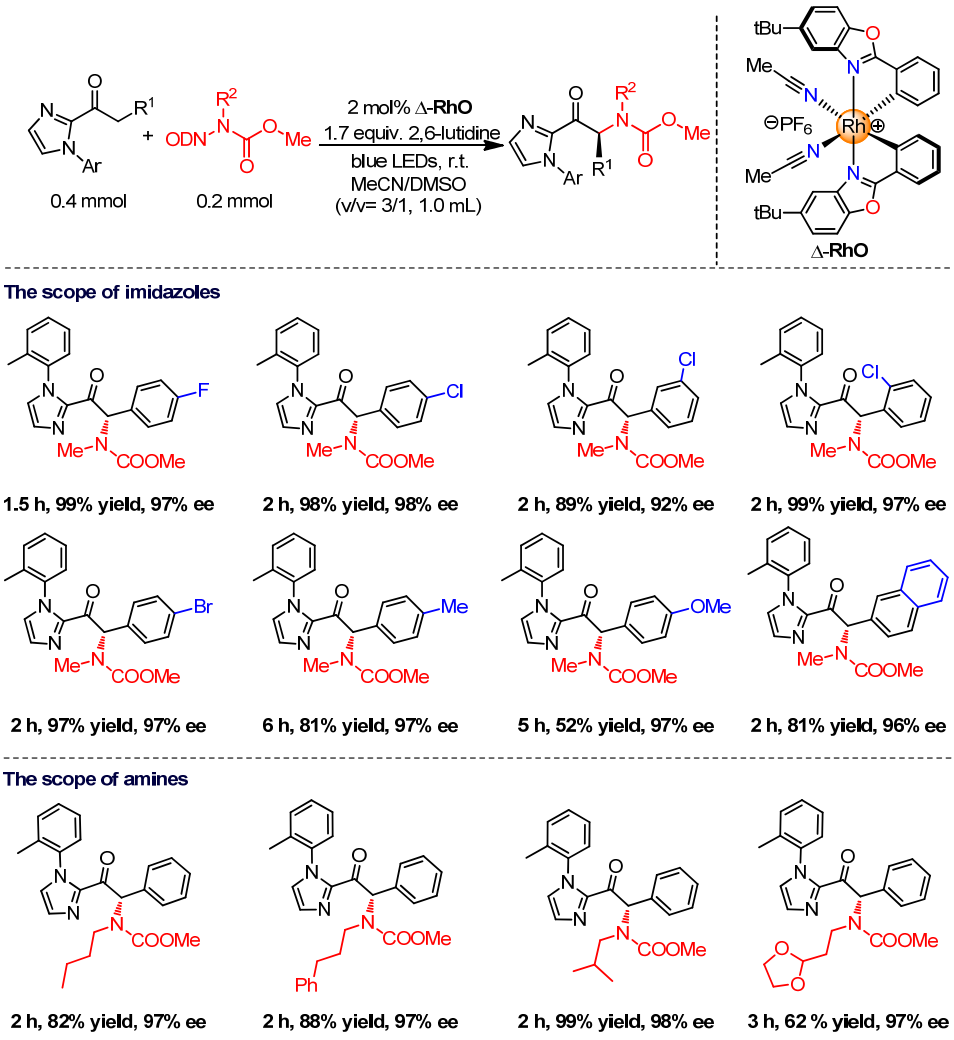


**Scheme 46** Scope of Substrates for Visible-Light-Induced Enantioselective C-N Formation#

A mechanism was carefully proposed: the acyl imidazole substrate coordinates to the rhodium complex in a bidentate fashion (intermediate **I**) followed by a deprotonation of the α-methylene group which affords a neutral rhodium enolate complex (intermediate **II**, the crystal structure of **II** is obtained). It is believed that this enolate **II** has a crucial dual function. Firstly, it serves as an initiator and reinitiator upon photoactivation (**II** + $h\nu \rightarrow$ **II***) by transfering a single electron (**II*** $\rightarrow$ $\mathbf{II}^{+}$ + $e^{-}$) to the ODN-carbamate which then fragments into a sulfonate anion and an aminyl radical (the aminyl radical can be trapped by *N*-methylindole). Secondly, enolate **II** contains a very electron rich double bond that reacts with the electrophilic nitrogen-centered radical in a stereocontrolled fashion. This provides a rhodium-coordinated ketyl (intermediate **III**) which is highly reducing and either donates

an electron to the photosensitizer redox cycle to regenerate the oxidized photosensitizer ($\mathbf{II}^{+} + e^{-} \rightarrow \mathbf{II}$) or directly transfers a single electron to the ODN-carbamate, thereby propagating a chain process which is further confirmed by a determined quantum yield of 14 for this photochemical reaction.

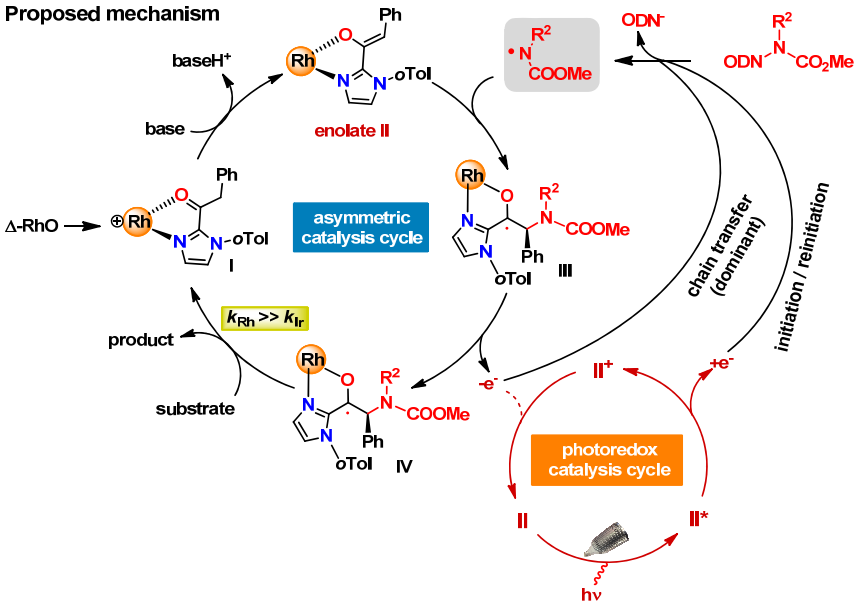


**Figure 54** Proposed mechanism for the visible-light-activated enantioselective C-N formation.

Notably, related previously reported iridium-based photoredox catalysts fail for the here described enantioselective radical C-N bond formation. This surprising preference for rhodium over iridium is pinpointed to much faster ligand exchange kinetics of the rhodium complexes involved in the catalytic cycle, which is crucial to keep pace with the highly reactive and therefore short-lived nitrogen-centered radical intermediate.

### 4) Outlook

Future work will be focused on designing and synthesizing more types of octahedral chiral-at-metal complexes, and exploring more reactions (such as C-H activiations, cascade reactions). In addition, the novel asymmetric photoinduced catalytic reactions by using boryl radicals/ alkoxyl radicals/ phosphonyl radicals/ sulfur radicals will also be explored.

# Chapter 5. Experimental Part

## 5.1 Materials and Methods

All reactions were carried out under an atmosphere of nitrogen with magnetic stirring. Catalytic reactions were performed using standard Schlenk glassware or simple glass vials.

### Solvents and Reagents

Solvents were distilled under nitrogen from calcium hydride ($CH_3CN$, $CH_2Cl_2$, DMF), sodium/benzophenone (THF), or magnesium turnings/iodine (MeOH). Dry dimethylsulfoxide (DMSO) is purchased from Sigma-Aldrich without further purification. 2,3-Dihydrofuran and isoprene were used after freshly distilled from calcium hydride. All other reagents were purchased from Sigma Aldrich, Alfa aesar, TCI, Acros, Fluorochem, and ChemPUR and used without further purification.

### Chromatographic Methods

Flash column chromatography was performed with silica gel 60 M from Macherey-Nagel (irregular shaped, 230–400 mesh, pH 6.8, pore volume: 0.81 mL × $g^{-1}$, mean pore size: 66 Å, specific surface: 492 $m^2$ × $g^{-1}$, particle size distribution: 0.5% < 25 μm and 1.7% > 71 μm, water content: 1.6%). For thin layer chromatography (TLC) analysis throughout this work, Merck precoated TLC plates (silica gel 60 F254, 0.25 mm) were employed.

### Nuclear Magnetic Resonance Spectroscopy (NMR)

$^1$H NMR, proton coupled $^{19}$F NMR and proton decoupled $^{13}$C NMR spectra were measured at room temperature on a Bruker Avance 300 system ($^1$H-NMR resonance: 300 MHz, $^{19}$F-NMR resonance: 282 MHz, $^{13}$C-NMR resonance: 75 MHz) or Bruker Avance 500 system ($^1$H-NMR resonance: 500 MHz, $^{13}$C-NMR resonance: 125 MHz), equipped with an autosampler BACS-60 and analyzed using MESTRENOVA software.

Chemical shifts are given in ppm on the $\delta$ scale, and were determined after calibration to the residual signals of the solvents, which were used as an internal standard. NMR standards were used as follows: $^1$H NMR spectroscopy: $\delta$ = 7.26 ppm (residual $CHCl_3$ in $CDCl_3$), $\delta$ = 5.32 ppm (residual $CHDCl_2$ in

$CD_2Cl_2$), $\delta$ = 1.94 ppm (residual $CHD_2CN$ in $CD_3CN$). Data are reported as: br = broad, s = singlet, d = doublet, t = triplet, q = quartet, m = multiplet; coupling constant(s) *J* is given in Hert (Hz) and was calculated by the program. Multiplicities of the signals are assigned as observed in the spectra, not according to theoretical expectations. $^{13}C\{^1H\}$ NMR spectroscopy: $\delta$ = 77.0 ppm ($CDCl_3$), $\delta$ = 53.8 ppm ($CD_2Cl_2$), $\delta$ = 1.3 ppm and 118.3 ppm ($CD_3CN$).

**Infrared Spectroscopy (IR)**

IR spectra were recorded on a Bruker Alpha FT-IR spectrophotometer. The absorption bands were indicated a wave numbers *v* ($cm^{-1}$). All substances were measured as films or solids.

**Mass Spectrometry**

High-resolution mass spectra were recorded on a Bruker En Apex Ultra 7.0 TFT-MS instrument using ESI technique. Ionic masses are given in units of m/z for the isotopes with the highest natural abundance.

**High Performance Liquid Chromatography (HPLC)**

Chiral HPLC chromatography was performed with an Agilent 1200 HPLC system equipped with a quaternary pump, autosampler, column oven and variable wavelength detector and analyzed using CHEMSTATION B03.01 software. All the compounds in the thesis were detected by UV at λ = 254 nm or 220 nm. The corresponding mobile phase, the type of the columns and the flow rate were specified in the individual procedures.

**Circular Dichroism Spectroscopy (CD)**

CD spectra were recorded on a JASCO J-810 CD spectropolarimeter in a 1 mm path length quartz cuvette. The parameters we used as follows: from 600 nm to 200 nm; data pitch (0.5 nm); bandwdith (1 nm); response (1 second); sensitivity (standard); scanning speed (50 nm/min); accumulation (3 times). The concentration of the compounds for the measurements was 0.1 mM.

**Crystal Structure Analysis**

X-ray data were collected with a Bruker 3 circuit D8 Quest diffractometer with MoKa radiation (microfocus tube with multilayer optics) and Photon 100 CMOS detector at 115 K. Scaling and absorption correction was performed by using the SADABS[1] software package of Bruker. Structures were solved using direct methods in SHELXS or SHELXT[2], refined using the full matrix least squares procedure in SHELXL-2015[3], and drawn using DIAMOND[4]. The Flack parameter is a factor used to estimate the absolute configuration of the compounds.[5] The hydrogen atoms were placed in calculated

positions and refined as riding on their respective C atom, and Uiso(H) was set at 1.2 Ueq($Csp^2$) and 1.5 Ueq($Csp^3$). Disorder of $PF_6$ ions, solvent molecules or phenyl and *t*-butyl groups was refined using restraints for both the geometry and the anisotropic displacement factors.

**Other Analysis**

Optical rotations were measured with a Perkin-Elmer 241 polarimeter or Krüss P8000-T polarimeter at 20 °C or 25 °C in DCM. UV/Vis measurements were taken on a Spectra Max M5 microplate reader in a 10.0 mm quartz cuvette. Cut off and band-pass photochemical experiments have been performed using a 150W Xenon short arc lamp (USHIO INC. JAPAN) to irradiate the reaction mixture.

## 5.2 Synthesis of Catalysts

### 5.2.1 Synthesis of ligands

**5-*tert*-Butyl-2-phenylbenzo[*d*]oxazole (1)**

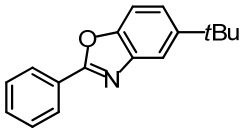


The compound was synthesized following a published procedure with slight modifications[6]. A solution of 2-amino-4-*tert*-butylphenol (0.825 g, 5.0 mmol) and benzaldehyde (0.530g, 0.5 mL, 5.0 mmol) in *m*-xylene (16 mL) was stirred at 120 °C for 30 minutes. 4-Methoxy-TEMPO (46.5 mg, 5 mol%) was added to the mixture and the reaction mixture was stirred at this temperature for a further 8 h under an oxygen atmosphere. The reaction mixture was cooled to room temperature and concentrated under reduced pressure. The residue was purified by flash chromatography on silica gel (EtOAc/*n*-hexane = 1: 20) to obtain the product **1** (1.152 g, 4.6 mmol, 92% yield) as a white solid.
$^1$H NMR (300 MHz, $CDCl_3$) $\delta$ 8.29 – 8.22 (m, 2H), 7.81 (d, $J$ = 1.8 Hz, 1H), 7.56 – 7.48 (m, 4H), 7.42 (dd, $J$ = 8.6, 1.9 Hz, 1H), 1.40 (s, 9H). All spectroscopic data were in agreement with the literature.[7]

**5-(*tert*-Butyl)-2-phenylbenzo[*d*]thiazole (2)**

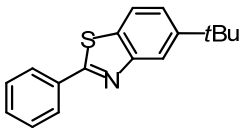


5-(*tert*-Butyl)-2-phenylbenzo[*d*]thiazole **2** could be synthesized according to the literature with slight modifications,[8] a mixture of 1-bromo-4-(*tert*-butyl)-2-nitrobenzene[9] (2.29 g, 8.9 mmol), sulfur (430 mg, 13.4 mmol), and phenylmethanamine (2.38 g, 22.3 mmol) in pyridine (1.8 mL) was stirred under an atmosphere of nitrogen in a Schlenk tube at 100 °C for 16 h. After being cooled to room temperature, the volatiles were removed in *vacuo*. The crude reaction mixture was triturated with $CH_2Cl_2$ (3 mL × 5). The combined $CH_2Cl_2$ layers were concentrated and purified by silica gel column

chromatography (EtOAc/*n*-hexane = 1: 100) to afford the desired product **2** (1.92 g, 7.2 mmol, 81% yield) as a pale yellow solid. $^{1}$H NMR (300 MHz, $CDCl_3$) $\delta$ 8.02 (dd, $J$ = 1.9, 0.4 Hz, 1H), 7.95 – 7.99 (m, 2H), 7.67 (dd, $J$ = 8.5, 0.4 Hz, 1H), 7.32 – 7.38 (m, 4H), 1.30 (s, 9H). $^{13}$C NMR (75 MHz, $CDCl_3$) $\delta$ 168.3, 154.7, 150.2, 133.9, 132.1, 131.0, 129.1, 127.6, 123.6, 121.1, 119.9, 35.1, 31.7. IR (film): $\nu$ ($cm^{-1}$) 2960, 2903, 2863, 1542, 1508, 1474, 1453, 1442, 1412, 1361 1316, 1282, 1260, 1243, 1210, 1098, 1064, 1023, 963, 921, 880, 812, 770, 762, 736, 704, 687, 660, 606, 480, 411. HRMS (ESI, *m*/*z*) calcd for $C_{17}H_{18}N_1S_1$ $[M+H]^+$: 268.1154, found: 268.1152.

**5-(*tert*-Butyl)-2-(4-fluorophenyl)benzo[*d*]oxazole (3)**

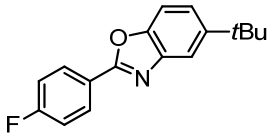


Starting from 4-fluorobenzaldehyde (0.737 g, 5.94 mmol), 2-amino-4-*tert*-butylphenol (1.000 g, 6.06 mmol) and 4-methoxy-TEMPO (56 mg, 5 mol%) according to the *general procedure* for **1** to give **3** as a white solid (EtOAc/*n*-hexane = 1: 10; 1.520 g, 5.65 mmol, 95% yield). $^{1}$H NMR (300 MHz, $CDCl_3$) $\delta$ 8.26 – 8.12 (m, 2H), 7.78 (dd, $J$ = 1.8, 0.7 Hz, 1H), 7.42 (dd, $J$ = 8.6, 0.7 Hz, 1H), 7.37 (dd, $J$ = 8.6, 1.8 Hz, 1H), 7.19 – 7.06 (m, 2H), 1.39 (s, 9H). $^{13}$C NMR (75 MHz, $CDCl_3$) $\delta$ 166.3, 163.0, 162.2, 148.8, 148.1, 142.0, 129.7, 129.5, 123.7, 123.6, 122.8, 116.5, 116.2, 115.9, 109.6, 34.9, 31.7. $^{19}$F NMR (282 MHz, $CDCl_3$) $\delta$ – 107.6 (s, 1F). IR (film): $\nu$ ($cm^{-1}$) 2955, 2904, 2872, 1597, 1559, 1492, 1475, 1460, 1426, 1411, 1389, 1362, 1330, 1286, 1266, 1219, 1199, 1152, 1127, 1095, 1078, 1053, 1008, 926, 872, 840, 822, 803, 734, 710, 693, 650, 638, 630, 588, 540, 512, 459, 427, 413. HRMS (ESI, *m*/*z*) calcd for $C_{17}H_{17}F_1N_1O_1$ $[M+H]^+$: 270.1289, found: 270.1291.

**5-(*tert*-Butyl)-2-(4-(trifluoromethyl)phenyl)benzo[*d*]oxazole (4)**

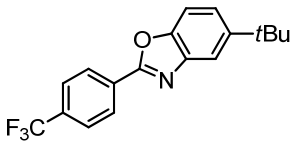


Starting from 4-(trifluoromethyl)benzaldehyde (1.033 g, 5.94 mmol), 2-amino-4-*tert*-butylphenol (1.000 g, 6.06 mmol) and 4-methoxy-TEMPO (56 mg, 5 mol%) according to the *general procedure* for **1** to give **4** as a white solid (EtOAc/*n*-hexane = 1: 20; 1.850 g, 5.80 mmol, 98% yield). $^{1}$H NMR (300 MHz, $CDCl_3$) $\delta$ 8.41 – 8.31 (m, 2H), 7.83 (d, $J$ = 1.7 Hz, 1H), 7.81 – 7.73 (m, 2H), 7.52 (d, J = 8.6 Hz, 1H), 7.46 (dd, $J$ = 8.7, 1.8 Hz, 1H), 1.41 (s, 9H). $^{13}$C NMR (75 MHz, $CDCl_3$) $\delta$ 161.6, 148.9, 148.6, 141.8, 133.0, 132.6, 130.6, 127.7, 126.0, 125.91, 125.86, 125.8, 125.6, 123.6, 122.0, 116.8, 109.9, 35.0, 31.7. $^{19}$F NMR (282 MHz, $CDCl_3$) $\delta$ – 63.9 (s, 1F). IR (film): $\nu$ ($cm^{-1}$) 2972, 2956, 2869, 1622, 1557, 1478, 1465, 1413, 1367, 1319, 1266, 1202, 1185, 1162, 1118, 1079, 1067, 1053, 1013,

926, 882, 846, 812, 749, 703, 650, 591, 553, 503, 461, 431, 407. HRMS (ESI, *m*/*z*) calcd for $C_{18}H_{17}F_3N_1O_1$ $[M+H]^+$: 320.1257, found: 320.1261.

**5-(*tert*-Butyl)-2-(4-nitrophenyl)benzo[*d*]oxazole (5)**

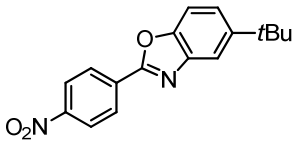


Starting from 4-nitrobenzaldehyde (0.896 g, 5.94 mmol), 2-amino-4-*tert*-butylphenol (1.000 g, 6.06 mmol) and 4-methoxy-TEMPO (56 mg, 5 mol%) according to the *general procedure* for **1** to give **5** as a pale yellow solid (put it in the fridge (4 $^oC$) over night to give pale yellow crystal which was washed by *n*-hexane; 1.278 g, 4.32 mmol, 73% yield). $^1H$ NMR (300 MHz, $CDCl_3$) $\delta$ 8.45 – 8.37 (m, 4H), 8.37 – 8.32 (m, 2H), 7.83 (dd, $J$ = 1.8, 0.8 Hz, 1H), 7.53 (dd, $J$ = 8.7, 0.8 Hz, 2H), 7.49 (dd, $J$ = 8.7, 1.7 Hz, 1H), 1.40 (s, 9H). $^{13}C$ NMR (75 MHz, $CDCl_3$) $\delta$ 160.7, 149.2, 149.0, 148.9, 141.8, 132.9, 128.2, 124.2, 124.1, 117.0, 110.0, 77.4, 77.0, 76.6, 35.0, 31.7. IR (film): $\nu$ ($cm^{-1}$) 2964, 2907, 2869, 1617, 1604, 1552, 1521, 1477, 1422, 1409, 1396, 1366, 1342, 1321, 1303, 1291, 1270, 1221, 1196, 1135, 1107, 1081, 1054, 1007, 937, 928, 877, 853, 814, 759, 718, 703, 648, 532, 484, 469, 457, 420. HRMS (ESI, *m*/*z*) calcd for $C_{17}H_{17}N_2O_3$ $[M+H]^+$: 297.1234, found: 297.1237.

**5-(*tert*-Butyl)-2-(4-methoxyphenyl)benzo[*d*]oxazole (6)**

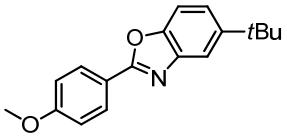


Starting from 4-fluorobenzaldehyde (0.809 g, 5.94 mmol), 2-amino-4-*tert*-butylphenol (1.000 g, 6.06 mmol) and 4-methoxy-TEMPO (56 mg, 5 mol%) according to the *general procedure* for **1** to give **6** as a white solid (EtOAc/*n*-hexane = 1: 15; 1.650 g, 5.87 mmol, 99% yield). $^1H$ NMR (300 MHz, $CDCl_3$) $\delta$ 8.22 – 8.14 (m, 1H), 7.77 (dd, $J$ = 1.9, 0.6 Hz, 1H), 7.46 (d, $J$ = 8.6 Hz, 1H), 7.38 (dd, $J$ = 8.6, 1.9 Hz, 1H), 7.06 – 6.99 (m, 2H), 3.88 (s, 3H), 1.39 (s, 9H). $^{13}C$ NMR (75 MHz, $CDCl_3$) $\delta$ 163.3, 162.2, 148.7, 147.9, 142.1, 129.3, 122.3, 119.9, 116.2, 114.3, 109.5, 55.4, 34.9, 31.8. IR (film): $\nu$ ($cm^{-1}$) 3071, 2973, 2952, 2905, 1606, 1582, 1559, 1498, 1474, 1463, 1440, 1417, 1390, 1361, 1338, 1318, 1302, 1253, 1224, 1202, 1184, 1169, 1118, 1108, 1056, 1025, 1006, 933, 922, 868, 835, 811, 787, 737, 699, 652, 643, 629, 588, 553, 516. HRMS (ESI, *m*/*z*) calcd for $C_{18}H_{20}N_1O_2$ $[M+H]^+$: 282.1489, found: 282.1489.

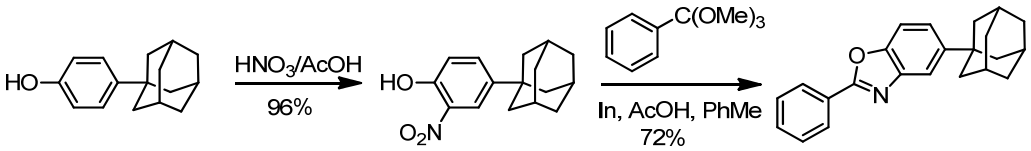


**4-((3*r*,5*r*,7*r*)-Adamantan-1-yl)-2-nitrophenol 144**

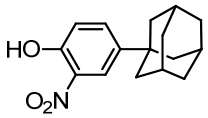


Compound **144** was synthesized following a published procedure.[10] To a solution of 175 μL 94% $HNO_3$ in 1.5 mL of glacial acetic acid was added to a suspension of 1.00 g (4.38 mmol) of 4-(1-adamantyl)phenol in 15 mL of glacial acetic acid dropwise under vigorous stirring at room temperature. The reaction mixture was stirred for 30 min and poured into crushed ice, and the precipitate was separated by filtration and washed with water until the washings were neutral. The precipitale was dried under reduced pressure to give the crude product **144** (1.15 g, 4.21 mmol, 96% yield) which was used without further purification. $^1$H NMR (300 MHz, $CDCl_3$) $\delta$ 10.47 (s, 1H), 8.02 (d, $J$ = 2.4 Hz, 1H), 7.63 (dd, $J$ = 8.8, 2.4 Hz, 1H), 7.10 (d, $J$ = 8.8 Hz, 1H), 2.12 (p, $J$ = 3.0 Hz, 3H), 2.00 – 1.84 (m, 6H), 1.84 – 1.70 (m, 6H). All spectroscopic data were in agreement with the literature.[10]

**5-((3*r*,5*r*,7*r*)-Adamantan-1-yl)-2-phenylbenzo[*d*]oxazole (7)**

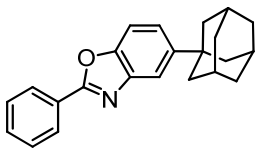


5-((3*r*,5*r*,7*r*)-Adamantan-1-yl)-2-phenylbenzo[*d*]oxazole **7** was synthesized according to a published procedure with some modifications.[11] 4-((3*r*,5*r*,7*r*)-Adamantan-1-yl)-2-nitrophenol **144** (500 mg, 1.83 mmol) was added to a mixture of indium powder (420 mg, 3.66 mmol) and acetic acid (1.0 mL, 18.3 mmol) in toluene (6 mL), and then trimethyl orthoester (689 mg, 3.66 mmol) was added. The reaction mixture was stirred at 100 $^o$C under a nitrogen atmosphere. After the reaction was complete, the reaction mixture was diluted with $CH_2Cl_2$ (20 mL), filtered through Celite, poured into sat. aq. $NH_4Cl$ solution (20 mL), and then extracted with $CH_2Cl_2$ (20 mL×3). The combined organic extracts were dried over $Na_2SO_4$, filtered, and concentrated. The residue was eluted with ethyl acetate/hexane (EtOAc/*n*-hexane = 1: 15) through a silica gel column to give the corresponding the desired product **7** (431 mg, 1.31 mmol, 72% yield) as a white solid. $^1$H NMR (300 MHz, $CDCl_3$) $\delta$ 8.33 – 8.19 (m, 2H), 7.78 (d, $J$ = 1.8 Hz, 1H), 7.52 (dd, $J$ = 7.5, 3.8 Hz, 4H), 7.41 (dd, $J$ = 8.6, 1.9 Hz, 1H), 2.14 (s, 3H), 2.03 – 1.89 (m, 6H), 1.88 – 1.72 (m, 6H). $^{13}$C NMR (75 MHz, $CDCl_3$) $\delta$ 163.1, 148.8, 148.5, 142.1, 131.3, 128.9, 127.5, 127.4, 122.4, 116.2, 109.7, 43.7, 36.8, 36.4, 29.0. IR (film): $\nu$ ($cm^{-1}$) 2908, 2846, 1550, 1474, 1448, 1425, 1332, 1321, 1283, 1263, 1246, 1203, 1186, 1127, 1102, 1052, 1023, 977, 933,

925, 870, 851, 813, 798, 778, 706, 687, 649, 637, 489, 455, 435, 422. HRMS (ESI, *m*/*z*) calcd for $C_{23}H_{24}N_1O_1$ $[M+H]^+$: 330.1852, found: 330.1855.

**5-(*tert*-Butyl)-2-(naphthalen-1-yl)benzo[*d*]oxazole (8)**

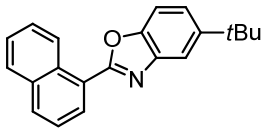


Starting from 1-naphthaldehyde (0.928 g, 5.94 mmol), 2-amino-4-*tert*-butylphenol (1.000 g, 6.06 mmol) and 4-methoxy-TEMPO (56 mg, 5 mol%) according to the *general procedure* for **1** to give **8** as a brown oil (EtOAc/*n*-hexane = 1: 10; 1.780 g, 5.91 mmol, 99% yield). $^1$H NMR (300 MHz, $CDCl_3$) $\delta$ 9.49 (d, $J$ = 8.6 Hz, 1H), 8.43 (dd, $J$ = 7.4, 1.3 Hz, 1H), 8.03 (d, $J$ = 8.2 Hz, 1H), 7.98 – 7.84 (m, 2H), 7.78 – 7.66 (m, 1H), 7.66 – 7.53 (m, 3H), 7.48 (dd, $J$ = 8.6, 1.9 Hz, 1H), 1.44 (s, 9H). $^{13}$C NMR (75 MHz, $CDCl_3$) $\delta$ 162.7, 148.0, 147.7, 142.2, 133.8, 131.9, 130.5, 128.9, 128.4, 127.6, 126.3, 126.1, 124.7, 123.5, 122.8, 116.6, 109.4, 34.8, 31.7. IR (film): $\nu$ ($cm^{-1}$) 3050, 2958, 2902, 2864, 1541, 1509, 1479, 1459, 1424, 1396, 1362, 1327, 1284, 1269, 1257, 1218, 1202, 1180, 1134, 1110, 1072, 973, 918, 875, 852, 803, 771, 741, 719, 662, 651, 578, 538, 432. HRMS (ESI, *m*/*z*) calcd for $C_{21}H_{20}N_1O_1$ $[M+H]^+$: 302.1539, found: 302.1543.

**5-(*tert*-Butyl)-2-(pyren-1-yl)benzo[*d*]oxazole (9)**

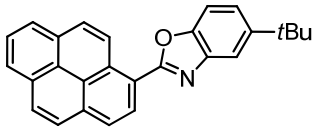


Starting from pyrene-1-carbaldehyde (1.380 g, 6.00 mmol), 2-amino-4-*tert*-butylphenol (1.000 g, 6.06 mmol) and 4-methoxy-TEMPO (56 mg, 5 mol%) according to the *general procedure* for **1** to give **9** as a yellow solid (EtOAc/*n*-hexane = 1: 10; 2.050 g, 5.47 mmol, 91% yield). $^1$H NMR (300 MHz, $CDCl_3$) $\delta$ 9.76 (d, $J$ = 9.4 Hz, 1H), 8.88 (d, $J$ = 8.1 Hz, 1H), 8.36 – 8.22 (m, 4H), 8.17 (d, $J$ = 9.0 Hz, 1H), 8.08 (dd, $J$ = 15.1, 7.6 Hz, 2H), 7.99 (d, $J$ = 1.7 Hz, 1H), 7.62 (d, $J$ = 8.6 Hz, 1H), 7.50 (dd, $J$ = 8.6, 1.9 Hz, 1H), 1.47 (s, 9H). $^{13}$C NMR (75 MHz, $CDCl_3$) $\delta$ 1163.5, 148.3, 148.0, 142.5, 133.2, 131.0, 130.5, 129.7, 129.2, 129.0, 127.3, 127.0, 126.1, 126.0, 125.8, 125.3, 124.8, 124.4, 124.2, 122.8, 120.2, 116.7, 109.6, 35.0, 31.8. IR (film): $\nu$ ($cm^{-1}$) 3040, 2949, 2899, 2863, 1596, 1584, 1548, 1533, 1504, 1478, 1433, 1423, 1386, 1330, 1259, 1214, 1189, 1135, 1118, 1073, 1016, 969, 937, 922, 879, 879, 870, 855, 843, 817, 798, 764, 753, 730, 706, 680, 648, 596, 504, 456, 410, 400. HRMS (ESI, *m*/*z*) calcd for $C_{27}H_{22}N_1O_1$ $[M+H]^+$: 376.1696, found: 376.1698.

**5-(*tert*-Butyl)-1-butyl-2-(pyren-1-yl)-1*H*-benzo[*d*]imidazole (10)**

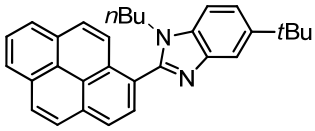


Pyrene-1-carbaldehyde (920 mg, 4.00 mmol) and 4-(*tert*-butyl)benzene-1,2-diamine (656 mg, 4.00 mmol) were heated at 120°C in nitrobenzene (14 mL) for 18 h. After cooling to room temperature, the mixture was concentrated in vacuo. The residue was purified by flash chromatography on silica gel (n-hexane to EtOAc/n-hexane = 1: 3) to afford the 5-(*tert*-butyl)-2-(pyren-1-yl)-1*H*-benzo[*d*]imidazole (1.20 g, 3.21 mmol, 80% yield) as a yellow solid. To a mixture of 5-(*tert*-butyl)-2-(pyren-1-yl)-1*H*-benzo[*d*]imidazole (374 mg, 1.00 mmol), 1-bromobutane (158 mg, 1.15 mmol) and tetrabutylammonium iodide (152 mg, 0.41 mmol) was added sodium hydroxide solution (in 12.5 mL of pentan-3-one). The mixture was stirred at 100 °C for 12 h. The solution was then removed in vacuo. The crude product was dissolved in DCM (15 mL), and washed with water. The organic phase was concentrated and purified by flash chromatography on silica gel (EtOAc/n-hexane = 1: 4) to afford the target product **10** (184 mg, 0.43 mmol, 43% yield) as a yellow oil. $^{1}$H NMR (300 MHz, $CDCl_3$) $\delta$ 8.35 – 8.13 (m, 6H), 8.12 – 8.01 (m, 3H), 7.93 (d, J = 9.2 Hz, 1H), 7.53 (dd, J = 8.6, 1.7 Hz, 1H), 7.48 (d, J = 8.5 Hz, 1H), 4.07 (t, J = 7.3 Hz, 2H), 1.68 – 1.55 (m, 2H), 1.48 (s, 9H), 1.11 – 0.95 (m, 2H), 0.60 (t, J = 7.3 Hz, 3H). $^{13}$C NMR (75 MHz, $CDCl_3$) $\delta$153.0, 145.8, 143.4, 133.0, 132.2, 131.2, 130.8, 130.4, 128.7, 128.5, 127.9, 127.2, 126.3, 125.8, 125.6, 125.1, 124.7, 124.6, 124.43, 124.37, 120.8, 116.3, 109.5, 44.4, 34.9, 31.9, 31.7, 19.7, 13.3. IR (film): $\nu$ ($cm^{-1}$) 3041, 2956, 2865, 1618, 1604, 1583, 1477, 1455, 1431, 1393, 1363, 1330, 1282, 1260, 1243, 1198, 1179, 1081, 1032, 925, 925, 906, 845, 817, 760, 726, 717, 682, 655, 638, 613, 505, 458, 399. HRMS (ESI, *m*/*z*) calcd for $C_{31}H_{31}N_2$ $[M+H]^+$: 431.2482, found: 431.2484.

## 5.2.2 Synthesis of chloro-bridged Ir or Rh dimers

***N,N-trans*-Iridium Complex *rac*-11**

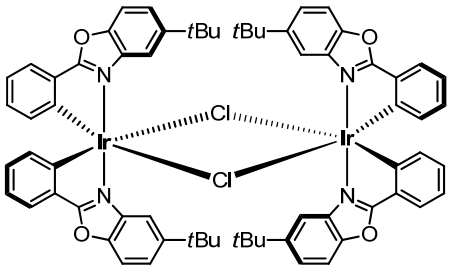


The *N,N-trans*-iridium complex *rac*-**11** was synthesized according to a route developed by Nonoyama for iridium(III) $\mu$-chloro-bridged dimers with related cyclometalated ligands, which involves refluxing $IrCl_3 \bullet nH_2O$ with 2–2.5 equivalents of cyclometalating ligand in a 3:1 mixture of 2-methoxyethanol and water.[12] Accordingly, 5-*tert*-butyl-2-phenylbenzo[*d*]oxazole **1** (979 mg, 3.90 mmol) was added to iridium chloride hydrate (671 mg, 1.90 mmol) in a mixture of 2-ethoxyethanol/water (3:1, 80 mL).

The reaction mixture was heated at 130 °C for 24 h under nitrogen. The resulting precipitate was collected by centrifugation, washed with diethyl ether and dried to yield the product *rac*-**11** (1.16 g, 0.80 mmol, 84% yield) as a yellow solid. $^1$H NMR (300 MHz, $CD_2Cl_2$) $\delta$ 8.40 – 8.27 (m, 4H), 7.58 (dd, $J$ = 7.6, 1.3 Hz, 4H), 7.36 – 7.16 (m, 8H), 6.88 (dd, $J$ = 11.0, 3.9 Hz, 4H), 6.64 (td, $J$ = 7.5, 1.3 Hz, 4H), 6.09 (d, $J$ = 7.8 Hz, 4H), 1.25 (s, 36H). All spectroscopic data were in agreement with the literature.[12]

***N,N-trans*-Rhodium Complex *rac*-12**

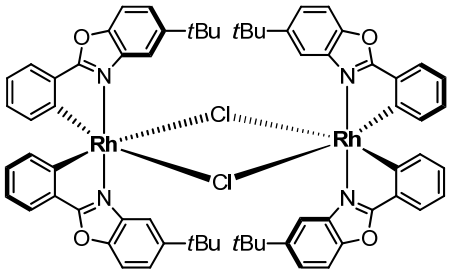


The *N,N-trans*-rhodium complex *rac*-**12** was synthesized according to a route reported by Mesmaeker for rhodium(III) $\mu$-chloro-bridged dimers with related cyclometalated ligands. Accordingly, 5-*tert*-butyl-2-phenyl-benzo[*d*]oxazole **1** (1.014 g, 4.04 mmol) was added to $RhCl_3$•$3H_2O$ (524 mg, 2.00 mmol) in a mixture of 2-ethoxyethanol and water (3:1, 88 mL). The reaction mixture was heated at 120°C for 21 h under an atmosphere of nitrogen. The resulting precipitate was collected by centrifugation, washed with methanol and dried to obtain the product *rac*-**12** (940 mg, 0.74 mmol, 74% yield) as a pale yellow solid. $^1$H NMR (300 MHz, $CD_2Cl_2$) $\delta$ 8.38 (t, $J$ = 1.3 Hz, 4H), 7.65 (dd, $J$ = 7.6, 1.2 Hz, 4H), 7.22 (d, $J$ = 1.2 Hz, 8H), 6.97 (td, $J$ = 7.4, 1.1 Hz, 4H), 6.76 (td, $J$ = 7.6, 1.6 Hz, 4H), 6.12 (d, $J$ = 7.8 Hz, 4H), 1.22 (s, 36H). All spectroscopic data were in agreement with the literature.[15]

***N,N-trans*-Iridium Complex *rac*-13**

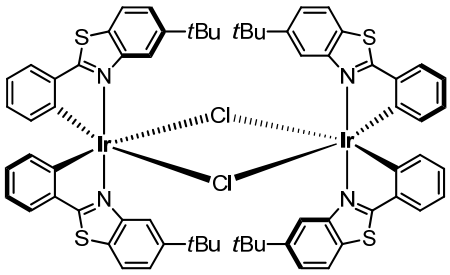


The *N,N-trans*-iridium complex *rac*-**13** was synthesized by the same method for synthesizing *rac*-**11**. 5-(*tert*-butyl)-2-phenylbenzo[*d*]thiazole **2** (1040 mg, 3.90 mmol) was added to iridium chloride hydrate (686 mg, 1.95 mmol) in a mixture of 2-ethoxyethanol/water (3:1, 88 mL). The reaction mixture was heated at 130 °C for 18 h under nitrogen. The resulting precipitate was collected by centrifugation, washed with *n*-hexane and dried to yield the product *rac*-**13** (1.07 g, 0.70 mmol, 72% yield) as a yellow solid. $^1$H NMR (300 MHz, $CDCl_3$) $\delta$ 8.86 (d, $J$ = 1.5 Hz, 4H), 7.44 (dd, $J$ = 7.6, 0.9

Hz, 4H), 7.38 (d, $J$ = 8.5 Hz, 4H), 7.26 (dd, $J$ = 8.5, 1.8 Hz, 4H), 6.73 (t, $J$ = 7.4 Hz, 4H), 6.44 – 6.28 (m, 4H), 6.01 (d, $J$ = 7.7 Hz, 4H), 1.24 (s, 36H). $^{13}$C NMR (75 MHz, $CDCl_3$) $\delta$ 179.0, 151.5, 149.9, 146.3, 141.9, 134.0, 128.9, 127.5, 125.1, 122.1, 121.4, 121.2, 120.3, 35.5, 31.8. IR (film): $\nu$ ($cm^{-1}$) 2961, 1580, 1460, 1438, 1411, 1292, 1280, 1262, 1247, 1104, 1079, 1025, 993, 808, 797, 781, 753, 731, 720, 697, 689, 668, 459, 381.

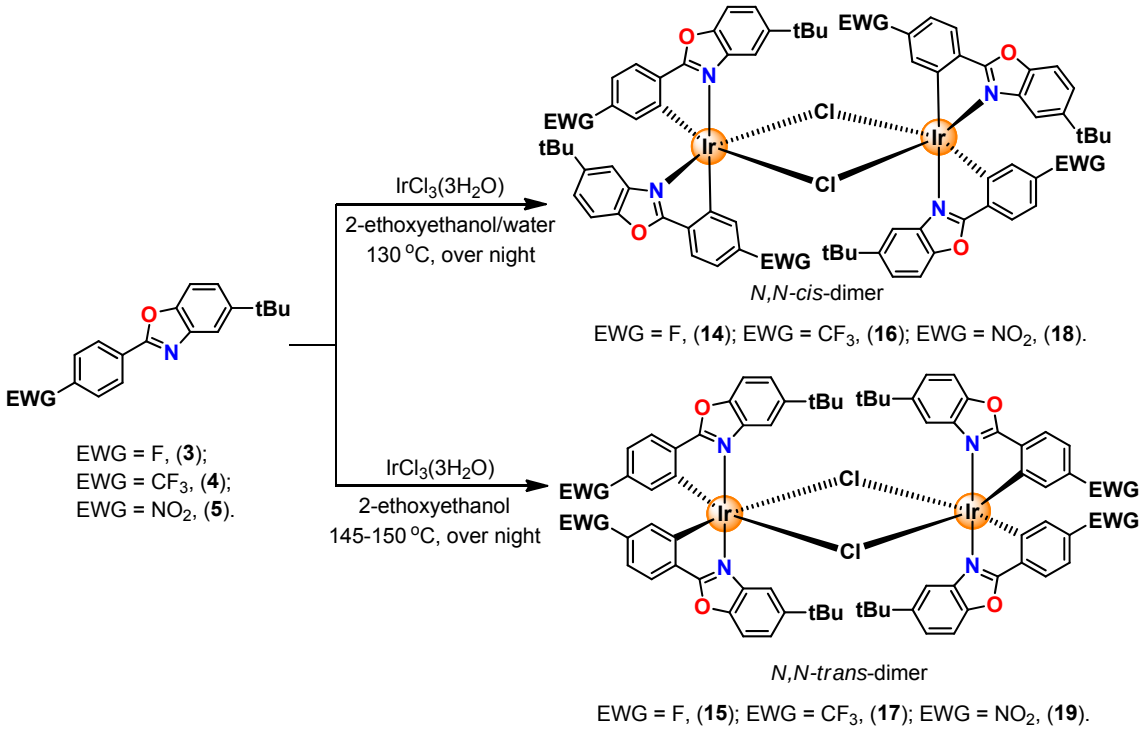


### *N,N-cis*-Iridium Complex *rac*-14

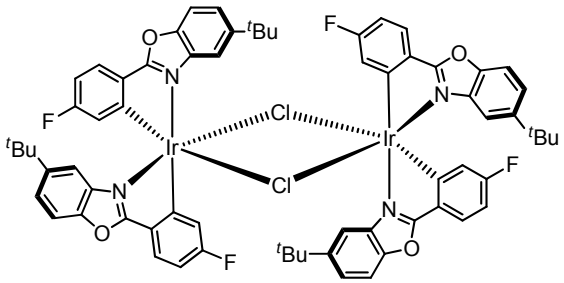


The *N,N-cis*-iridium complex *rac*-**14** was synthesized by the same method for synthesizing *rac*-**11**. 5-(*tert*-Butyl)-2-(4-fluorophenyl)benzo[*d*]oxazole **3** (928 mg, 3.45 mmol) was added to iridium chloride hydrate (608 mg, 1.73 mmol) in a mixture of 2-ethoxyethanol/water (3:1, 76 mL). The reaction mixture was heated at 130 °C for 18 h under nitrogen. The resulting precipitate was collected by centrifugation, washed with MeOH and dried to yield *cis*-iridium product *rac*-**14** (1.04 g, 0.68 mmol, 79% yield, contained 33% *trans rac*-**14**) as a yellow solid. $^1$H NMR (300 MHz, $CDCl_3$) $\delta$ 8.15 – 8.10 (m, 2H), 7.80 (dd, $J$ = 8.5, 5.7 Hz, 2H), 7.61 – 7.52 (m, 2H), 7.39 (dd, $J$ = 11.2, 2.4 Hz, 2H), 7.30 – 7.27 (m, 4H), 7.25 (d, $J$ = 3.4 Hz, 2H), 7.08 (dd, $J$ = 8.7, 1.9 Hz, 2H), 6.99 (td, $J$ = 8.7, 2.5 Hz, 2H), 6.50 (td, $J$ = 8.6, 2.5 Hz, 2H), 6.01 (dd, $J$ = 10.3, 2.5 Hz, 2H), 5.82 (d, $J$ = 1.5 Hz, 2H), 1.24 (s, 18H), 0.60 (s, 18H). IR (film): $\nu$ ($cm^{-1}$) 2960, 2908, 2868, 1596, 1562, 1520, 1480, 1450, 1428, 1391,

1367, 1325, 1297, 1272, 1244, 1197, 1128, 1116, 1082, 1055, 1029, 931, 886, 865, 833, 804, 754, 745, 701, 647, 592, 572, 452.

***N,N-trans*-Iridium Complex *rac*-15**

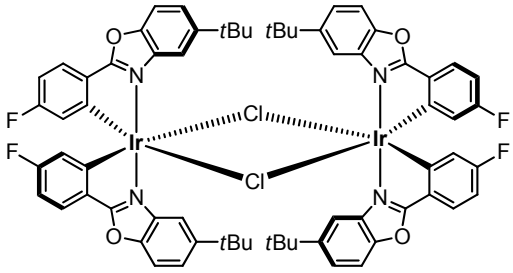


The *N,N-trans*-iridium *rac*-**15** was synthesized by the silimar method for synthesizing *rac*-**11** with some modifications. 5-(*tert*-Butyl)-2-(4-fluorophenyl)benzo[*d*]oxazole **3** (307 mg, 1.14 mmol) was added to iridium chloride hydrate (168 mg, 0.48 mmol) in 2-ethoxyethanol (16 mL). The reaction mixture was heated at 145 °C for 18 h under nitrogen. After cooling to room temperature, the mixture was added 1 *N* HCl. The colored precipitate was filtered off, washed with 1 *N* HCl and MeOH, and then dried to yield the product *rac*-**15** (308 mg, 0.20 mmol, 84% yield) as a yellow solid. $^{1}$H NMR (300 MHz, $CDCl_3$) $\delta$ 8.23 (d, $J$ = 1.8 Hz, 4H), 7.55 (dd, $J$ = 8.4, 5.7 Hz, 4H), 7.23 (dd, $J$ = 8.9, 1.9 Hz, 4H), 7.16 (d, $J$ = 8.8 Hz, 4H), 6.58 (td, $J$ = 8.7, 2.4 Hz, 4H), 5.74 (dd, $J$ = 10.0, 2.4 Hz, 4H), 1.25 (s, 36H). $^{19}$F NMR (282 MHz, $CDCl_3$) $\delta$ – 106.4 (s, 4F). IR (film): $\nu$ ($cm^{-1}$) 2961, 2908, 2871, 1618, 1597,1561, 1519, 1481, 1457, 1428, 1385, 1364, 1296, 1273, 1243, 1196, 1127, 1114, 1080, 978, 932, 888, 859, 834, 812, 803, 754, 744, 702, 673, 646, 598, 582, 572, 452.

***N,N-cis*-Iridium Complex *rac*-16**

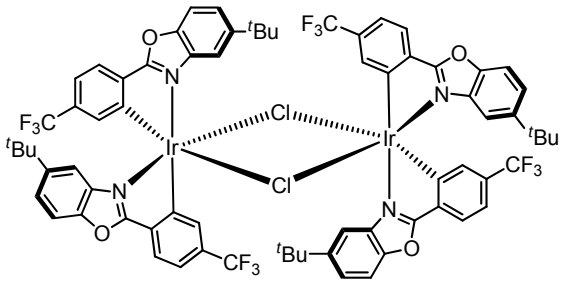


The *N,N-cis*-iridium complex *rac*-**16** was synthesized by the same method for synthesizing *rac*-**11**. 5-(*tert*-Butyl)-2-(4-(trifluoromethyl)phenyl)benzo[*d*]oxazole **4** (1140 mg, 3.57 mmol) was added to iridium chloride hydrate (615 mg, 1.74 mmol) in a mixture of 2-ethoxyethanol/water (3:1, 76 mL). The reaction mixture was heated at 130 °C over night under nitrogen. The resulting precipitate was collected by centrifugation, washed with MeOH and dried to yield the *cis*-iridium product *rac*-**16** (1.16 g, 0.67 mmol, 77% yield) as an orange solid. $^{1}$H NMR (300 MHz, $CDCl_3$) $\delta$ 8.23 (t, $J$ = 1.3 Hz, 2H), 8.07 (d, $J$ = 1.6 Hz, 2H), 7.88 (d, $J$ = 8.0 Hz, 2H), 7.67 (dd, $J$ = 8.0, 0.9 Hz, 2H), 7.42 (dd, $J$ = 8.0, 1.7

Hz, 2H), 7.37 – 7.30 (m, 6H), 7.16 (dd, $J$ = 8.8, 1.9 Hz, 2H), 7.01 (ddd, $J$ = 8.0, 1.8, 0.8 Hz, 2H), 6.37 – 6.31 (m, 2H), 5.93 (d, $J$ = 1.6 Hz, 2H), 1.26 (s, 18H), 0.61 (s, 18H). $^{19}$F NMR (282 MHz, $CDCl_3$) $\delta$ – 62.5 (s, 2F), – 63.4 (s, 2F). IR (film): $\nu$ ($cm^{-1}$) 2963, 2905, 2869, 1598, 1574, 1480, 1461, 1428, 1388, 1366, 1312, 1273, 1250, 1195, 1161, 1117, 1094, 1069, 1040, 932, 898, 885, 829, 812, 794, 764, 702, 671, 639, 453, 383.

***N,N-trans*-Iridium Complex *rac*-17**

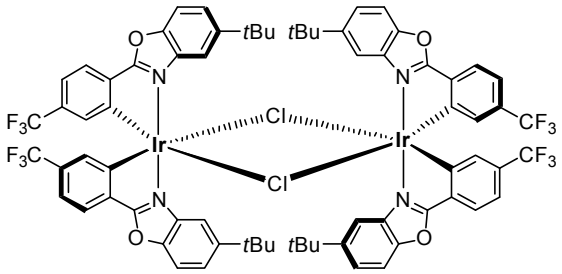


The *N,N-trans*-iridium complex *rac*-**17** was synthesized by the same method for synthesizing *rac*-**15**. 5-(*tert*-Butyl)-2-(4-(trifluoromethyl)phenyl)benzo[*d*]oxazole **4** (268 mg, 0.84 mmol) was added to iridium chloride hydrate (123 mg, 0.35 mmol) in 2-ethoxyethanol (12 mL). The reaction mixture was heated at 145 °C for 20 h under nitrogen. After cooling to room temperature, the mixture was added 1 *N* HCl. The colored precipitate was filtered off, washed with 1 *N* HCl and MeOH, and then dried to yield the product *rac*-**17** (270 mg, 0.16 mmol, 91% yield) as an orange solid. $^1$H NMR (300 MHz, $CDCl_3$) $\delta$ 8.12 (dd, $J$ = 2.0, 0.6 Hz, 4H), 7.64 (d, $J$ = 7.9 Hz, 4H), 7.31 (dd, $J$ = 8.9, 1.9 Hz, 4H), 7.22 (dd, $J$ = 8.8, 0.6 Hz, 4H), 7.10 (ddd, $J$ = 7.9, 1.6, 0.7 Hz, 4H), 6.43 – 6.34 (m, 4H), 1.28 (s, 36H). $^{19}$F NMR (282 MHz, $CDCl_3$) $\delta$ – 64.2 (s, 12F). IR (film): $\nu$ ($cm^{-1}$) 2965, 2909, 2870, 1599, 1574, 1479, 1459, 1388, 1366, 1310, 1271, 1252, 1157, 1118, 1093, 1081, 1068, 1040, 1015, 978, 932, 883, 847, 821, 806, 793, 762, 702, 674, 639, 454.

***N,N-cis*-Iridium Complex *rac*-18**

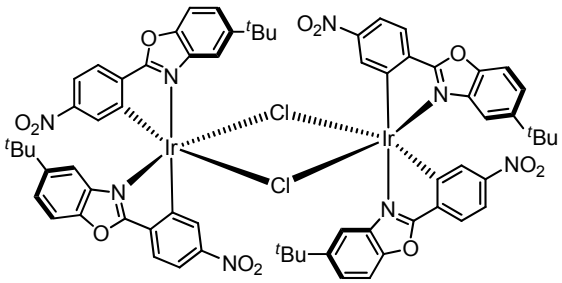


The *N,N-cis*-iridium complex *rac*-**18** was synthesized by the same method for synthesizing *rac*-**9**. 5-(*tert*-Butyl)-2-(4-nitrophenyl)benzo[*d*]oxazole **5** (1037 mg, 3.50 mmol) was added to iridium chloride hydrate (618 mg, 1.75 mmol) in a mixture of 2-ethoxyethanol/water (3:1, 76 mL). The reaction mixture was heated at 130 °C for 24 h under nitrogen. The resulting precipitate was collected

by centrifugation, washed with MeOH and dried to yield the product *rac*-**18** (1.05 g, 0.64 mmol, 73% yield) as a red solid. $^1$H NMR (300 MHz, $CD_2Cl_2$) $\delta$ 8.53 (d, $J$ = 1.5 Hz, 2H), 8.26 – 8.18 (m, 2H), 8.00 – 7.97 (m, 2H), 7.87 – 7.75 (m, 4H), 7.63 (dd, $J$ = 8.4, 2.1 Hz, 2H), 7.49 – 7.44 (m, 4H), 7.40 (d, $J$ = 8.7 Hz, 2H), 7.26 (dd, $J$ = 8.8, 1.7 Hz, 2H), 6.84 (d, $J$ = 2.0 Hz, 2H), 5.90 (d, $J$ = 1.4 Hz, 2H), 1.28 (s, 18H), 0.63 (s, 18H). IR (film): $\nu$ (cm$^{-1}$) 2960, 2905, 2870, 1599, 1538, 1504, 1479, 1448, 1428, 1393, 1365, 1334, 1298, 1272, 1244, 1190, 1163, 1119, 1107, 1069, 1036, 932, 886, 867, 828, 814, 739, 728, 706, 699, 668, 646, 452.

***N,N-trans*-Iridium Complex *rac*-19**

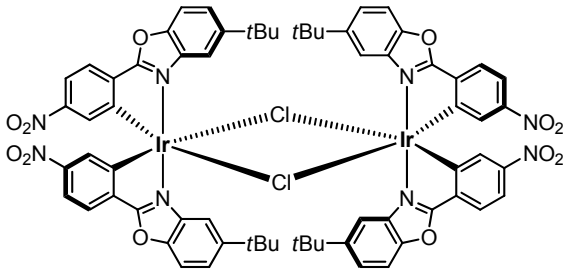


The *N,N-trans*-iridium complex *rac*-**19** was synthesized by the same method for synthesizing *rac*-**15**. 5-(*tert*-Butyl)-2-(4-nitrophenyl)benzo[*d*]oxazole **5** (200 mg, 0.68 mmol) was added to iridium chloride hydrate (108 mg, 0.31 mmol) in 2-ethoxyethanol (10 mL). The reaction mixture was heated at 150 °C for 20 h under nitrogen. After cooling to room temperature, the mixture was added 1 *N* HCl. The colored precipitate was filtered off, washed with 1 *N* HCl and MeOH, and then dried to yield the product *rac*-**19** (217 mg, 0.13 mmol, 84% yield) as a red solid. IR (film): $\nu$ (cm$^{-1}$) 2967, 2907, 2869, 1601, 1554, 1537, 1523, 1505, 1479, 1447, 1427, 1389, 1364, 1337, 1301, 1272, 1246, 1135, 1107, 1082, 1056, 1036, 932, 886, 869, 855, 833806, 740, 727, 706, 645, 452, 402.

***N,N-trans*-Iridium Complex *rac*-20**

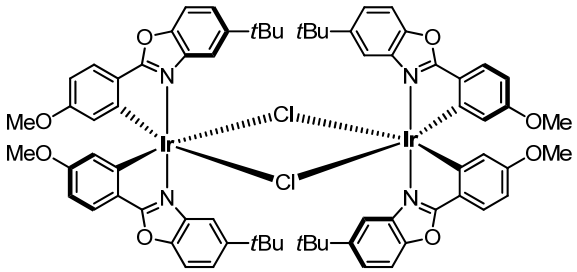


The *N,N-trans*-iridium complex *rac*-**20** was synthesized by the same method for synthesizing *rac*-**15**. 5-(*tert*-Butyl)-2-(4-methoxyphenyl)benzo[*d*]oxazole **6** (375 mg, 1.33 mmol) was added to iridium chloride hydrate (196 mg, 0.56 mmol) in 2-ethoxyethanol (18 mL). The reaction mixture was heated at 150 °C for 20 h under nitrogen. After cooling to room temperature, the mixture was added 1 *N* HCl. The colored precipitate was filtered off, washed with 1 *N* HCl and MeOH, and then dried to yield the product *rac*-**20** (380 g, 0.24 mmol, 86% yield) as a yellow solid. $^1$H NMR (300 MHz, $CDCl_3$) $\delta$ 8.41 (dd, $J$ = 1.6, 0.9 Hz, 4H), 7.59 (d, $J$ = 8.5 Hz, 4H), 7.40 (s, 4H), 7.26 (s, 5H), 6.54 (dd, $J$ = 8.5, 2.4 Hz,

4H), 5.82 (d, $J$ = 2.4 Hz, 4H), 3.28 (s, 12H), 1.37 (s, 36H). IR (film): $\nu$ ($cm^{-1}$) 2965, 2936, 2905, 2872, 2833, 1616, 1587, 1564, 1506, 1480, 1460, 1429, 1379, 1362, 1309, 1262, 1230, 1214, 1166, 1141, 1130, 1116, 1082, 1039, 1020, 975, 930, 890, 861, 851, 843, 804, 794, 754, 744, 704, 676, 646, 610, 585, 569, 449, 405.

***N,N-trans*-Iridium Complex *rac*-21**

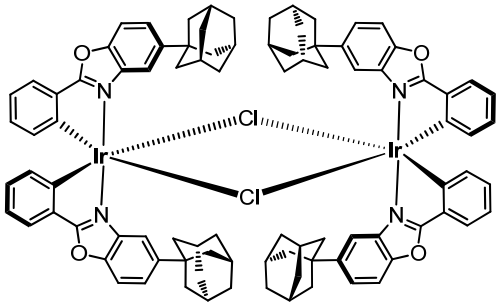

The *N,N-trans*-iridium complex *rac*-**21** was synthesized by the same method for synthesizing *rac*-**15**. Accordingly, 5-((3*r*,5*r*,7*r*)-adamantan-1-yl)-2-phenylbenzo[*d*]oxazole **7** (384.0 mg, 1.17 mmol) was added to iridium chloride hydrate (200 mg, 0.57 mmol) in 2-ethoxyethanol (18 mL). The reaction mixture was heated at 150 °C for 18 h under nitrogen. After cooling to room temperature, the mixture was added 1 *N* HCl. The colored precipitate was filtered off, washed with 1 *N* HCl and MeOH, and then dried to yield the product *rac*-**21** (440.0 mg, 0.25 mmol, 88% yield) as a yellow solid. $^1$H NMR (300 MHz, $CDCl_3$) $\delta$ 8.27 (s, 4H), 7.58 – 7.48 (m, 4H), 7.21 (d, $J$ = 1.2 Hz, 8H), 6.80 (td, $J$ = 7.4, 1.1 Hz, 4H), 6.58 (td, $J$ = 7.5, 1.5 Hz, 4H), 6.09 (d, $J$ = 7.8 Hz, 4H), 2.07 (s, 12H), 1.90 – 1.67 (m, 48H). IR (film): $\nu$ ($cm^{-1}$) 2901, 2847, 1590, 1554, 1519, 1476, 1447, 1425, 1385, 1345, 1316, 1298, 1263, 1244, 1155, 1132, 1102, 1075, 1052, 1038, 1016, 975, 929, 886, 823, 792, 767, 736, 726, 705, 651, 634, 583, 451, 441, 384.

***N,N-trans*-Iridium Complex *rac*-22**

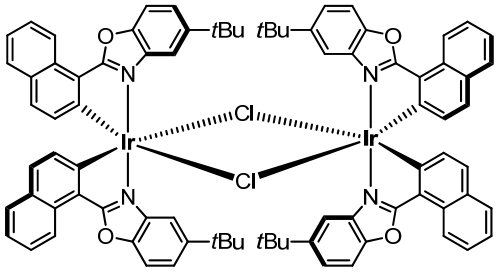

The *N,N-trans*-iridium complex *rac*-**22** was synthesized by the same method for synthesizing *rac*-**15**. 5-(*tert*-Butyl)-2-(naphthalen-1-yl)benzo[*d*]oxazole **8** (316 mg, 1.05 mmol) was added to iridium chloride hydrate (154 mg, 0.44 mmol) in 2-ethoxyethanol (15 mL). The reaction mixture was heated at 145 °C for 20 h under nitrogen. After cooling to room temperature, the mixture was added 1 *N* HCl. The colored precipitate was filtered off, washed with 1 *N* HCl and MeOH, and then dried to yield the

product *rac*-**22** (340 mg, 0.21 mmol, 95% yield) as a red solid. $^1$H NMR (300 MHz, $CDCl_3$) $\delta$ 8.87 (d, $J$ = 8.9 Hz, 4H), 8.42 (d, $J$ = 1.6 Hz, 4H), 7.57 – 7.50 (m, 8H), 7.35 (dd, $J$ = 8.8, 0.6 Hz, 4H), 7.33 – 7.26 (m, 8H), 6.95 (d, $J$ = 8.6 Hz, 4H), 6.29 (d, $J$ = 8.6 Hz, 4H), 1.27 (s, 36H). IR (film): $\nu$ ($cm^{-1}$) 3055, 2960, 2906, 2868, 1616, 1575, 1551, 1511, 1479, 1461, 1435, 1425, 1399, 1360, 1304, 1270, 1255, 1210, 1191, 1136, 1096, 1030, 1022, 926, 888, 862, 829, 815, 802, 785, 744, 727, 663, 643, 630, 606, 522, 455, 427.

### 5.2.3 Synthesis of racemic iridium and rhodium catalysts

**Racemic Iridium Catalyst *rac*-IrO**

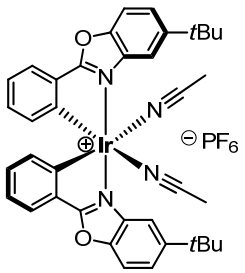


*rac*-**IrO** was synthesized according to the literature procedure[13] with some modifications. *rac*-**11** (434 mg, 0.298 mmol) in 50 mL of acetonitrile was added $AgPF_6$ (266 mg, 0.895 mmol). Heat this mixture in the dark at 70 °C over night. The solvent was removed in vacuum, and the residue was purified by flash chromatography on silica gel (DCM/MeCN = 20: 1 to 10: 1) to afford the *rac*-**IrO** (540 mg, 99% yield) as a yellow solid. $^1$H NMR (300 MHz, $CD_2Cl_2$) $\delta$ 7.85 (d, $J$ = 1.3 Hz, 2H), 7.82 – 7.64 (m, 6H), 7.02 (td, $J$ = 7.5, 1.0 Hz, 2H), 6.85 (td, $J$ = 7.5, 1.5 Hz, 2H), 6.37 (d, $J$ = 7.4 Hz, 2H), 2.44 (s, 6H), 1.46 (s, 18H). All spectroscopic data were in agreement with the literature.[13]

**Racemic Rhodium Catalyst *rac*-RhO**

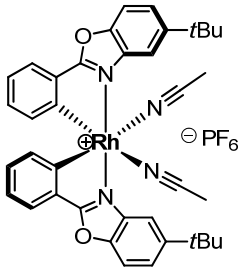


*rac*-**RhO** was synthesized according to the literature procedure[13] with some modifications. *rac*-**12** (344 mg, 0.27 mmol) in 15 mL of acetonitrile was added $AgPF_6$ (149 mg, 0.59 mmol). Heat this mixture in the dark at 50 °C for 16 h. The solvent was removed in vacuum, and the residue was purified by flash chromatography on silica gel (DCM/MeCN = 20: 1) to afford the *rac*-**RhO** (443 mg, 0.52 mmol, 99% yield) as a pale yellow solid. $^1$H NMR (300 MHz, $CD_2Cl_2$) $\delta$ 7.88 (d, $J$ = 1.6 Hz, 2H),

7.80 – 7.74 (m, 6H), 7.09 (td, J = 7.5, 0.9 Hz, 2H), 6.94 (td, *J* = 7.6, 1.5 Hz, 2H), 6.40 (d, *J* = 7.8 Hz, 2H), 2.31 (s, 6H), 1.46 (s, 18H). All spectroscopic data were in agreement with the literature.[15]

**Racemic Iridium Catalyst *rac*-IrS**

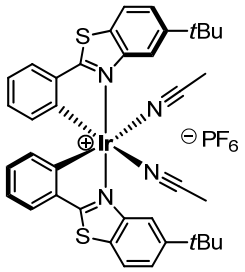


*rac*-**IrS** was synthesized by the same procedure of synthesizing *rac*-**IrO**. *rac*-**13** (453 mg, 0.298 mmol) in 50 mL of acetonitrile was added $AgPF_6$ (266 mg, 0.895 mmol). Heat this mixture in the dark at 70 °C over night. The solvent was removed in vacuum, and the residue was purified by flash chromatography on silica gel (DCM/ MeCN = 20: 1 to 10: 1) to afford the *rac*-**IrS** (562 mg, 99% yield) as a yellow solid. $^1$H NMR (300 MHz, $CD_2Cl_2$) $\delta$ 8.42 (d, *J* = 1.5 Hz, 2H), 8.02 (d, *J* = 8.6 Hz, 2H), 7.73 (dd, *J* = 8.6, 1.8 Hz, 2H), 7.67 (dd, *J* = 7.7, 0.9 Hz, 2H), 6.96 (td, *J* = 7.5, 1.1 Hz, 2H), 6.74 (td, *J* = 7.6, 1.4 Hz, 2H), 6.18 (d, *J* = 7.3 Hz, 2H), 2.35 (s, 6H), 1.47 (s, 18H). $^{13}$C NMR (75 MHz, $CD_2Cl_2$) $\delta$ 181.3, 153.0, 150.3, 142.7, 141.0, 132.9, 131.5, 128.7, 126.1, 125.4, 123.6, 123.1, 121.6, 116.7, 35.6, 31.6, 4.0. IR (film): $\nu$ ($cm^{-1}$) 3060, 2961, 2289, 1583, 1555, 1461, 1444, 1413, 1363, 1321, 1295, 1270, 1253, 1169, 1156, 1126, 1103, 1053, 1020, 998, 936, 874, 835, 787, 757, 732, 700, 669, 616, 589, 458, 403. HRMS (ESI, *m*/*z*) calcd for $C_{38}H_{38}IrN_4S_2$ $[M–PF_6]^+$: 807.2162, found: 807.2163.

**Racemic Iridium Catalyst *rac*-IrO(F)**

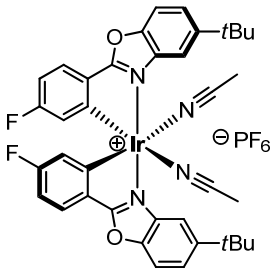


*rac*-**IrO(F)** was synthesized by the same procedure of synthesizing *rac*-**IrO**. *rac*-**15** (40 mg, 0.026 mmol) in 13 mL of acetonitrile was added $AgPF_6$ (15 mg, 0.059 mmol). Heat this mixture in the dark at 70 °C for 24 h. The solvent was removed in vacuum, and the residue was purified by flash chromatography on silica gel (DCM/MeCN = 20: 1 to 10: 1) to afford the *rac*-**IrO(F)** (43 mg, 0.045 mmol, 86% yield) as a yellow solid. $^1$H NMR (300 MHz, $CD_2Cl_2$) $\delta$ 7.83 (dd, *J* = 1.8, 0.7 Hz, 2H), 7.79 – 7.69 (m, 6H), 6.77 (ddd, *J* = 9.0, 8.5, 2.4 Hz, 2H), 6.05 (dd, *J* = 9.5, 2.4 Hz, 2H), 2.46 (s, 6H), 1.47 (s, 18H). $^{13}$C NMR (75 MHz, $CD_2Cl_2$) $\delta$ 176.3, 166.5, 163.1, 151.2, 148.6, 144.9, 144.8, 137.9,

128.4, 128.3, 126.3, 125.1, 121.2, 119.8, 112.7, 112.0, 111.4, 111.0, 35.6, 31.7, 3.8. IR (film): $\nu$ ($cm^{-1}$) 2969, 2957, 2867, 1600, 1562, 1522, 1482, 1467, 1397, 1365, 1284, 1200, 1127, 1117, 937, 849, 825, 807, 757, 649, 574, 557, 453.

**Racemic Iridium Catalyst *rac*-IrO($CF_3$)**

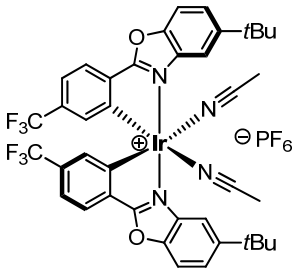


*rac*-**IrO($CF_3$)** was synthesized by the same procedure of synthesizing *rac*-**IrO**. *rac*-**17** (40 mg, 0.022 mmol) in 22 mL of acetonitrile was added $AgPF_6$ (12 mg, 0.049 mmol). Heat this mixture in the dark at 70 °C over night. The solvent was removed in vacuum, and the residue was purified by flash chromatography on silica gel (DCM/MeCN = 20: 1 to 10: 1) to afford the *rac*-**IrO($CF_3$)** (37 mg, 0.035 mmol, 80% yield) as a yellow solid. $^1$H NMR (300 MHz, $CD_2Cl_2$) $\delta$ 7.89 (dd, $J$ = 1.8, 0.7 Hz, 2H), 7.87 – 7.83 (m, 2H), 7.81 (d, $J$ = 0.8 Hz, 2H), 7.78 (dd, $J$ = 8.9, 1.7 Hz, 2H), 7.29 (ddd, $J$ = 8.0, 1.7, 0.8 Hz, 2H), 6.55 (s, 2H), 2.47 (s, 6H), 1.47 (s, 18H). IR (film): $\nu$ ($cm^{-1}$) 2937, 1621, 1594, 1518, 1441, 1390, 1345, 1323, 1271, 1242, 1167, 1120, 1083, 1051, 1041, 1017, 926, 837, 777, 734, 711, 680, 656, 600, 556, 451, 426, 388.

**Racemic Iridium Catalyst *rac*-IrO($NO_2$)**

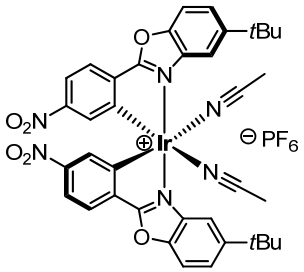


*rac*-**IrO($NO_2$)** was synthesized by the same procedure of synthesizing *rac*-**IrO**. *rac*-**19** (48 mg, 0.029 mmol) in 15 mL of acetonitrile was added $AgPF_6$ (16 mg, 0.065 mmol). Heat this mixture in the dark at 70 °C for 17 h. The solvent was removed in vacuum, and the residue was purified by flash chromatography on silica gel (DCM/MeCN = 20: 1 to 10: 1) to afford the *rac*-**IrO($NO_2$)** (47 mg, 0.047 mmol, 81% yield) as a brown solid. $^1$H NMR (300 MHz, $CD_2Cl_2$) $\delta$ 7.93 – 7.91 (m, 2H), 7.89 (d, $J$ = 0.6 Hz, 2H), 7.88 – 7.83 (m, 6H), 7.05 (dd, $J$ = 2.0, 0.6 Hz, 2H), 2.48 (s, 6H), 1.48 (s, 18H). IR (film): $\nu$ ($cm^{-1}$) 2959, 2939, 2868, 1602, 1544, 1513, 1481, 1449, 1393, 1340, 1300, 1273, 1244, 1107,

1094, 1036, 933, 870, 842, 813, 740, 728, 705, 647, 556, 454.

**Racemic Iridium Catalyst *rac*-IrO(OMe)**

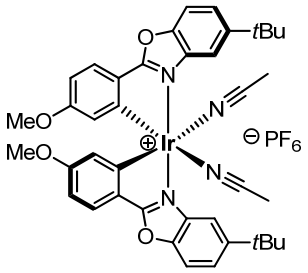


*rac*-**IrO(OMe)** was synthesized by the same procedure of synthesizing *rac*-**IrO**. *rac*-**20** (62 mg, 0.039 mmol) in 20 mL of acetonitrile was added $AgPF_6$ (22 mg, 0.086 mmol). Heat this mixture in the dark at 70 °C over night. The solvent was removed in vacuum, and the residue was purified by flash chromatography on silica gel (DCM/MeCN = 20: 1 to 10: 1) to afford the *rac*-**IrO(OMe)** (72 mg, 0.073 mol, 94% yield) as a yellow solid. $^1$H NMR (300 MHz, $CD_2Cl_2$) $\delta$ 7.78 (d, $J$ = 1.8 Hz, 2H), 7.75 – 7.68 (m, 4H), 7.65 (dd, $J$ = 8.8, 1.8 Hz, 2H), 6.62 (dd, $J$ = 8.6, 2.4 Hz, 2H), 5.86 (d, $J$ = 2.3 Hz, 2H), 3.50 (s, 6H), 2.44 (s, 6H), 1.45 (s, 18H). $^{13}$C NMR (75 MHz, $CD_2Cl_2$) $\delta$ 177.1, 162.9, 150.8, 148.5, 144.2, 138.4, 128.0, 124.2, 122.5, 120.7, 118.4, 112.5, 111.7, 109.0, 55.2, 35.5, 31.8, 3.8. IR (film): $\nu$ ($cm^{-1}$) 2968, 2954, 2941, 1621, 1595, 1566, 1508, 1460, 1434, 1400, 1388, 1313, 1269, 1216, 1175, 1144, 1048, 1037, 1022, 935, 847, 828, 806, 756, 746, 706, 650, 572, 557, 538, 450.

**Racemic Iridium Catalyst *rac*-IrO(ada)**

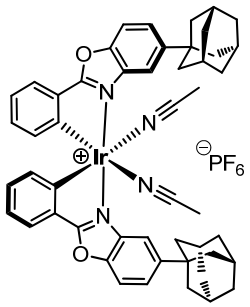


*rac*-**IrO(ada)** was synthesized by the same procedure of synthesizing *rac*-**IrO**. *rac*-**21** (206 mg, 0.117 mmol) in 58 mL of acetonitrile was added $AgPF_6$ (88 mg, 0.350 mmol). Heat this mixture in the dark at 70 °C for 2 days. The solvent was removed in vacuum, and the residue was purified by flash chromatography on silica gel (DCM/MeCN = 100: 1 to 20: 1) to afford the *rac*- **IrO(ada)** (220 mg, 0.204 mmol, 87% yield) as a yellow solid. $^1$H NMR (300 MHz, $CD_2Cl_2$) $\delta$ 7.82 (d, $J$ = 1.5 Hz, 2H), 7.78 (d, $J$ = 8.8 Hz, 2H), 7.71 (dt, $J$ = 7.0, 1.6 Hz, 4H), 7.02 (td, $J$ = 7.5, 1.1 Hz, 2H), 6.85 (td, $J$ = 7.5, 1.5 Hz, 2H), 6.37 (d, $J$ = 7.6 Hz, 2H), 2.47 (s, 6H), 2.15 (s, 6H), 2.12 – 1.98 (m, 12H), 1.90 – 1.74 (m, 12H). $^{13}$C NMR (75 MHz, $CD_2Cl_2$) $\delta$ 177.2, 151.3, 148.7, 141.9, 138.4, 132.8, 132.5, 130.0, 126.2,

124.3, 123.5, 120.8, 112.8, 111.9, 43.9, 37.1, 36.9, 29.4, 3.9. IR (film): $\nu$ ($cm^{-1}$) 2901, 2847, 1593, 1523, 1476, 1449, 1432, 1388, 1265, 1041, 933, 874, 838, 796, 774, 740, 729, 705, 651, 637, 556, 454, 446.

**Racemic Iridium Catalyst *rac*-IrO(nap)**

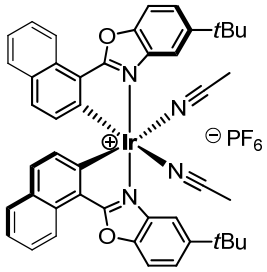


*rac*-**IrO(nap)** was synthesized by the same procedure of synthesizing *rac*-**IrO**. *rac*-**22** (78 mg, 0.047 mmol) in 24 mL of acetonitrile was added $AgPF_6$ (26 mg, 0.10 mmol). Heat this mixture in the dark at 70 °C over night. The solvent was removed in vacuum, and the residue was purified by flash chromatography on silica gel (DCM/MeCN = 20: 1 to 10: 1) to afford the *rac*-**IrO(nap)** (96 mg, 0.094 mmol, 99% yield) as a yellow solid. $^1$H NMR (300 MHz, $CD_2Cl_2$) $\delta$ 9.00 – 8.90 (m, 2H), 7.96 – 7.88 (m, 4H), 7.77 (dd, $J$ = 8.8, 1.9 Hz, 2H), 7.72 – 7.60 (m, 4H), 7.40 (ddd, $J$ = 8.2, 7.0, 1.1 Hz, 2H), 7.27 (d, $J$ = 8.4 Hz, 2H), 6.61 (d, $J$ = 8.5 Hz, 2H), 2.42 (s, 6H), 1.49 (s, 18H). IR (film): $\nu$ ($cm^{-1}$) 2964, 2935, 1618, 1576, 1555, 1516, 1481, 1432, 1404, 1361, 1269, 1192, 1035, 1023, 930, 869, 835, 813, 787, 746, 731, 698, 658, 645, 556, 523, 425.

**Racemic Iridium Catalyst *rac*-IrO(pyrene)**

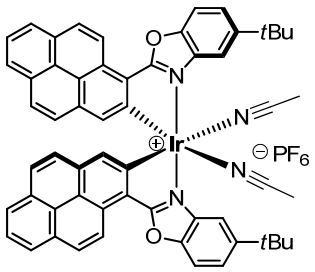


5-(*tert*-Butyl)-2-(pyren-1-yl)benzo[*d*]oxazole **9** (769 mg, 2.05 mmol) was added to iridium chloride hydrate (353 mg, 1.00 mmol) in 2-ethoxyethanol (33 mL). The reaction mixture was heated at 145 °C for 80 h under nitrogen. After cooling to room temperature, the mixture was added 1 *N* HCl. The colored precipitate was filtered off, washed with 1 *N* HCl and MeOH, and then dried to yield the iridium dimer **23** (950 mg, 0.49 mmol, 98% yield) as a red powder which was used without further purification. The iridium dimer **23** (195 mg, 0.10 mmol) in 50 mL of acetonitrile was added $AgPF_6$ (56 mg, 0.22 mmol). Heat this mixture in the dark at 70 °C for 39 h. The solvent was removed in vacuum, and the residue was purified by flash chromatography on silica gel (DCM/MeCN = 10: 1) to afford the *rac*-**IrO(pyrene)** (102 mg, 0.087 mmol, 87% yield) as a yellow solid. $^1$H NMR (300 MHz, $CD_2Cl_2$) $\delta$

9.34 (d, *J* = 9.3 Hz, 2H), 8.29 (d, *J* = 9.4 Hz, 2H), 8.23 – 8.17 (m, 2H), 8.12 – 8.05 (m, 4H), 8.04 (d, *J* = 3.1 Hz, 2H), 7.93 (d, *J* = 7.6 Hz, 2H), 7.90 – 7.83 (m, 4H), 7.52 (d, *J* = 9.0 Hz, 2H), 7.23 (s, 2H), 2.40 (s, 6H), 1.53 (s, 18H). IR (film): *v* ($cm^{-1}$) 2953, 2937, 1624, 1583, 1543, 1498, 1478, 1459, 1427, 1400, 1382, 1366, 1341, 1310, 1270, 1236, 1187, 1144, 1085, 1048, 984, 938, 877, 838, 780, 757, 733, 708, 653, 636, 626, 581, 556, 459, 405. HRMS (ESI, *m*/*z*) calcd for $C_{58}H_{46}IrN_4O_2$ $[M–PF_6]^+$: 1023.3249, found: 1023.3255.

**Racemic Iridium Catalyst *rac*-IrN(pyrene)**

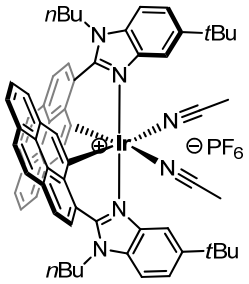


5-(*tert*-Butyl)-1-butyl-2-(pyren-1-yl)-1*H*-benzo[*d*]imidazole **10** (68.8 mg, 0.16 mmol) was added to iridium chloride hydrate (28.2 mg, 0.08 mmol) in 2-ethoxyethanol (3 mL). The reaction mixture was heated at 145 °C over night under nitrogen. After cooling to room temperature, the mixture was added 1 *N* HCl. The colored precipitate was filtered off, washed with 1 *N* HCl and MeOH, and then dried to yield iridium dimer **24** (65 mg, 0.03 mmol, 75% yield) as a red powder which was used without further purification. Iridium dimer **24** (62 mg, 0.029 mmol) in 14 mL of acetonitrile was added $AgPF_6$ (22 mg, 0.086 mmol). Heat this mixture in the dark at 65 °C over night. The solvent was removed in vacuum, and the residue was purified by flash chromatography on silica gel (DCM/MeCN = 20: 1) to afford the *rac*-**IrN(pyrene)** (59 mg, 0.046 mmol, 80% yield) as a dark red solid (not pure, contained 14% isomer). $^1$H NMR (300 MHz, $CD_2Cl_2$) $\delta$ 8.56 (d, *J* = 8.1 Hz, 2H), 8.42 (d, *J* = 8.1 Hz, 2H), 8.22 (s, 4H), 8.00 (d, *J* = 7.4 Hz, 2H), 7.62 (t, *J* = 7.6 Hz, 2H), 7.37 (d, *J* = 8.6 Hz, 2H), 7.20 (d, *J* = 5.9 Hz, 4H), 7.08 (dd, *J* = 8.6, 1.8 Hz, 2H), 5.99 (d, *J* = 1.8 Hz, 2H), 4.53 (t, *J* = 8.0 Hz, 4H), 2.14 – 1.99 (m, 4H), 1.94 (s, 6H), 1.45 (dt, *J* = 14.7, 7.3 Hz, 4H), 1.00 (t, *J* = 7.4 Hz, 6H), 0.20 (s, 18H). IR (film): *v* ($cm^{-1}$) 2957, 2929, 2864, 1556, 1505, 1471, 1438, 1415, 1402, 1333, 1174, 871, 836, 758, 711, 677, 651, 627, 576, 556, 424, 404, 393. HRMS (ESI, *m*/*z*) calcd for $C_{66}H_{64}IrN_6$ $[M–PF_6]^+$: 1133.4822, found: 1133.4821.

## 5.2.4 Synthesis of non-racemic iridium catalysts

The synthesis of non-racemic **IrO**[14] or chiral **RhO**[15] is followed published procedures.

### 5.2.4.1 Synthesis of the Chiral Auxiliary (*S*)-25

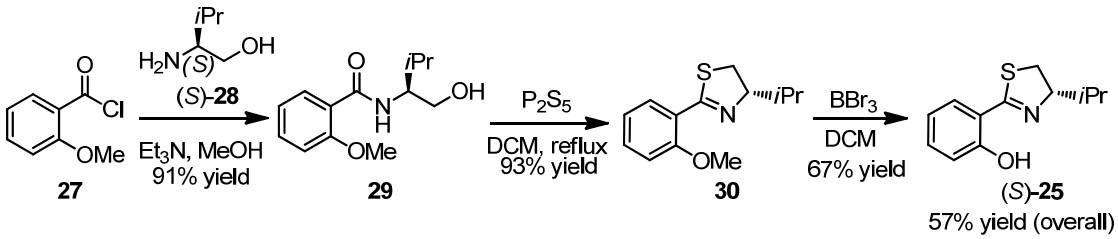


**(*S*)-*N*-(1-hydroxy-3-methylbutan-2-yl)-2-methoxybenzamide (29)**

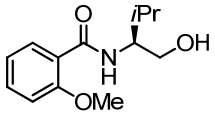

(*S*)-**28** (3.43 g, 33.3 mmol) and triethylamine (4.63 mL, 33.3 mmol) were dissolved in 175 mL of MeOH. 2-Methoxybenzoyl chloride **27** (6.23 g, 36.6 mmol) was added at 0 °C. The reaction mixture was stirred at 0 °C for one hour. The solvent was evaporated and the white residue was dissolved in 200 mL of ethyl acetate / $H_2O$ (v/v = 1: 1). The aqueous layer was separated and extracted twice with ethyl acetate. The combined organic layers were dried over $MgSO_4$, filtered and the solvent was removed *in vacuo*. The residue was purified by flash chromatography on silica gel (short column, EtOAc/*n*-hexane = 1: 2 to 2: 1) to give the compound **29** (7.20 g, 30.4 mmol, 91% yield) as a white solid. $^1$H NMR (300 MHz, $CDCl_3$) $\delta$ 8.17 (dd, $J$ = 7.8, 1.9 Hz, 1H), 8.13 (s, 1H), 7.45 (ddd, $J$ = 8.3, 7.3, 1.9 Hz, 1H), 7.13 – 7.02 (m, 1H), 6.97 (dd, $J$ = 8.3, 1.1 Hz, 1H), 4.08 – 3.90 (m, 1H), 3.97 (s, 3H), 3.86 – 3.65 (m, 2H), 3.50 (s, 1H), 2.12 – 1.92 (m, 1H), 1.02 (d, $J$ = 7.1 Hz, 3H), 1.00 (d, $J$ = 7.1 Hz, 3H). $^{13}$C NMR (75 MHz, $CDCl_3$) $\delta$ 166.8, 157.6, 133.1, 132.5, 121.6, 121.5, 111.5, 65.4, 58.3, 56.2, 29.3, 19.9, 18.5. IR (film): $\nu$ (cm$^{-1}$) 3374, 2958, 2942, 2878, 2839, 1642, 1627, 1598, 1552, 1484, 1464, 1436, 1420, 1385, 1365, 1354, 1313, 1295, 1239, 1179, 1165, 1156, 1138, 1123, 1103, 1075, 1054, 1034, 1021, 969, 864, 824, 786, 755, 695, 638, 608, 567, 535, 519, 448. HRMS (ESI, *m*/*z*) calcd for $C_{13}H_{20}N_1O_3$ $[M+H]^+$: 238.1438, found: 238.1443.

**(*S*)-4-Isopropyl-2-(2-methoxyphenyl)-4,5-dihydrothiazole (30)**

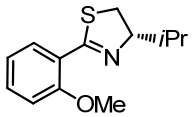

A mixture of compound **29** (4.50g, 19.0 mmol) and phosphorus pentasulfide (7.00 g, 31.6 mmol) in $CH_2Cl_2$ (100mL) was heated under reflux with vigorous stirring for 40 h. The resulting suspension was filtered and the filtrate was washed with 2 *N* sodium hydroxide (3 × 40 mL) and water (2 × 40 mL), dried and the solvent was evaporated. The crude product was purified by flash chromatography on silica gel (EtOAc/*n*-hexane = 1: 4) to give the compound **30** (4.16 g, 17.7 mmol, 93% yield) as a colorless oil. $^1$H NMR (300 MHz, $CDCl_3$) $\delta$ 7.86 (dd, $J$ = 7.7, 1.8 Hz, 1H), 7.38 (ddd, $J$ = 8.3, 7.4, 1.8 Hz, 1H), 7.04 – 6.89 (m, 2H), 4.35 (ddd, $J$ = 9.8, 8.8, 6.2 Hz, 1H), 3.89 (s, 3H), 3.32 (dd, $J$ = 10.9, 8.8 Hz, 1H), 3.05 (dd, $J$ = 10.8, 9.7 Hz, 1H), 2.21 – 2.03 (m, 1H), 1.11 (d, $J$ = 6.8 Hz, 3H), 1.02 (d, $J$ = 6.8 Hz, 3H). $^{13}$C NMR (75 MHz, $CDCl_3$) $\delta$ 163.6, 157.7, 131.8, 130.4, 123.1, 120.8, 112.0, 82.1, 56.0,

35.2, 33.2, 19.9, 19.0. IR (film): $\nu$ ($cm^{-1}$) 2957, 2870, 2836, 1590, 1486, 1460, 1434, 1383, 1365, 1283, 1249, 1222, 1178, 1160, 1114, 1049, 1021, 986, 955, 937, 887, 788, 752, 674, 616, 602, 572, 529, 495. HRMS (ESI, *m*/*z*) calcd for $C_{13}H_{18}N_1O_1S_1$ $[M+H]^+$: 236.1104, found: 236.1105.

**(*S*)-2-(4-Isopropyl-4,5-dihydrothiazol-2-yl)phenol (25)**

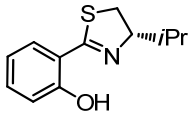


A flame-dried flask (500 mL) was equipped with the compound **30** (8.97 g, 38.1 mmol, 1.0 eq) and dried for 30 min in *vacuo*. Subsequently, the compound **30** was dissolved with dry DCM (180 mL) and the resulting solution was cooled to −78 °C. Neat $BBr_3$ (7.30 mL, 75.8 mmol, 2.0 eq) was added dropwise via syringe over a perdiod of 10 min. The resulting mixture was stirred at −78 °C for 20 min and then stirred at 0 °C for 3 h. Then, the mixture was quenched at 0 °C by addition of MeOH (80 mL) and $N(EtOH)_3$ (33 mL, 248 mmol, 6.5 equiv). Subsequently, DCM was selectively removed in *vacuo* and additional MeOH (170 mL) was added. The resulting yellow suspension was stirred at 70 °C (reflux) for 12 h. After cooling to room temperature, the white precipitate was filtered off and washed thoroughly with MeOH. All volatiles were removed from the filtrate in *vacuo* and the residue was dissolved in DCM and adsorbed on silica gel. The adsorbed crude product was purified by flash chromatography on silica gel (short column, EtOAc/*n*-hexane = 1: 20). After solvent removal and drying in *vacuo*, the desired product (*S*)-**25** was obtained as a yellow viscous oil (5.65 g, 25.5 mmol, 67%). $^1$H NMR (300 MHz, $CDCl_3$) $\delta$ 12.85 (s, 1H), 7.43 – 7.32 (m, 2H), 7.05 (dd, $J$ = 8.3, 1.2 Hz, 1H), 6.88 (td, $J$ = 7.8, 1.2 Hz, 1H), 4.48 (ddd, $J$ = 9.5, 8.7, 6.6 Hz, 1H), 3.41 (dd, $J$ = 11.0, 8.7 Hz, 1H), 3.11 (dd, $J$ = 11.0, 9.5 Hz, 1H), 2.14 – 1.97 (m, $J$ = 6.8 Hz, 1H), 1.08 (dd, $J$ = 17.4, 6.7 Hz, 6H). All spectroscopic data were in agreement with the literature.[16]

### 5.2.4.2 Synthesis of Λ and Δ-IrS

Catalysts Λ and Δ-**IrS** were synthesized following a recently published procedure.[17]

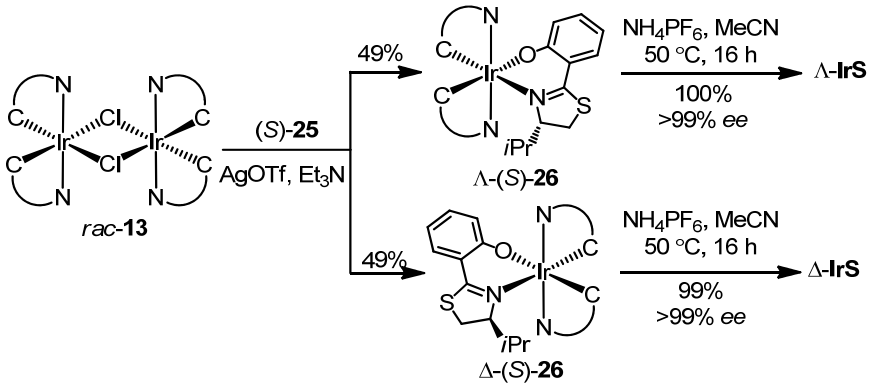

**Iridium Auxiliary Complexes Λ and Δ-(*S*)-26**

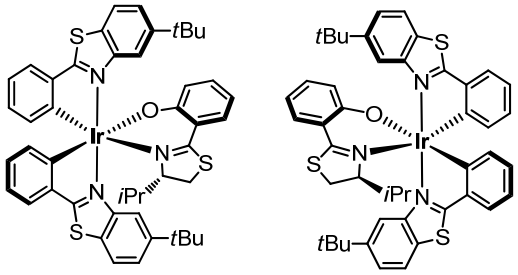

A mixture of iridium (III) dimer complex *rac*-**13** (500 mg, 0.329 mmol), the chiral auxiliary (*S*)-4-isopropyl-2-(2'-hydroxyphenyl)-2-thiazoline {(*S*)-**25**} (160 mg, 0.724 mmol), AgOTf (186 mg, 0.724 mmol) and triethylamine (460 μL, 3.29 mmol) in ethanol (33 mL) was purged with nitrogen for 5 min and then heated at reflux overnight. The reaction mixture was cooled to room temperature and concentrated to dryness. The residue was subjected to a flash silica gel chromatography (EtOAc / *n*-hexane = 1: 25 to 1: 10) to separate the two diastereomers. The first eluting diastereomer was assigned as Λ-(*S*)-**26** (orange solid, 305 mg, 0.323 mmol, 49%) and the second eluting diastereomer was assigned as Δ-(*S*)-**26** (orange solid, 305 mg, 0.324 mmol, 49%).

Λ-(*S*)-**26**: $^{1}$H NMR (300 MHz, $CD_2Cl_2$) $\delta$ 9.00 (d, $J$ = 1.7 Hz, 1H), 7.87 (d, $J$ = 8.5 Hz, 1H), 7.77 (d, $J$ = 1.6 Hz, 1H), 7.75 (dd, $J$ = 7.7, 0.9 Hz, 1H), 7.73 (d, $J$ = 8.5 Hz, 1H), 7.62 (dd, $J$ = 7.6, 1.0 Hz, 1H), 7.51 (ddd, $J$ = 8.5, 4.1, 1.8 Hz, 2H), 7.19 (dd, $J$ = 8.1, 1.7 Hz, 1H), 6.98 – 6.80 (m, 4H), 6.72 (td, $J$ = 7.5, 1.4 Hz, 1H), 6.69 – 6.62 (m, 1H), 6.58 (dd, $J$ = 8.6, 1.1 Hz, 1H), 6.21 – 6.00 (m, 2H), 4.45 (dt, $J$ = 9.7, 2.1 Hz, 1H), 3.38 (dd, $J$ = 11.6, 9.8 Hz, 1H), 2.97 (dd, $J$ = 11.7, 1.9 Hz, 1H), 1.48 (s, 9H), 1.17 (s, 9H), 0.72 – 0.58 (m, 1H), 0.34 (d, $J$ = 7.0 Hz, 3H), 0.06 (d, $J$ = 6.9 Hz, 3H). $^{13}$C NMR (75 MHz, $CD_2Cl_2$) $\delta$ 181.3, 180.4, 170.1, 169.3, 152.2, 152.1, 152.0, 151.5, 151.3, 150.4, 142.9, 142.6, 136.4, 133.3, 133.1, 132.2, 130.6, 129.7, 128.7, 128.2, 126.4, 126.0, 124.3, 124.1, 123.5, 122.4, 122.1, 121.7, 120.8, 119.9, 119.8, 116.3 113.4, 83.8, 35.4, 35.3, 32.0 (3 C), 31.4 (3 C), 31.2, 28.4, 19.8, 14.7. CD (MeOH): λ, nm (Δε, $M^{-1}cm^{-1}$) 458 (–14), 369 (+27), 340 (+38), 304 (–11), 268 (+13), 252 (+2).

Δ-(*S*)-**26**: $^{1}$H NMR (300 MHz, $CD_2Cl_2$) $\delta$ 8.79 (d, $J$ = 1.8 Hz, 1H), 7.88 (s, 1H), 7.82 (dd, $J$ = 28.4, 9.6 Hz, 2H), 7.64 (ddd, $J$ = 15.8, 7.6, 0.9 Hz, 2H), 7.50 (ddd, $J$ = 21.2, 8.6, 1.8 Hz, 2H), 7.31 (dd, $J$ = 8.0, 1.7 Hz, 1H), 6.95 (ddd, $J$ = 8.6, 6.9, 1.8 Hz, 1H), 6.91 – 6.79 (m, 2H), 6.69 (td, $J$ = 7.5, 1.4 Hz, 1H), 6.63 (td, $J$ = 7.5, 1.3 Hz, 1H), 6.57 – 6.47 (m, 2H), 6.31 – 6.19 (m, 2H), 3.49 (ddd, $J$ = 9.0, 5.0, 3.8 Hz, 1H), 2.90 (dd, $J$ = 11.3, 5.1 Hz, 1H), 2.45 (dd, $J$ = 11.2, 9.2 Hz, 1H), 1.92 (m, 1H), 1.25 (s, 9H), 1.11 (s, 9H), 0.81 (d, $J$ = 6.8 Hz, 3H), 0.14 (d, $J$ = 7.0 Hz, 3H). $^{13}$C NMR (75 MHz, $CD_2Cl_2$) $\delta$ 181.62, 180.87, 169.81, 168.16, 153.17, 152.49, 151.87, 151.53, 151.06, 150.08, 142.42, 142.07, 135.73, 133.31, 132.62, 132.17, 130.53, 130.43, 128.65, 128.42, 126.46, 125.75, 124.26, 124.15, 124.06, 122.12, 121.91, 121.89, 121.32, 120.80, 118.80, 117.62, 113.04, 83.20, 35.45, 35.28, 31.69 (3 C), 31.30 (3 C), 30.72, 30.26, 20.75, 17.93. CD (MeOH): λ, nm (Δε, $M^{-1}cm^{-1}$) 488 (+15), 443 (+5), 425 (+10), 344 (–52), 319 (+43), 293 (+22), 285 (+26), 268 (–10), 253 (+9).

IR (film): $\nu$ ($cm^{-1}$) 3055, 2953, 2906, 2866, 1601, 1580, 1556, 1522, 1459, 1436, 1407, 1361, 1331,

1314, 1290, 1278, 1244, 1194, 1151, 1123, 1101, 1045, 1030, 1006, 992, 928, 844, 808, 780, 755, 736, 725, 697, 670, 658, 587, 555, 523, 466. HRMS (ESI, *m*/*z*) calcd for $C_{46}H_{47}IrN_3OS_3Na$ $[M+Na]^+$: 968.2324, found: 968.2323.

**Enantiopure Iridium Catalysts Λ and Δ-IrS**

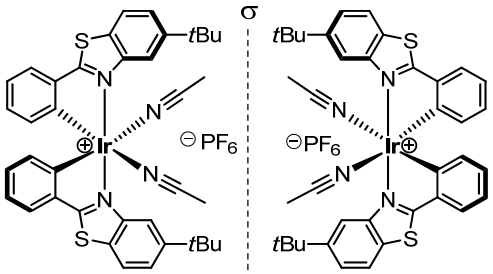


A suspension of the auxiliary complex Λ-(*S*)-**26** (220 mg, 0.233 mmol) or Δ-(*S*)-**26** (113.0 mg, 0.120 mmol) and $NH_4PF_6$ (for Λ-(*S*)-**26**: 1.14 g, 6.99 mmol; for Δ-(*S*)-**26**: 0.59 g, 3.60 mmol,) in acetonitrile (5 mM, 47.0 mL for Λ-(*S*)-**26**; 24.0 mL for Δ-(*S*)-**26**) was heated at 50 °C for 16 h under argon in the dark. The reaction mixture was concentrated to dryness and subjected to a flash silica gel chromatography ($CH_2Cl_2$/$CH_3CN$ = 100:1 to 30:1) to give the enantiopure catalyst Λ-**IrS** (221 mg, 0.232 mmol, >99% yield) or Δ-**IrS** (113 mg, 0.119 mmol, >99% yield) as yellow solids. The chiral auxiliary (*S*)-**25** can be recovered (Δ-(*S*)-**26**→Δ-**IrS** + (*S*)-**25**, 25.5 mg, 96% yield, > 99.9% ee). The absolute configurations of the obtained Λ- and Δ-configured iridium (III) complexes were verified by CD spectroscopy and confirmed by an X-ray crystal structure of Λ-**IrS**. The enantiomeric purity was verified by chiral HPLC analysis. $^1$H NMR (300 MHz, $CD_2Cl_2$) $\delta$ 8.42 (d, $J$ = 1.5 Hz, 2H), 8.02 (d, $J$ = 8.6 Hz, 2H), 7.73 (dd, $J$ = 8.6, 1.8 Hz, 2H), 7.67 (dd, $J$ = 7.7, 0.9 Hz, 2H), 6.96 (td, $J$ = 7.5, 1.1 Hz, 2H), 6.74 (td, $J$ = 7.6, 1.4 Hz, 2H), 6.18 (d, $J$ = 7.3 Hz, 2H), 2.35 (s, 6H), 1.47 (s, 18H). All spectroscopic data were in agreement with *rac*-**IrS**.

Λ-**IrS**: CD (MeOH, 0.2 mM): λ, nm (Δε, $M^{-1}cm^{-1}$) 460 (–7), 358 (+29), 287 (–17), 256 (+11), 242 (–9).

Δ-**IrS**: CD (MeOH, 0.2 mM): λ, nm (Δε, $M^{-1}cm^{-1}$) 461 (+14), 359 (–34), 289 (+27), 255 (–9), 243 (+17).

### 5.2.4.3 Synthesis of Λ and Δ-IrO(ada)

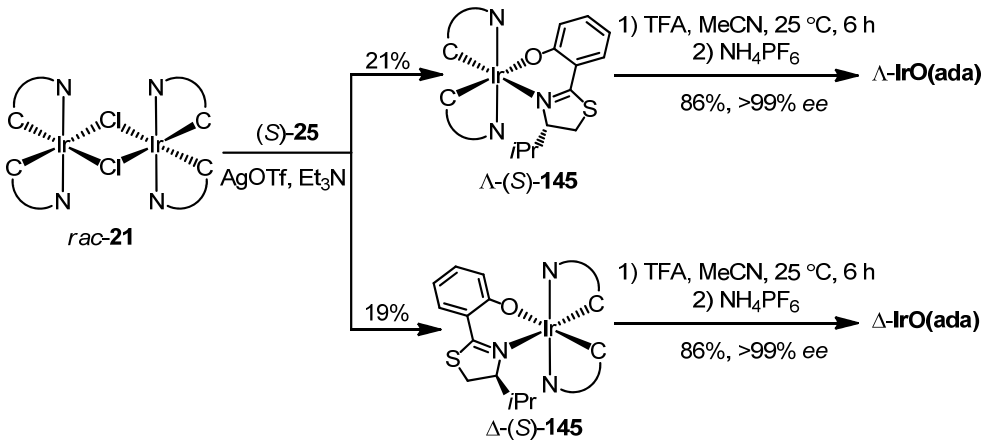


**Iridium Auxiliary Complexes Λ and Δ-(*S*)-145**

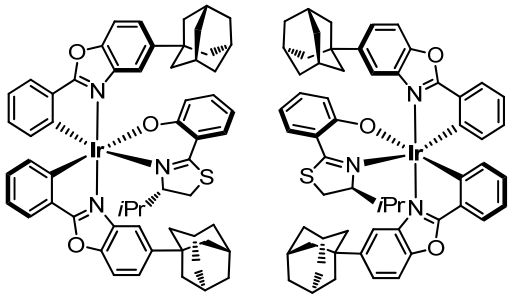

Iridium auxiliary complexes Λ and Δ-(*S*)-**145** were synthesized according to the procedure of Λ and Δ-(*S*)-**26** with some modifications. A mixture of iridium (III) dimer complex *rac*-**21** (520 mg, 0.29 mmol), the chiral auxiliary (*S*)-4-isopropyl-2-(2'-hydroxyphenyl)-2-thiazoline {(*S*)-**25**} (143 mg, 0.65 mmol), and triethylamine (409 μL, 2.94 mmol) in ethanol (30 mL) was purged with argon for 5 min and then heated at 95 °C for 38 h. The reaction mixture was cooled to room temperature and separated by centrifugation. The main comound in filtrate is Λ-(*S*)-**145** and the main compound in solid is Δ-(*S*)-**145** and iridium (III) dimer. They are subjected to a flash silica gel chromatography (*n*-hexane/$CH_2Cl_2$ = 4: 1 to 1: 2) to afford Λ-(*S*)-**145** (orange solid, 127 mg, 0.12 mmol, 21%) and Δ-(*S*)-**145** (orange solid, 116 mg, 0.11 mmol, 19%).

Λ-(*S*)-**145**: $^1$H NMR (300 MHz, $CD_2Cl_2$) $\delta$ 7.93 (d, $J$ = 1.9 Hz, 1H), 7.71 (d, $J$ = 7.6 Hz, 1H), 7.68 – 7.40 (m, 7H), 7.23 – 7.14 (m, 1H), 7.02 – 6.68 (m, 6H), 6.38 (d, $J$ = 7.6 Hz, 1H), 6.31 (t, $J$ = 7.5 Hz, 1H), 4.88 – 4.74 (m, 1H), 3.48 (t, $J$ = 10.6 Hz, 1H), 3.05 (d, $J$ = 11.6 Hz, 1H), 2.24 – 1.95 (m, 12H), 1.92 – 1.62 (m, 18H), 0.85 – 0.72 (m, 1H), 0.23 (d, $J$ = 6.9 Hz, 3H), 0.14 (d, $J$ = 6.9 Hz, 3H). $^{13}$C NMR (75 MHz, $CD_2Cl_2$) $\delta$ 178.3, 178.0, 167.7, 167.1, 150.8, 150.7, 150.5, 149.9, 148.8, 148.5, 139.4, 138.9, 135.2, 133.6, 133.5, 131.9, 131.8, 131.5, 131.3, 126.2, 125.9, 124.7, 122.6, 122.5, 122.0, 120.9, 118.3, 115.0, 113.3, 112.9, 111.1, 110.6, 85.5, 43.9, 43.6, 37.2, 37.0, 36.9, 36.9, 31.8, 30.1, 29.5, 29.5, 28.1, 19.1, 14.1. CD (DCM/MeOH = 1/4, 0.2 mM): λ, nm (Δε, $M^{-1}cm^{-1}$) 454 (–10), 361 (+32), 338 (+26), 326 (+42), 304 (–34), 300 (–30), 293 (–38), 262 (+10), 251 (+12).

Δ-(*S*)-**145**: $^1$H NMR (300 MHz, $CD_2Cl_2$) $\delta$ 7.92 (d, $J$ = 1.9 Hz, 1H), 7.75 – 7.65 (m, 2H), 7.61 (d, $J$ = 8.7 Hz, 1H), 7.55 (d, $J$ = 8.6 Hz, 1H), 7.49 – 7.34 (m, 4H), 7.05 (ddd, $J$ = 8.6, 6.8, 1.8 Hz, 1H), 6.96 – 6.83 (m, 3H), 6.81 – 6.73 (m, 2H), 6.62 (dd, $J$ = 8.6, 1.2 Hz, 1H), 6.44 (d, $J$ = 7.4 Hz, 1H), 6.30 (ddd, $J$ = 8.1, 6.8, 1.3 Hz, 1H), 3.64 – 3.59 (m, 1H), 2.88 (dd, $J$ = 11.2, 2.0 Hz, 1H), 2.73 – 2.60 (m, 1H), 2.25 – 2.12 (m, 1H), 2.08 (s, 3H), 1.95 (s, 3H), 1.87 – 1.57 (m, 24H), 1.07 (d, $J$ = 6.8 Hz, 3H), 0.03 (d, $J$ = 7.0 Hz, 3H). $^{13}$C NMR (75 MHz, $CD_2Cl_2$) $\delta$ 178.9, 178.7, 167.4, 167.3, 151.97, 151.50, 150.5, 149.8, 149.0, 148.5, 139.9, 138.7, 135.9, 133.2, 132.6, 132.4, 131.5, 131.4, 131.2, 130.5, 126.3, 126.0, 124.3, 122.5, 122.4, 121.7, 120.9, 119.6, 114.9, 114.0, 113.1, 110.9, 110.7, 82.4, 43.7, 43.5, 37.1, 37.0, 36.9, 36.9, 32.2, 29.9, 29.5, 29.5, 20.4, 17.3. CD (DCM/MeOH = 1/4, 0.2 mM): λ, nm (Δε, $M^{-1}cm^{-1}$) 458 (+18), 407 (+10), 329 (–52), 306 (+45), 300 (+34), 289 (+36), 284 (+37), 261 (–9), 250 (–15).
IR (film): $\nu$ ($cm^{-1}$) 2899, 2846, 1590, 1559, 1520, 1475, 1462, 1441, 1379, 1356, 1345, 1291, 1263, 1253, 1244, 1194, 1153, 1132, 1115, 1102, 1070, 1035, 1010, 973, 960, 943, 929, 845, 823, 796, 770, 739, 729, 705, 693, 650, 635, 600, 581, 554, 522, 455, 444, 400, 385. HRMS (ESI, $m/z$) calcd for $C_{58}H_{59}IrN_3OS_1$ $[M+H]^+$: 1070.3904, found: 1070.3908.

**Enantiopure Iridium Catalyst Λ-IrO(ada)**

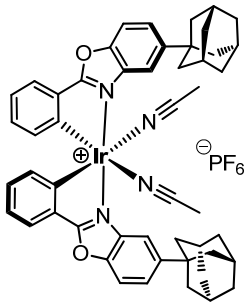


The suspension of Λ-(*S*)-**145** (38 mg, 0.036 mmol) in MeCN (6 mL) was added TFA (13.6 μL, 0.18 mmol) at room temperature and the mixture was stirred for 6 hour. After the solvent was removed, ethanol was added to dissolve the product. Then the product was transferred to the centrifugal tube, $NH_4PF_6$ and $H_2O$ were added. The mixture was under ultra sonic for 10 min. After centrifugation, reserve the solid. Purified the solid by flash silica gel chromatography ($CH_2Cl_2$/$CH_3CN$ = 100:1 to 20:1) to give the enantiopure catalyst Λ-**IrO(ada)** (33 mg, 0.031 mmol, 86%) as a yellow solid. **Δ-IrO(ada)** can be obtained by the same method as **Λ-IrO(ada)**. The absolute configurations of the obtained Λ- and Δ-configured iridium (III) complexes were verified by CD spectroscopy. $^1$H NMR (300 MHz, $CD_2Cl_2$) $\delta$ 7.82 (d, $J$ = 1.5 Hz, 2H), 7.78 (d, $J$ = 8.8 Hz, 2H), 7.71 (dt, $J$ = 7.0, 1.6 Hz, 4H), 7.02 (td, $J$ = 7.5, 1.1 Hz, 2H), 6.85 (td, $J$ = 7.5, 1.5 Hz, 2H), 6.37 (d, $J$ = 7.6 Hz, 2H), 2.47 (s, 6H), 2.15 (s, 6H), 2.12 – 1.98 (m, 12H), 1.90 – 1.74 (m, 12H). All spectroscopic data were in agreement with *rac*-**IrO(ada)**.
Λ-**IrO(ada):** CD (MeOH, 0.2 mM): λ, nm (Δε, $M^{-1}cm^{-1}$) 436 (–14), 368 (+38), 360 (+36), 344 (+52), 288 (–38), 269 (–48), 251 (+3).

Δ-**IrO(ada):** CD (MeOH, 0.2 mM): λ, nm (Δε, $M^{-1}cm^{-1}$) 436 (+15), 367 (–37), 361 (–35), 344 (–53), 289 (+40), 269 (+52), 251 (–2).

## 5.3 Synthesis of Substrates

### 5.3.1 Synthesis of the α,β-unsaturated substrates

Substrate **67** is purchased from Sigma-Aldrich. All other substrates were synthesized according to reported procedures with some modifications.

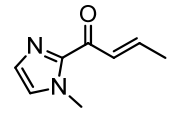
**31**

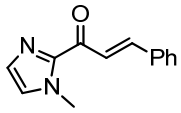
**32**

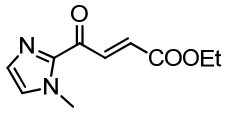
**33**

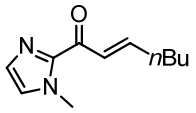
**34**

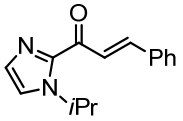
**35**

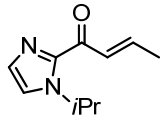
**45**

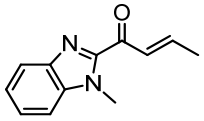
**57**

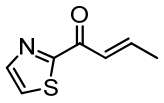
**58**

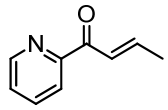
**59**

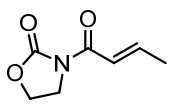
**60**

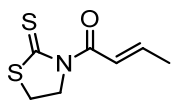
**61**

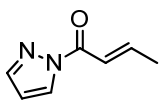
**62**

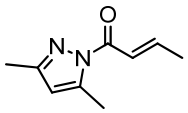
**63**

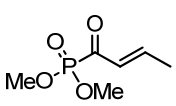
**64**

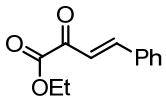
**65**

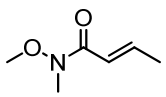
**66**

**(*E*)-1-(1-Methyl-1*H*-imidazol-2-yl)but-2-en-1-one (31)**

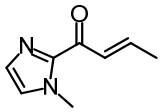

To a solution of *N*-methyl-imidazole (5.2 mL, 66.0 mmol) in THF (100 mL) at −78 °C was added dropwise *n*-BuLi (26.4 mL, 2.5 M in hexane, 66.0 mmol). The reaction mixture was stirred at −78 °C for 10 min, and then stirred at room temperature for additional 30 min. (*E*)-but-2-enoic acid (2.580 g, 30.0 mmol) was added to the flask after the reaction mixture was cooled back down to −78 °C. The reaction mixture was allowed to warm to room temperature slowly (over a period of 3-4 h) and stirred over night. The reaction mixture was quenched with a saturated aqueous solution of $Na_2CO_3$ (30 mL, about 1 mL/ mmol of carboxylic acid) and extracted with EtOAc (4 × 100 mL). The combined organic layers were dried over anhydrous $Na_2SO_4$, filtered, and concentrated under reduced pressure. The residue was purified by flash chromatography on silica gel (EtOAc/*n*-hexane = 1:1) to give **3** (1.67 g, 11.1 mmol, 37% yield, *E* / *Z* > 100: 1) as a white solid. $^1$H NMR (300 MHz, $CDCl_3$) $\delta$ 7.42 (dq, *J* =

15.5, 1.6 Hz, 1H), 7.23 – 7.06 (m, 2H), 7.03 (s, 1H), 4.03 (s, 3H), 1.98 (dd, $J$ = 6.9, 1.6 Hz, 3H). All spectroscopic data were in agreement with the literature.[18]

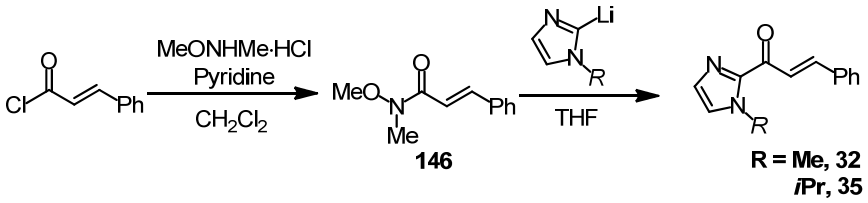


***N*-Methoxy-*N*-methylcinnamamide (146)**

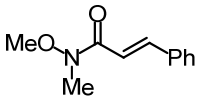

To a solution of *N, O*-dimethylhydroxylamine hydrochloride (2.93 g, 30.0 mmol) in $CH_2Cl_2$ (60 mL) at 0 °C were added *trans*- cinnamoyl chloride (5.00 g, 33.0 mmol) and pyridine (5.3 mL, 66.0 mmol) successively. The reaction mixture was stirred at 0 °C for 30 min, then stirred at room temperature for additional 30 min. The reaction mixture was diluted with EtOAc (100 mL). The organic layer was washed with 1 *N* HCl (3 × 25 mL), aqueous saturated $NaHCO_3$ (3 × 40 mL), and brine (40 mL). The combined organic layers were dried over anhydrous $Na_2SO_4$, filtered, and concentrated under reduced pressure. The residue was purified by flash chromatography on silica gel (EtOAc/*n*-hexane = 1:10 to 1:5) to give **146** (5.67 g, 29.7 mmol, 99% yield) as a white solid. $^1$H NMR (300 MHz, $CDCl_3$) $\delta$ 7.73 (d, $J$ = 15.8 Hz, 1H), 7.62 – 7.52 (m, 2H), 7.45 – 7.32 (m, 3H), 7.03 (d, $J$ = 15.8 Hz, 1H), 3.75 (s, 3H), 3.30 (s, 3H). All spectroscopic data were in agreement with the literature.[18]

**(*E*)-1-(1-Methyl-1*H*-imidazol-2-yl)-3-phenylprop-2-en-1-one (32)**

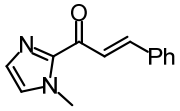

To a solution of *N*-methyl-imidazole (0.96 mL, 12.0 mmol) in THF (25 mL) at −78 °C was added *n*-BuLi (4.8 mL, 2.5 M in hexane, 12.0 mmol) dropwise. The reaction mixture was stirred at −78 °C for 10 min, and then stirred at room temperature for 30 min. The Weinreb amide **146** (1.91 g, 10.0 mmol) was added to the flask after the reaction mixture was cooled back down to −78 °C. The reaction mixture was allowed to warm to room temperature slowly (over a period of 3–4 h) and stirred overnight. The reaction mixture was quenched with acetic acid (6 equiv) at 0 °C and then the reaction mixture was allowed to warm to room temperature before being diluted with EtOAc (100 mL). The organic layer was washed with a saturated aqueous solution of $Na_2CO_3$ and extracted with EtOAc (4 × 30 mL), and dried with anhydrous $Na_2SO_4$, filtered, and concentrated under reduced pressure. The residue was purified by flash chromatography on silica gel (EtOAc/*n*-hexane = 1: 3 to 1: 2) to produce **32** (1.78 g, 8.4 mmol, 84% yield, $E/Z$ > 100: 1) as a white solid. $^1$H NMR (300 MHz, $CDCl_3$) $\delta$ 8.08 (d,

*J* = 16.0 Hz, 1H), 7.82 (d, *J* = 16.1 Hz, 1H), 7.74 – 7.60 (m, 2H), 7.49 – 7.30 (m, 3H), 7.21 (s, 1H), 7.07 (s, 1H), 4.08 (s, 3H). All spectroscopic data were in agreement with the literature.[18]

**(*E*)-1-(1-Isopropyl-1*H*-imidazol-2-yl)-3-phenylprop-2-en-1-one (35)**

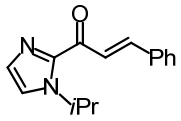


Following the procedure for the preparation of **32**, *N*-isopropylimidazole (1.36 mL, 12.0 mmol) was converted to α,β-unsaturated 2-acylimidazole **35** (2.20 g, 9.2 mmol, 92% yield, *E*/*Z* > 100: 1) as a white solid. $^1$H NMR (300 MHz, $CDCl_3$) $\delta$ 8.12 (d, *J* = 16.0 Hz, 1H), 7.80 (d, *J* = 16.0 Hz, 1H), 7.73 – 7.64 (m, 2H), 7.45 – 7.35 (m, 3H), 7.31 (d, *J* = 0.7 Hz, 1H), 7.25 (s, 1H), 5.72 (hept, *J* = 6.7 Hz, 1H), 1.48 (d, *J* = 6.7 Hz, 6H). All spectroscopic data were in agreement with the literature.[18]

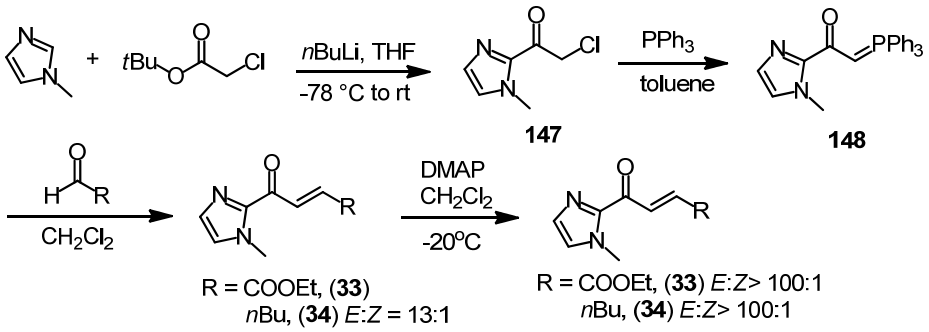


**2-Chloro-1-(1-methyl-1*H*-imidazol-2-yl) ethanone (147)**

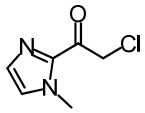


To a solution of *N*-methylimidazole (1.6 mL, 20.0 mmol) in THF (50 mL) at −78 °C was added dropwise *n*-BuLi (8.0 mL, 2.5 M in hexane, 20.0 mmol). The reaction mixture was stirred at −78 °C for 10 min, and then stirred at room temperature for additional 30 min. Next, *tert*-butyl 2-chloroacetate (30.0 mmol) was added to the flask at −78 °C. After being stirred at −78 °C for 2.5 h, the reaction mixture was quenched with $H_2O$ and extracted with EtOAc (4 × 50 mL). The combined organic layers were dried over anhydrous $Na_2SO_4$, filtered, and concentrated under reduced pressure. The residue was purified by flash chromatography on silica gel (EtOAc/*n*-hexane = 1: 1) to afford **147** (2.16 g, 13.7 mmol, 68%) as a white solid. $^1$H NMR (300 MHz, $CDCl_3$) $\delta$ 7.16 (d, *J* = 0.8 Hz, 1H), 7.11 (s, 1H), 4.93 (s, 2H), 4.03 (s, 3H). All spectroscopic data were in agreement with the literature.[18]

**1-(1-Methyl-1*H*-imidazol-2-yl)-2-(triphenyl-phosphoranylidene) ethanone (148)**

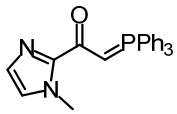

To a solution of **147** (2.12 g, 13.4 mmol) in toluene (28 mL) at room temperature was added $PPh_3$ (3.87 g, 14.8 mmol). After being stirred at 95 °C for overnight, the reaction mixture was diluted with 1 *N* HCl (90 mL) and $Et_2O$ (80 mL). The aqueous layer was separated and organic layer was extracted with 1 *N* HCl (2 × 20 mL). The combined aqueous layers were washed with $Et_2O$ (2 × 60 mL) and neutralized with aqueous saturated $Na_2CO_3$. Then the aqueous layer was extracted with EtOAc (3 × 60 mL). The combined organic layers were dried over anhydrous $Na_2SO_4$, filtered, and concentrated under reduced pressure to produce Wittig reagent **148** (4.70 g, 12.2 mmol, 91%) as a pale yellow solid which was used for the next reaction without further purification. $^1$H NMR (300 MHz, $CDCl_3$) $\delta$ 7.81 – 7.66 (m, 6H), 7.62 – 7.51 (m, 3H), 7.50 – 7.40 (m, $J$ = 8.3, 2.9, 1.3 Hz, 6H), 6.99 (d, $J$ = 1.0 Hz, 1H), 6.82 (s, 1H), 4.97 (d, $J$ = 24.0 Hz, 1H), 4.00 (s, 3H). All spectroscopic data were in agreement with the literature.[18]

**(*E*)-Ethyl 4-(1-methyl-1*H*-imidazol-2-yl)-4-oxobut-2-enoate (33)**

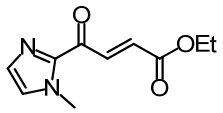


To a solution of Wittig reagent **148** (1.29 g, 3.3 mmol) in toluene (14 mL) at room temperature was added ethyl 2-oxoacetate (~50% in toluene, 1.3 mL, 6.5 mmol). The reaction mixture was stirred at room temperature over night. After the solvent was removed in vacuum, the material was dissolved in 10 mL of $CH_2Cl_2$ and 67 mg of DMAP was added to the flask. The flask was sealed with a septum and purged with dried $N_2$. The reaction mixture was stirred until homogeneous and stored in a freezer (–20 °C) for several days. The reaction mixture was directed loaded on a $SiO_2$ and purified by flash silica chromatography (EtOAc/*n*-hexane = 1: 1) to afford **33** (438 mg, 2.1 mmol, 65% yield, *E*/Z > 100: 1). $^1$H NMR (300 MHz, $CDCl_3$) $\delta$ 8.26 (d, $J$ = 15.9 Hz, 1H), 7.20 (d, $J$ = 0.8 Hz, 1H), 7.10 (s, 1H), 6.88 (d, $J$ = 15.9 Hz, 1H), 4.24 (q, $J$ = 7.1 Hz, 2H), 4.03 (s, 3H), 1.30 (t, $J$ = 7.1 Hz, 3H). All spectroscopic data were in agreement with the literature.[18]

**(*E*)-1-(1-Methyl-1*H*-imidazol-2-yl)hept-2-en-1-one (34)**

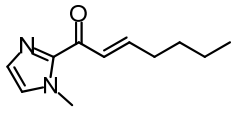

To a solution of Wittig reagent **148** (1.99 g, 5.0 mmol) in toluene (25 mL) at room temperature was added pentanal (8.0 mL, 75 mmol). The reaction mixture was stirred at room temperature for 24 h (monitored by TLC). After the solvent was removed in *vacuo*, the material was dissolved in 20 mL of $CH_2Cl_2$ and 95 mg of DMAP (0.17 equiv) was added to the flask. The flask was sealed with a septum and purged with dried $N_2$. The reaction mixture was stirred until homogeneous and stored in a freezer (–20 °C) for several days. The reaction mixture was directed loaded on a $SiO_2$ and the disired compound was purified by flash silica chromatography (EtOAc/*n*-hexane = 1: 3 to 1: 2) to afford **34**

(920 mg, 4.8 mmol, 96% yield, *E*/*Z* > 100: 1). $^1$H NMR (300 MHz, $CDCl_3$) $\delta$ 7.38 (dt, *J* = 15.6, 1.4 Hz, 1H), 7.20 – 6.95 (m, 3H), 4.02 (s, 3H), 2.50 – 2.02 (m, 2H), 1.58 – 1.42 (m, 2H), 1.42 – 1.28 (m, 2H), 0.89 (t, *J* = 7.2 Hz, 3H). All spectroscopic data were in agreement with the literature.[18]

**(*E*)-1-(1-Isopropyl-1*H*-imidazol-2-yl) but-2-en-1-one (45)**

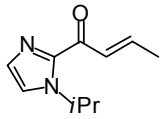

Following the procedure of **31**, *N*-isopropyl-imidazole (7.50 mL, 66.0 mmol) was converted to α,β-unsaturated 2-acylimidazole **45** (1.76 g, 9.9 mmol, 33% yield) as a white solid. $^1$H NMR (300 MHz, $CDCl_3$) $\delta$ 7.46 (dq, *J* = 15.5, 1.6 Hz, 1H), 7.28 (d, *J* = 0.9 Hz, 1H), 7.20 (d, *J* = 0.8 Hz, 1H), 7.18-7.03 (m, 1H), 5.74 – 5.56 (m, 1H), 1.99 (dd, *J* = 6.9, 1.6 Hz, 3H), 1.46 (d, *J* = 6.7 Hz, 6H). All spectroscopic data were in agreement with the literature.[14]

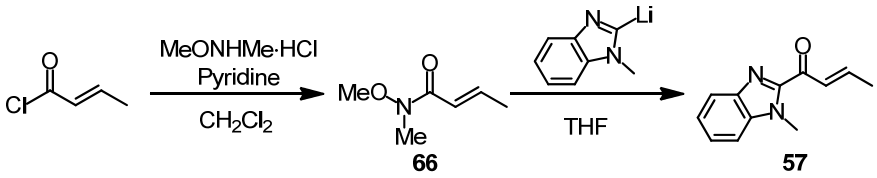


**(*E*)-*N*-Methoxy-*N*-methylbut-2-enamide (66)**

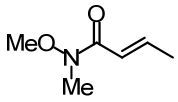

According to the procedure for the preparation of **146**, (*E*)-but-2-enoyl chloride (4.2 mL, 44.0 mmol) was converted to **66** (3.20 g, 9.2 mmol, 62% yield, *E*/*Z* > 100: 1) as a colorless oil. $^1$H NMR (300 MHz, $CDCl_3$) $\delta$ 6.97 (dq, *J* = 15.4, 6.9 Hz, 1H), 6.41 (dq, *J* = 15.3, 1.7 Hz, 1H), 3.69 (s, 3H), 3.22 (s, 3H), 1.90 (dd, *J* = 6.9, 1.7 Hz, 3H). All spectroscopic data were in agreement with the literature.[18]

**(*E*)-1-(1-Methyl-1*H*-benzo[d]imidazol-2-yl)but-2-en-1-one (57)**

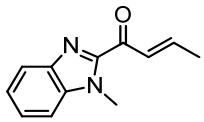

To a solution of 1-methyl-1*H*-benzo[d]imidazoles (0.41 g, 3.1 mmol) in THF (5 mL) at −78 °C was added dropwise *n*-BuLi (1.24 mL, 2.5 M in hexane, 3.1 mmol). The reaction mixture was stirred at −78 °C for 10 min, and then stirred at −40 °C for 1.5 h. To a solution of **66** in THF (10 mL) at −78 °C was added the anionic benzimidazole solution via cannula. The mixture was stirred at −40 °C over night. The reaction mixture was quenched by 0.70 mL of AcOH, diluted with 50 mL of EtOAc, and

washed with $NaHCO_3$ (50 mL) and brine (50 mL). The organic layer was dried over anhydrous $Na_2SO_4$, filtered, and concentrated under reduced pressure. The residue was purified by flash chromatography on silica gel (EtOAc/*n*-hexane = 1: 2) to afford **57** (0.21 g, 1.1 mmol, 35% yield, *E* / *Z* > 100: 1) as a white solid. $^1$H NMR (300 MHz, $CDCl_3$) $\delta$ 7.90 (dt, *J* = 8.0, 1.0 Hz, 1H), 7.60 (dq, *J* = 15.5, 1.6 Hz, 1H), 7.48 – 7.42 (m, 2H), 7.42 – 7.33 (m, 1H), 7.31 – 7.18 (m, 1H), 4.18 (s, 3H), 2.05 (dd, *J* = 6.9, 1.6 Hz, 3H). All spectroscopic data were in agreement with the literature.[19]

**(*E*)-1-(Thiazol-2-yl)but-2-en-1-one (58)**

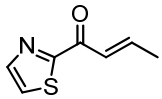

To a solution of thiazole in 15 mL of THF at –15 $^o$C was added *i*PrMgCl (1.8 mL, 2.0 M, 3.6 mmol) slowly. After stirring for 40 min at –15 $^o$C, a solution of **66** (0.39 g, 3.0 mmol) in 5 mL of THF was added slowly. The reaction mixture was allowed to warm to room temperature and stirred over night. It was quenched by aqueous $NH_4Cl$ and extracted once with EtOAc (15 mL). The organic layer was dried over anhydrous $Na_2SO_4$, filtered, and concentrated under reduced pressure. The residue was purified by flash chromatography on silica gel (EtOAc/*n*-hexane = 1: 10) to afford **58** (78 mg, 0.51 mmol, 17% yield, *E*/*Z* > 100: 1) as a colorless oil. $^1$H NMR (300 MHz, $CDCl_3$) $\delta$ 8.01 (d, *J* = 3.0 Hz, 1H), 7.66 (d, *J* = 3.0 Hz, 1H), 7.45 – 7.28 (m, 2H), 2.03 (d, *J* = 5.4 Hz, 3H). All spectroscopic data were in agreement with the literature.[19]

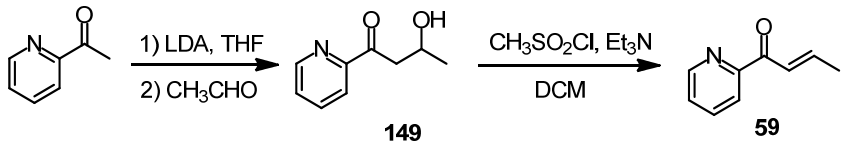


**3-Hydroxy-1-pyridin-2-ylbutan-1-one (149)**

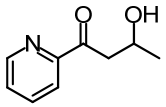

2-Acetylpyridine (1.5 mL, 13.4 mmol) was added dropwise to a solution of LDA (20 mmol in 20 mL of THF) at –20 $^o$C. The resulting solution was stirred at –20 $^o$C for 2 h. Acetaldehyde (1.50 mL, 26.8 mmol) was added dropwise. After the reaction mixture was stirred for 0.5 h, a saturated solution of $NH_4Cl$ (15 mL) was added. The organic phase was collected, and the aqueous was extracted with 10 mL of $Et_2O$. The combined organic layers were dried over anhydrous $Na_2SO_4$, filtered, and concentrated under reduced pressure. The residue was purified by flash chromatography on silica gel (EtOAc/*n*-hexane = 1: 2) to afford **149** (1.30 g, 7.9 mmol, 59% yield) as a colorless oil. $^1$H NMR (300 MHz, $CDCl_3$) $\delta$ 8.66 (ddd, *J* = 4.8, 1.7, 0.9 Hz, 1H), 8.03 (dt, *J* = 7.8, 1.1 Hz, 1H), 7.84 (td, *J* = 7.7, 1.7 Hz, 1H), 7.48 (ddd, *J* = 7.6, 4.8, 1.3 Hz, 1H), 4.33 (tq, *J* = 9.0, 2.7 Hz, 1H), 3.82 (s, 1H), 3.41 (dd,

*J* = 17.0, 2.8 Hz, 1H), 3.22 (dd, *J* = 17.1, 8.8 Hz, 1H), 1.29 (d, *J* = 6.3 Hz, 3H). All spectroscopic data were in agreement with the literature.[20]

**(*E*)-1-(Pyridin-2-yl)but-2-en-1-one (59)**

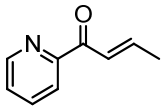

To a solution of **149** (1.25 g, 7.6 mmol) in 32 mL of dry DCM was added TEA (3.2 mL, 22.7 mmol) at −30 °C, and then sulfonyl chloride (0.70 mL, 9.1 mmol) was added dropwise. The reaction mixture was allowed to reach room temperature over night. The solution was quenched by water, and extract by DCM. The combined organic layers were dried over anhydrous $Na_2SO_4$, filtered, and concentrated under reduced pressure. The residue was purified by flash chromatography on silica gel (EtOAc/*n*-hexane = 1: 5) to afford **59** (0.87 g, 5.9 mmol, 78% yield, *E*/*Z* = 40: 1) as a pale yellow oil. $^1$H NMR (300 MHz, $CDCl_3$) $\delta$ 8.74 – 8.67 (m, 1H), 8.18 – 8.07 (m, 1H), 7.90 – 7.80 (m, 1H), 7.61 (dq, *J* = 15.6, 1.6 Hz, 1H), 7.46 (ddd, *J* = 7.3, 4.5, 1.3 Hz, 1H), 7.35 – 7.16 (m, 1H), 2.08 – 1.99 (m, 3H). All spectroscopic data were in agreement with the literature.[20]

**(*E*)-3-(But-2-enoyl)oxazolidin-2-one (60)**

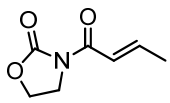

To the solution of 2-oxazolinone (0.87 g, 10 mmol) in THF (20 mL), *n*-BuLi (4.0 mL, 2.5 M in hexane, 10 mmol) was added dropwise at −78 °C. After stirring for 3 h, crotonoyl chloride (1.04 mL, 11 mmol) was added slowly. The mixture was stirred for 30 min at −78 °C and other 15 min at 0 °C. Then the reaction mixture was quenched by a saturated solution of $NH_4Cl$ and extracted with EtOAc. The combined organic layers were dried over anhydrous $Na_2SO_4$, filtered, and concentrated under reduced pressure. The residue was purified by flash chromatography on silica gel (EtOAc/*n*-hexane = 1: 2) to afford **60** (1.01 g, 6.5 mmol, 65%) as a colorless oil. $^1$H NMR (300 MHz, $CDCl_3$) $\delta$ 7.26 (dq, *J* = 15.0, 1.2 Hz, 1H), 7.18 (dq, *J* = 15.0, 6.4 Hz, 1H), 4.41 (t, *J* = 8.0 Hz, 2H), 4.07 (t, *J* = 8.0 Hz, 2H), 1.96 (dd, *J* = 6.4, 1.2 Hz, 3H). All spectroscopic data were in agreement with the literature.[21]

**(*E*)-1-(2-Thioxothiazolidin-3-yl)but-2-en-1-one (61)**

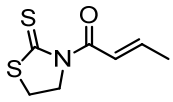

Triethylamine (4.6 mL, 33.0 mmol) was added dropwise to stirred solution of 1,3-thiazolidine-2-thione (3.58 g, 30.0 mmol) and crotonoyl chloride (2.9 mL, 30.0 mmol) in $CH_2Cl_2$ (46 mL) at −78 °C. The mixture was stirred at −78 °C for 30 min and 0 °C for another 30 min. Then, it was diluted with $Et_2O$, and washed with saturated $NaHCO_3$ and water. The combined organic layers were dried

over anhydrous $Na_2SO_4$, filtered, and concentrated under reduced pressure. The residue was purified by flash chromatography on silica gel (EtOAc/*n*-hexane = 1: 3) to afford **61** (2.09 g, 11.2 mmol, 37%, *E* / *Z* = 30: 1) as a yellow oil (stored at –20 °C). $^1$H NMR (300 MHz, $CDCl_3$) $\delta$ 7.21 (dq, *J* = 15.1, 1.5 Hz, 1H), 7.02 (dq, *J* = 14.9, 6.8 Hz, 1H), 4.51 (t, *J* = 7.4 Hz, 2H), 3.32 (t, *J* = 7.4 Hz, 2H), 1.94 (dd, *J* = 6.9, 1.5 Hz, 3H). All spectroscopic data were in agreement with the literature.[22]

**(*E*)-1-(1*H*-Pyrazol-1-yl)but-2-en-1-one (62)**

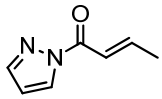

To a solution of pyrazole (2.75 g, 40.4 mmol) in 60 mL of $CH_2Cl_2$ was added $SOCl_2$ (0.88 mL, 12.2 mol) and stirred at room temperature for 1 h. Then, (*E*)-but-2-enoic acid (0.87 g, 9.9 mmol) was added in one portion. The mixture was stirred for additional 3 h. The resulting solution was diluted with $CH_2Cl_2$ (60 mL), washed with aqueous NaOH solution (0.50 M, 3 × 20 mL) and water (3 × 20 mL). The organic layer was dried over anhydrous $Na_2SO_4$, filtered, and concentrated under reduced pressure. The residue was purified by flash chromatography on silica gel (EtOAc/*n*-hexane = 1: 20) to afford **62** (1.13 g, 8.3 mmol, 84% yield, *E*/*Z* > 100: 1) as a colorless oil. $^1$H NMR (300 MHz, $CDCl_3$) $\delta$ 8.33 (d, *J* = 2.8 Hz, 1H), 7.80 – 7.68 (m, 1H), 7.44 – 7.24 (m, 2H), 6.46 (dd, *J* = 2.9, 1.5 Hz, 1H), 2.05 (d, *J* = 5.5 Hz, 3H). All spectroscopic data were in agreement with the literature.[23]

**(*E*)-1-(3,5-Dimethyl-1*H*-pyrazol-1-yl)but-2-en-1-one (63)**

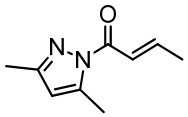

A toluene (5 mL) solution of $SOCl_2$ (1.55g, 13 mmol) was added dropwise to a mixture of pyrazole (0.96g, 10 mmol), (*E*)-but-2-enoic acid (1.12g, 13 mmol) and TEA (5.56 mL, 40 mmol) in toluene (25 mL) at 5 °C. After being continuously stirred for 2 hours, it is quenched by water, and washed with 1 *N* HCl, aqueous NaOH and aqueous NaCl. Then it was extracted with DCM. The combined organic layers were dried over anhydrous $Na_2SO_4$, filtered, and concentrated under reduced pressure. The residue was purified by flash chromatography on silica gel (EtOAc/*n*-hexane = 1: 10) to afford **63** (1.45 g, 8.8 mmol, 88% yield, *E*/*Z* > 100: 1) as a colorless oil. $^1$H NMR (300 MHz, $CDCl_3$) $\delta$ 7.36 – 7.28 (m, 1H), 7.28 – 7.14 (m, 1H), 5.98 (s, 1H), 2.57 (d, *J* = 1.0 Hz, 3H), 2.26 (s, 3H), 2.01 (dd, *J* = 6.4, 1.2 Hz, 3H). All spectroscopic data were in agreement with the literature.[24]

**(*E*)-Dimethyl but-2-enoylphosphonate (64)**

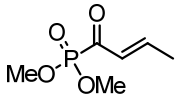

4.25 mL (4.47 g, 36.0 mmol) of trimethyphosphite was added to 3.83 mL (4.18 g, 40.0 mmol) of crotonoyl chloride very slowly (3-4 drops per minute) at 0 °C. The reaction mixture was stirred at 0 °C for 1 h and at room temperature for 5 h. The reaction mixture was directed loaded on a $SiO_2$ and the disired compound was purified by flash silica chromatography (EtOAc/*n*-hexane = 2: 3) to afford **64** (2.31 g, 13.0 mmol, 36% yield, *E*/*Z* = 15:1) as a yellow oil. $^1$H NMR (300 MHz, $CDCl_3$) $\delta$ 7.53 (dq, *J* = 16.0, 6.9 Hz, 1H), 6.41 (ddq, *J* = 16.6, 15.9, 1.6 Hz, 1H), 3.87 (s, 3H), 3.84 (s, 3H), 2.02 (dd, *J* = 6.9, 1.6 Hz, 3H). All spectroscopic data were in agreement with the literature.[25]

**(*E*)-Ethyl 2-oxo-4-phenylbut-3-enoate (65)**

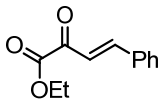


To a solution of alkyl pyruvate (3.460 g, 30 mmol) and aldehyde (2.120 g, 20 mmol) in 50 mL of dry dichloromethane was added $Cu(OTf)_2$ (720 mg, 0.2 mmol). After reflux over a period of 46 h, the cooled reaction mixture was deposited on a short pad of basic alumina and filtered with additional dichloromethane (200 mL). The homogeneous organic solution was evaporated and the residue was purified by column chromatography on silica gel (EtOAc/*n*-hexane = 1: 50) and recrystallisation (in EtOH at –20 °C) to afford **65** (1.72 g, 8.4 mmol, 42%) as a yellow oil (r.t.). $^1$H NMR (300 MHz, $CDCl_3$) $\delta$ 7.87 (d, *J* = 16.1 Hz, 1H), 7.68 – 7.59 (m, 2H), 7.52 – 7.37 (m, 3H), 7.36 (d, *J* = 16.1 Hz, 1H), 4.40 (q, *J* = 7.1 Hz, 2H), 1.42 (t, *J* = 7.2 Hz, 3H). All spectroscopic data were in agreement with the literature.[26]

## 5.3.2 Synthesis of the 2-acylpyridine *N*-oxides

### 5.3.2.1 Synthesis of 2-acylpyridine

2-Acylpyridines **150** and **152** are commercial. All other substrates were synthesized according to reported procedures with some modifications.

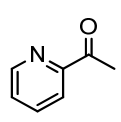


**150**

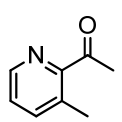


**151**

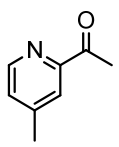


**152**

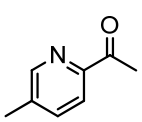


**153**

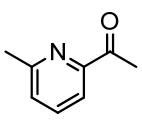


**154**

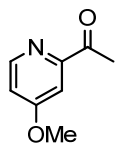


**155**

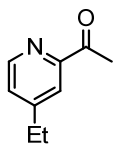


**156**

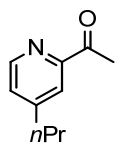


**157**

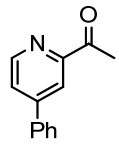


**158**

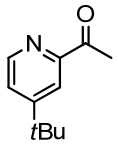


**159**

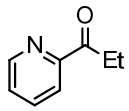


**160**

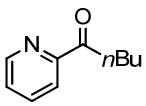


**161**

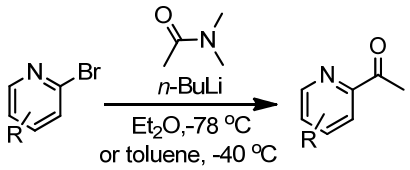


**1-(3-Methylpyridin-2-yl)ethanone (151)**

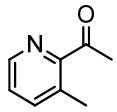


To a solution of 2-bromo-3-methylpyridine (1.720 g, 10.0 mmol, 1.0 equiv) in dry toluene (100 mL, 0.1 M), cooled to –40 °C (dry ice/MeCN bath), was added *n*-butyllithium (4.0 mL, 2.5 M solution in hexanes, 1.0 equiv) dropwise. The reaction mixture was stirred at this temperature for 60 min, then *N*,*N*-dimethylacetamide (1.568 g, 18 mmol, 1.8 equiv) was added dropwise and the mixture was allowed to warm to –15 °C for 1 h. Saturated aqueous ammonium chloride was added and the organic layer was separated. The aqueous layer was extracted with EtOAc and the combined organic layers were dried over anhydrous sodium sulfate, filtered, and concentrated in *vacuo* to give **151** as a yellow oil (EtOAc/*n*-hexane = 1: 20; 774 mg, 5.73 mmol, 57% yield). $^1$H NMR (300 MHz, $CDCl_3$) $\delta$ 8.51 (d, $J$ = 4.5 Hz, 1H), 7.59 (d, $J$ = 7.8 Hz, 1H), 7.33 (dd, $J$ = 7.8, 4.6 Hz, 1H), 2.71 (d, $J$ = 1.0 Hz, 3H), 2.58 (s, 3H). All spectroscopic data were in agreement with the literature.[27]

**1-(5-Methylpyridin-2-yl)ethanone (153)**

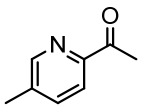


To a solution of 2-bromo-5-methylpyridine (1.720 g, 10.0 mmol, 1.0 equiv) in dry ether (20 mL, 0.5 M), cooled to –78 °C, was added *n*-butyllithium (4.0 mL, 2.5 M solution in hexanes, 1.0 equiv) dropwise. The reaction mixture was allowed to warm to –40° C for 15 min, and then cooled back to –78 °C again. *N*,*N*-dimethylacetamide (1.568 g, 18 mmol, 1.8 equiv) was added dropwise and the mixture was stirred at –78 °C for 2 h. Saturated aqueous ammonium chloride was added and the organic layer was separated. The aqueous layer was extracted with EtOAc and the combined organic layers were dried over anhydrous sodium sulfate, filtered, and concentrated in *vacuo* to give **153** as a yellow oil (EtOAc/*n*-hexane = 1: 10; 1.03 g, 7.63 mmol, 76% yield). $^1$H NMR (300 MHz, $CDCl_3$) $\delta$ 8.50 – 8.48 (m, 1H), 7.94 (d, $J$ = 7.8 Hz, 1H), 7.63 – 7.60 (m, 1H), 2.70 (s, 3H), 2.41 (s, 3H). All spectroscopic data were in agreement with the literature.[28]

**1-(6-Methylpyridin-2-yl)ethanone (154)**

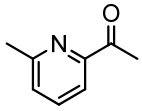

Starting from 2-bromo-6-methylpyridine (302 mg, 1.76 mmol) and *N*,*N*-dimethylacetamide (230 mg, 2.64 mmol) according to the *general procedure* for **153** to give **154** as a yellow oil (EtOAc/*n*-hexane = 1: 30 to 1/20; 110 mg, 0.81 mmol, 46% yield). $^1$H NMR (300 MHz, $CDCl_3$) $\delta$ 7.83 (d, $J$ = 7.7 Hz, 1H), 7.69 (t, $J$ = 7.7 Hz, 1H), 7.31 (d, $J$ = 7.6 Hz, 1H), 2.71 (s, 3H), 2.61 (s, 3H). All spectroscopic data were in agreement with the literature.[29]

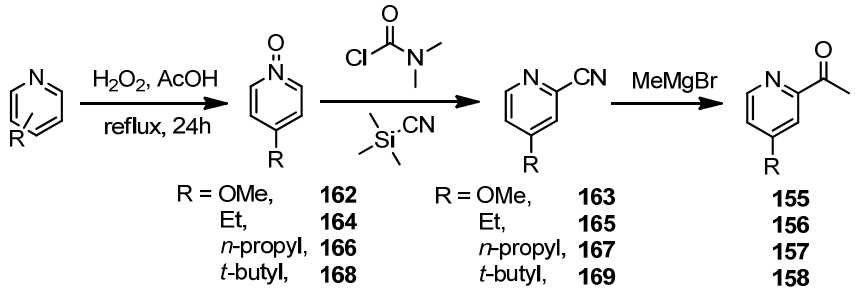


**4-Methoxypyridine 1-oxide (162)**

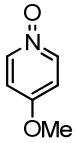

4-Methoxylpyridine (1.6 mL, 15.0 mmol, 1.0 equiv) was dissolved in glacial acetic acid (10.0 mL), 30% hydrogen peroxide (1.87 mL, 16.5 mmol, 1.1 equiv) was added, and the reaction mixture was refluxed for 24 h. The reaction mixture was concentrated in *vacuo* and washed with aqueous sat. $NaHCO_3$. Remove the water from the reaction mixture under the reducing pressure, and then DCM was added to the mixture. After centrifugation, the solution was concentrated in *vacuo* and the resulting crude product was purified by flash chromatography on silica gel (very short colomn, EtOAc/MeOH = 10: 1) to provide the target compound **162** (1.730 g, 13.84 mmol, 92% yield). $^1$H NMR (300 MHz, $CDCl_3$) $\delta$ 8.35 – 8.22 (m, 1H), 6.98 – 6.74 (m, 2H), 3.88 (s, 3H). All spectroscopic data were in agreement with the literature.[30]

**4-Methoxypicolinonitrile (163)**

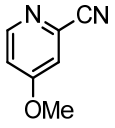

To a solution of pyridine *N*-oxide **162** (make sure no water in **162**) (500 mg, 4.0 mmol) in dry DCM (4 mL, 1.0 M), was added trimethylsilyl cyanide (498 mg, 5.0 mmol, 1.25 equiv) at the room temperature. Dimethylcarbamyl chloride (538 mg, 5.0 mmol, 1.25 equiv) in dry DCM was added to the reaction mixture dropwise (over a 30 min period). After the reaction mixture was stirred at the room

temperature for 24 hours, a solution of 10% $K_2CO_3$ (4 mL) was added dropwise, and stirring was continued for another 15 min. The organic layer was separated, and the aqueous layer was extracted two times with DCM. The combined organic layers was concentrated in *vacuo* to give the disired compound **163** (475 mg, 3.54 mmol, 89% yield) as a white solid without further purification. $^1$H NMR (300 MHz, $CDCl_3$) $\delta$ 8.51 (d, $J$ = 5.8 Hz, 1H), 7.22 (d, $J$ = 2.5 Hz, 1H), 7.00 (dd, $J$ = 5.8, 2.6 Hz, 1H), 3.91 (s, 3H). All spectroscopic data were in agreement with the literature.[30]

**1-(4-Methoxypyridin-2-yl)ethanone (155)**

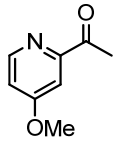


To a stirred solution of 4-methoxypicolinonitrile **163** (402 mg, 3.00 mmol, 1.0 equiv) in dry THF (5 mL, 0.64 M; the solubility of B1 is not good in $Et_2O$) was added a 1.2 equivalents of a solution of the methylmagnesium bromide (3.0 M, 1.2 mL, 3.6 mmol, 1.2 equiv) dropwise at –15 °C (NaCl/ice bath) under $N_2$ atmosphere. After the addition, the reaction mixture was further stirred at this temperature for 1 h and the cooling bath was removed. After warming to room temperature (3 h), the reaction mixture was quenched by the addition of 1 *N* HCl and stirring continued for another 30 min. After separation of the two phases, the water phase was neutralized to pH 8 with 2 *N* NaOH solution and extracted with $CH_2Cl_2$. The combined organic layers were washed with water, saturated brine, dried over anhydrous $Na_2SO_4$, and filtered. The resulting crude oil was purified by flash chromatography on silica gel (EtOAc/*n*-hexane = 1: 4) to provide the target compound **155** as a white solid (280 mg, 1.85 mmol, 62% yield). $^1$H NMR (300 MHz, $CDCl_3$) $\delta$ 8.46 (d, $J$ = 5.6 Hz, 1H), 7.54 (d, $J$ = 2.6 Hz, 1H), 6.96 (dd, $J$ = 5.6, 2.7 Hz, 1H), 3.88 (s, 3H), 2.69 (s, 3H). All spectroscopic data were in agreement with the literature.[31]

**4-Ethylpyridine 1-oxide (164)**

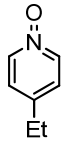


Starting from 4-ethylpyridine (2.143 g, 20.0 mmol) and 30% hydrogen peroxide (2.493 g, 2.5 mL, 22.0 mmol, 1.1 equiv) according to the *general procedure* for **162** to give **164** as a white solid (without further purification; 2.250 g, 18.3 mmol, 92% yield). $^1$H NMR (300 MHz, $CDCl_3$) $\delta$ 8.14 (d, $J$ = 7.0 Hz, 2H), 7.11 (d, $J$ = 6.9 Hz, 2H), 2.65 (q, $J$ = 7.6 Hz, 2H), 1.24 (t, $J$ = 7.6 Hz, 3H). All spectroscopic data were in agreement with the literature.[32]

**4-Ethylpicolinonitrile (165)**

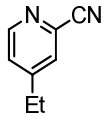

Starting from pyridine *N*-oxide **164** (984 mg, 8.0 mmol), trimethylsilyl cyanide (992 mg, 10.0 mmol, 1.25 equiv) and dimethylcarbamyl chloride (1075 mg, 10.0 mmol, 1.25 equiv) according to the *general procedure* for **163** to give **165** as a colorless oil (EtOAc/*n*-hexane = 1: 4; 1.050 g, 7.95 mmol, 99% yield). $^{1}$H NMR (300 MHz, $CDCl_3$) $\delta$ 8.58 (d, $J$ = 5.1 Hz, 1H), 7.54 (dt, $J$ = 1.5, 0.8 Hz, 1H), 7.34 (ddt, $J$ = 5.1, 1.6, 0.7 Hz, 1H), 2.72 (q, $J$ = 7.6 Hz, 3H), 1.28 (t, $J$ = 7.6 Hz, 3H). $^{13}$C NMR (75 MHz, $CDCl_3$) $\delta$ 154.5, 150.8, 133.9, 128.2, 126.5, 117.4, 27.9, 13.9. IR (film): $\nu$ ($cm^{-1}$) 3052, 2973, 2937, 2878, 2235, 1736, 1595, 1555, 1463, 1431, 1403, 1376, 1328, 1292, 1250, 1153, 1096, 1061, 992, 895, 881, 852, 791, 741, 673, 638, 565, 531, 475, 420, 401, 386. HRMS (ESI, *m*/*z*) calcd for $C_8H_8N_2Na_1$ $[M+Na]^+$: 155.0580, found: 155.0579.

**1-(4-Ethylpyridin-2-yl)ethanone (156)**

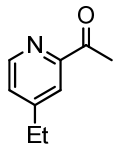

Starting from 4-ethylpicolinonitrile **165** (400 mg, 3.0 mmol) and methylmagnesium bromide (3.0 M, 1.2 mL, 3.6 mmol, 1.2 equiv) according to the *general procedure* for **155** to give **156** as a colorless oil (EtOAc/*n*-hexane = 1: 10; 320 mg, 2.15 mmol, 72% yield). $^{1}$H NMR (300 MHz, $CDCl_3$) $\delta$ 8.54 (d, $J$ = 4.9 Hz, 1H), 7.87 (s, 1H), 7.30 – 7.26 (m, 1H), 2.77 – 2.60 (m, 5H), 1.25 (t, $J$ = 7.6 Hz, 3H). $^{13}$C NMR (75 MHz, $CDCl_3$) $\delta$ 200.3, 154.0, 153.6, 148.9, 126.7, 121.2, 28.2, 25.8, 14.2. IR (film): $\nu$ ($cm^{-1}$) 3052, 2970, 2935, 2877, 1697, 1599, 1555, 1461, 1416, 1378, 1352, 1282, 1185, 1115, 1087, 1060, 1019, 995, 958, 908, 843, 744, 728, 591, 555, 483, 394. HRMS (ESI, *m*/*z*) calcd for $C_9H_{11}N_1O_1Na_1$ $[M+Na]^+$: 172.0733, found: 172.0735.

**4-Propylpyridine 1-oxide (166)**

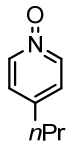

Starting from 4-propylpyridine (2.424 g, 20.0 mmol) and 30% hydrogen peroxide (2.493 g, 2.5 mL, 22.0 mmol, 1.1 equiv) according to the *general procedure* for **162** to give **166** as a white solid (without further purification; 2.470 g, 18.0 mmol, 90% yield). $^{1}$H NMR (300 MHz, $CDCl_3$) $\delta$ 8.07 (d, $J$ = 6.9 Hz, 2H), 7.03 (d, $J$ = 6.6 Hz, 2H), 2.53 (t, $J$ = 7.6 Hz, 2H), 1.60 (h, $J$ = 7.4 Hz, 2H), 0.90 (t, $J$ = 7.3 Hz, 3H). $^{13}$C NMR (75 MHz, $CDCl_3$) $\delta$ 141.94, 138.62, 125.88, 36.21, 23.21, 13.35. IR (film): $\nu$ ($cm^{-1}$) 3119, 3093, 3055, 3023, 2958, 2926, 2867, 1481, 1462, 1426, 1372, 1238, 1195, 1176, 1090, 1044, 1030, 915, 888, 864, 838, 786, 770, 714, 660, 615, 563, 547, 525, 511, 481, 416, 380. HRMS (ESI,

*m*/*z*) calcd for $C_8H_{12}N_1O_1$ $[M+H]^+$: 138.0913, found: 138.0912.

**4-Propylpicolinonitrile (167)**

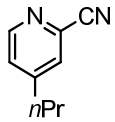


Starting from pyridine *N*-oxide **166** (1.370 g, 10.0 mmol), trimethylsilyl cyanide (1.240 g, 12.5 mmol, 1.25 equiv) and Dimethylcarbamyl chloride (1.340 g, 12.5 mmol, 1.25 equiv) according to the *general procedure* for **163** to give **167** as a colorless oil (EtOAc/*n*-hexane = 1: 8; 1.450 g, 9.9 mmol, 99% yield). $^1$H NMR (300 MHz, $CDCl_3$) $\delta$ 8.57 (dd, $J$ = 5.0, 0.8 Hz, 1H), 7.51 (dd, $J$ = 1.7, 0.8 Hz, 1H), 7.32 (ddd, $J$ = 5.0, 1.6, 0.8 Hz, 1H), 2.64 (d, $J$ = 7.8 Hz, 2H), 1.68 (h, $J$ = 7.4 Hz, 2H), 0.96 (t, $J$ = 7.3 Hz, 3H). All spectroscopic data were in agreement with the literature.[33]

**1-(4-Propylpyridin-2-yl)ethanone (157)**

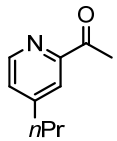


Starting from 4-propylpicolinonitrile **167** (400 mg, 3.0 mmol) and methylmagnesium bromide (3.0 M, 1.2 mL, 3.6 mmol, 1.2 equiv) according to the *general procedure* for **155** to give **157** as a colorless oil (EtOAc/*n*-hexane = 1: 10; 320 mg, 2.15 mmol, 72% yield). $^1$H NMR (300 MHz, $CDCl_3$) $\delta$ 8.55 (d, $J$ = 4.9 Hz, 1H), 7.87 (dd, $J$ = 1.7, 0.8 Hz, 1H), 7.28 (dd, $J$ = 5.0, 1.7 Hz, 1H), 2.72 (s, 3H), 2.65 (t, $J$ = 7.8 Hz, 2H), 1.68 (dq, $J$ = 14.8, 7.4 Hz, 2H), 0.94 (t, $J$ = 7.4 Hz, 3H). $^{13}$C NMR (75 MHz, $CDCl_3$) $\delta$ 200.4, 153.6, 152.7, 148.8, 127.3, 121.8, 37.3, 25.9, 23.4, 13.6. IR (film): $\nu$ ($cm^{-1}$) 2961, 2932, 2872, 1696, 1599, 1554, 1465, 1415, 1352, 1282, 1254, 1186, 1087, 995, 968, 912, 868, 831, 781, 732, 724, 592, 580, 562, 489, 396. HRMS (ESI, *m*/*z*) calcd for $C_{10}H_{14}N_1O_1$ $[M+H]^+$: 164.1070, found: 164.1069.

**4-(*tert*-Butyl)pyridine 1-oxide (168)**

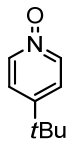


Starting from 4-(*tert*-butyl)pyridine (2.030 g, 15.0 mmol) and 30% hydrogen peroxide (1870 mg, 1.87 mL, 16.5 mmol, 1.1 equiv) according to the *general procedure* for **162** to give **168** as a pale yellow solid (without further purification; 1.909 g, 12.6 mmol, 84% yield). $^1$H NMR (300 MHz, $CDCl_3$) $\delta$ 8.17 – 8.05 (m, 2H), 7.25 – 7.17 (m, 2H), 1.28 (s, 9H). All spectroscopic data were in agreement with the literature.[34]

**4-(*tert*-Butyl)picolinonitrile (169)**

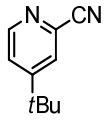

Starting from 4-(*tert*-butyl)pyridine *N*-oxide **168** (1.510 g, 10.0 mmol), trimethylsilyl cyanide (1.240 g, 12.5 mmol, 1.25 equiv) and dimethylcarbamyl chloride (1.340 g, 12.5 mmol, 1.25 equiv) according to the *general procedure* for **163** to give **169** as a colorless oil (EtOAc/*n*-hexane = 1: 10; 1.571 g, 9.8 mmol, 98% yield). $^1$H NMR (300 MHz, $CDCl_3$) $\delta$ 8.60 (dd, $J$ = 5.2, 0.8 Hz, 1H), 7.68 (dd, $J$ = 2.0, 0.8 Hz, 1H), 7.48 (dd, $J$ = 5.3, 1.9 Hz, 1H), 1.33 (s, 9H). All spectroscopic data were in agreement with the literature.[35]

**1-(4-(*tert*-Butyl)pyridin-2-yl)ethanone (159)**

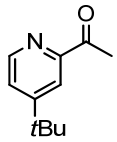

Starting from 4-(*tert*-butyl)picolinonitrile **169** (480 mg, 3.0 mmol) and methylmagnesium bromide (3.0 M, 1.2 mL, 3.6 mmol, 1.2 equiv) according to the *general procedure* for **155** to give **159** as a colorless oil (EtOAc/*n*-hexane = 1: 10; 388 mg, 2.19 mmol, 73% yield). $^1$H NMR (300 MHz, $CDCl_3$) $\delta$ 8.57 (d, $J$ = 5.2 Hz, 1H), 8.05 (d, $J$ = 2.0 Hz, 1H), 7.44 (dd, $J$ = 5.2, 2.0 Hz, 1H), 2.71 (s, 3H), 1.32 (s, 9H). All spectroscopic data were in agreement with the literature.[35]

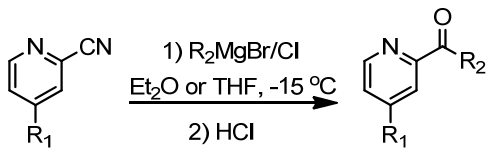


**1-(4-Phenylpyridin-2-yl)ethanone (158)**

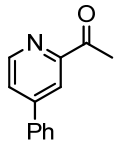

To a stirred solution of 4-phenylpicolinonitrile (901 mg, 5.0 mmol, 1.0 equiv) in dry diethyl ether (7.8 mL, 0.64 M) was added a solution of methylmagnesium bromide (3.0 M, 2.0 mL, 6.0 mmol 1.2 equiv) dropwise at –15 °C (NaCl/ice bath) under $N_2$ atmosphere. After the addition, the reaction mixture was further stirred at this temperature for 1 h and the cooling bath was removed. After warming to room temperature (3 h) the reaction mixture was quenched by the addition of 2 *N* HCl and stirring continued for another 15 min. After separation of the two phases, the water phase was neutralized to pH = 8 with 2 *N* NaOH solution and extracted with $CH_2Cl_2$. The combined organic layers were washed with water, saturated brine, dried over anhydrous $Na_2SO_4$, and filtered. The resulting crude oil was purified by flash chromatography on silica gel (EtOAc/*n*-hexane = 1: 4) to provide **158** as a colorless oil (EtOAc/*n*-hexane = 1: 10; 895 mg, 4.54 mmol, 91% yield). $^1$H NMR (300 MHz, $CDCl_3$) $\delta$ 8.70 (d, $J$ = 5.1 Hz, 1H), 8.30 – 8.24 (m, 1H), 7.73 – 7.59 (m, 3H), 7.57 – 7.37 (m, 3H), 2.76 (s, 3H). $^{13}$C NMR (75

MHz, $CDCl_3$) $\delta$ 200.0, 154.2, 149.4, 149.3, 137.4, 129.4, 129.2, 127.0, 124.6, 119.4, 25.8. IR (film): $\nu$ ($cm^{-1}$) 3059, 1695, 1593, 1540, 1469, 1404, 1347, 1300, 1222, 1114, 1081, 1047, 995, 961, 901, 851, 810, 767, 700, 644, 615, 585, 546, 517, 476, 397. HRMS (ESI, *m*/*z*) calcd for $C_{13}H_{11}N_1O_1Na$ $[M+Na]^+$: 220.0733, found: 220.0732.

**1-(Pyridin-2-yl)propan-1-one (160)**

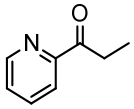

Starting from 2-cyanopydine (1.04 g, 10.0 mmol) and ethylmagnesium bromide (1.0 M in $Et_2O$, 12 mL, 12.0 mmol 1.2 equiv) according to the *general procedure* for **158** to give **160** as a pale yellow oil (EtOAc/*n*-hexane = 1: 4; 578 mg, 4.28 mmol, 43% yield) (The yield is low due to the bad quality of Grignard reagents). $^1$H NMR (300 MHz, $CDCl_3$) $\delta$ 8.68 (ddd, $J$ = 4.8, 1.7, 0.9 Hz, 1H), 8.05 (dt, $J$ = 7.8, 1.1 Hz, 1H), 7.84 (td, $J$ = 7.7, 1.7 Hz, 1H), 7.47 (ddd, $J$ = 7.6, 4.8, 1.3 Hz, 1H), 3.25 (q, $J$ = 7.3 Hz, 2H), 1.22 (t, $J$ = 7.3 Hz, 3H). All spectroscopic data were in agreement with the literature.[36]

**1-(Pyridin-2-yl)pentan-1-one (161)**

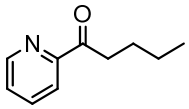

Starting from 2-cyanopydine (1.04 g, 10.0 mmol) and *n*-butylmagnesium chloride (2.0 M in $Et_2O$, 6.0 mL, 12.0 mmol 1.2 equiv) according to the *general procedure* for **158** to give **161** as a colorless oil (EtOAc/*n*-hexane = 1: 8; 1.160 g, 7.12 mmol, 71% yield). $^1$H NMR (300 MHz, $CDCl_3$) $\delta$ 8.65 (ddd, $J$ = 4.8, 1.8, 0.9 Hz, 1H), 8.01 (dt, $J$ = 7.9, 1.1 Hz, 1H), 7.81 (tt, $J$ = 7.7, 1.6 Hz, 1H), 7.43 (ddd, $J$ = 7.5, 4.8, 1.3 Hz, 1H), 3.19 (t, $J$ = 7.4 Hz, 2H), 1.69 (p, $J$ = 7.6 Hz, 2H), 1.40 (dq, $J$ = 14.6, 7.3 Hz, 2H), 0.92 (t, $J$ = 7.3 Hz, 3H). All spectroscopic data were in agreement with the literature.[37]

### 5.3.2.2 Synthesis of 2-acylpyridine N-oxides

All substrates were synthesized according to reported procedures with some modifications.

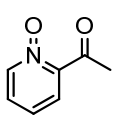

**81**

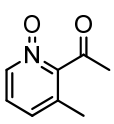

**82**

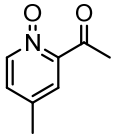

**83**

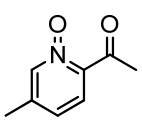

**84**

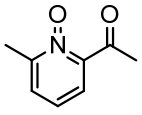

**85**

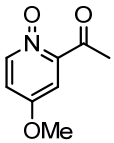


**86**

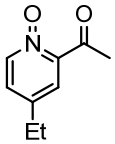


**87**

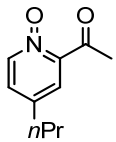


**88**

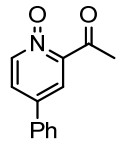


**89**

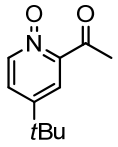


**90**

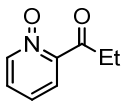


**91**

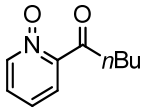


**92**

***Gernaral Procedure:*** *m*-chloroperbenzoic acid (MCPBA, 70% purity, 3.2 equiv) was added to a solution of 2-acylpyridines **150-161** (1.0 equiv) in $CH_2Cl_2$ (0.11 M for 2-acylpyridines) at 0 °C. The mixture was stirred at the room temperature over night. After that, the solvent was removed under reduced pressure and the residue chromatographed on silica gel eluting with EtOAc and EtOAc-EtOH mixtures to give compounds **81-92**.

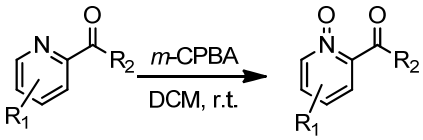


**2-Acetylpyridine 1-oxide (81)**

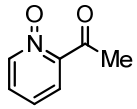


Starting from 2-acyl pyridine **150** (1.210 g, 10.0 mmol) and *m*-chloroperbenzoic acid (6.040 g, 35.0 mmol) according to the *general procedure* to give **81** as a grey solid (28 h, 0.860 g, 6.28 mmol, 63% yield). $^1$H NMR (300 MHz, $CDCl_3$) $\delta$ 8.20 (d, $J$ = 6.2 Hz, 1H), 7.68 (dd, $J$ = 7.6, 2.8 Hz, 1H), 7.43 – 7.24 (m, 2H), 2.80 (s, 3H). All spectroscopic data were in agreement with the literature.[38]

**2-Acetyl-3-methylpyridine 1-oxide (82)**

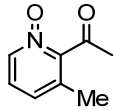


Starting from 1-(3-methylpyridin-2-yl)ethanone **151** (405 mg, 3.00 mmol) and *m*-chloroperbenzoic acid (1810 mg, 10.50 mmol) according to the *general procedure* to give **82** as a white solid (28 h, 441 mg, 2.92 mmol, 97% yield). $^1$H NMR (300 MHz, $CDCl_3$) $\delta$ 8.17 – 8.07 (m, 1H), 7.29 – 7.18 (m, 2H), 2.64 (s, 3H), 2.27 (s, 3H). All spectroscopic data were in agreement with the literature.[38]

**2-Acetyl-4-methylpyridine 1-oxide (83)**

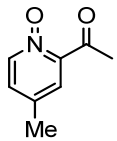


Starting from 1-(4-methylpyridin-2-yl)ethanone **152** (554 mg, 4.10 mmol) and *m*-chloroperbenzoic acid (2480 mg, 14.40 mmol) according to the *general procedure* to give **83** as a grey solid (19 h, 441 mg, 3.51 mmol, 86% yield). $^1$H NMR (300 MHz, $CDCl_3$) $\delta$ 8.09 (d, $J$ = 6.6 Hz, 1H), 7.48 (d, $J$ = 2.6

Hz, 1H), 7.16 (dd, *J* = 6.2, 2.6 Hz, 1H), 2.80 (s, 3H), 2.36 (s, 3H). All spectroscopic data were in agreement with the literature.[38]

**2-Acetyl-5-methylpyridine 1-oxide (84)**

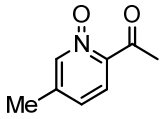

Starting from 1-(5-methylpyridin-2-yl)ethanone **153** (554 mg, 4.10 mmol) and *m*-chloroperbenzoic acid (2480 mg, 14.40 mmol) according to the *general procedure* to give **84** as a pale yellow solid (19 h, 520 mg, 3.44 mmol, 84% yield). $^1$H NMR (300 MHz, $CDCl_3$) $\delta$ 8.05 (dt, *J* = 1.5, 0.8 Hz, 1H), 7.63 (d, *J* = 8.2 Hz, 1H), 7.11 (ddd, *J* = 8.2, 1.5, 0.7 Hz, 1H), 2.80 (s, 3H), 2.34 (s, 3H). All spectroscopic data were in agreement with the literature.[38]

**2-Acetyl-6-methylpyridine 1-oxide (85)**

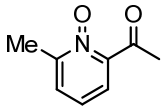

Starting from 1-(6-methylpyridin-2-yl)ethanone **154** (540 mg, 4.00 mmol) and *m*-chloroperbenzoic acid (2416 mg, 14.00 mmol) according to the *general procedure* to give **85** as a pale yellow solid (20 h, 490 mg, 3.25 mmol, 81% yield). $^1$H NMR (300 MHz, $CDCl_3$) $\delta$ 7.55 (dd, *J* = 7.7, 2.1 Hz, 1H), 7.40 (dd, *J* = 7.7, 2.1 Hz, 1H), 7.26 (t, *J* = 7.8 Hz, 1H), 2.81 (s, 3H), 2.57 (s, 3H). All spectroscopic data were in agreement with the literature.[38]

**2-Acetyl-4-methoxypyridine 1-oxide (86)**

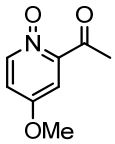

Starting from 1-(4-methoxypyridin-2-yl)ethanone **155** (227 mg, 1.50 mmol) and *m*-chloroperbenzoic acid (906 mg, 5.25 mmol) according to the *general procedure* to give **86** as a pale yellow solid (3 days, 180 mg, 1.08 mmol, 72% yield). $^1$H NMR (300 MHz, $CDCl_3$) $\delta$ 8.21 (d, *J* = 7.2 Hz, 1H), 7.22 (d, *J* = 3.6 Hz, 1H), 6.97 (dd, *J* = 7.3, 3.6 Hz, 1H), 3.92 (s, 3H), 2.85 (s, 3H). All spectroscopic data were in agreement with the literature.[38]

**2-Acetyl-4-ethylpyridine 1-oxide (87)**

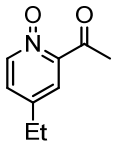

Starting from 1-(4-ethylpyridin-2-yl)ethanone **156** (290 mg, 2.00 mmol) and *m*-chloroperbenzoic acid

(1.201 g, 7.00 mmol) according to the *general procedure* to give **87** as a pale yellow solid (21 h, 284 mg, 1.72 mmol, 86% yield). $^{1}$H NMR (300 MHz, $CDCl_3$) $\delta$ 8.08 (d, $J$ = 6.6 Hz, 1H), 7.51 – 7.43 (m, 1H), 7.16 (dd, $J$ = 6.6, 2.8 Hz, 1H), 2.78 (s, 3H), 2.63 (q, $J$ = 7.6 Hz, 2H), 1.23 (t, $J$ = 7.6 Hz, 3H). $^{13}$C NMR (75 MHz, $CDCl_3$) $\delta$ 195.2, 146.1, 142.9, 140.0, 127.5, 125.7, 30.6, 27.3, 14.0. IR (film): $\nu$ ($cm^{-1}$) 2970, 2932, 2874, 1687, 1614, 1537, 1463, 1431, 1353, 1289, 1236, 1191, 1133, 1070, 1017, 903, 878, 836, 781, 705, 581, 535, 488, 453. HRMS (ESI, *m*/*z*) calcd for $C_9H_{12}N_1O_2$ $[M+H]^+$: 166.0863, found: 166.0861.

**2-Acetyl-4-propylpyridine 1-oxide (88)**

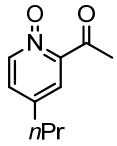


Starting from 1-(4-propylpyridin-2-yl)ethanone **157** (326 mg, 2.00 mmol) and *m*-chloroperbenzoic acid (1.201 g, 7.00 mmol) according to the *general procedure* to give **88** as a colorless oil (21 h, 290 mg, 1.62 mmol, 81% yield). $^{1}$H NMR (300 MHz, $CDCl_3$) $\delta$ 8.08 (d, $J$ = 6.6 Hz, 1H), 7.46 (d, $J$ = 2.7 Hz, 1H), 7.14 (dd, $J$ = 6.6, 2.7 Hz, 1H), 2.78 (s, 3H), 2.57 (t, $J$ = 7.8 Hz, 2H), 1.63 (h, $J$ = 7.4 Hz, 2H), 0.93 (t, $J$ = 7.3 Hz, 3H). $^{13}$C NMR (75 MHz, $CDCl_3$) $\delta$ 195.2, 146.0, 141.6, 134.0, 128.0, 126.3, 36.3, 30.7, 23.2, 13.4. IR (film): $\nu$ ($cm^{-1}$) 2960, 2930, 2868, 1686, 1614, 1536, 1462, 1431, 1352, 1288, 1242, 1189, 1131, 1072, 1018, 978, 908, 834, 803, 761, 705, 583, 548, 452. HRMS (ESI, *m*/*z*) calcd for $C_{10}H_{13}N_1O_2Na_1$ $[M+Na]^+$: 202.0838, found: 202.0839.

**2-Acetyl-4-phenylpyridine 1-oxide (89)**

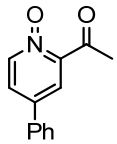


Starting from 1-(4-phenylpyridin-2-yl)ethanone **158** (865 mg, 4.39 mmol) and *m*-chloroperbenzoic acid (2.650 g, 15.27 mmol) according to the *general procedure* to give **89** as a white solid (19 h, 792 mg, 3.72 mmol, 85% yield). $^{1}$H NMR (300 MHz, $CDCl_3$) $\delta$ 8.22 (d, $J$ = 6.8 Hz, 1H), 7.92 (d, $J$ = 2.8 Hz, 1H), 7.64 – 7.54 (m, 3H), 7.53 – 7.35 (m, 3H), 2.84 (s, 3H). All spectroscopic data were in agreement with the literature.[38]

**2-Acetyl-4-(*tert*-butyl)pyridine 1-oxide (90)**

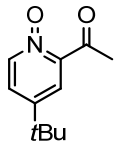


Starting from 1-(4-(*tert*-butyl)pyridin-2-yl)ethanone **159** (368 mg, 2.08 mmol) and *m*-chloroperbenzoic acid (1.260 g, 7.28 mmol) according to the *general procedure* to give **90** as a

white solid (38 h, 334 mg, 1.73 mmol, 83% yield). $^{1}$H NMR (300 MHz, $CDCl_3$) $\delta$ 8.11 (d, $J$ = 6.9 Hz, 1H), 7.64 (d, $J$ = 2.9 Hz, 1H), 7.33 (dd, $J$ = 6.9, 2.9 Hz, 1H), 2.81 (s, 3H), 1.31 (s, 9H). $^{13}$C NMR (75 MHz, $CDCl_3$) $\delta$ 195.4, 150.2, 145.9, 139.9, 125.2, 123.5, 34.7, 30.7, 30.4. IR (film): $\nu$ ($cm^{-1}$) 2960, 2917, 2869, 1672, 1605, 1477, 1453, 1418, 1394, 1358, 1293, 1263, 1241, 1181, 1137, 969, 918, 829, 747, 677, 580, 554, 511, 465. HRMS (ESI, $m/z$) calcd for $C_{11}H_{16}N_1O_2$ $[M+H]^+$: 194.1176, found: 194.1175.

**2-Propionylpyridine 1-oxide (91)**

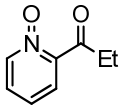


Starting from 1-(pyridin-2-yl)propan-1-one **160** (270 mg, 2.00 mmol) and *m*-chloroperbenzoic acid (1.208 g, 7.0 mmol) according to the *general procedure* to give **91** as a pale yellow oil (23 h, 204 mg, 1.35 mmol, 68% yield). $^{1}$H NMR (300 MHz, $CDCl_3$) $\delta$ 8.33 – 8.24 (m, 1H), 7.73 – 7.66 (m, 1H), 7.43 – 7.35 (m, 2H), 3.24 (q, $J$ = 7.2 Hz, 2H), 1.22 (t, $J$ = 7.2 Hz, 3H). All spectroscopic data were in agreement with the literature.[38]

**2-Pentanoylpyridine 1-oxide (92)**

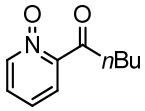


Starting from 1-(pyridin-2-yl)pentan-1-one **161** (652 mg, 4.00 mmol) and *m*-chloroperbenzoic acid (2.416 g, 14.0 mmol) according to the *general procedure* to give **92** as a colorless oil (26 h, 401 mg, 2.24 mmol, 56% yield). $^{1}$H NMR (300 MHz, $CDCl_3$) $\delta$ 8.25 – 8.20 (m, 1H), 7.62 (dd, $J$ = 7.2, 2.7 Hz, 1H), 7.43 – 7.29 (m, 2H), 1.69 (p, $J$ = 7.4 Hz, 2H), 1.38 (dq, $J$ = 14.5, 7.3 Hz, 2H), 0.92 (t, $J$ = 7.3 Hz, 3H). All spectroscopic data were in agreement with the literature.[38]

## 5.3.3 Synthesis of 2-acyl imidazoles

### 5.3.3.1 Synthesis of weinreb amides

All substrates were synthesized according to reported procedures with slightly modifications.[17,39]

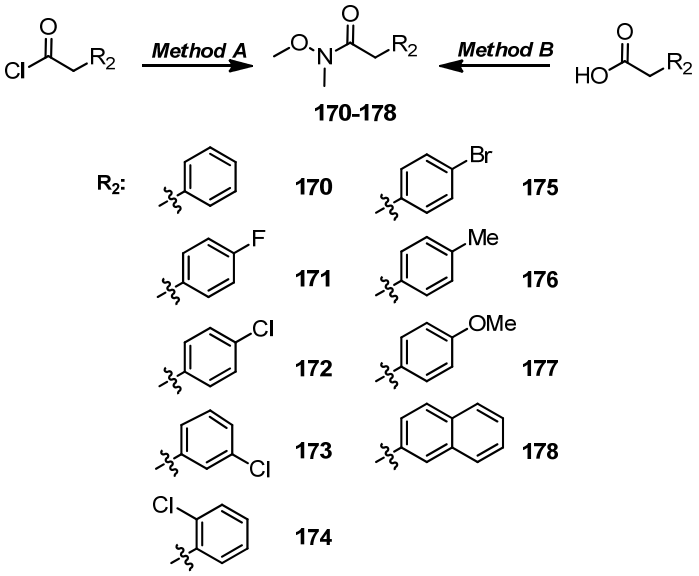


***Gernaral Procedure A:*** To a mixture of *N*,*O*-dimethylhydroxylamine hydrochloride (1.1 equiv) and pyridine (2.5 equiv) in $CH_2Cl_2$ (0.5 M for acyl chloride) were added the corresponding acyl chloride (1.0 equiv) at 0 $^oC$. The reaction mixture was stirred at the room temperature for additional 2 hours. The reaction mixture was diluted with EtOAc. The organic layer was washed with 2 *N* HCl (twice), aqueous saturated $NaHCO_3$ (twice) and brine. The combined organic layers were dried over anhydrous $Na_2SO_4$. The crude mixture was purified by flash chromatography on silica gel (EtOAc/*n*-hexane = 1: 3) to give the pure Weinreb amide.

***Gernaral Procedure B:*** To a solution of corresponding carboxylic acid (1.0 equiv) in $CH_2Cl_2$ (0.16 M for carboxylic acid) were added stepwise *N, O*-dimethylhydroxylamine hydrochloride (1.5 equiv), 1-(3- dimethylaminopropyl)-3-ethylcarbodiimide hydrochloride (1.5 equiv) and 4-dimethylamino-pyridine (1.5 equiv). The reaction mixture was stirred over night at room temperature. After that, the reaction mixture was quenched by water, and then was extracted with $CH_2Cl_2$. The combined organic layers were washed with 1 *N* HCl and brine, dried over $Na_2SO_4$ and the solvent was evaporated in *vacuo*. The crude mixtute was purified by flash chromatography on silica gel (EtOAc/*n*-hexane = 1: 3) to give the pure Weinreb amide.

**_N_-Methoxy-_N_-methyl-2-phenylacetamide (170)**

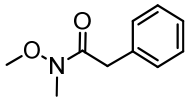

Following the *Gernaral Procedure A*, 2-phenylacetyl chloride (6.960 g, 45.0 mmol) was converted to Weinreb amide **170** (8.027 g, 44.8 mmol, >99% yield) as a colorless oil. $^1H$ NMR (300 MHz, $CDCl_3$) $\delta$ 7.46 – 7.15 (m, 5H), 3.79 (s, 2H), 3.62 (s, 3H), 3.21 (s, 3H). All spectroscopic data were in agreement with the literature.[40]

**2-(4-Fluorophenyl)-*N*-methoxy-*N*-methylacetamide (171)**

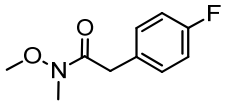

Following the *Gernaral Procedure B*, 2-(4-fluorophenyl)acetic acid (1.232 g, 8.00 mmol) was convert to Weinreb amide **171** (1.520 g, 7.72 mmol, 97% yield) as a white solid. $^{1}$H NMR (300 MHz, $CDCl_3$) $\delta$ 7.32 – 7.23 (m, 2H), 7.07 – 6.96 (m, 2H), 3.76 (s, 2H), 3.66 (s, 3H), 3.21 (s, 3H). $^{19}$F NMR (282 MHz, $CDCl_3$) $\delta$ –117.22 (s, 1F). All spectroscopic data were in agreement with the literature.[41]

**2-(4-Chlorophenyl)-*N*-methoxy-*N*-methylacetamide (172)**

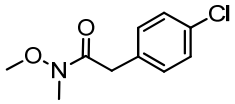

Following the *Gernaral Procedure A*, 2-(4-chlorophenyl)acetyl chloride (1.087 g, 5.75 mmol) was converted to Weinreb amide **172** (0.990 g, 4.65 mmol, 81% yield) as a colorless oil. $^{1}$H NMR (300 MHz, $CDCl_3$) $\delta$ 7.30 (d, $J$ = 8.7 Hz, 2H), 7.24 (d, $J$ = 8.5 Hz, 2H), 3.75 (s, 2H), 3.65 (s, 3H), 3.20 (s, 3H). All spectroscopic data were in agreement with the literature.[42]

**2-(3-Chlorophenyl)-*N*-methoxy-*N*-methylacetamide (173)**

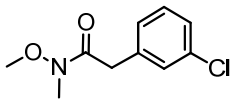

Following the *Gernaral Procedure B*, 2-(3-chlorophenyl)acetic acid (1.706 g, 10.0 mmol) was convert to Weinreb amide **173** (1.490 g, 7.00mmol, 70% yield) as a colorless oil. $^{1}$H NMR (300 MHz, $CDCl_3$) $\delta$ 7.32 – 7.27 (m, 1H), 7.26 – 7.13 (m, 3H), 3.74 (s, 2H), 3.64 (s, 3H), 3.20 (s, 3H). All spectroscopic data were in agreement with the literature.[43]

**2-(2-Chlorophenyl)-*N*-methoxy-*N*-methylacetamide (174)**

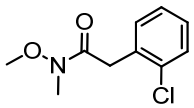

Following the *Gernaral Procedure B*, 2-(2-chlorophenyl)acetic acid (1.706 g, 10.0 mmol) was convert to Weinreb amide **174** (2.123 g, 9.97 mmol, >99% yield) as a colorless oil. $^{1}$H NMR (300 MHz, $CDCl_3$) $\delta$ 7.42 – 7.35 (m, 1H), 7.33 – 7.28 (m, 1H), 7.26 – 7.16 (m, 2H), 3.92 (s, 2H), 3.71 (s, 3H), 3.23 (s, 3H). All spectroscopic data were in agreement with the literature.[44]

**2-(4-Bromophenyl)-*N*-methoxy-*N*-methylacetamide (175)**

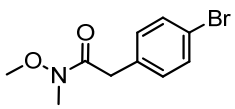

Following the *Gernaral Procedure B*, 2-(4-bromophenyl)acetic acid (1.720 g, 8.00 mmol) was convert

to Weinreb amide **175** (1.990 g, 7.74 mmol, 97% yield) as a white solid. $^1$H NMR (300 MHz, $CDCl_3$) $\delta$ 7.44 (d, $J$ = 8.4 Hz, 1H), 7.17 (d, $J$ = 8.4 Hz, 2H), 3.72 (s, 2H), 3.63 (s, 3H), 3.19 (s, 3H). All spectroscopic data were in agreement with the literature.[39]

***N*-Methoxy-*N*-methyl-2-(*p*-tolyl)acetamide (176)**

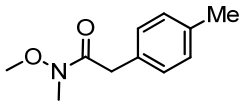


Following the *Gernaral Procedure B*, 2-(*p*-tolyl)acetic acid (1.200 g, 8.00 mmol) was convert to Weinreb amide **176** (1.540 g, 7.98 mmol, >99% yield) as a white solid. $^1$H NMR (300 MHz, $CDCl_3$) $\delta$ 7.18 (d, $J$ = 8.1 Hz, 2H), 7.12 (d, $J$ = 7.8 Hz, 2H), 3.73 (s, 2H), 3.61 (s, 3H), 3.19 (s, 3H), 2.32 (s, 3H). All spectroscopic data were in agreement with the literature.[39]

***N*-Methoxy-2-(4-methoxyphenyl)-*N*-methylacetamide (177)**

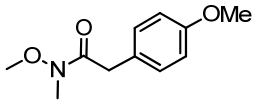


Following the *Gernaral Procedure A*, 2-(4-methoxyphenyl)acetyl chloride (1.477 g, 8.00 mmol) was converted to Weinreb amide **177** (1.401 g, 6.70 mmol, 84% yield) as a colorless oil. $^1$H NMR (300 MHz, $CDCl_3$) $\delta$ 7.21 (d, $J$ = 8.7 Hz, 2H), 6.85 (d, $J$ = 8.7 Hz, 2H), 3.78 (s, 3H), 3.71 (s, 2H), 3.61 (s, 3H), 3.18 (s, 3H). All spectroscopic data were in agreement with the literature.[17]

***N*-Methoxy-*N*-methyl-2-(naphthalen-2-yl)acetamide (178)**

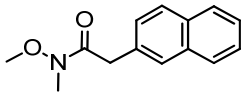


Following the *Gernaral Procedure B*, 2-(naphthalen-2-yl) acetic acid (1.488 g, 8.00 mmol) was converted to Weinreb amide **178** (1.778g, 7.76 mmol, 97% yield) as a colorless oil. $^1$H NMR (300 MHz, $CDCl_3$) $\delta$ 7.85 – 7.77 (m, 3H), 7.77 – 7.73 (m, 1H), 7.51 – 7.39 (m, 3H), 3.94 (s, 2H), 3.61 (s, 3H), 3.22 (s, 3H). All spectroscopic data were in agreement with the literature.[17]

### 5.3.3.2 Synthesis of 2-acyl imidazoles

2-Acyl imidazoles **105-115** were synthesized starting from corresponding Weinreb amide following a published literature with slight modification[44] and **116** was synthesized starting from propionic anhydride according to a reported procedure.[45]

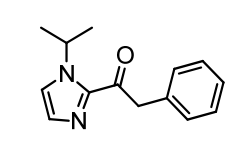

**105**

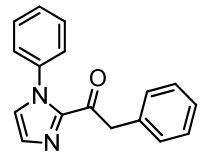

**106**

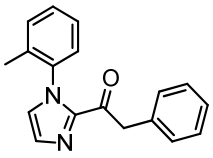

**107**

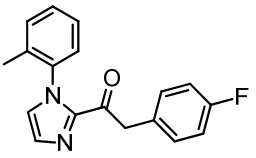

**108**

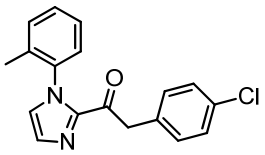

**109**

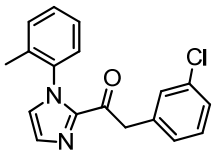

**110**

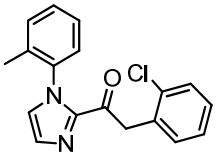

**111**

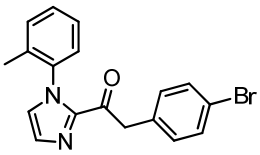

**112**

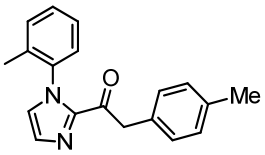

**113**

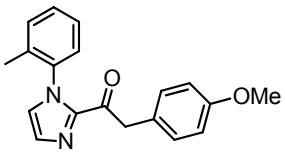

**114**

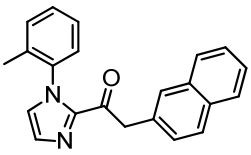

**115**

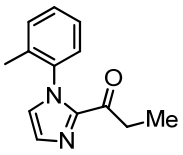

**116**

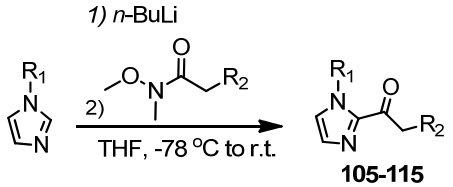


**105-115**

***General procedure:*** To a solution of *N*-isopropylimidazole, or *N*-phenylimidazole, or *N*-(*o*-tolyl)-imidazole (1.1 equiv) in anhydrous THF (0.4 M for the Weinreb amide) at –78 °C added *n*-BuLi (1.1 equiv, 2.5 M in hexanes) dropwise. The reaction mixture was stirred at –78 °C for 30 min, and then stirred at room temperature for 30 min. The corresponding Weinreb amide **170-178** (1.0 equiv in THF) was added dropwise to the flask after the reaction mixture was cooled back down to –78 °C. The reaction mixture was allowed to warm to room temperature slowly and stirred over night. The reaction mixture was quenched with water, diluted with EtOAc. The organic phase was washed with aqueous saturated $NaHCO_3$, brine, dried over anhydrous $Na_2SO_4$ and concentrated in *vacuo*. The crude product was subjected to a silica gel flash chromatography (EtOAc/*n*-hexane = 1: 5) to afford the corresponding 2-acyl imidazole **105-115**.

**1-(1-Isopropyl-1*H*-imidazol-2-yl)-2-phenylethanone (105)**

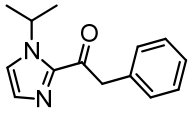

Following the general procedure, the Weinreb amide **170** (1.432 g, 8.0 mmol) was converted to 2-acyl imidazole **105** (1.544 g, 6.77 mmol, 85% yield) as a colorless oil. $^1$H NMR (300 MHz, $CDCl_3$) $\delta$ 7.39 – 7.23 (m, 7H), 5.77 – 5.33 (m, 1H), 4.49 (s, 2H), 1.43 (d, $J$ = 6.7 Hz, 6H). All spectroscopic data were in agreement with the literature.[17]

**2-Phenyl-1-(1-phenyl-1*H*-imidazol-2-yl)ethanone (106)**

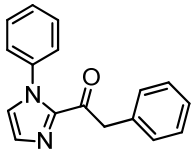

Following the general procedure, the Weinreb amide **170** (1.521g, 9.00 mmol) was converted to 2-acyl imidazole **106** (1.550 g, 5.92 mmol, 66% yield) as a white solid. 1H NMR (300 MHz, $CDCl_3$) $\delta$ 7.46–7.37 (m, 3H), 7.34–7.20 (m, 8H), 7.19 (d, $J$ = 1.0 Hz, 1H), 4.45 (s, 2H). All spectroscopic data were in agreement with the literature.[44]

**2-Phenyl-1-(1-(*o*-tolyl)-1*H*-imidazol-2-yl)ethanone (107)**

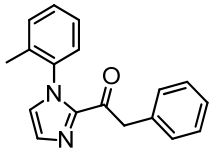

Following the general procedure, the Weinreb amide **170** (1.790 g, 10.0 mmol) was converted to 2-acyl imidazole **107** (2.230 g, 8.08 mmol, 81% yield) as a white solid. $^1$H NMR (300 MHz, $CDCl_3$) $\delta$ 7.40 – 7.16 (m, 9H), 7.15 – 7.01 (m, 2H), 4.50 (d, $J$ = 15.3 Hz, 1H), 4.40 (d, $J$ = 15.3 Hz, 1H), 1.90 (s, 3H). $^{13}$C NMR (75 MHz, $CDCl_3$) $\delta$ 188.3, 143.2, 137.7, 134.4, 134.3, 130.6, 129.9, 129.8, 128.9, 128.3, 126.7, 126.7, 126.5, 126.2, 45.3, 17.0. IR (film): $v$ ($cm^{-1}$) 3105, 3030, 2914, 1685, 1592, 1494, 1452, 1390, 1340, 1307, 1208, 1147, 1079, 1023, 991, 958, 912, 887, 840, 789, 761, 721, 696, 590, 542, 512, 480, 454. HRMS (ESI, $m/z$) calcd for $C_{18}H_{16}N_2O_1Na_1$ $[M+ Na]^+$: 299.1155, found: 299.1156.

**2-(4-Fluorophenyl)-1-(1-(*o*-tolyl)-1*H*-imidazol-2-yl)ethanone (108)**

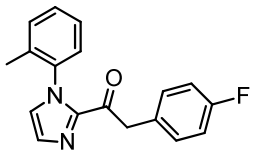

Following the general procedure, the Weinreb amide **171** (0.985 g, 5.0 mmol) was converted to 2-acyl imidazole **108** (1.104 g, 3.76 mmol, 75% yield) as a white solid. $^1$H NMR (300 MHz, $CDCl_3$) $\delta$ 7.38 (d, $J$ = 1.0 Hz, 1H), 7.37 – 7.32 (m, 1H), 7.32 – 7.22 (m, 5H), 7.15 – 7.07 (m, 2H), 7.03 – 6.93 (m, 2H), 4.48 (d, $J$ = 15.4 Hz, 1H), 4.38 (d, $J$ = 15.4 Hz, 1H), 1.91 (s, 3H). $^{13}$C NMR (75 MHz, $CDCl_3$) $\delta$ 188.10, 188.09, 163.5, 160.2, 143.0, 137.7, 134.3, 131.4, 131.3, 130.7, 130.00, 129.95, 129.0, 126.8, 126.5, 126.2, 115.3, 115.0, 44.4, 17.0. $^{19}$F NMR (282 MHz, $CDCl_3$) $\delta$ –116.32 (s, 1F). IR (film): $v$ ($cm^{-1}$) 3051, 2925, 1683, 1603, 1502, 1454, 1397, 1305, 1221, 1151, 1092, 1027, 966, 912, 863, 832, 792, 763, 715, 669, 608,516 355. HRMS (ESI, $m/z$) calcd for $C_{18}H_{15}F_1N_2O_1Na_1$ $[M+ Na]^+$: 317.1061, found: 317.1051.

**2-(4-Chlorophenyl)-1-(1-(*o*-tolyl)-1*H*-imidazol-2-yl)ethanone (109)**

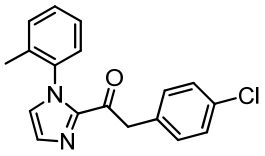

Following the general procedure, the Weinreb amide **172** (0.980 g, 4.60 mmol) was converted to 2-acyl imidazole **109** (1.027 g, 3.31 mmol, 72% yield) as a white solid. $^{1}$H NMR (300 MHz, $CDCl_3$) $\delta$ 7.37 (d, $J$ = 1.0 Hz, 1H), 7.35 – 7.31 (m, 1H), 7.30 – 7.20 (m, 6H), 7.11 (d, $J$ = 1.0 Hz, 1H), 7.08 (dd, $J$ = 7.7, 1.4 Hz, 1H), 4.45 (d, $J$ = 15.3 Hz, 1H), 4.36 (d, $J$ = 15.4 Hz, 1H), 1.90 (s, 3H). $^{13}$C NMR (75 MHz, $CDCl_3$) $\delta$ 187.8, 143.0, 137.7, 134.4, 132.8, 131.2, 130.7, 123.0, 129.1, 128.5, 126.9, 126.6, 126.2, 44.7, 17.1. IR (film): $v$ ($cm^{-1}$) 3111, 3029, 2913, 1684, 1591, 1494, 1451, 1392, 1306, 1207, 1145, 1079, 1023, 958, 912, 841, 788, 764, 718, 591, 543, 454. HRMS (ESI, $m/z$) calcd for $C_{18}H_{15}Cl_1N_2O_1Na_1$ $[M+Na]^+$: 333.0765, found: 333.0766.

**2-(3-Chlorophenyl)-1-(1-(*o*-tolyl)-1*H*-imidazol-2-yl)ethanone (110)**

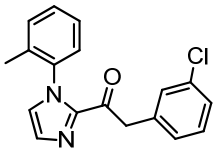

Following the general procedure, the Weinreb amide **173** (1.065 g, 5.00 mmol) was converted to 2-acyl imidazole **110** (0.810 g, 2.61 mmol, 52% yield) as a white solid. $^{1}$H NMR (300 MHz, $CDCl_3$) $\delta$ 7.41 – 7.25 (m, 5H), 7.24 – 7.16 (m, 3H), 7.15 – 7.05 (m, 2H), 4.47 (d, $J$ = 15.5 Hz, 1H), 4.38 (d, $J$ = 15.4 Hz, 1H), 1.92 (s, 3H). $^{13}$C NMR (75 MHz, $CDCl_3$) $\delta$ 187.6, 143.0, 137.7, 136.3, 134.4, 134.1, 130.7, 130.1, 130.0, 129.6, 129.1, 128.1, 127.0, 126.6, 126.2, 44.9, 17.0. IR (film): $v$ ($cm^{-1}$) 3131, 1682, 1600, 1574, 1498, 1478, 1459, 1431, 1409, 1392, 1344, 1311, 1216, 1168, 1146, 1081, 1043, 1021, 960, 910, 893, 883, 865, 855, 811, 794, 759, 717, 705, 683, 593, 550, 542, 505, 453, 415. HRMS (ESI, $m/z$) calcd for $C_{18}H_{15}Cl_1N_2O_1Na_1$ $[M+Na]^+$: 333.0765, found: 333.0767.

**2-(2-Chlorophenyl)-1-(1-(*o*-tolyl)-1*H*-imidazol-2-yl)ethanone (111)**

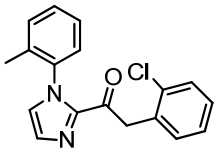

Following the general procedure, the Weinreb amide **174** (1.065 g, 5.00 mmol) was converted to 2-acyl imidazole **111** (0.960 g, 3.10 mmol, 62% yield) as a white solid. $^{1}$H NMR (300 MHz, $CDCl_3$) $\delta$ 7.39 (d, $J$ = 1.0 Hz, 1H), 7.37 – 7.20 (m, 5H), 7.20 – 7.14 (m, 3H), 7.13 (d, $J$ = 1.0 Hz, 1H), 4.77 (d, $J$ = 17.6 Hz, 1H), 4.57 (d, $J$ = 17.7 Hz, 1H), 1.99 (s, 3H). $^{13}$C NMR (75 MHz, $CDCl_3$) $\delta$ 187.0, 143.0, 137.7, 134.7, 134.5, 132.9, 132.1, 130.7, 129.9, 129.3, 129.0, 128.4, 126.6, 126.5, 126.2, 43.6, 17.1. IR (film): $v$ ($cm^{-1}$) 3089, 1683, 1501, 1488, 1472, 1460, 1444, 1400, 1344, 1309, 1150, 1094, 1050, 1032, 963, 948, 915, 811, 802, 787, 766, 751, 717, 692, 678, 598, 573, 554, 535, 504, 459, 448, 436.

HRMS (ESI, *m*/*z*) calcd for $C_{18}H_{15}Cl_1N_2O_1Na_1$ $[M+Na]^+$: 333.0765, found: 333.0766.

**2-(4-Bromophenyl)-1-(1-(*o*-tolyl)-1*H*-imidazol-2-yl)ethanone (112)**

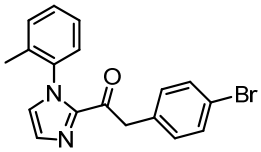

Following the general procedure, the Weinreb amide **175** (1.290 g, 5.0 mmol) was converted to 2-acyl imidazole **112** (1.153 g, 3.26 mmol, 65% yield) as a white solid. $^1$H NMR (300 MHz, $CDCl_3$) $\delta$ 7.45 – 7.38 (m, 2H), 7.37 (d, $J$ = 1.0 Hz, 1H), 7.36 – 7.22 (m, 3H), 7.22 – 7.16 (m, 2H), 7.12 (d, $J$ = 1.0 Hz, 1H), 7.09 (dd, $J$ = 7.7, 1.4 Hz, 1H), 4.45 (d, $J$ = 15.3 Hz, 1H), 4.35 (d, $J$ = 15.3 Hz, 1H), 1.91 (s, 3H). $^{13}$C NMR (75 MHz, $CDCl_3$) $\delta$ 187.7, 143.0, 137.7, 134.4, 133.3, 131.6, 131.5, 130.7, 130.0, 129.1, 126.9, 126.5, 126.2, 120.8, 44.7, 17.0. IR (film): $v$ ($cm^{-1}$) 3113, 2896, 1688, 1487, 1456, 1442, 1408, 1391, 1338, 1313, 1281, 1199, 1150, 1068, 1048, 1021, 1011, 969, 910, 861, 801, 766, 717, 708, 691, 672, 627, 556, 538, 517, 469, 455. HRMS (ESI, *m*/*z*) calcd for $C_{18}H_{15}Br_1N_2O_1Na_1$ $[M+Na]^+$: 377.0260, 379.0241, found: 377.0261, 379.0241.

**2-(*p*-Tolyl)-1-(1-(*o*-tolyl)-1*H*-imidazol-2-yl)ethanone (113)**

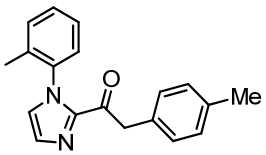

Following the general procedure, the Weinreb amide **176** (0.965 g, 5.0 mmol) was converted to 2-acyl imidazole **113** (1.050 g, 3.62 mmol, 72% yield) as a white solid. $^1$H NMR (300 MHz, $CDCl_3$) $\delta$ 7.38 (d, $J$ = 1.0 Hz, 1H), 7.36 – 7.31 (m, 1H), 7.31 – 7.24 (m, 2H), 7.24 – 7.19 (m, 2H), 7.15 – 7.08 (m, 4H), 4.47 (d, $J$ = 15.2 Hz, 1H), 4.38 (d, $J$ = 15.3 Hz, 1H), 2.32 (s, 3H), 1.93 (s, 3H). $^{13}$C NMR (75 MHz, $CDCl_3$) $\delta$ 188.5, 143.2, 137.8, 136.2, 134.4, 131.2, 130.6, 129.8, 129.7, 129.1, 128.9, 126.6, 126.4, 126.2, 44.9, 21.0, 17.0. IR (film): $v$ ($cm^{-1}$) 3025, 2922, 1680, 1512, 1492, 1459, 1398, 1341, 1304, 1147, 1089, 1050, 1039, 1023, 963, 913, 761, 735, 714, 674, 610, 564, 550, 524, 499, 477, 457. HRMS (ESI, *m*/*z*) calcd for $C_{19}H_{19}N_2O_1$ $[M+H]^+$: 291.1492, found: 291.1493.

**2-(4-Methoxyphenyl)-1-(1-(*o*-tolyl)-1*H*-imidazol-2-yl)ethanone (114)**

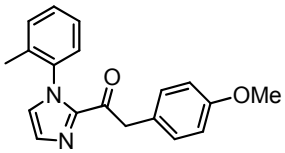

Following the general procedure, the Weinreb amide **177** (1.045 g, 5.0 mmol) was converted to 2-acyl imidazole **114** (1.106 g, 3.61 mmol, 72% yield) as a white solid. $^1$H NMR (300 MHz, $CDCl_3$) $\delta$ 7.36 (d, $J$ = 1.0 Hz, 1H), 7.34 – 7.29 (m, 1H), 7.29 – 7.17 (m, 4H), 7.11 – 7.06 (m, 2H), 6.87 – 6.78 (m, 2H),

4.42 (d, $J$ = 15.3 Hz, 1H), 4.32 (d, $J$ = 15.3 Hz, 1H), 3.77 (s, 3H), 1.89 (s, 3H). $^{13}$C NMR (75 MHz, $CDCl_3$) $\delta$ 188.7, 158.5, 143.3, 137.8, 134.5, 130.9, 130.7, 129.8, 129.0, 126.7, 126.5, 126.4, 126.3, 113.9, 55.2, 44.5, 17.0. IR (film): $v$ ($cm^{-1}$) 3158, 2916, 1668, 1607, 1583, 1509, 1488, 1460, 1447, 1421, 1394, 1302, 1261, 1239, 1179, 1146, 1114, 1087, 1057, 1037, 975, 941, 916, 830, 818, 787, 768, 714, 671, 615, 567, 549, 530, 518, 458, 445, 419. HRMS (ESI, $m/z$) calcd for $C_{19}H_{18}N_2O_2Na_1$ [M+ Na]$^+$: 329.1260, found: 329.1263.

**2-(Naphthalen-2-yl)-1-(1-(*o*-tolyl)-1*H*-imidazol-2-yl)ethanone (115)**

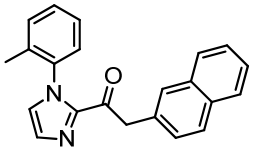

Following the general procedure, the Weinreb amide **178** (0.641 g, 2.8 mmol) was converted to 2-acyl imidazole **115** (0.600 g, 1.84 mmol, 66% yield) as a white solid. $^1$H NMR (300 MHz, $CDCl_3$) $\delta$ 7.83 – 7.73 (m, 4H), 7.49 – 7.40 (m, 3H), 7.39 (d, $J$ = 1.0 Hz, 1H), 7.37 – 7.29 (m, 1H), 7.28 – 7.19 (m, 2H), 7.11 (d, $J$ = 1.0 Hz, 1H), 7.08 (dd, $J$ = 7.7, 1.5 Hz, 1H), 4.65 (d, $J$ = 15.0 Hz, 1H), 4.56 (d, $J$ = 15.0 Hz, 1H), 1.89 (s, 3H). $^{13}$C NMR (75 MHz, $CDCl_3$) $\delta$ 188.3, 143.2, 137.8, 134.4, 133.5, 132.4, 131.9, 130.7, 129.9, 129.0, 128.6, 128.0, 128.0, 127.7, 127.6, 126.8, 126.5, 126.2, 125.9, 125.5, 45.6, 17.1. IR (film): $v$ ($cm^{-1}$) 3115, 2955, 1682, 1550, 1457, 1394, 1311, 1305, 1147, 1023, 964, 911, 867, 795, 760, 747, 709, 675, 632, 621, 568, 540, 518, 480, 454, 404. HRMS (ESI, $m/z$) calcd for $C_{22}H_{18}N_2O_1Na_1$ [M+ Na]$^+$: 349.1311, found: 349.1312.

**1-(1-(*o*-Tolyl)-1*H*-imidazol-2-yl)propan-1-one (116)**

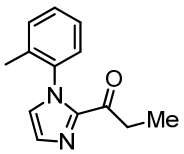

According to the literature[7], *n*-BuLi (2.64 mL, 6.60 mmol, 2.5 M in hexane, 1.10 equiv) was added to a solution of *N*-(*o*-tolyl)-imidazole (0.948 g, 6.00 mmol, 1.0 equiv) in THF (10 mL) at –78°C. The solution was stirred for 30 min, transferred via cannula into propionic anhydride (0.848 g, 6.60 mmol, 1.1 equiv) in THF (4 mL) at –78°C. After 30 min, the reaction mixture was allowed to warm to room temperture and quenched with sodium hydroxide solution (2.0 M, 12 mL) and stirred vigorously for 1 hour. The aqueous phase was extracted with ethyl acetate (3 × 20 mL). The combined organic phases were washed with brine (20 mL), dried over sodium sulfate, and concentrated. The crude product was subjected to a silica gel flash chromatography (EtOAc/*n*-hexane = 1: 2) to afford the 2-acyl imidazole **116** (0.773 g, 3.61 mmol, 60% yield) as a white solid. $^1$H NMR (300 MHz, $CDCl_3$) $\delta$ 7.45 – 7.24 (m, 4H), 7.13 (dd, $J$ = 7.7, 1.3 Hz, 1H), 7.08 (d, $J$ = 1.0 Hz, 1H), 3.36 – 2.97 (m, 2H), 1.99 (s, 3H), 1.13 (t, $J$ = 7.3 Hz, 3H). All spectroscopic data were in agreement with the literature.[45]

## 5.3.4 Synthesis of amines

All substrates were synthesized according to reported procedures with slightly modifications.[46]

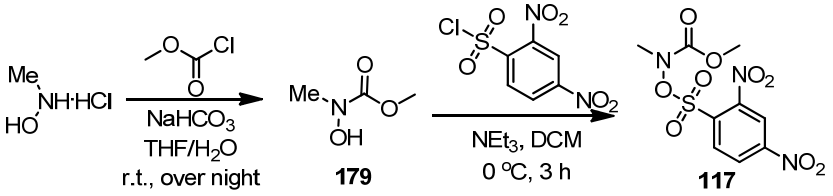


**Methyl hydroxy(methyl)carbamate (179)**

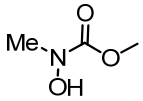

To a stirred suspension of *N*-methylhydroxylamine hydrochloride (2.500 g, 30.1 mmol) in THF (50 mL) and $H_2O$ (5 mL) was added $NaHCO_3$ (5.000 g, 59.5 mmol) and methylchloroformate (2.5 mL, 32.4 mmol). The resulting clear suspension was stirred over night at room temperature, then diluted with $H_2O$ (25 mL) and extracted with $CH_2Cl_2$ (3 × 25 mL). The combined organic extracts were dried ($Na_2SO_4$) and concentrated in *vacuo* to yield the disired compound **179** (2.969 g, 94% yield) as a colorless oil which was used without further purification. $^1$H NMR (300 MHz, $CDCl_3$) $\delta$ 7.94 (s, 1H), 3.72 (s, 3H), 3.19 (s, 3H). All spectroscopic data were in agreement with the literature.[46]

**Methyl ((2,4-dinitrophenyl)sulfonyl)oxy(methyl)carbamate (117)**

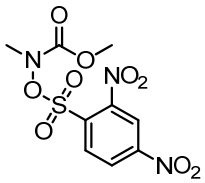

To a stirred solution of methyl hydroxy(methyl)carbamate **179** (1.000 g, 9.5 mmol) in $CH_2Cl_2$ (60 mL) at 0 °C was added $NEt_3$ (1.7 mL, 12.4 mmol) and 2,4-dinitrobenzenesulfonyl chloride (2.666 g, 10.0 mmol). The resulting orange solution was stirred at 0 °C for 3 h, then diluted with 0.5 M aqueous citric acid (30 mL) and extracted with $CH_2Cl_2$ (2 × 30 mL). The combined organic extracts were washed with saturated aqueous $NaHCO_3$ (30 mL) and brine (30 mL), dried ($Na_2SO_4$) and concentrated under reduced pressure. The residue was purified by flash chromatography on silica gel (dichloromethane /*n*-hexane = 1: 1) to give **117** (2.410 g, 7.2 mmol, 76% yield) as a white solid. $^1$H NMR (300 MHz, $CDCl_3$) $\delta$ 8.67 (d, $J$ = 2.2 Hz, 1H), 8.56 (dd, $J$ = 8.7, 2.2 Hz, 1H), 8.42 (d, $J$ = 8.6 Hz, 1H), 3.61 (d, $J$ = 1.3 Hz, 3H), 3.39 (s, 3H). All spectroscopic data were in agreement with the literature.[46]

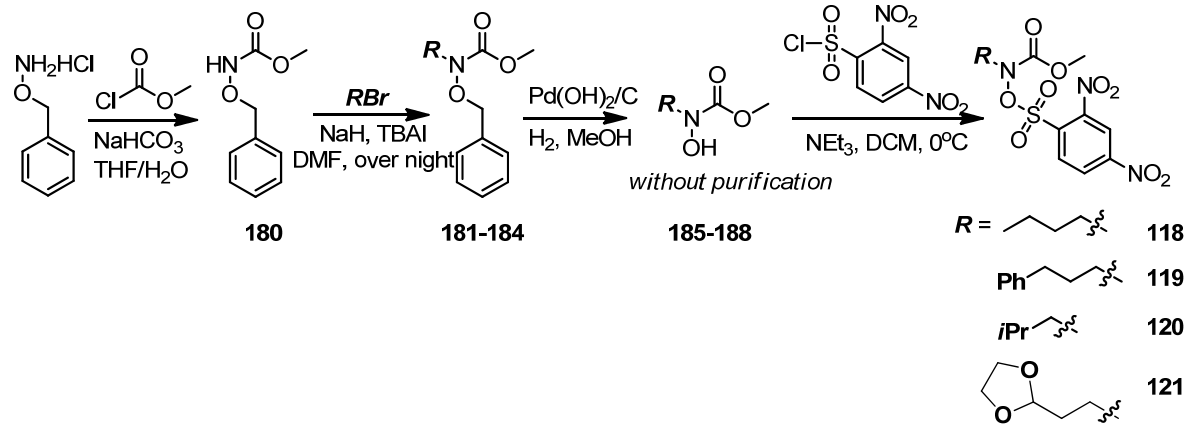


**Methyl benzyloxycarbamate (180)**

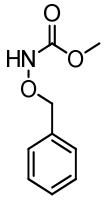

To a stirred suspension of *O*-benzylhydroxylamine hydrochloride (3.800 g, 23.8 mmol) in THF (50 mL) and $H_2O$ (5 mL) was added $NaHCO_3$ (4.000 g, 47.6 mmol) and methylchloroformate (2.0 mL, 26.2 mmol). The resulting clear suspension was stirred over night at room temperature, then diluted with $H_2O$ (20 mL) and extracted with EtOAc (3 × 20 mL). The combined organic extracts were dried ($Na_2SO_4$) and concentrated under reduced pressure to yield the disired compound **180** (4.288 g, > 99% yield) as a colorless oil which was used without further purification. $^1$H NMR (300 MHz, $CDCl_3$) $\delta$ 7.45 – 7.30 (m, 5H), 7.24 (s, 1H), 4.87 (s, 2H), 3.77 (s, 3H). All spectroscopic data were in agreement with the literature.[46]

**Methyl benzyloxy(butyl)carbamate (181)**

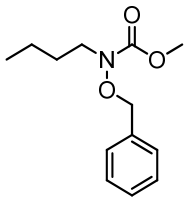

To a stirred solution of methyl benzyloxycarbamate **180** (1.000 g, 5.5 mmol) in DMF (30 mL) at 0 °C was added NaH (60% dispersion in mineral oil, 330 mg, 8.25 mmol). The reaction mixture was stirred for 10 min at 0 °C then 1-butylbromide (0.77 mL, 7.15 mmol) and TBAI (203 mg, 0.55 mmol) were added. The resulting suspension was stirred at room temperature for 4 h before being quenched by the addition of 0.5 M aqueous citric acid (25 mL). The mixture was poured into a separatory funnel and extracted with MTBE (3 × 25 mL). The combined organic extracts were washed with brine (25 mL), dried ($Na_2SO_4$) and concentrated under reduced pressure. The residue was purified by flash chromatography on silica gel (EtOAc/*n*-hexane = 1: 10) to provide the pure title compound **181** (1.204 g, 92% yield) as a colorless oil. $^1$H NMR (300 MHz, $CDCl_3$) $\delta$ 7.48 – 7.29 (m, 5H), 4.85 (s, 2H), 3.78

(s, 3H), 3.50 – 3.37 (m, 2H), 1.67 – 1.47 (m, 2H), 1.40 – 1.24 (m, 2H), 0.90 (t, $J$ = 7.3 Hz, 3H). All spectroscopic data were in agreement with the literature.[46]

**Methyl butyl(((2,4-dinitrophenyl)sulfonyl)oxy)carbamate (118)**

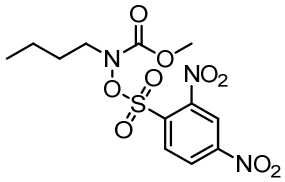

To a solution of methyl benzyloxy(butyl)carbamate **181** (711 mg, 3.0 mmol) in MeOH (24 mL), was added $Pd(OH)_2/C$ (142 mg, 20 wt.%) under nitrogen and the resulting suspension was degassed by bubbling hydrogen (balloon) for 5 min. The mixture was stirred over night at room temperature under hydrogen atmosphere and then filtered directly through a pad of celite. The filter cake was washed with MeOH (10 mL) and the filtrate was concentrated in *vacuo* to give **185** as a colorless oil. The crude product **185** was dissolved in $CH_2Cl_2$ (27 mL), and cooled to 0 °C, then $NEt_3$ (543 µL, 3.9 mmol) and 2,4-dinitrobenzenesulfonyl chloride (880 mg, 3.3 mmol) were added stepwise. The resulting solution was stirred at 0 °C for 30 min, then diluted with 0.5 M aqueous citric acid (20 mL) and extracted with $CH_2Cl_2$ (2 × 20 mL). The combined organic extracts were washed with saturated aqueous $NaHCO_3$ (20 mL) and brine (20 mL), dried ($Na_2SO_4$) and concentrated in *vacuo*. The resultant was purified by flash chromatography on silica gel (EtOAc/*n*-hexane = 1: 8) to provide the pure disired compound **118** (964 mg, 85% yield) as a pale yellow solid. $^1$H NMR (300 MHz, $CDCl_3$) $\delta$ 8.66 (d, $J$ = 2.2 Hz, 1H), 8.56 (dd, $J$ = 8.6, 2.2 Hz, 1H), 8.40 (d, $J$ = 8.6 Hz, 1H), 3.69 (t, $J$ = 7.5 Hz, 2H), 3.61 (s, 3H), 1.72 – 1.62 (m, 2H), 1.40 – 1.27 (m, 2H), 0.94 (t, $J$ = 7.3 Hz, 3H). All spectroscopic data were in agreement with the literature.[46]

**Methyl benzyloxy(3-phenylpropyl)carbamate (182)**

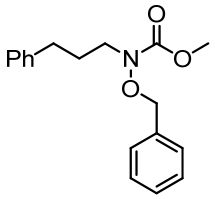

To a stirred solution of methyl benzyloxycarbamate **180** (1.000 g, 5.5 mmol) in DMF (19 mL) at 0 °C was added NaH (60% dispersion in mineral oil, 330 mg, 8.25 mmol). The reaction mixture was stirred for 10 min at 0 °C then (3-bromopropyl)benzene (1.20 mL, 7.7 mmol) and TBAI (408 mg, 1.10 mmol) were added stepwise. The resulting suspension was stirred at room temperature for 3 h before being quenched by the addition of 0.5 M aqueous citric acid (25 mL). The mixture was poured into a separatory funnel and extracted with MTBE (3 × 25 mL). The combined organic extracts were washed with brine (25 mL), dried ($Na_2SO_4$) and concentrated under reduced pressure. The residue was purified by flash chromatography on silica gel (EtOAc/*n*-hexane = 1: 8) to provide the pure disired compound

**182** (1.457 g, 88% yield) as a colorless oil. $^1$H NMR (300 MHz, $CDCl_3$) $\delta$ 7.43 – 7.31 (m, 5H), 7.31 – 7.23 (m, 2H), 7.23 – 7.13 (m, 3H), 4.79 (s, 2H), 3.78 (s, 3H), 3.59 – 3.40 (m, 2H), 2.71 – 2.55 (m, 2H), 2.04 – 1.79 (m, 2H) (Contained the minor rotamer). All spectroscopic data were in agreement with the literature.[46]

**Methyl ((2,4-dinitrophenyl)sulfonyl)oxy(3-phenylpropyl)carbamate (119)**

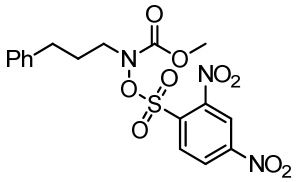

To a solution of methyl benzyloxy(butyl)carbamate **182** (1.457 g, 4.87 mmol) in MeOH (16 mL), was added $Pd(OH)_2$/C (291 mg, 20 wt.%) under nitrogen and the resulting suspension was degassed by bubbling hydrogen (balloon) for 5 minutes. The mixture was stirred over night at room temperature under hydrogen atmosphere and then filtered directly through a pad of celite. The filter cake was washed with MeOH (10 mL) and the filtrate was concentrated in *vacuo* to give **186** as a colorless oil. The crude product **186** was dissolved in $CH_2Cl_2$ (10 mL), cooled to 0 °C, then $NEt_3$ (880 µL, 6.3 mmol) and 2,4-dinitrobenzenesulfonyl chloride (1.560 g, 5.84 mmol) were added stepwise. The resulting solution was stirred at 0 °C for 40 min, then diluted with 0.5 M aqueous citric acid (30 mL) and extracted with $CH_2Cl_2$ (2 × 30 mL). The combined organic extracts were washed with saturated aqueous $NaHCO_3$ (30 mL) and brine (30 mL), dried ($Na_2SO_4$) and concentrated in *vacuo*. The resultant was purified by flash chromatography on silica gel (EtOAc/*n*-hexane = 1: 10 to 1: 5) to provide the pure disired compound **119** (1.905 g, 89% yield) as a pale yellow oil. $^1$H NMR (300 MHz, $CDCl_3$) $\delta$ 8.60 (d, $J$ = 2.2 Hz, 1H), 8.52 (dd, $J$ = 8.6, 2.2 Hz, 1H), 8.36 (d, $J$ = 8.7 Hz, 1H), 7.33 – 7.06 (m, 5H), 3.63 (s over m, 5H), 2.64 (t, $J$ = 7.6 Hz, 2H), 2.06 – 1.96 (m, 2H) (Contained the minor rotamer). All spectroscopic data were in agreement with the literature.[46]

**Methyl benzyloxy(isobutyl)carbamate (183)**

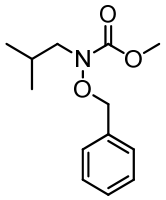

To a stirred solution of methyl benzyloxycarbamate **180** (1.000 g, 5.52 mmol) in DMF (19 mL) at 0 °C was added NaH (60% dispersion in mineral oil, 330 mg, 8.25 mmol). The reaction mixture was stirred for 10 min at 0 °C then 1-bromo-2-methylpropane (840 µL, 7.73 mmol) and TBAI (408 mg, 1.10 mmol) were added. The resulting suspension was stirred at 60°C over night before being quenched by the addition of 0.5 M aqueous citric acid (25 mL). The mixture was poured into a separatory funnel and extracted with MTBE (3 × 25 mL). The combined organic extracts were washed

with brine (25 mL), dried ($Na_2SO_4$) and concentrated under reduced pressure. The residue was purified by flash chromatography on silica gel (EtOAc/*n*-hexane = 1: 4) to provide the pure disired compound **183** (1.010 g, 77% yield) as a colorless oil. $^1$H NMR (300 MHz, $CDCl_3$) $\delta$ 7.45 – 7.28 (m, 5H), 4.86 (s, 2H), 3.78 (s, 3H), 3.29 (d, $J$ = 7.3 Hz, 2H), 2.11 – 1.98 (m, 1H), 0.91 (d, $J$ = 6.7 Hz, 6H). $^{13}$C NMR (75 MHz, $CDCl_3$) $\delta$ 157.8, 135.5, 129.2, 128.5, 128.4, 76.8, 56.9, 52.9, 26.6, 20.0. IR (film): $\nu$ ($cm^{-1}$) 3032, 2956, 2872, 1703, 1497, 1448, 1376, 1330, 1250, 1193, 1154, 1124, 1066, 982, 911, 852, 805, 747, 697, 622, 546, 499, 386. HRMS (ESI, *m*/*z*) calcd for $C_{13}H_{19}N_1O_3Na$ $[M+Na]^+$: 260.1257, found: 260.1258.

**Methyl ((2,4-dinitrophenyl)sulfonyl)oxy(isobutyl)carbamate (120)**

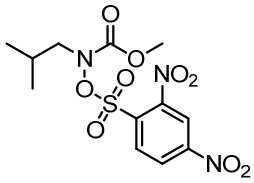

To a solution of methyl benzyloxy(butyl)carbamate **183** (948 mg, 4.00 mmol) in MeOH (32 mL), was added $Pd(OH)_2$/C (190 mg, 20 wt.%) under nitrogen and the resulting suspension was degassed by bubbling hydrogen (balloon) for 5 minutes. The mixture was stirred over night at room temperature under hydrogen atmosphere and then filtered directly through a pad of celite. The filter cake was washed with MeOH (10 mL) and the filtrate was concentrate in *vacuo* to give **187** as a colorless oil. The crude product **187** was dissolved in $CH_2Cl_2$ (8 mL), cooled to 0 °C, then $NEt_3$ (720 µL, 5.20 mmol) and 2,4-dinitrobenzenesulfonyl chloride (1.280 g, 4.80 mmol) were added stepwise. The resulting solution was stirred at 0 °C for 40 min, then diluted with 0.5 M aqueous citric acid (20 mL) and extracted with $CH_2Cl_2$ (2 × 20 mL). The combined organic extracts were washed with saturated aqueous $NaHCO_3$ (20 mL) and brine (20 mL), dried ($Na_2SO_4$) and concentrated in *vacuo*. The resultant yellow solid was purified by flash chromatography on silica gel (EtOAc/*n*-hexane = 1: 10 to 1: 5) to provide the pure disired compound **120** (1.186 g, 79% yield) as a white solid. $^1$H NMR (300 MHz, $CDCl_3$) $\delta$ 8.66 (d, $J$ = 2.2 Hz, 1H), 8.56 (dd, $J$ = 8.7, 2.2 Hz, 1H), 8.40 (d, $J$ = 8.7 Hz, 1H), 3.60 (s, 3H), 3.56 (d, $J$ = 7.3 Hz, 2H), 2.25 – 2.11 (m, 1H), 0.94 (d, $J$ = 6.7 Hz, 6H). $^{13}$C NMR (75 MHz, $CDCl_3$) $\delta$ 156.7, 151.0, 149.0, 134.2, 133.6, 126.2, 120.1, 60.6, 54.1, 26.1, 19.8. IR (film): $\nu$ ($cm^{-1}$) 3113, 2990, 1722, 1606, 1568, 1538, 1472, 1443, 1403, 1389, 1376, 1343, 1330, 1306, 1268, 1189, 1167, 1130, 1100, 1017, 972, 953, 918, 903, 880, 842, 831, 790, 757, 744, 732, 662, 651, 626, 612, 591, 549, 515, 471, 456, 390. HRMS (ESI, *m*/*z*) calcd for $C_{12}H_{15}N_3O_9S_1Na_1$ $[M+Na]^+$: 400.0421, found: 400.0424.

**Methyl (2-(1,3-dioxolan-2-yl)ethyl)(benzyloxy)carbamate (184)**

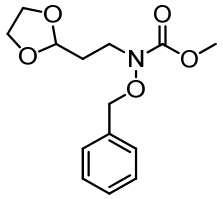

To a stirred solution of methyl benzyloxycarbamate **180** (543 mg, 3.00 mmol) in DMF (12 mL) at 0 °C was added NaH (60% dispersion in mineral oil, 180 mg, 4.50 mmol). The reaction mixture was stirred for 10 min at 0 °C then 2-(2-bromoethyl)-1,3-dioxolane (493 μL, 4.20 mmol) and TBAI (220 mg, 0.60 mmol) were added. The resulting suspension was stirred at 60°C over night before being quenched by the addition of 0.5 M aqueous citric acid (15 mL). The mixture was poured into a separatory funnel and extracted with MTBE (3 × 15 mL). The combined organic extracts were washed with brine (15 mL), dried ($Na_2SO_4$) and concentrated under reduced pressure. The residue was purified by flash chromatography on silica gel (EtOAc/*n*-hexane = 1: 4) to provide the pure disired compound **184** (694 mg, 82% yield) as a colorless oil. $^1$H NMR (300 MHz, $CDCl_3$) $\delta$ 7.45 – 7.29 (m, 5H), 4.91 (t, $J$ = 4.6 Hz, 1H), 4.86 (s, 2H), 3.98 – 3.89 (m, 2H), 3.88 – 3.79 (m, 2H), 3.78 (s, 3H), 3.64 – 3.55 (m, 2H), 2.03 – 1.92 (m, 2H). $^{13}$C NMR (75 MHz, $CDCl_3$) $\delta$ 157.8, 135.4, 129.2, 128.5, 128.4, 102.6, 77.1, 64.9, 53.1, 45.2, 31.2. IR (film): $\nu$ ($cm^{-1}$) 2954, 2881, 1705, 1497, 1450, 1364, 1286, 1260, 1206, 1137, 1112, 1047, 943, 894, 853, 749, 698, 620, 499, 385. HRMS (ESI, *m*/*z*) calcd for $C_{14}H_{19}N_1O_5Na_1$ [M+ Na]$^+$: 304.1155, found: 304.1157.

**Methyl (2-(1,3-dioxolan-2-yl)ethyl)(((2,4-dinitrophenyl)sulfonyl)oxy)carbamate (121)**

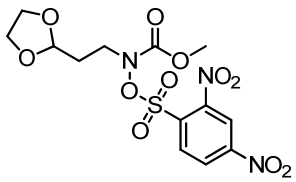

To a solution of methyl benzyloxy(butyl)carbamate **184** (650 mg, 2.31 mmol) in MeOH (18 mL), was added $Pd(OH)_2$/C (130 mg, 20 wt.%) under nitrogen and the resulting suspension was degassed by bubbling hydrogen (balloon) for 5 minutes. The mixture was stirred over night at room temperature under hydrogen atmosphere and then filtered directly through a pad of celite. The filter cake was washed with MeOH (10 mL) and the filtrate was concentrate in *vacuo* to give **188** as a colorless oil. The crude product **188** was dissolved in $CH_2Cl_2$ (21 mL), cooled to 0 °C, then $NEt_3$ (420 μL, 3.00 mmol) and 2,4-dinitrobenzenesulfonyl chloride (648 mg, 2.43 mmol) were added stepwise. The resulting solution was stirred at 0 °C for 60 min, then diluted with 0.5 M aqueous citric acid (20 mL) and extracted with $CH_2Cl_2$ (2 × 20 mL). The combined organic extracts were washed with saturated aqueous $NaHCO_3$ (20 mL) and brine (20 mL), dried ($Na_2SO_4$) and concentrated in *vacuo*. The resultant yellow solid was purified by flash chromatography on silica gel (EtOAc/*n*-hexane = 1: 3) to provide the pure disired compound **121** (920 mg, 95% yield) as a pale yellow solid. $^1$H NMR (300 MHz, $CDCl_3$) $\delta$ 8.65 (d, $J$ = 2.2 Hz, 1H), 8.55 (dd, $J$ = 8.6, 2.2 Hz, 1H), 8.40 (d, $J$ = 8.7 Hz, 1H), 4.93

(t, $J$ = 4.3 Hz, 1H), 3.99 – 3.91 (m, 2H), 3.90 – 3.76 (m, 4H), 3.61 (s, 3H), 2.06 (td, $J$ = 7.3, 4.3 Hz, 2H). $^{13}$C NMR (75 MHz, $CDCl_3$) $\delta$ 156.5, 151.0, 149.0, 134.4, 133.2, 126.2, 120.1, 101.9, 65.0, 54.3, 49.0, 29.9. IR (film): $\nu$ (cm$^{-1}$) 3114, 2966, 2872, 1736, 1604, 1559, 1541, 1475, 1446, 1428, 1401, 1389, 1337, 1305, 1288, 1244, 1225, 1194, 1130, 1106, 1060, 1016, 1000, 973, 946, 906, 892, 840, 833, 804, 770, 752, 736, 707, 684, 658, 633, 609, 576, 564, 535, 469, 440, 423, 395, 381. HRMS (ESI, $m/z$) calcd for $C_{13}H_{15}N_3O_{11}S_1Na_1$ [M+ Na]$^+$: 444.0320, found: 444.0323.

## 5.4 Application for Asymmetric Lewis Acids Catalysis

### 5.4.1 Asymmetric conjugate additions by chiral Lewis acids

#### 5.4.1.1 Asymmetric Friedel-Crafts alkylations

**(*S*)-3-(1*H*-Indol-3-yl)-1-(1-methyl-1*H*-imidazol-2-yl)butan-1-one (36)**

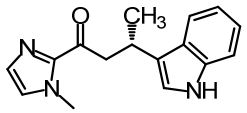


To a solution of catalyst Λ-**IrS** (1.9 mg, 0.002 mmol, 1 mol%) in distilled, anhydrous THF (0.2 mL) in a glass vial was added 2-acyl imidazole **31** (30.2 mg, 0.20 mmol). After being stirred at room temperature for 20 min, 1*H*-indole (58.6 mg, 0.50 mmol) was added at room temperature. The reaction mixture was stirred for the indicated time (monitored by TLC) under argon atmosphere. Afterwards, the mixture was concentrated under reduced pressure. The residue was purified by flash chromatography on silica gel (EtOAc/*n*-hexane = 1: 2 to 1: 1) to give (*S*)-**36** as a white solid (25 °C, 40 h, 50.2 mg, 94% yield, 99% ee). Enantiomeric excess was established by HPLC analysis using a Chiralpak AD-H column (HPLC: AD-H, 254 nm, *n*-hexane/isopropanol = 90: 10, flow rate 0.80 mL/min, 40 °C, $t_r$ (major) = 49.0 min, $t_r$ (minor) = 38.5 min). $[\alpha]_D^{25}$ = –11.3° (*c* 0.8, $CH_2Cl_2$) (Lit.[14] $[\alpha]_D^{20}$ = –14.5° (*c* 2.7, $CH_2Cl_2$) for 96% ee of product with *S*-configuration). $^1$H NMR (300 MHz, $CDCl_3$) $\delta$ 8.81 (br s, 1H), 7.67 (d, $J$ = 7.7 Hz, 1H), 7.30 (d, $J$ = 7.6 Hz, 1H), 7.22 – 7.18 (m, 1H), 7.17 – 7.05 (m, 2H), 6.99 (s, 1H), 6.98 – 6.95 (m, 1H), 3.93 (s, 3H), 3.91 – 3.79 (m, 1H), 3.58 (dd, $J$ = 16.0, 6.2 Hz, 1H), 3.50 (dd, $J$ = 16.0, 8.4 Hz, 1H), 1.42 (d, $J$ = 6.9 Hz, 3H). All spectroscopic data are in agreement with the literature.[14]

**(*S*)-3-(4-(Dimethylamino)-2-methoxyphenyl)-1-(1-methyl-1*H*-imidazol-2-yl)butan-1-one (37)**

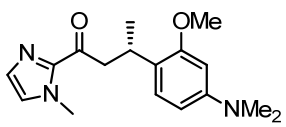


To a solution of catalyst Λ-**IrO** (3.7 mg, 0.004 mmol, 2 mol%) or Λ-**IrS** (3.8 mg, 0.004 mmol, 2 mol%) in distilled, anhydrous THF (0.1 – 0.2 mL) was added the 2-acyl imidazole **31** (30.0 mg, 0.20

mmol) in a Schlenk tube. After being stirred at room temperature for 20 min, 3-methoxy-*N*,*N*-dimethylaniline (90.6 mg, 88.0 μL, 0.6 mmol) was added at room temperature. The reaction mixture was stirred for the indicated time (monitored by TLC) under nitrogen atmosphere. Afterwards, the mixture was concentrated under reduced pressure. The residue was purified by flash chromatography on silica gel (EtOAc/*n*-hexane = 1: 2 to 1: 1) to afford the product (*S*)-**37** as a colorless oil (catalyzed by Λ-**IrO**: 1.0 M for **31**, 25 °C, 20 h, 59.0 mg, 98% yield, 94% ee; catalyzed by Λ-**IrS**: 2.0 M for **31**, 25 °C, 66 h, 58.0 mg, 97% yield, >99% ee). Enantiomeric excess established by HPLC analysis using a Chiralpak AD-H column (HPLC: AD-H, 254 nm, *n*-hexane/isopropanol = 90:10, flow rate 0.8 mL/min, 25 °C, $t_r$ (major) = 15.6 min, $t_r$ (minor) = 13.5 min). $[\alpha]_D^{25}$ = –3.0° (*c* 0.5, $CH_2Cl_2$). $^1$H NMR (300 MHz, $CDCl_3$) $\delta$ 7.13 – 7.07 (m, 2H), 6.97 (s, 1H), 6.32 – 6.23 (m, 2H), 3.93 (s, 3H), 3.80 (s, 3H), 3.78 – 3.68 (m, 1H), 3.50 – 3.30 (m, 2H), 2.91 (s, 6H), 1.25 (d, *J* = 6.9 Hz, 3H). $^{13}$C NMR (75 MHz, $CDCl_3$) $\delta$ 192.6, 157.7, 150.4, 143.6, 128.8, 127.5, 126.7, 123.2, 105.0, 96.8, 55.3, 45.9, 40.9 (2C), 36.1, 28.6, 21.1. IR (film): $\nu$ ($cm^{-1}$) 2956, 2837, 2800, 1671, 1612, 1567, 1513, 1459, 1404, 1351, 1288, 1234, 1188, 1125, 1092, 1032, 980, 911, 867, 813, 773, 694, 641, 606, 553, 512, 471. HRMS (ESI, *m*/*z*) calcd for $C_{17}H_{24}N_3O_2$ $[M+H]^+$: 302.1863, found: 302.1863.

**(*S*)-3-(5-Methoxyfuran-2-yl)-1-(1-methyl-1*H*-imidazol-2-yl)butan-1-one (38)**

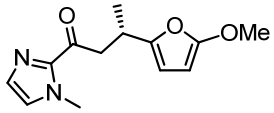


To a solution of catalyst Λ-**IrO** (2.8 mg, 0.003 mmol, 1 mol%) or Λ-**IrS** (2.9 mg, 0.003 mmol, 1 mol%) in distilled, anhydrous THF (0.3 mL) was added 2-acyl imidazole **31** (45.0 mg, 0.30 mmol) in a Schlenk tube. After being stirred at room temperature for 20 min, 2-methoxyfuran (88.3 mg, 82.9 μL, 0.9 mmol) was added at room temperature. The reaction mixture was stirred for the indicated time (monitored by TLC) under nitrogen atmosphere. Afterwards, the mixture was concentrated under reduced pressure. The residue was purified by flash chromatography on silica gel (EtOAc/*n*-hexane = 1: 2 to 1: 1) to afford the product (*S*)-**38** as a colorless oil (catalyzed by Λ-**IrO**: 25 °C, 20 h, 67.8 mg, 91% yield, 94% ee; catalyzed by Λ-**IrS**: 25 °C, 36 h, 66.4 mg, 89% yield, 94% ee). Enantiomeric excess established by HPLC analysis using a Chiralpak IC column (HPLC: IC, 254 nm, *n*-hexane/isopropanol = 85:15, flow rate 0.5 mL/min, 40 °C, $t_r$ (major) = 26.8 min, $t_r$ (minor) = 24.6 min). $[\alpha]_D^{25}$ = –3.3° (*c* 1.1, $CH_2Cl_2$) for 94% ee (Lit.[18] $[\alpha]_D^{25}$ = +4.1° (*c* 1.7, $CH_2Cl_2$) for 98% ee of product with *S*-configuration). $^1$H NMR (300 MHz, $CDCl_3$) δ 7.17 (d, *J* = 1.0 Hz, 1H), 7.05 (d, *J* = 0.9 Hz, 1H), 6.04 – 5.95 (m, 1H), 5.88 (dd, *J* = 11.5, 0.7 Hz, 1H), 4.00 (s, 3H), 3.71 (s, 3H), 3.66 – 3.52 (m, 1H), 3.31 (dd, *J* = 5.2, 4.2 Hz, 1H), 2.17 – 2.06 (m, 1H), 1.29 (d, *J* = 6.4 Hz, 3H). All spectroscopic data are in agreement with the literature.[18]

**(*S*)-1-(1-Methyl-1*H*-imidazol-2-yl)-3-(1*H*-pyrrol-2-yl)butan-1-one (39)**

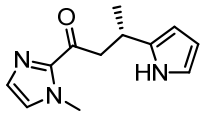

To a solution of catalyst Λ-**IrO** (3.7 mg, 0.004 mmol, 2 mol%) or Λ-**IrS** (3.8 mg, 0.004 mmol, 2 mol%) in distilled, anhydrous THF (0.2 mL) was added 2-acyl imidazole **31** (30.0 mg, 0.20 mmol) in a Schlenk tube. After being stirred at room temperature for 20 min, 1*H*-pyrrole (201.0 mg, 208.1 μL, 3.0 mmol) was added at room temperature. The reaction mixture was stirred for the indicated time (monitored by TLC) under nitrogen atmosphere. Afterwards, the mixture was concentrated under reduced pressure. The residue was purified by flash chromatography on silica gel (EtOAc/*n*-hexane = 1: 2 to 1: 1) to afford the product (*S*)-**39** as a white solid (catalyzed by Λ-**IrO**: 25 °C, 20 h, 35.1 mg, 81% yield, 95% ee; catalyzed by Λ-**IrS**: 25 °C, 22 h, 38.6 mg, 89% yield, 94% ee). Enantiomeric excess established by HPLC analysis using a Chiralpak OD-H column (HPLC: OD-H, 254 nm, *n*-hexane/isopropanol = 97:3, flow rate 0.8 mL/min, 25 °C, $t_r$ (major) = 27.5 min, $t_r$ (minor) = 26.0 min). $[\alpha]_D^{25}$ = +77.5° (*c* 0.4, $CH_2Cl_2$) for 94% ee (Lit.[47] $[\alpha]_D^{25}$ = –66.8° (*c* 1.2, $CH_2Cl_2$) for 87% ee of product with *R*-configuration). $^1$H NMR (300 MHz, $CDCl_3$) $\delta$ 8.86 (brs, 1H), 7.13 (d, *J* = 0.7 Hz, 1H), 7.01 (s, 1H), 6.66 (dd, *J* = 4.1, 2.6 Hz, 1H), 6.09 (dd, *J* = 5.9, 2.8 Hz, 1H), 5.95 (m, 1H), 3.99 (s, 3H), 3.58 – 3.45 (m, 2H), 3.33 (m, 1H), 1.38 (d, *J* = 6.8 Hz, 3H). All spectroscopic data are in agreement with the literature.[47]

**(*R*)-3-(4-(Dimethylamino)-2-methoxyphenyl)-1-(1-methyl-1*H*-imidazol-2-yl)-3-phenylpropan-1-one (40)**

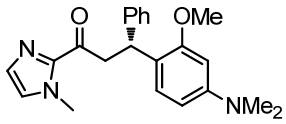

To a solution of catalyst Λ-**IrS** (3.8 mg, 0.004 mmol, 2 mol%) in distilled, anhydrous THF (0.1 mL) was added the 2-acyl imidazole **32** (42.4 mg, 0.20 mmol) in a Schlenk tube. After being stirred at room temperature for 20 min, 3-methoxy-*N*,*N*-dimethylaniline (90.6 mg, 88.0 μL, 0.6 mmol) was added at room temperature. The reaction mixture was stirred 40 °C for 18 h under nitrogen atmosphere. Afterwards, the mixture was concentrated under reduced pressure. The residue was purified by flash chromatography on silica gel (EtOAc/*n*-hexane = 1: 2 to 1: 1) to afford the product (*R*)-**40** as a colorless oil (72.5 mg, 99% yield, 99% ee). Enantiomeric excess established by HPLC analysis using a Chiralpak AD-H column (HPLC: AD-H, 254 nm, *n*-hexane/isopropanol = 90: 10, flow rate 1.0 mL/min, 25 °C, $t_r$ (major) = 18.6 min, $t_r$ (minor) = 23.4 min). $[\alpha]_D^{25}$ = +15.4° (*c* 0.9, $CH_2Cl_2$). $^1$H NMR (300 MHz, $CDCl_3$) $\delta$ 7.37 – 7.29 (m, 2H), 7.24 – 7.18 (m, 2H), 7.15 – 7.03 (m, 3H), 6.94 (d, *J* = 0.9 Hz, 1H), 6.32 – 6.19 (m, 2H), 5.07 (t, *J* = 7.8 Hz, 1H), 3.96 (dd, *J* = 17.2, 8.3 Hz, 1H), 3.88 (s, 3H), 3.79 (dd, *J* = 17.2, 8.3 Hz, 1H), 3.77 (s, 3H), 2.90 (s, 6H). $^{13}$C NMR (75 MHz, $CDCl_3$) $\delta$ 191.5, 157.8, 150.5, 144.9, 143.5, 128.9 (2C), 128.5, 128.1 (3C), 126.7, 125.7, 121.5, 104.9, 96.9, 55.5, 44.0, 40.9

(2C), 38.7, 36.1. IR (film): $\nu$ ($cm^{-1}$) 2993, 2904, 1672, 1611, 1561, 1514, 1491, 1469, 1452, 1441, 1406, 1356, 1290, 1240, 1206, 1195, 1184, 1172, 1154, 1116, 1075, 1052, 1032, 986, 955, 915, 868, 860, 844, 814, 799, 779, 739, 697, 687, 642, 561, 537, 510, 497, 465, 383. HRMS (ESI, *m*/*z*) calcd for $C_{22}H_{26}N_3O_2$ $[M+H]^+$: 364.2020, found: 364.2021.

**(*S*)-Ethyl**

**2-(4-(dimethylamino)-2-methoxyphenyl)-4-(1-methyl-1*H*-imidazol-2-yl)-4-oxobutanoate (41)**

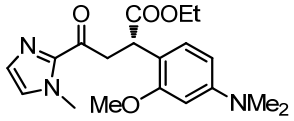


To a solution of catalyst Λ-**IrS** (3.8 mg, 0.004 mmol, 2 mol%) in distilled, anhydrous THF (0.1 mL) was added the 2-acyl imidazole **33** (41.6 mg, 0.20 mmol) in a Schlenk tube. After being stirred at room temperature for 20 min, 3-methoxy-*N*,*N*-dimethylaniline (90.6 mg, 88.0 μL, 0.6 mmol) was added at room temperature. The reaction mixture was stirred 40 °C for 24 h under nitrogen atmosphere. Afterwards, the mixture was concentrated under reduced pressure. The residue was purified by flash chromatography on silica gel (EtOAc/*n*-hexane = 1: 2) to afford the product (*S*)-**41** as a colorless oil (68.1 mg, 95% yield, 99% ee). Enantiomeric excess established by HPLC analysis using a Chiralpak AD-H column (HPLC: AD-H, 254 nm, hexane/isopropanol = 90:10, flow rate 1.0 mL/min, 25 °C, $t_r$ (major) = 18.1 min, $t_r$ (minor) = 13.0 min). $[\alpha]_D^{25}$ = +108.9° (*c* 0.7, $CH_2Cl_2$). $^1$H NMR (300 MHz, $CDCl_3$) $\delta$ 7.09 (d, *J* = 1.0 Hz, 1H), 7.05 (d, *J* = 8.3 Hz, 1H), 6.98 (d, *J* = 0.9 Hz, 1H), 6.33 – 6.18 (m, 2H), 4.49 (dd, *J* = 9.9, 4.4 Hz, 1H), 4.13 (q, *J* = 7.1 Hz, 2H), 4.07 – 3.97 (m, 1H), 3.96 (s, 3H), 3.79 (s, 3H), 3.30 (dd, *J* = 18.2, 4.4 Hz, 1H), 2.93 (s, 6H), 1.18 (t, *J* = 7.1 Hz, 3H). $^{13}$C NMR (75 MHz, $CDCl_3$) $\delta$ 191.3, 174.3, 157.8, 151.2, 143.1, 129.2, 129.1, 126.7, 115.8, 105.0, 96.6, 60.7, 55.5, 42.2, 40.9 (2C), 39.9, 36.1, 14.3. IR (film): $\nu$ ($cm^{-1}$) 2938, 2804, 1726, 1674, 1612, 1568, 1516, 1462, 1407, 1353, 1288, 1236, 1157, 1107, 1030, 981, 913, 848, 811, 773, 687, 641, 530, 496, 469. HRMS (ESI, *m*/*z*) calcd for $C_{19}H_{26}N_3O_4$ $[M+H]^+$: 360.1918, found: 360.1929.

**(*S*)-3-(4-(Dimethylamino)-2-methoxyphenyl)-1-(1-methyl-1*H*-imidazol-2-yl)heptan-1-one (42)**

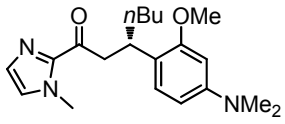


To a solution of catalyst Λ-**IrS** (3.8 mg, 0.004 mmol, 2 mol%) in distilled, anhydrous THF (0.1 mL) was added the 2-acyl imidazole **34** (38.4 mg, 0.20 mmol) in a Schlenk tube. After being stirred at room temperature for 20 min, 3-methoxy-*N*,*N*-dimethylaniline (90.6 mg, 88.0 μL, 0.6 mmol) was added at room temperature. The reaction mixture was stirred at 40 °C for 48 h under nitrogen atmosphere. Afterwards, the mixture was concentrated under reduced pressure. The residue was purified by flash chromatography on silica gel (EtOAc/*n*-hexane = 1: 2) to afford the product (*S*)-**42** as a colorless oil

(55.8 mg, 81% yield, 96% ee). Enantiomeric excess established by HPLC analysis using a Chiralpak IC column (HPLC: IC, 254 nm, hexane/isopropanol = 70:30, flow rate 1.0 mL/min, 25 °C, $t_r$ (major) = 8.3 min, $t_r$ (minor) = 12.4 min). $[\alpha]_D^{25}$ = +3.2° (*c* 0.7, $CH_2Cl_2$). $^1$H NMR (300 MHz, $CDCl_3$) $\delta$ 7.09 (d, *J* = 0.9 Hz, 1H), 7.03 (d, *J* = 8.2 Hz, 1H), 6.94 (d, *J* = 0.9 Hz, 1H), 6.33 – 6.18 (m, 2H), 3.89 (s, 3H), 3.78 (s, 3H), 3.68 – 3.55 (m, 1H), 3.52 – 3.29 (m, 2H), 2.90 (s, 6H), 1.80 – 1.48 (m, 2H), 1.32 – 1.13 (m, 4H), 0.80 (t, *J* = 6.9 Hz, 3H). $^{13}$C NMR (75 MHz, $CDCl_3$) $\delta$ 192.8, 158.4, 150.2, 143.7, 128.8, 128.6, 126.5, 121.8, 105.1, 97.0, 55.5, 44.9, 40.9 (2C), 36.1, 35.4, 34.2, 29.8, 22.9, 14.1. IR (film): $\nu$ ($cm^{-1}$) 2952, 2926, 2855, 2798, 1671, 1612, 1567, 1513, 1461, 1439, 1403, 1349, 1287, 1235, 1203, 1180, 1152, 1124, 1108, 1078, 1059, 1034, 978, 914, 812, 779, 733, 693, 642, 505, 470. HRMS (ESI, *m*/*z*) calcd for $C_{20}H_{30}N_3O_2$ $[M+H]^+$: 344.2333, found: 344.2340.

### 5.4.1.2 Asymmetric Michael additions

**(*S*)-2-(4-(1-Methyl-1*H*-imidazol-2-yl)-4-oxobutan-2-yl)malononitrile (43)**

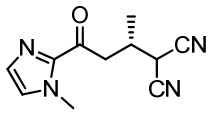


To a solution of catalyst Λ-**IrO** (1.8 mg, 0.002 mmol, 1 mol%) or Λ-**IrS** (1.9 mg, 0.002 mmol, 1 mol%) in distilled, anhydrous THF (0.4 mL) was added 2-acyl imidazole **31** (30.2 mg, 0.20 mmol) in a Schlenk tube. After being stirred at room temperature for 20 min, malononitrile (15.8 mg, 0.24 mmol) was added at room temperature. The reaction mixture was stirred at 25 °C for the indicated time (monitored by TLC) under nitrogen atmosphere. Afterwards, the mixture was concentrated under reduced pressure. The residue was purified by flash chromatography on silica gel (EtOAc/*n*-hexane = 1: 2 to 1: 1) to afford the product (*S*)-**43** as a colorless oil (catalyzed by Λ-**IrO**: 16 h, 41.5 mg, 96% yield, 88% ee; catalyzed by Λ-**IrS**: 24 h, 40.9 mg, 95% yield, 90% ee). Enantiomeric excess established by HPLC analysis using a Chiralpak AD-H column (254 nm, hexane/isopropanol = 90:10, flow rate 1.0 mL/min, 25 °C, $t_r$ (major) = 23.0 min, $t_r$ (minor) = 21.8 min). $[\alpha]_D^{25}$ = +30.0° (*c* 0.4, $CH_2Cl_2$) for 90% ee of the product (Lit.[15] $[\alpha]_D^{20}$ = –33.2°, *c* 0.4, $CH_2Cl_2$) for 92% ee of product with *R*-configuration). It is worth noting that 97% ee of (*S*)-**22** (albeit reduced yield of just 43% yield) can be obtained when malononitrile reacts instead with 2 equivalents of 2-acyl imidazole **11** catalyzed by Λ-**IrO** under otherwise identical conditions. $^1$H NMR (300 MHz, $CDCl_3$) $\delta$ 7.15 (s, 1H), 7.08 (s, 1H), 4.37 (d, *J* = 4.9 Hz, 1H), 3.99 (s, 3H), 3.47 (dd, *J* = 18.0, 5.3 Hz, 1H), 3.28 (dd, *J* = 18.0, 8.2 Hz, 1H), 2.89-2.71 (m, 1H), 1.36 (d, *J*= 6.9 Hz, 3H). All spectroscopic data were in agreement with the literature.[15]

**(*S*)-2,2-Dimethyl-5-(4-(1-methyl-1*H*-imidazol-2-yl)-4-oxobutan-2-yl)-1,3-dioxane-4,6-dione (44)**

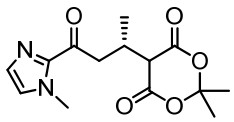

To a solution of catalyst Λ-**IrO** (3.7 mg, 0.004 mmol, 2 mol%) or Λ-**IrS** (3.8 mg, 0.004 mmol, 2 mol%) in distilled, anhydrous THF (0.2 mL) was added 2-acyl imidazole **31** (30.2 mg, 0.20 mmol) in a Schlenk tube. After being stirred at room temperature for 20 min, 2,2-dimethyl- 1,3-dioxane-4,6-dione (86.5 mg, 0.6 mmol) was added at room temperature. The reaction mixture was stirred at 25 °C for 6 h under nitrogen atmosphere. Afterwards, the mixture was concentrated under reduced pressure. The residue was purified by flash chromatography on silica gel (EtOAc/*n*-hexane = 1: 2 to 1: 1) to afford the product (*S*)-**44** as a white solid (catalyzed by Λ-**IrO**: 54.5 mg, 93% yield, 81% ee; catalyzed by Λ-**IrS**: 55.3 mg, 94% yield, 91% ee). Enantiomeric excess established by HPLC analysis using a Chiralpak AD-H column (254 nm, hexane/isopropanol = 90:10, flow rate 0.8 mL/min, 40 °C, $t_r$ (major) = 28.1 min, $t_r$ (minor) = 26.4 min). $[\alpha]_D^{25}$ = +2.1° (*c* 0.8, $CH_2Cl_2$) for 91% ee of the product (Lit.[15] $[\alpha]_D^{20}$ = –3.3° (*c* 0.8, $CH_2Cl_2$) for 95% ee of product with *R*-configuration). $^1$H NMR (300 MHz, $CDCl_3$) $\delta$ 7.13 (d, *J* = 0.9 Hz, 1H), 7.03 (s, 1H), 3.98 (s, 3H), 3.56 (dd, *J* = 7.2, 5.0 Hz, 2H), 3.24 – 3.10 (m, 1H), 1.77 (d, *J* = 5.8 Hz, 6H), 1.21 (d, *J* = 7.0 Hz, 3H). All spectroscopic data were in agreement with the literature.[15]

**(*S*)-*tert*-Butyl**

**1-((*S*)-4-(1-methyl-1*H*-imidazol-2-yl)-4-oxobutan-2-yl)-2-oxocyclopentanecarboxylate (46)**

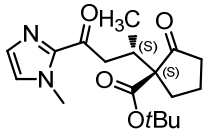

To a solution of catalyst Λ-**IrO** (3.7 mg, 0.004 mmol, 2 mol%) or Λ-**IrS** (3.8 mg, 0.004 mmol, 2 mol%) in distilled, anhydrous THF (0.4 mL) was added 2-acyl imidazole **31** (30.2 mg, 0.20 mmol) in a Schlenk tube. After being stirred at 40 °C for 20 min, *tert*-butyl 2-oxocyclopentanecarboxylate (73.7 mg, 0.40 mmol) was added at room temperature. The reaction mixture was stirred at 40 °C for the indicated time (monitored by TLC) under nitrogen atmosphere. Afterwards, the mixture was concentrated under reduced pressure. The residue was purified by flash chromatography on silica gel (EtOAc/*n*-hexane = 1: 2 to 1: 1) to afford the product (*S,S*)-**46** as a colorless oil (catalyzed by Λ-**IrO**: 25 h, 35.1 mg, 53% yield, 90% ee, *dr* = 1.8:1; catalyzed by Λ-**IrS**: 25 h, 56.7 mg, 85% yield, 96% ee, *dr* = 1.5:1). Enantiomeric excess established by HPLC analysis using a Chiralpak AD-H column (254 nm, hexane/isopropanol = 95:5, flow rate 0.5 mL/min, 40 °C, $t_r$ (major) = 26.9 min, $t_r$ (minor) = 29.5 min). $[\alpha]_D^{20}$ = –11.5° (*c* 0.4, $CH_2Cl_2$) for 96% ee of the product. (Lit.[15] $[\alpha]_D^{20}$ = +13.1° (*c* 1.4, $CH_2Cl_2$) for 99% ee of the product with *R,R*-configuration). $^1$H NMR (300 MHz, $CDCl_3$) $\delta$ 7.08 (d, *J* = 0.8 Hz, 1H), 6.99 (s, 1H), 3.96 (s, 3H), 3.22 (dd, *J* = 16.6, 10.3 Hz, 1H), 3.08 – 2.97 (m, 1H), 2.74 (dd, *J* = 16.6, 2.6 Hz, 1H), 2.50 – 2.30 (m, 2H), 2.21 – 2.06 (m, 1H), 2.01 – 1.85 (m, 3H), 1.42 (s, 9H), 0.94 (d,

$J$ = 6.7 Hz, 3H). All spectroscopic data are in agreement with the literature.[15]

**(*S*)-*tert*-Butyl 2-((*S*)-4-(1-methyl-1*H*-imidazol-2-yl)-4-oxobutan-2-yl)-1-oxo-2,3-dihydro-1*H*-indene-2-carboxylate (47)**

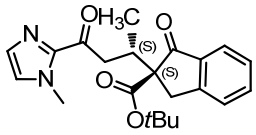

To a solution of catalyst Λ-**IrO** (1.8 mg, 0.002 mmol, 1 mol%) or Λ-**IrS** (1.9 mg, 0.002 mmol, 1 mol%) in distilled, anhydrous THF (0.2 mL) was added 2-acyl imidazole **31** (30.2 mg, 0.20 mmol) in a Schlenk tube. After being stirred at 40 °C for 20 min, *tert*-butyl 1-oxo-2,3-dihydro-1*H*-indene-2-carboxylate (92.8 mg, 0.4 mmol) was added at room temperature. The reaction mixture was stirred at 25 °C for the indicated time (monitored by TLC) under nitrogen atmosphere. Afterwards, the mixture was concentrated under reduced pressure. The residue was purified by flash chromatography on silica gel (EtOAc/*n*-hexane = 1: 2 to 1: 1) to afford the product (*S,S*)-**47** as a colorless oil (catalyzed by Λ-**IrO**: 72 h, 68.1 mg, 89% yield, 97% ee, *dr* = 10:1; catalyzed by Λ-**IrS**: 70.4 mg, 93% yield, 97% ee, *dr* = 22:1). Enantiomeric excess established by HPLC analysis using a Chiralpak AD-H column (254 nm, hexane/isopropanol = 85:15, flow rate 0.8 mL/min, 25 °C, $t_r$ (major) = 17.1 min, $t_r$ (minor) = 11.2 min). $[\alpha]_D^{25}$ = +94.1° (*c* 1.0, $CH_2Cl_2$) for 97% ee of the product. (Lit.[15] $[\alpha]_D^{20}$ = –96.9° (*c* 0.7, $CH_2Cl_2$) for 97% ee of the product with *R,R*-configuration). $^1$H NMR (300 MHz, $CDCl_3$) $\delta$ 7.74 (d, $J$ = 7.6 Hz, 1H), 7.65 – 7.56 (m, 1H), 7.50 (d, $J$ = 7.7 Hz, 1H), 7.40 – 7.32 (m, 1H), 7.13 (d, $J$ = 0.9 Hz, 1H), 7.03 (s, 1H), 4.01 (s, 3H), 3.69 (d, $J$ = 17.5 Hz, 1H), 3.51 – 3.39 (m, 1H), 3.32 – 3.18 (m, 2H), 3.09 (dd, $J$ = 16.3, 2.8 Hz, 1H), 1.36 (s, 9H), 0.76 (d, $J$ = 6.7 Hz, 3H). All spectroscopic data were in agreement with the literature.[15]

**(*S*)-*tert*-Butyl 6-((*S*)-4-(1-methyl-1*H*-imidazol-2-yl)-4-oxobutan-2-yl)-5-oxo-6,7-dihydro-5*H*-indeno[5,6-*d*][1,3]dioxole-6-carboxylate (48)**

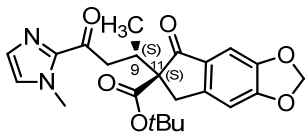

Starting from **31** (30.0 mg, 0.2 mmol) and *tert*-butyl 5-oxo-6,7-dihydro-5*H*-indeno[5,6-*d*][1,3]dioxole-6-carboxylate (110.4 mg, 0.4 mmol) according to the *general procedure* for **47** to give (*S,S*)-**48** as a colorless oil (catalyzed by 1 mol % Λ-**IrS**: 61 mg, 72% yield, 97% ee, *dr* = 13:1). Enantiomeric excess established by HPLC analysis using a Chiralpak AD-H column (HPLC: AD-H, 254 nm, hexane/isopropanol = 85:15, flow rate 0.8 mL/min, 25 °C, $t_r$ (major) = 33.8 min, $t_r$ (minor) = 19.5 min); $[\alpha]_D^{25}$ = +103.0° (*c* 0.60, $CH_2Cl_2$) for 97% ee of the product. $^1$H NMR (300 MHz, $CDCl_3$) $\delta$ 7.08 (d, $J$ = 0.9 Hz, 1H), 7.04 (s, 1H), 7.01 (d, $J$ = 0.5 Hz, 1H), 6.83 (s, 1H), 6.03 (dd, $J$ = 2.1, 1.1 Hz,

2H), 3.97 (s, 3H), 3.52 (d, $J$ = 17.4 Hz, 1H), 3.44 – 3.29 (m, 1H), 3.26 – 3.13 (m, 1H), 3.06 – 2.95 (m, 2H), 1.34 (s, 9H), 0.72 (d, $J$ = 6.7 Hz, 3H). $^{13}$C NMR (75 MHz, $CDCl_3$) $\delta$ 200.0, 191.2, 169.4, 154.8, 151.8, 148.5, 143.4, 130.5, 129.0, 127.1, 105.5, 102.9, 102.4, 81.9, 66.5, 42.3, 36.2, 33.0, 32.8, 27.8 (3 C), 15.1. IR (film): $\nu$ (cm$^{-1}$) 2973, 2928, 1731, 1696, 1674, 1608, 1502, 1470, 1405, 1367, 1310, 1249, 1217, 1145, 1073, 1033, 984, 937, 913, 864, 844, 796, 770, 734, 697, 580, 427. HRMS (ESI, $m/z$) calcd for $C_{23}H_{27}N_2O_6$ [M+H]$^+$: 427.1864, found: 427.1855.

**(*S*)-*tert*-Butyl 2-((*S*)-1-ethoxy-4-(1-methyl-1*H*-imidazol-2-yl)-1,4-dioxobutan-2-yl)-1-oxo-2,3-dihydro-1*H*-indene-2-carboxylate (49)**

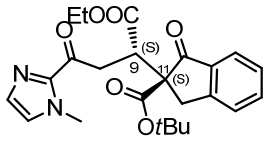


Starting from **33** (30.0 mg, 0.2 mmol) and 1-oxo-2,3-dihydro-1*H*-indene-2-carboxylate (92.8 mg, 0.4 mmol) according to the *general procedure* for **47** to give (*S,S*)-**49** as a colorless oil (catalyzed by Λ-**IrS**: 71 mg, 81% yield, 96% ee, *dr* = 15:1). Enantiomeric excess established by HPLC analysis using a Chiralpak AD-H column (HPLC: AD-H, 254 nm, hexane/isopropanol = 70:30, flow rate 0.8 mL/min, 25 °C, $t_r$ (major) = 10.3 min, $t_r$ (minor) = 11.8 min); $[\alpha]_D^{25}$ = +112.1° (*c* 1.04, $CH_2Cl_2$) for 96% ee of the product. $^1$H NMR (300 MHz, $CDCl_3$) $\delta$ 7.75 (d, $J$ = 7.6 Hz, 1H), 7.57 (td, $J$ = 7.6, 1.1 Hz, 1H), 7.46 (d, $J$ = 7.7 Hz, 1H), 7.35 (t, $J$ = 7.4 Hz, 1H), 7.14 (d, $J$ = 0.6 Hz, 1H), 7.03 (s, 1H), 4.31 (dd, $J$ = 10.1, 3.0 Hz, 1H), 3.99 (s, 3H), 3.97 – 3.87 (m, 1H), 3.86 – 3.68 (m, 3H), 3.27 (dd, $J$ = 17.5, 3.0 Hz, 1H), 3.24 (d, $J$ = 17.2 Hz, 1H), 1.35 (s, 9H), 0.80 (t, $J$ = 7.1 Hz, 3H). $^{13}$C NMR (75 MHz, $CDCl_3$) $\delta$ 200.2, 189.7, 172.3, 168.0, 153.4, 135.3, 135.1, 129.1, 127.6, 127.0, 126.4, 124.7, 82.9, 63.3, 61.1, 44.1, 38.2, 36.2, 34.6, 31.6, 30.3, 27.8 (3 C), 13.6. IR (film): $\nu$ (cm$^{-1}$) 2979, 2934, 1712, 1677, 1607, 1590, 1464, 1410, 1368, 1348, 1329, 1246, 1212, 1147, 1088, 1024, 983, 914, 842, 776, 742, 691, 515, 472, 454. HRMS (ESI, $m/z$) calcd for $C_{24}H_{28}N_2O_6Na$ [M+Na]$^+$: 463.1840, found: 463.1840.

**(*S*)-*tert*-Butyl 2-((*S*)-1-(1-methyl-1*H*-imidazol-2-yl)-1-oxoheptan-3-yl)-1-oxo-2,3-dihydro-1*H*-indene-2-carboxylate (50)**

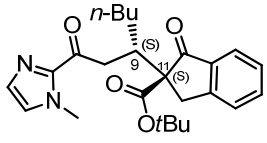


Starting from **34** (30.0 mg, 0.2 mmol) and 1-oxo-2,3-dihydro-1*H*-indene-2-carboxylate (92.8 mg, 0.4 mmol) according to the *general procedure* for **47** except higher temperature (40 °C) to give (*S,S*)-**50** as a colorless oil (catalyzed by 2 mol% Λ-**IrS**: 20% yield, 85% ee, *dr* = 9:1). Enantiomeric excess

established by HPLC analysis using a Chiralpak AD-H column (HPLC: AD-H, 254 nm, hexane/isopropanol = 85:15, flow rate 0.8 mL/min, 25 °C, $t_r$ (major) = 14.3 min, $t_r$ (minor) = 10.1 min). $^1$H NMR (300 MHz, $CDCl_3$) $\delta$ 7.73 (d, $J$ = 7.6 Hz, 1H), 7.64 – 7.55 (m, 1H), 7.49 (d, $J$ = 7.7 Hz, 1H), 7.36 (t, $J$ = 7.4 Hz, 1H), 7.12 (d, $J$ = 0.8 Hz, 1H), 7.02 (s, 1H), 4.01 (s, 3H), 3.70 (d, $J$ = 17.5 Hz, 1H), 3.32 (s, 1H), 3.29 – 3.10 (m, 3H), 1.30 (s, 9H), 1.20 – 1.05 (m, 6H), 0.71 (t, $J$ = 6.8 Hz, 3H). $^{13}$C NMR (75 MHz, $CDCl_3$) $\delta$ 202.6, 191.3, 169.6, 154.0, 136.3, 135.1, 128.7, 127.6, 126.9, 126.4, 124.6, 82.0, 66.6, 41.7, 37.8, 36.3, 34.2, 31.6, 30.2, 27.9, 27.8 (3 C), 22.9, 14.0. IR (film): $\nu$ (cm$^{-1}$) 2956, 2930, 2870, 1735, 1704, 1674, 1606, 1590, 1464, 1405, 1367, 1275, 1246, 1212, 1148, 1081, 1020, 984, 914, 845, 768, 742, 691, 612, 472, 454. HRMS (ESI, *m*/*z*) calcd for $C_{25}H_{32}N_2O_4Na$ [M+Na]$^+$: 447.2254, found: 447.2257.

**(*S*)-*tert*-Butyl 2-((*S*)-4-(1-isopropyl-1*H*-imidazol-2-yl)-4-oxobutan-2-yl)-1-oxo-2,3-dihydro-1*H*-indene-2-carboxylate (51)**

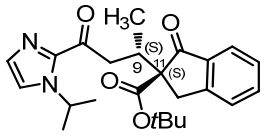


Starting from **45** (35.6 mg, 0.2 mmol) and 1-oxo-2,3-dihydro-1*H*-indene-2-carboxylate (92.8 mg, 0.4 mmol) according to the *general procedure* for **47** to give (*S,S*)-**51** as a white solid (catalyzed by 2 mol % Λ-**IrS**: 71 mg, 87% yield, 96% ee, *dr* = 49:1). Enantiomeric excess established by HPLC analysis using a Chiralpak AD-H column (HPLC: AD-H, 254 nm, hexane/isopropanol = 85:15, flow rate 0.5 mL/min, 25 °C, $t_r$ (major) = 21.4 min, $t_r$ (minor) = 13.1 min); $[\alpha]_D^{20}$ = +92.3° (*c* 0.7, $CH_2Cl_2$) for 96% ee of the product. $^1$H NMR (300 MHz, $CDCl_3$) $^1$H NMR (300 MHz, $CDCl_3$) $\delta$ 7.75 (d, $J$ = 7.7 Hz, 1H), 7.66 – 7.57 (m, 1H), 7.51 (d, $J$ = 7.7 Hz, 1H), 7.37 (t, $J$ = 7.4 Hz, 1H), 7.28 (d, $J$ = 1.2 Hz, 1H), 7.17 (s, 1H), 5.67 – 5.50 (m, 1H), 3.71 (d, $J$ = 17.5 Hz, 1H), 3.54 – 3.37 (m, 1H), 3.35 – 3.07 (m, 3H), 1.45 (d, $J$ = 6.7 Hz, 6H), 1.38 (s, 9H), 0.77 (d, $J$ = 6.7 Hz, 3H). $^{13}$C NMR (75 MHz, $CDCl_3$) $\delta$ 202.4, 191.4, 169.4, 154.1, 142.7, 136.1, 135.2, 129.4, 127.6, 126.4, 124.6, 121.2, 82.1, 66.0, 49.4, 43.0, 33.3, 33.1, 27.9 (3 C), 23.8 (2 C), 15.3. IR (film): $\nu$ (cm$^{-1}$) 2976, 2928, 2875, 1705, 1668, 1602, 1463, 1397, 1371, 1340, 1252, 1143, 1094, 1032, 1011, 985, 916, 879, 841, 809, 773, 744, 708, 621, 566, 523, 463. HRMS (ESI, *m*/*z*) calcd for $C_{24}H_{30}N_2O_4Na$ [M+Na]$^+$: 433.2098, found: 433.2093.

### 5.4.1.3 Asymmetric cycloadditions

**((*3S,4R,5S*)-2-Benzyl-5-methyl-3-phenylisoxazolidin-4-yl)(1-methyl-1*H*-imidazol-2-yl)methanone (52)**

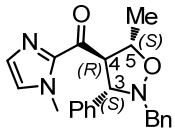

To a solution of catalyst Λ-**IrO** (3.7 mg, 0.004 mmol, 2 mol%) or Λ-**IrS** (3.8 mg, 0.004 mmol, 2 mol%) in distilled, anhydrous $CH_2Cl_2$ (0.2 mL) was added the 2-acyl imidazole **31** (30.0 mg, 0.20 mmol) in a Schlenk tube containing 80 mg of 4 Å molecular sieves. After being stirred at room temperature for 20 min, (*Z*)-*N*-benzylidene(phenyl)methanamine oxide (49.0 mg, 0.22 mmol) was added. The reaction mixture was stirred for the indicated time (monitored by TLC) under nitrogen atmosphere. Afterwards, the mixture was concentrated under reduced pressure. The residue was purified by flash chromatography on silica gel (EtOAc/*n*-hexane = 1: 2 to 1: 1) to give **52** as a white solid (catalyzed by Λ-**IrO**: 36 h, 71.2 mg, 99% yield, 92% ee, *endo*/*exo* > 99:1; catalyzed by Λ-**IrS**: 72 h, 62.1 mg, 86% yield, 98% ee, *endo*/*exo* > 99:1). Enantiomeric excess established by HPLC analysis using a Chiralpak AD-H column (254 nm, hexane/isopropanol = 90:10, flow rate 0.8 mL/min, 40 °C, $t_r$ (major) = 12.6 min, $t_r$ (minor) = 17.8 min). $[\alpha]_D^{25}$ = +9.9° (*c* 0.5, $CH_2Cl_2$) for 98% ee of the product. (Lit.[48] $[\alpha]_D^{25}$ = –7.7° (*c* 3.2, $CH_2Cl_2$) for 97% ee of product with *(3R,4S,5R)*-configuration). $^1$H NMR (300 MHz, $CDCl_3$) $\delta$ 7.55 – 7.47 (m, 2H), 7.47 – 7.41 (m, 2H), 7.39 – 7.20 (m, 6H), 7.12 (d, *J* = 0.9 Hz, 1H), 7.03 (d, *J* = 0.9 Hz, 1H), 4.63 – 4.52 (m, 2H), 4.48 – 4.36 (m, 1H), 4.14 (d, *J* = 14.3 Hz, 1H), 4.03 (s, 3H), 3.98 (d, *J* = 14.3 Hz, 1H), 1.69 (d, *J* = 6.1 Hz, 3H). All spectroscopic data are in agreement with the literature.[48]

**1-Methyl-2-((3a*S*,4*S*,7a*R*)-4-methyl-3,3a,4,7a-tetrahydro-2*H*-furo[2,3-b]pyran-6-yl)-1*H*-imidazole (53)**

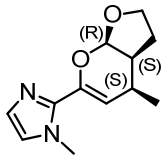

To a solution of catalyst Λ-**IrO** (3.7 mg, 0.004 mmol, 2 mol%) or Λ-**IrS** (3.8 mg, 0.004 mmol, 2 mol%) in distilled, anhydrous $CH_2Cl_2$ (0.2 mL) was added the 2-acyl imidazole **31** (30.0 mg, 0.20 mmol) in a Schlenk tube containing 5.0 mg of 3 Å molecular sieves powder. After being stirred at room temperature for 20 min, 2,3-dihydrofuran (140.0 mg, 151.0 μL, 2.0 mmol) was added. The reaction mixture was stirred for the indicated time (monitored by TLC) under nitrogen atmosphere. Afterwards, the mixture was concentrated under reduced pressure. The residue was purified by flash chromatography on silica gel (EtOAc/*n*-hexane = 1: 1 to 2: 1) to afford the **53** as colorless oil (catalyzed by Λ-**IrO**: 48 h, 43.9 mg, 99% yield, 98% ee, *endo*:*exo* > 50:1; catalyzed by Λ-**IrS**: 68 h, 35.0 mg, 80% yield, 95% ee, *endo*:*exo* > 30:1). Enantiomeric excess established by HPLC analysis using a Chiralpak IC column (HPLC: IC, 254 nm, hexane/isopropanol = 70:30, flow rate 1.0 mL/min, 25 °C, $t_r$ (major) = 19.1 min, $t_r$ (minor) = 15.8 min). $[\alpha]_D^{25}$ = –15.5° (*c* 0.4, $CH_2Cl_2$) for 98% ee of the

product. $^1$H NMR (300 MHz, $CDCl_3$) $\delta$ 6.90 (d, $J$ = 1.2 Hz, 1H), 6.76 (d, $J$ = 1.1 Hz, 1H), 5.54 (d, $J$ = 4.0 Hz, 1H), 5.33 (dd, $J$ = 2.3, 1.3 Hz, 1H), 4.13 (td, $J$ = 8.5, 3.3 Hz, 1H), 4.00 – 3.90 (m, 1H), 3.72 (s, 3H), 2.96 – 2.83 (m, 1H), 2.46 – 2.34 (m, 1H), 1.94 – 1.78 (m, 2H), 1.09 (d, $J$ = 7.3 Hz, 3H). $^{13}$C NMR (75 MHz, $CDCl_3$) $\delta$ 142.7, 142.1, 127.8, 122.5, 104.6, 101.3, 68.5, 43.6, 34.9, 26.5, 23.5, 18.5. IR (film): $\nu$ ($cm^{-1}$) 3111, 2958, 2929, 2874, 1733, 1711, 1677, 1456, 1407, 1281, 1231, 1158, 1118, 1026, 981, 916, 864, 836, 765, 693, 660, 620, 600, 557, 500, 462, 388. HRMS (ESI, $m/z$) calcd for $C_{12}H_{17}N_2O_2$ $[M+H]^+$: 221.1285, found: 221.1283.

**1-Isopropyl-2-((3a*S*,4*S*,7a*R*)-4-phenyl-3,3a,4,7a-tetrahydro-2*H*-furo[2,3-b]pyran-6-yl)-1*H*-imidazole (54)**

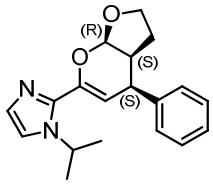


To a solution of catalyst Λ-**IrO** (3.7 mg, 0.004 mmol, 2 mol%) or Λ-**IrS** (3.8 mg, 0.004 mmol, 2 mol%) in distilled, anhydrous $CH_2Cl_2$ (0.2 mL) was added the 2-acyl imidazole **35** (48.0 mg, 0.20 mmol) in a Schlenk tube containing 5.0 mg of 3 Å molecular sieves powder. After being stirred at room temperature for 20 min, 2,3-dihydrofuran (140.0 mg, 151.0 μL, 2.0 mmol) was added. The reaction mixture was stirred for the indicated time (monitored by TLC) under nitrogen atmosphere. Afterwards, the mixture was concentrated under reduced pressure. The residue was purified by flash chromatography on silica gel (EtOAc/*n*-hexane = 1: 1 to 2: 1) to afford **54** as a colorless oil (catalyzed by Λ-**IrO**: 24 h, 50.4 mg, 81% yield, 99% ee, *endo:exo* > 50:1; catalyzed by Λ-**IrS**: 60 h, 25.2 mg, 40% yield, 99% ee, *endo:exo* > 20:1). Enantiomeric excess established by HPLC analysis using a Chiralpak IC column (254 nm, hexane/isopropanol = 70:30, flow rate 1.0 mL/min, 25 °C, $t_r$ (major) = 19.1 min, $t_r$ (minor) = 10.3 min). $[\alpha]_D^{25}$ = –8.0° (*c* 0.6, $CH_2Cl_2$) for 98% ee of the product. $^1$H NMR (300 MHz, $CDCl_3$) $\delta$ 7.28 (d, $J$ = 4.4 Hz, 4H), 7.25 – 7.17 (m, 1H), 6.99 (d, $J$ = 1.1 Hz, 1H), 6.98 (d, $J$ = 1.2 Hz, 1H), 5.67 (d, $J$ = 3.7 Hz, 1H), 5.62 (dd, $J$ = 2.4, 1.3 Hz, 1H), 4.92 (hept, $J$ = 6.6 Hz, 1H), 4.18 (dd, $J$ = 6.4, 2.4 Hz, 1H), 4.14 – 4.03 (m, 1H), 3.91 – 3.75 (m, 1H), 2.75 – 2.54 (m, 1H), 1.84 (tt, $J$ = 12.3, 9.7 Hz, 1H), 1.41 (dd, $J$ = 9.1, 6.7 Hz, 6H), 1.37 – 1.33 (m, 1H). $^{13}$C NMR (75 MHz, $CDCl_3$) $\delta$ 144.1, 142.1, 142.0, 128.6 (2C), 128.3, 127.7 (2C), 126.8, 116.6, 102.4, 101.1, 68.5, 48.5, 44.3, 37.9, 24.6, 23.8 (2C). IR (film): $\nu$ ($cm^{-1}$) 2973, 1719, 1666, 1393, 1256, 1202, 1117, 1059, 1020, 983, 768, 701, 620, 554, 499, 461, 403. HRMS (ESI, $m/z$) calcd for $C_{19}H_{23}N_2O_2$ $[M+H]^+$: 311.1754, found: 311.1753.

**((1*R*,6*R*)-4,6-Dimethylcyclohex-3-en-1-yl)(1-methyl-1*H*-imidazol-2-yl)methanone (55)**

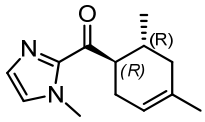

To a solution of catalyst Λ-**IrO** (3.7 mg, 0.004 mmol, 2 mol%) or Λ-**IrS** (3.8 mg, 0.004 mmol, 2 mol%) in distilled, anhydrous $CH_2Cl_2$ (0.2 mL) was added 2-acyl imidazole **31** (30.0 mg, 0.20 mmol) in a Schlenk tube containing 10.0 mg of 4 Å molecular sieves powder. After being stirred at room temperature for 20 min, isoprene (136.2 mg, 200.0 μL, 2.0 mmol) was added. The reaction mixture was stirred for the indicated time (monitored by TLC) under nitrogen atmosphere. Afterwards, the mixture was concentrated under reduced pressure. The residue was purified by flash chromatography on silica gel (EtOAc/*n*-hexane = 1: 4) to afford **55** as a colorless oil (catalyzed by Λ-**IrO**: 48 h, 32.8 mg, 76% yield, 98% ee, *dr* > 99:1; catalyzed by Λ-**IrS**: 48 h, 24.0 mg, 56% yield, 99% ee, *dr* > 99:1). Enantiomeric excess established by HPLC analysis using a Chiralpak IC column (254 nm, hexane/isopropanol = 97:3, flow rate 1.0 mL/min, 25 °C, $t_r$ (major) = 9.9 min, $t_r$ (minor) = 14.2 min). $[\alpha]_D^{20}$= –46.6° (*c* 0.3, $CH_2Cl_2$) for 99% ee of the product. $^1$H NMR (300 MHz, $CDCl_3$) $\delta$ 7.10 (d, *J* = 0.84 Hz, 1H), 7.01(s, 1H), 5.36 (s, 1H), 3.98 (s, 3H), 3.75 – 3.66 (m, 1H), 2.20 – 1.96 (m, 4H), 1.82 – 1.72 (m. 1H), 1.61 (s, 3H), 0.88(d, *J* = 6.36 Hz, 3H). $^{13}$C NMR (300 MHz, $CDCl_3$) $\delta$ 197.3, 143.6, 133.4, 129.0, 127.2, 119.3, 48.1, 38.6, 36.3, 31.2, 29.8, 23.3, 19.8. IR (film): *v* ($cm^{-1}$) 2956, 2919, 1665, 1453, 1403, 1284, 1236, 1152, 1089, 1005, 907, 861, 829, 769, 697, 662, 623, 514, 426. HRMS (ESI, m/z) calcd for $C_{13}H_{19}N_2O$ $[M+H]^+$: 219.1435, found: 219.1493.

### 5.4.1.4 Scope of acceptor-substituted alkenes

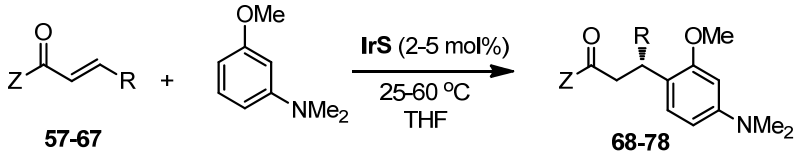


**57-67** **68-78**

**(*S*)-3-(4-(Dimethylamino)-2-methoxyphenyl)-1-(1-methyl-1*H*-benzo[*d*]imidazol-2-yl)butan-1-one (68)**

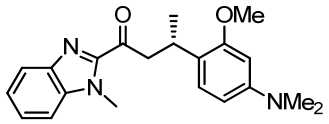

To a solution of catalyst Λ-**IrS** (9.5 mg, 0.01 mmol, 5 mol%) in distilled, anhydrous THF (0.1 mL) was added the benzimidazole **57** (40.0 mg, 0.20 mmol) in a Schlenk tube. After being stirred at room temperature for 3 min, 3-methoxy-*N*,*N*-dimethylaniline (90.6 mg, 88.0 μL, 0.6 mmol) was added at room temperature. The reaction mixture was stirred at 60 °C for 24 h under nitrogen atmosphere. Afterwards, the mixture was purified by flash chromatography on silica gel (EtOAc/*n*-hexane = 1: 4) to afford (*S*)-**68** as a colorless oil (60.1 mg, 86% yield, 96% ee). Enantiomeric excess established by HPLC analysis using a Chiralpak AD-H column (HPLC: AD-H, 254 nm, hexane/isopropanol = 90:10,

flow rate 1.0 mL/min, 25 °C, $t_r$ (major) = 12.2 min, $t_r$ (minor) = 11.1 min). $[\alpha]_D^{25}$ = –14.3° (*c* 0.7, $CH_2Cl_2$). $^1$H NMR (300 MHz, $CDCl_3$) $\delta$ 7.90 (dt, *J* = 7.9, 1.1 Hz, 1H), 7.45 – 7.30 (m, 3H), 7.12 (d, *J* = 8.3 Hz, 1H), 6.29 (dd, *J* = 8.3, 2.5 Hz, 1H), 6.25 (d, *J* = 2.5 Hz, 1H), 4.05 (s, 3H), 3.89 – 3.78 (m, 1H), 3.79 (s, 3H), 3.62 (dd, *J* = 7.2, 1.4 Hz, 2H), 2.91 (s, 6H), 1.33 (d, *J* = 6.9 Hz, 3H). $^{13}$C NMR (75 MHz, $CDCl_3$) $\delta$ 195.5, 157.8, 150.5, 146.8, 141.8, 137.0, 128.3, 127.7, 125.6, 123.6, 122.0, 110.5, 105.1, 96.9, 55.4, 47.1, 41.0 (2C), 32.3, 28.9, 21.1. IR (film): $\nu$ ($cm^{-1}$) 2955, 2833, 1683, 1612, 1567, 1513, 1479, 1456, 1394, 1349, 1335, 1289, 1235, 1179, 1153, 1120, 1096, 1059, 1032, 997, 978, 895, 812, 794, 767, 741, 640, 505, 481, 433. HRMS (ESI, *m*/*z*) calcd for $C_{21}H_{26}N_3O_2$ $[M+H]^+$: 352.2020, found: 352.2030.

**(*S*)-3-(4-(Dimethylamino)-2-methoxyphenyl)-1-(thiazol-2-yl)butan-1-one (69)**

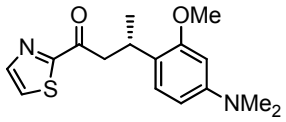


To a solution of catalyst Λ-**IrS** (3.8 mg, 0.004 mmol, 2 mol%) in distilled, anhydrous THF (0.1 mL) was added the 2-thiazole **58** (30.6 mg, 0.20 mmol) in a Schlenk tube. After being stirred at room temperature for 3 min, 3-methoxy-*N*,*N*-dimethylaniline (90.6 mg, 88.0 μL, 0.6 mmol) was added at room temperature. The reaction mixture was stirred at 40 °C for 18 h under nitrogen atmosphere. Afterwards, the mixture was purified by flash chromatography on silica gel (EtOAc/*n*-hexane = 1: 5) to afford (*S*)-**69** (purified by flash chromatography on silica gel, EtOAc/*n*-hexane = 1: 5) as a colorless oil (60.6 mg, 99% yield, 98% ee). Enantiomeric excess established by HPLC analysis using a Chiralpak OD-H column (HPLC: OD-H, 254 nm, hexane/isopropanol = 95:5, flow rate 1.0 mL/min, 25 °C, $t_r$ (major) = 10.5 min, $t_r$ (minor) = 11.1 min). $[\alpha]_D^{25}$ = + 20.8° (*c* 0.7, $CH_2Cl_2$). $^1$H NMR (300 MHz, $CDCl_3$) $\delta$ 7.98 (dd, *J* = 3.0, 1.2 Hz, 1H), 7.62 (dd, *J* = 3.0, 1.2 Hz, 1H), 7.10 (dd, *J* = 8.4, 1.1 Hz, 1H), 6.47 – 5.91 (m, 2H), 3.86 – 3.70 (m, 1H), 3.78 (d, *J* = 1.2 Hz, 3H), 3.50 – 3.33 (m, 2H), 2.92 (d, *J* = 1.2 Hz, 6H), 1.30 (dd, *J* = 6.9, 1.2 Hz, 3H). $^{13}$C NMR (75 MHz, $CDCl_3$) $\delta$ 193.5, 168.0, 157.8, 150.6, 144.7, 127.6, 125.9, 122.8 105.1, 96.9, 55.3, 45.9, 41.0 (2C), 29.0, 20.8. IR (film): $\nu$ ($cm^{-1}$) 2957, 2930, 2872, 2833, 1680, 1612, 1567, 1514, 1479, 1453, 1439, 1423, 1388, 1348, 1281, 1236, 1192, 1181, 1122, 1094, 1060, 1035, 978, 879, 812, 792, 640, 630, 510. HRMS (ESI, *m*/*z*) calcd for $C_{16}H_{21}N_2O_2S$ $[M+H]^+$: 305.1318, found: 305.1335.

**(*S*)-3-(4-(Dimethylamino)-2-methoxyphenyl)-1-(pyridin-2-yl)butan-1-one (70)**

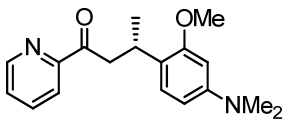


To a solution of catalyst Λ-**IrS** (9.5 mg, 0.01 mmol, 5 mol%) in distilled, anhydrous MeCN (0.1 mL) was added the pyridine **59** (88.2 mg, 0.60 mmol) in a Schlenk tube. After being stirred at room temperature for 3 min, 3-methoxy-*N*,*N*-dimethylaniline (30.2 mg, 29.3 μL, 0.2 mmol) was added at

room temperature. The reaction mixture was stirred at 60 °C for 24 h under nitrogen atmosphere. Afterwards, the mixture was purified by flash chromatography on silica gel (EtOAc/*n*-hexane = 1: 4) to afford (*S*)-**70** as a colorless oil (52.0 mg, 87% yield, 97% ee). Enantiomeric excess established by HPLC analysis using a Chiralpak IC column (HPLC: IC, 254 nm, hexane/isopropanol = 95:5, flow rate 1.0 mL/min, 25 °C, $t_r$ (major) = 17.8 min, $t_r$ (minor) = 20.3 min). $[\alpha]_D^{20}$ = –1.2° (*c* 0.6, $CH_2Cl_2$). $^1$H NMR (300 MHz, $CDCl_3$) $\delta$ 8.67 (ddd, *J* = 4.8, 1.7, 0.9 Hz, 1H), 7.99 (dt, *J* = 7.9, 1.1 Hz, 1H), 7.79 (td, *J* = 7.7, 1.8 Hz, 1H), 7.43 (ddd, *J* = 7.5, 4.7, 1.3 Hz, 1H), 7.11 (d, *J* = 8.3 Hz, 1H), 6.31 (dd, *J* = 8.3, 2.5 Hz, 1H), 6.27 (d, *J* = 2.4 Hz, 1H), 3.86 – 3.71 (m, 1H), 3.78 (s, 3H), 3.58 – 3.39 (m, 2H), 2.92 (s, 6H), 1.28 (d, *J* = 6.9 Hz, 3H). $^{13}$C NMR (75 MHz, $CDCl_3$) $\delta$ 201.5, 157.9, 154.2, 150.4, 148.9, 136.8, 127.6, 126.8, 123.7, 121.9, 105.2, 97.1, 55.4, 45.0, 41.1 (2C), 28.6, 21.0. IR (film): $\nu$ ($cm^{-1}$) 2958, 2931, 2872, 2833, 1693, 1613, 1582, 1567, 1513, 1481, 1461, 1436, 1348, 1309, 1284, 1235, 1191, 1122, 1091, 1060, 1033, 993, 978, 812, 792, 769, 742, 662, 640, 617, 508, 406. HRMS (ESI, *m*/*z*) calcd for $C_{18}H_{23}N_2O_2$ $[M+H]^+$: 299.1754, found: 299.1762.

**3-(3-(4-(Dimethylamino)-2-methoxyphenyl)butanoyl)oxazolidin-2-one (71)**

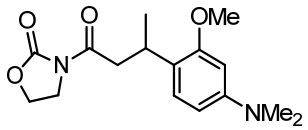


To a solution of catalyst Λ-**IrS** (9.5 mg, 0.01 mmol, 5 mol%) in distilled, anhydrous THF or $CHCl_3$ or Toluene (0.1 mL) was added the 2-oxazolidinone **60** (31.0 mg, 0.20 mmol) in a Schlenk tube. After being stirred at room temperature for 3 min, 3-methoxy-*N*,*N*-dimethylaniline (90.6 mg, 88.0 μL, 0.6 mmol) was added at room temperature. The reaction mixture was stirred at 40 °C or 60 °C for 24 h under nitrogen atmosphere. No product (**71**) was observed.

**(*S*)-3-(4-(Dimethylamino)-2-methoxyphenyl)-1-(2-thioxothiazolidin-3-yl)butan-1-one (72)**

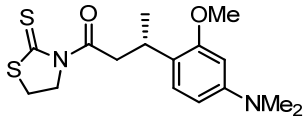


To a solution of catalyst Λ-**IrS** (5.7 mg, 0.006 mmol, 2 mol%) in distilled, anhydrous THF (0.15 mL) was added the 2-thiazolidinethione **61** (55.8 mg, 0.30 mmol) in a Schlenk tube. After being stirred at room temperature for 3 min, 3-methoxy-*N*,*N*-dimethylaniline (135.9 mg, 131.2 μL, 0.9 mmol) was added at room temperature. The reaction mixture was stirred at 40 °C for 22 h under nitrogen atmosphere. Afterwards, the mixture was purified by flash chromatography on silica gel (EtOAc/*n*-hexane = 1: 2) to afford (*S*)-**72** as a colorless oil (47.1 mg, 47% yield, 68% ee). Enantiomeric excess established by HPLC analysis using a Chiralpak OD-H column (HPLC: OD-H, 254 nm, hexane/isopropanol = 70:30, flow rate 1.0 mL/min, 25 °C, $t_r$ (major) = 11.1 min, $t_r$ (minor) = 14.0 min). $[\alpha]_D^{20}$ = +11.4° (*c* 0.5, $CH_2Cl_2$). $^1$H NMR (300 MHz, $CDCl_3$) $\delta$ 7.03 (d, *J* = 8.2 Hz, 1H),

6.34 – 6.24 (m, 2H), 4.40 (td, *J* = 7.5, 1.5 Hz, 2H), 3.83 (s, 3H), 3.70 – 3.53 (m, 3H), 3.22 – 3.10 (m, 2H), 2.93 (s, 6H), 1.26 (d, *J* = 6.6 Hz, 3H). $^{13}$C NMR (75 MHz, $CDCl_3$) $\delta$ 201.4, 174.5, 158.0, 150.5, 128.1, 122.3, 105.1, 97.0, 56.3, 55.5, 45.0, 41.1 (2C), 30.5, 28.5, 20.9. IR (film): $\nu$ ($cm^{-1}$) 2931, 2832, 2799, 1697, 1612, 1566, 1513, 1461, 1439, 1352, 1277, 1234, 1144, 1122, 1048, 1031, 999, 977, 908, 878, 812, 793, 728, 674, 642, 568, 506, 474, 453. HRMS (ESI, *m*/*z*) calcd for $C_{16}H_{22}N_2O_2S_2Na$: $[M+Na]^+$: 361.1015, found: 361.1025.

**(*S*)-3-(4-(Dimethylamino)-2-methoxyphenyl)-1-(1*H*-pyrazol-1-yl)butan-1-one (73)**

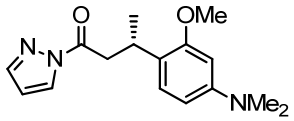


To a solution of catalyst Λ-**IrS** (5.7 mg, 0.006 mmol, 2 mol%) in distilled, anhydrous THF (0.15 mL) was added the pyrazole **62** (40.8 mg, 0.30 mmol) in a Schlenk tube. After being stirred at room temperature for 3 min, 3-methoxy-*N*,*N*-dimethylaniline (135.9 mg, 131.2 μL, 0.9 mmol) was added at room temperature. The reaction mixture was stirred at 40 °C for 26 h under nitrogen atmosphere. Afterwards, the mixture was purified by flash chromatography on silica gel (EtOAc/*n*-hexane = 1: 10) to afford (*S*)-**73** as a colorless oil (74.2 mg, 86% yield, 98% ee). Enantiomeric excess established by HPLC analysis using a Chiralpak OD-H column (HPLC: OD-H, 254 nm, hexane/isopropanol = 95:5, flow rate 1.0 mL/min, 25 °C, $t_r$ (major) = 8.2 min, $t_r$ (minor) = 7.7 min). $[\alpha]_D^{25}$ = –3.2° (*c* 0.7, $CH_2Cl_2$). $^1$H NMR (300 MHz, $CDCl_3$) $\delta$ 8.24 (dd, *J* = 2.8, 0.7 Hz, 1H), 7.70 (dd, *J* = 1.5, 0.7 Hz, 1H), 7.10 (d, *J* = 8.3 Hz, 1H), 6.41 (dd, *J* = 2.9, 1.5 Hz, 1H), 6.31 (dd, *J* = 8.3, 2.5 Hz, 1H), 6.27 (d, *J* = 2.5 Hz, 1H), 3.80 (s, 3H), 3.83 – 3.72 (m, 1H), 3.42 (d, *J* = 7.3 Hz, 2H), 2.94 (s, 6H), 1.34 (d, *J* = 7.0 Hz, 3H). $^{13}$C NMR (75 MHz, $CDCl_3$) $\delta$ 171.5, 157.9, 150.6, 143.6, 128.2, 127.6, 122.3, 109.3, 105.0, 96.8, 55.3, 41.1, 40.9 (2C), 29.4, 20.6. IR (film): $\nu$ ($cm^{-1}$) 2958, 2932, 2874, 2834, 1729, 1613, 1567, 1514, 1482, 1453, 1439, 1411, 1380, 1342, 1323, 1261, 1236, 1197, 1125, 1087, 1036, 978, 925, 912, 813, 768, 736, 644, 609, 507, 478. HRMS (ESI, *m*/*z*) calcd for $C_{16}H_{22}N_3O_2$ $[M+H]^+$: 288.1707 found: 288.1712.

**(*S*)-1-(3,5-Dimethyl-1*H*-pyrazol-1-yl)-3-(4-(dimethylamino)-2-methoxyphenyl)butan-1-one (74)**

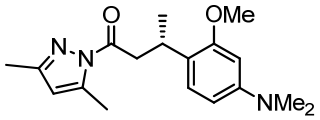


To a solution of catalyst Λ-**IrS** (9.5 mg, 0.01 mmol, 5 mol%) in distilled, anhydrous THF (0.1 mL) was added the pyrazole **63** (98.4 mg, 0.60 mmol) in a Schlenk tube. After being stirred at room temperature for 3 min, 3-methoxy-*N*,*N*-dimethylaniline (30.2 mg, 29.3 μL, 0.2 mmol) was added at room temperature. The reaction mixture was stirred at 60 °C for 24 h under nitrogen atmosphere. Afterwards, the mixture was purified by flash chromatography on silica gel (EtOAc/*n*-hexane = 1: 10) to afford (*S*)-**74** as a colorless oil (24 h, 62.5 mg, 99% yield, 95% ee). Enantiomeric excess established

by HPLC analysis using a Chiralpak AD-H column (HPLC: AD-H, 254 nm, hexane/isopropanol = 98:2, flow rate 1.0 mL/min, 25 °C, $t_r$ (major) = 8.2 min, $t_r$ (minor) = 9.0 min). $[\alpha]_D^{25}$ = –27.0° (*c* 0.7, $CH_2Cl_2$). $^1$H NMR (300 MHz, $CDCl_3$) $\delta$ 7.11 (d, *J* = 8.2 Hz, 1H), 6.35 – 6.25 (m, 2H), 5.93 (d, *J* = 1.1 Hz, 1H), 3.82 (s, 3H), 3.74 (dt, *J* = 8.1, 6.7 Hz, 1H), 3.46 – 3.30 (m, 2H), 2.94 (s, 6H), 2.52 (d, *J* = 1.0 Hz, 3H), 2.24 (s, 3H), 1.32 (d, *J* = 6.9 Hz, 3H). $^{13}$C NMR (75 MHz, $CDCl_3$) $\delta$ 173.4, 157.9, 151.4, 150.5, 143.9, 127.5, 122.9, 110.8, 105.0, 96.9, 55.4, 42.3, 41.0 (2C), 28.9, 20.6, 14.6, 13.9. IR (film): $\nu$ ($cm^{-1}$) 2958, 2928, 2873, 2833, 2797, 1722, 1613, 1568, 1514, 1454, 1439, 1410, 1375, 1342, 1324, 1236, 1196, 1177, 1124, 1095, 1061, 1036, 978, 961, 923, 896, 810, 764, 735, 679, 641, 586, 557, 508, 478, 413. HRMS (ESI, *m*/*z*) calcd for $C_{18}H_{26}N_3O_2$ $[M+H]^+$: 316.2020, found: 316.2026.

**(*S*)-Methyl 3-(4-(dimethylamino)-2-methoxyphenyl)butanoate (75')**

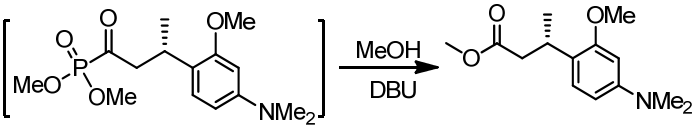


To a solution of catalyst Λ-**IrS** (9.5 mg, 0.01 mmol, 5 mol%) in distilled, anhydrous THF (0.1 mL) was added the phosphonate **64** (35.6 mg, 0.20 mmol) in a Schlenk tube. After being stirred at room temperature for 3 min, 3-methoxy-*N*,*N*-dimethylaniline (90.6 mg, 88.0 μL, 0.6 mmol) was added at room temperature. The reaction mixture was stirred at 60 °C for 24 h under nitrogen atmosphere. Methanol (0.50 mL), followed by DBU (0.10 mL), were added directly to the reaction mixture at room temperature. The reaction mixture was stirred for 30 min. After removing the solvent, the residue was purified by flash chromatography on silica gel (EtOAc/*n*-hexane = 1: 5) directly to give (*S*)-**75'** as a colorless oil (24.8 mg, 49% yield, 82% ee). Enantiomeric excess established by HPLC analysis using a Chiralpak OD-H column (HPLC: OD-H, 254 nm, hexane/isopropanol = 98:2, flow rate 1.0 mL/min, 25 °C, $t_r$ (major) = 12.1 min, $t_r$ (minor) = 10.9 min). $[\alpha]_D^{20}$ = +20.1° (*c* 0.2, $CH_2Cl_2$). $^1$H NMR (300 MHz, $CDCl_3$) $\delta$ 7.02 (d, *J* = 8.1 Hz, 1H), 6.41 – 6.20 (m, 2H), 3.83 (s, 3H), 3.64 (s, 3H), 3.61 – 3.44 (m, 1H), 2.94 (s, 6H), 2.67 (dd, *J* = 14.9, 5.8 Hz, 1H), 2.47 (dd, *J* = 14.9, 9.1 Hz, 1H), 1.25 (d, *J* = 7.0 Hz, 3H). All spectroscopic data are in agreement with the literature.[25]

**(*R*)-Ethyl 4-(4-(dimethylamino)-2-methoxyphenyl)-2-oxo-4-phenylbutanoate (76)**

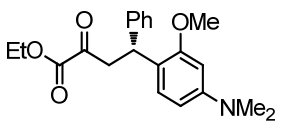


To a solution of catalyst Λ-**IrS** (3.8 mg, 0.004 mmol, 2 mol%) in distilled, anhydrous THF (0.1 mL) was added the α-ketoester **65** (40.8 mg, 0.20 mmol) in a Schlenk tube. After being stirred at room temperature for 3 min, 3-methoxy-*N*,*N*-dimethylaniline (90.6 mg, 88.0 μL, 0.6 mmol) was added at room temperature. The reaction mixture was stirred at 25 °C for 24 h under nitrogen atmosphere. Afterwards, the mixture was purified by flash chromatography on silica gel (EtOAc/*n*-hexane = 1: 8)

to afford (*R*)-**76** as a colorless oil (70.8 mg, 99% yield, 95% ee). Enantiomeric excess established by HPLC analysis using a Chiralpak AD-H column (HPLC: AD-H, 254 nm, hexane/isopropanol = 90:10, flow rate 1.0 mL/min, 25 °C, $t_r$ (major) = 11.2 min, $t_r$ (minor) = 9.8 min). $[\alpha]_D^{20}$ = +33.3° (*c* 0.8, $CH_2Cl_2$). $^1$H NMR (300 MHz, $CDCl_3$) $\delta$ 7.32 – 7.27 (m, 4H), 7.24 – 7.15 (m, 1H), 6.95 (d, *J* = 8.3 Hz, 1H), 6.33 – 6.22 (m, 2H), 4.95 (t, *J* = 7.6 Hz, 1H), 4.29 (q, *J* = 7.1 Hz, 2H), 3.80 (s, 3H), 3.63 (dd, *J* = 16.5, 7.7 Hz, 1H), 3.49 (dd, *J* = 16.5, 7.6 Hz, 1H), 2.94 (s, 6H), 1.35 (t, *J* = 7.1 Hz, 3H). $^{13}$C NMR (75 MHz, $CDCl_3$) $\delta$ 193.3, 161.2, 157.6, 150.9, 143.8, 128.7, 128.3 (2C), 128.0 (2C), 126.2, 120.0, 104.9, 96.6, 62.3, 55.3, 44.8, 40.8 (2C), 38.9, 14.1. IR (film): $\nu$ ($cm^{-1}$) 2935, 2836, 2801, 1722, 1613, 1567, 1514, 1492, 1451, 1440, 1408, 1354, 1274, 1235, 1180, 1154, 1111, 1063, 1031. 979, 950, 855, 812, 759, 728, 698, 641, 543, 510, 464. HRMS (ESI, *m*/*z*) calcd for $C_{21}H_{25}N_1O_4Na_1$ $[M+Na]^+$: 378.1687 found: 378.1704.

**3-(4-(Dimethylamino)-2-methoxyphenyl)-*N*-methoxy-*N*-methylbutanamide (77)**

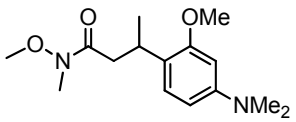


To a solution of catalyst Λ-**IrS** (9.5 mg, 0.01 mmol, 5 mol%) in distilled, anhydrous THF (0.1 mL) was added the Weinreb amide **66** (25.8 mg, 0.20 mmol) in a Schlenk tube. After being stirred at room temperature for 3 min, 3-methoxy-*N*,*N*-dimethylaniline (90.6 mg, 88.0 μL, 0.6 mmol) was added at room temperature. The reaction mixture was stirred at 60 °C for 24 h under nitrogen atmosphere. No product (**77**) was observed.

**Methyl 3-(4-(dimethylamino)-2-methoxyphenyl)butanoate (78)**

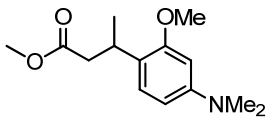


To a solution of catalyst Λ-**IrS** (9.5 mg, 0.01 mmol, 5 mol%) in distilled, anhydrous THF (0.1 mL) was added the carboxylic ester **67** (20.0 mg, 0.20 mmol) in a Schlenk tube. After being stirred at room temperature for 3 min, 3-methoxy-*N*,*N*-dimethylaniline (90.6 mg, 88.0 μL, 0.6 mmol) was added at room temperature. The reaction mixture was stirred at 60 °C for 24 h under nitrogen atmosphere. No product (**78**) was observed.

### 5.4.1.5 Assignment of the absolute and relative configuration of the Diels-Alder product

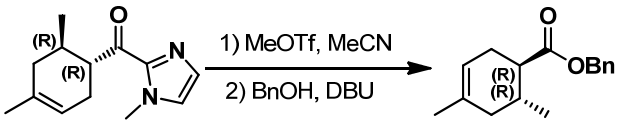


**55**
98% ee

**56**
99% yield, 98% ee

**(1*R*,6*R*)-Benzyl 4,6-dimethylcyclohex-3-enecarboxylate (56)**

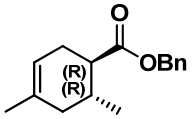


The mixture of **55** (60.5 mg, 0.28 mmol) and 4Å molecular sieves (140 mg) in acetonitrile (2.8 mL) was stirred vigorously for 2 hours. Then methyl trifluoromethanesulfonate (86.9 mg, 0.53 mmol, 60 µL, 1.90 equiv.) was added. After 40 minutes benzyl alcohol (302.0 mg, 2.8 mmol, 290 µL, 10.0 equiv) and diazabicyclo[5.4.0]undec-7-ene (127.7 mg, 0.84 mmol, 125 µL, 3.00 equiv) were added stepwise. After one hour stirring at room temperature the solvent was removed in *vacuo*. Purification by flash chromatography (EtOAc/*n*-hexane = 1: 20) afforded the disired compound **56** (68.1 mg, 99%) as a colorless oil. $^{1}$H NMR (300 MHz, $CDCl_3$) $\delta$ 7.81 – 6.71 (m, 5H), 5.35 (br s, 1H), 5.15 (d, $J$ = 0.9 Hz, 2H), 2.41 – 2.12 (m, 3H), 2.11 – 1.85 (m, 2H), 1.70 (d, $J$ = 10.0 Hz, 1H), 1.65 (s, 3H), 0.95 (d, $J$ = 6.3 Hz, 3H). $^{13}$C NMR (75 MHz, $CDCl_3$) $\delta$ 176.0, 136.3, 133.3, 128.5, 128.2, 128.1, 118.7, 66.0, 47.0, 38.1, 31.1, 28.9, 23.3, 19.7. All spectroscopic data were in agreement with the literature.[49]

**Optical rotation of (1*R*, 6*R*)-56:**

$[\alpha]_D^{20}$ = –131.6° (*c* 0.7, $CH_2Cl_2$, 98% ee).

Lit.[49] : $[\alpha]_D^{20}$ = +54° (*c* 0.055, $CH_2Cl_2$), (1*S*,6*S*)-**56**.

Lit.[50] : $[\alpha]_D$ = +171° (*c* 1.0, $CH_2Cl_2$, 99% ee), (1*S*,6*S*)-**56**.

**Chiral HPLC with (1*R*, 6*R*)-31:**

$t_r$ (major) = 9.6 min, $t_r$ (minor) = 11.0 min (as shown in **Figure 55**).

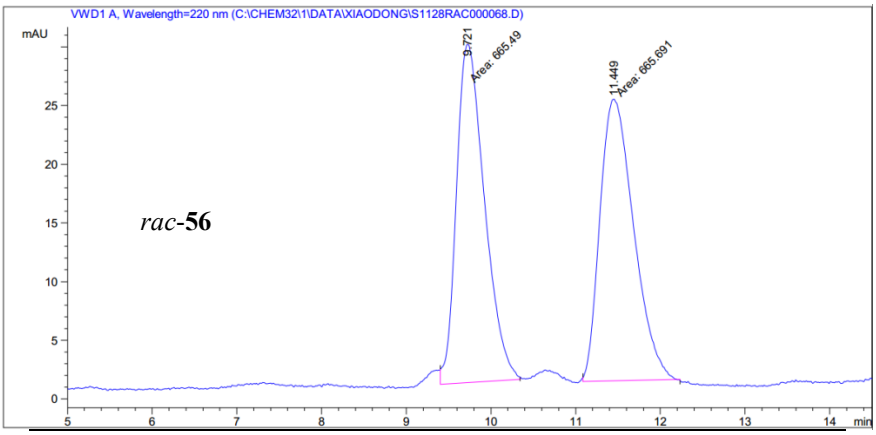


| Peak # | RetTime [min] | Type | Width [min] | Area [mAU*s] | Height [mAU] | Area % |
|---|---|---|---|---|---|---|
| 1 | 9.721 | FM | 0.3845 | 665.48962 | 28.84762 | 49.9924 |
| 2 | 11.449 | MM | 0.4618 | 665.69080 | 24.02469 | 50.0076 |

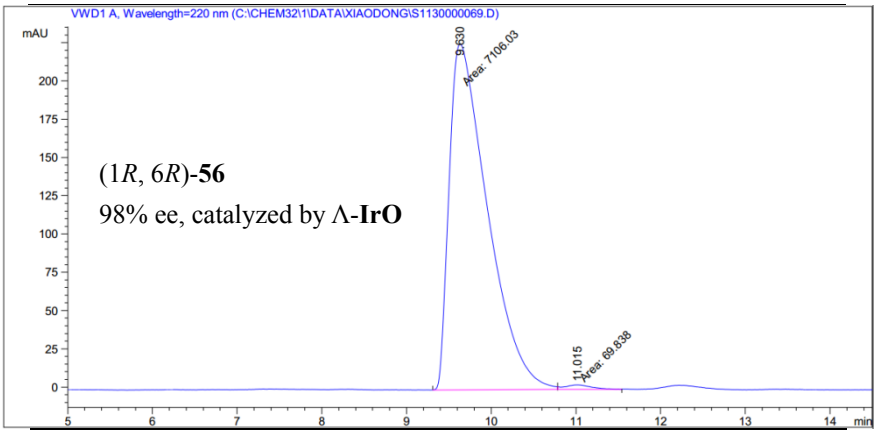


| Peak # | RetTime [min] | Type | Width [min] | Area [mAU*s] | Height [mAU] | Area % |
|---|---|---|---|---|---|---|
| 1 | 9.630 | MF | 0.5238 | 7106.03076 | 226.12300 | 99.0268 |
| 2 | 11.015 | FM | 0.3810 | 69.83804 | 3.05505 | 0.9732 |

**Figure 55** HPLC traces of compound **56**

*HPLC: Daicel Chiralpak OB-H column, 220 nm, heptane/isopropanol = 99.5/0.5, flow rate 1.0 mL/min, 25 ℃.*

### 5.4.1.6 Kinetic experiments

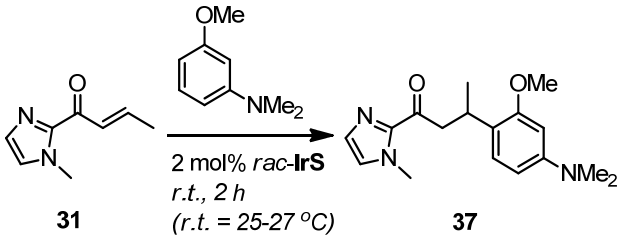


***Procedure:*** To a solution of catalyst *rac*-**IrS** (2 mol%) in distilled, anhydrous THF was added the 2-acyl imidazole **31** in a Schlenk tube. After being stirred at room temperature for 20 min, 3-methoxy-*N*,*N*-dimethylaniline was added at room temperature (detail information was shown in Table 10). 2 hours later, the solvent was removed and the crude sample was tested by $^{1}$H NMR at once. Every experiment was done three times (the results were shown in Table 11).

**Table 10** Detail Information for Kinetic Experiments

| *Entry* | *1* | *2* | *3* | *4* | *5* | *6* | *7* | *8* | *9* |
|---|---|---|---|---|---|---|---|---|---|
| ***31/aniline*** | ***1/3*** | ***1/2.5*** | ***1/2*** | ***1/1.5*** | ***1/1*** | ***1.5/1*** | ***2/1*** | ***2.5/1*** | ***3/1*** |
| ***31*** *(μL;mmol)* | *27;0.2* | *27;0.2* | *27;0.2* | *27;0.2* | *27;0.2* | *41;0.3* | *54;0.4* | *68;0.5* | *81;0.6* |
| ***Aniline*** *(μL;mmol)* | *90;0.6* | *75;0.5* | *60;0.4* | *45;0.3* | *30;0.2* | *30;0.2* | *30;0.2* | *30;0.2* | *30;0.2* |
| *THF (μL)* | *83* | *98* | *113* | *128* | *143* | *129* | *116* | *102* | *89* |
| $V_{total}$ *(μL)* | *200* | *200* | *200* | *200* | *200* | *200* | *200* | *200* | *200* |
| Conditions: 2 mol% catalyst loading; 2 hours; at room temperature. | | | | | | | | | |

**Table 11** Conversions *vs* Substrate Concentrations

| **[31] (M)** | Conv.1 (%) | Conv.2 (%) | Conv.3 (%) | Mean (%) | Standard Diviation | Standard Error |
|---|---|---|---|---|---|---|
| 1 | 9.0 | 11.2 | 11.2 | ***10.5*** | 1.27 | 0.73 |
| 1.5 | 13.6 | 14.3 | 14.9 | ***14.3*** | 0.65 | 0.38 |
| 2 | 16.6 | 17.8 | 16.3 | ***16.9*** | 0.79 | 0.46 |
| 2.5 | 20.5 | 20.6 | 18.7 | ***19.9*** | 1.07 | 0.62 |
| 3 | 25.2 | 24.0 | 22.7 | ***24.0*** | 1.25 | 0.72 |
| **[aniline] (M)** | | | | | | |
| 1 | 9.0 | 11.2 | 11.2 | ***10.5*** | 1.27 | 0.73 |
| 1.5 | 9.8 | 11.1 | 10.5 | ***10.5*** | 0.65 | 0.38 |
| 2 | 10.0 | 10.0 | 10.5 | ***10.2*** | 0.29 | 0.17 |
| 2.5 | 9.2 | 10.5 | 10.6 | ***10.1*** | 0.78 | 0.45 |
| 3 | 8.9 | 10.1 | 11.2 | ***10.1*** | 1.15 | 0.66 |

## 5.4.2 Generation of asymmetric quaternary stereocenters with the Henry reaction

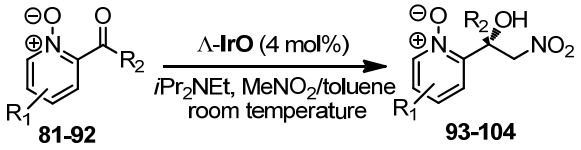


***General Procedure:*** To an oven-dried 10 mL Schlenk tube equipped with a magnetic stir bar was added Λ-**IrO** (4 mol%), 2-acyl-pyridine *N*-oxides **81-92** (0.2 mmol, 1.0 equiv), toluene (0.4 mL, contain 20 mol% $i$Pr$_2$NEt), and $MeNO_2$ (0.1 mL). The reaction mixture was stirred at room temperature for a certain time. And then, the reaction mixture was concentrated in *vacuo*. The resulting crude oil was purified by flash chromatography on silica gel (short column, EtOAc/*n*-hexane = 1: 1 to 2: 1) to provide the target compound **93-104**.

**(*R*)-2-(2-Hydroxy-1-nitropropan-2-yl)pyridine 1-oxide (93)**

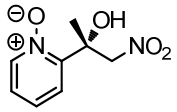

Starting from 2-acyl-pyridine *N*-oxides **81** (27.7 mg, 0.20 mmol) according to the *general procedure* to give **93** as a white solid (8 hours, 23.3 mg, 0.118 mmol, 56% yield). Enantiomeric excess established by HPLC analysis using a Chiralpak AD-H column, ee = 94% (HPLC: AD-H, 254 nm, hexane/isopropanol = 70: 30, flow rate 2.0 mL/min, 25 $^oC$), $t_r$ (minor) = 3.5 min, $t_r$ (major) = 7.5 min). $^1H$ NMR (300 MHz, $CDCl_3$) $\delta$ 8.25 (dt, $J$ = 6.2, 1.0 Hz, 1H), 7.79 (s, 1H), 7.46 – 7.40 (m, 2H), 7.38 – 7.30 (m, 1H), 5.34 (d, $J$ = 11.2 Hz, 1H), 4.82 (d, $J$ = 11.1 Hz, 1H), 1.79 (s, 3H). All spectroscopic data were in agreement with the literature.[38]

**(*R*)-2-(2-Hydroxy-1-nitropropan-2-yl)-3-methylpyridine 1-oxide (94)**

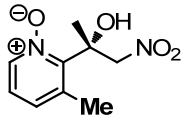

No product **94** was formed according to the *general procedure*.

**(*R*)-2-(2-Hydroxy-1-nitropropan-2-yl)-4-methylpyridine 1-oxide (95)**

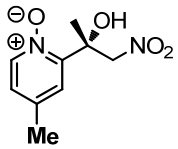

Starting from 2-acyl-pyridine *N*-oxides **83** (30.2 mg, 0.20 mmol) according to the *general procedure* to give **95** as a pale yellow solid (23 hours, 26.1 mg, 0.123 mmol, 62% yield). Enantiomeric excess established by HPLC analysis using a Chiralpak AD-H column, ee = 93% (HPLC: AD-H, 254 nm, hexane/isopropanol = 80:20, flow rate 2.0 mL/min, 25 $^oC$), $t_r$ (minor) = 4.7 min, $t_r$ (major) = 16.0 min).

$^1$H NMR (300 MHz, $CDCl_3$) $\delta$ 8.21 (s, 1H), 8.14 (d, $J$ = 6.5 Hz, 1H), 7.19 (s, 1H), 7.16 (d, $J$ = 6.8 Hz, 1H), 5.44 (d, $J$ = 11.0 Hz, 1H), 4.74 (d, $J$ = 11.0 Hz, 1H), 2.40 (s, 3H), 1.80 (s, 3H). All spectroscopic data were in agreement with the literature.[38]

**(*R*)-2-(2-Hydroxy-1-nitropropan-2-yl)-5-methylpyridine 1-oxide (96)**

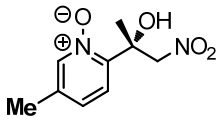


Starting from 2-acyl-pyridine *N*-oxides **84** (30.2 mg, 0.20 mmol) according to the *general procedure* to give **96** as a white solid (5 hours, 31.4 mg, 0.148 mmol, 74% yield). Enantiomeric excess established by HPLC analysis using a Chiralpak AD-H column, ee = 98% (HPLC: AD-H, 254 nm, hexane/isopropanol = 70:30, flow rate 2.0 mL/min, 25 $^o$C), $t_r$ (minor) = 4.9 min, $t_r$ (major) = 7.0 min). $^1$H NMR (300 MHz, $CDCl_3$) $\delta$ 8.12 (d, $J$ = 0.6 Hz, 1H ), 8.01 (s, 1H), 7.29 (d, $J$ = 8.1 Hz, 1H), 7.24 (dd, $J$ = 8.1 Hz, 0.6 Hz, 1H), 5.42 (d, $J$ = 10.8 Hz, 1H), 4.72 (d, $J$ = 11.1 Hz, 1H), 2.36 (s, 3H), 1.80 (s, 3H). All spectroscopic data were in agreement with the literature.[38]

**(*R*)-2-(2-Hydroxy-1-nitropropan-2-yl)-6-methylpyridine 1-oxide (97)**

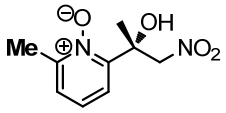


Starting from 2-acyl-pyridine *N*-oxides **85** (30.2 mg, 0.20 mmol) according to the *general procedure* to give **97** as a colorless oil (7 hours, 25.9 mg, 0.122 mmol, 61% yield). Enantiomeric excess established by HPLC analysis using a Chiralpak AD-H column, ee = 91% (HPLC: AD-H, 254 nm, hexane/isopropanol = 80:20, flow rate 1.0 mL/min, 25 $^o$C), $t_r$ (minor) = 8.5 min, $t_r$ (major) = 12.2 min). $^1$H NMR (300 MHz, $CDCl_3$) $\delta$ 8.20 (brs, 1H), 7.31 (td, $J$ = 7.3, 3.6 Hz, 3H), 5.40 (d, $J$ = 10.9 Hz, 1H), 4.74 (d, $J$ = 10.9 Hz, 1H), 2.55 (s, 3H), 1.80 (s, 3H). All spectroscopic data were in agreement with the literature.[38]

**(*R*)-2-(2-Hydroxy-1-nitropropan-2-yl)-4-methoxypyridine 1-oxide (98)**

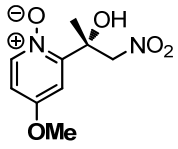


Starting from 2-acyl-pyridine *N*-oxides **86** 33.4 mg, 0.20 mmol) according to the *general procedure* to give **98** as a whote solid (18 hours, 37.6 mg, 0.165 mmol, 82% yield). Enantiomeric excess established by HPLC analysis using a Chiralpak AD-H column, ee = 84% (HPLC: AD-H, 254 nm, hexane/isopropanol = 80:20, flow rate 1.0 mL/min, 25 $^o$C), $t_r$ (minor) = 4.2 min, $t_r$ (major) = 18.6 min). $^1$H NMR (300 MHz, $CDCl_3$) $\delta$ 8.18 (d, $J$ = 7.2 Hz, 1H), 6.94 (d, $J$ = 3.4 Hz, 1H), 6.88 (dd, $J$ = 7.2, 3.4 Hz, 1H), 5.42 (d, $J$ = 11.1 Hz, 1H), 4.80 (d, $J$ = 11.1 Hz, 1H), 3.89 (s, 3H), 1.79 (s, 3H). All

spectroscopic data were in agreement with the literature.[38]

**(*R*)-4-Ethyl-2-(2-hydroxy-1-nitropropan-2-yl)pyridine 1-oxide (99)**

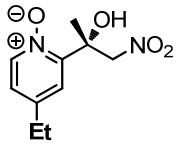


Starting from 2-acyl-pyridine *N*-oxides **87** (33.0 mg, 0.20 mmol) according to the *general procedure* to give **99** as a pale yellow solid (5 hours, 33.6 mg, 0.149 mmol, 75% yield). Enantiomeric excess established by HPLC analysis using a Chiralpak AD-H column, ee = 92% (HPLC: AD-H, 254 nm, hexane/isopropanol = 80:20, flow rate 2.0 mL/min, 25 $^{o}$C), $t_r$ (minor) = 4.3 min, $t_r$ (major) = 10.9 min). $^{1}$H NMR (300 MHz, $CDCl_3$) $\delta$ 8.16 (d, $J$ = 6.5 Hz, 1H), 7.21 (d, $J$ = 2.4 Hz, 1H), 7.18 (dd, $J$ = 6.6, 2.4 Hz, 1H), 5.43 (d, $J$ = 11.0 Hz, 1H), 4.75 (d, $J$ = 11.0 Hz, 1H), 2.69 (q, $J$ = 7.6 Hz, 3H), 1.80 (s, 3H), 1.26 (t, $J$ = 7.6 Hz, 3H). $^{13}$C NMR (75 MHz, $CDCl_3$) $\delta$ 148.7, 146.1, 139.9, 125.0, 124.2, 80.6, 72.5, 27.8, 23.2, 14.1. IR (film): $v$ (cm$^{-1}$) 3038, 2976, 1542, 1475, 1422, 1378, 1364, 1269, 1209, 1159, 1131, 1089, 1077, 1059, 949, 896, 865, 852, 838, 794, 757, 730, 710, 634, 587, 532, 488, 450, 406, 389. HRMS (ESI, $m/z$) calcd for $C_{10}H_{14}N_2O_4Na_1$ $[M+Na]^+$: 249.0846, found: 249.0847.

**(*R*)-2-(2-Hydroxy-1-nitropropan-2-yl)-4-propylpyridine 1-oxide (100)**

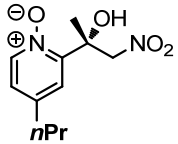


Starting from 2-acyl-pyridine *N*-oxides **88** (33.0 mg, 0.20 mmol) according to the *general procedure* to give **100** as a pale yellow solid (4 hours, 41.3 mg, 0.172 mmol, 86% yield). Enantiomeric excess established by HPLC analysis using a Chiralpak AD-H column, ee = 91% (HPLC: AD-H, 254 nm, hexane/isopropanol = 80:20, flow rate 2.0 mL/min, 25 $^{o}$C), $t_r$ (minor) = 4.2 min, $t_r$ (major) = 7.7 min). $^{1}$H NMR (300 MHz, $CDCl_3$) $\delta$ 8.16 (d, $J$ = 6.5 Hz, 1H), 7.24 – 7.04 (m, 2H), 5.43 (d, $J$ = 11.0 Hz, 1H), 4.75 (d, $J$ = 11.1 Hz, 1H), 2.62 (t, $J$ = 7.6 Hz, 2H), 1.66 (h, $J$ = 7.4 Hz, 2H), 0.96 (t, $J$ = 7.3 Hz, 3H). $^{13}$C NMR (75 MHz, $CDCl_3$) $\delta$ 148.5, 144.7, 139.7, 125.5, 124.7, 80.5, 72.5, 36.7, 23.4, 23.2, 13.4. IR (film): $v$ (cm$^{-1}$) 3050, 2960, 2926, 1541, 1475, 1460, 1447, 1416, 1379, 1340, 1313, 1266, 1237, 1208, 1156, 1137, 1105, 1078, 988, 953, 900, 874, 863, 841, 809, 781, 750, 732, 705, 649, 635, 587, 528, 495, 417, 396. HRMS (ESI, $m/z$) calcd for $C_{11}H_{16}N_2O_4Na_1$ $[M+Na]^+$: 263.1002, found: 263.1003.

**(*R*)-2-(2-Hydroxy-1-nitropropan-2-yl)-4-phenylpyridine 1-oxide (101)**

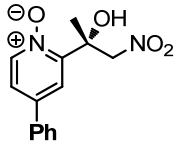

Starting from 2-acyl-pyridine *N*-oxides **89** (42.6 mg, 0.20 mmol) according to the *general procedure* to give **101** as a white solid (11 hours, 40.0 mg, 0.145 mmol, 73% yield). Enantiomeric excess established by HPLC analysis using a Chiralpak AD-H column, ee = 93% (HPLC: AD-H, 254 nm, hexane/isopropanol = 80:20, flow rate 2.0 mL/min, 25 °C), $t_r$ (minor) = 7.0 min, $t_r$ (major) = 8.0 min). $^1$H NMR (300 MHz, $CDCl_3$) $\delta$ 8.30 (d, $J$ = 6.7 Hz, 1H), 7.67 – 7.43 (m, 7H), 5.47 (d, $J$ = 11.2 Hz, 1H), 4.83 (d, $J$ = 11.2 Hz, 1H), 1.88 (s, 3H). All spectroscopic data were in agreement with the literature.[38]

**(*R*)-4-(*tert*-Butyl)-2-(2-hydroxy-1-nitropropan-2-yl)pyridine 1-oxide (102)**

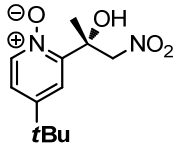


Starting from 2-acyl-pyridine *N*-oxides **90** (38.6 mg, 0.20 mmol) according to the *general procedure* to give **102** as a pale yellow oil (8 hours, 33.0 mg, 0.130 mmol, 65% yield). Enantiomeric excess established by HPLC analysis using a Chiralpak AD-H column, ee = 52% (HPLC: AD-H, 254 nm, hexane/isopropanol = 80:20, flow rate 2.0 mL/min, 25 °C), $t_r$ (minor) = 4.2 min, $t_r$ (major) = 4.8 min). $^1$H NMR (300 MHz, $CDCl_3$) $\delta$ 8.17 (dd, $J$ = 6.6, 0.7 Hz, 1H), 7.38 – 7.28 (m, 2H), 5.41 (d, $J$ = 11.1 Hz, 1H), 4.78 (d, $J$ = 11.1 Hz, 1H), 1.82 (s, 3H), 1.32 (s, 9H). $^{13}$C NMR (75 MHz, $CDCl_3$) $\delta$ 153.3, 148.3, 139.6, 122.8, 121.7, 80.6, 72.6, 34.9, 30.4, 23.2. IR (film): $\nu$ ($cm^{-1}$) 2966, 2872, 1550, 1479, 1466, 1416, 1377, 1368, 1308, 1270, 1224, 1190, 1160, 1126, 1077, 950, 907, 872, 827, 748, 733, 684, 633, 596, 530, 513, 397. HRMS (ESI, *m*/*z*) calcd for $C_{12}H_{18}N_2O_4Na_1$ $[M+Na]^+$: 277.1159, found: 277.1160.

**(*R*)-2-(2-Hydroxy-1-nitrobutan-2-yl)pyridine 1-oxide (103)**

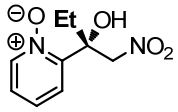


Starting from 2-acyl-pyridine *N*-oxides **91** (30.2 mg, 0.20 mmol) according to the *general procedure* to give **103** as a colorless oil (8 hours, 18.6 mg, 0.088 mmol, 44% yield). Enantiomeric excess established by HPLC analysis using a Chiralpak AD-H column, ee = 95% (HPLC: AD-H, 254 nm, hexane/isopropanol = 70:30, flow rate 2.0 mL/min, 25 °C), $t_r$ (minor) = 3.8 min, $t_r$ (major) = 8.0 min). $^1$H NMR (300 MHz, $CDCl_3$) $\delta$ 8.27 (dt, J = 6.3, 1.1 Hz, 1H), 7.68 (s, 1H), 7.43 (dd, J = 5.1, 1.1 Hz, 1H), 7.35 (m, 1H), 5.29 (d, J = 11.4 Hz, 1H), 4.97 (d, J = 11.4 Hz, 1H), 2.25 (m, 1H), 2.08 (m, 1H), 1.07 (t, J = 7.4 Hz, 3H). All spectroscopic data were in agreement with the literature.[38]

**(*R*)-2-(2-Hydroxy-1-nitrohexan-2-yl)pyridine 1-oxide (104)**

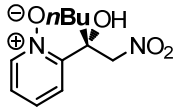


Starting from 2-acyl-pyridine *N*-oxides **92** (35.8 mg, 0.20 mmol) according to the *general procedure* to

give **104** as a pale yellow oil (10 hours, 18.3 mg, 0.076 mmol, 38% yield). Enantiomeric excess established by HPLC analysis using a Chiralpak AD-H column, ee = 92% (HPLC: AD-H, 254 nm, hexane/isopropanol = 80:20, flow rate 1.0 mL/min, 25 $^{o}$C), $t_r$ (minor) = 7.7 min, $t_r$ (major) = 9.5 min). $^1$H NMR (300 MHz, $CDCl_3$) $\delta$ 8.27 (dt, $J$ = 6.3, 1.0 Hz, 1H), 7.48 – 7.37 (m, 2H), 7.39 – 7.30 (m, 1H), 5.29 (d, $J$ = 11.4 Hz, 1H), 4.97 (d, $J$ = 11.4 Hz, 1H), 2.28 – 1.93 (m, 2H), 1.66 – 1.30 (m, 4H), 0.93 (t, $J$ = 7.1 Hz, 3H). All spectroscopic data were in agreement with the literature.[38]

## 5.5 Application for Asymmetric Photoredox Catalysis

### 5.5.1 Visible-Light-Induced enantioselective C-N bond formation

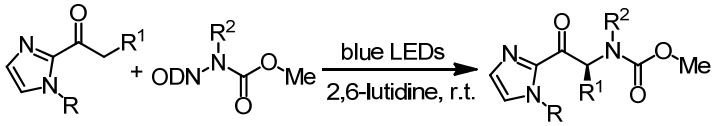


***General Procedure:*** To an oven-dried 10 mL Schlenk tube equipped with a magnetic stir bar was added Δ-**RhO** (2 mol%), 2-acyl imidazoles **105-116** (0.4 mmol, 2.0 equiv), and the amine reagent **117-121** (0.20 mmol, 1.0 equiv). The Schlenk tube was then degassed by alternative evacuation and back filling with nitrogen. DMSO (0.25 mL), $CH_3CN$ (0.75 mL), and 2, 6-lutidine (36.4 mg, 40 μL, 0.34 mmol, 1.7 equiv) were then added to the Schlenk tube via syringe addition. The resulting clear solution was degassed for 5 min by bubbling nitrogen through the reaction medium. The reaction mixture was stirred at room temperature and positioned approximately 10 cm from 24 W Blue LEDs. Upon completion, the reaction mixture was concentrated in *vacuo*. The resulting crude oil was purified by flash chromatography on silica gel (EtOAc/*n*-hexane = 1: 4 to 1: 2) to provide the target compounds **122-137**.

**(*S*)-Methyl (2-(1-isopropyl-1*H*-imidazol-2-yl)-2-oxo-1-phenylethyl)(methyl)carbamate (122)**

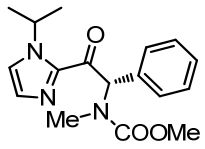

Starting from 2-acyl imidazole **105** (91.2 mg, 0.40 mmol) and the amine reagent **117** (67.0 mg, 0.20 mmol) according to the *general procedure* to give **122** as a colorless oil (14 h, 32.3 mg, 0.103 mmol, 52% yield). Enantiomeric excess established by HPLC analysis using a Chiralpak OD-H column, ee = 80% (HPLC: OD-H, 254 nm, hexane/isopropanol = 85:15, flow rate 1.0 mL/min, 25 $^{o}$C), $t_r$ (minor) = 18.1 min, $t_r$ (major) = 13.1 min). $[\alpha]_D^{20}$ = +107.0° (*c* 0.8, $CH_2Cl_2$). $^1$H NMR (300 MHz, $CDCl_3$) $\delta$ 7.36 – 7.22 (m, 6H), 7.11 – 7.06 (m, 2H), 5.59 – 5.50 (m, 1H), 3.72 (s, 3H), 2.83 (s, 3H), 1.46 (dd, appear t, $J$ = 6.6 Hz, 6H). $^{13}$C NMR (75 MHz, $CDCl_3$) $\delta$ 189.7, 157.5 (156.8, the rotamer), 141.1, 135.2, 130.1, 129.4, 128.7, 128.1, 121.2, 65.2 (64.5, the rotamer), 52.9, 49.2, 32.3, 23.7, 23.4. IR (film): $\nu$ ($cm^{-1}$)

2956, 1677, 1453, 1393, 1372, 1305, 1254, 1190, 1146, 1086, 1031, 1000, 991, 955, 915, 860, 817, 769, 734, 701, 670, 646, 617, 586, 555, 516, 492, 390. HRMS (ESI, *m*/*z*) calcd for $C_{17}H_{22}N_3O_3$ $[M+H]^+$: 316.1656, found: 316.1657.

**(*S*)-Methyl methyl(2-oxo-1-phenyl-2-(1-phenyl-1*H*-imidazol-2-yl)ethyl)carbamate (123)**

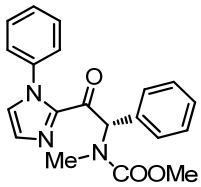

Starting from 2-acyl imidazole **106** (104.8 mg, 0.40 mmol) and the amine reagent **117** (67.0 mg, 0.20 mmol) according to the *general procedure* to give **123** as a pale yellow solid (2 hours, 64.4 mg, 0.185 mmol, 93% yield). Enantiomeric excess established by HPLC analysis using a Chiralpak OD-H column, ee = 89% (HPLC: OD-H, 254 nm, hexane/isopropanol = 85:15, flow rate 1.0 mL/min, 25 $^oC$), $t_r$ (minor) = 11.1 min, $t_r$ (major) = 14.7 min). $[\alpha]_D^{20}$ = +251.1° (*c* 0.8, $CH_2Cl_2$). $^1H$ NMR (300 MHz, $CDCl_3$) $\delta$ 7.55 – 7.42 (m, 3H), 7.40 – 7.27 (m, 7H), 7.21 (d, *J* = 1.1 Hz, 1H), 7.13 – 7.06 (m, 2H), 3.71 (s, 3H), 2.74 (s, 3H). $^{13}C$ NMR (75 MHz, $CDCl_3$) $\delta$ 188.1, 157.4 (156.5, the rotamer), 141.7, 138.1, 134.7, 130.1, 129.6, 129.0, 128.8, 128.7, 128.2, 126.9, 125.8, 64.9 (64.2, the rotamer), 52.8, 32.2. IR (film): *v* ($cm^{-1}$) 2954, 1683, 1596, 1491, 1446, 1401, 1375, 1344, 1306, 1243, 1209, 1188, 1146, 1074, 1036, 1022, 1001, 983, 974, 951, 913, 859, 817, 760, 734, 693, 587, 547, 523, 387. HRMS (ESI, *m*/*z*) calcd for $C_{20}H_{20}N_3O_3$ $[M+H]^+$: 350.1499, found: 350.1500.

**(*S*)-Methyl methyl(2-oxo-1-phenyl-2-(1-(*o*-tolyl)-1*H*-imidazol-2-yl)ethyl)carbamate (124)**

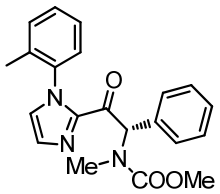

Starting from 2-acyl imidazole **107** (104.8 mg, 0.40 mmol) and the amine reagent **117** (67.0 mg, 0.20 mmol) according to the *general procedure* to give **124** as a pale yellow solid (2 hours, 69.4 mg, 0.191 mmol, 96% yield). Enantiomeric excess established by HPLC analysis using a Chiralpak OD-H column, ee = 97% (HPLC: OD-H, 254 nm, hexane/isopropanol = 85:15, flow rate 1.0 mL/min, 25 $^oC$), $t_r$ (minor) = 7.9 min, $t_r$ (major) = 12.3 min). $[\alpha]_D^{20}$ = +328.6° (*c* 0.8, $CH_2Cl_2$). $^1H$ NMR (300 MHz, $CDCl_3$) $\delta$ 7.46 – 7.17 (m, 10H), 7.17 – 6.97 (m, 2H), 3.70 (s, 3H), 2.73 and 2.69 (s and s, 3H, contained the rotamer), 2.04 and 1.97 (s and s, 3H, contained the rotamer). $^{13}C$ NMR (126 MHz, $CDCl_3$) $\delta$ 188.4, 188.2, 188.0, 187.8, 157.3, 156.5, 142.0, 142.0, 137.5, 137.4, 135.1, 134.7, 134.4, 134.0, 130.7, 130.6, 130.5, 130.3, 129.64, 129.61, 129.5, 129.3, 129.2, 129.1, 128.7, 128.6, 128.2, 128.2, 126.8, 126.7, 126.5, 126.4, 126.2, 126.0, 64.4, 64.0, 52.7, 32.1, 31.8, 31.7, 17.2, 17.0 (Contained the rotamer). IR (film): *v* ($cm^{-1}$) 2954, 1685, 1490, 1453, 1403, 1374, 1344, 1303, 1241,

1214, 1188, 1146, 1088, 1046, 1029, 973, 951, 914, 859, 818, 799, 762, 735, 718, 701, 676, 588, 560, 458, 390. HRMS (ESI, *m*/*z*) calcd for $C_{21}H_{21}N_3O_3Na_1$ $[M+Na]^+$: 386.1475, found: 386.1475.

**(*S*)-Methyl (1-(4-fluorophenyl)-2-oxo-2-(1-(*o*-tolyl)-1*H*-imidazol-2-yl)ethyl)(methyl)carbamate (125)**

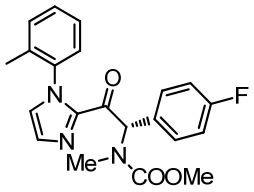

Starting from 2-acyl imidazole **108** (117.6 mg, 0.40 mmol) and the amine reagent **117** (67.0 mg, 0.20 mmol) according to the *general procedure* to give **125** as a white solid (1.5 hours, 76.2 mg, 0.200 mmol, >99% yield). Enantiomeric excess established by HPLC analysis using a Chiralpak OD-H column, ee = 97% (HPLC: OD-H, 254 nm, hexane/isopropanol = 90:10, flow rate 1.0 mL/min, 25 $^oC$), $t_r$ (minor) = 9.0 min, $t_r$ (major) = 12.4 min). $[\alpha]_D^{20}$ = +273.4° (*c* 0.9, $CH_2Cl_2$). $^1H$ NMR (300 MHz, $CDCl_3$) $\delta$ 7.43 – 7.19 (m, 7H), 7.16 – 6.98 (m, 4H), 3.71 (s, 3H), 2.74 and 2.70 (s and s, 3H, contained the rotamer), 2.04 and 1.97 (s and s, 3H, contained the rotamer). $^{19}F$ NMR (282 MHz, $CDCl_3$) $\delta$ – 114.13 and – 113.86 (s and s, 1F, contained the rotamer). $^{13}C$ NMR (126 MHz, $CDCl_3$) $\delta$ 188.1, 187.8, 163.5, 161.5, 157.3, 156.5, 141.9, 137.5, 137.4, 135.1, 134.9, 134.0, 131.4, 131.2, 130.8, 130.6, 130.4, 130.4, 129.3, 129.2, 126.8, 126.7, 126.6, 126.5, 126.0, 115.9, 115.8, 115.72, 115.65, 63.8, 63.2, 52.9, 32.1, 32.0, 31.8, 17.2, 17.1, 17.0 (Contained the rotamer). IR (film): *v* ($cm^{-1}$) 2956, 1684, 1604, 1508, 1490, 1452, 1402, 1376, 1345, 1304, 1223, 1189, 1147, 1099, 1047, 1028, 974, 953, 915, 865, 846, 816, 797, 762, 717, 674, 646, 588, 560, 454, 520, 500, 458. HRMS (ESI, *m*/*z*) calcd for $C_{21}H_{20}F_1N_3O_3Na_1$ $[M+Na]^+$: 404.1381, found: 404.1381.

**(*S*)-Methyl (1-(4-chlorophenyl)-2-oxo-2-(1-(*o*-tolyl)-1*H*-imidazol-2-yl)ethyl)(methyl)carbamate (126)**

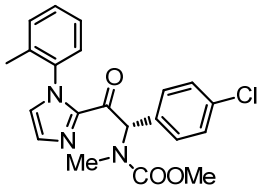

Starting from 2-acyl imidazole **109** (124.0 mg, 0.40 mmol) and the amine reagent **117** (67.0 mg, 0.20 mmol) according to the *general procedure* to give **126** as a pale yellow solid (2 hours, 77.8 mg, 0.196 mmol, 98% yield). Enantiomeric excess established by HPLC analysis using a Chiralpak OD-H column, ee = 98% (HPLC: OD-H, 254 nm, hexane/isopropanol = 95:5, flow rate 1.0 mL/min, 25 $^oC$), $t_r$ (minor) = 9.6 min, $t_r$ (major) = 15.0 min). $[\alpha]_D^{20}$ = +311.3° (*c* 1.0, $CH_2Cl_2$). $^1H$ NMR (300 MHz, $CDCl_3$) $\delta$ 7.49 – 7.17 (m, 8H), 7.16 – 6.98 (m, 3H), 3.72 (s, 3H), 2.75 and 2.71 (s and s, 3H, contained the rotamer), 2.04 and 1.98 (s and s, 3H, contained the rotamer). $^{13}C$ NMR (75 MHz, $CDCl_3$) $\delta$ 187.8,

187.5, 157.3, 156.5, 141.9, 137.4, 135.1, 134.3, 134.0, 133.4, 131.0, 130.8, 130.6, 130.5, 129.3, 129.0, 129.0, 126.8, 126.7, 126.5, 126.0, 63.8, 63.4, 52.9, 32.1, 17.1 (Contained the rotamer). IR (film): $\nu$ ($cm^{-1}$) 2954, 1686, 1592, 1490, 1455, 1400, 1375, 1345, 1304, 1242, 1190, 1149, 1090, 1046, 1029, 1015, 984, 952, 915, 863, 806, 764, 731, 717, 693, 675, 587, 560, 506, 458, 434, 389. HRMS (ESI, *m*/*z*) calcd for $C_{21}H_{21}Cl_1N_3O_3$ $[M+H]^+$: 398.1266, found:398.1267.

**(*S*)-Methyl (1-(3-chlorophenyl)-2-oxo-2-(1-(*o*-tolyl)-1*H*-imidazol-2-yl)ethyl)(methyl)carbamate (127)**

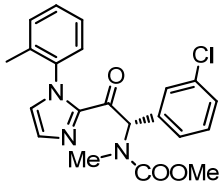


Starting from 2-acyl imidazole **110** (124.0 mg, 0.40 mmol) and the amine reagent **117** (67.0 mg, 0.20 mmol) according to the *general procedure* to give **127** as a pale yellow solid (2 hours, 70.6 mg, 0.178 mmol, 89% yield). Enantiomeric excess established by HPLC analysis using a Chiralpak OD-H column, ee = 92% (HPLC: OD-H, 254 nm, hexane/isopropanol = 90:10, flow rate 1.0 mL/min, 25 $^oC$), $t_r$ (minor) = 8.7 min, $t_r$ (major) = 11.0 min). $[\alpha]_D^{20}$ = +253.3° (*c* 0.8, $CH_2Cl_2$). $^1H$ NMR (300 MHz, $CDCl_3$) $\delta$ 7.48 – 7.30 (m, 4H), 7.30 – 7.22 (m, 4H), 7.14 – 7.02 (m, 3H), 3.73 (s, 3H), 2.76 and 2.72 (s and s, 3H, contained the rotamer), 2.05 and 2.00 (s and s, 3H, contained the rotamer). $^{13}C$ NMR (126 MHz, $CDCl_3$) $\delta$ 187.7, 187.5, 157.3, 156.4, 142.0, 141.9, 137.5, 137.3, 137.0, 136.8, 136.6, 135.1, 134.8, 134.6, 134.5, 134.1, 130.8, 130.7, 130.5, 130.0, 129.6, 129.6, 129.4, 129.2, 128.5, 127.8, 127.8, 127.6, 127.5, 127.0, 126.8, 126.7, 126.6, 126.5, 126.1, 63.9, 63.4, 52.9, 32.3, 32.2, 32.1, 31.9, 17.2, 17.0 (Contained the rotamer). IR (film): $\nu$ ($cm^{-1}$) 2954, 1685, 1595, 1573, 1489, 1476, 1454, 1400, 1375, 1346, 1303, 1241, 1214, 1188, 1147, 1081, 1046, 1028, 999, 958, 915, 888, 857, 820, 762, 714, 692, 678, 657, 589, 566, 547, 527, 459, 441, 422, 389. HRMS (ESI, *m*/*z*) calcd for $C_{21}H_{20}Cl_1N_3O_3Na_1$ $[M+Na]^+$: 420.1085, found:420.1088.

**(*S*)-Methyl (1-(2-chlorophenyl)-2-oxo-2-(1-(*o*-tolyl)-1*H*-imidazol-2-yl)ethyl)(methyl)carbamate (128)**

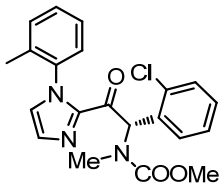


Starting from 2-acyl imidazole **111** (124.0 mg, 0.40 mmol) and the amine reagent **117** (67.0 mg, 0.20 mmol) according to the *general procedure* to give **128** as a pale yellow solid (2 hours, 78.8 mg, 0.198 mmol, 99% yield). Enantiomeric excess established by HPLC analysis using a Chiralpak OD-H column, ee = 97% (HPLC: OD-H, 254 nm, hexane/isopropanol = 90:10, flow rate 1.0 mL/min, 25 $^oC$),

$t_r$ (minor) = 10.6 min, $t_r$ (major) = 20.1 min). $[\alpha]_D^{20}$ = +307.9° (*c* 0.9, $CH_2Cl_2$). $^1$H NMR (300 MHz, $CDCl_3$) $\delta$ 7.46 – 7.28 (m, 4H), 7.25 – 6.98 (m, 7H), 3.70 (s, 3H), 2.76 and 2.69 (s and s, 3H, contained the rotamer), 2.03 and 2.01 (s and s, 3H, contained the rotamer). $^{13}$C NMR (126 MHz, $CDCl_3$) $\delta$ 187.5, 187.4, 187.0, 186.7, 157.0, 156.6, 141.9, 141.8, 137.54, 137.49, 137.4, 137.3, 135.3, 135.2, 135.1, 134.9, 134.8, 134.4, 134.3, 134.1, 133.23, 133.15, 132.9, 132.1, 130.8, 130.7, 130.64, 130.57, 130.52, 130.46, 130.39, 130.36, 130.24, 130.20, 130.0, 129.9, 129.7, 129.54, 129.51, 129.3, 129.2, 129.13, 129.07, 128.9, 128.4, 126.9, 126.8, 126.62, 126.59, 126.56, 126.50, 126.46, 126.4, 126.3, 126.1, 126.0, 63.1, 63.0, 62.5, 62.2, 53.1, 53.0, 52.9, 52.8, 32.5, 32.3, 32.1, 32.0, 17.22, 17.17, 17.13, 17.05, 17.0 (Contained the rotamer). IR (film): $\nu$ ($cm^{-1}$) 2956, 1685, 1446, 1401, 1376, 1301, 1246, 1188, 1147, 1028, 973, 955, 915, 865, 854, 819, 759, 717, 697, 675, 589, 560, 530, 506, 458, 428. HRMS (ESI, *m*/*z*) calcd for $C_{21}H_{20}Cl_1N_3O_3Na_1$ $[M+Na]^+$: 420.1085, found:420.1089.

**(*S*)-Methyl (1-(4-bromophenyl)-2-oxo-2-(1-(*o*-tolyl)-1*H*-imidazol-2-yl)ethyl)(methyl)carbamate (129)**

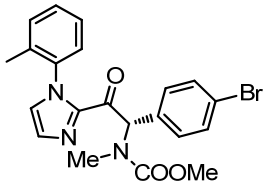


Starting from 2-acyl imidazole **112** (141.6 mg, 0.40 mmol) and the amine reagent **117** (67.0 mg, 0.20 mmol) according to the *general procedure* to give **129** as a pale yellow solid (2 hours, 85.2 mg, 0.193 mmol, 97% yield). Enantiomeric excess established by HPLC analysis using a Chiralpak OD-H column, ee = 97% (HPLC: OD-H, 254 nm, hexane/isopropanol = 90:10, flow rate 1.0 mL/min, 25 $^o$C), $t_r$ (minor) = 10.0 min, $t_r$ (major) = 15.9 min). $[\alpha]_D^{20}$ = +275.6° (*c* 1.1, $CH_2Cl_2$). $^1$H NMR (300 MHz, $CDCl_3$) $\delta$ 7.50 – 7.43 (m, 2H), 7.43 – 7.09 (m, 7H), 7.09 – 6.98 (m, 2H), 3.69 (s, 3H), 2.73 and 2.69 (s and s, 3H, contained the rotamer), 2.02 and 1.96 (s and s, 3H, contained the rotamer). $^{13}$C NMR (126 MHz, $CDCl_3$) $\delta$ 187.8, 187.5, 157.3, 156.4, 141.9, 137.5, 137.3, 135.1, 134.8, 134.0, 133.6, 131.94, 131.87, 131.3, 131.2, 131.0, 130.8, 130.6, 130.47, 130.46, 129.3, 129.2, 126.8, 126.6, 126.5, 126.0, 122.5, 63.9, 63.4, 52.9, 32.1, 32.0, 31.9, 17.2, 17.1, 17.0 (Contained the rotamer). IR (film): $\nu$ ($cm^{-1}$) 2954, 1686, 1587, 1501, 1486, 1405, 1370, 1344, 1323, 1311, 1301, 1287, 1257, 1211, 1192, 1179, 1146, 1108, 1086, 1072, 1058, 1027, 1009, 981, 953, 915, 868, 836, 808, 763, 727, 717, 686, 677, 663, 588, 559, 527, 501, 457, 397. HRMS (ESI, *m*/*z*) calcd for $C_{21}H_{20}Br_1N_3O_3Na_1$ $[M+Na]^+$: 464.0580, 486.0562, found: 464.0584, 486.0564.

**(*S*)-Methyl methyl(2-oxo-1-(*p*-tolyl)-2-(1-(*o*-tolyl)-1*H*-imidazol-2-yl)ethyl)carbamate (130)**

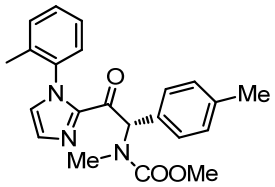

Starting from 2-acyl imidazole **113** (116.0 mg, 0.40 mmol) and the amine reagent **117** (67.0 mg, 0.20 mmol) according to the *general procedure* to give **130** as a pale yellow solid (6 h, 61.4 mg, 0.163 mmol, 81% yield). Enantiomeric excess established by HPLC analysis using a Chiralpak OD-H column, ee = 97% (HPLC: OD-H, 254 nm, hexane/isopropanol = 90:10, flow rate 1.0 mL/min, 25 $^{o}$C), $t_r$ (minor) = 7.5 min, $t_r$ (major) = 11.2 min). $[\alpha]_D^{20}$ = +347.5° (*c* 0.8, $CH_2Cl_2$). $^1$H NMR (300 MHz, $CDCl_3$) $\delta$ 7.46 – 7.21 (m, 5H), 7.21 – 7.03 (m, 6H), 3.70 (s, 3H), 2.72 and 2.68 (s and s, 3H, contained the rotamer), 2.33 (s, 3H), 2.05 and 1.97 (s and s, 3H, contained the rotamer). $^{13}$C NMR (126 MHz, $CDCl_3$) $\delta$ 188.7, 188.5, 188.3, 188.1, 157.4, 156.6, 142.1, 142.1, 138.2, 138.1, 137.7, 137.5, 135.2, 134.9, 134.1, 131.6, 131.2, 130.8, 130.70, 130.5, 130.4, 129.7, 129.5, 129.5, 129.3, 129.1, 126.9, 126.8, 126.6, 126.4, 126.3, 126.1, 126.0, 64.3, 63.8, 52.7, 32.1, 31.8, 31.7, 21.1, 17.3, 17.12, 17.05 (Contained the rotamer). IR (film): $\nu$ (cm$^{-1}$) 2953, 1685, 1500, 1489, 1451, 1402, 1373, 1309, 1242, 1190, 1146, 1046, 1023, 974, 952, 914, 863, 826, 804, 786, 762, 738, 717, 675, 645, 634, 588, 560, 515, 493, 458, 395. HRMS (ESI, *m*/*z*) calcd for $C_{22}H_{23}N_3O_3Na_1$ $[M+Na]^+$: 400.1632, found: 420.1635.

**(*S*)-Methyl (1-(4-methoxyphenyl)-2-oxo-2-(1-(*o*-tolyl)-1*H*-imidazol-2-yl)ethyl)(methyl)carbamate (131)**

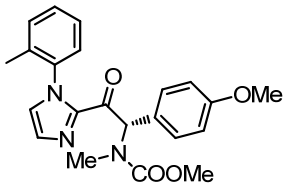

Starting from 2-acyl imidazole **114** (122.4mg, 0.40 mmol) and the amine reagent **117** (67.0 mg, 0.20 mmol) according to the *general procedure* to give **131** as a pale yellow solid (6 h, 41.0 mg, 0.104 mmol, 52% yield). Enantiomeric excess established by HPLC analysis using a Chiralpak OD-H column, ee = 97% (HPLC: OD-H, 254 nm, hexane/isopropanol = 90:10, flow rate 1.0 mL/min, 25 $^{o}$C), $t_r$ (minor) = 12.4 min, $t_r$ (major) = 20.5 min). $[\alpha]_D^{20}$ = +313.3° (*c* 0.5, $CH_2Cl_2$). $^1$H NMR (300 MHz, $CDCl_3$) $\delta$ 7.47 – 7.30 (m, 4H), 7.31 – 7.14 (m, 2H), 7.14 – 6.98 (m, 3H), 6.88 (d, *J* = 8.6 Hz, 2H), 3.80 (s, 3H), 3.70 (s, 3H), 2.72 and 2.68 (s and s, 3H, contained the rotamer), 2.05 and 1.96 (s and s, 3H, contained the rotamer). $^{13}$C NMR (75 MHz, $CDCl_3$) $\delta$ 189.8, 188.4, 159.5, 158.3, 142.1, 137.7, 134.1, 131.1, 130.8, 130.6, 130.4, 130.2, 129.9, 129.2, 128.7, 126.9, 126.6, 126.5, 126.4, 126.3, 126.0, 125.8, 125.7, 114.23, 114.17, 113.61, 113.58, 63.9, 63.5, 55.2, 55.0, 52.8, 32.0, 31.8, 17.3, 17.1 (Contained the rotamer). IR (film): $\nu$ (cm$^{-1}$) 2955, 1684, 1608, 1510, 1491, 1458, 1401, 1376, 1302, 1248, 1176, 1146, 1028, 981, 952, 914, 863, 808, 787, 762, 717, 675, 588, 559, 526, 458. HRMS (ESI, *m*/*z*) calcd

for $C_{22}H_{24}N_3O_4$ $[M+H]^+$: 394.1761, found: 394.1762.

**(*S*)-Methyl methyl(1-(naphthalen-2-yl)-2-oxo-2-(1-(*o*-tolyl)-1*H*-imidazol-2-yl)ethyl)carbamate (132)**

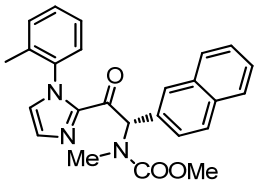


Starting from 2-acyl imidazole **115** (130.4 mg, 0.40 mmol) and the amine reagent **117** (67.0 mg, 0.20 mmol) according to the *general procedure* to give **132** as a pale yellow solid (2 h, 67.0 mg, 0.162 mmol, 81% yield). Enantiomeric excess established by HPLC analysis using a Chiralpak OD-H column, ee = 96% (HPLC: OD-H, 254 nm, hexane/isopropanol = 90:10, flow rate 1.0 mL/min, 25 $^oC$), $t_r$ (minor) = 12.1 min, $t_r$ (major) = 17.5 min). $[\alpha]_D^{20}$ = +341.9° (*c* 0.9, $CH_2Cl_2$). $^1H$ NMR (300 MHz, $CDCl_3$) $\delta$ 7.93 – 7.74 (m, 3H), 7.69 (s, 1H), 7.59 – 7.29 (m, 7H), 7.25 (d, *J* = 4.1 Hz, 1H), 7.15 (d, *J* = 7.6 Hz, 1H), 7.05 (s, 1H), 3.77 (s, 3H), 2.78 and 2.74 (s and s, 3H, contained the rotamer), 2.10 and 2.03 (s and s, 3H, contained the rotamer). $^{13}C$ NMR (75 MHz, $CDCl_3$) $\delta$ 188.5, 188.3, 157.5, 156.6, 142.2, 142.1, 137.6, 135.3, 134.0, 133.07, 133.05, 132.9, 132.3, 131.9, 130.9, 130.7, 130.4, 129.2, 128.9, 128.8, 128.0, 127.9, 127.6, 127.3, 127.0, 126.7, 126.5, 126.3, 126.1, 64.5, 64.1, 52.9, 32.2, 32.0, 17.3, 17.1; (Contained the rotamer). IR (film): $\nu$ ($cm^{-1}$) 2954, 1684, 1501, 1490, 1454, 1403, 1376, 1344, 1302, 1236, 1191, 1148, 1125, 1047, 1028, 968, 944, 915, 905, 894, 866, 817, 792, 761, 732, 717, 692, 676, 646, 559, 478, 459. HRMS (ESI, *m*/*z*) calcd for $C_{25}H_{23}N_3O_3Na_1$ $[M+Na]^+$: 436.1634, found: 436.1634.

**(*S*)-Methyl butyl(2-oxo-1-phenyl-2-(1-(*o*-tolyl)-1*H*-imidazol-2-yl)ethyl)carbamate (133)**

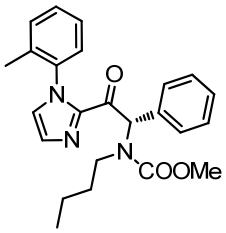


Starting from 2-acyl imidazole **107** (110.4 mg, 0.40 mmol) and the amine reagent **118** (75.4 mg, 0.20 mmol) according to the *general procedure* to give **133** as a pale yellow oil (2 h, 66.6 mg, 0.164 mmol, 82% yield). Enantiomeric excess established by HPLC analysis using a Chiralpak OD-H column, ee = 97% (HPLC: OD-H, 254 nm, hexane/isopropanol = 95:5, flow rate 1.0 mL/min, 25 $^oC$), $t_r$ (minor) = 11.6 min, $t_r$ (major) = 17.3 min). $[\alpha]_D^{20}$ = +251.1° (*c* 0.8, $CH_2Cl_2$). $^1H$ NMR (300 MHz, $CDCl_3$) $\delta$ 7.43 – 7.27 (m, 7H), 7.23 (d, *J* = 4.5 Hz, 2H), 7.06 – 6.97 (m, 3H), 3.67 (s, 3H), 3.41 – 3.16 (m, 1H), 3.15 – 2.86 (m, 1H), 2.04 and 1.91 (s and s, 3H, contained the rotamer), 1.33 – 1.23 (m, 1H), 1.06 – 0.66 (m, 3H), 0.63 and 0.58 (d and d, *J* = 7.4 Hz and 7.5 Hz, 3H, contained the rotamer). $^{13}C$ NMR (75 MHz,

$CDCl_3$) $\delta$ 187.9, 187.6, 157.4, 156.4, 142.2, 137.6, 135.1, 134.7, 134.5, 134.2, 130.8, 130.6, 130.20, 130.17, 129.1, 128.7, 128.6, 128.4, 128.3, 126.9, 126.6, 126.4, 126.3, 126.2, 126.1, 65.0, 52.6, 52.6, 45.3, 31.1, 19.7, 17.2, 17.1, 13.43, 13.41; (Contained the rotamer). IR (film): $v$ ($cm^{-1}$) 2955, 2929, 1686, 1493, 1453, 1393, 1290, 1258, 1200, 1145, 1085, 1047, 1029, 961, 930, 913, 860, 823, 798, 761, 736, 717, 701, 676, 616, 557, 458, 444, 405, 393. HRMS (ESI, $m/z$) calcd for $C_{24}H_{27}N_3O_3Na_1$ $[M+Na]^+$: 428.1945, found: 428.1950.

**(*S*)-Methyl (2-oxo-1-phenyl-2-(1-(*o*-tolyl)-1*H*-imidazol-2-yl)ethyl)(3-phenylpropyl)carbamate (134)**

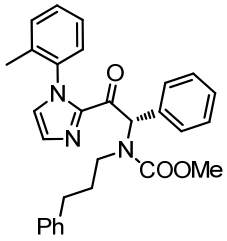


Starting from 2-acyl imidazole **107** (110.4 mg, 0.40 mmol) and the amine reagent **119** (87.8 mg, 0.20 mmol) according to the *general procedure* to give **134** as a pale yellow oil (2 h, 80.1 mg, 0.177 mmol, 89% yield). Enantiomeric excess established by HPLC analysis using a Chiralpak AD-H column, ee = 97% (HPLC: AD-H, 254 nm, hexane/isopropanol = 70:30, flow rate 1.0 mL/min, 25 $^oC$), $t_r$ (minor) = 6.4 min, $t_r$ (major) = 16.2 min). $[\alpha]_D^{20}$ = +173.8° ($c$ 0.7, $CH_2Cl_2$). $^1H$ NMR (300 MHz, $CDCl_3$) $\delta$ 7.46 – 7.19 (m, 9H), 7.21 – 7.11 (m, 3H), 7.14 – 6.96 (m, 3H), 6.89 (t, $J$ = 6.6 Hz, 2H), 3.68 (s, 3H), 3.46 – 3.24 (m, 1H), 3.19 – 2.90 (m, 1H), 2.38 – 2.13 (m, 2H), 2.04 and 1.92 (s and s, 3H, contained the rotamer), 1.74 – 1.50 (m, 1H), 1.37 – 1.01 (m, 1H). $^{13}C$ NMR (126 MHz, $CDCl_3$) $\delta$ 187.9, 187.6, 157.3, 156.3, 142.1, 141.5, 137.7, 135.2, 134.6, 134.1, 130.8, 130.6, 130.3, 130.2, 130.1, 129.1, 128.8, 128.7, 128.5, 128.5, 128.4, 128.3, 128.3, 128.2, 128.1, 128.0, 126.9, 126.6, 126.4, 126.3, 126.2, 126.1, 125.5, 65.1, 64.8, 52.73, 52.69, 45.2, 45.00, 33.0, 30.7, 30.2, 17.3, 17.1; (Contained the rotamer). IR (film): $v$ ($cm^{-1}$) 2953, 2925, 1686, 1602, 1584, 1495, 1452, 1392, 1295, 1248, 1188, 1167, 1151, 1113, 1079, 1047, 1028, 1003, 954, 913, 865, 847, 830, 819, 799, 762, 749, 737, 717, 698, 677, 619, 559, 493, 458, 389. HRMS (ESI, $m/z$) calcd for $C_{29}H_{29}N_3O_3Na_1$ $[M+Na]^+$: 490.2101, found: 490.2106.

**(*S*)-Methyl isobutyl(2-oxo-1-phenyl-2-(1-(*o*-tolyl)-1*H*-imidazol-2-yl)ethyl)carbamate (135)**

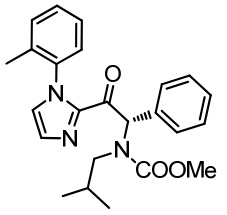


Starting from 2-acyl imidazole **107** (110.4 mg, 0.40 mmol) and the amine reagent **120** (75.4 mg, 0.20 mmol) according to the *general procedure* to give **135** as a pale yellow solid (2 h, 78.5 mg, 0.194

mmol, 97% yield). Enantiomeric excess established by HPLC analysis using a Chiralpak OD-H column, ee = 97% (HPLC: OD-H, 254 nm, hexane/isopropanol = 95:5, flow rate 1.0 mL/min, 25 $^{o}$C), $t_r$ (minor) = 10.1 min, $t_r$ (major) = 14.0 min). $[\alpha]_D^{20}$ = +216.7° (*c* 0.5, $CH_2Cl_2$). $^1$H NMR (300 MHz, $CDCl_3$) $\delta$ 7.43 – 7.25 (m, 7H), 7.23 (d, *J* = 3.8 Hz, 2H), 7.09 – 6.78 (m, 3H), 3.65 (s, 3H), 3.38 – 3.13 (m, 1H), 3.06 – 2.80 (m, 1H), 2.04 and 1.87 (s and s, 3H, contained the rotamer), 1.36 – 1.12 (m, 1H), 0.67 (d and d, appear t, *J* = 6.5 Hz, 3H, contained the rotamer), 0.46 and 0.42 (d and d, *J* = 6.6 Hz and 6.7 Hz, 3H, contained the rotamer). $^{13}$C NMR (126 MHz, $CDCl_3$) $\delta$ 187.8, 187.5, 157.9, 142.2, 137.6, 134.5, 134.3, 130.8, 130.6, 130.4, 130.1, 130.0, 129.1, 128.6, 128.54, 128.46, 128.4, 126.9, 126.5, 126.4, 126.1, 65.8, 65.4, 52.9, 52.6, 27.8, 27.8, 19.9, 19.8, 19.7, 17.3, 17.0; (Contained the rotamer). IR (film): *v* ($cm^{-1}$) 2955, 1685, 1493, 1454, 1435, 1394, 1335, 1302, 1260, 1209, 1190, 1148, 1086, 1047, 1028, 985, 962, 913, 858, 825, 800, 761, 736, 717, 703, 677, 663, 617, 559, 457. HRMS (ESI, *m*/*z*) calcd for $C_{24}H_{27}N_3O_3Na_1$ $[M+Na]^+$: 428.1945, found: 428.1947.

**(*S*)-Methyl (2-(1,3-dioxolan-2-yl)ethyl)(2-oxo-1-phenyl-2-(1-(*o*-tolyl)-1*H*-imidazol-2-yl)ethyl) carbamate (136)**

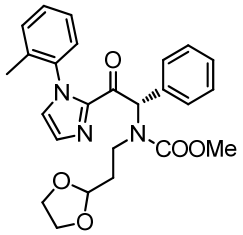


Starting from 2-acyl imidazole **107** (110.4 mg, 0.40 mmol) and the amine reagent **121** (84.2 mg, 0.20 mmol) according to the *general procedure* to give **136** as a pale yellow oil (3 h, 56.6 mg, 0.126 mmol, 63% yield). Enantiomeric excess established by HPLC analysis using a Chiralpak OD-H column, ee = 97% (HPLC: OD-H, 254 nm, hexane/isopropanol = 90:10, flow rate 1.0 mL/min, 25 $^{o}$C), $t_r$ (minor) = 22.2 min, $t_r$ (major) = 25.4 min). $[\alpha]_D^{20}$ = +196.4° (*c* 0.58, $CH_2Cl_2$). $^1$H NMR (300 MHz, $CDCl_3$) $\delta$ 7.49 – 7.26 (m, 8H), 7.22 (d, *J* = 4.4 Hz, 2H), 7.05 (d, *J* = 7.0 Hz, 1H), 7.00 (s, 1H), 4.52 (s, 1H), 3.87 – 3.53 (m, 7H), 3.53 – 3.32 (m, 1H), 3.30 – 3.02 (m, 1H), 1.97 (d, *J* = 37.5 Hz, 3H), 1.70 (tt, *J* = 10.6, 5.4 Hz, 1H), 1.38 – 1.09 (m, 1H); (Contained the rotamer). $^{13}$C NMR (126 MHz, $CDCl_3$) $\delta$ 187.7, 187.4, 157.2, 142.0, 137.6, 135.2, 134.5, 134.1, 130.8, 130.5, 130.23, 130.20, 130.1, 129.1, 128.83, 128.76, 128.4, 126.9, 126.6, 126.4, 126.3, 126.2, 126.1, 102.6, 65.1, 64.6, 64.5, 64.4, 52.80, 52.77, 40.7, 40.5, 33.4, 33.0, 17.3, 17.1; (Contained the rotamer). IR (film): *v* ($cm^{-1}$)2956, 2883, 1686, 1492, 1455, 1442, 1393, 1299, 1264, 1215, 1195, 1144, 1121, 1048, 1026, 986, 955, 913, 902, 858, 826, 798, 763, 717, 701, 676, 665, 616, 559, 517, 487, 458, 395. HRMS (ESI, *m*/*z*) calcd for $C_{25}H_{27}N_3O_5Na_1$ $[M+Na]^+$: 472.1843, found: 472.1847.

**(*S*)-Methyl methyl(1-oxo-1-(1-(*o*-tolyl)-1*H*-imidazol-2-yl)propan-2-yl)carbamate (137)**

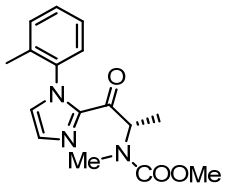

Starting from 2-acyl imidazole **116** (85.6 mg, 0.40 mmol) and the amine reagent **117** (67.0 mg, 0.20 mmol) according to the *general procedure*, no product (**137**) was observed after 38 hours.

## 5.5.2 Mechanistic study

### 5.5.2.1 The UV/vis absorbance spectra of *rac*-RhO, *rac*-IrO, RhO-enolate and IrO-enolate

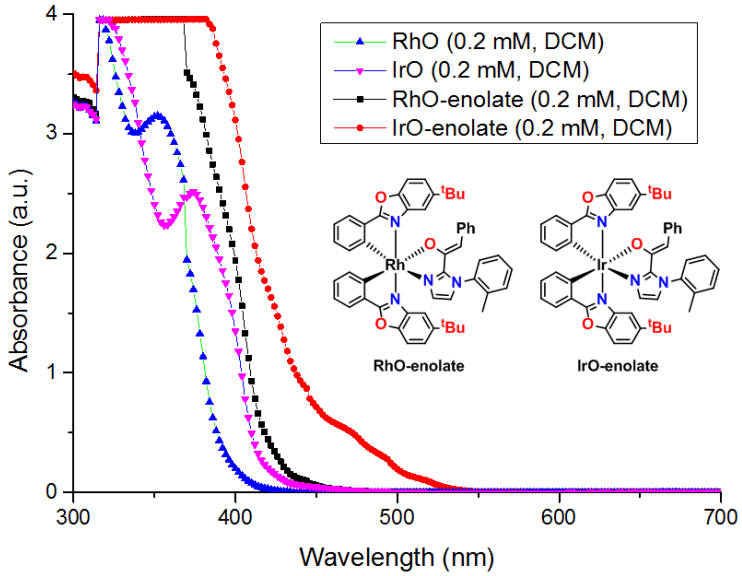


**Figure 56** The UV/vis absorbance spectra of *rac*-**RhO**, *rac*-**IrO**, **RhO**-enolate and **IrO**-enolate.#

### 5.5.2.2 Catalytic behavior of RhO-enolate complex

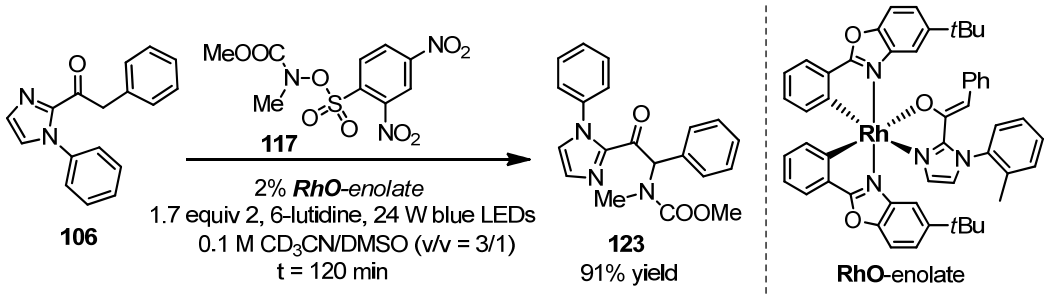


***Procedure:*** To an oven-dried 10 mL Schlenk tube equipped with a magnetic stir bar was added **RhO**-enolate (2 mol%), 2-acyl imidazole **106** (0.2 mmol, 2.0 equiv), and the amine reagent **117** (0.10 mmol, 1.0 equiv). The Schlenk tube was then degassed by alternative evacuation and back filling with nitrogen. DMSO (0.25 mL), $CH_3CN$ (0.75 mL), and 2, 6-lutidine (20 μL, 0.17 mmol, 1.7 equiv) were

then added to the Schlenk tube via syringe addition. The resulting clear solution was degassed for 5 min by bubbling nitrogen through the reaction medium. The reaction mixture was stirred at room temperature and positioned approximately 10 cm from 24 W Blue LEDs. 2 hours later, the reaction mixture was concentrated in *vacuo*. The resulting crude oil was purified by flash chromatography on silica gel (EtOAc/*n*-hexane = 1: 4 to 1: 2) to provide the target compound **123** as a pale yellow solid (91% yield).

### 5.5.2.3 Trapping experiments by *N*-methylindole

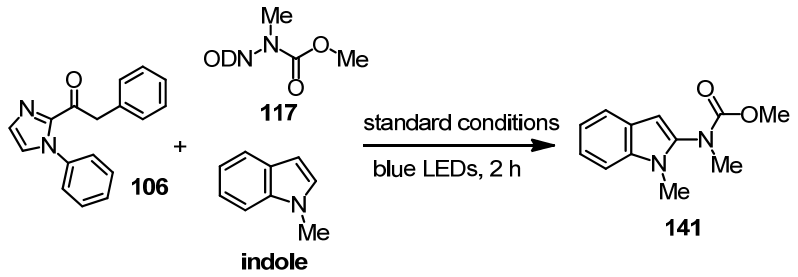


***Procedure:*** To an oven-dried 10 mL Schlenk tube equipped with a magnetic stir bar was added *rac*-**IrO**, *rac*-**IrS** or *rac*-**RhO** (each 2 mol%), 2-acyl imidazoles **106** (5.2 mg, 0.02 mmol, 0.2 equiv), and the amine reagent **117** (33.5 mg, 0.10 mmol, 1.0 equiv). The Schlenk tube was then degassed by alternative evacuation and back filling with nitrogen. DMSO (0.125 mL), $CH_3CN$ (0.375 mL), 2,6-lutidine (20 μL, 0.17 mmol, 1.7 equiv) and *N*-methylindole (26.2 mg, 0.2 mmol, 2.0 equiv) were then added to the Schlenk tube via syringe addition. The resulting clear solution was degassed for 5 min by bubbling nitrogen through the reaction medium. The reaction mixture was stirred at room temperature and positioned approximately 10 cm from 24 W blue LEDs. 2 hours later, the reaction mixture was concentrated in *vacuo*. The yield is determined by crude $^1$HNMR and based on trimethyl(phenyl)silane as an internal standard. After that, the reaction mixture was concentrated in *vacuo*. The resulting crude oil was purified by flash chromatography on silica gel (EtOAc/*n*-hexane = 1: 10 to 1: 5) to provide the target compound **141** as a colorless oil.

**Methyl methyl(1-methyl-1*H*-indol-2-yl)carbamate (141)**

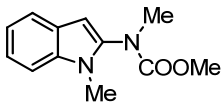


$^1$H NMR (300 MHz, $CDCl_3$) $\delta$ 7.60 (ddd, $J$ = 7.9, 1.2, 0.8 Hz, 1H), 7.32 (ddt, $J$ = 8.3, 1.5, 0.8 Hz, 1H), 7.30 – 7.23 (m, 1H), 7.14 (ddd, $J$ = 8.0, 6.8, 1.4 Hz, 1H), 6.34 (d, $J$ = 0.8 Hz, 1H), 3.73 (s, 3H), 3.58 (s, 3H), 3.33 (s, 3H). $^{13}$C NMR (75 MHz, $CDCl_3$) $\delta$ 156.5, 137.9, 134.8, 126.4, 121.9, 120.8, 119.8, 109.4, 95.9, 53.3, 38.7, 28.6. IR (film): $\nu$ ($cm^{-1}$) 3075, 2952, 2847, 1710, 1579, 1558, 1447, 1434, 1392, 1367, 1339, 1309, 1255, 1228, 1191, 1156, 1092, 1000, 934, 893, 818, 772, 749, 734, 680, 525, 446, 404. HRMS (ESI, *m*/*z*) calcd for $C_{12}H_{14}N_2O_2Na_1$ $[M+Na]^+$:241.0947, found: 241.0954.

### 5.5.2.4 Trapping experiment by TEMPO

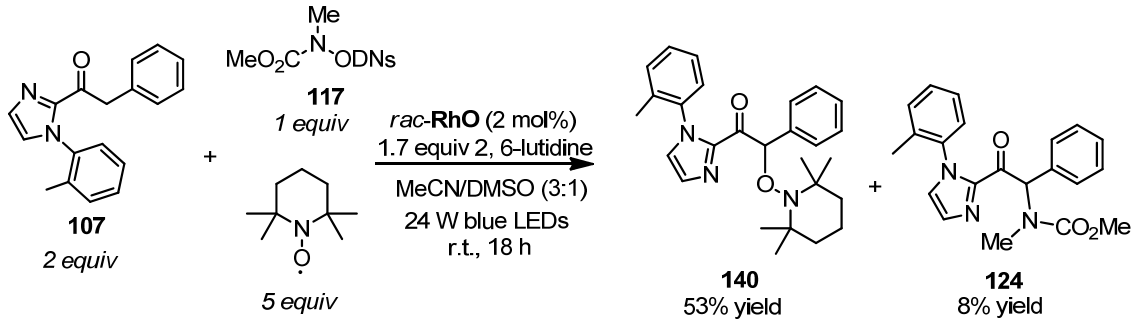


***Procedure:*** To an oven-dried 10 mL Schlenk tube equipped with a magnetic stir bar was added *rac*-**RhO** (2 mol%), 2-acyl imidazoles **107** (0.40 mmol, 2.0 equiv), the amine reagent **117** (0.20 mmol, 1.0 equiv) and *TEMPO* (1.00 mmol, 5.0 equiv). The Schlenk tube was then degassed by alternative evacuation and back filling with nitrogen. DMSO (0.25 mL), $CH_3CN$ (0.75 mL), and 2, 6-lutidine (40 μL, 0.34 mmol, 1.7 equiv) were then added to the Schlenk tube via syringe addition. The resulting clear solution was degassed for 5 min by bubbling nitrogen through the reaction medium. The reaction mixture was stirred at room temperature and positioned approximately 10 cm from 24 W Blue LEDs. 18 hours later, the reaction mixture was concentrated in *vacuo*. The resulting crude oil was purified by flash chromatography on silica gel (EtOAc/*n*-hexane = 1: 20 to 1: 2) to provide the target compound **140** as a white solid (53% yield) and **124** as a colorless oil (8% yield).

**2-Phenyl-2-((2,2,6,6-tetramethylpiperidin-1-yl)oxy)-1-(1-(*o*-tolyl)-1*H*-imidazol-2-yl)ethanone (140)**

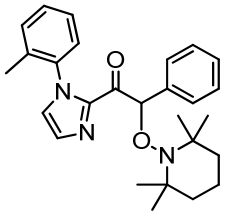

$^1$H NMR (300 MHz, $CDCl_3$) $\delta$ 7.51 (t, $J$ = 6.9 Hz, 2H), 7.40 – 7.04 (m, 8H), 7.03 (d, $J$ = 0.8 Hz, 1H), 6.62 (dd, $J$ = 22.7, 8.9 Hz, 1H), 2.04 (s, 1H), 1.46 (q, $J$ = 10.2, 6.8 Hz, 5H), 1.34 – 1.24 (m, 1H), 1.22 (s, 2H), 1.18 (s, 3H), 1.06 (s, 6H), 0.75 (d, $J$ = 6.2 Hz, 3H); (Contained the rotamer). $^{13}$C NMR (75 MHz, $CDCl_3$) $\delta$ 188.9, 188.7, 142.8, 142.7, 138.1, 138.0, 137.4, 137.3, 134.5, 134.2, 130.5, 129.9, 128.9, 128.8, 128.1, 128.0, 127.3, 126.4, 126.2, 126.1, 89.6, 89.4, 59.8, 59.4, 40.0, 33.7, 33.1, 20.0, 17.1, 17.1, 15.7; (Contained the rotamer). IR (film): $v$ ($cm^{-1}$) 2962, 2926, 2846, 1682, 1490, 1454, 1392, 1378, 1360, 1340, 1301, 1277, 1241, 1208, 1183, 1146, 1131, 1083, 1053, 1044, 1030, 1008, 954, 923, 908, 881, 870, 828, 790, 775, 759, 734, 717, 696, 680, 664, 646, 623, 564, 553, 520, 496, 458. HRMS (ESI, $m/z$) calcd for $C_{27}H_{34}N_3O_2$ $[M+H]^+$: 432.2646, found: 432.2646.

### 5.5.2.5 "Dark and Light" experiments

***Procedure:*** To an oven-dried 10 mL Schlenk tube equipped with a magnetic stir bar was added *rac*-**RhO** (2 mol%), 2-acyl imidazole **106** (0.20 mmol, 2.0 equiv), the amine reagent **117** (0.10 mmol, 1.0 equiv) and 9.2 μL tetradecane. The Schlenk tube was then degassed by alternative evacuation and back filling with nitrogen. DMSO (0.25 mL), $CH_3CN$ (0.75 mL), and 2, 6-lutidine (20 μL, 0.17 mmol, 1.7 equiv) were then added to the Schlenk tube via syringe addition. The resulting clear solution was degassed for 5 min by bubbling nitrogen through the reaction medium. The reaction mixture was stirred at room temperature and positioned approximately 10 cm from 24 W Blue LEDs for specified time intervals (Table 12). After irradiation for 5 min, turn off the light, and 5 μL samples were taken by a microsyringe and diluted with 200 μL DCM. The yield of the product was detected by GC (FID detector, tetradecane as reference standard). After 60 min in the dark, 5 μL samples were taken for testing by the same method. Repeat this "dark and light" experiment three times. (Figure 57)

**Table 12** The Data for "Dark and Light" Experiments

| Time / min | Yield / % (by GC) | Remarks |
|---|---|---|
| 0 | 0 | / |
| 5 | 1.8 | Light (5min) |
| 65 | 4.2 | Dark (60min) |
| 70 | 12.0 | Light (5min) |
| 130 | 16.4 | Dark (60min) |
| 135 | 23.3 | Light (5min) |
| 195 | 24.3 | Dark (60min) |
| 200 | 29.2 | Light (5min) |

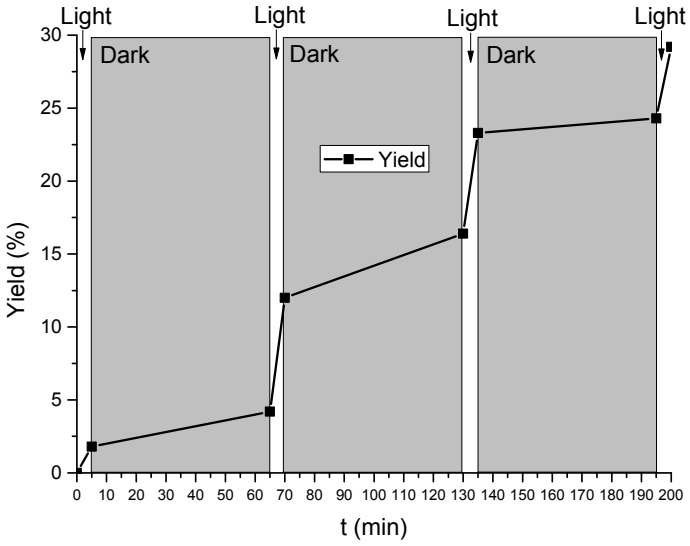


**Figure 57** "Dark and Light" experiments.

### 5.5.2.6 Quantum yield measurement

The quantum yield was measured by standard ferrioxalate actinometry.[51] A 150 W Xenon lamp (50% of light intensity, 420±5 nm bandpass filter high transmittance) was used as the light source. The measured method was designed according to published procedures with modifications. [52,53]

The solutions were prepared under the red light (1.1 W red LED) and stored in the dark:

Potassium ferrioxalate solution (0.15 M): 736.9 mg of potassium ferrioxalate hydrate was dissolved in 10 mL of 0.05 M $H_2SO_4$.

Buffered solution of phenanthroline: 50 mg of 1,10-phenanthroline and 11.25 g of sodium acetate were dissolved in 50 mL of 0.5 M $H_2SO_4$.

*1) Measurement of light intensity at 420 nm.*

1 mL of the ferrioxalate solution was added to a quartz cuvette (l = 10 mm). The actinometry solution was irradiated with 150 W Xenon lamp (50% of light intensity, 420 nm ± 5 nm bandpass filter high transmittance) for specified time intervals (30s, 60s, 90s, 120s). After irradiation, 175 μL of the phenanthroline solution was added to the cuvette. The solution was kept in dark for 30 min to make sure the complete coordination. The absorbance of the actinometry solution was monitored at 510 nm. The absorbance of a non-irradiated (in dark) sample was also measured at 510 nm. (Table 13)

**Table 13** The Absorbance of the Actinometry Solution at 510 nm

| ***t/s*** | *30* | *60* | *90* | *120* |
|---|---|---|---|---|
| ***ΔA/a.u.*** | *0.350* | *0.738* | *1.108* | *1.399* |

The moles of $Fe^{2+}$ formed were determined using Beer's Law (eq 1):

$$\text{mol } Fe^{2+} = \frac{V \times \Delta A(510\text{ nm})}{l \times \varepsilon(510\text{ nm})} \quad (1)$$

- V is the final volume (0.01175 L) after complexation with phenanthroline;
- ΔA (510 nm) is the optical difference in absorbance between the irradiated and non-irradiated solutions;
- l is the path length (1 cm);
- ε(510 nm) is the molar absorptivity of $Fe(phen)_3^{2+}$(11100 $L \cdot mol^{-1} \cdot cm^{-1}$).

The photon flux (it is defined as the number of photons per second per unit area) can be calculated using eq 2:

$$\text{photon flux} = \frac{d(\text{mol } Fe^{2+})/dt}{\Phi \times f} \quad (2)$$

- Φ is the quantum yield for the ferrioxalate actinometer (1.05 for a 0.15 solution at 412 nm; ***1.04 for a 0.15 solution at 422 nm***; 1.03 for a 0.15 solution at 433 nm)[51];
- $f = 1 - 10^{-A}$ (3)
- f is the fraction of light absorbed which was calculated using eq 3; where A is the absorbance of

above ferrioxalate solution at 420 nm (as shown in Figure 58, A > 3, indicating f is > 0.999 ≈ 1).

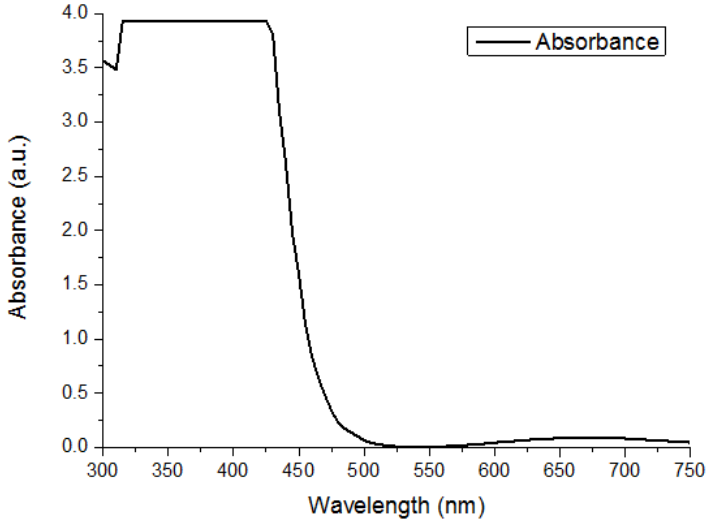


**Figure 58** Absorbance of the ferrioxalate actinometer solution (0.15 M).

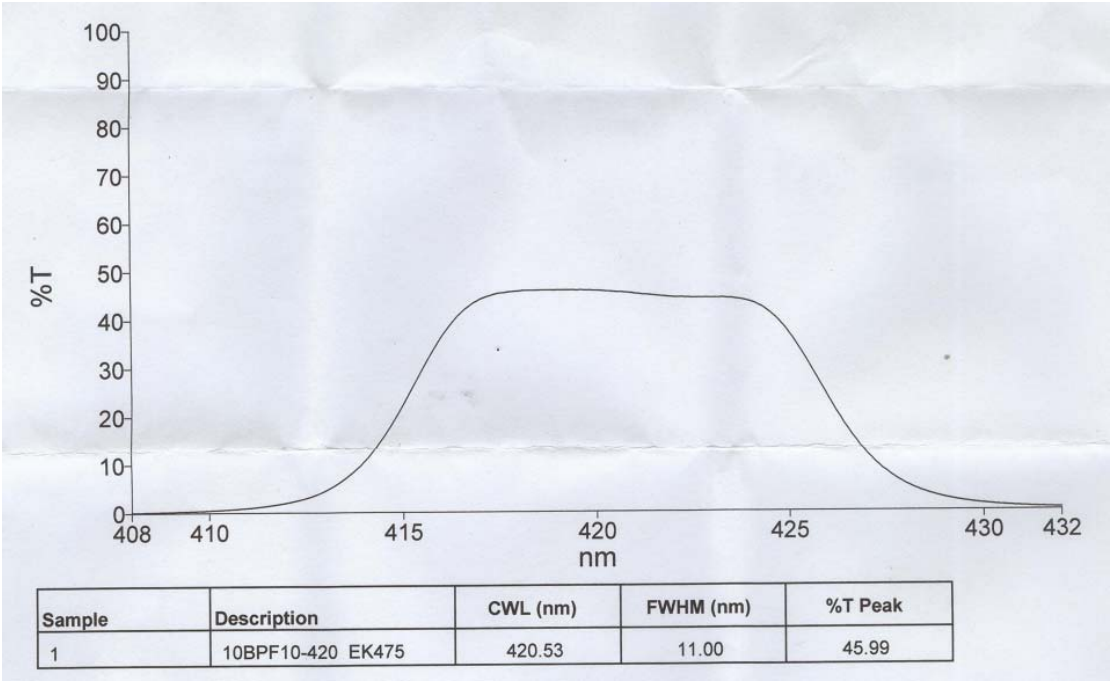


| Sample | Description | CWL (nm) | FWHM (nm) | %T Peak |
|---|---|---|---|---|
| 1 | 10BPF10-420 EK475 | 420.53 | 11.00 | 45.99 |

**Figure 59** The bandpass filter (420±5 nm).

According to Table 13 and equation (1), the moles of $Fe^{2+}$ are plotted as a function of time (t) in Figure 60 (the slope in Figure 60 is d(mol $Fe^{2+}$)/dt). Combine the equation (2), equation (3) with the slope, the photon flux can be calculated as follows:

$$\text{photon flux} = \frac{1.27 \times 10^{-9}}{1.04 \times 1} = 1.22 \times 10^{-9} \text{einstein} \cdot s^{-1}$$

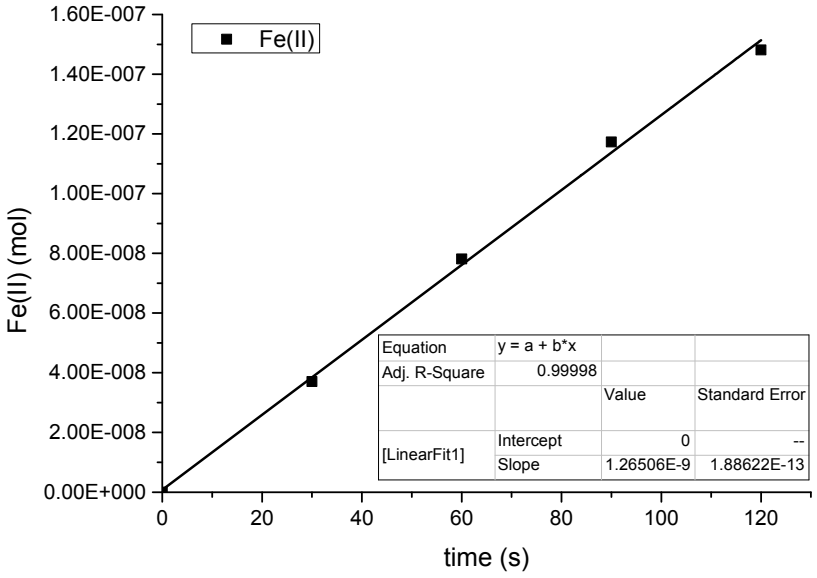


**Figure 60** The moles of $Fe^{2+}$ are plotted as a function of time (t).

*2) Determination of the response factor (GC, FID detector, tetradecane as reference standard)*

Before a yield can be calculated, the gas chromatograph (GC) needs to be calibrated to determine the response factors for each individual component (reference standard and amination product **123**). The response factor is effectively the calibration factor for each individual component and it can be measured by using the following formula:

$$\text{Rf (Response Factor)} = \frac{\text{Peak Area}}{\text{Calibration Concentration}} \quad (4)$$

Tetradecane is chosen as reference standard. According to equation (4), Rf(tetradecane)/Rf(product) can be calculated as follows:

$$\text{Rf (tetradecane)/Rf (product)} = \frac{\dfrac{\text{peak area (tetradecane)}}{\text{concentration (tetradecane)}}}{\dfrac{\text{peak area (product)}}{\text{concentration (product)}}} = \frac{\text{ratio of peak area (tetradecane/product)}}{\text{ratio of mass (tetradecane/product)}} \quad (5)$$

The tetradecane and product **123** (the mass ratio is specified) are mixed in DCM and determined by GC. The ratio of integrated areas (tetradecane/ product) is shown in Table 14. Accoring to Table 14, fit linear of the integrated areas ratio (tetradecane /product) to the mass ratio (tetradecane /product) to give a slope of 1.645 (see Figure 61). Combined with equation (5), Rf(tetradecane)/Rf(product) is equal to 1.645.

**Table 14** Determination of the Response Factor

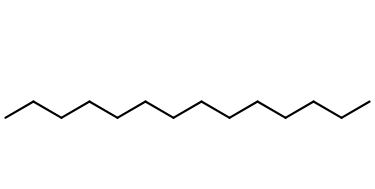

tetradecane as reference standard

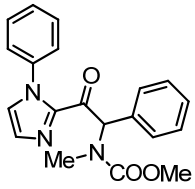

product

| *entry* | 1 | 2 | 3 | 4 |
|---|---|---|---|---|
| *Mass of tetradecane/product (mg)* | 0.17/1.7 | 0.34/1.7 | 0.51/1.7 | 0.68/1.7 |
| *Mass ratio of tetradecane/product* | 0.1 | 0.2 | 0.3 | 0.4 |
| *Ratio of integrated areas tetradecane/product (GC)* | 0.185 | 0.335 | 0.504 | 0.642 |

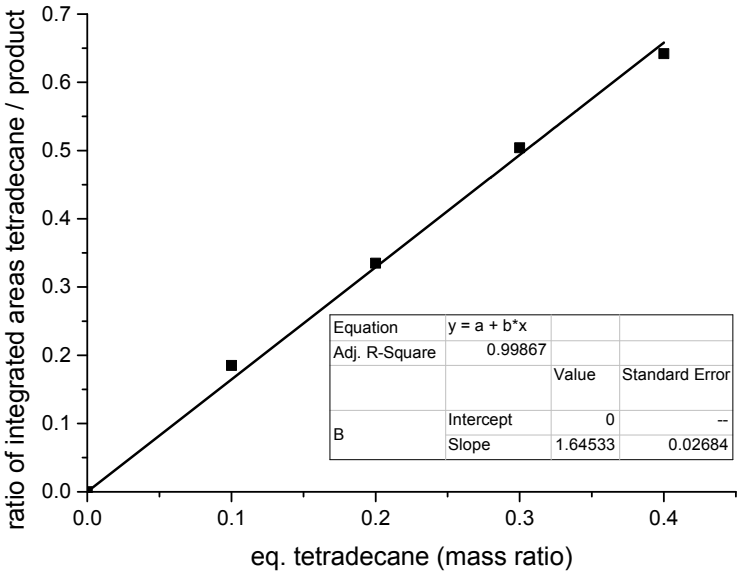


**Figure 61** Fit linear of the integrated areas ratio (tetradecane /product) to the mass ratio (tetradecane /product).

*3) Measurement of quantum yield*

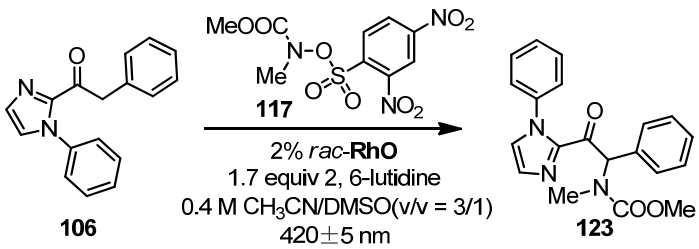


To an dried 1.0 mL cuvette (with rubber cap) equipped with a magnetic stir bar was added *rac*-**RhO** (2 mol%), 2-phenyl-1-(1-phenyl-1*H*-imidazol-2-yl)ethanone **106** (209.6 mg, 0.80 mmol, 2.0 equiv), and the amine reagent methyl ((2,4-dinitrophenyl)sulfonyl)oxy(methyl)carbamate **117** (134.0 mg, 0.40

mmol, 1.0 equiv). The cuvette was then degassed by alternative evacuation and back filling with nitrogen. The mixture solvents of DMSO/$CH_3CN$ (v/v = 1/3), 2, 6-lutidine (80 μL, 0.68 mmol, 1.7 equiv), and tetredacane (14.0 mg) were then added to the cuvette (the total volume is 1.0 mL) via syringe addition. The resulting clear solution was degassed for 5 min by bubbling nitrogen through the reaction medium. The reaction mixture was stirred at room temperature and irradiated with 150 W Xenon lamp (50% of light intensity, 420 nm ± 5 nm bandpass filter high transmittance) for specified time intervals (3 minutes, 6 minutes, 9 minutes, 12 minutes). The yield of product was detected by GC (FID detector, tetradecane as reference standard).

According to the ratio of integrated areas tetradecane/product in GC and the response factor (Rf(tetradecane)/Rf(product) = 1.645), we calculate the yield of product, which is shown in Table 15.

**Table 15** The Yield of Product at Different Time

| ***t/min*** | 0 | 3 | 6 | 9 | 12 |
|---|---|---|---|---|---|
| ***Yield%*** | 0 | 0.68 | 1.76 | 2.31 | 2.75 |

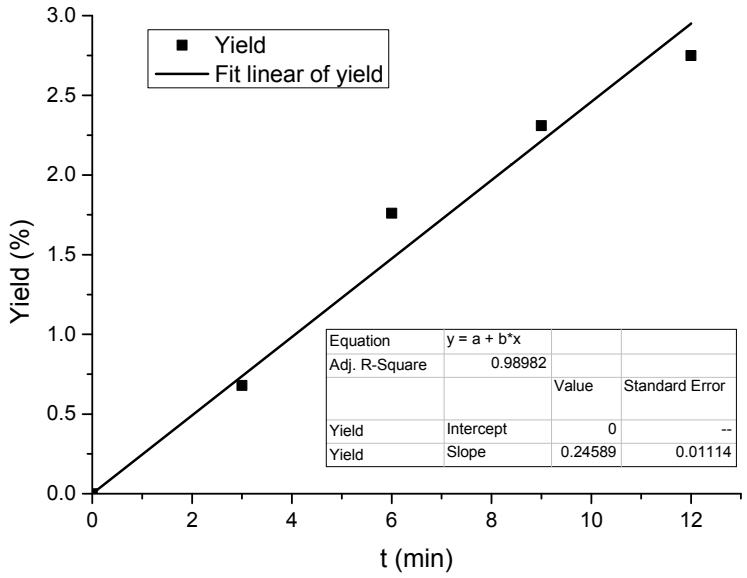


**Figure 62** Fit linear of yield.

According to the Figure 62, the quantum yield is,

$$\mathbf{\Phi} = \text{mol product/ mol photons} = 0.4\times10^{-3}\times0.246\%/(1.206\times10^{-9}\times60) = \mathbf{13.6}$$

### 5.5.3 Photo reaction in flow

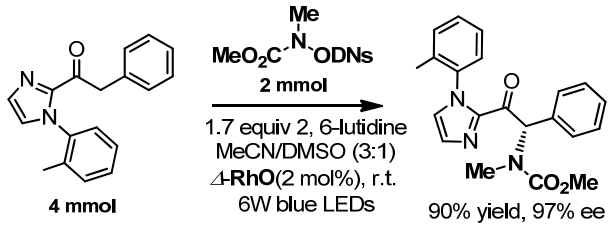


***Flow rate: 0.15 mL/min***
***total reaction time: 180 min***

***Procedure:*** To a dried 50 mL centrifugal tube was added Δ-**RhO** (33.2 mg, 2 mol%), 2-acyl imidazoles **107** (4.0 mmol, 2.0 equiv), and the amine reagent **117** (2.0 mmol, 1.0 equiv). Dry DMSO (5.0 mL), dry $CH_3CN$ (15.0 mL), and 2,6-lutidine (400 μL, 3.4 mmol, 1.7 equiv) were then added to the centrifugal tube via syringe addition. The resulting clear solution was degassed for 5 min by bubbling nitrogen through the reaction medium. The reaction mixture is then pumped through the photo reactor at a flow rate (0.15 mL/min). After 180 min, the collected mixture was concentrated in *vacuo*, and then diluted with EtOAc and wahed by water. The organic phase was dried over anhydrous $Na_2SO_4$ and concentrated in *vacuo*. The resulting crude product was purified by flash chromatography on silica gel (EtOAc/*n*-hexane = 1:4 to 1:2) to provide the target compound **124** as a pale yellow solid (653 mg, 1.80 mmol, 90% yield and 97% ee).

## 5.6 Single Crystal X-ray Diffraction

Crystal data and the detailed information are listed in the **Appendix 8**.

*rac*-**18**

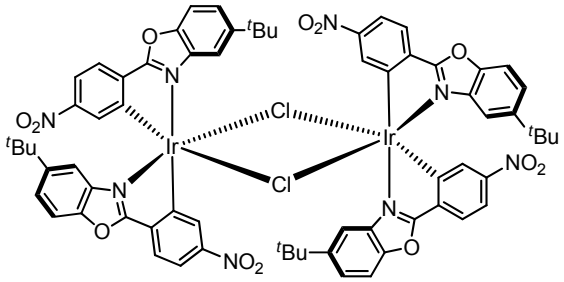

Crystals of *rac*-**18** suitable for single-crystal X-ray diffraction were obtained by slow diffusion from a solution of *rac*-**18** (10 mg) in $CH_2Cl_2$ (1.5 mL) layered with *n*-hexane (0.5 mL) at room temperature for several days in a NMR tube.

*rac*-**IrO($NO_2$)**

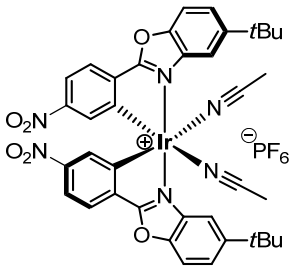

Crystals of *rac*-**IrO($NO_2$)** suitable for single-crystal X-ray diffraction were obtained by slow diffusion from a solution of *rac*-**IrO($NO_2$)** (20 mg) in $CH_2Cl_2$ (0.5 mL) layered with *n*-hexane (1.5 mL) at room temperature for several days in a NMR tube.

*rac*-**IrO(nap)**

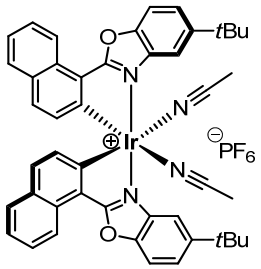

Crystals of *rac*-**IrO(nap)** suitable for single-crystal X-ray diffraction were obtained by slow diffusion from a solution of *rac*-**IrO(nap)** (20 mg) in $CH_2Cl_2$ (0.5 mL) layered with *n*-hexane (1.5 mL) at room temperature for several days in a NMR tube.

Λ-**IrS**

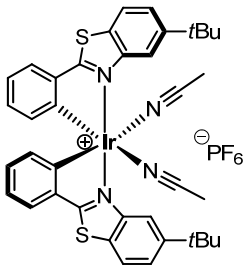

Crystals of Λ-**IrS** suitable for single-crystal X-ray diffraction were obtained by slow diffusion from a solution of Λ-**IrS** (30 mg) in $CH_2Cl_2$ (0.5 mL) layered with *n*-hexane (1.5 mL) at room temperature for several days in a NMR tube.

*rac*-**IrO(ada)**

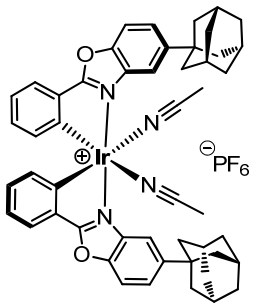

Crystals of *rac*-**IrO(ada)** suitable for single-crystal X-ray diffraction were obtained by slow diffusion from a solution of *rac*-**IrO(ada)** (30 mg) in $CH_2Cl_2$ (0.5 mL) layered with *n*-hexane (1.5 mL) at room temperature for several days in a NMR tube.

(*S,S*)-**51**

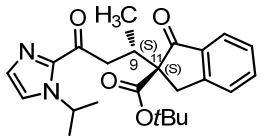

Crystals of (*S,S*)-**51** suitable for single-crystal X-ray diffraction were obtained by slow diffusion from a solution of (*S,S*)-**51** (71 mg) in $CH_2Cl_2$ (0.5 mL) layered with *n*-hexane (1.5 mL) at room temperature for several days in a NMR tube.

**Iridium-coordinated substrate (79)**

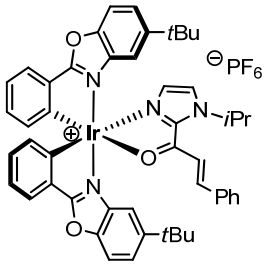

To a solution of *rac*-**IrO** (50.0 mg, 0.054 mmol) in distilled, anhydrous $CH_2Cl_2$ (0.55 mL) at room temperature was added **35** (13.2 mg, 0.055 mmol) under $N_2$ in a Schlenk tube. The reaction mixture was stirred at room temperature over night. Then, distilled anhydrous *n*-hexane (2 mL) was added slowly. Dark brown crystals were obtained after one day by slow diffusion.

**Iridium-coordinated product (80)**

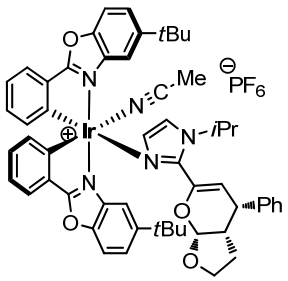


To a solution of *rac*-**IrO** (40.0 mg, 0.043 mmol) in distilled, anhydrous $CH_2Cl_2$ (0.42 mL) at room temperature was added **35** (10.4 mg, 0.043 mmol) under $N_2$ in a Schlenk tube. The reaction mixture was stirred at room temperature over night. 2,3-Dihydrofuran (9.1 mg, 0.13 mmol) was added and stirred for two hours. Then distilled anhydrous *n*-hexane (2 mL) was added slowly. Yellow crystals were obtained after one day by slow diffusion.

**Rhodium-coordinated product (138)**

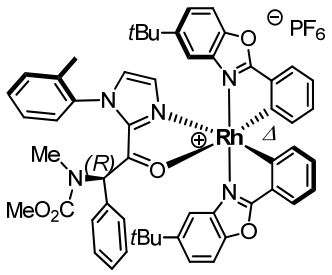


To a solution of Δ-**RhO** (21.8 mg, 0.026mmol) in $CH_2Cl_2$ (5 mL) at room temperature was added (*R*)-**124** (catalyzed by Λ-**RhO**; 13.8 mg, 0.0380 mmol) in a bottom flask. And then the solvent was removed under reduced pressure. The residue was dissolved in 0.5 mL of $CH_2Cl_2$. Single crystals of **138** suitable for X-ray diffraction were obtained by slow diffusion from a solution of residue in $CH_2Cl_2$ (0.5 mL) layered with *n*-hexane (2 mL) at room temperature for one day in a NMR tube.

**Rhodium-coordinated substrate (139)**

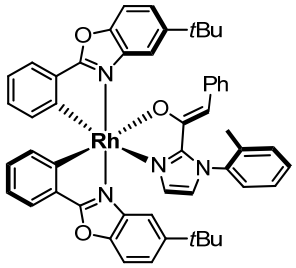

To a mixture of ***rac*-RhO** (83.1 mg, 0.1 mmol), imidazole substrate **117** (33.1mg, 0.12 mmol) and NaOMe (8.1 mg, 0.15 mmol) was added MeOH (0.4 mL) and DCM (1.6 mL). The mixture was stirred under $N_2$ over night. The solvents were removed in *vacuo*. Then 10 mL of $CH_2Cl_2$ was added. After centrifugation, the clear solution was reserved and concentrated. Single crystals of complex **139** suitable for X-ray diffraction were obtained by slow diffusion from a solution of residue in $CH_2Cl_2$ (1.0 mL) layered with *n*-hexane (4 mL) at room temperature for two days in a glass tube.

***rac*-IrO(pyrene)**

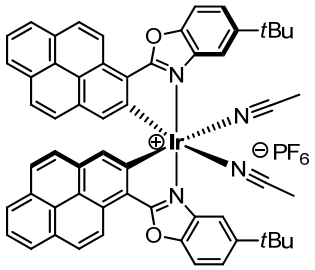


Crystals of *rac*-**IrO(pyrene)** suitable for single-crystal X-ray diffraction were obtained by slow diffusion from a solution of *rac*-**IrO(pyrene)** (10 mg) in $CH_2Cl_2$ (0.5 mL) layered with *n*-hexane (0.5 mL) at room temperature for several days in a NMR tube.

***rac*-IrN(pyrene)**

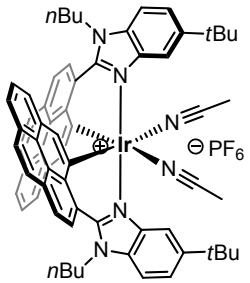


Crystals of *rac*-**IrN(pyrene)** suitable for single-crystal X-ray diffraction were obtained by slow diffusion from a solution of *rac*-**IrN(pyrene)** (20 mg) in $CH_2Cl_2$ (0.5 mL) layered with *n*-hexane (1.5 mL) at room temperature for several days in a NMR tube. (The quality of this crystal is not good enough.)

## 5.7 References


1 *SADABS. Bruker AXS area detector scaling and absorption correction*, Bruker AXS Inc., Madison, Wisconsin, USA, **2014**.

2 G. M. Sheldrick, *Acta Crystallogr. A Found Adv.* **2015**, *71*, 3−8.

3 G. M. Sheldrick, *Actacrystallographica. Section C, Structural chemistry* **2015**, *71*, 3−8.

4 K. Brandenburg, *Diamond-Crystal and Molecular Structure Visualization*, Crystal Impact - Dr. H. Putz & Dr. K. Brandenburg GbR, Bonn, Germany, **2014**.

5 H. D. Flack, *Chimia* **2014**, *68*, 26−30.

6 Y.-X. Chen, L.-F. Qian, W. Zhang, B. Han, *Angew. Chem. Int. Ed.* **2008**, *47*, 9330–9333.

7 R.-G. Xing, Y.-N. Li, Q. Liu, Q.-Y. Meng, J. Li, X.-X. Shen, Z. Liu, B. Zhou, X. Yao, Z.-L. Liu, *Eur. J. Org. Chem.* **2010**, *2010*, 6627−6632.

8 T. B. Nguyen, L. Ermolenko, P. Retailleau, A. Al-Mourabit, *Angew. Chem. Int. Ed.* **2014**, *53*, 13808−13812.

9 H. A. Wegner, H. Reisch, K. Rauch, A. Demeter, K. A. Zachariasse, A. de Meijere, L. T. Scott, *J. Org. Chem.* **2006**, *71*, 9080−9087.

10 V. A. Osyanin, E. A. Ivleva, Y. N. Klimochkin, *Synth. Commun.* **2012**, *42*, 1832−1847.

11 J. J. Lee, J. Kim, Y. M. Jun, B. M. Lee, B. H. Kim, *Tetrahedron* **2009**, *65*, 8821−8831.

12 M. Nonoyama, *Bull. Chem. Soc. Jpn.* **1974**, *47*, 767−768.

13 K. A. McGee, K. R. Mann, *Inorg. Chem.* **2007**, *46*, 7800−7809.

14 H. Huo, C. Fu, K. Harms, E. Meggers, *J. Am. Chem. Soc.* **2014**, *136*, 2990–2993.

15 C. Wang, L.-A. Chen, H. Huo, X. Shen, K. Harms, L. Gong, E. Meggers, *Chem. Sci.* **2015**, *6*, 1094–1100.

16 L.-A. Chen, W. Xu, B. Huang, J. Ma, L. Wang, J. W. Xi, K. Harms, L. Gong, E. Meggers, *J. Am. Chem. Soc.* **2013**, *135*, 10598−10601.

17 H. Huo, X. Shen, C. Wang, L. Zhang, P. Rose, L.-A. Chen, K. Harms, M. Marsch, G. Hilt, E. Meggers, *Nature* **2014**, *515*, 100−103.

18 D. A. Evans, K. R. Fandrick, H.-J. Song, *J. Am. Chem. Soc.* **2005**, *127*, 8942−8943.

19 D. A. Evans, K. R. Fandrick, H.-J. Song, K. A. Scheidt, R. Xu, *J. Am. Chem. Soc.* **2007**, *129*, 10029−10041.

20 H. Wolpher, S. Sinha, J. Pan, A. Johansson, M. J. Lundqvist, P. Persson, R. Lomoth, J. Bergquist, L. Sun, V. Sundström, B. Åkermark, T. Polívka, *Inorg. Chem.* **2007**, *46*, 638−651.

21 T. Nakamura, M. Oshida, T. Nomura, A. Nakazaki, S. Kobayashi, *Org. Lett.* **2007**, *9*, 5533−5536.

22 D. A. Evans, R. J. Thomson, F. Franco, *J. Am. Chem. Soc.* **2005**, *127*, 10816−10817.

23 J. Ma, X. Ding, Y. Hu, Y. Huang, L. Gong, E. Meggers, *Nat. Commun.* **2014**, *5*, 4531

24 K. Itoh, M. Hasegawa, J. Tanaka, S. Kanemasa, *Org. Lett.* **2005**, *7*, 979−981.

25 D. A. Evans, K. A. Scheidt, K. R. Fandrick, H. W. Lam, J. Wu, *J. Am. Chem. Soc.* **2003**, *125*,

10780−10781.

26 G. Dujardin, S. Leconte, A. Bénard, E. Brown, *Synlett* **2001**, 0147−0149.

27 L. Zheng, S. Sonzini, M. Ambarwati, E. Rosta, O. A. Scherman, A. Herrmann, *Angew. Chem. Int. Ed.* **2015**, *54*, 13007−13011.

28 B. Champin, V. Sartor, J.-P. Sauvage, *New J. Chem.* **2008**, *32*, 1048–1054.

29 S. Nayab, H. Lee, J. H. Jeong, *Polyhedron* **2012**, *43*, 55–62.

30 H. J. Park, J. N. Kim, H.-J. Yoo, K.-R. Wee, S. O. Kang, D. W. Cho, U. C. Yoon, *J. Org. Chem.* **2013**, *78*, 8054–8064.

31 D. Bhuniya, R. Mukkavilli, R. Shivahare, D. Launay, R. T. Dere, A. Deshpande, A. Verma, P. Vishwakarma, M. Moger, A. Pradhan, H. Pati, V. S. Gopinath, S. Gupta, S. K. Puri, D. Martin, *Eur. J. Med. Chem.* **2015**, *102*, 582–593.

32 F. Napoly, R. Kieffer, L. Jean-Gérard, C. Goux-Henry, M. Draye, B. Andrioletti, *Tetrahedron Lett.* **2015**, *56*, 2517-2520.

33 J. G. Lewis, S. K. Anandan, H. O'Dowd, M. F. Gordeev, L. Li, Patent No. US 20060148722 A1, July 06, **2006**.

34 S. Duric, C. C. Tzschucke, *Org. Lett.* **2011**, *13*, 2310–2313.

35 R. Custelcean, P. V. Bonnesen, N. C. Duncan, X. Zhang, L. A. Watson, G. Van Berkel, W. B. Parson, B. P. Hay, *J. Am. Chem. Soc.* **2012**, *134*, 8525–8534.

36 H. Huo, C. Wang, K. Harms, E. Meggers, *J. Am. Chem. Soc.* **2015**, *137*, 9551–9554.

37 H. Yang, N. Huo, P. Yang, H. Pei, H. Lv, X. Zhang, *Org. Lett.* **2015**, *17*, 4144–4147.

38 M. Holmquist, G. Blay, M. C. Muñoz, J. R. Pedro, *Org. Lett.* **2014**, *16*, 1204–1207.

39 Y. Tan, W. Yuan, L. Gong, E. Meggers, *Angew. Chem. Int. Ed.* **2015**, *53*, 13045–13048.

40 T. Niu, W. Zhang, D. Huang, C. Xu, H. Wang, Y. Hu, *Org. Lett.* **2009**, *11*, 4474−4477.

41 J. Jiang, J. L. Bunda, G. A. Doss, G. G. Chicchi, M. M. Kurtz, K.-L. C. Tsao, X. Tong, S. Zheng, A. Upthagrove, K. Samuel, R. Tschirret-Guth, S. Kumar, A. Wheeldon, E. J. Carlson, R. Hargreaves, D. Burns, T. Hamill, C. Ryan, S. M. Krause, W. Eng, R. J. DeVita, S. G. Mills, *J. Med. Chem.* **2009**, *52*, 3039−3046.

42 J. R. Denton, H. M. L. Davies, *Org. Lett.* **2009**, *11*, 787−790.

43 T. Kambe, T. Maruyama, M. Nakano, Y. Yamaura, T. Shono, A. Seki, K. Sakata, T. Maruyama, H. Nakai, M. Toda, *Chem. Pharm. Bull.* **2011**, *59*, 1523−1534.

44 H. Huo, X. Huang, X. Shen, K. Harms, E. Meggers, *Synlett* **2016**, *27*, 749−753.

45 B. M. Trost, K. Lehr, D. J. Michaelis, J. Xu, A. K. Buckl, *J. Am. Chem. Soc.* **2010**, *132*, 8915−8917.

46 G. Cecere, C. M. König, J. L. Alleva, D. W. C. MacMillan, *J. Am. Chem. Soc.* **2013**, *135*, 11521−11524.

47 D. A. Evans, K. R. Fandrick, *Org. Lett.* **2006**, *8*, 2249−2252.

48 D. A. Evans, H.-J. Song, K. R. Fandrick, *Org. Lett.* **2006**, *8*, 3351−3354.

49 D. A. Evans, K. T. Chapman, J. Bisaha, *J. Am. Chem. Soc.* **1988**, *110*, 1238–1256.

50 I. W. Davies, C. H. Senanayake, L. Castonguay, R. D. Larsen, T. R. Verhoeven, P. J. Reider, *Tetrahedron Lett.* **1995**, *36*, 7619–7622.

51 S. L. Murov, I. Carmichael, G. L. Hug, Handbook of Photochemistry (Second Edition), New York, **1993**.

52 Ł. Woźniak, J. J. Murphy, P. Melchiorre, *J. Am. Chem. Soc.* **2015**, *137*, 5678−5681.

53 M. A. Cismesia, T. P. Yoon, *Chem. Sci.* **2015**, *6*, 5426−5434.

# Chapter 6. Appendices

## Appendix 1. List of Abbreviations

| | |
|---|---|
| $^{1}$H NMR | proton nuclear magnetic resonance spectroscopy |
| $^{13}$C NMR | carbon nuclear magnetic resonance spectroscopy |
| $^{9}$F NMR | fluorine nuclear magnetic resonance spectroscopy |
| $\delta$ | chemical shift |
| J | coupling constant |
| br | broad |
| s | singlet |
| d | doublet |
| t | triplet |
| q | quartet |
| m | multiplet |
| ppm | parts per million |
| AcOH | acetic acid |
| ada | adamantane |
| aq | aqueous |
| Ar | argon |
| bpy | 2,2′-bipyridine |
| Calcd | calculated |
| CBSA | *p*-Cl-benzenesulfonic acid |
| CD | circular dichroism |
| $CH_2Cl_2$/ DCM | dichloromethane |
| $CD_2Cl_2$ | dideuteromethylenechloride |
| $CHCl_3$ | chloroform |
| $CDCl_3$ | deuterochloroform |
| $CH_3CN$/ MeCN | acetonitrile |
| conc | concentrated |

| | |
|---|---|
| DBU | 1,8-diazabicycloundec-7-ene |
| DIPEA | *N,N*-diisopropylethylamine |
| DMAc | dimethylacetamide |
| DMAP | 4-dimethylaminopyridine |
| DMF | dimethylformamide |
| DMSO | dimethyl sulfoxide |
| dr | diastereomeric ratio |
| EDA | electron donor-acceptor |
| EDC | 1-ethyl-3-(3-dimethylaminopropyl)carbodiimide hydrochloride |
| ee | enantiomeric excesses |
| e.g. | exempli gratia (lat.: for example) |
| en | ethylenediamine |
| er | enantiomeric ratio |
| EROCM | enantioselective ring opening/cross-metathesis |
| et al. | et alii (lat.: and others) |
| ESI | electrospray ionization |
| EtOH | ethanol |
| $Et_2O$ | diethyl ether |
| $Et_2NH$ | diethyl amine |
| $Et_3N$ | triethyl amine |
| EtOAc | ethyl acetate |
| h | hour(s) |
| HPLC | high performance liquid chromatography |
| HRMS | high resolution mass spectrometry |
| Hz | Hertz |
| IR spectra | infrared spectra |
| Ir | iridium |
| L | liter(s) |
| M | mol/liter |
| min | minute(s) |
| mL | milliliter(s) |
| MLCT | metal-to-ligand charge transfer |
| mmol | millimole |
| MS | mass spectroscopy |
| $N_2$ | nitrogen |
| NBS | *N*-bromosuccinimide |

| | |
|---|---|
| NCRs | nitrogen-centered radicals |
| Nu | nucleophile |
| ODN | 2,4-dinitrophenylsulfonyloxy |
| PCET | proton-coupled electron transfer |
| Ph | phenyl |
| $PPh_3$ | triphenylphosphine |
| ppm | parts per million |
| ppy | 2-phenylpyridine |
| *rac* | racemate |
| RCM | ring closing metathesis |
| Rh | rhodium |
| r.t. | room temperature |
| *sec* | secondary |
| SET | single-electron transfer |
| TEMPO | 2,2,6,6-tetramethyl-1-piperidinyloxy |
| 4-MeO-TEMPO | 4-methoxy-2,2,6,6-tetramethyl-1-piperidinyloxy |
| TFA | trifluoroacetic acid |
| THF | tetrahydrofuran |
| TLC | thin layer chromatography |
| UV | ultraviolet |

## Appendix 2. List of Figures

## Appendix 3. List of Schemes

## Appendix 4. List of Tables

# Appendix 5. List of Synthesized Compounds

## Appendix 5.1 List of Ir/Rh complexes

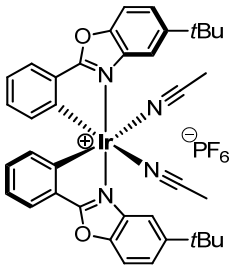

*rac*-, Λ- and Δ-**IrO**

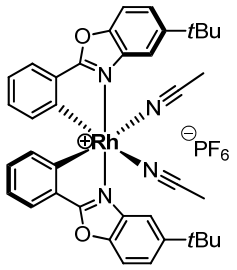

*rac*-, Λ- and Δ-**RhO**

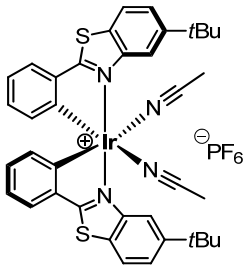

*rac*-, Λ- and Δ-**IrS**

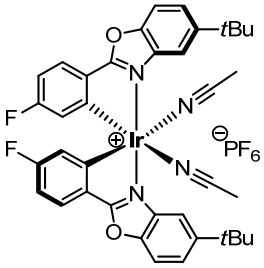

*rac*-**IrO(F)**

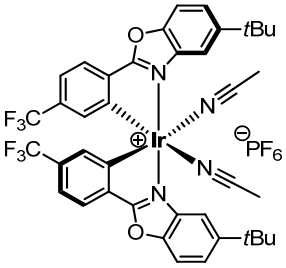

*rac*-**IrO(CF$_3$)**

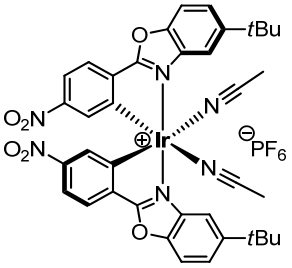

*rac*-**IrO(NO$_2$)**

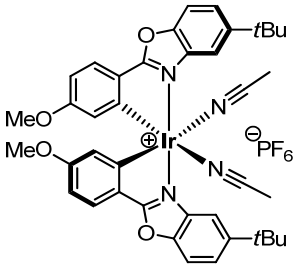

*rac*-**IrO(OMe)**

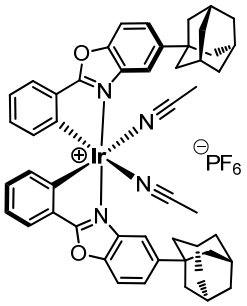

*rac*-, Λ- and Δ-**IrO(ada)**

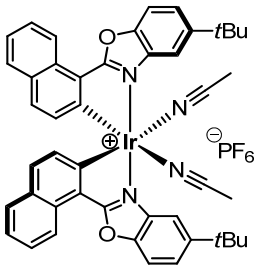

*rac*-**IrO(nap)**

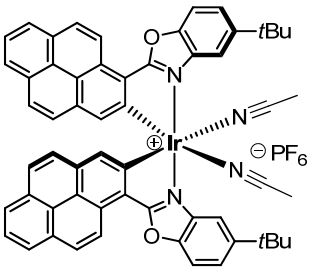

*rac*-**IrO(pyrene)**

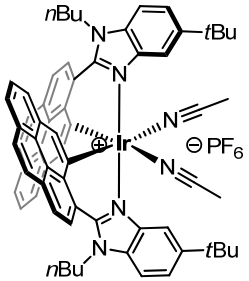

*rac*-**IrN(pyrene)**

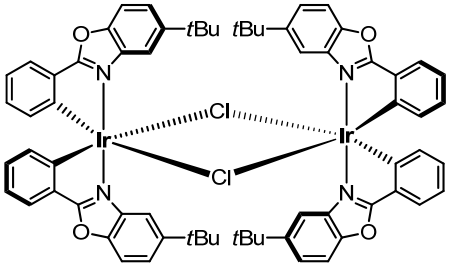

*rac*-**11**

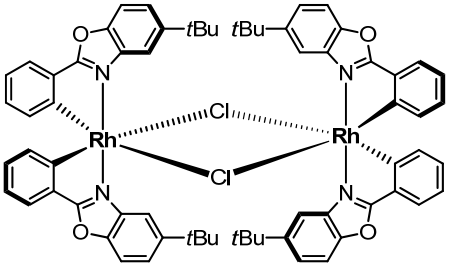

*rac*-**12**

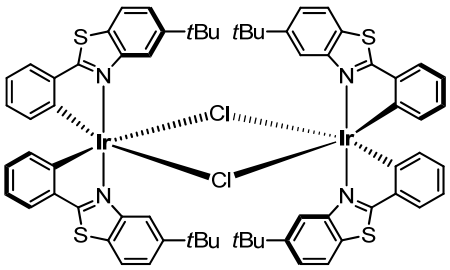

*rac*-**13**

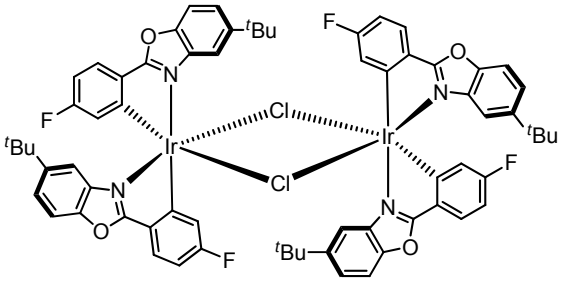

*rac*-**14**

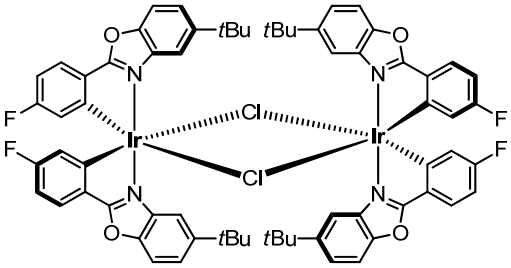

*rac*-**15**

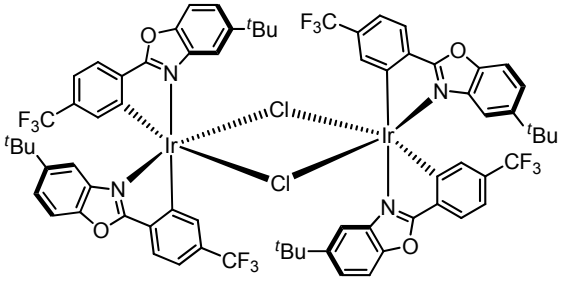

*rac*-**16**

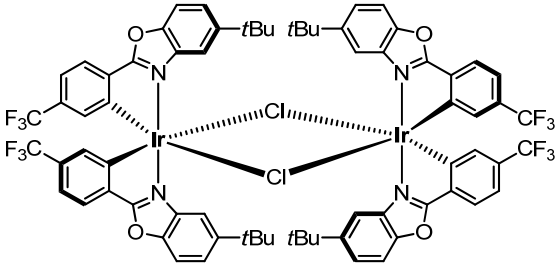

*rac*-**17**

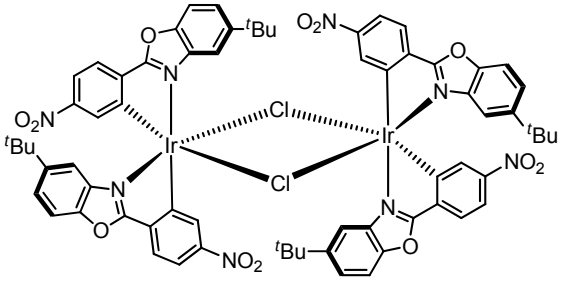

*rac*-**18**

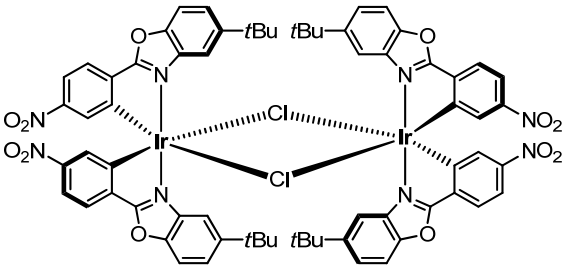

*rac*-**19**

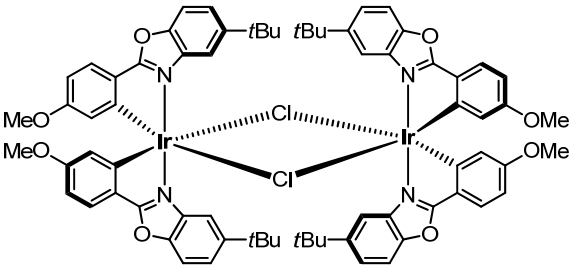

*rac*-**20**

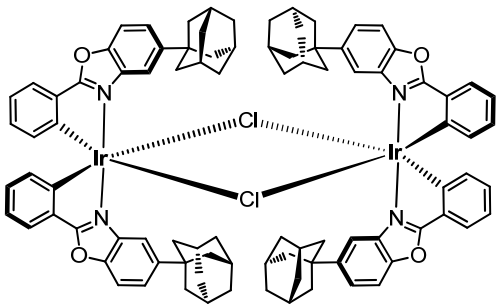

*rac*-**21**

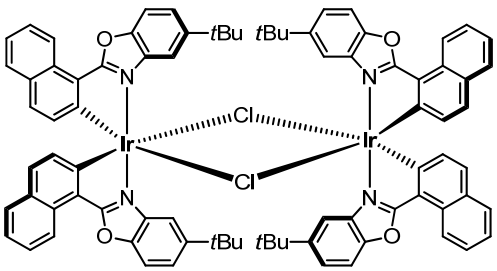

*rac*-**22**

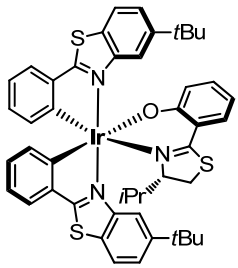


Λ-(*S*)-**26**

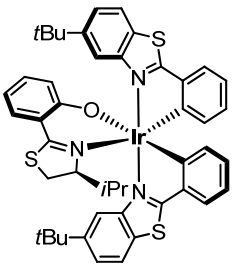


Δ-(*S*)-**26**

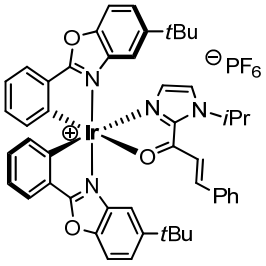


**79**

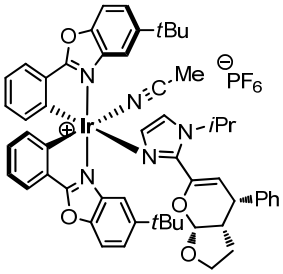


**80**

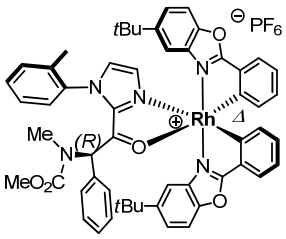


**138**

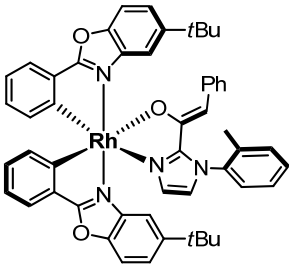


**139**

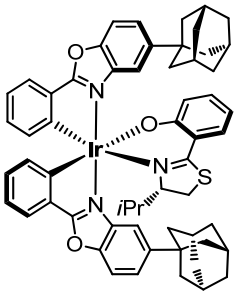


Λ-(*S*)-**145**

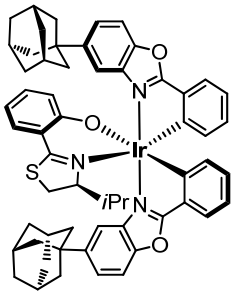


Δ-(*S*)-**145**

## Appendix 5.2 List of organic compounds

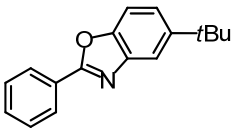


**1**

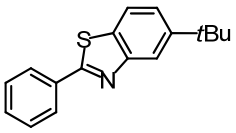


**2**

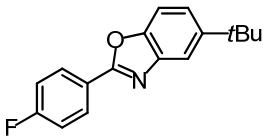


**3**

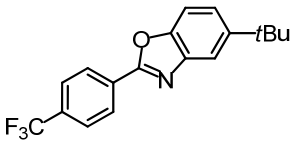


**4**

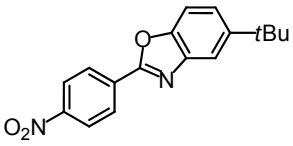


**5**

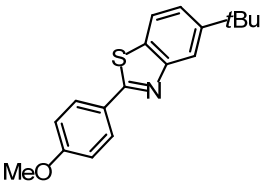


**6**

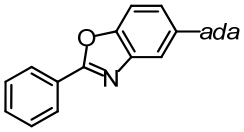


**7**

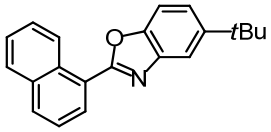


**8**

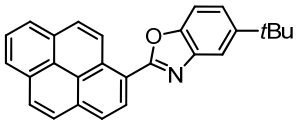


**9**

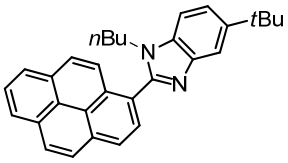


**10**

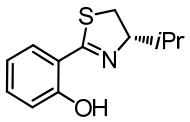


*(S)*-**25**

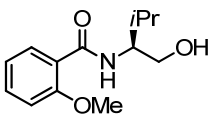


*(S)*-**29**

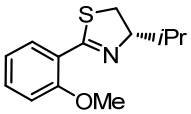


*(S)*-**30**

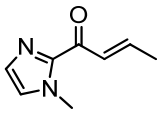


**31**

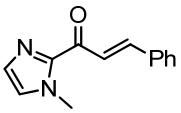


**32**

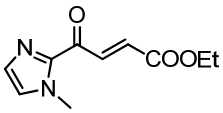


**33**

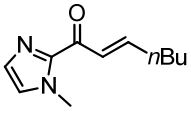


**34**

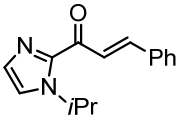


**35**

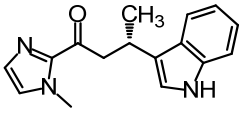


(*S*)-**36**

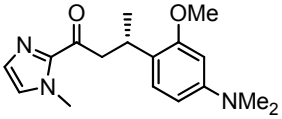


(*S*)-**37**

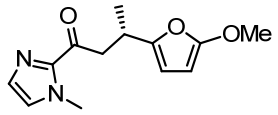

(*S*)-**38**

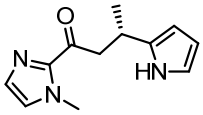

(*S*)-**39**

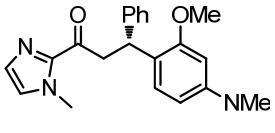

(*R*)-**40**

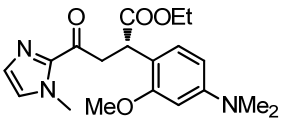

(*S*)-**41**

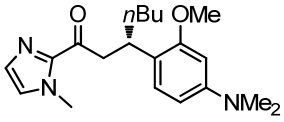

(*S*)-**42**

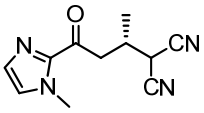

(*S*)-**43**

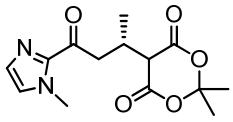

(*S*)-**44**

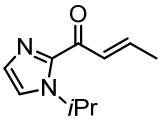

**45**

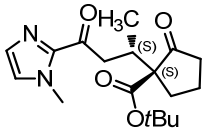

(*S,S*)-**46**

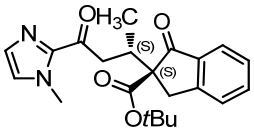

(*S,S*)-**47**

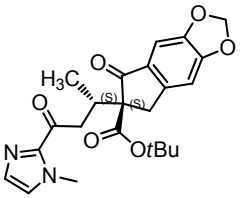

(*S,S*)-**48**

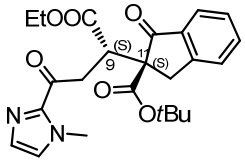

(*S,S*)-**49**

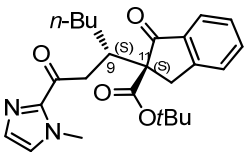

(*S,S*)-**50**

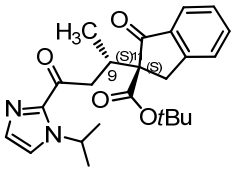

(*S,S*)-**51**

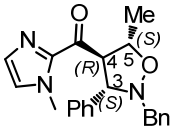

**52**

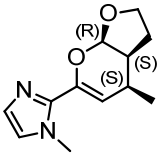

**53**

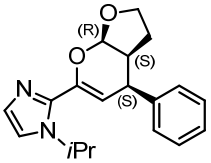

**54**

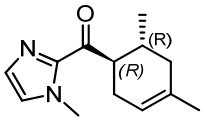

**55**

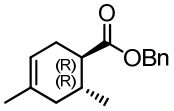

(1*R*, 6*R*)-**56**

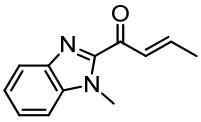

**57**

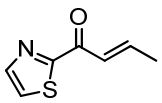

**58**

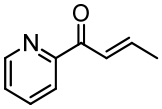

**59**

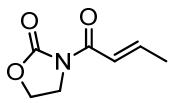

**60**

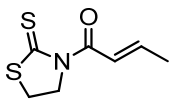

**61**

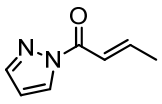

**62**

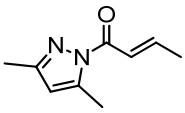

**63**

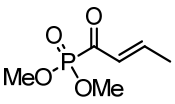

**64**

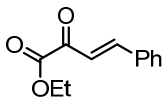

**65**

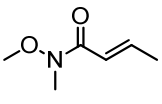

**66**

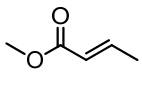

**67**

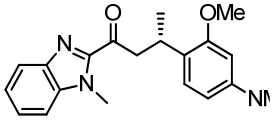

(*S*)-**68**

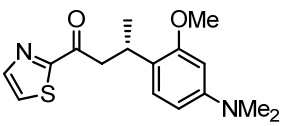

(*S*)-**69**

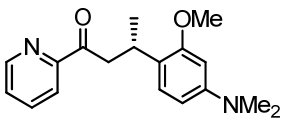

(*S*)-**70**

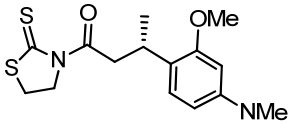

(*S*)-**72**

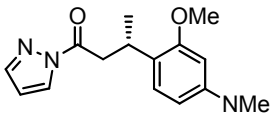

(*S*)-**73**

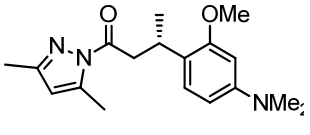

(*S*)-**74**

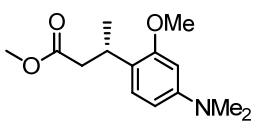

(*S*)-**75'**

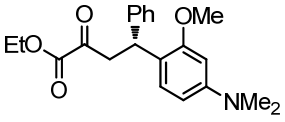

(*S*)-**76**

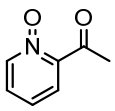

**81**

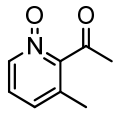

**82**

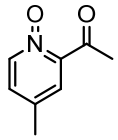

**83**

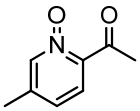

**84**

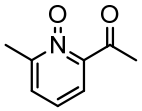

**85**

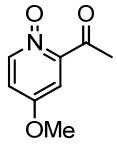

**86**

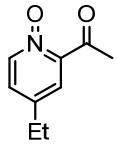

**87**

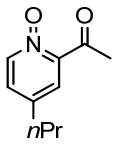

**88**

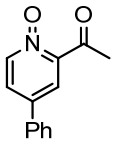

**89**

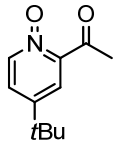

**90**

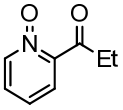

**91**

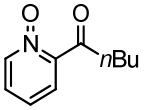

**92**

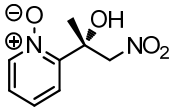

(*R*)-**93**

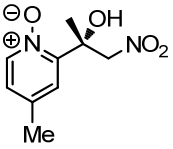

(*R*)-**95**

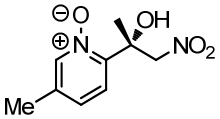

(*R*)-**96**

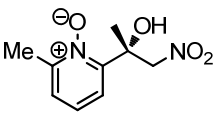

(*R*)-**97**

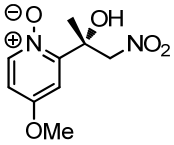

(*R*)-**98**

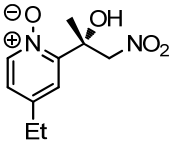

(*R*)-**99**

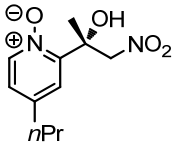

(*R*)-**100**

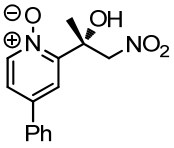

(*R*)-**101**

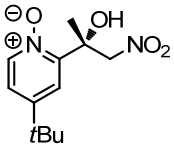

(*R*)-**102**

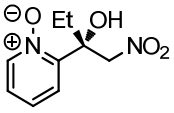

(*R*)-**103**

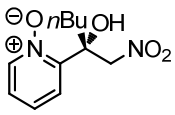

(*R*)-**104**

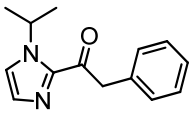

**105**

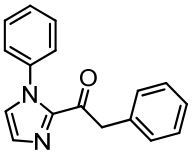

**106**

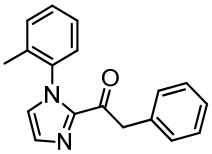

**107**

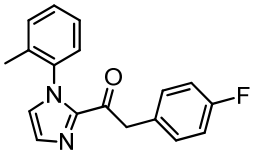

**108**

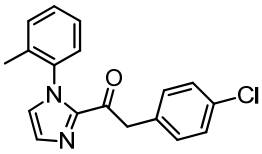

**109**

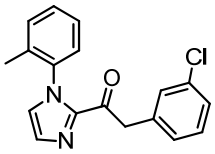

**110**

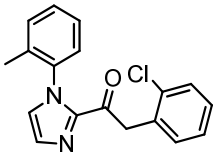

**111**

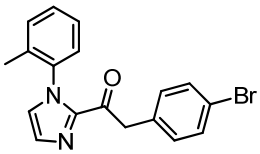

**112**

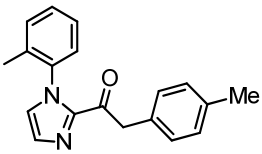

**113**

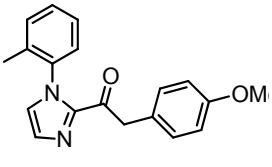

**114**

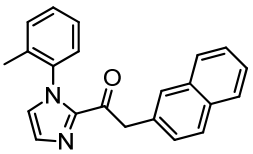

**115**

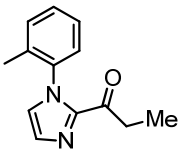

**116**

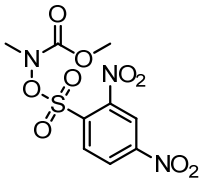

**117**

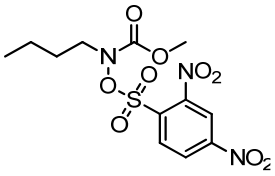

**118**

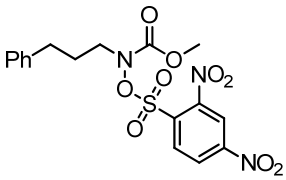

**119**

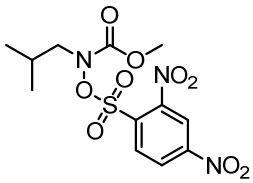

**120**

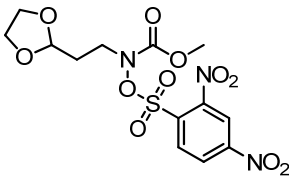

**121**

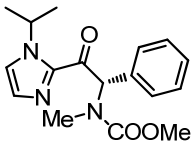

(*S*)-**122**

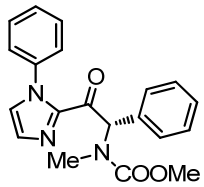

(*S*)-**123**

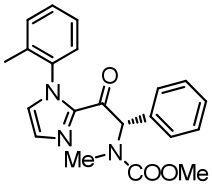

(*S*)-**124**

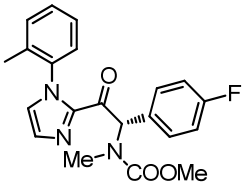

(*S*)-**125**

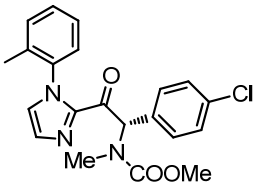

(*S*)-**126**

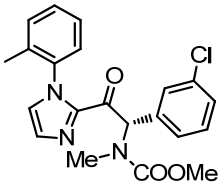

(*S*)-**127**

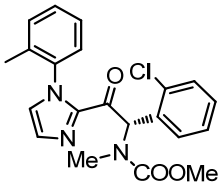

(*S*)-**128**

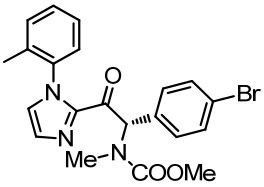

(*S*)-**129**

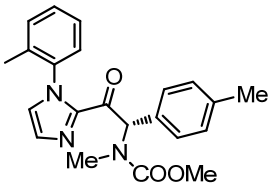

(*S*)-**130**

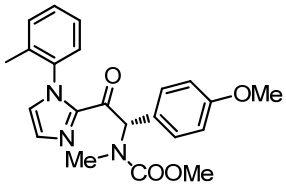

(*S*)-**131**

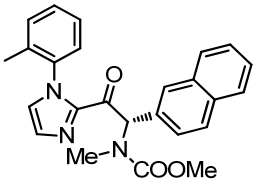

(*S*)-**132**

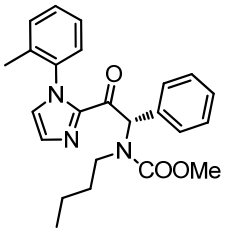

(*S*)-**133**

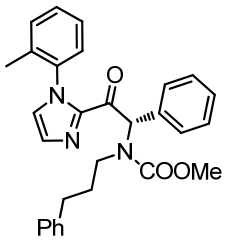

(*S*)-**134**

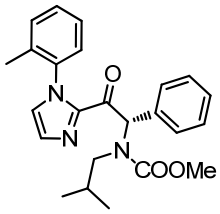

(*S*)-**135**

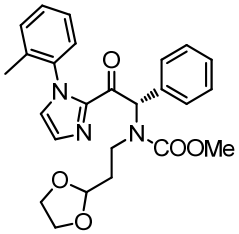

(*S*)-**136**

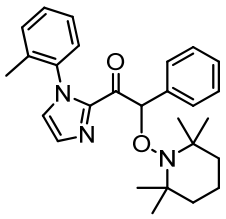

**140**

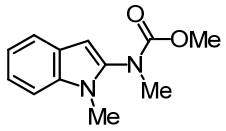

**141**

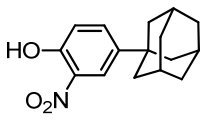

**144**

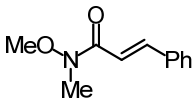

**146**

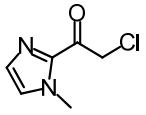

**147**

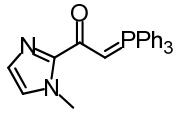

**148**

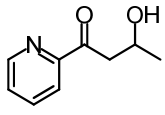

**149**

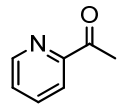


**150**

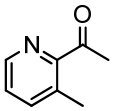


**151**

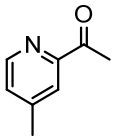


**152**

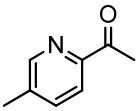


**153**

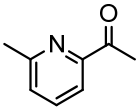


**154**

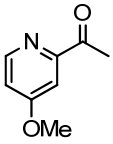


**155**

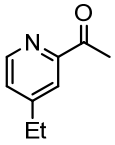


**156**

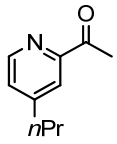


**157**

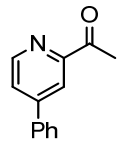


**158**

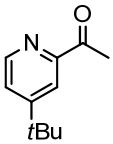


**159**

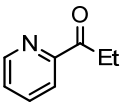


**160**

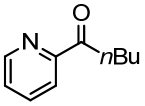


**161**

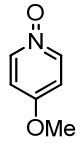


**162**

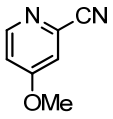


**163**

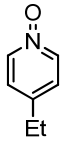


**164**

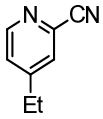


**165**

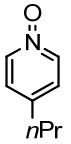


**166**


**167**

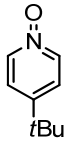


**168**

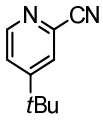


**169**

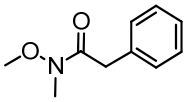


**170**

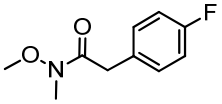


**171**

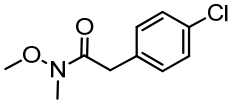


**172**

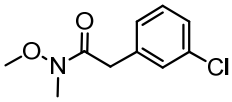


**173**

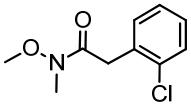


**174**

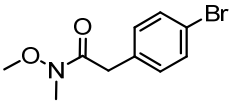


**175**

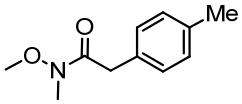


**176**

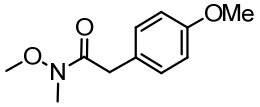


**177**

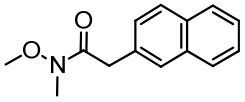


**178**

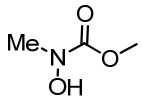


**179**

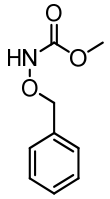


**180**

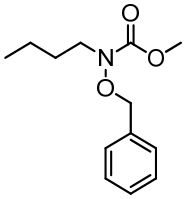


**181**

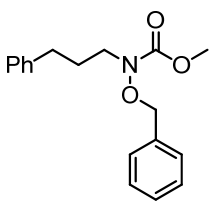


**182**

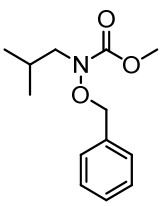


**183**

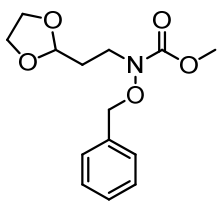


**184**

# Appendix 6. Spectra of Enantiopure Iridium Complexes

## Appendix 6.1 NMR spectra of enantiopure iridium complexes

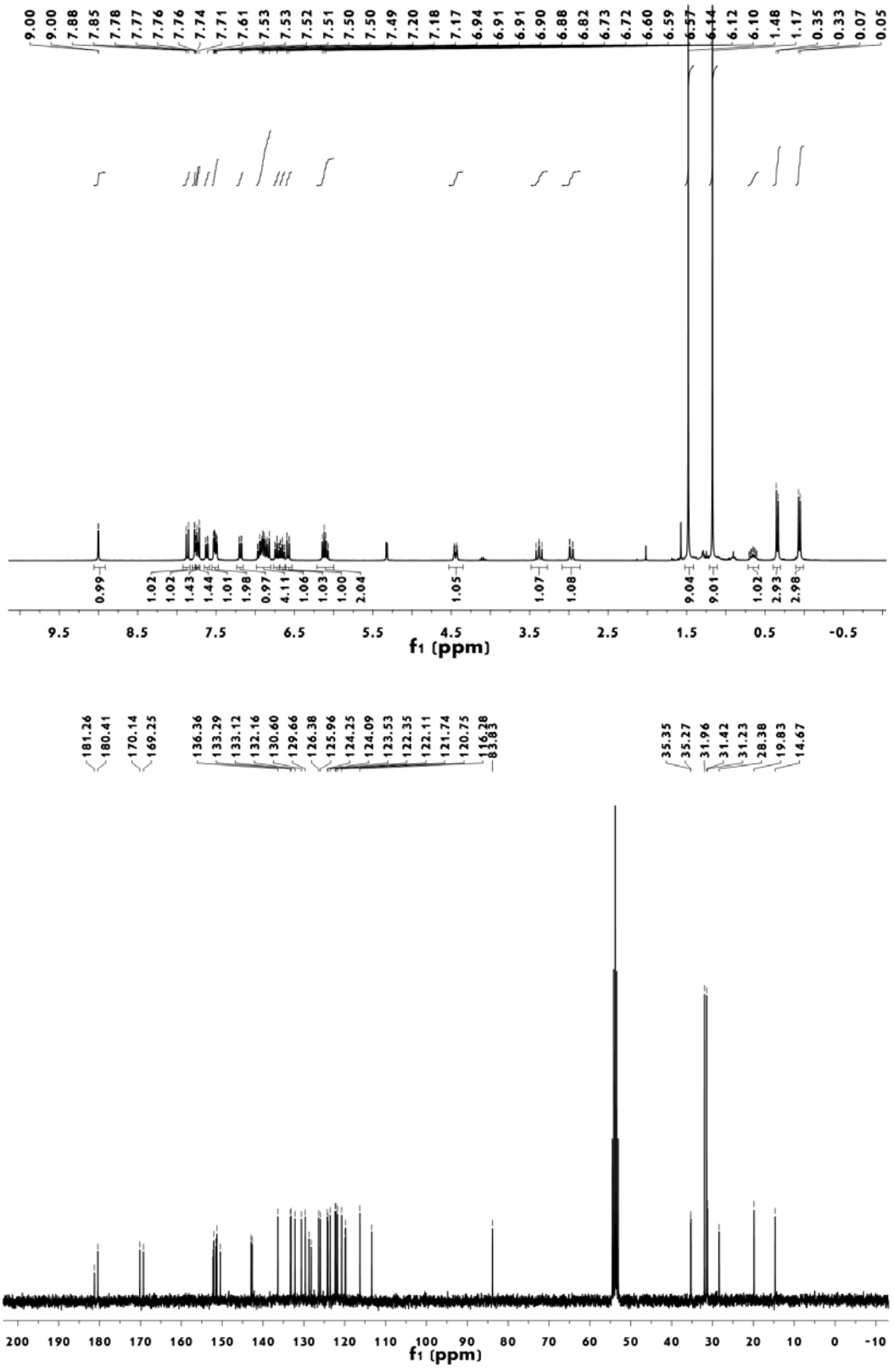


**Figure 63** $^{1}$H NMR and $^{13}$C NMR spectrum of iridium auxiliary complex Λ-(*S*)-**26**.

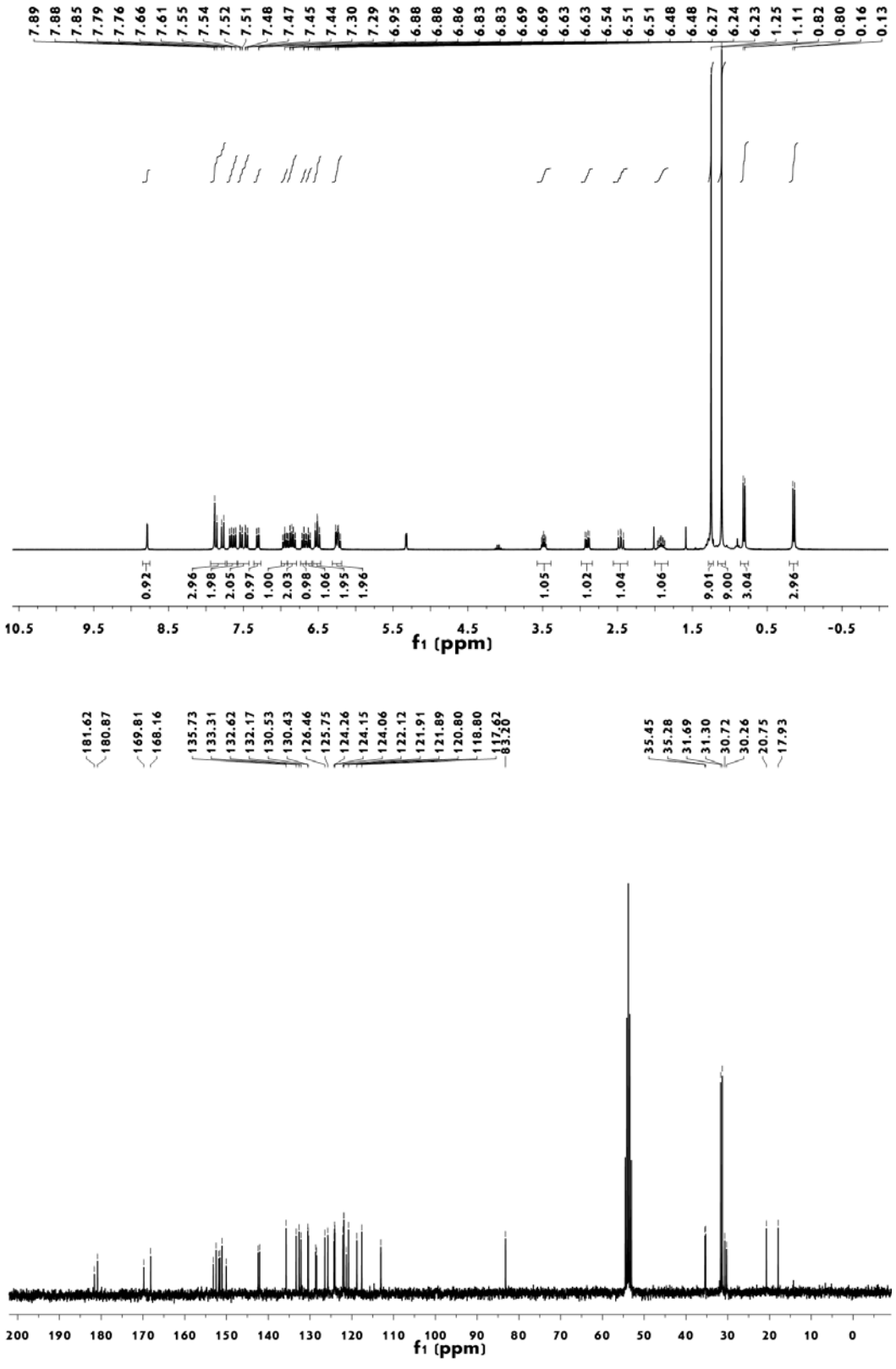


**Figure 64** $^{1}$H NMR and $^{13}$C NMR spectrum of iridium auxiliary complex Δ-(*S*)-**26**.

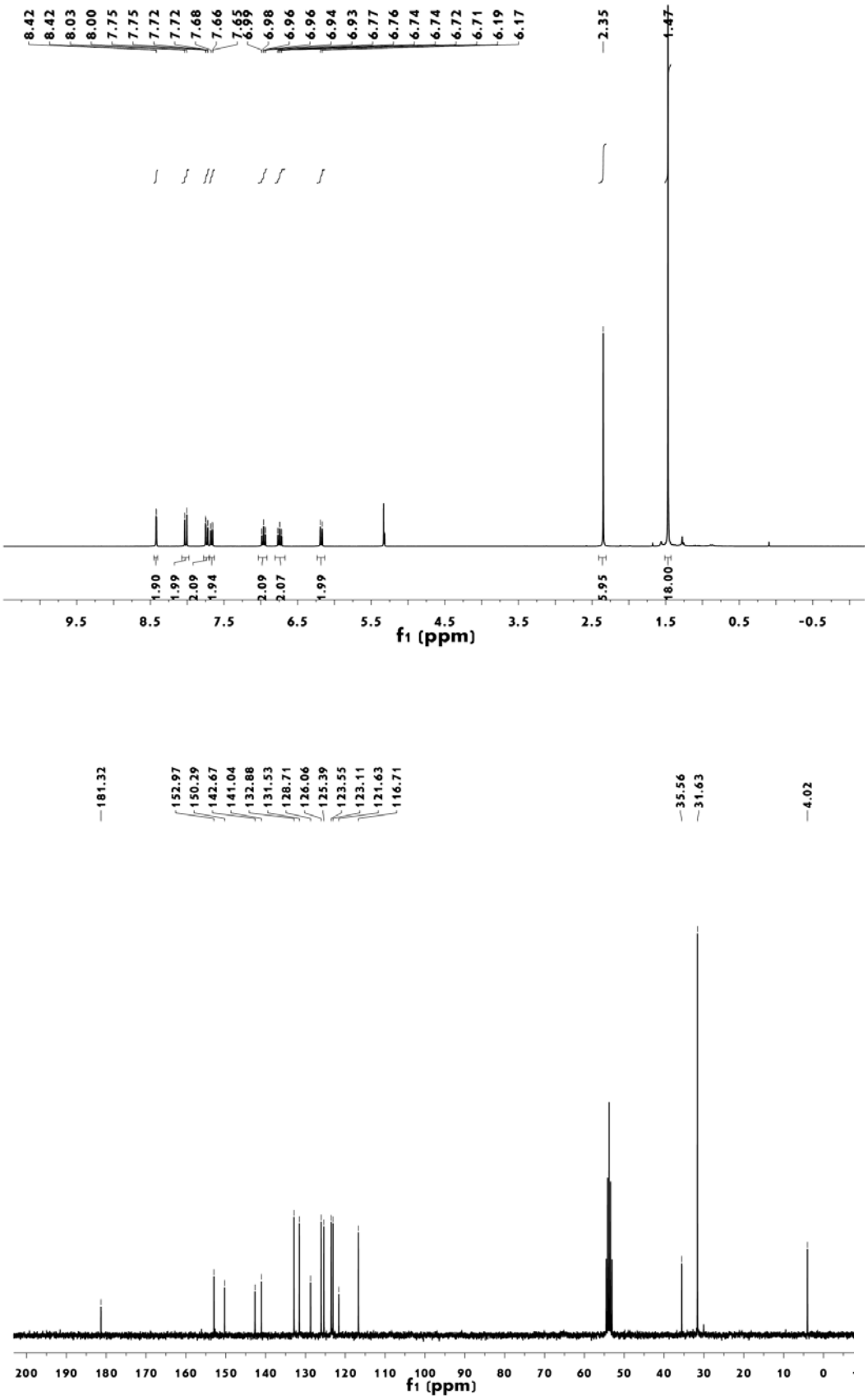


**Figure 65** $^{1}$H NMR and $^{13}$C NMR spectrum of Λ-**IrS**

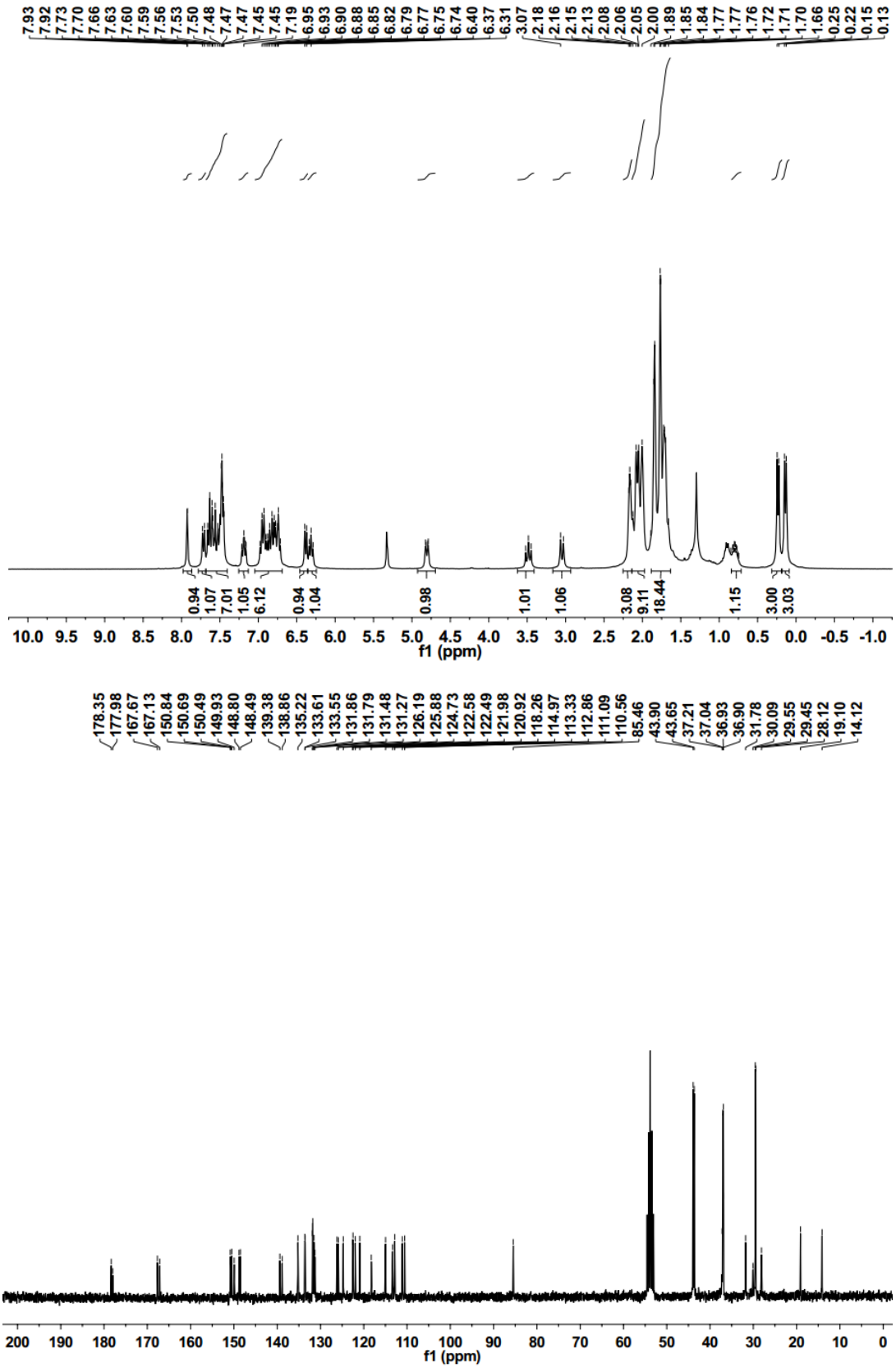


**Figure 66** $^{1}$H NMR and $^{13}$C NMR spectrum of iridium auxiliary complex Λ-(*S*)-**145**.

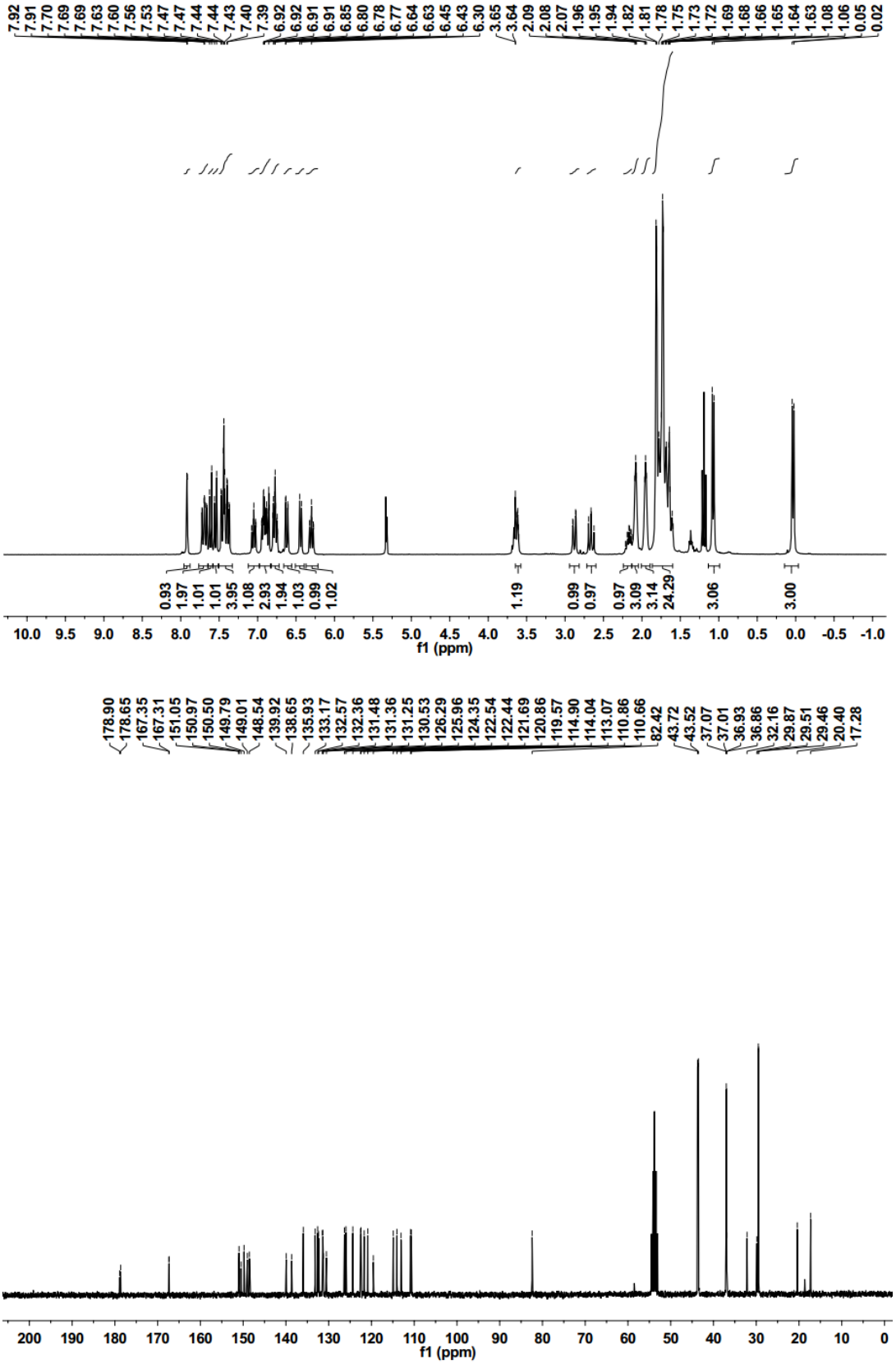


**Figure 67** $^{1}$H NMR and $^{13}$C NMR spectrum of iridium auxiliary complex Δ-(*S*)-**145**.

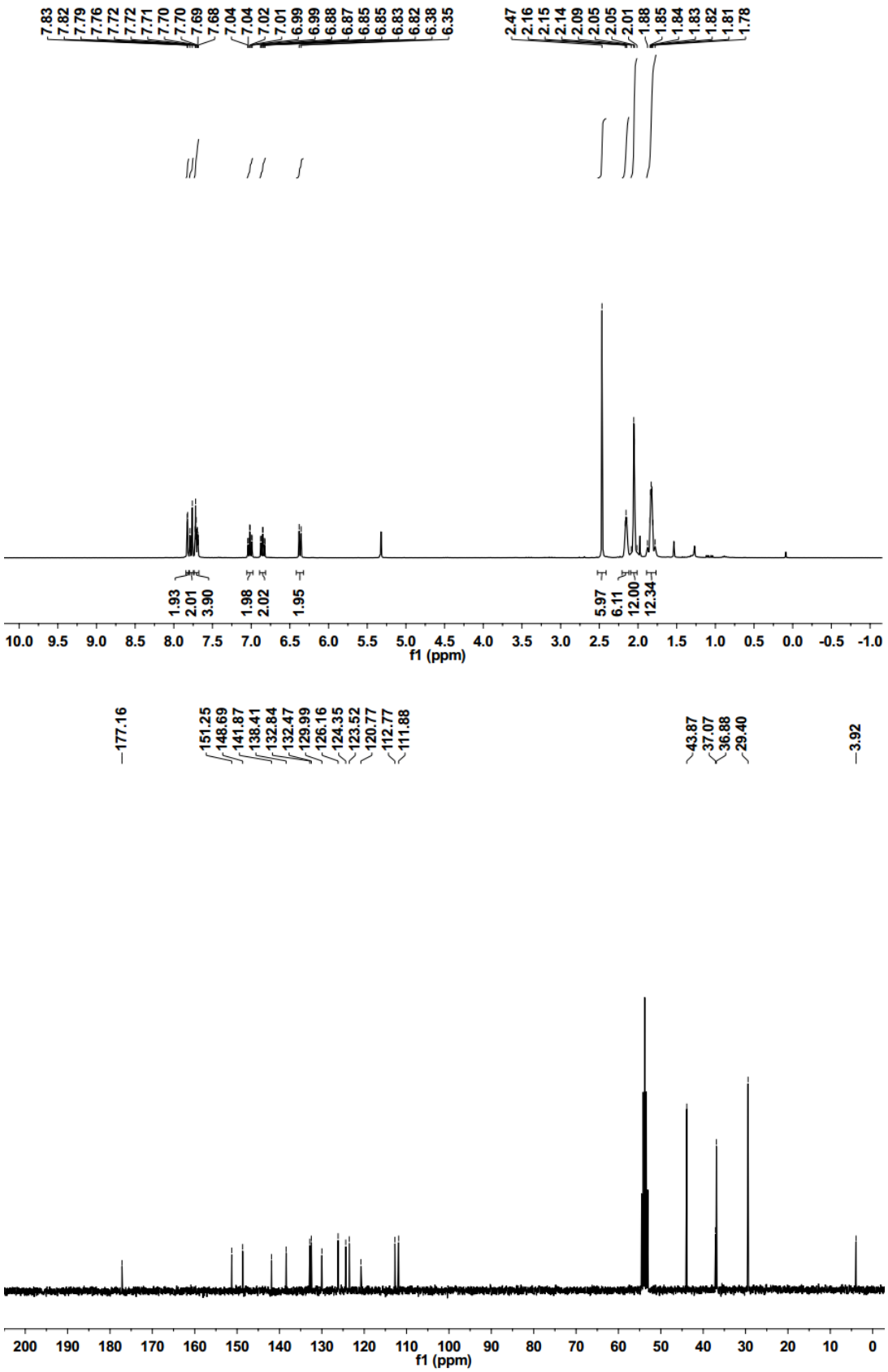


**Figure 68** $^{1}$H NMR and $^{13}$C NMR spectrum of iridium auxiliary complex Λ-**IrO(ada)**.

## Appendix 6.2 CD spectra of enantiopure iridium complexes

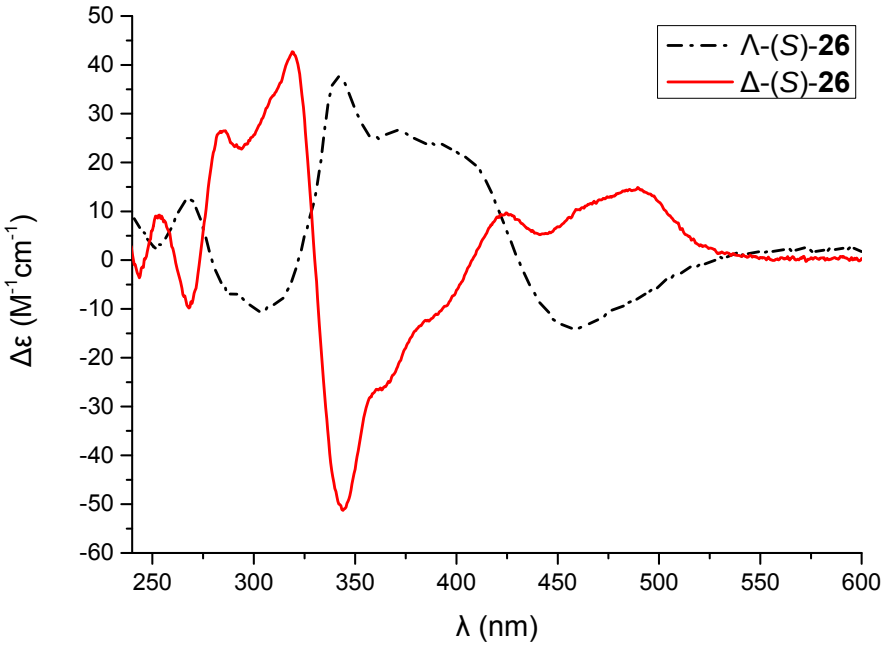


**Figure 69** CD spectra of complexes Λ-(*S*)-**26** and Δ-(*S*)-**26**.
Recorded in $CH_3OH$ (0.2 mM).

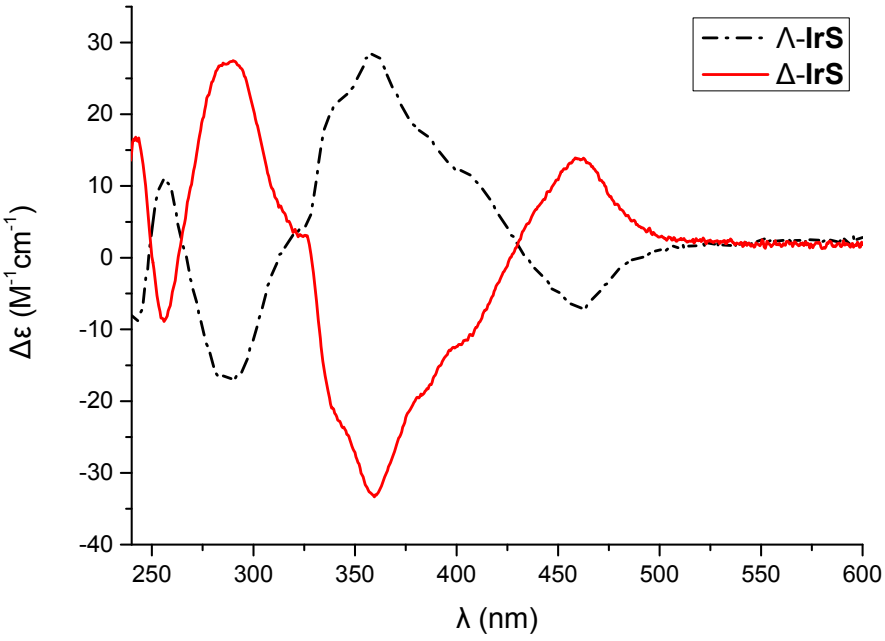


**Figure 70** CD spectra of complexes Λ-**IrS** and Δ-**IrS**.
Recorded in $CH_3OH$ (0.2 mM).

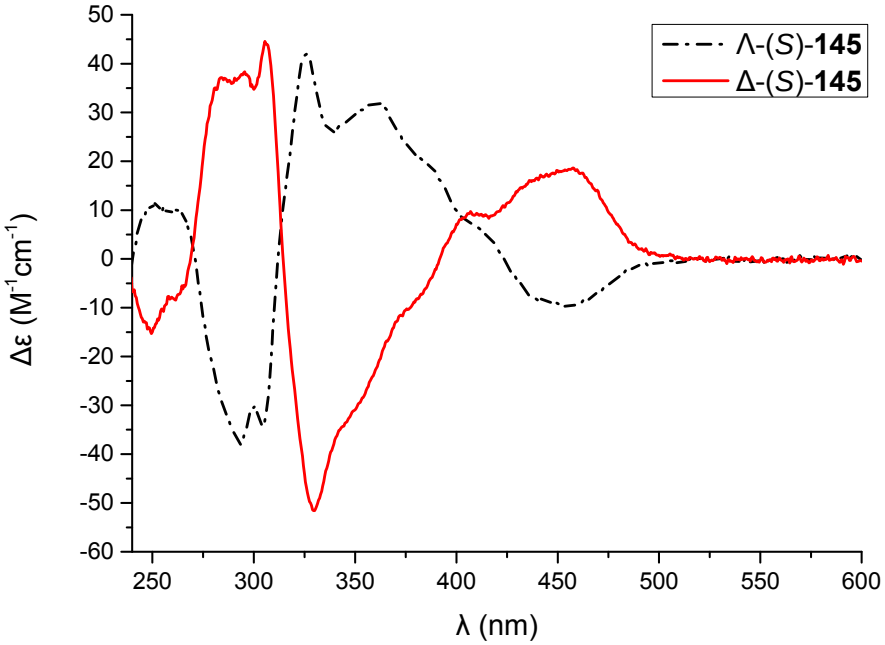


**Figure 71** CD spectra of complexes Λ-(*S*)-**145** and Δ-(*S*)-**145**.
Recorded in DCM/$CH_3OH$ (v/v = 1/4, 0.2 mM).

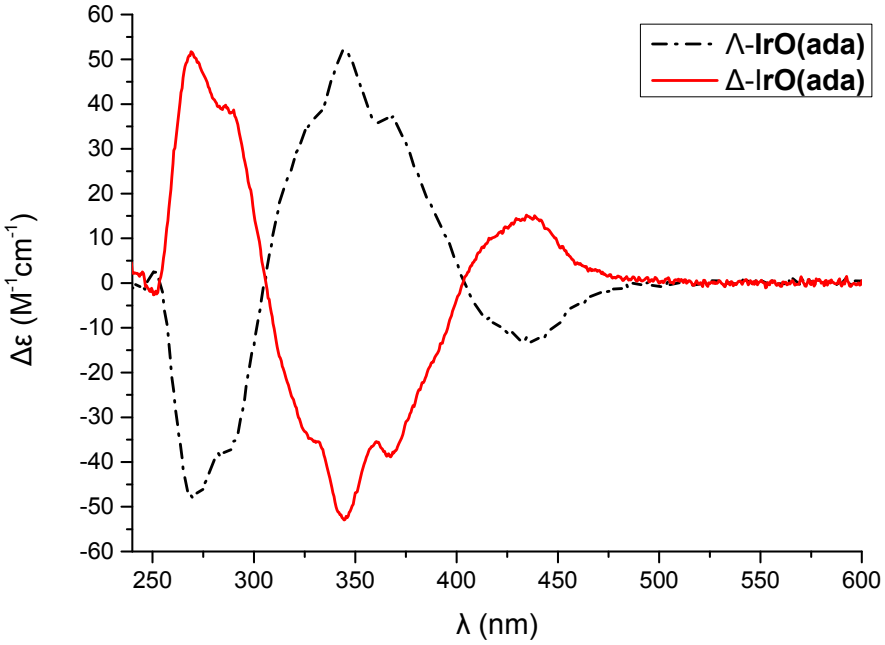


**Figure 72** CD spectra of complexes Λ-**IrO(ada)** and Δ-**IrO(ada)**.
Recorded in $CH_3OH$ (0.2 mM).

# Appendix 7. HPLC Traces on Chiral Stationary Phase

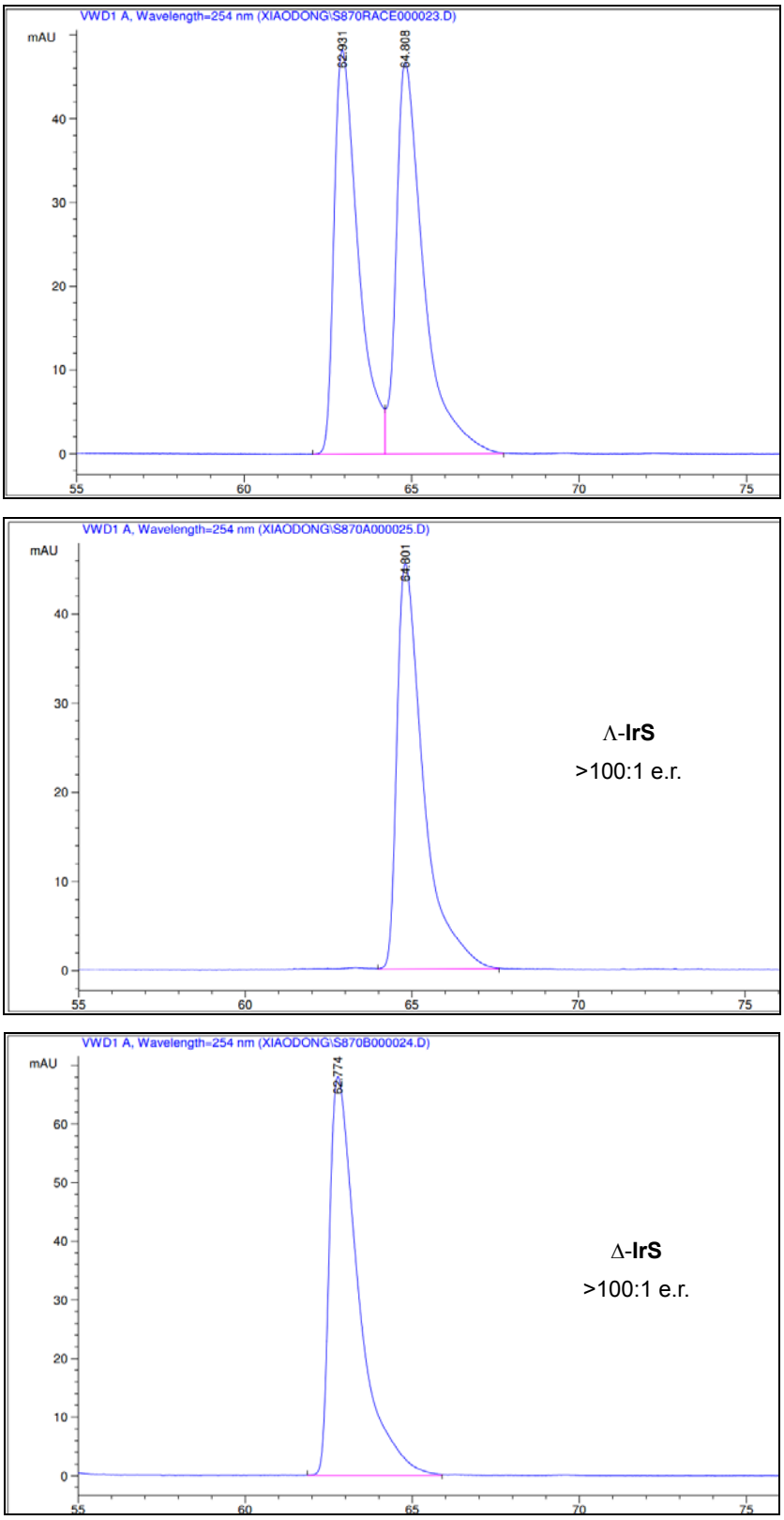


**Figure 73** Enantiomeric purities of the catalysts Λ-**IrS** and Δ-**IrS**.

*HPLC conditions: Daicel Chiralpak IB (250 × 4.6 mm); mobile phase: A = 0.1% TFA, B = MeCN; gradient: 38% to 46% B in 60 min; flow rate: 1.0 mL/min; 254 nm; 20 °C.*

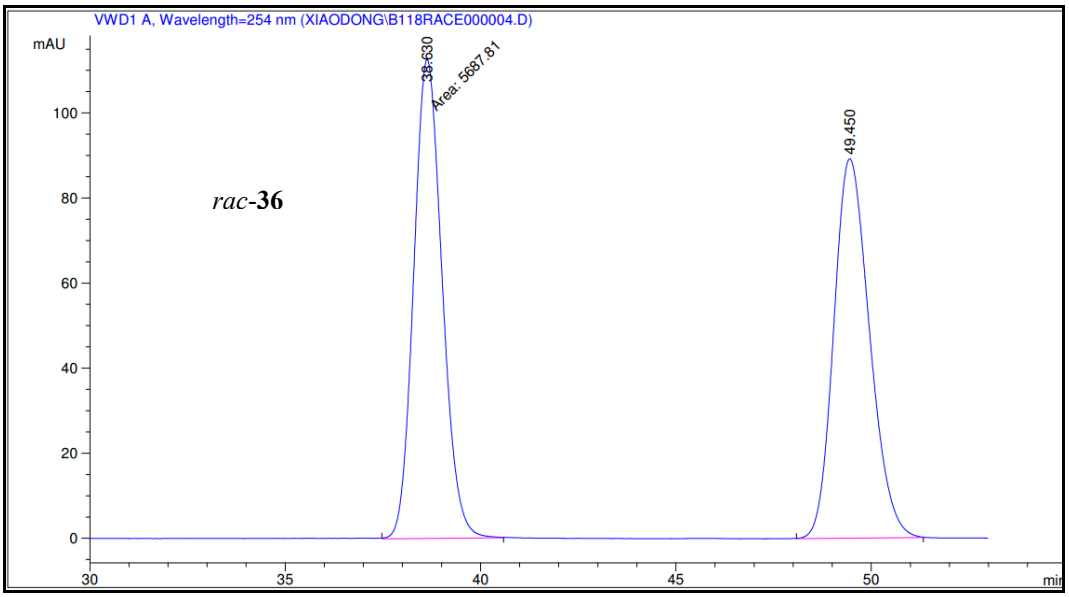


| Peak # | RetTime [min] | Type | Width [min] | Area [mAU*s] | Height [mAU] | Area % |
|---|---|---|---|---|---|---|
| 1 | 38.630 | MM | 0.8421 | 5687.81396 | 112.56605 | 50.0425 |
| 2 | 49.450 | BB | 0.9830 | 5678.14893 | 89.18725 | 49.9575 |

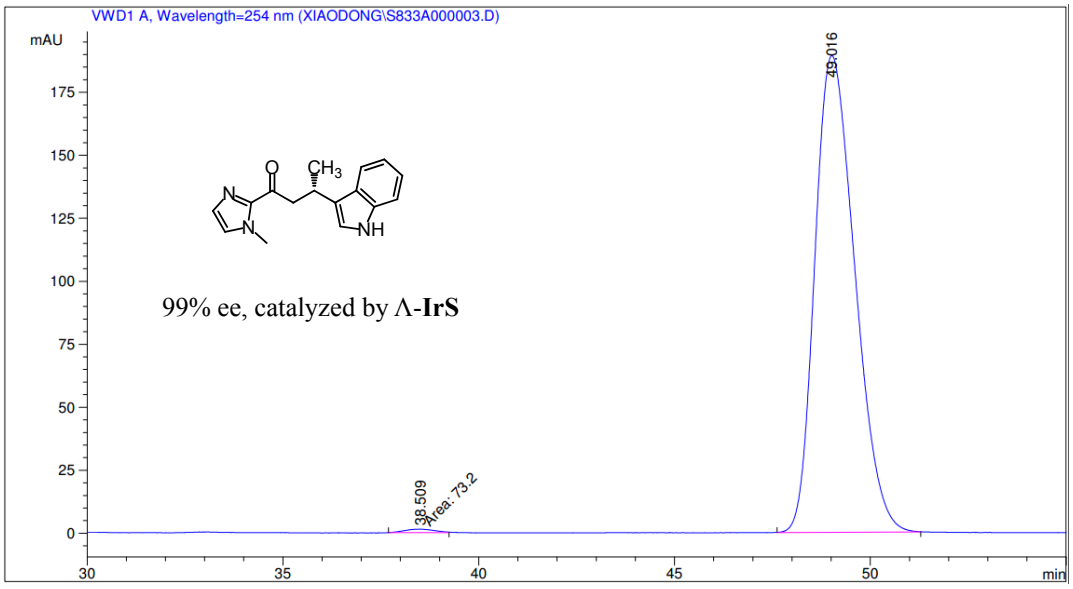


| Peak # | RetTime [min] | Type | Width [min] | Area [mAU*s] | Height [mAU] | Area % |
|---|---|---|---|---|---|---|
| 1 | 38.509 | MF | 0.8772 | 73.19995 | 1.39082 | 0.5423 |
| 2 | 49.016 | BB | 1.1190 | 1.34259e4 | 189.22839 | 99.4577 |

**Figure 74** HPLC traces of compound **36**.

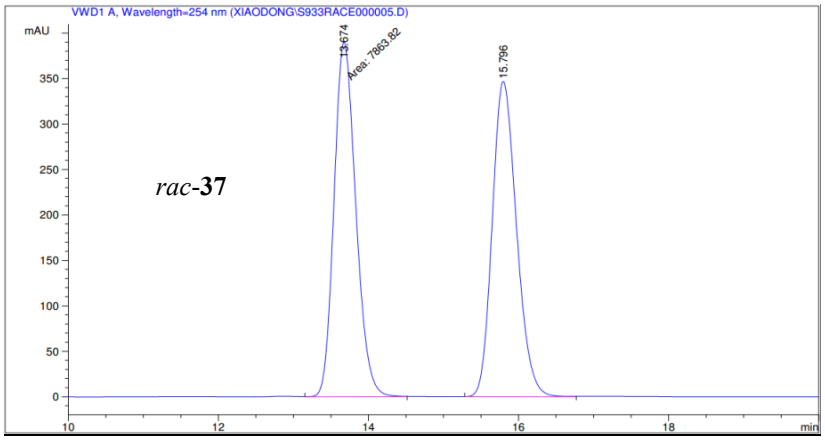


| Peak # | RetTime [min] | Type | Width [min] | Area [mAU*s] | Height [mAU] | Area % |
|---|---|---|---|---|---|---|
| 1 | 13.674 | MF | 0.3360 | 7863.81982 | 390.08548 | 50.2211 |
| 2 | 15.796 | BB | 0.3482 | 7794.58643 | 346.69852 | 49.7789 |

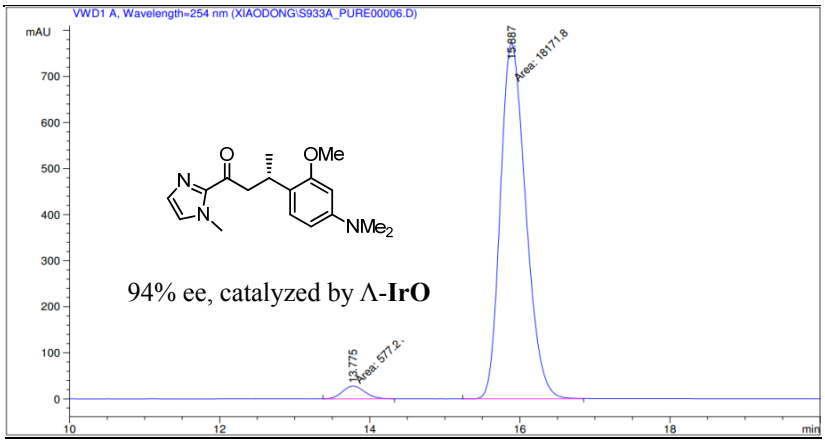


| Peak # | RetTime [min] | Type | Width [min] | Area [mAU*s] | Height [mAU] | Area % |
|---|---|---|---|---|---|---|
| 1 | 13.775 | MF | 0.3488 | 577.21741 | 27.57767 | 3.0786 |
| 2 | 15.887 | MF | 0.3924 | 1.81718e4 | 771.81403 | 96.9214 |

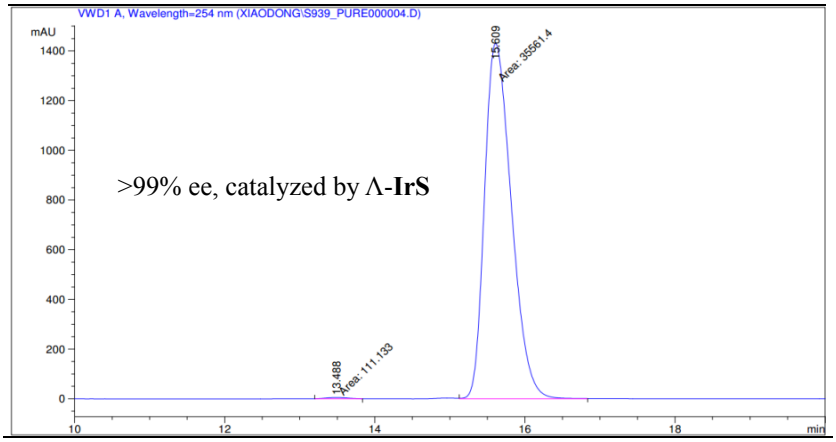


| Peak # | RetTime [min] | Type | Width [min] | Area [mAU*s] | Height [mAU] | Area % |
|---|---|---|---|---|---|---|
| 1 | 13.488 | MM | 0.3583 | 111.13294 | 5.16895 | 0.3115 |
| 2 | 15.608 | MF | 0.4145 | 3.55614e4 | 1430.05347 | 99.6885 |

**Figure 75** HPLC traces of compound **37**.

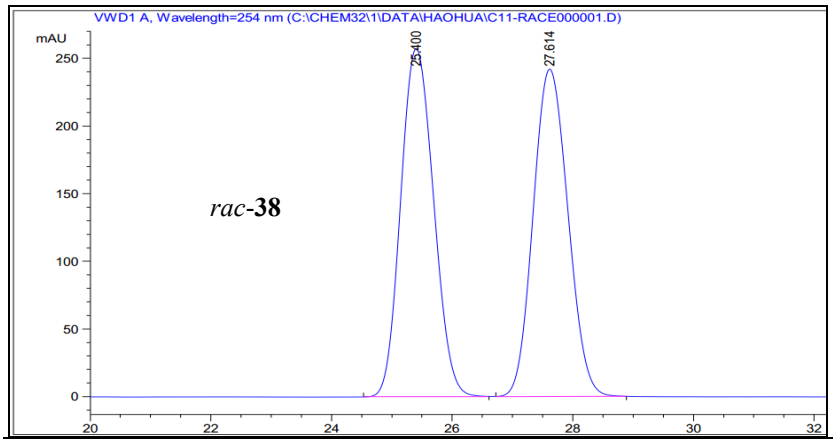


| Peak # | RetTime [min] | Type | Width [min] | Area [mAU*s] | Height [mAU] | Area % |
|---|---|---|---|---|---|---|
| 1 | 25.400 | BB | 0.6097 | 9759.82031 | 257.47388 | 50.1778 |
| 2 | 27.614 | BB | 0.6390 | 9690.65625 | 242.01826 | 49.8222 |

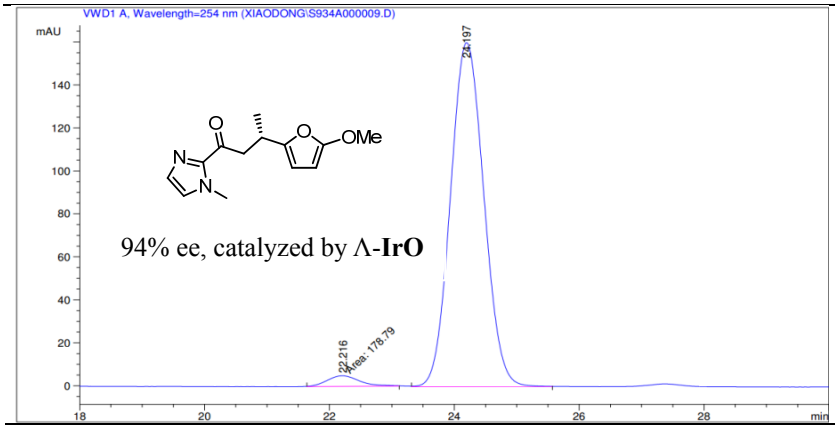


| Peak # | RetTime [min] | Type | Width [min] | Area [mAU*s] | Height [mAU] | Area % |
|---|---|---|---|---|---|---|
| 1 | 22.216 | MM | 0.6064 | 178.79048 | 4.91376 | 2.9155 |
| 2 | 24.197 | VB | 0.5866 | 5953.63574 | 160.16139 | 97.0845 |

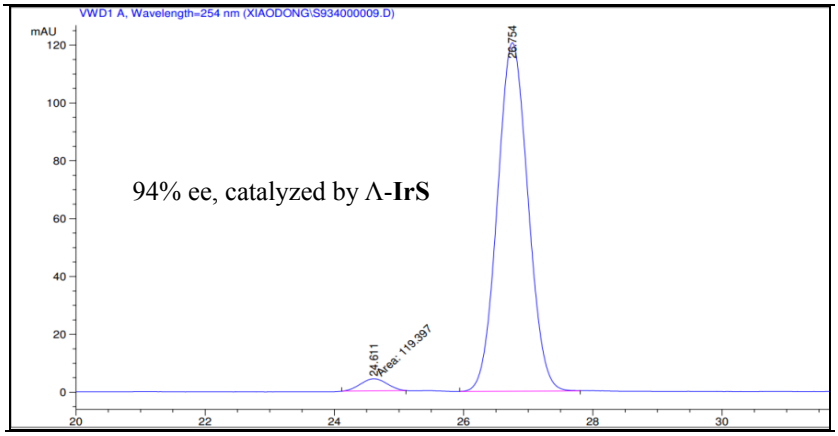


| Peak # | RetTime [min] | Type | Width [min] | Area [mAU*s] | Height [mAU] | Area % |
|---|---|---|---|---|---|---|
| 1 | 24.611 | MM | 0.4763 | 119.39693 | 4.17802 | 2.9294 |
| 2 | 26.754 | BB | 0.5114 | 3956.39990 | 120.44363 | 97.0706 |

**Figure 76** HPLC traces of compound **38**.

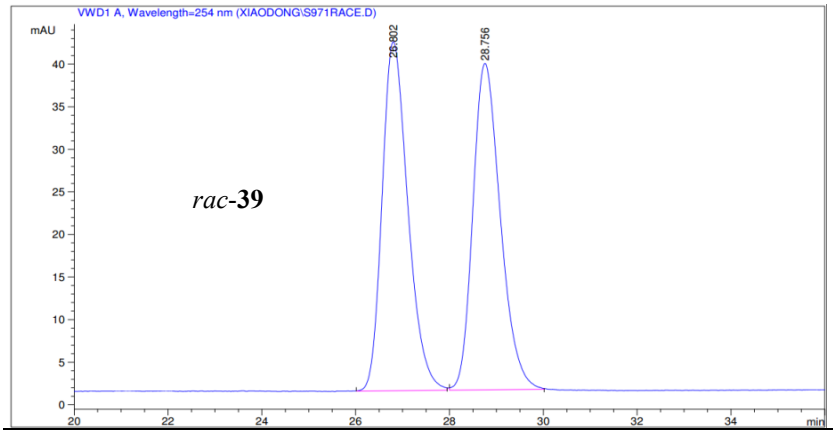


| Peak # | RetTime [min] | Type | Width [min] | Area [mAU*s] | Height [mAU] | Area % |
|---|---|---|---|---|---|---|
| 1 | 26.802 | BB | 0.5849 | 1563.96350 | 40.99169 | 50.0679 |
| 2 | 28.756 | BB | 0.6188 | 1559.71899 | 38.33744 | 49.9321 |

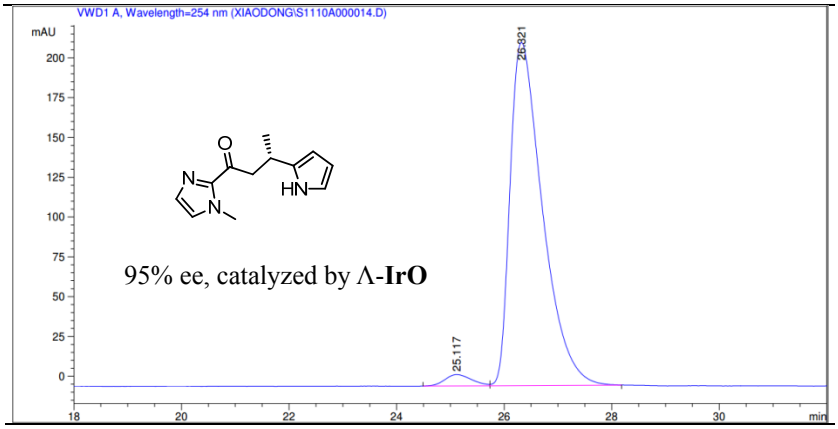


| Peak # | RetTime [min] | Type | Width [min] | Area [mAU*s] | Height [mAU] | Area % |
|---|---|---|---|---|---|---|
| 1 | 25.117 | BV | 0.4952 | 246.83122 | 7.08670 | 2.6586 |
| 2 | 26.321 | VB | 0.6289 | 9037.34082 | 215.55846 | 97.3414 |

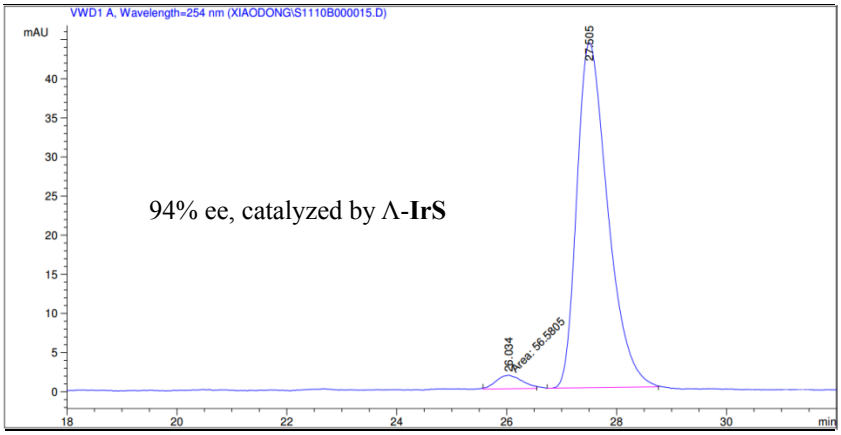


| Peak # | RetTime [min] | Type | Width [min] | Area [mAU*s] | Height [mAU] | Area % |
|---|---|---|---|---|---|---|
| 1 | 26.034 | MF | 0.5450 | 56.58051 | 1.73042 | 3.1815 |
| 2 | 26.505 | VB | 0.6000 | 1721.82935 | 44.06918 | 96.8185 |

**Figure 77** HPLC traces of compound **39**.

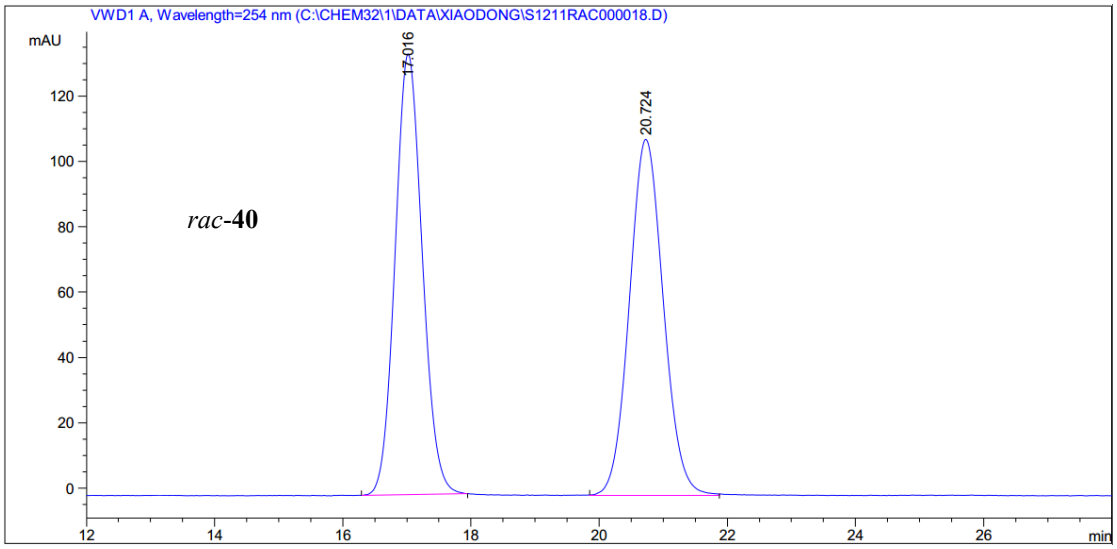


| Peak # | RetTime [min] | Type | Width [min] | Area [mAU*s] | Height [mAU] | Area % |
|---|---|---|---|---|---|---|
| 1 | 17.016 | VB | 0.4572 | 3975.10522 | 134.95076 | 49.7398 |
| 2 | 20.724 | BB | 0.5652 | 4016.68677 | 109.03468 | 50.2602 |

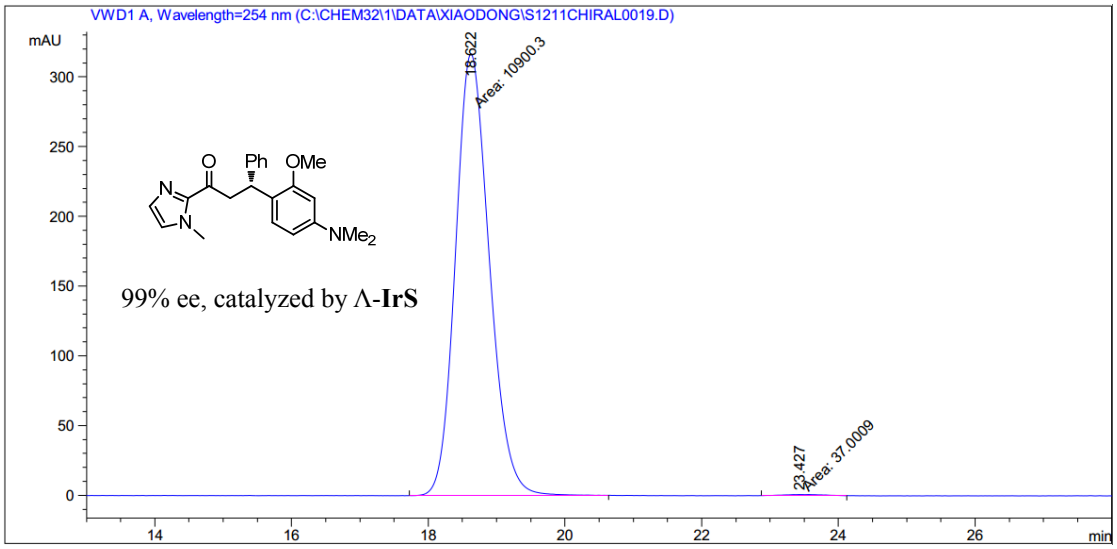


| Peak # | RetTime [min] | Type | Width [min] | Area [mAU*s] | Height [mAU] | Area % |
|---|---|---|---|---|---|---|
| 1 | 18.622 | MM | 0.5737 | 1.09003e4 | 316.65167 | 99.6617 |
| 2 | 23.427 | MM | 0.7214 | 37.00091 | 8.54818e-1 | 0.3383 |

**Figure 78** HPLC traces of compound **40**.

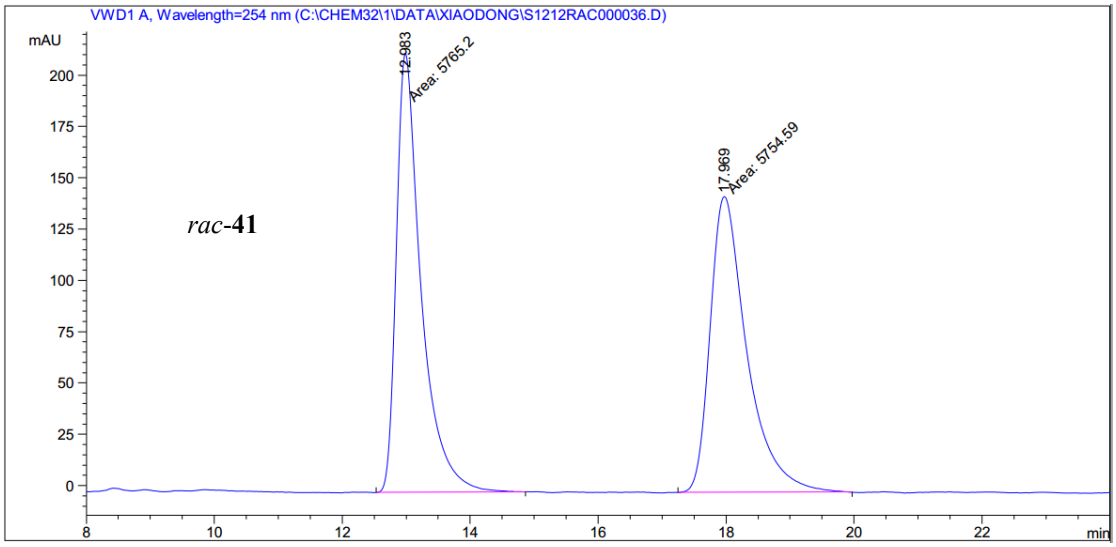


| Peak # | RetTime [min] | Type | Width [min] | Area [mAU*s] | Height [mAU] | Area % |
|---|---|---|---|---|---|---|
| 1 | 12.983 | MM | 0.4494 | 5765.20459 | 213.81839 | 50.0461 |
| 2 | 17.969 | MM | 0.6655 | 5754.58984 | 144.10692 | 49.9539 |

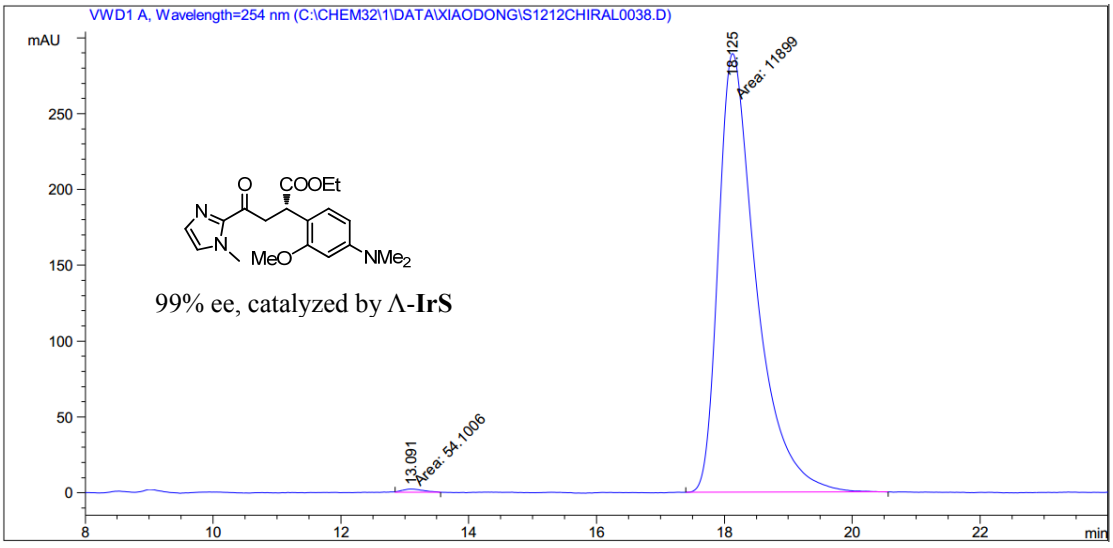


| Peak # | RetTime [min] | Type | Width [min] | Area [mAU*s] | Height [mAU] | Area % |
|---|---|---|---|---|---|---|
| 1 | 13.091 | MM | 0.4011 | 54.10061 | 2.24792 | 0.4526 |
| 2 | 18.125 | MM | 0.6854 | 1.18990e4 | 289.35458 | 99.5474 |

**Figure 79** HPLC traces of compound **41**.

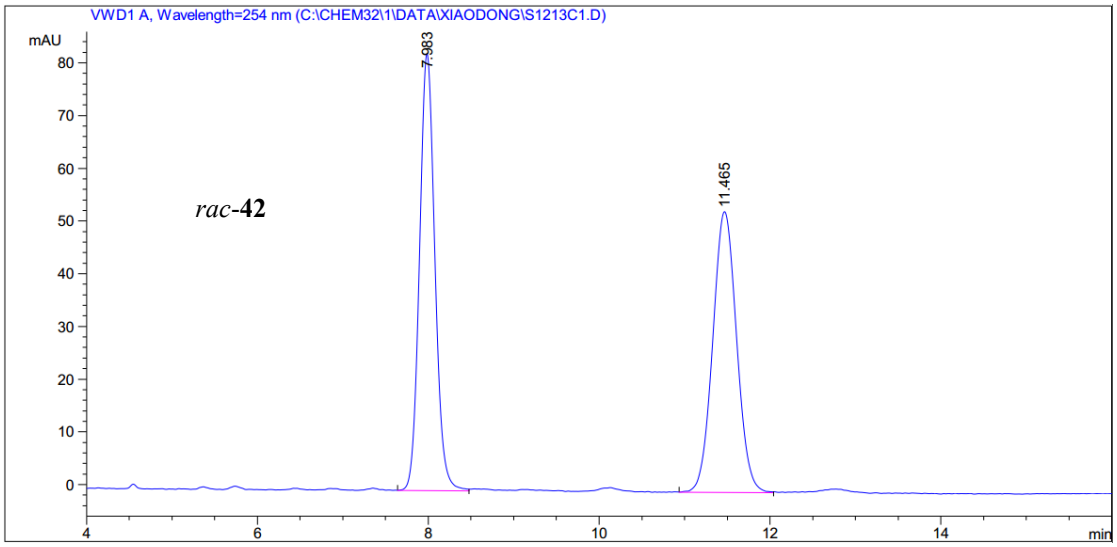


| Peak # | RetTime [min] | Type | Width [min] | Area [mAU*s] | Height [mAU] | Area % |
|---|---|---|---|---|---|---|
| 1 | 7.983 | VB | 0.1929 | 1040.57227 | 82.96185 | 50.1166 |
| 2 | 11.465 | VB | 0.3009 | 1035.72949 | 53.32177 | 49.8834 |

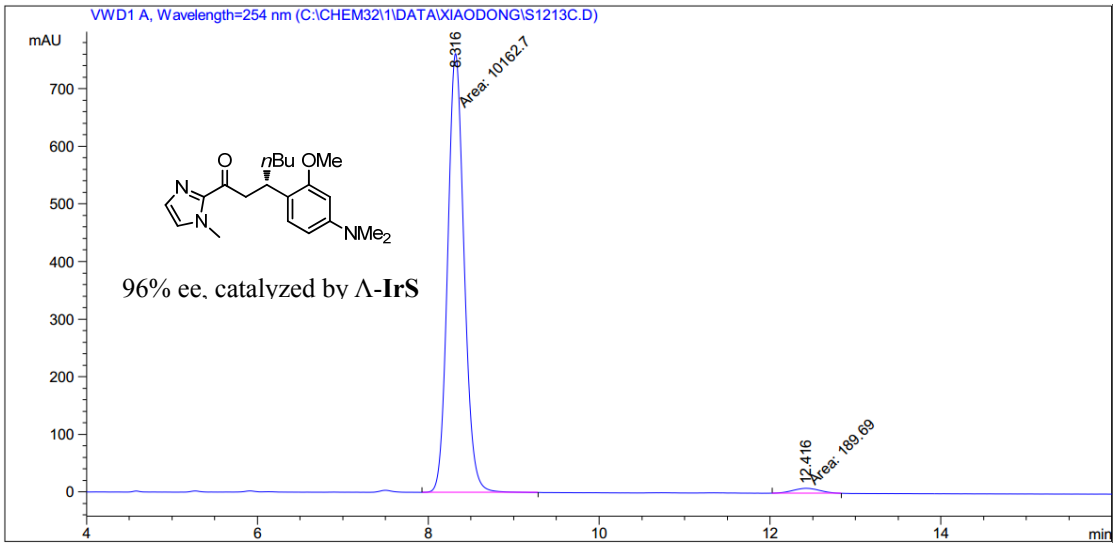


| Peak # | RetTime [min] | Type | Width [min] | Area [mAU*s] | Height [mAU] | Area % |
|---|---|---|---|---|---|---|
| 1 | 8.316 | MM | 0.2223 | 1.01627e4 | 762.09894 | 98.1677 |
| 2 | 12.416 | MM | 0.3664 | 189.69049 | 8.62937 | 1.8323 |

**Figure 80** HPLC traces of compound **42**.

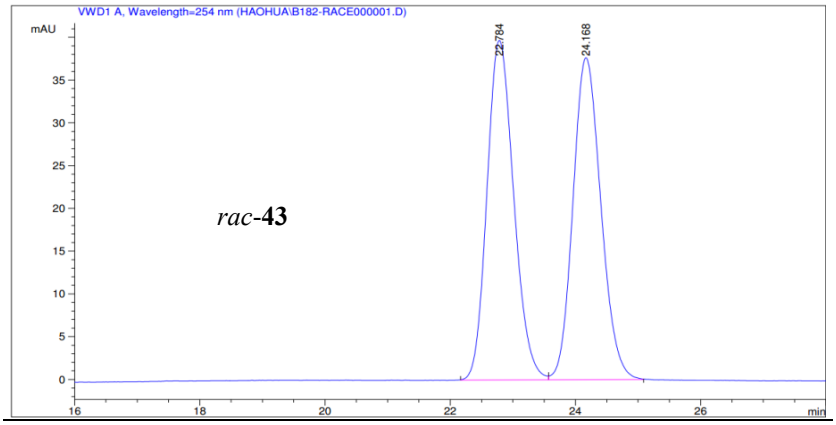


| Peak # | RetTime [min] | Type | Width [min] | Area [mAU*s] | Height [mAU] | Area % |
|---|---|---|---|---|---|---|
| 1 | 22.784 | BB | 0.4613 | 1178.59717 | 39.71305 | 50.2401 |
| 2 | 24.168 | BB | 0.4840 | 1167.33130 | 37.64820 | 49.7599 |

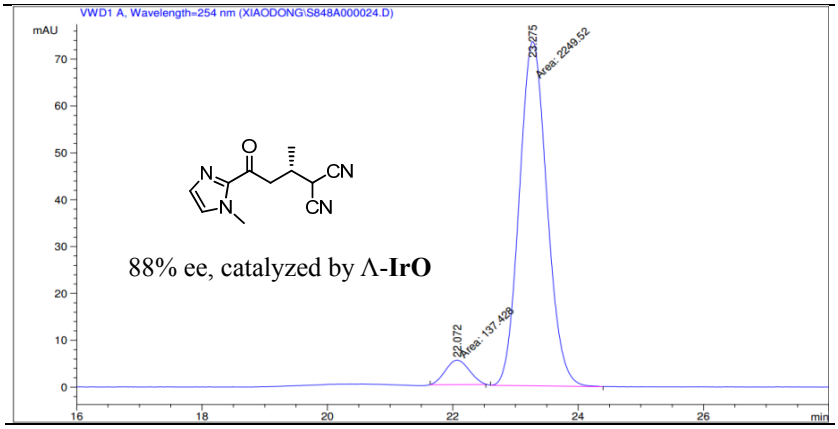


| Peak # | RetTime [min] | Type | Width [min] | Area [mAU*s] | Height [mAU] | Area % |
|---|---|---|---|---|---|---|
| 1 | 22.072 | MM | 0.4410 | 137.42838 | 5.19432 | 5.7575 |
| 2 | 23.275 | MM | 0.5102 | 2249.52100 | 73.47902 | 94.2425 |

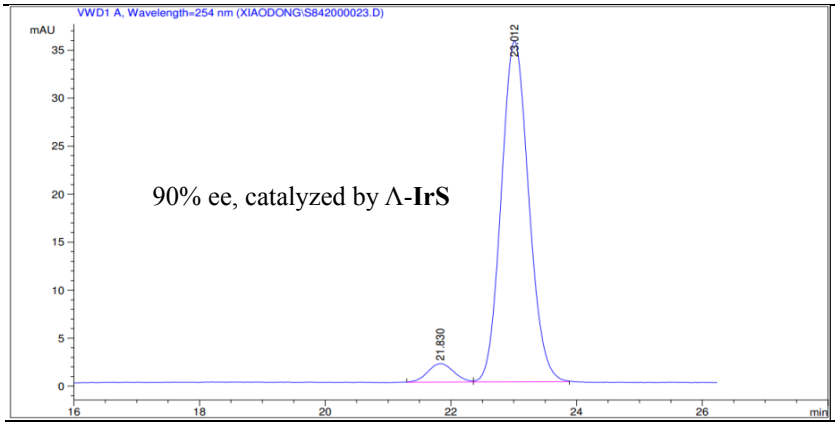


| Peak # | RetTime [min] | Type | Width [min] | Area [mAU*s] | Height [mAU] | Area % |
|---|---|---|---|---|---|---|
| 1 | 21.830 | BV | 0.3479 | 55.00225 | 1.92494 | 4.8563 |
| 2 | 23.012 | VB | 0.4751 | 1077.59302 | 35.48796 | 95.1437 |

**Figure 81** HPLC traces of compound **43**.

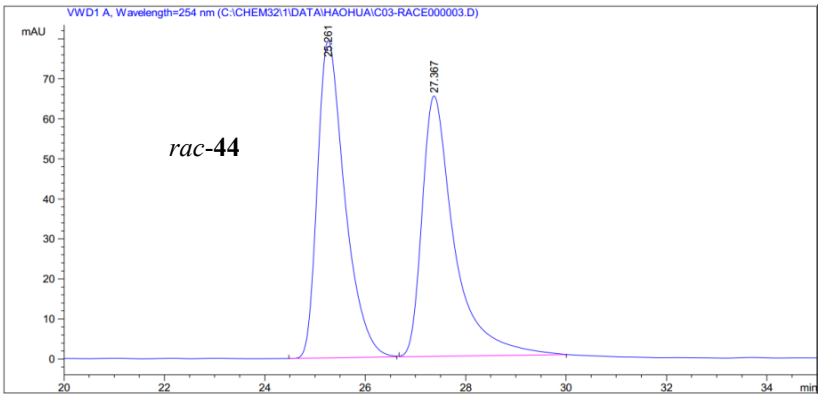


| Peak # | RetTime [min] | Type | Width [min] | Area [mAU*s] | Height [mAU] | Area % |
|---|---|---|---|---|---|---|
| 1 | 25.261 | BB | 0.5682 | 3008.80444 | 79.23686 | 50.8097 |
| 2 | 27.367 | BB | 0.6604 | 2912.91357 | 65.08873 | 49.1903 |

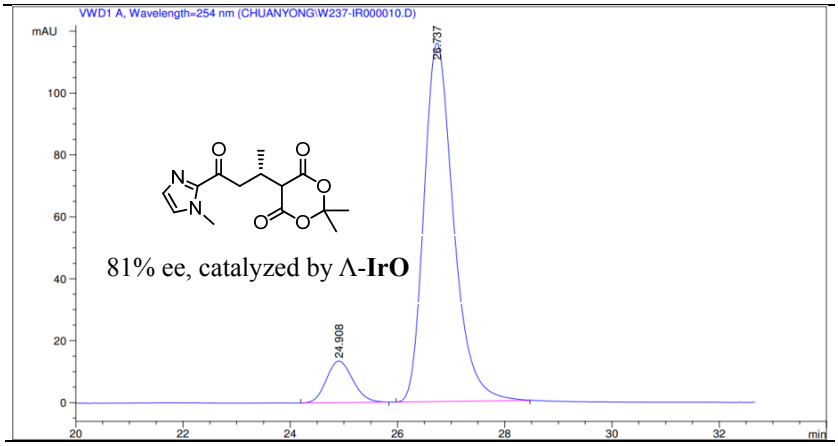


| Peak # | RetTime [min] | Type | Width [min] | Area [mAU*s] | Height [mAU] | Area % |
|---|---|---|---|---|---|---|
| 1 | 24.908 | BB | 0.5208 | 457.89447 | 13.40493 | 9.3503 |
| 2 | 26.737 | BB | 0.5855 | 4439.24023 | 115.80431 | 90.6497 |

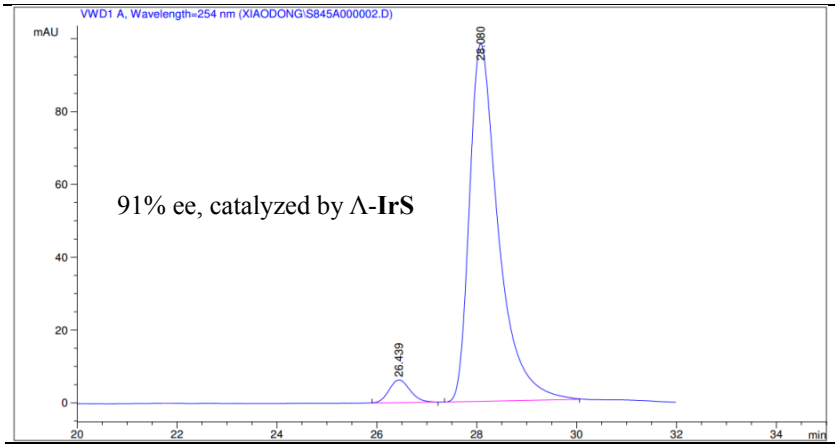


| Peak # | RetTime [min] | Type | Width [min] | Area [mAU*s] | Height [mAU] | Area % |
|---|---|---|---|---|---|---|
| 1 | 26.439 | BB | 0.4459 | 183.35036 | 6.24568 | 4.4242 |
| 2 | 28.080 | BB | 0.5988 | 3960.94531 | 98.18440 | 95.5758 |

**Figure 82** HPLC traces of compound **44**.

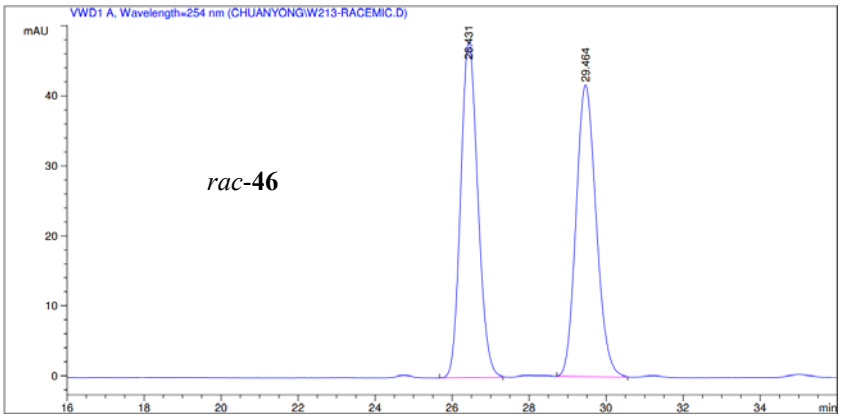


| Peak # | RetTime [min] | Type | Width [min] | Area [mAU*s] | Height [mAU] | Area % |
|---|---|---|---|---|---|---|
| 1 | 26.431 | BB | 0.4790 | 1483.64502 | 47.93988 | 49.5918 |
| 2 | 29.464 | BB | 0.5640 | 1508.06726 | 41.61650 | 50.4082 |

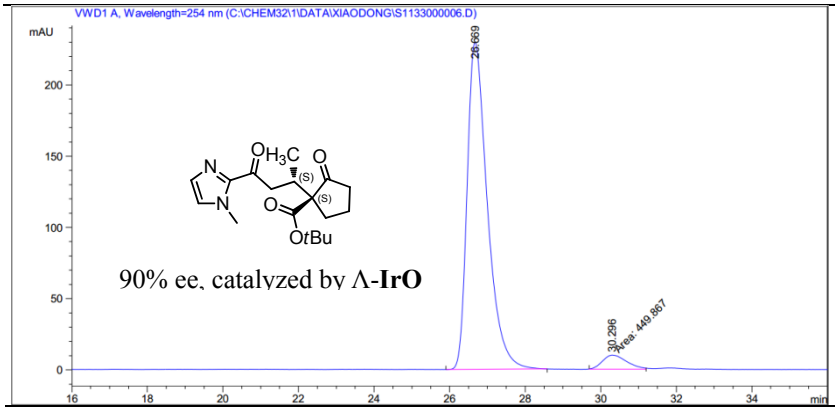


| Peak # | RetTime [min] | Type | Width [min] | Area [mAU*s] | Height [mAU] | Area % |
|---|---|---|---|---|---|---|
| 1 | 26.669 | VB | 0.5623 | 8525.45313 | 229.84721 | 94.9877 |
| 2 | 30.296 | FM | 0.7476 | 449.86661 | 10.02874 | 5.0123 |

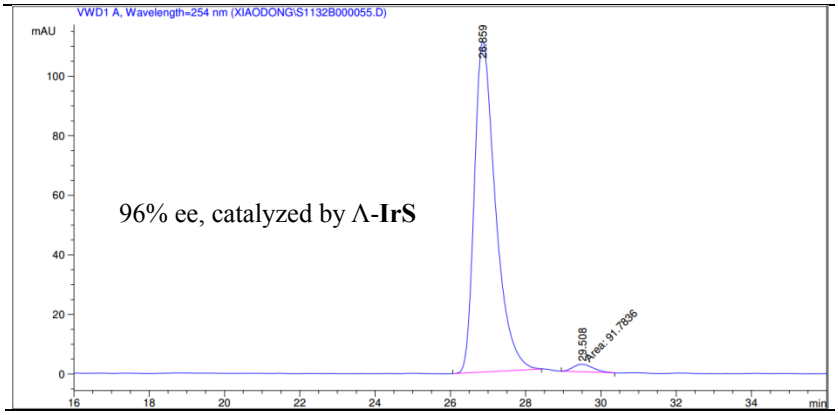


| Peak # | RetTime [min] | Type | Width [min] | Area [mAU*s] | Height [mAU] | Area % |
|---|---|---|---|---|---|---|
| 1 | 26.859 | VB | 0.5915 | 4339.95752 | 111.01386 | 97.9289 |
| 2 | 29.508 | MF | 0.6054 | 91.78365 | 2.52667 | 2.0711 |

**Figure 83** HPLC traces of compound **46**.

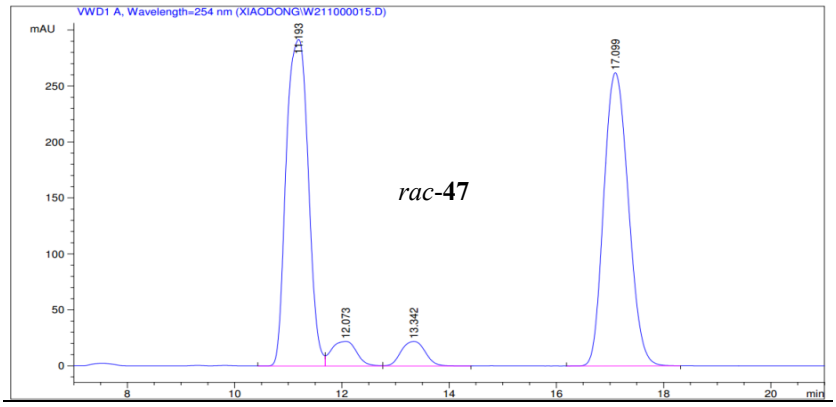


| Peak # | RetTime [min] | Type | Width [min] | Area [mAU*s] | Height [mAU] | Area % |
|---|---|---|---|---|---|---|
| 1 | 11.193 | VV | 0.4671 | 8330.63672 | 291.71237 | 46.1087 |
| 2 | 12.073 | VV | 0.5207 | 712.80756 | 21.91737 | 3.9453 |
| 3 | 13.342 | VB | 0.5064 | 682.27936 | 21.88411 | 3.7763 |
| 4 | 17.099 | VB | 0.5085 | 8341.64453 | 261.88049 | 46.1697 |

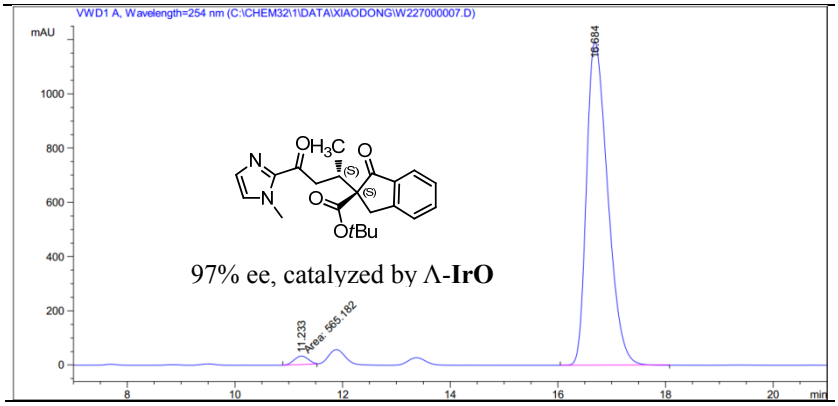


| Peak # | RetTime [min] | Type | Width [min] | Area [mAU*s] | Height [mAU] | Area % |
|---|---|---|---|---|---|---|
| 1 | 11.233 | MM | 0.3064 | 565.18250 | 30.74432 | 1.7059 |
| 2 | 16.684 | BB | 0.4232 | 3.25658e4 | 1193.21106 | 98.2941 |

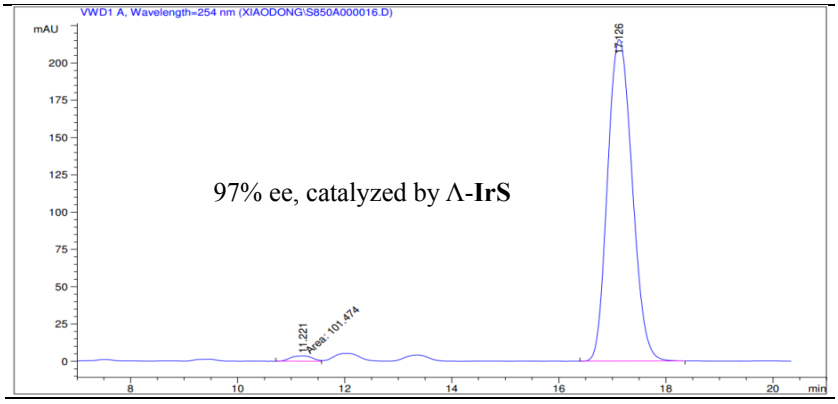


| Peak # | RetTime [min] | Type | Width [min] | Area [mAU*s] | Height [mAU] | Area % |
|---|---|---|---|---|---|---|
| 1 | 11.221 | MM | 0,4674 | 101.47427 | 3.61864 | 1.4540 |
| 2 | 17.126 | BB | 0.5091 | 6877.49023 | 215.57463 | 98.5460 |

**Figure 84** HPLC traces of compound **47**.

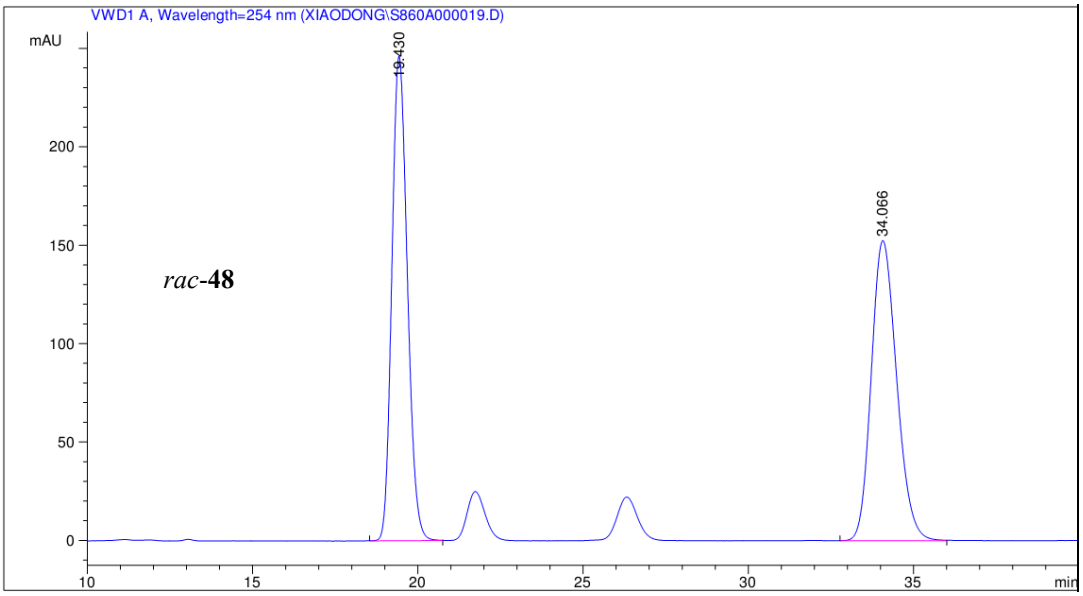


| Peak # | RetTime [min] | Type | Width [min] | Area [mAU*s] | Height [mAU] | Area % |
|---|---|---|---|---|---|---|
| 1 | 19.430 | VB | 0.5101 | 8026.8709 | 246.11972 | 49.6639 |
| 2 | 34.066 | BV | 0.8309 | 8135.50146 | 152.41451 | 50.3361 |

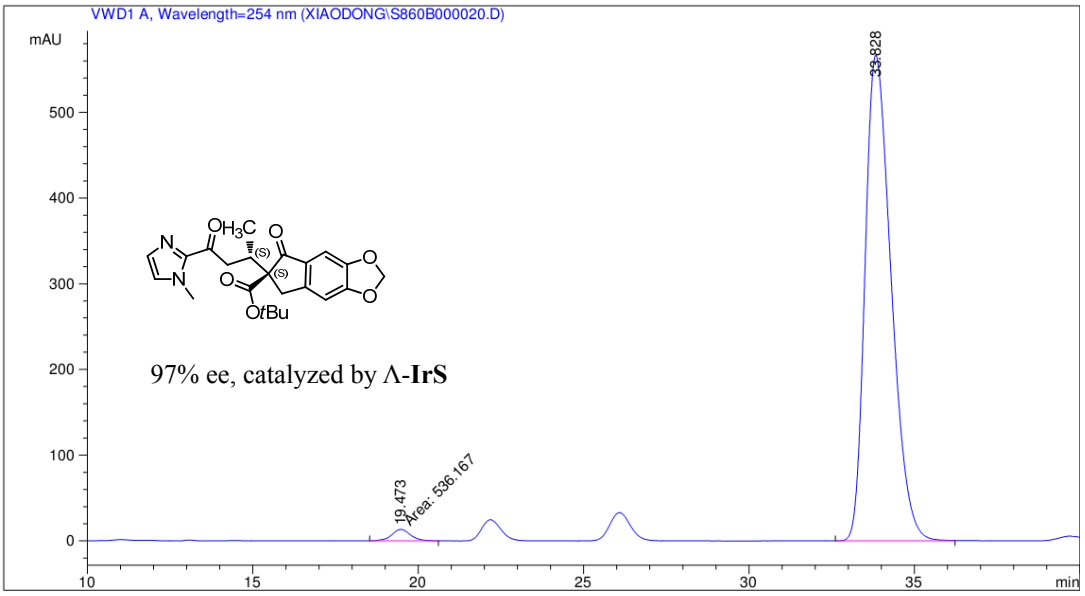


| Peak # | RetTime [min] | Type | Width [min] | Area [mAU*s] | Height [mAU] | Area % |
|---|---|---|---|---|---|---|
| 1 | 19.473 | FM | 0.6665 | 536.16663 | 13.40802 | 1.69810 |
| 2 | 33.828 | VV | 0.8502 | 3.10390e4 | 566.59875 | 98.3019 |

**Figure 85** HPLC traces of compound **48**.

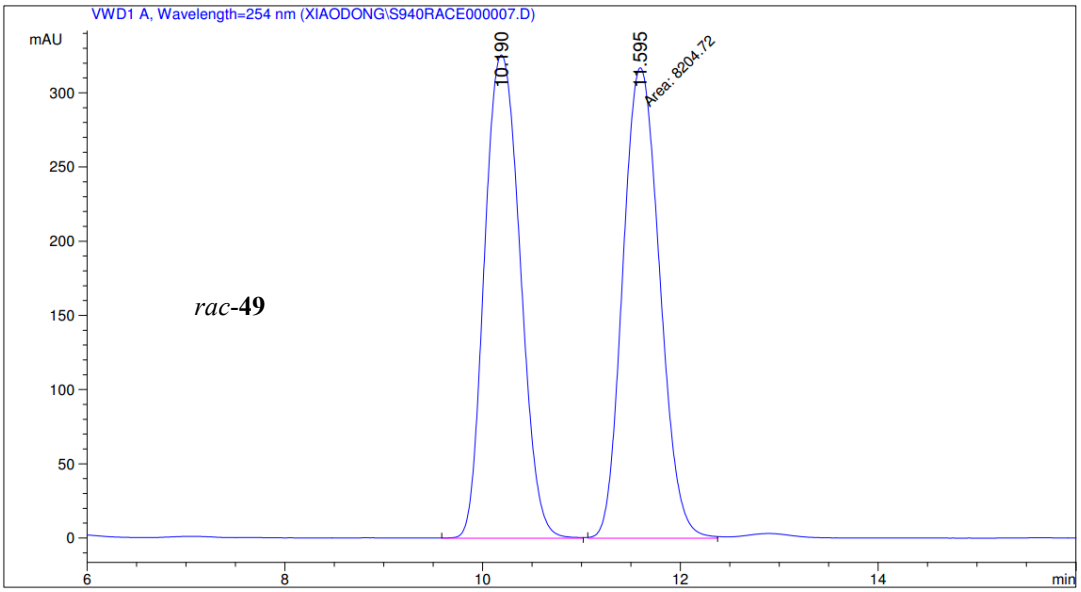


| Peak # | RetTime [min] | Type | Width [min] | Area [mAU*s] | Height [mAU] | Area % |
|---|---|---|---|---|---|---|
| 1 | 10.190 | VV | 0.4041 | 8150.41943 | 325.62277 | 49.8340 |
| 2 | 11.595 | FM | 0.4314 | 8204.71973 | 316.99832 | 50.1660 |

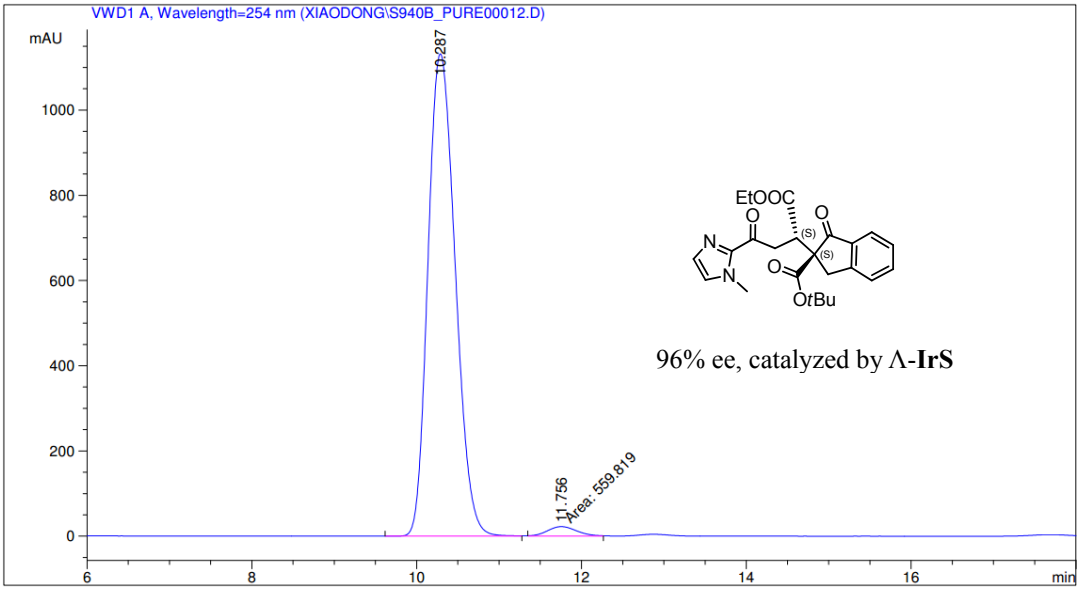


| Peak # | RetTime [min] | Type | Width [min] | Area [mAU*s] | Height [mAU] | Area % |
|---|---|---|---|---|---|---|
| 1 | 10.287 | VV | 0.3653 | 2.59844e4 | 1132.11560 | 97.8910 |
| 2 | 11.756 | FM | 0.4167 | 559.81915 | 22.38926 | 2.1090 |

**Figure 86** HPLC traces of compound **49**.

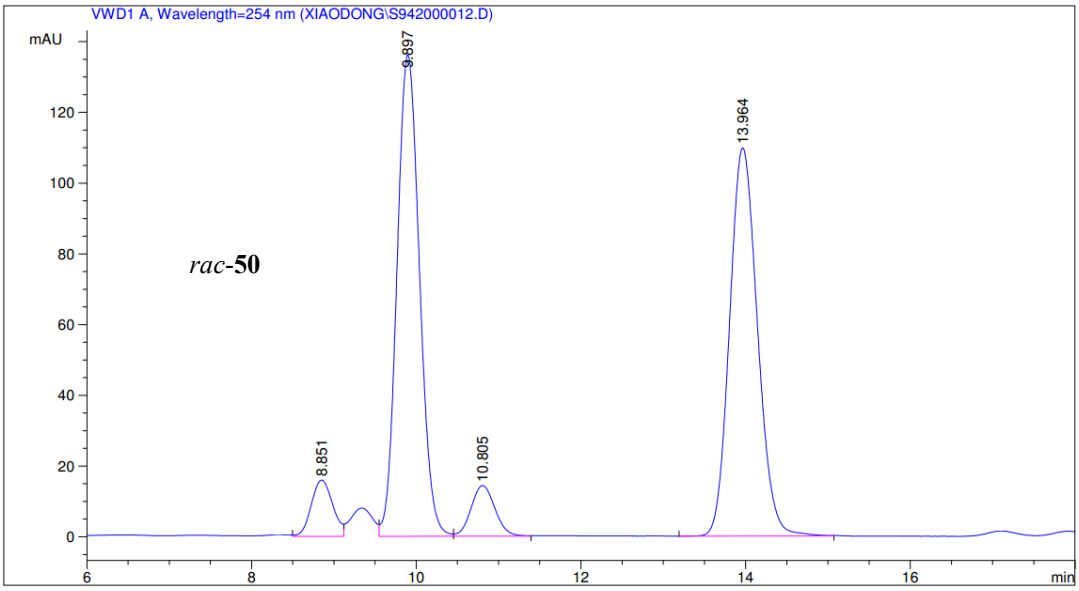


| Peak # | RetTime [min] | Type | Width [min] | Area [mAU*s] | Height [mAU] | Area % |
|---|---|---|---|---|---|---|
| 1 | 8.851 | VV | 0.2866 | 286.91385 | 15.87020 | 4.9980 |
| 2 | 9.897 | VV | 0.2985 | 2582.69116 | 136.14723 | 44.9900 |
| 3 | 10.805 | VB | 0.3157 | 290.28879 | 14.37609 | 5.0568 |
| 4 | 13.964 | VB | 0.3660 | 2580.69116 | 109.78651 | 44.9552 |

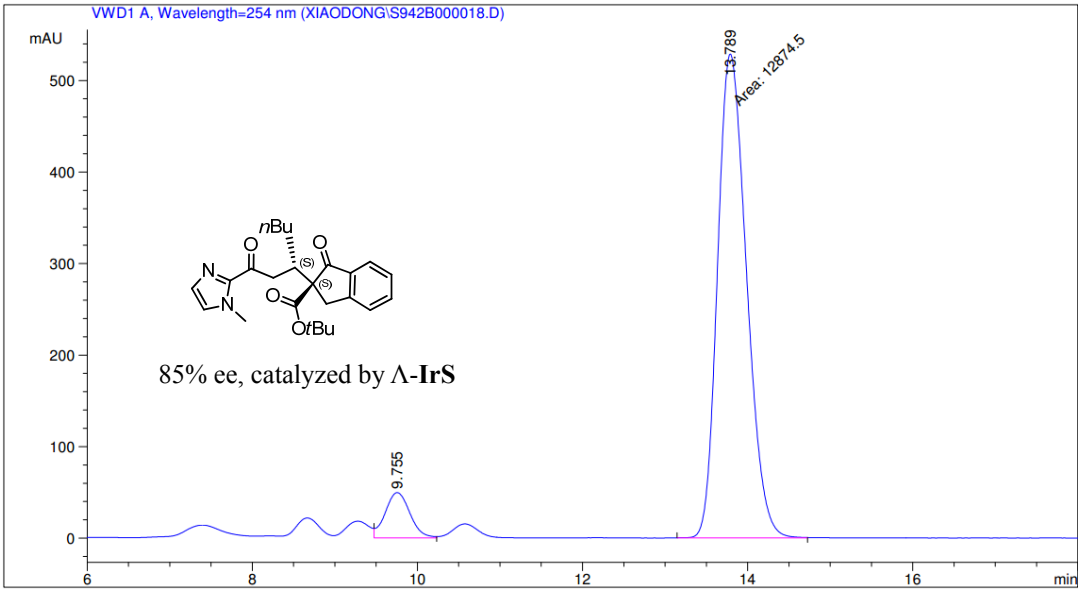


| Peak # | RetTime [min] | Type | Width [min] | Area [mAU*s] | Height [mAU] | Area % |
|---|---|---|---|---|---|---|
| 1 | 9.755 | VV | 0.3243 | 1030.00867 | 49.50636 | 7.4077 |
| 2 | 13.789 | FM | 0.4058 | 1.28745e4 | 528.78027 | 92.5923 |

**Figure 87** HPLC traces of compound **50**.

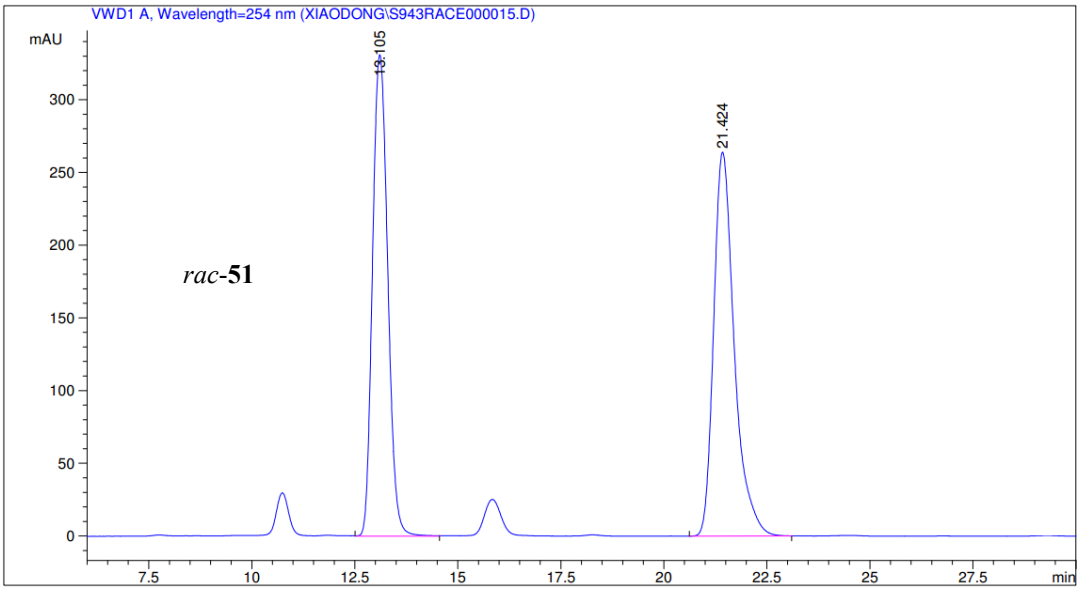


| Peak # | RetTime [min] | Type | Width [min] | Area [mAU*s] | Height [mAU] | Area % |
|---|---|---|---|---|---|---|
| 1 | 13.105 | VB | 0.4058 | 8485.14160 | 331.04080 | 48.0494 |
| 2 | 21.424 | VB | 0.5277 | 9174.05078 | 264.03427 | 51.9506 |

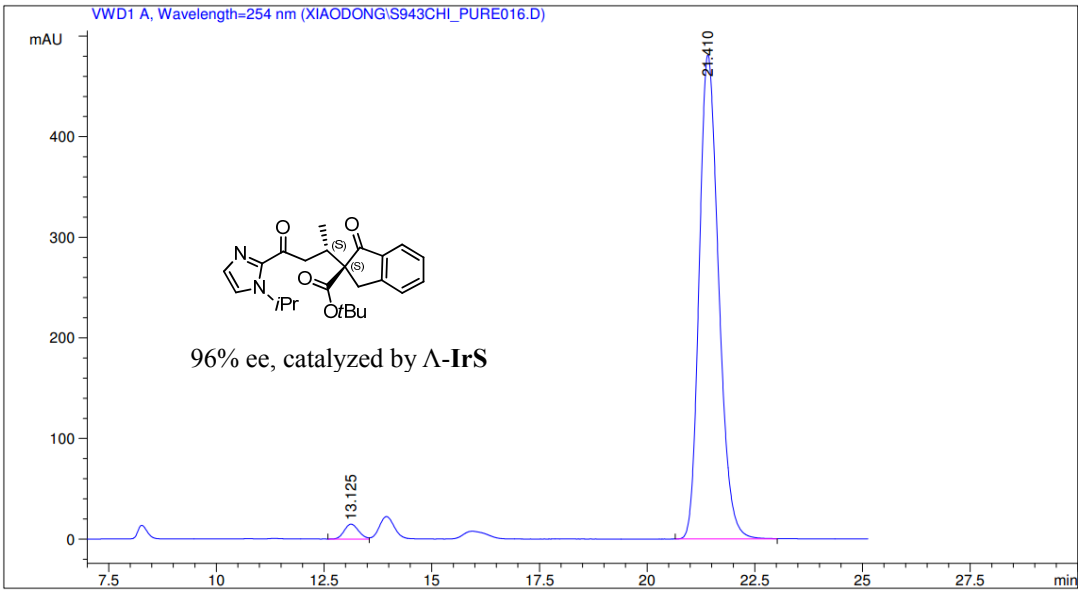


| Peak # | RetTime [min] | Type | Width [min] | Area [mAU*s] | Height [mAU] | Area % |
|---|---|---|---|---|---|---|
| 1 | 13.125 | VV | 0.3646 | 343.55960 | 14.84536 | 2.2266 |
| 2 | 21.410 | VB | 0.4881 | 1.50860e4 | 481.12292 | 97.7734 |

**Figure 88** HPLC traces of compound **51**.

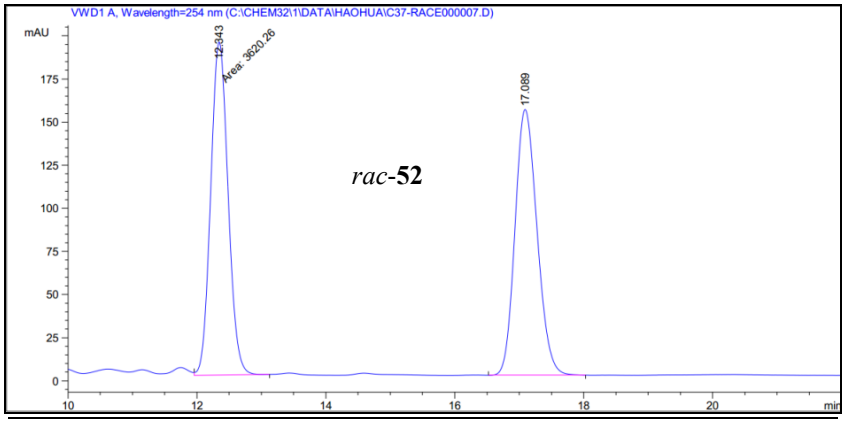


| Peak # | RetTime [min] | Type | Width [min] | Area [mAU*s] | Height [mAU] | Area % |
|---|---|---|---|---|---|---|
| 1 | 12.343 | MM | 0.3123 | 3620.26392 | 193.18588 | 49.6842 |
| 2 | 17.089 | VB | 0.3722 | 3666.28467 | 154.11316 | 50.3158 |

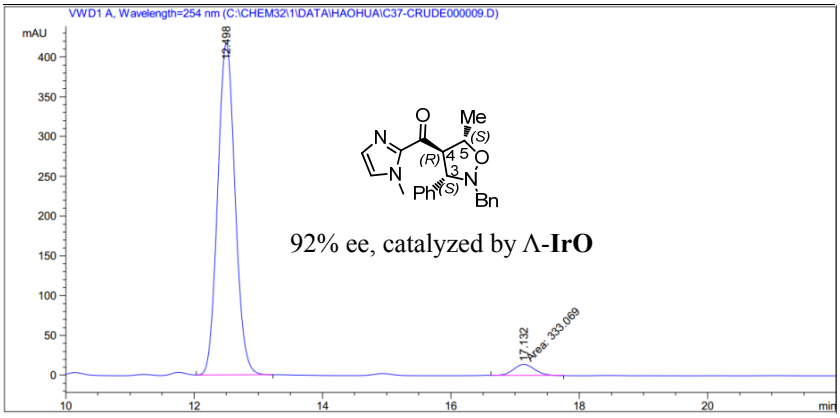


| Peak # | RetTime [min] | Type | Width [min] | Area [mAU*s] | Height [mAU] | Area % |
|---|---|---|---|---|---|---|
| 1 | 12.498 | VB | 0.2926 | 7870.44824 | 417.71896 | 95.9399 |
| 2 | 17.132 | FM | 0.3924 | 333.06882 | 14.14507 | 4.0601 |

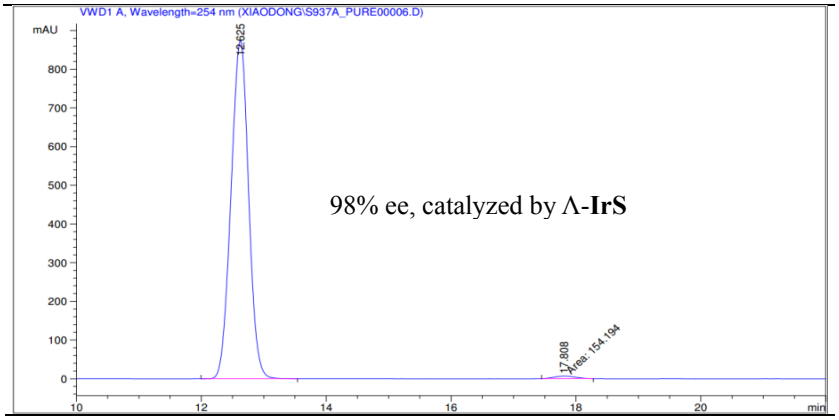


| Peak # | RetTime [min] | Type | Width [min] | Area [mAU*s] | Height [mAU] | Area % |
|---|---|---|---|---|---|---|
| 1 | 12.625 | VB | 0.3052 | 1.70790e4 | 873.86877 | 99.1053 |
| 2 | 17.808 | MM | 0.3924 | 154.19363 | 6.54996 | 0.8947 |

**Figure 89** HPLC traces of compound **52**.

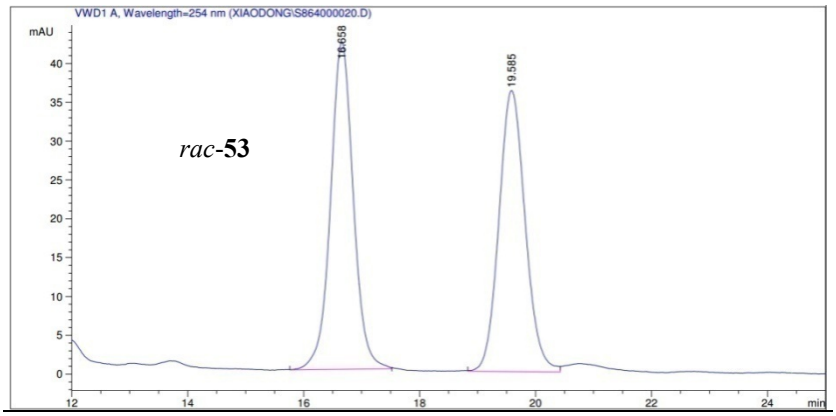


| Peak # | RetTime [min] | Type | Width [min] | Area [mAU*s] | Height [mAU] | Area % |
|---|---|---|---|---|---|---|
| 1 | 16.658 | VB | 0.4226 | 1153.26770 | 42.15503 | 50.3013 |
| 2 | 19.585 | BB | 0.4880 | 1139.45386 | 36.20518 | 49.6987 |

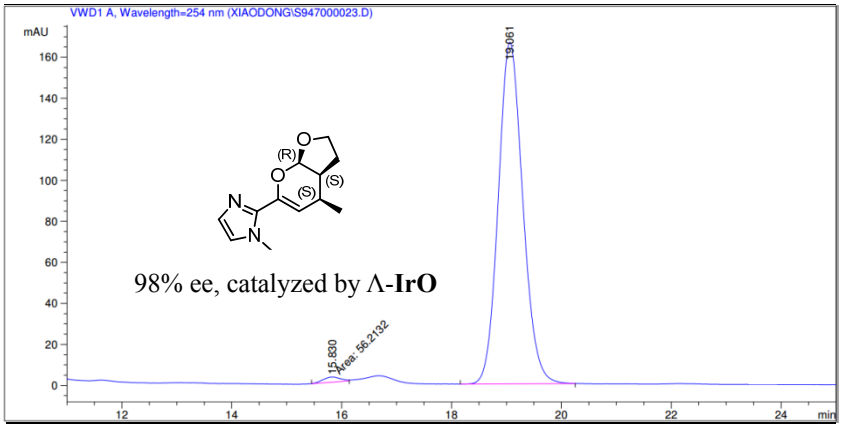


| Peak # | RetTime [min] | Type | Width [min] | Area [mAU*s] | Height [mAU] | Area % |
|---|---|---|---|---|---|---|
| 1 | 15.830 | MM | 0.3723 | 56.21323 | 2.51632 | 1.0767 |
| 2 | 19.061 | BB | 0.4769 | 5164.78027 | 166.51796 | 98.9233 |

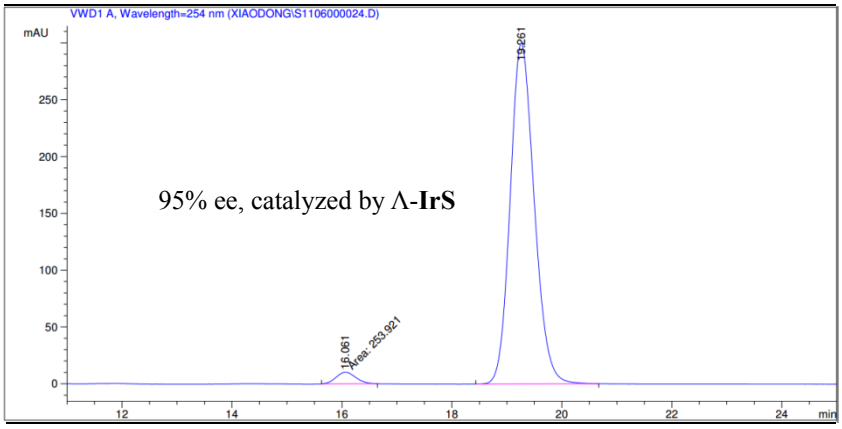


| Peak # | RetTime [min] | Type | Width [min] | Area [mAU*s] | Height [mAU] | Area % |
|---|---|---|---|---|---|---|
| 1 | 16.061 | MM | 0.4147 | 253.92087 | 10.20619 | 2.7101 |
| 2 | 19.261 | BB | 0.4695 | 9115.51074 | 300.00720 | 97.2899 |

**Figure 90** HPLC traces of compound **53**.

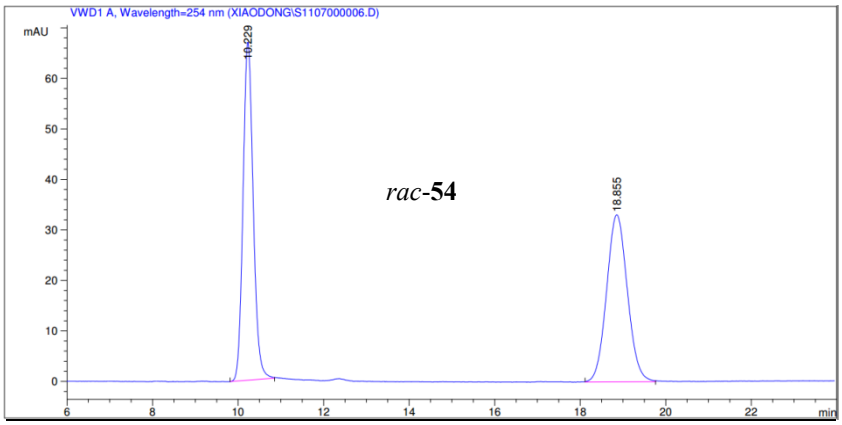


| Peak # | RetTime [min] | Type | Width [min] | Area [mAU*s] | Height [mAU] | Area % |
|---|---|---|---|---|---|---|
| 1 | 10.229 | BB | 0.2539 | 1105.66504 | 66.93617 | 49.7197 |
| 2 | 18.855 | BB | 0.5238 | 1118.12988 | 33.09314 | 50.2803 |

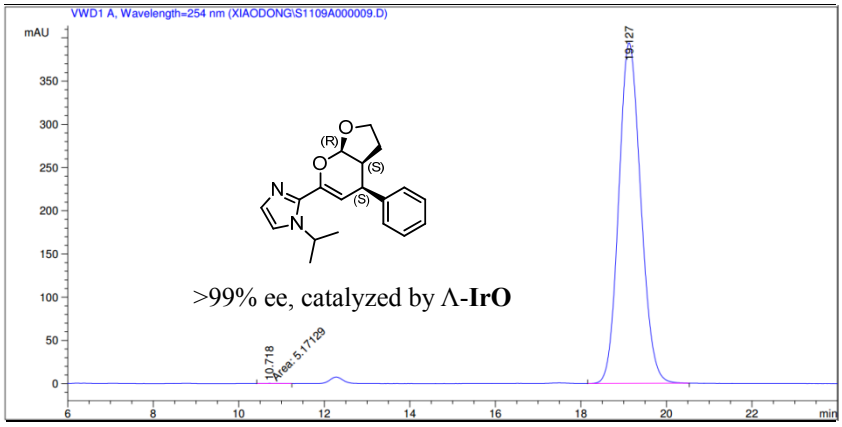


| Peak # | RetTime [min] | Type | Width [min] | Area [mAU*s] | Height [mAU] | Area % |
|---|---|---|---|---|---|---|
| 1 | 10.718 | MM | 0.4274 | 5.17129 | 2.01642e-1 | 0.0366 |
| 2 | 19.127 | VB | 0.5547 | 1.41132e4 | 394.08594 | 99.9634 |

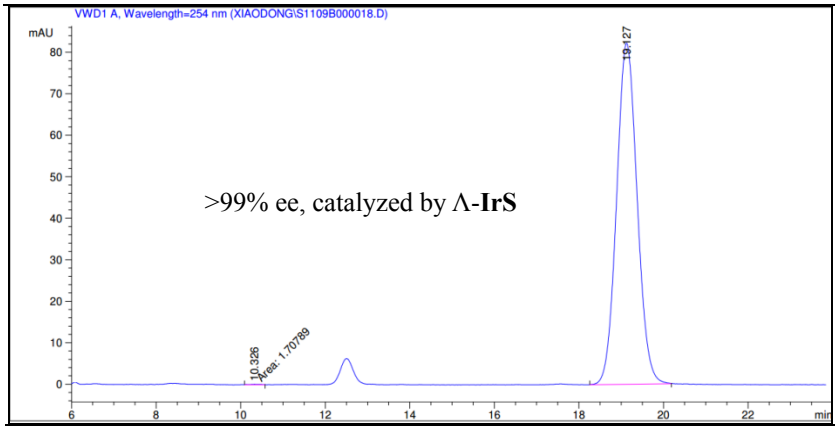


| Peak # | RetTime [min] | Type | Width [min] | Area [mAU*s] | Height [mAU] | Area % |
|---|---|---|---|---|---|---|
| 1 | 10.326 | MM | 0.2932 | 1.70789 | 9.70847e-2 | 0.0615 |
| 2 | 19..127 | BB | 0.5278 | 2775.66211 | 82.21273 | 99.9385 |

**Figure 91** HPLC traces of compound **54**.

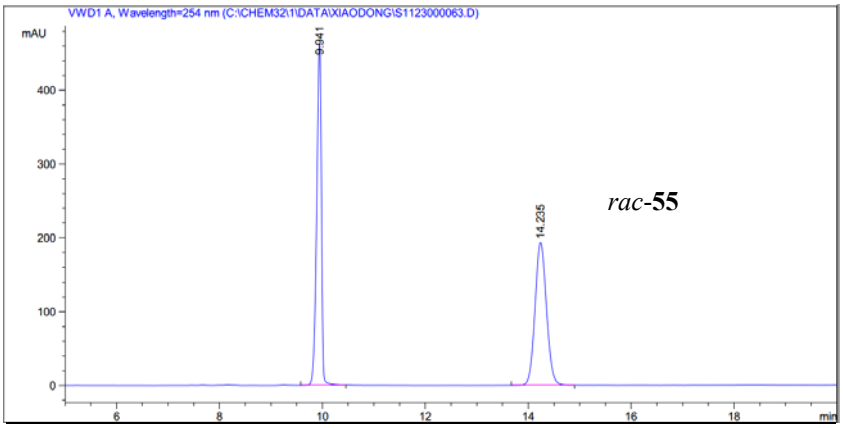


| Peak # | RetTime [min] | Type | Width [min] | Area [mAU*s] | Height [mAU] | Area % |
|---|---|---|---|---|---|---|
| 1 | 9.941 | BB | 0.0992 | 2960.62988 | 464.21027 | 49.7363 |
| 2 | 14.235 | VB | 0.2385 | 2992.02271 | 193.68895 | 50.2637 |

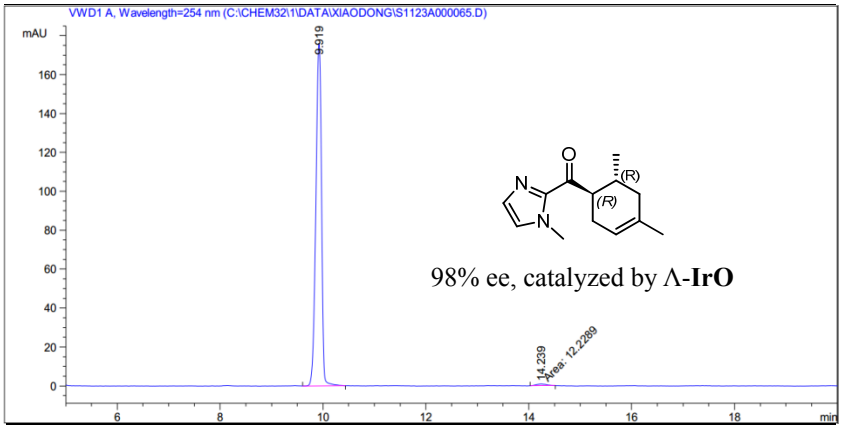


| Peak # | RetTime [min] | Type | Width [min] | Area [mAU*s] | Height [mAU] | Area % |
|---|---|---|---|---|---|---|
| 1 | 9.919 | VV | 0.1210 | 1344.09253 | 176.27159 | 99.0984 |
| 2 | 14.239 | MM | 0.2339 | 12.22889 | 8.71269e-1 | 0.9016 |

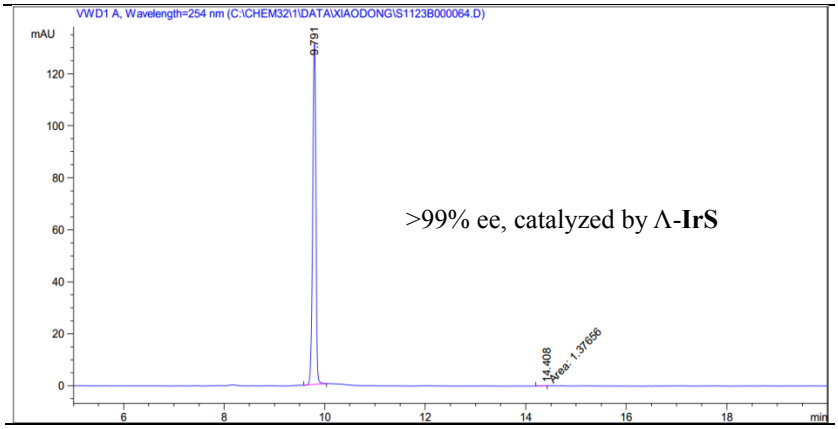


| Peak # | RetTime [min] | Type | Width [min] | Area [mAU*s] | Height [mAU] | Area % |
|---|---|---|---|---|---|---|
| 1 | 9.791 | BB | 0.0692 | 582.01080 | 131.38844 | 99.7640 |
| 2 | 14.408 | MM | 0.1505 | 1.37656 | 1.52444e-1 | 0.2360 |

**Figure 92** HPLC traces of compound **55**.

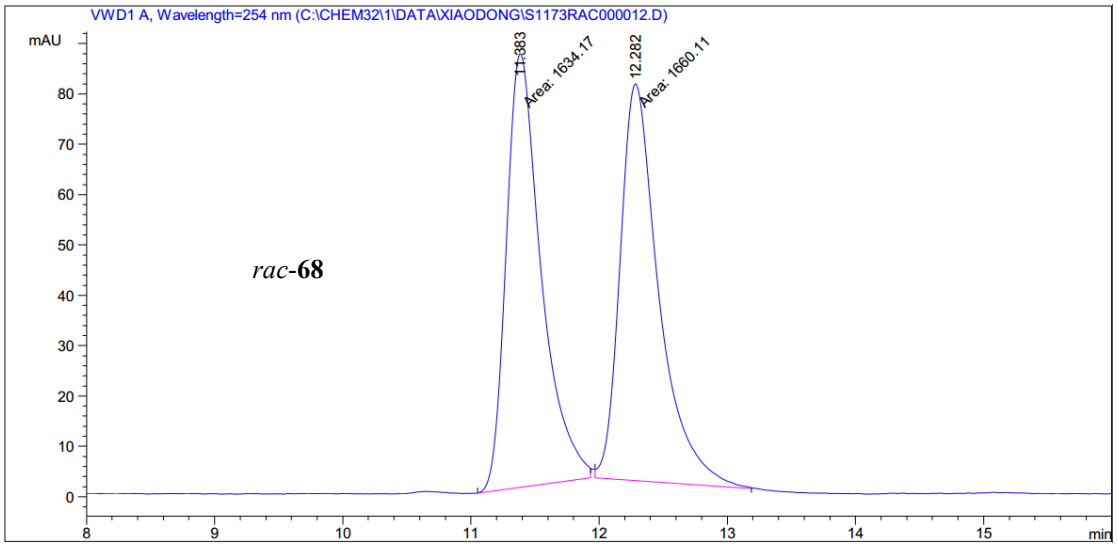


| Peak # | RetTime [min] | Type | Width [min] | Area [mAU*s] | Height [mAU] | Area % |
|---|---|---|---|---|---|---|
| 1 | 11.383 | MM | 0.3160 | 1634.16748 | 86.20078 | 49.6062 |
| 2 | 12.282 | MM | 0.3508 | 1660.11389 | 78.87221 | 50.3938 |

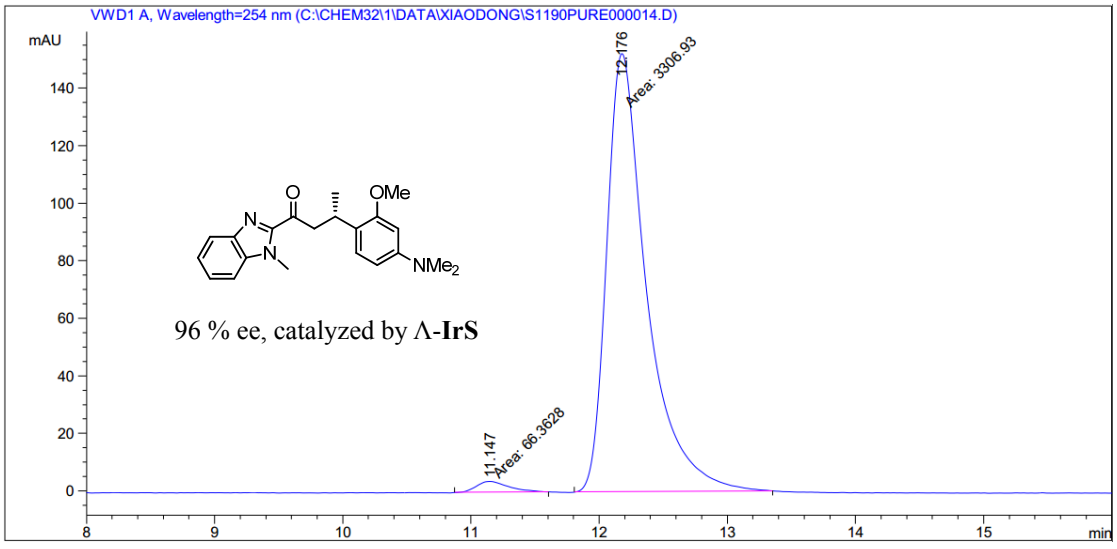


| Peak # | RetTime [min] | Type | Width [min] | Area [mAU*s] | Height [mAU] | Area % |
|---|---|---|---|---|---|---|
| 1 | 11.147 | MM | 0.2941 | 66.36278 | 3.76076 | 1.9673 |
| 2 | 12.176 | MM | 0.3618 | 3306.93433 | 152.34769 | 98.0327 |

**Figure 93** HPLC traces of compound **68**.

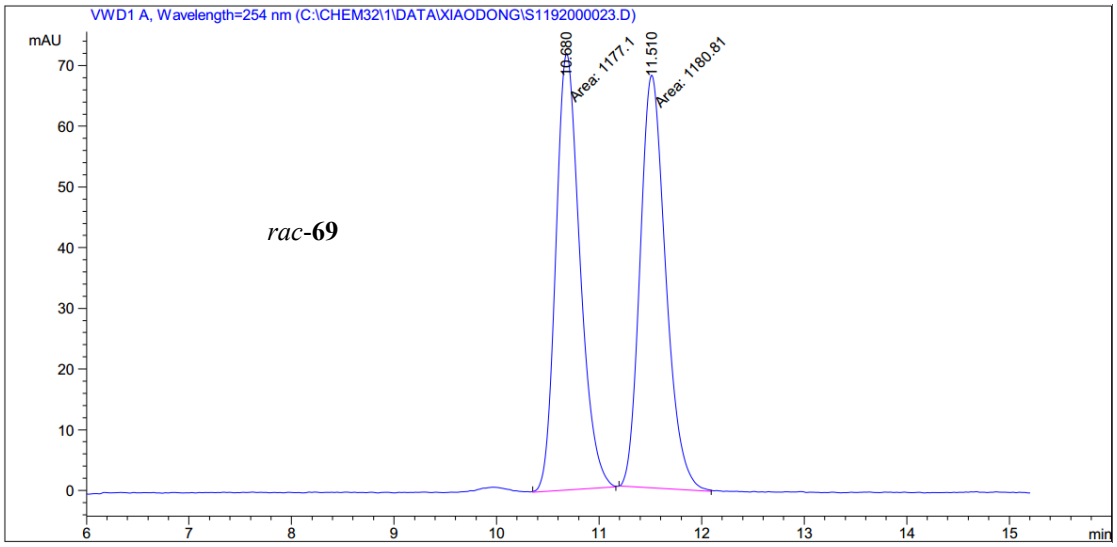


| Peak # | RetTime [min] | Type | Width [min] | Area [mAU*s] | Height [mAU] | Area % |
|---|---|---|---|---|---|---|
| 1 | 10.680 | MM | 0.2728 | 1177.10059 | 71.91488 | 49.9213 |
| 2 | 11.510 | MM | 0.2893 | 1180.81213 | 68.03181 | 50.0787 |

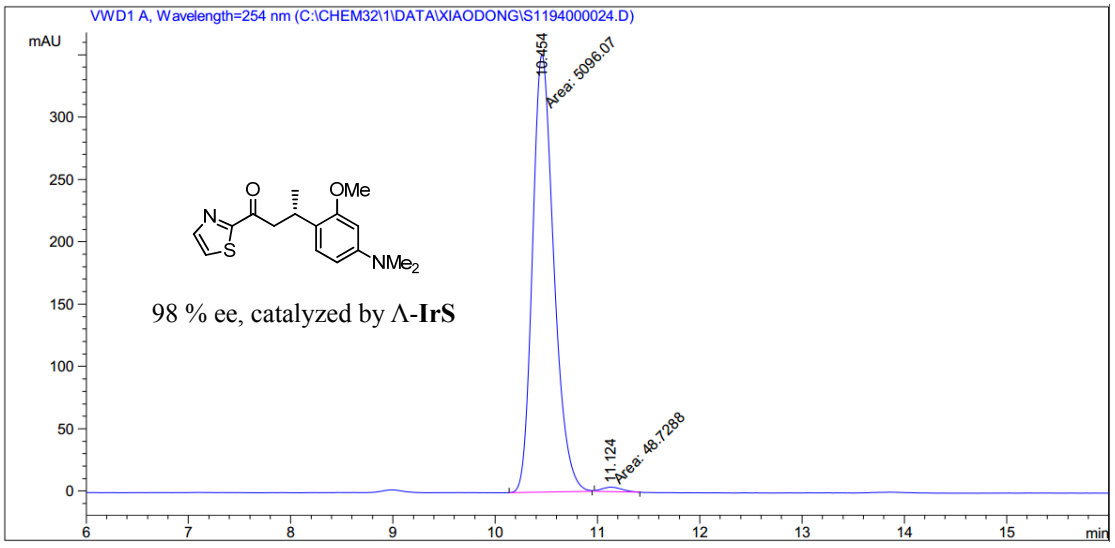


| Peak # | RetTime [min] | Type | Width [min] | Area [mAU*s] | Height [mAU] | Area % |
|---|---|---|---|---|---|---|
| 1 | 10.454 | MM | 0.2418 | 5096.07324 | 351.22644 | 99.0529 |
| 2 | 11.124 | MM | 0.2265 | 48.72881 | 3.58587 | 0.9471 |

**Figure 94** HPLC traces of compound **69**.

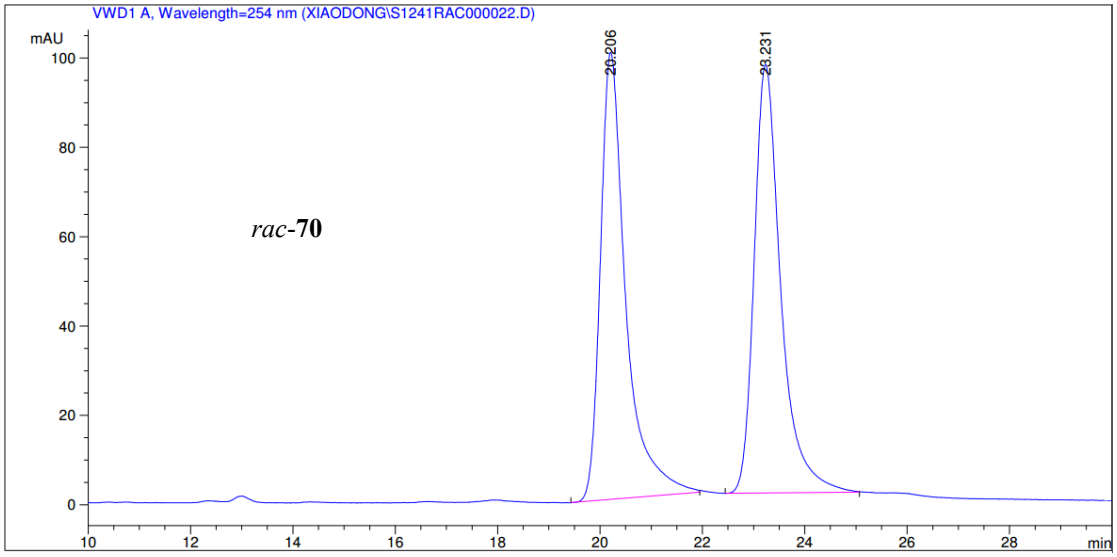


| Peak # | RetTime [min] | Type | Width [min] | Area [mAU*s] | Height [mAU] | Area % |
|---|---|---|---|---|---|---|
| 1 | 20.206 | BB | 0.5101 | 3451.11646 | 100.05773 | 49.8820 |
| 2 | 23.231 | BB | 0.5442 | 3467.44946 | 95.88226 | 50.1180 |

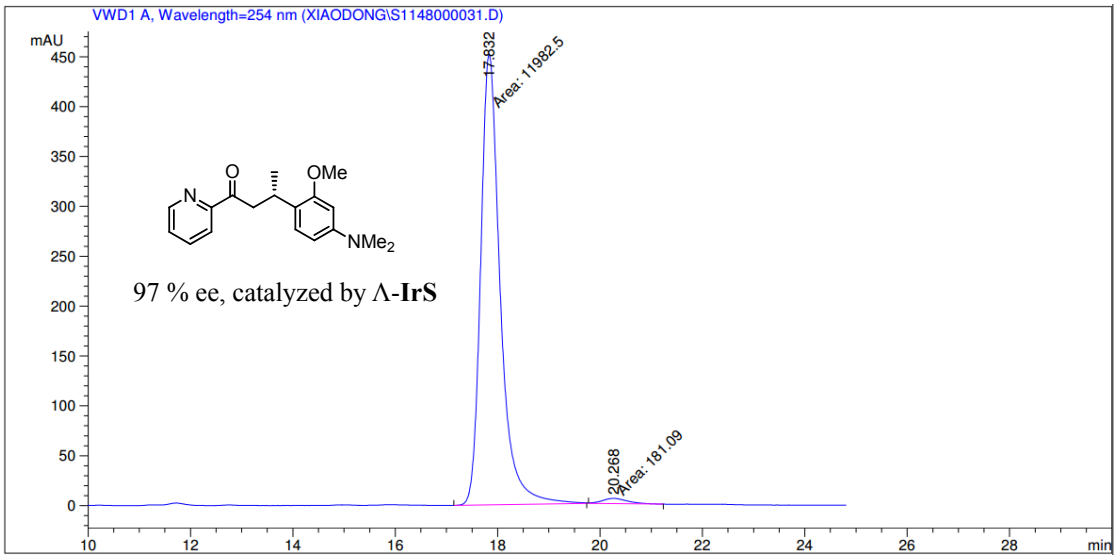


| Peak # | RetTime [min] | Type | Width [min] | Area [mAU*s] | Height [mAU] | Area % |
|---|---|---|---|---|---|---|
| 1 | 17.832 | MM | 0.4420 | 1.19825e4 | 451.84720 | 98.5112 |
| 2 | 20.268 | MM | 0.5743 | 181.09050 | 5.25510 | 1.4888 |

**Figure 95** HPLC traces of compound **70**.

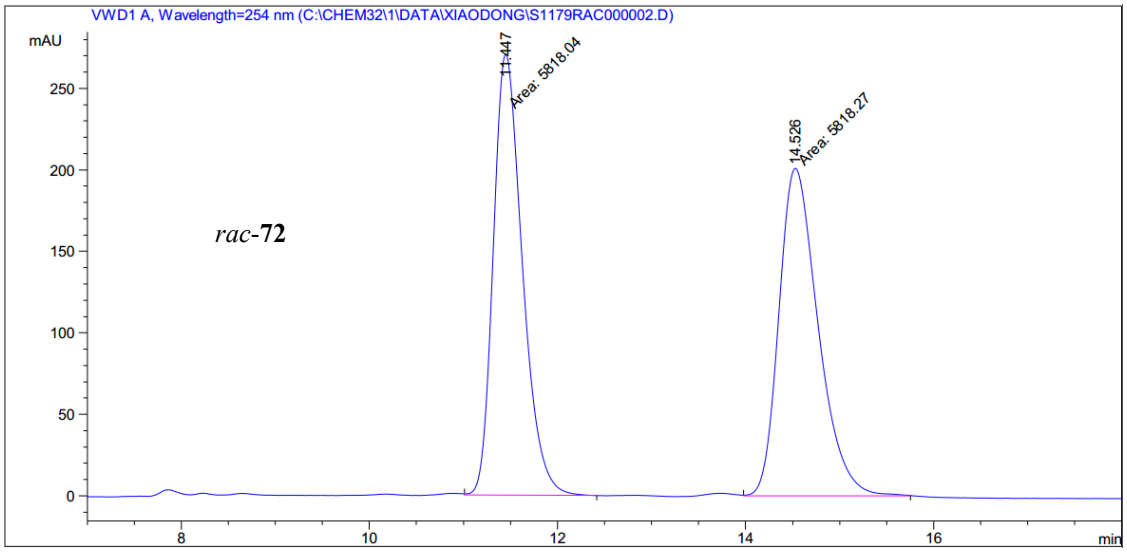


| Peak # | RetTime [min] | Type | Width [min] | Area [mAU*s] | Height [mAU] | Area % |
|---|---|---|---|---|---|---|
| 1 | 11.447 | MM | 0.3581 | 5818.03760 | 270.80154 | 49.9990 |
| 2 | 14.526 | MM | 0.4823 | 5818.27344 | 201.05034 | 50.0010 |

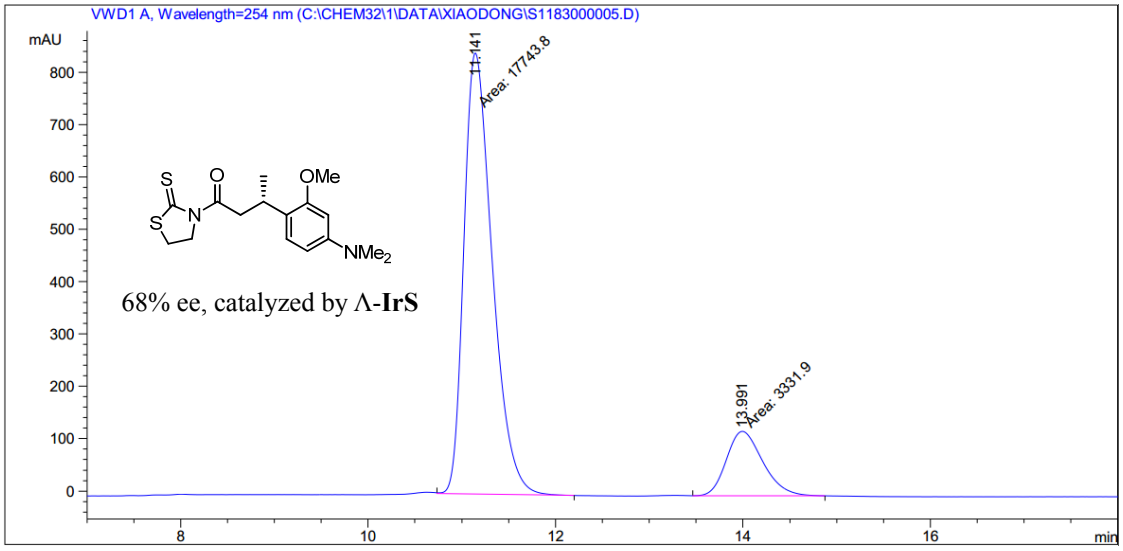


| Peak # | RetTime [min] | Type | Width [min] | Area [mAU*s] | Height [mAU] | Area % |
|---|---|---|---|---|---|---|
| 1 | 11.141 | MM | 0.3510 | 1.77438e4 | 842.64496 | 84.1908 |
| 2 | 13.991 | MM | 0.4508 | 3331.89551 | 123.17903 | 15.8092 |

**Figure 96** HPLC traces of compound **72**.

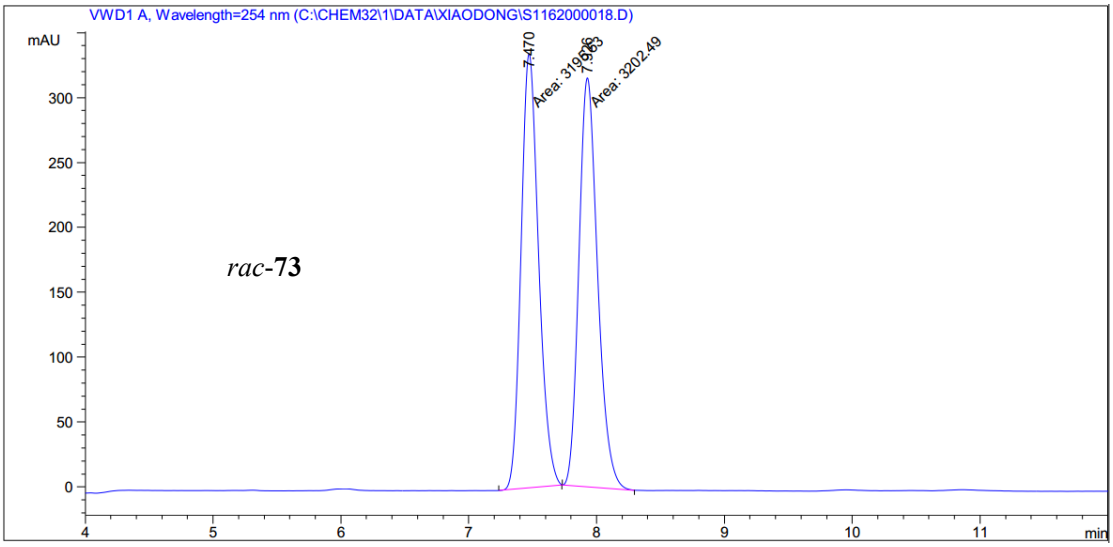


| Peak # | RetTime [min] | Type | Width [min] | Area [mAU*s] | Height [mAU] | Area % |
|---|---|---|---|---|---|---|
| 1 | 7.470 | MM | 0.1591 | 3195.52515 | 334.82138 | 49.9456 |
| 2 | 7.926 | MM | 0.1693 | 3202.48779 | 315.31531 | 50.0544 |

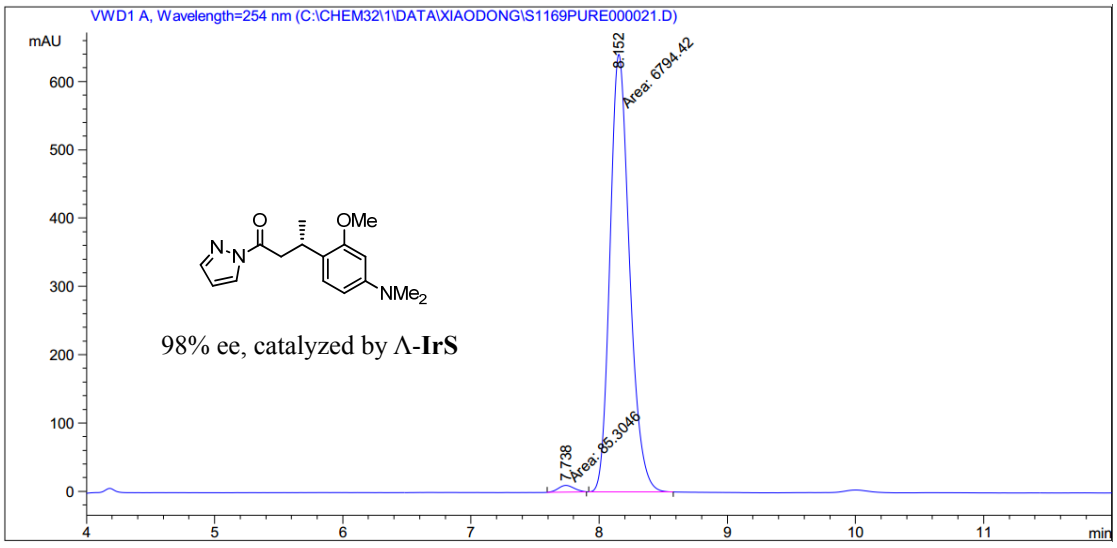


| Peak # | RetTime [min] | Type | Width [min] | Area [mAU*s] | Height [mAU] | Area % |
|---|---|---|---|---|---|---|
| 1 | 7.738 | MM | 0.1440 | 85.30462 | 9.87063 | 1.2399 |
| 2 | 8.152 | MM | 0.1767 | 6794.42139 | 640.84668 | 98.7601 |

**Figure 97** HPLC traces of compound **73**.

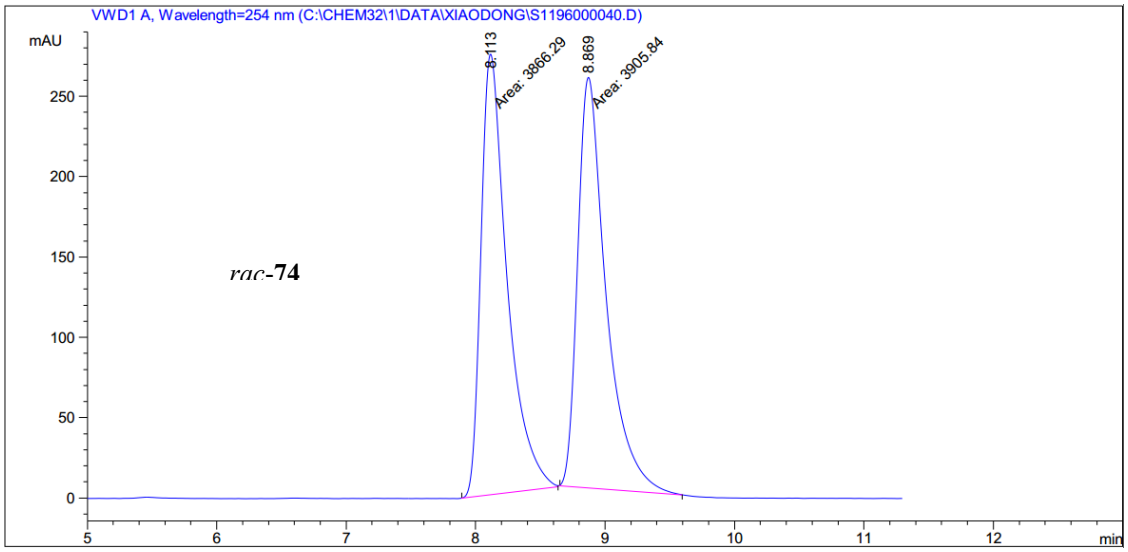


| Peak # | RetTime [min] | Type | Width [min] | Area [mAU*s] | Height [mAU] | Area % |
|---|---|---|---|---|---|---|
| 1 | 8.113 | MM | 0.2348 | 3866.28516 | 274.44803 | 49.7455 |
| 2 | 8.869 | MM | 0.2546 | 3905.83838 | 255.70940 | 50.2545 |

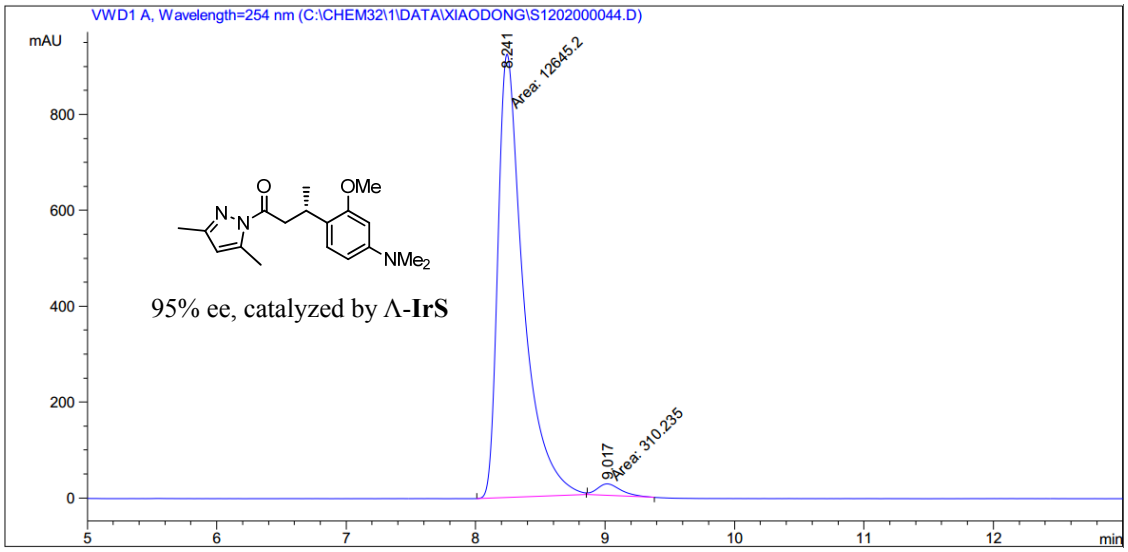


| Peak # | RetTime [min] | Type | Width [min] | Area [mAU*s] | Height [mAU] | Area % |
|---|---|---|---|---|---|---|
| 1 | 8.241 | MM | 0.2278 | 1.26452e4 | 925.19641 | 97.6054 |
| 2 | 9.017 | MM | 0.2138 | 310.23495 | 24.18731 | 2.3946 |

**Figure 98** HPLC traces of compound **74**.

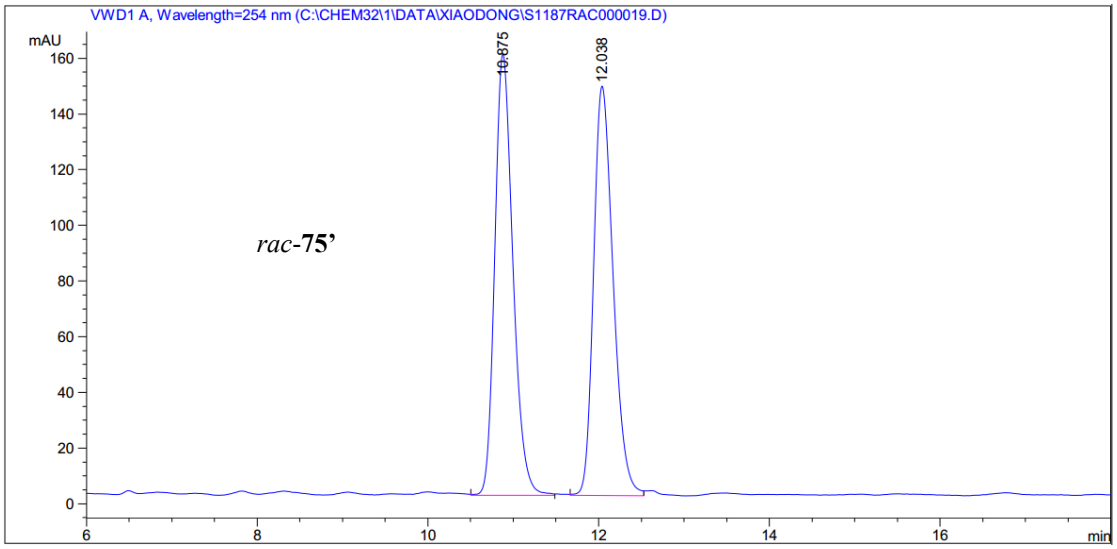


| Peak # | RetTime [min] | Type | Width [min] | Area [mAU*s] | Height [mAU] | Area % |
|---|---|---|---|---|---|---|
| 1 | 10.875 | VV | 0.2265 | 2348.59058 | 158.69167 | 50.0467 |
| 2 | 12.038 | BV | 0.2456 | 2344.21094 | 147.09657 | 49.9533 |

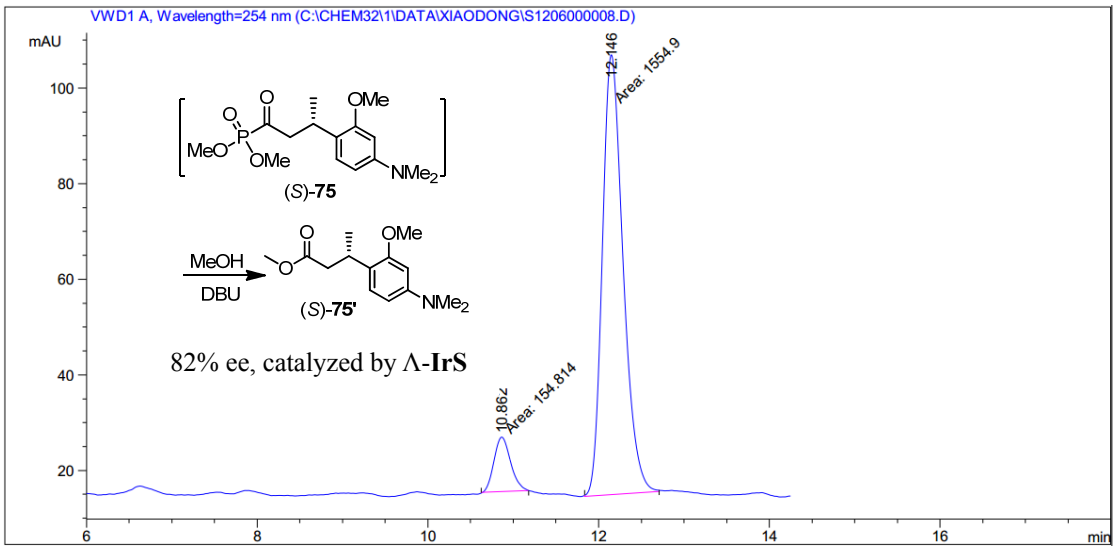


| Peak # | RetTime [min] | Type | Width [min] | Area [mAU*s] | Height [mAU] | Area % |
|---|---|---|---|---|---|---|
| 1 | 10.862 | MM | 0.2258 | 154.81367 | 11.42458 | 9.0550 |
| 2 | 12.146 | MM | 0.2815 | 1554.89880 | 92.06667 | 90.9450 |

**Figure 99** HPLC traces of compound **75'**.

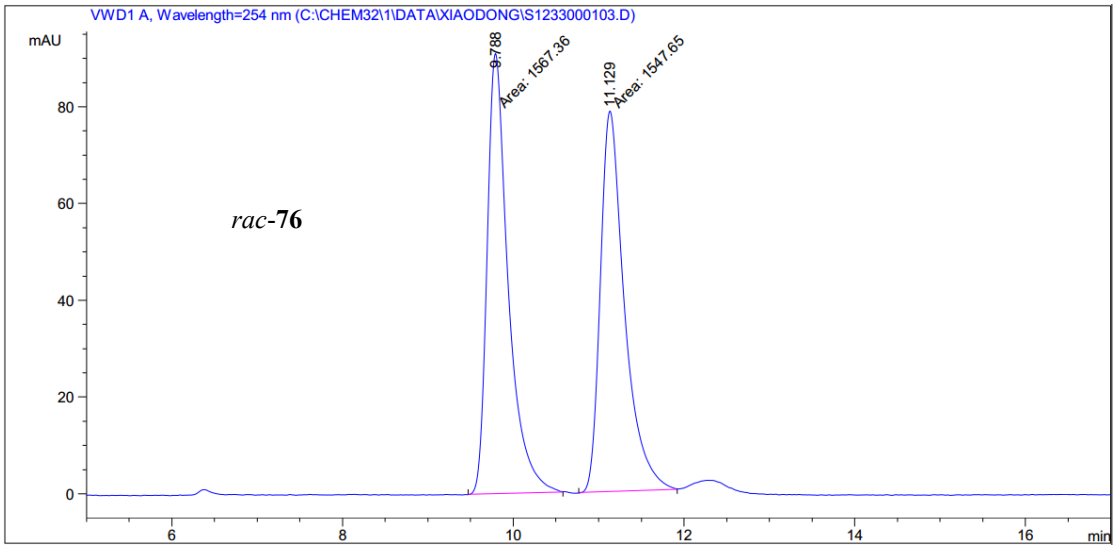


| Peak # | RetTime [min] | Type | Width [min] | Area [mAU*s] | Height [mAU] | Area % |
|---|---|---|---|---|---|---|
| 1 | 9.788 | MM | 0.2870 | 1567.36194 | 91.00428 | 50.3164 |
| 2 | 11.129 | MM | 0.3279 | 1547.64978 | 78.67178 | 49.6836 |

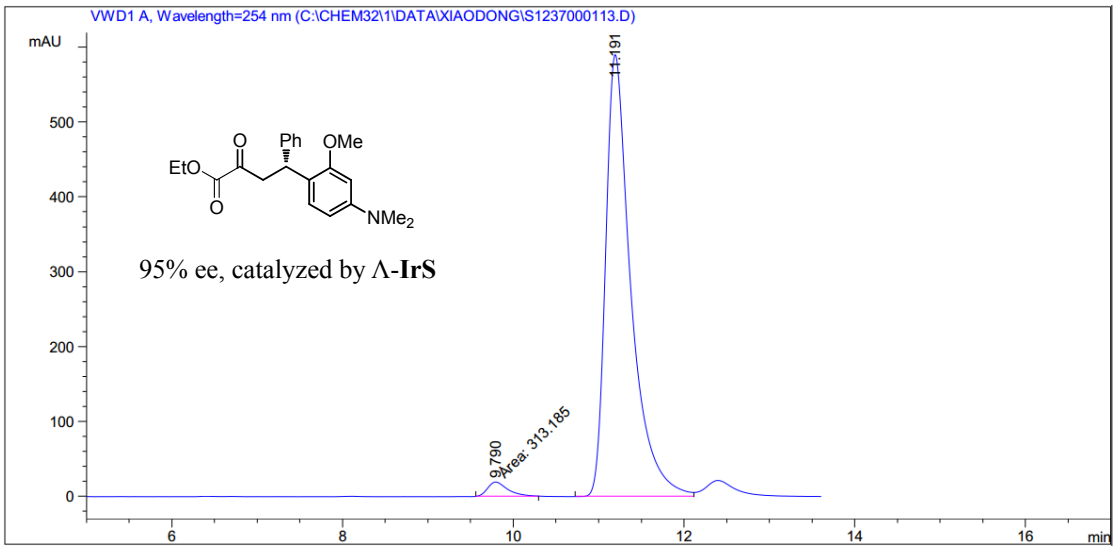


| Peak # | RetTime [min] | Type | Width [min] | Area [mAU*s] | Height [mAU] | Area % |
|---|---|---|---|---|---|---|
| 1 | 9.790 | MM | 0.2735 | 313.18546 | 19.08332 | 2.5121 |
| 2 | 11.191 | VV | 0.3040 | 1.21538e4 | 590.927998 | 97.4879 |

**Figure 100** HPLC traces of compound **76**.

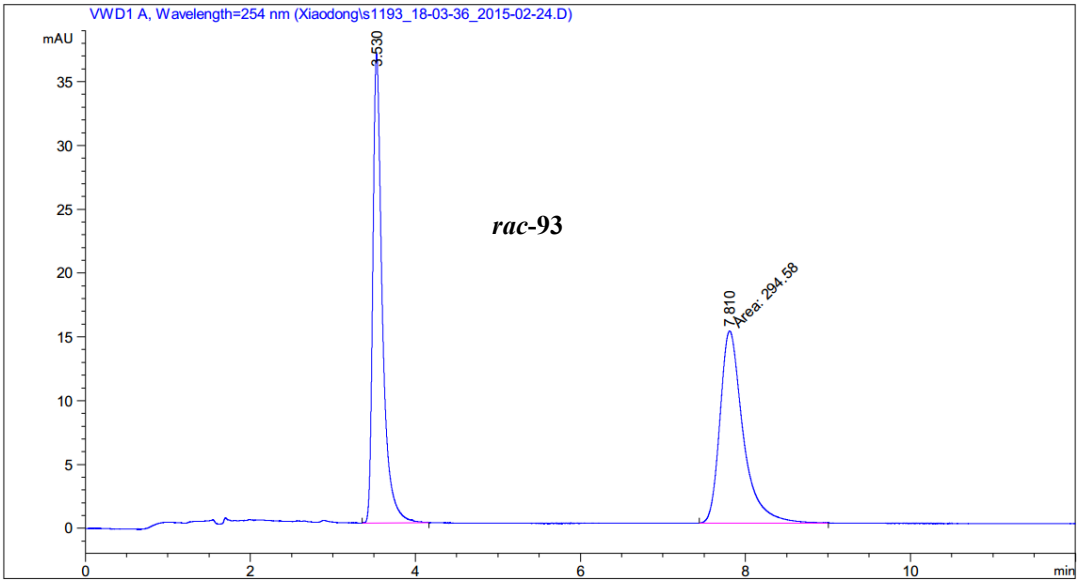


| Peak # | RetTime [min] | Type | Width [min] | Area [mAU*s] | Height [mAU] | Area % |
|---|---|---|---|---|---|---|
| 1 | 3.530 | BV R | 0.1181 | 294.79529 | 36.76015 | 50.0183 |
| 2 | 7.810 | MM | 0.3256 | 294.57977 | 15.07985 | 49.9817 |

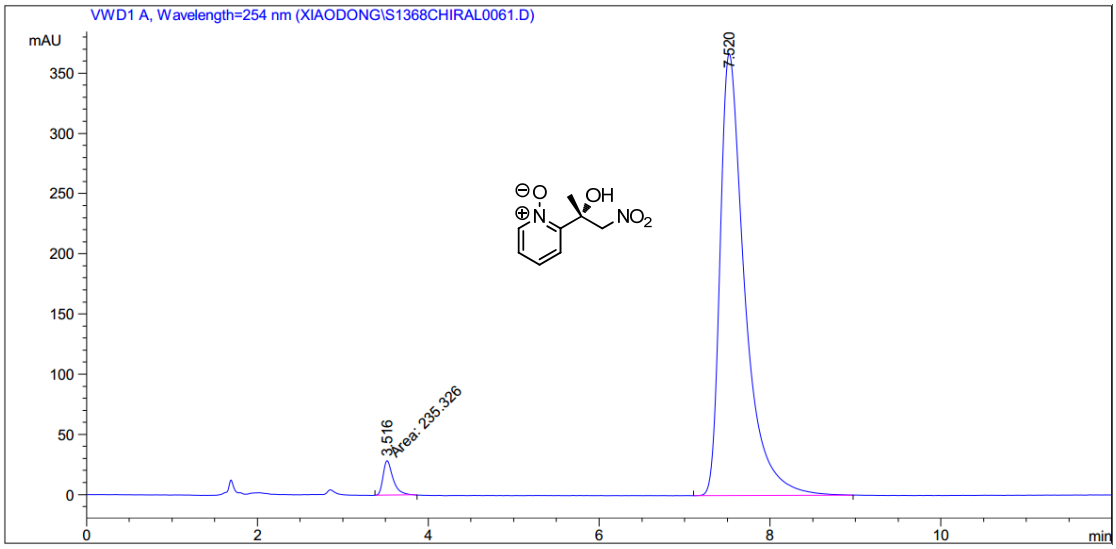


| Peak # | RetTime [min] | Type | Width [min] | Area [mAU*s] | Height [mAU] | Area % |
|---|---|---|---|---|---|---|
| 1 | 3.516 | MM | 0.1367 | 235.32608 | 28.69759 | 3.0954 |
| 2 | 7.520 | VV | 0.2981 | 7367.01807 | 367.17926 | 96.9046 |

**Figure 101** HPLC traces of compound **93**.

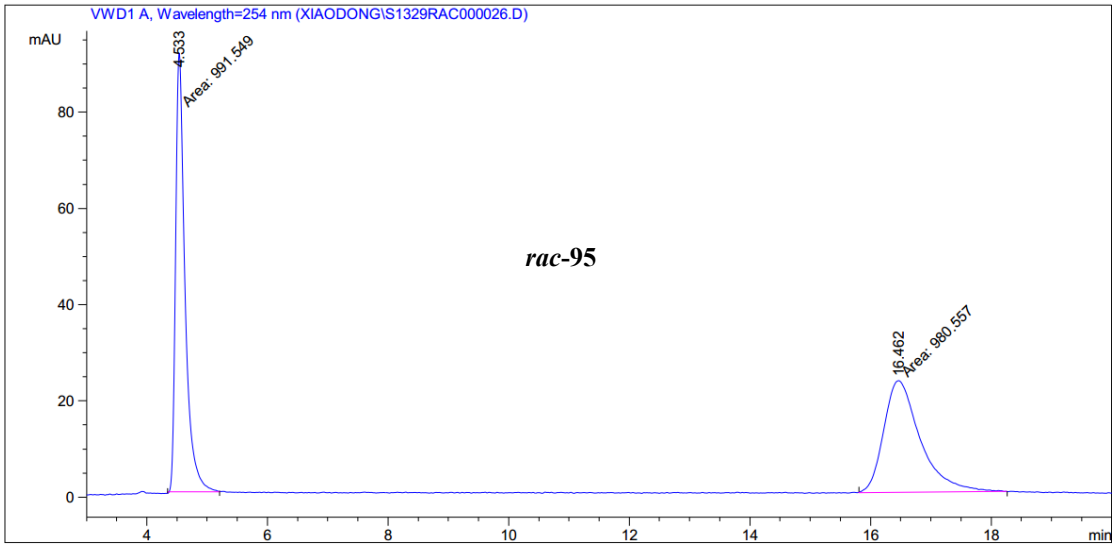


| Peak # | RetTime [min] | Type | Width [min] | Area [mAU*s] | Height [mAU] | Area % |
|---|---|---|---|---|---|---|
| 1 | 4.533 | MM | 0.1811 | 991.54883 | 91.25725 | 50.2787 |
| 2 | 16.462 | MM | 0.7036 | 980.55707 | 23.22625 | 49.7212 |

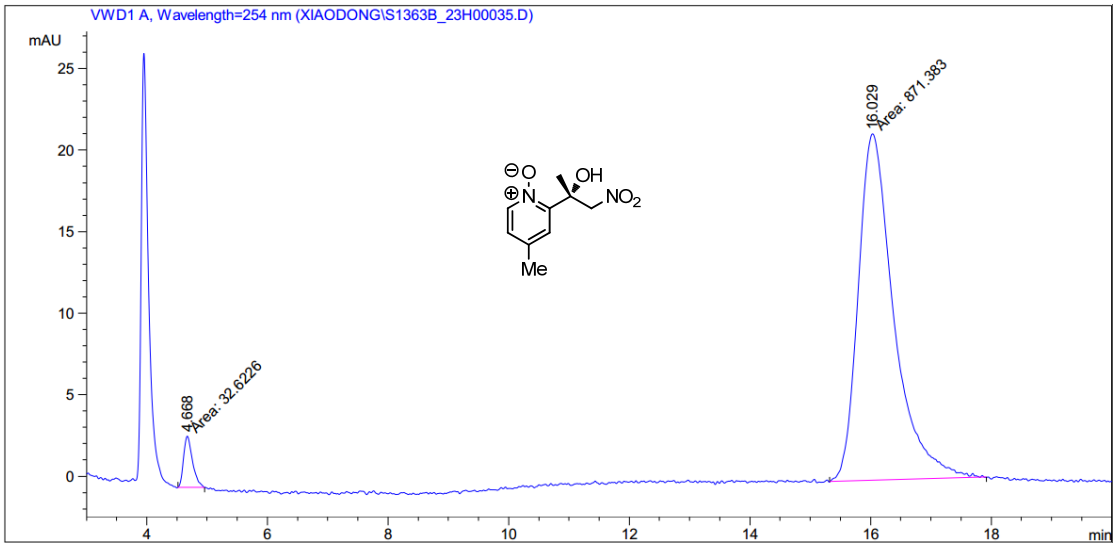


| Peak # | RetTime [min] | Type | Width [min] | Area [mAU*s] | Height [mAU] | Area % |
|---|---|---|---|---|---|---|
| 1 | 4.668 | MM | 0.1729 | 32.62260 | 3.14398 | 3.6087 |
| 2 | 16.029 | MM | 0.6833 | 871.38306 | 21.25500 | 96.3913 |

**Figure 102** HPLC traces of compound **95**.

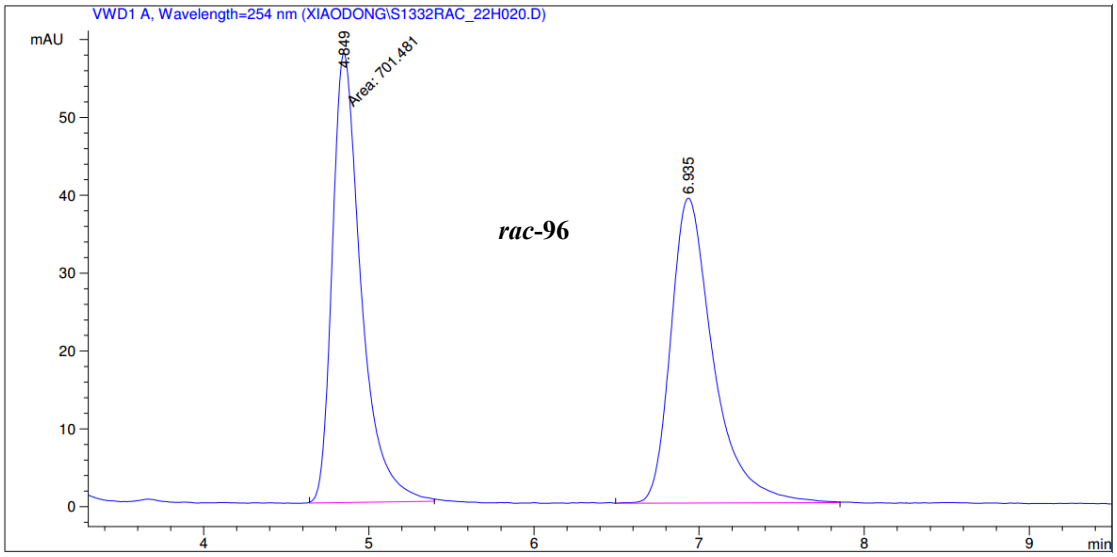


| Peak # | RetTime [min] | Type | Width [min] | Area [mAU*s] | Height [mAU] | Area % |
|---|---|---|---|---|---|---|
| 1 | 4.849 | MM | 0.2026 | 701.48132 | 57.71691 | 50.0611 |
| 2 | 6.935 | VB | 0.2667 | 699.76807 | 39.17224 | 49.9389 |

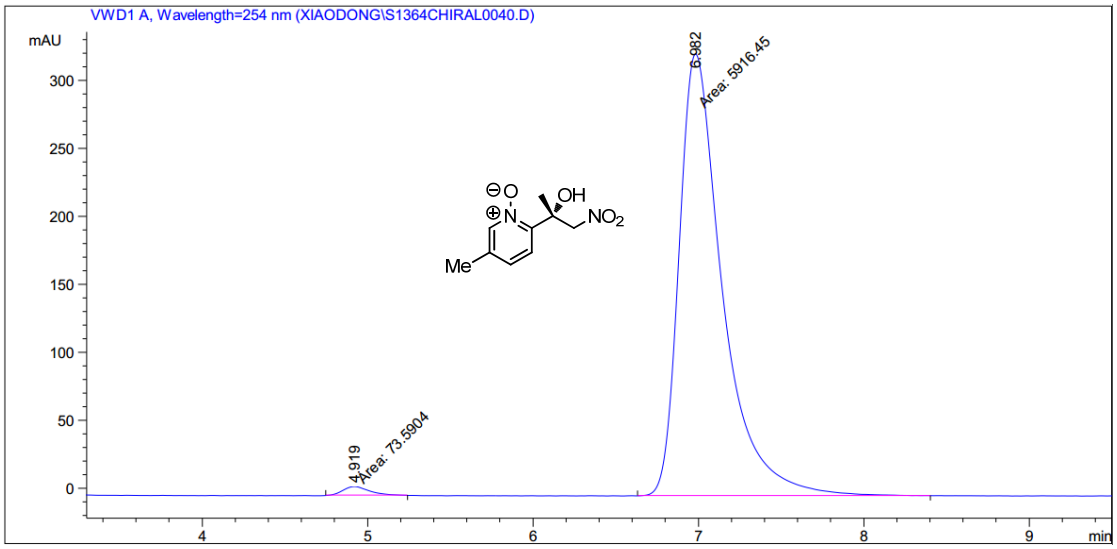


| Peak # | RetTime [min] | Type | Width [min] | Area [mAU*s] | Height [mAU] | Area % |
|---|---|---|---|---|---|---|
| 1 | 4.919 | MM | 0.1873 | 73.59045 | 6.54898 | 1.2285 |
| 2 | 6.982 | MM | 0.3033 | 5916.45020 | 325.07684 | 98.7715 |

**Figure 103** HPLC traces of compound **96**.

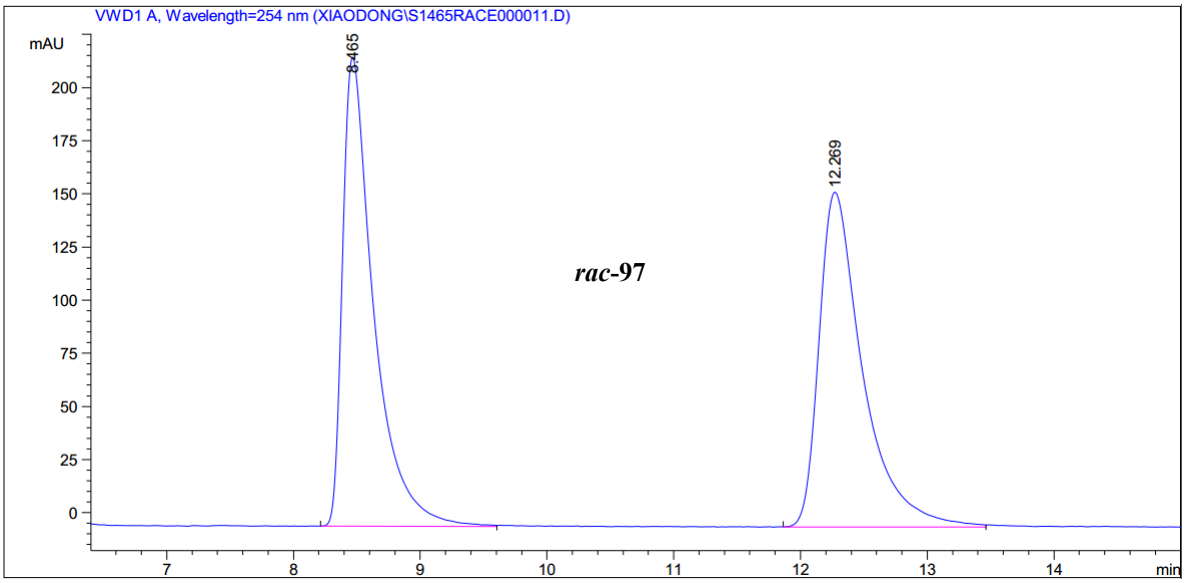


| Peak # | RetTime [min] | Type | Width [min] | Area [mAU*s] | Height [mAU] | Area % |
|---|---|---|---|---|---|---|
| 1 | 8.465 | BV | 0.2508 | 3781.31006 | 220.72137 | 50.0392 |
| 2 | 12.269 | VV | 0.3523 | 3775.39282 | 157.58440 | 49.9608 |

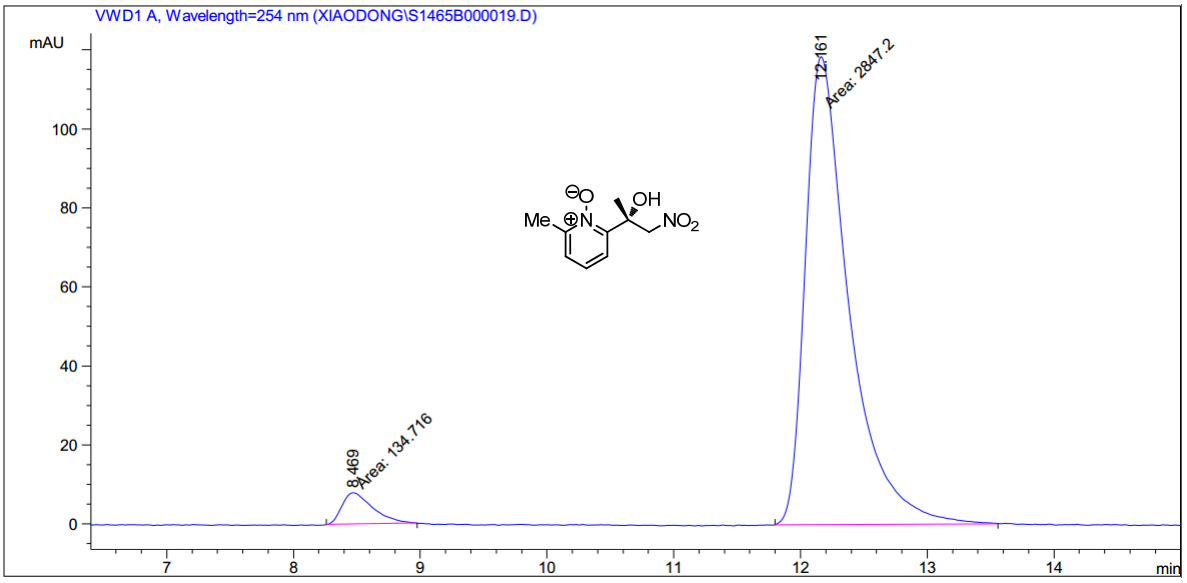


| Peak # | RetTime [min] | Type | Width [min] | Area [mAU*s] | Height [mAU] | Area % |
|---|---|---|---|---|---|---|
| 1 | 8.4679 | MM | 0.2825 | 134.71611 | 7.94660 | 4.5178 |
| 2 | 12.161 | MM | 0.4007 | 2847.20312 | 118.43519 | 95.4822 |

**Figure 104** HPLC traces of compound **97**.

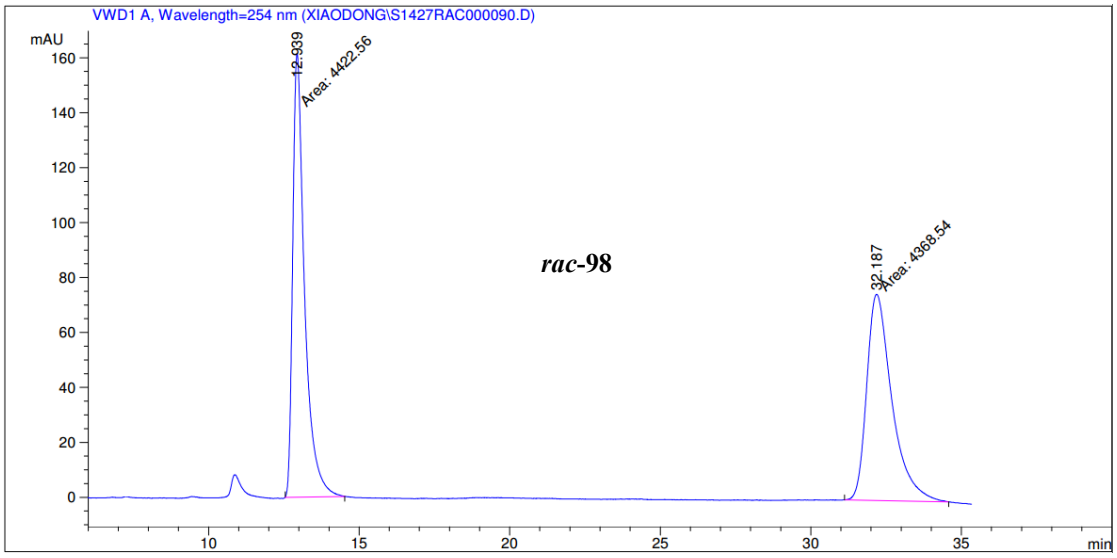


| Peak # | RetTime [min] | Type | Width [min] | Area [mAU*s] | Height [mAU] | Area % |
|---|---|---|---|---|---|---|
| 1 | 12.939 | MM | 0.4565 | 4422.56006 | 161.47766 | 50.3072 |
| 2 | 32.287 | MM | 0.9702 | 4368.54346 | 75.04665 | 49.6928 |

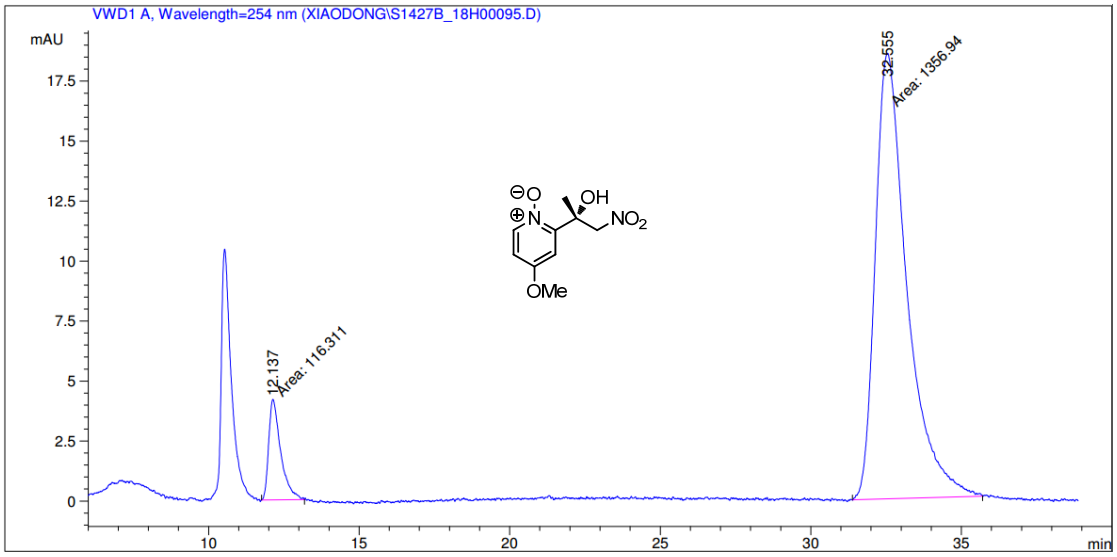


| Peak # | RetTime [min] | Type | Width [min] | Area [mAU*s] | Height [mAU] | Area % |
|---|---|---|---|---|---|---|
| 1 | 12.137 | MM | 0.4627 | 116.31055 | 4.18928 | 7.8948 |
| 2 | 32.555 | MM | 1.2179 | 1356.94080 | 18.57006 | 92.1052 |

**Figure 105** HPLC traces of compound **98**.

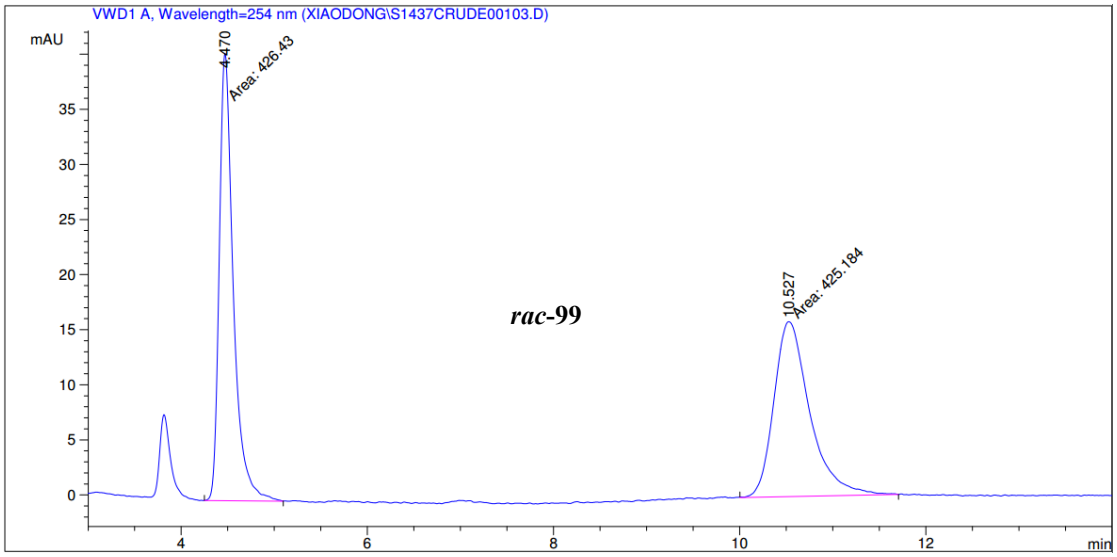


| Peak # | RetTime [min] | Type | Width [min] | Area [mAU*s] | Height [mAU] | Area % |
|---|---|---|---|---|---|---|
| 1 | 4.470 | MM | 0.1750 | 426.42999 | 40.61774 | 50.0731 |
| 2 | 10.527 | MM | 0.4465 | 425.18411 | 15.87054 | 49.9269 |

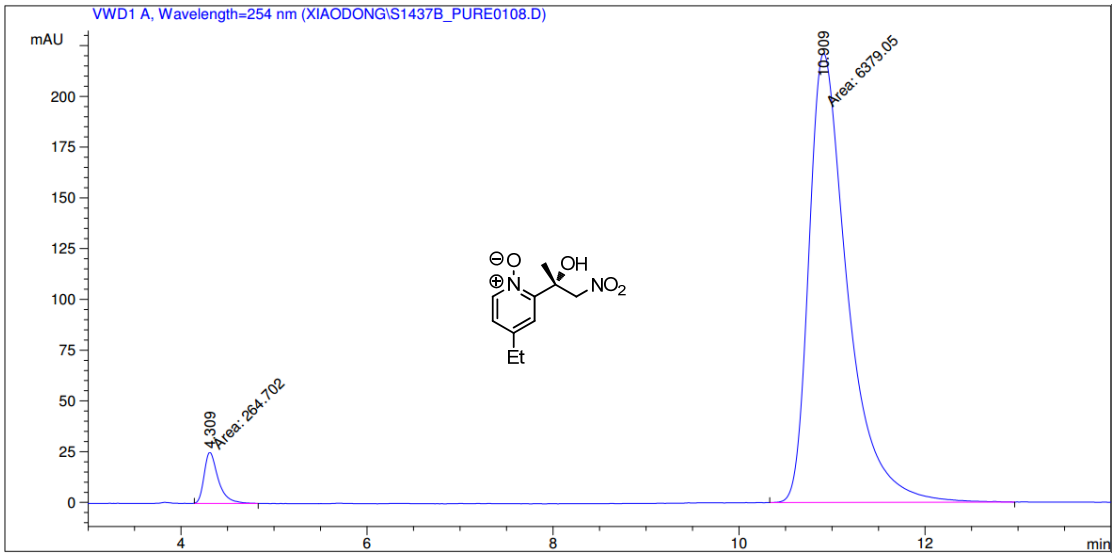


| Peak # | RetTime [min] | Type | Width [min] | Area [mAU*s] | Height [mAU] | Area % |
|---|---|---|---|---|---|---|
| 1 | 4.309 | MM | 0.1753 | 264.70172 | 25.15998 | 3.9842 |
| 2 | 10.909 | MM | 0.4805 | 6379.04590 | 221.24951 | 96.0158 |

**Figure 106** HPLC traces of compound **99**.

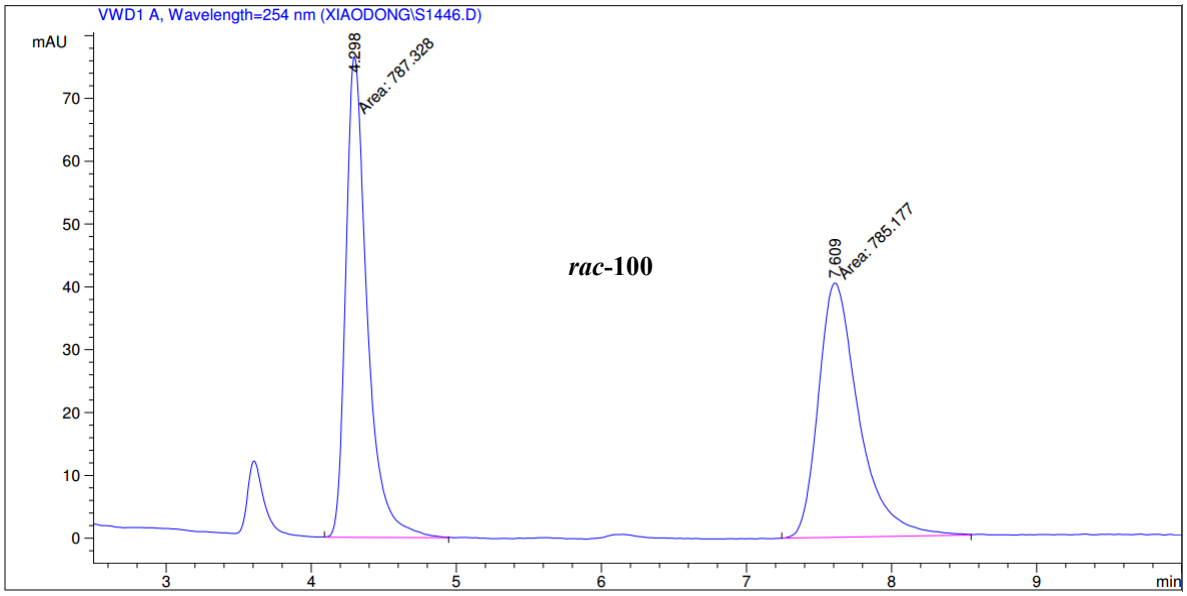


| Peak # | RetTime [min] | Type | Width [min] | Area [mAU*s] | Height [mAU] | Area % |
|---|---|---|---|---|---|---|
| 1 | 4.298 | MM | 0.1713 | 787.32776 | 76.60849 | 50.0684 |
| 2 | 7.609 | MM | 0.3232 | 785.17664 | 40.48538 | 49.9316 |

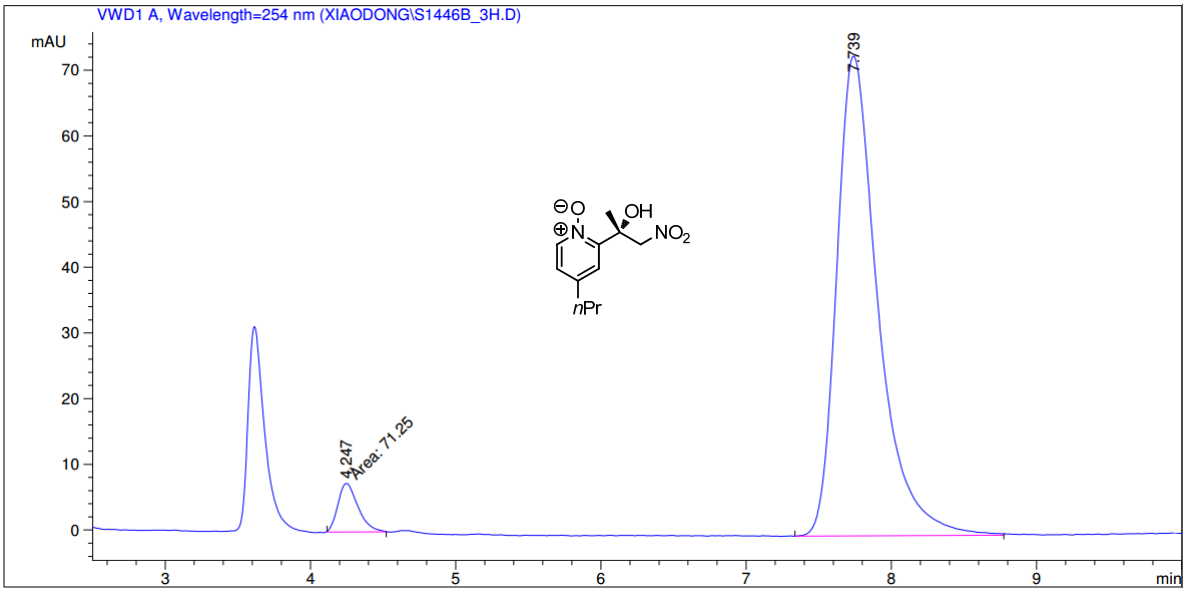


| Peak # | RetTime [min] | Type | Width [min] | Area [mAU*s] | Height [mAU] | Area % |
|---|---|---|---|---|---|---|
| 1 | 4.247 | MM | 0.1602 | 71.24998 | 7.41123 | 4.6982 |
| 2 | 7.729 | VB | 0.2978 | 1445.28589 | 73.04000 | 95.3018 |

**Figure 107** HPLC traces of compound **100**.

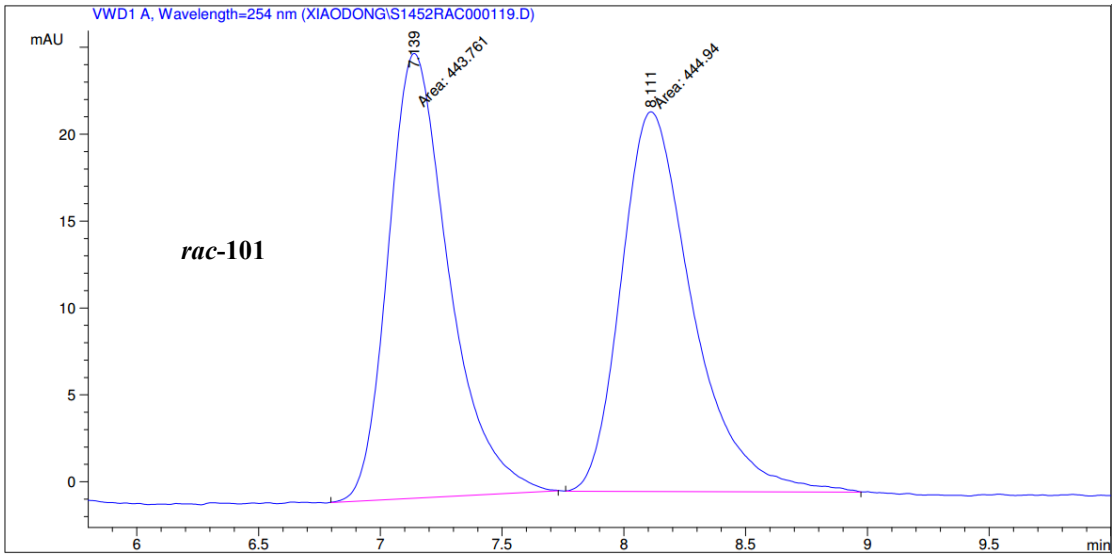


| Peak # | RetTime [min] | Type | Width [min] | Area [mAU*s] | Height [mAU] | Area % |
|---|---|---|---|---|---|---|
| 1 | 7.139 | MM | 0.2888 | 443.76120 | 25.60535 | 49.9337 |
| 2 | 8.111 | MM | 0.3393 | 444.94006 | 21.85354 | 50.0663 |

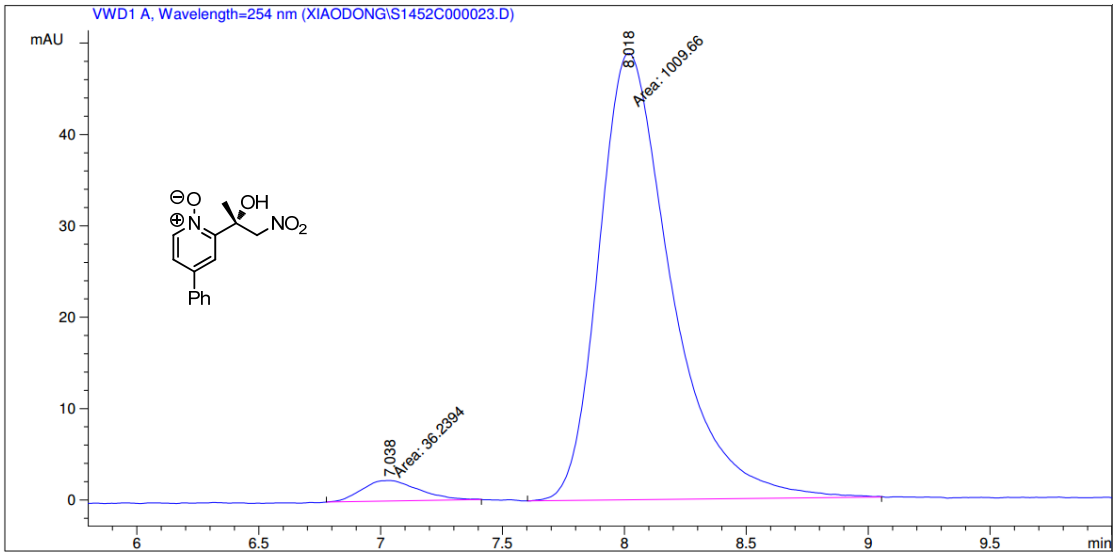


| Peak # | RetTime [min] | Type | Width [min] | Area [mAU*s] | Height [mAU] | Area % |
|---|---|---|---|---|---|---|
| 1 | 7.038 | MM | 0.2034 | 36.23938 | 2.23299 | 3.4649 |
| 2 | 8.018 | MM | 0.3441 | 1009.65521 | 48.90327 | 96.5351 |

**Figure 108** HPLC traces of compound **101**.

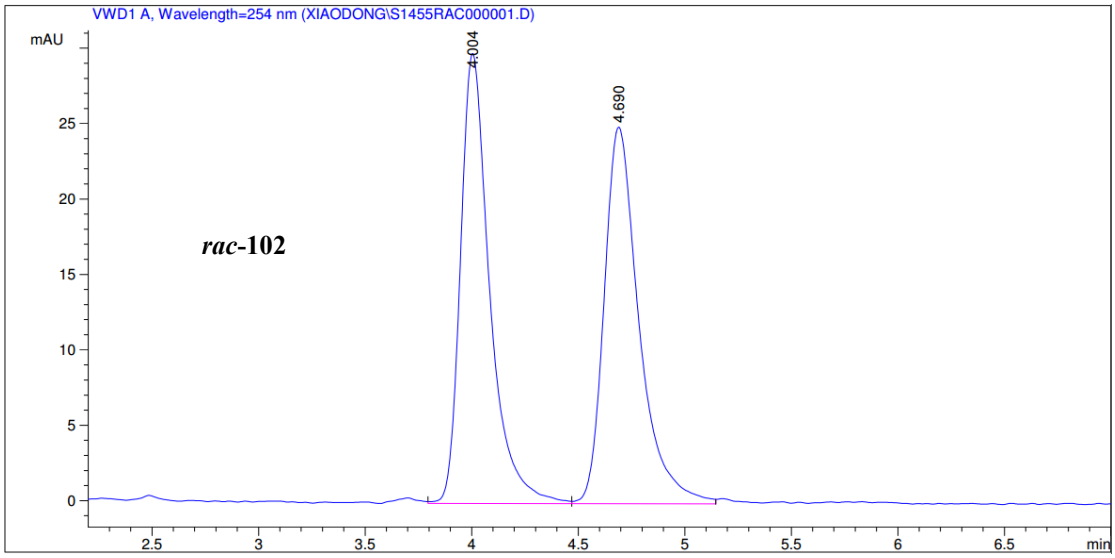


| Peak # | RetTime [min] | Type | Width [min] | Area [mAU*s] | Height [mAU] | Area % |
|---|---|---|---|---|---|---|
| 1 | 4.004 | VV | 0.1432 | 284.57932 | 29.85935 | 50.0020 |
| 2 | 4.690 | VV | 0.1722 | 284.55698 | 2498279 | 49.9980 |

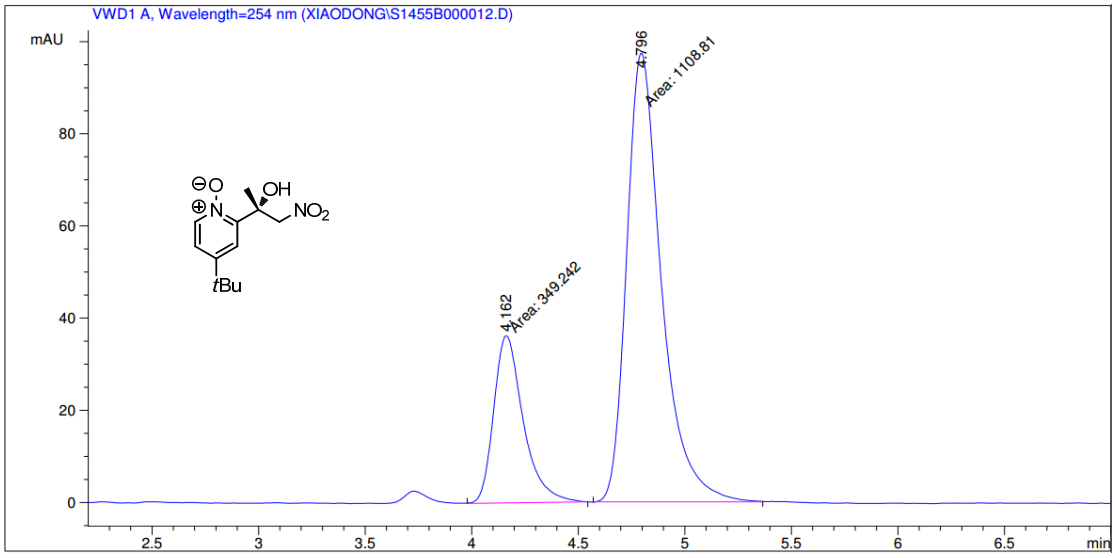


| Peak # | RetTime [min] | Type | Width [min] | Area [mAU*s] | Height [mAU] | Area % |
|---|---|---|---|---|---|---|
| 1 | 4.162 | MM | 0.1603 | 349.24155 | 36.31213 | 23.9526 |
| 2 | 4.796 | MM | 0.1897 | 1108.81396 | 97.44277 | 76.0474 |

**Figure 109** HPLC traces of compound **102**.

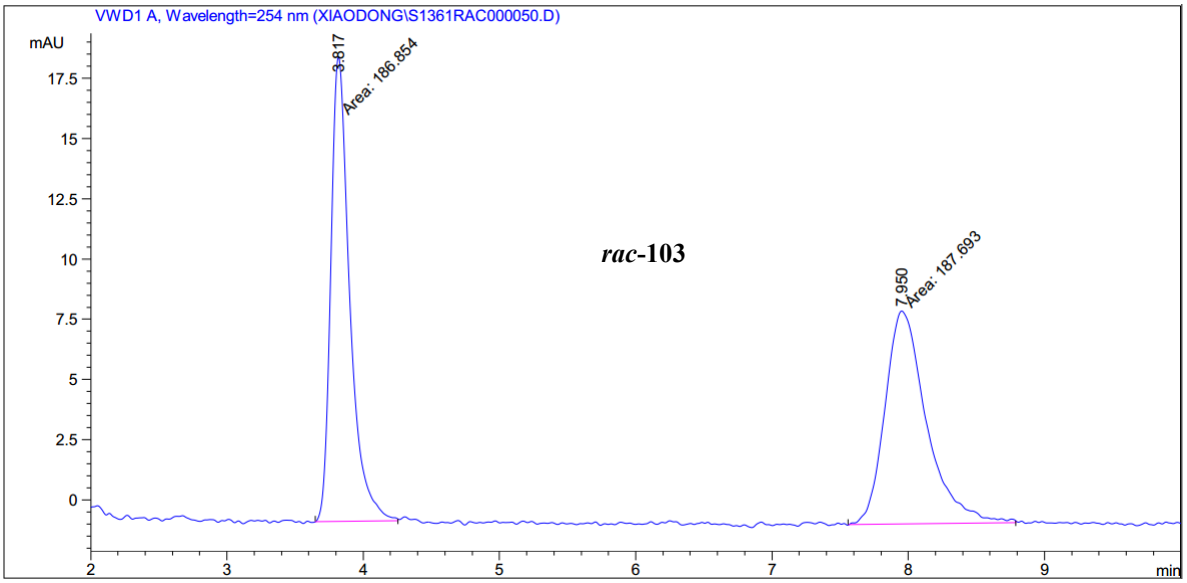


| Peak # | RetTime [min] | Type | Width [min] | Area [mAU*s] | Height [mAU] | Area % |
|---|---|---|---|---|---|---|
| 1 | 3.817 | MM | 0.1613 | 186.85374 | 19.31141 | 49.8880 |
| 2 | 7.950 | MM | 0.3537 | 187.69276 | 8.84525 | 50.1120 |

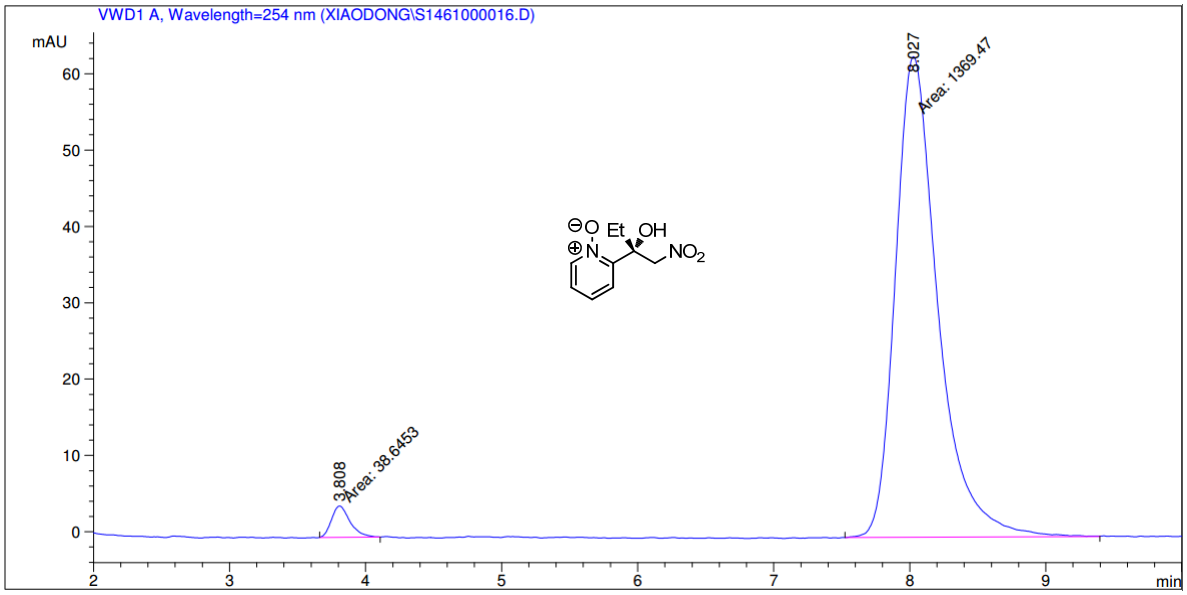


| Peak # | RetTime [min] | Type | Width [min] | Area [mAU*s] | Height [mAU] | Area % |
|---|---|---|---|---|---|---|
| 1 | 3.808 | MM | 0.1571 | 38.64534 | 4.09947 | 2.7445 |
| 2 | 8.027 | MM | 0.3626 | 1369.46814 | 62.95115 | 97.2555 |

**Figure 110** HPLC traces of compound **103**.

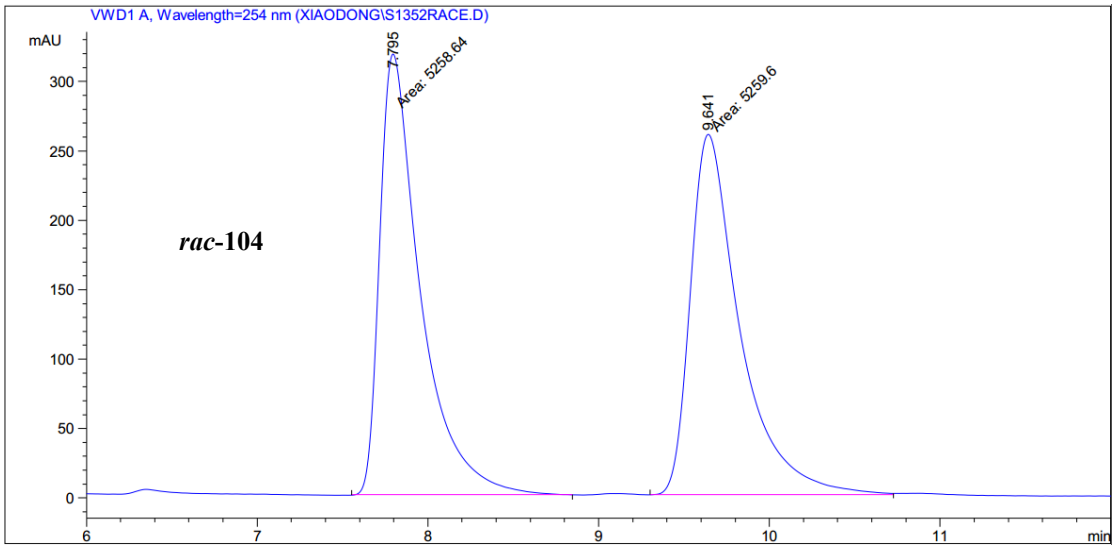


| Peak # | RetTime [min] | Type | Width [min] | Area [mAU*s] | Height [mAU] | Area % |
|---|---|---|---|---|---|---|
| 1 | 7.795 | MM | 0.2759 | 5258.63623 | 317.66507 | 49.9954 |
| 2 | 9.641 | MM | 0.3376 | 5259.60400 | 259.68253 | 50.0046 |

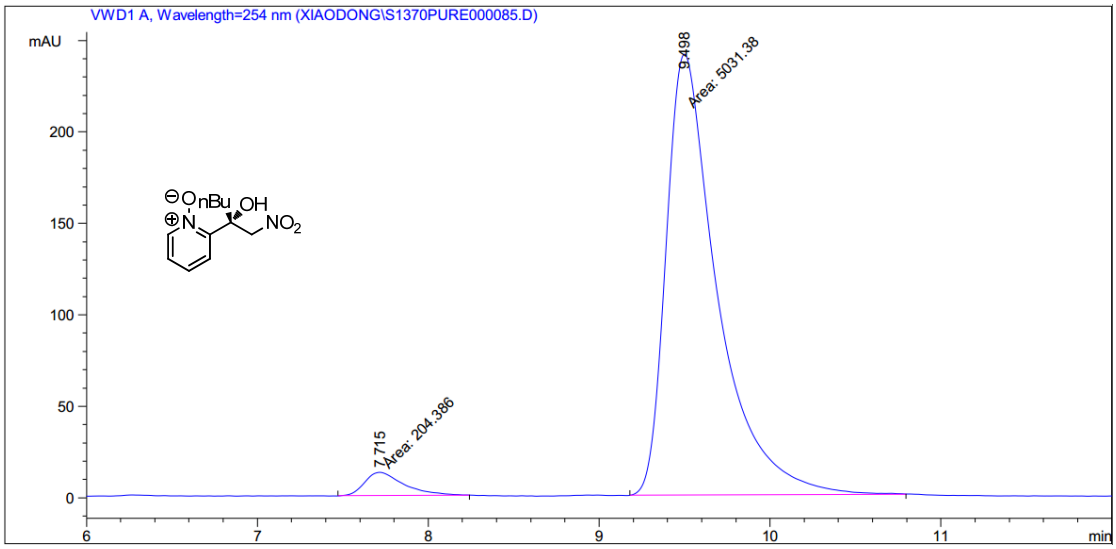


| Peak # | RetTime [min] | Type | Width [min] | Area [mAU*s] | Height [mAU] | Area % |
|---|---|---|---|---|---|---|
| 1 | 7.715 | MM | 0.2669 | 204.38618 | 12.76480 | 3.9037 |
| 2 | 9.498 | MM | 0.3478 | 5031.38428 | 241.11876 | 96.0963 |

**Figure 111** HPLC traces of compound **104**.

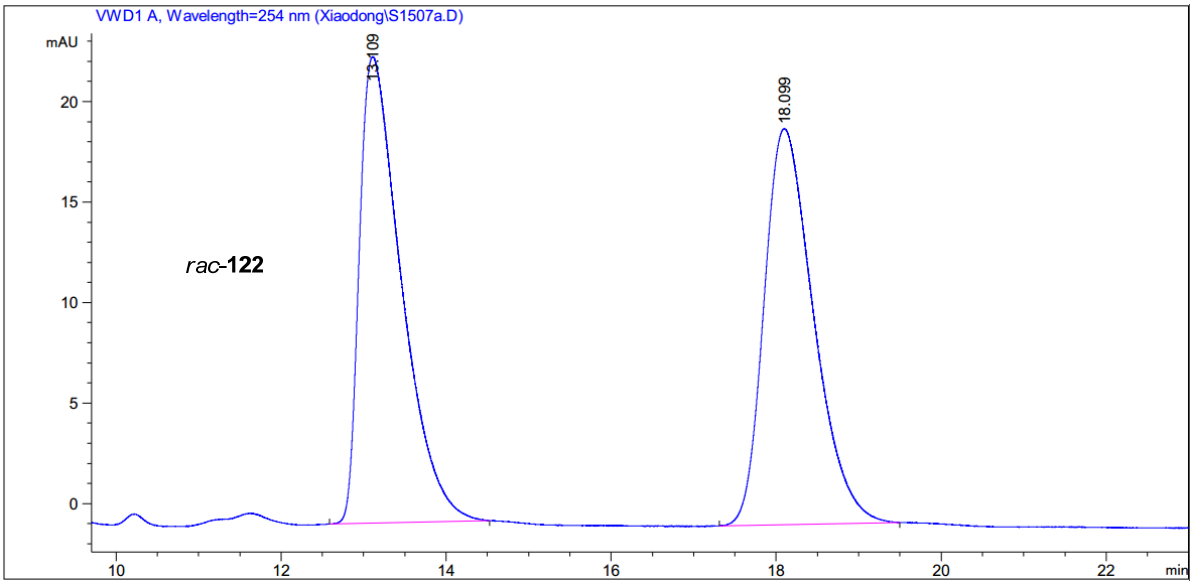


| Peak # | RetTime [min] | Type | Width [min] | Area [mAU*s] | Height [mAU] | Area % |
|---|---|---|---|---|---|---|
| 1 | 13.109 | BV R | 0.4142 | 821.12305 | 23.21243 | 50.0445 |
| 2 | 18.099 | BB | 0.4880 | 819.66125 | 19.69779 | 49.9555 |

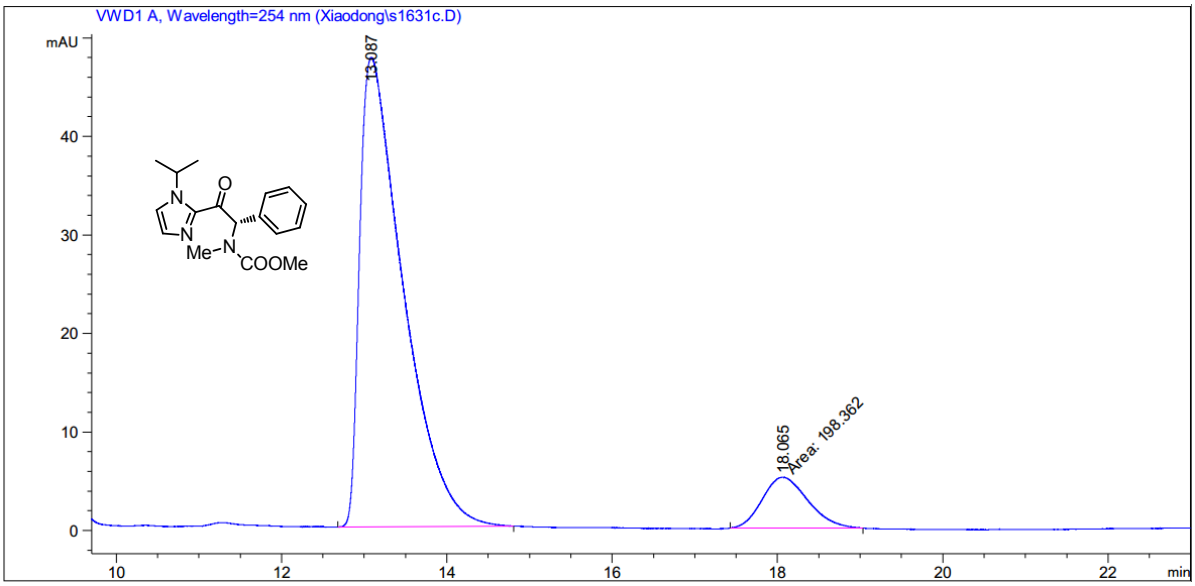


| Peak # | RetTime [min] | Type | Width [min] | Area [mAU*s] | Height [mAU] | Area % |
|---|---|---|---|---|---|---|
| 1 | 13.087 | BB | 0.4753 | 1738.34131 | 47.63286 | 89.7577 |
| 2 | 18.065 | MM | 0.6401 | 198.36226 | 5.16501 | 10.2423 |

**Figure 112** HPLC traces of compound **122**.

#

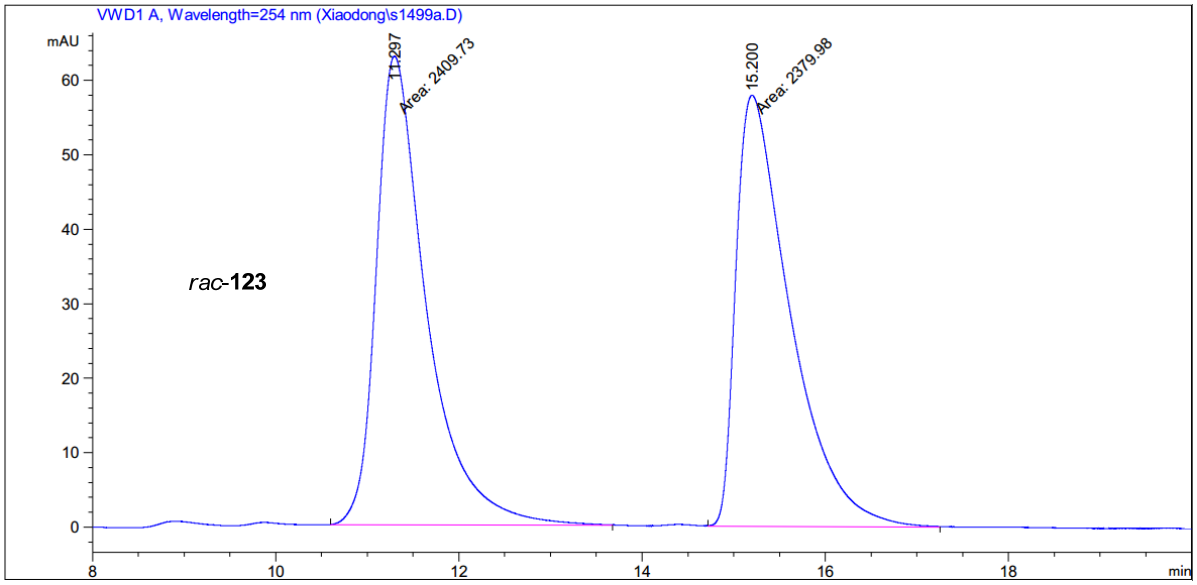


| Peak # | RetTime [min] | Type | Width [min] | Area [mAU*s] | Height [mAU] | Area % |
|---|---|---|---|---|---|---|
| 1 | 11.297 | MM | 0.6378 | 2409.72803 | 62.97132 | 50.3106 |
| 2 | 15.200 | MM | 0.6850 | 2379.97900 | 57.91004 | 49.6894 |

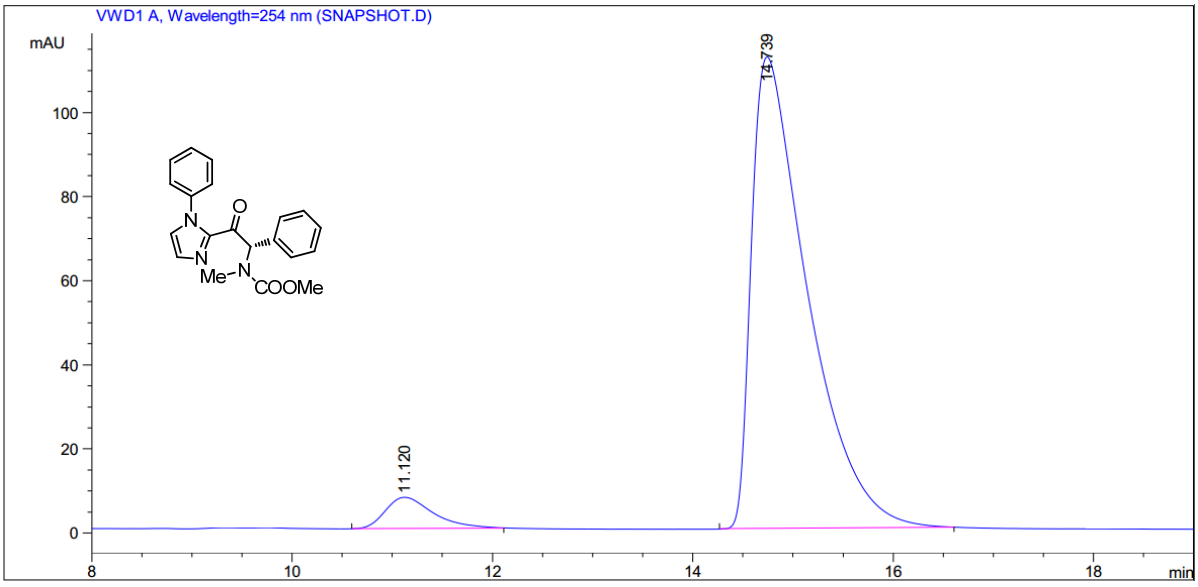


| Peak # | RetTime [min] | Type | Width [min] | Area [mAU*s] | Height [mAU] | Area % |
|---|---|---|---|---|---|---|
| 1 | 11.120 | BB | 0.4949 | 247.98788 | 7.44438 | 5.3775 |
| 2 | 14.739 | BB | 0.5731 | 4363.60791 | 112.21796 | 94.6225 |

**Figure 113** HPLC traces of compound **123**.

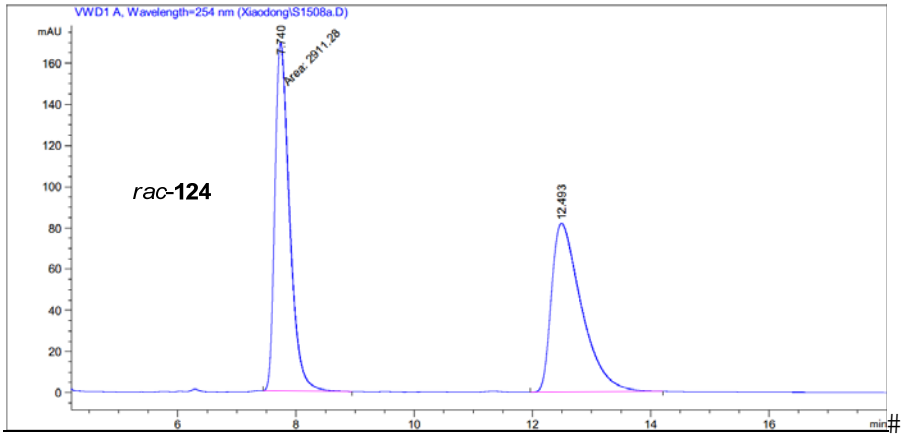


| Peak # | RetTime [min] | Type | Width [min] | Area [mAU*s] | Height [mAU] | Area % |
|---|---|---|---|---|---|---|
| 1 | 7.740 | MM | 0.2872 | 2911.27686 | 168.97226 | 50.1791 |
| 2 | 12.493 | BB | 0.4829 | 2890.49365 | 81.96684 | 49.8209 |

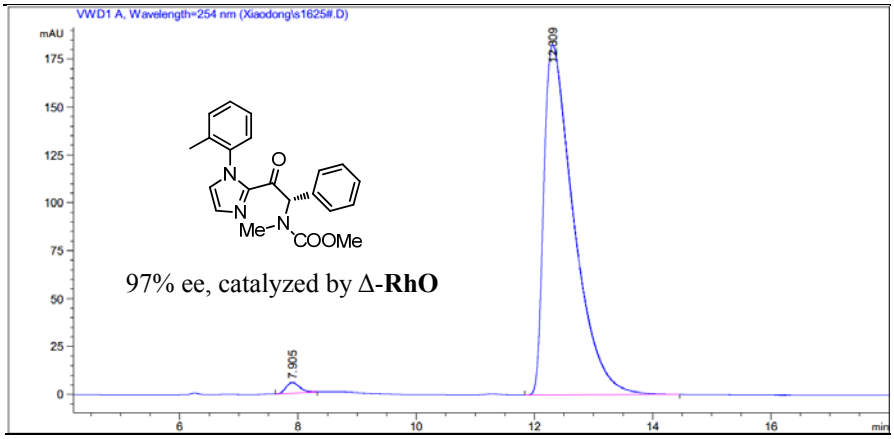


| Peak # | RetTime [min] | Type | Width [min] | Area [mAU*s] | Height [mAU] | Area % |
|---|---|---|---|---|---|---|
| 1 | 7.905 | BB | 0.1890 | 89.01913 | 5.62905 | 1.3691 |
| 2 | 12.309 | BB | 0.4909 | 6412.76904 | 182.73834 | 98.6309 |

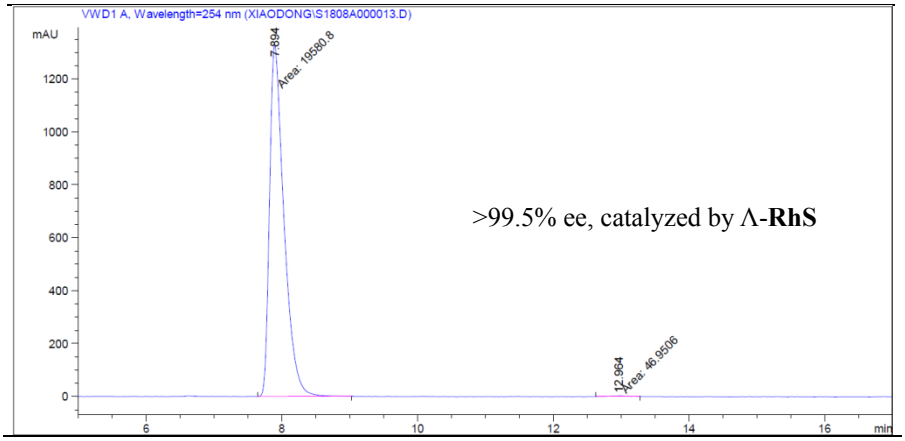


| Peak # | RetTime [min] | Type | Width [min] | Area [mAU*s] | Height [mAU] | Area % |
|---|---|---|---|---|---|---|
| 1 | 7.894 | MM | 0.2456 | 1.95808e4 | 1328.85364 | 99.7608 |
| 2 | 12.964 | MM | 0.3345 | 46.95055 | 2.33945 | 0.2392 |

**Figure 114** HPLC traces of compound **124**.

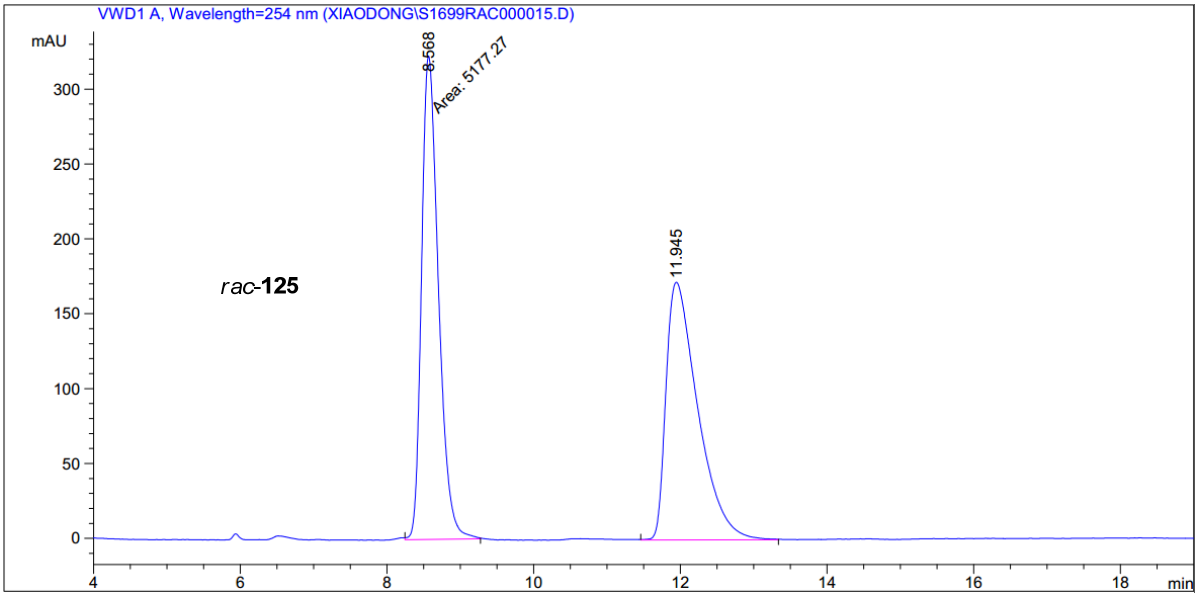


| Peak # | RetTime [min] | Type | Width [min] | Area [mAU*s] | Height [mAU] | Area % |
|---|---|---|---|---|---|---|
| 1 | 8.568 | MM | 0.2672 | 5177.27148 | 322.91907 | 49.9924 |
| 2 | 11.945 | VV | 0.4517 | 5178.84424 | 172.03442 | 50.0076 |

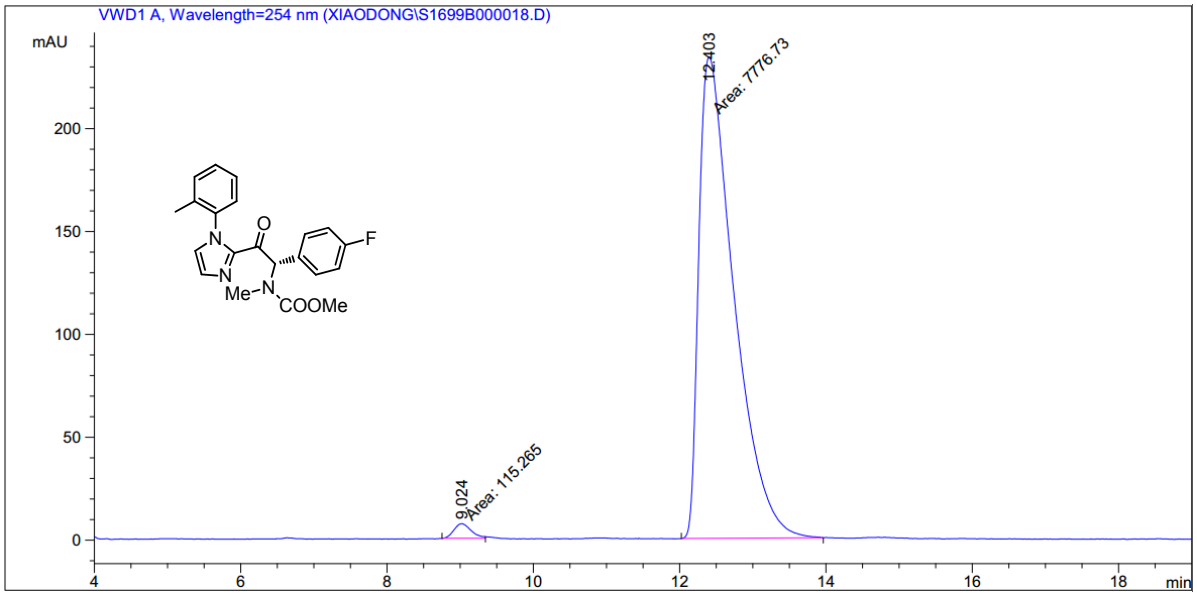


| Peak # | RetTime [min] | Type | Width [min] | Area [mAU*s] | Height [mAU] | Area % |
|---|---|---|---|---|---|---|
| 1 | 9.024 | MF | 0.2723 | 115.26480 | 7.05543 | 1.4605 |
| 2 | 12.403 | MM | 0.5537 | 7776.73096 | 234.10115 | 98.5395 |

**Figure 115** HPLC traces of compound **125**.

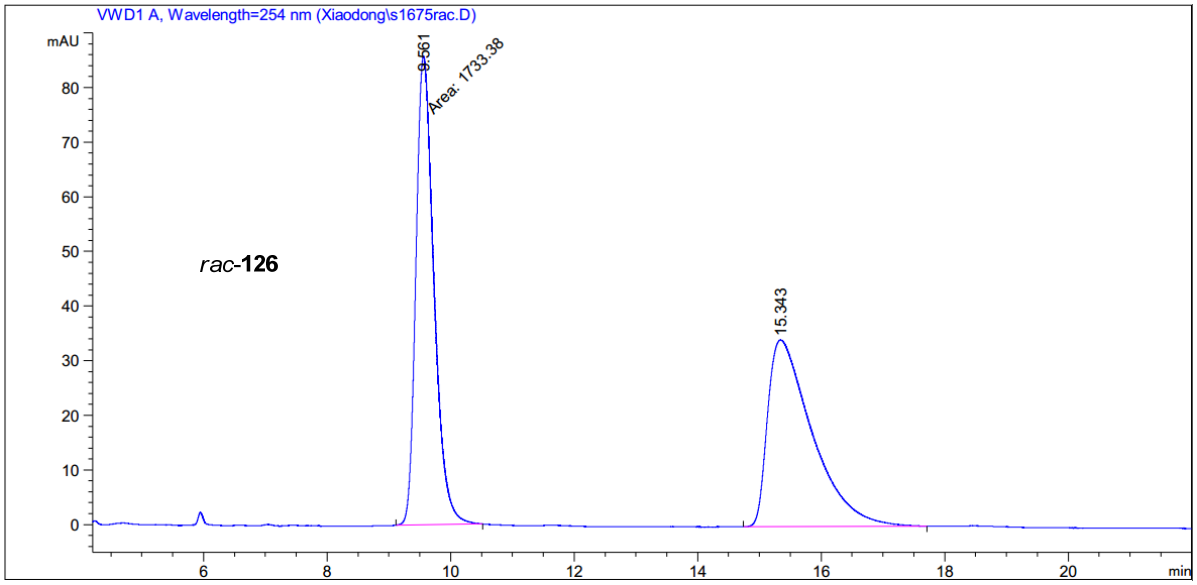


| Peak # | RetTime [min] | Type | Width [min] | Area [mAU*s] | Height [mAU] | Area % |
|---|---|---|---|---|---|---|
| 1 | 9.561 | MM | 0.3368 | 1733.38196 | 85.78720 | 50.2826 |
| 2 | 15.343 | BB | 0.6626 | 1713.89758 | 34.17424 | 49.7174 |

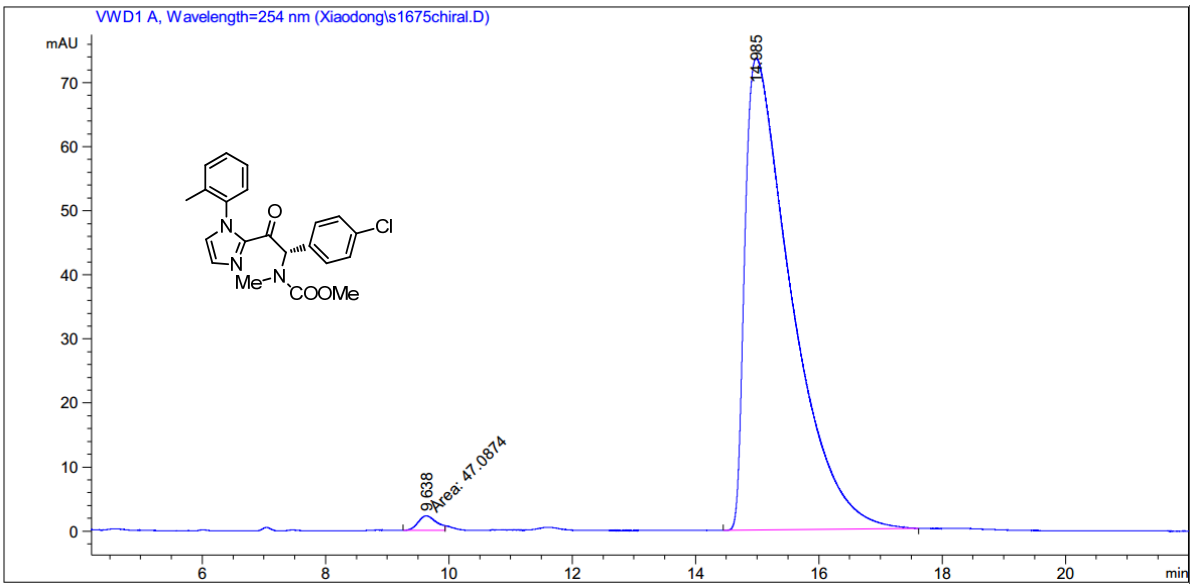


| Peak # | RetTime [min] | Type | Width [min] | Area [mAU*s] | Height [mAU] | Area % |
|---|---|---|---|---|---|---|
| 1 | 9.638 | MF | 0.3454 | 47.08741 | 2.27230 | 1.2125 |
| 2 | 14.985 | BB | 0.6719 | 3836.37622 | 73.68959 | 98.7875 |

**Figure 116** HPLC traces of compound **126**.

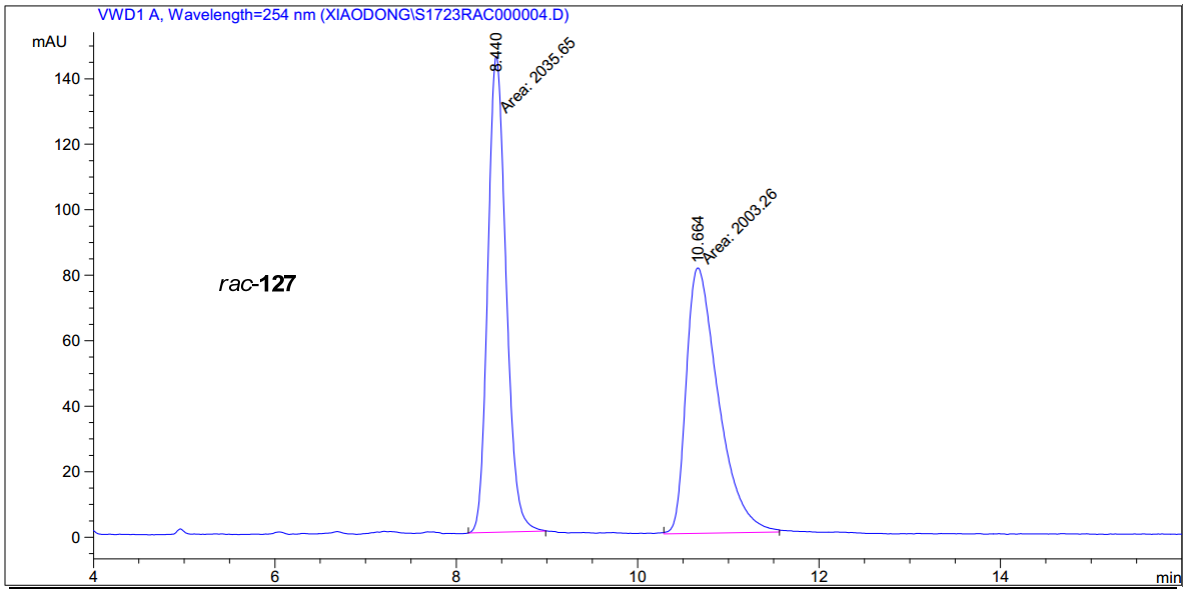


| Peak # | RetTime [min] | Type | Width [min] | Area [mAU*s] | Height [mAU] | Area % |
|---|---|---|---|---|---|---|
| 1 | 8.440 | MM | 0.2334 | 2035.65076 | 145.33856 | 50.4010 |
| 2 | 10.664 | MM | 0.4118 | 2003.26196 | 81.07648 | 49.5990 |

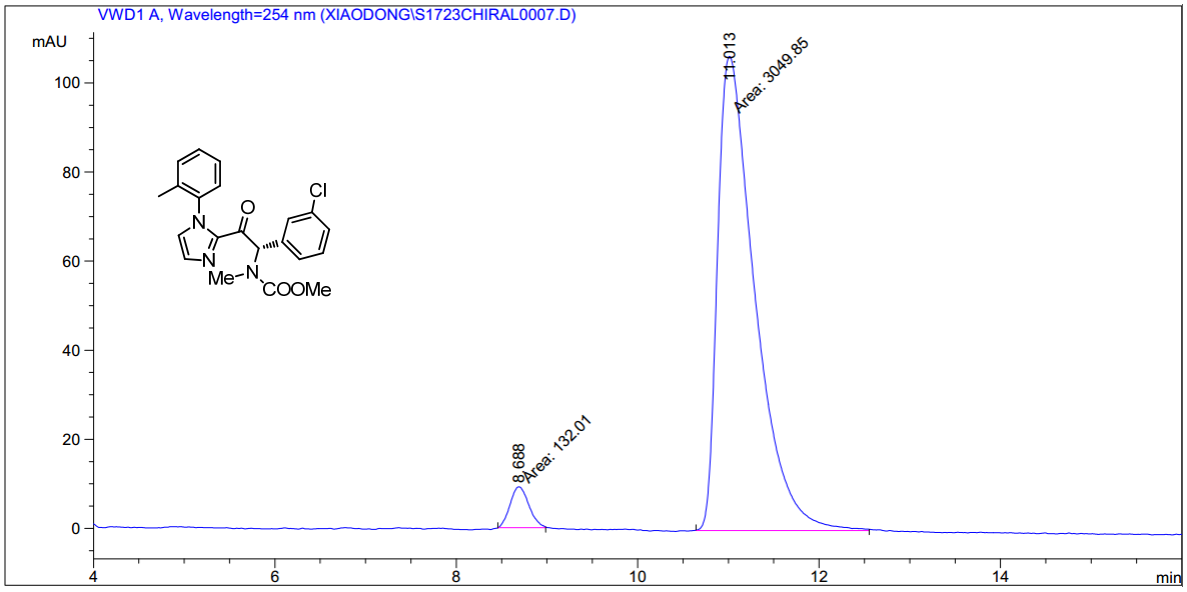


| Peak # | RetTime [min] | Type | Width [min] | Area [mAU*s] | Height [mAU] | Area % |
|---|---|---|---|---|---|---|
| 1 | 8.688 | MM | 0.2400 | 132.01024 | 9.16889 | 4.1488 |
| 2 | 11.013 | MM | 0.4774 | 3049.85327 | 106.48520 | 95.8512 |

**Figure 117** HPLC traces of compound **127**.

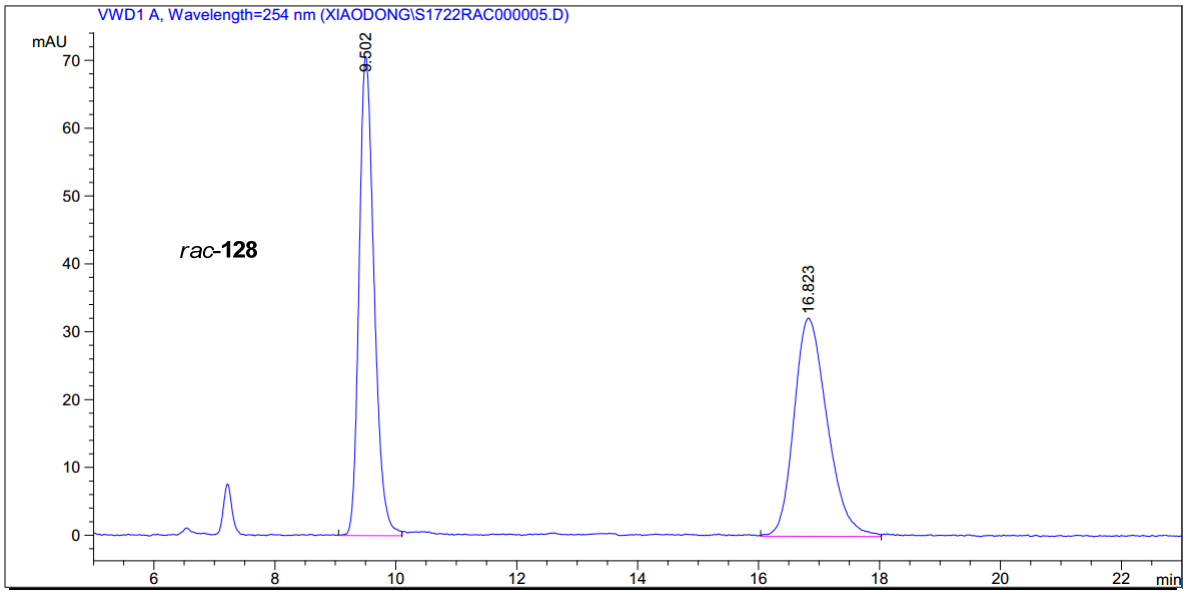


| Peak # | RetTime [min] | Type | Width [min] | Area [mAU*s] | Height [mAU] | Area % |
|---|---|---|---|---|---|---|
| 1 | 9.502 | VV | 0.2657 | 1220.65088 | 70.62157 | 49.8974 |
| 2 | 16.823 | VV | 0.5142 | 1225.67053 | 32.18125 | 50.1026 |

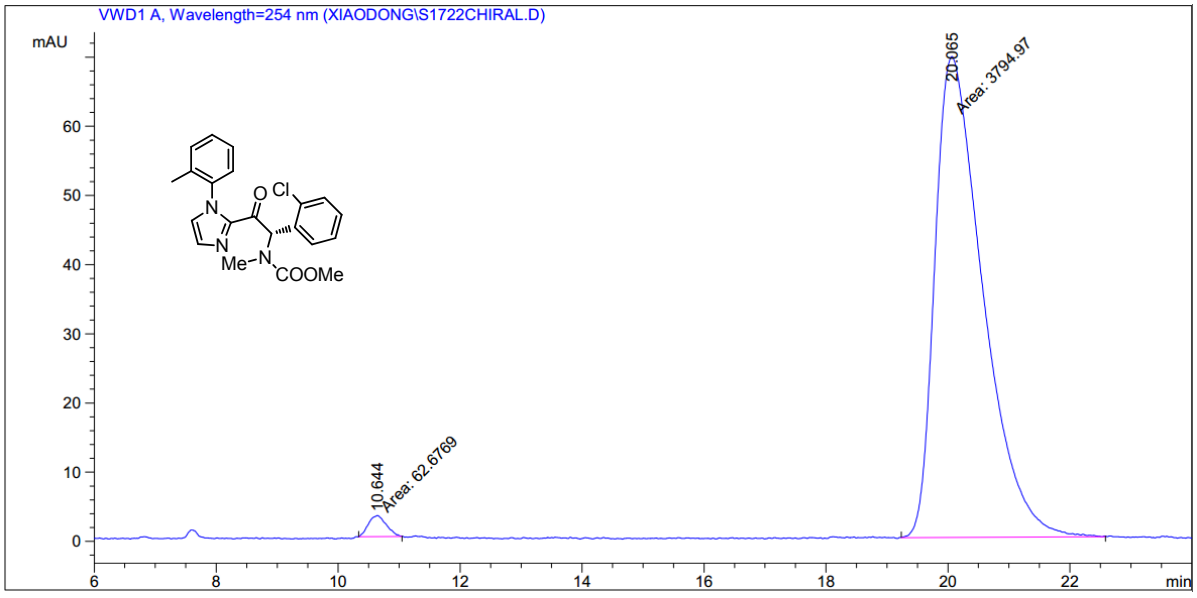


| Peak # | RetTime [min] | Type | Width [min] | Area [mAU*s] | Height [mAU] | Area % |
|---|---|---|---|---|---|---|
| 1 | 10.644 | MM | 0.3418 | 62.67695 | 3.05606 | 1.6247 |
| 2 | 20.065 | MM | 0.9098 | 3794.96924 | 69.51762 | 98.3753 |

**Figure 118** HPLC traces of compound **128**.

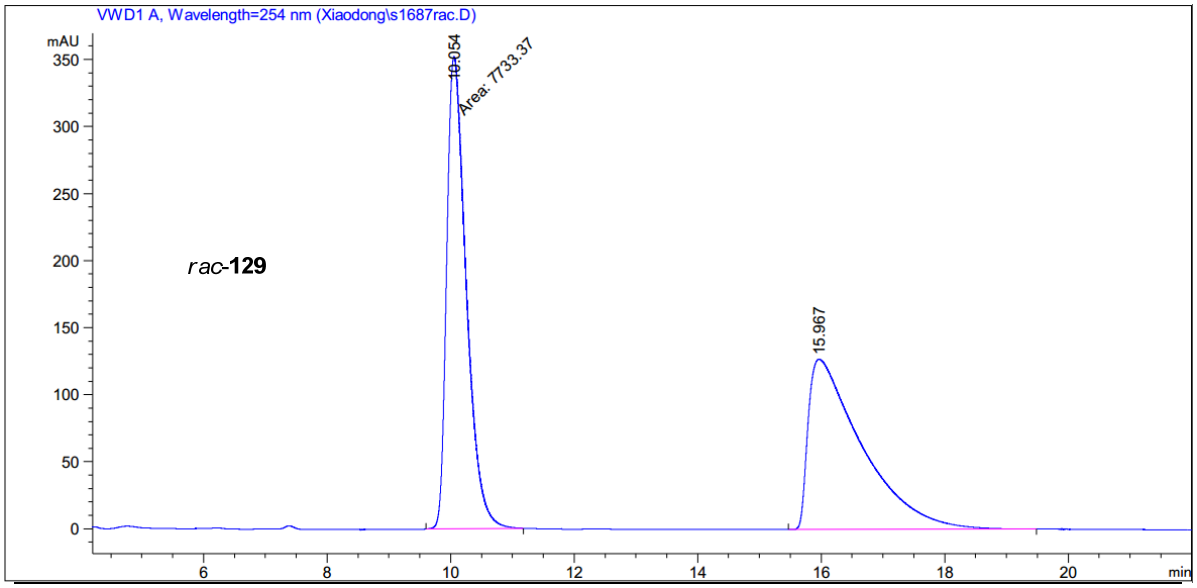


| Peak # | RetTime [min] | Type | Width [min] | Area [mAU*s] | Height [mAU] | Area % |
|---|---|---|---|---|---|---|
| 1 | 10.054 | MM | 0.3659 | 7733.37109 | 352.21219 | 50.2251 |
| 2 | 15.967 | BB | 0.7926 | 7664.04883 | 126.98806 | 49.7749 |

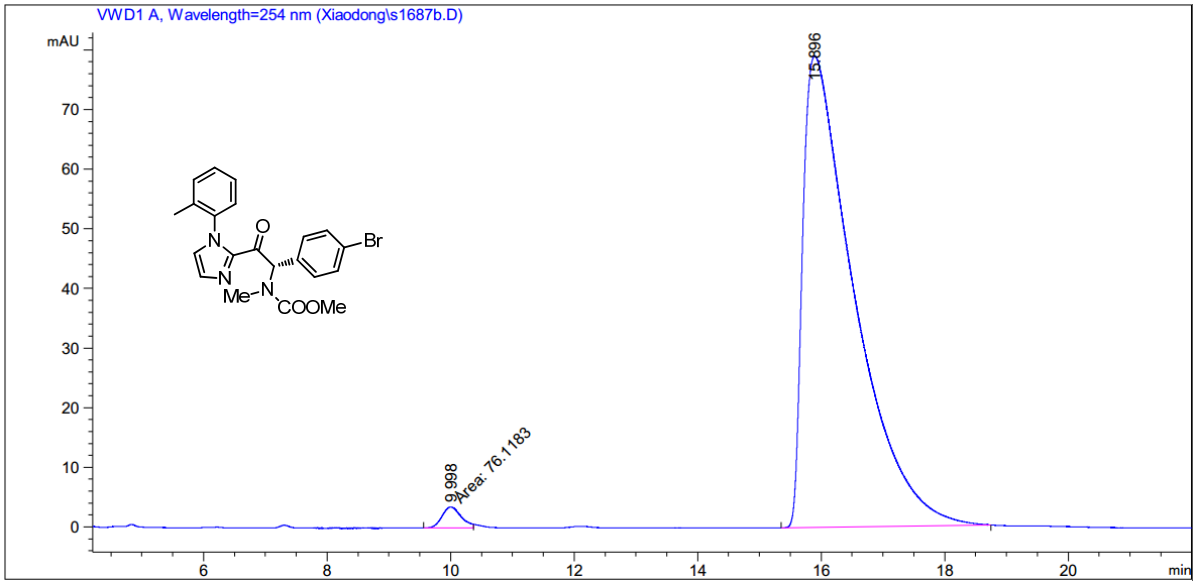


| Peak # | RetTime [min] | Type | Width [min] | Area [mAU*s] | Height [mAU] | Area % |
|---|---|---|---|---|---|---|
| 1 | 9.998 | MF | 0.3604 | 76.11834 | 3.52035 | 1.6423 |
| 2 | 15.896 | BB | 0.6787 | 4558.87988 | 79.06895 | 98.3577 |

**Figure 119** HPLC traces of compound **129**.

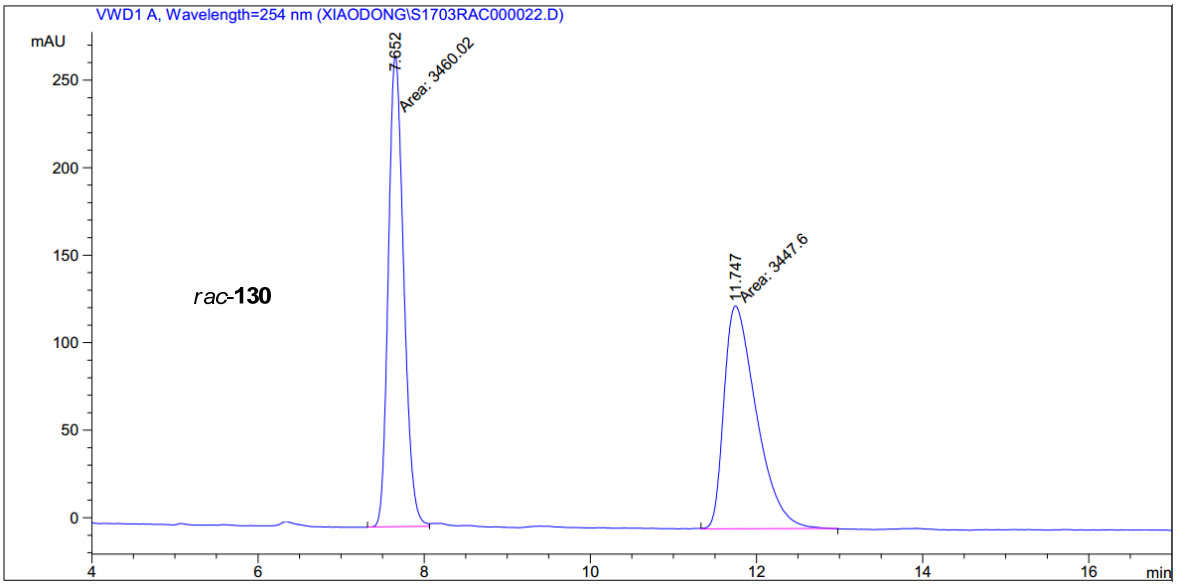


| Peak # | RetTime [min] | Type | Width [min] | Area [mAU*s] | Height [mAU] | Area % |
|---|---|---|---|---|---|---|
| 1 | 7.652 | MF | 0.2143 | 3460.02051 | 269.07526 | 50.0899 |
| 2 | 11.747 | MM | 0.4511 | 3447.60010 | 127.36810 | 49.9101 |

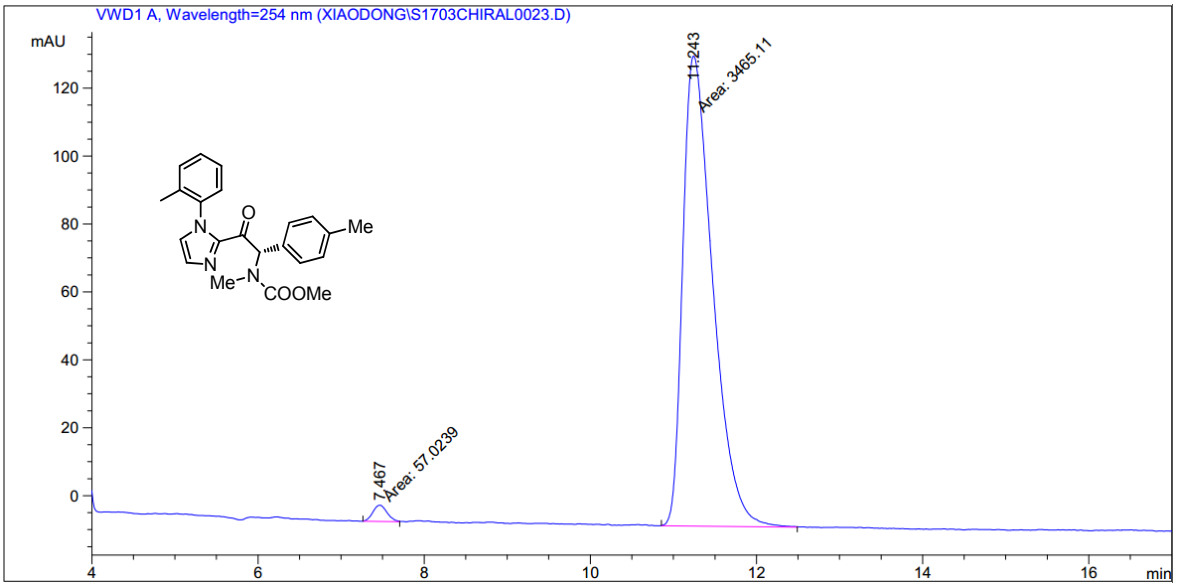


| Peak # | RetTime [min] | Type | Width [min] | Area [mAU*s] | Height [mAU] | Area % |
|---|---|---|---|---|---|---|
| 1 | 7.467 | MM | 0.1982 | 57.02394 | 4.79609 | 1.6190 |
| 2 | 11.243 | MM | 0.4173 | 3465.10693 | 138.39458 | 98.3810 |

**Figure 120** HPLC traces of compound **130**.

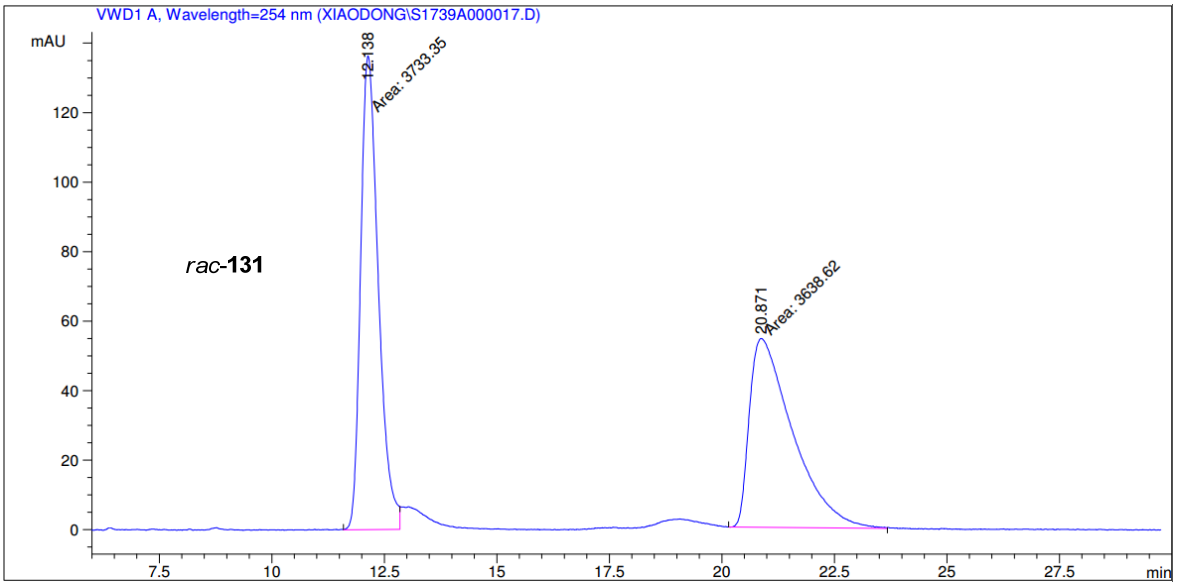


| Peak # | RetTime [min] | Type | Width [min] | Area [mAU*s] | Height [mAU] | Area % |
|---|---|---|---|---|---|---|
| 1 | 12.138 | MF | 0.4564 | 3733.34546 | 136.32205 | 50.6425 |
| 2 | 20.871 | MM | 1.1160 | 3638.61792 | 54.34027 | 49.3575 |

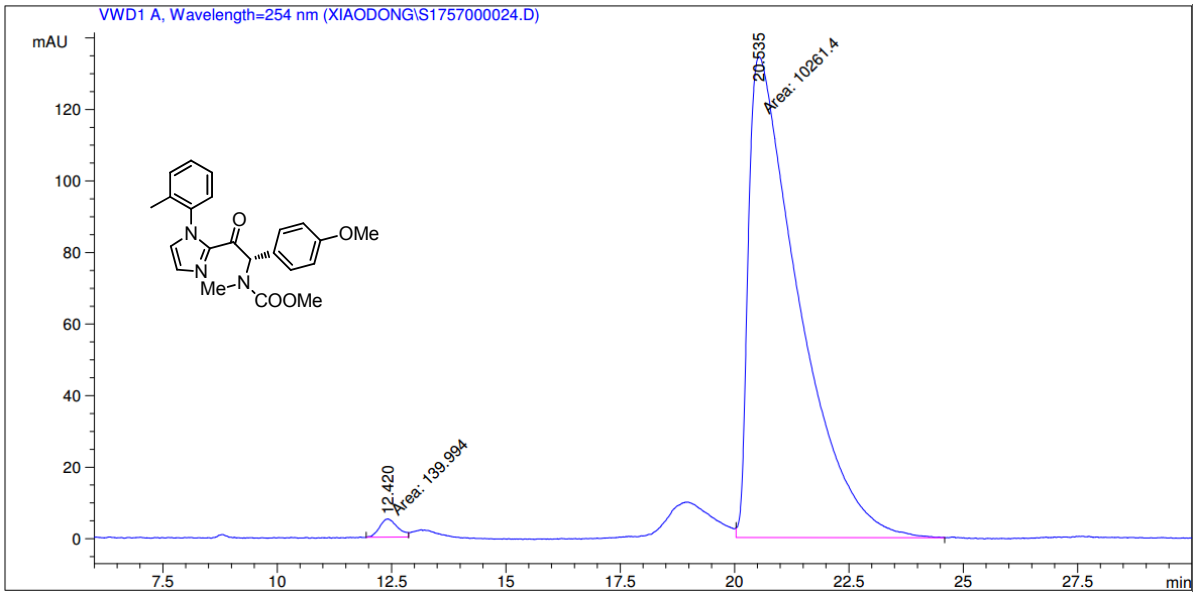


| Peak # | RetTime [min] | Type | Width [min] | Area [mAU*s] | Height [mAU] | Area % |
|---|---|---|---|---|---|---|
| 1 | 12.420 | MF | 0.4588 | 139.99443 | 5.08594 | 1.3459 |
| 2 | 20.535 | MM | 1.2725 | 1.02614e4 | 134.39609 | 98.6541 |

**Figure 121** HPLC traces of compound **131**

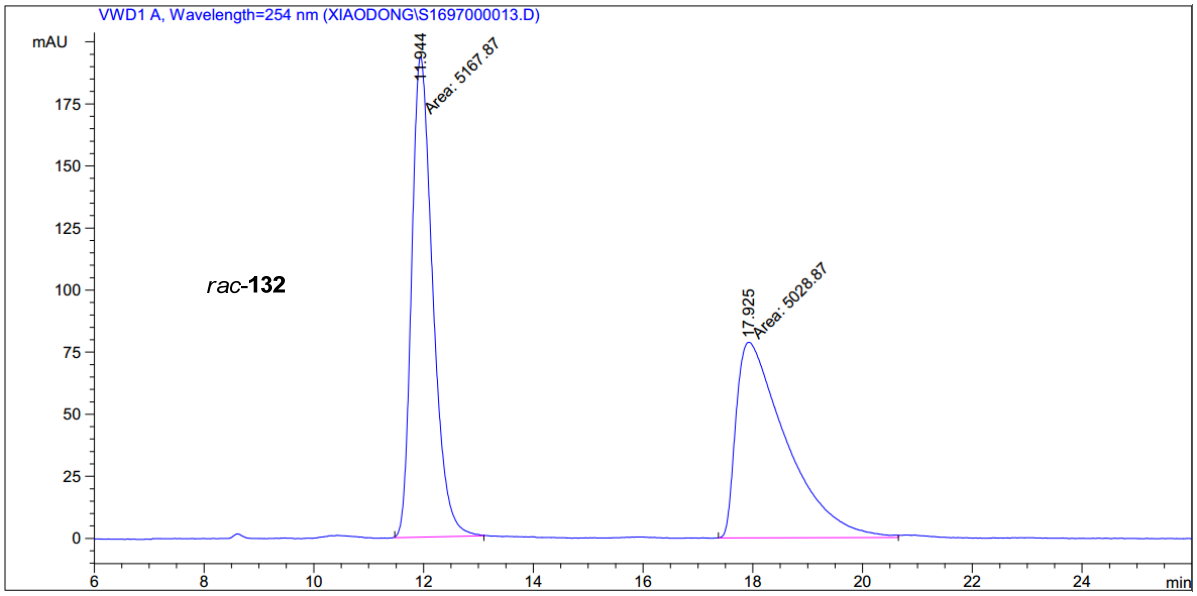


| Peak # | RetTime [min] | Type | Width [min] | Area [mAU*s] | Height [mAU] | Area % |
|---|---|---|---|---|---|---|
| 1 | 11.944 | MM | 0.4452 | 5167.86523 | 193.47052 | 50.6815 |
| 2 | 17.925 | MM | 1.0633 | 5028.87402 | 78.82182 | 49.3185 |

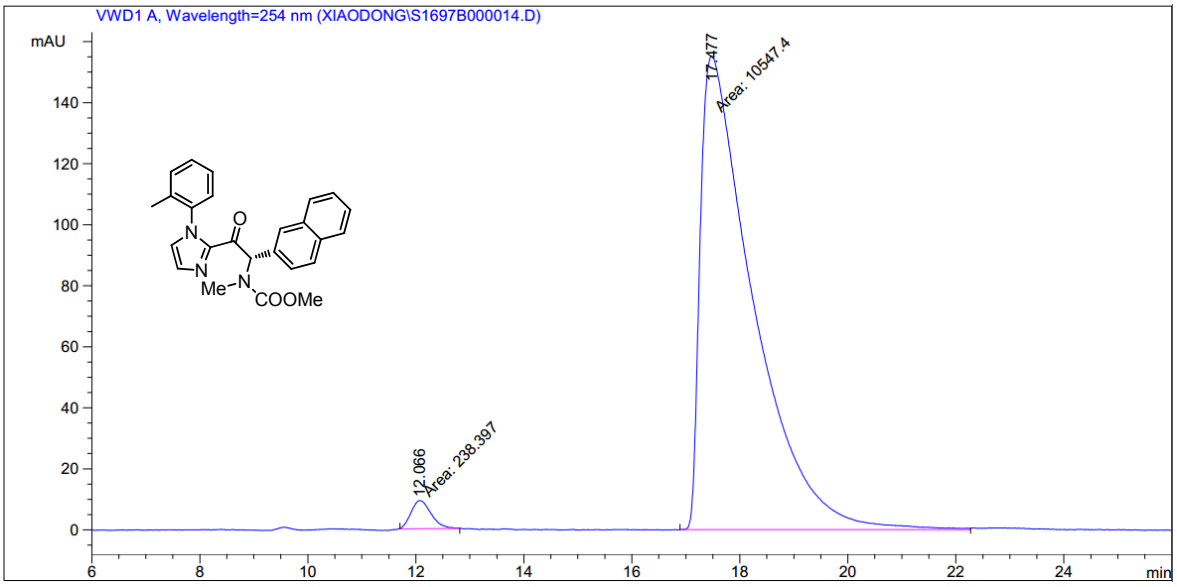


| Peak # | RetTime [min] | Type | Width [min] | Area [mAU*s] | Height [mAU] | Area % |
|---|---|---|---|---|---|---|
| 1 | 12.066 | MM | 0.4317 | 238.39705 | 9.20375 | 2.2103 |
| 2 | 17.477 | MM | 1.1328 | 1.05474e4 | 155.18494 | 97.7897 |

**Figure 122** HPLC traces of compound **132**.

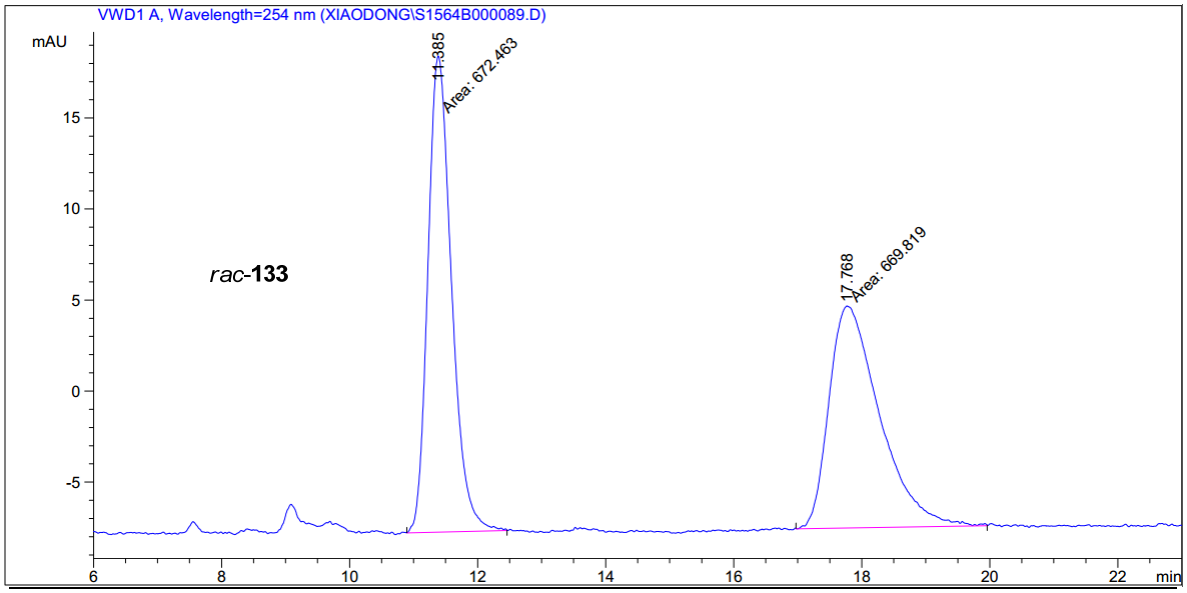


| Peak # | RetTime [min] | Type | Width [min] | Area [mAU*s] | Height [mAU] | Area % |
|---|---|---|---|---|---|---|
| 1 | 11.385 | MM | 0.4284 | 672.46295 | 26.15908 | 50.0985 |
| 2 | 17.768 | MM | 0.9150 | 669.81940 | 12.20044 | 49.9015 |

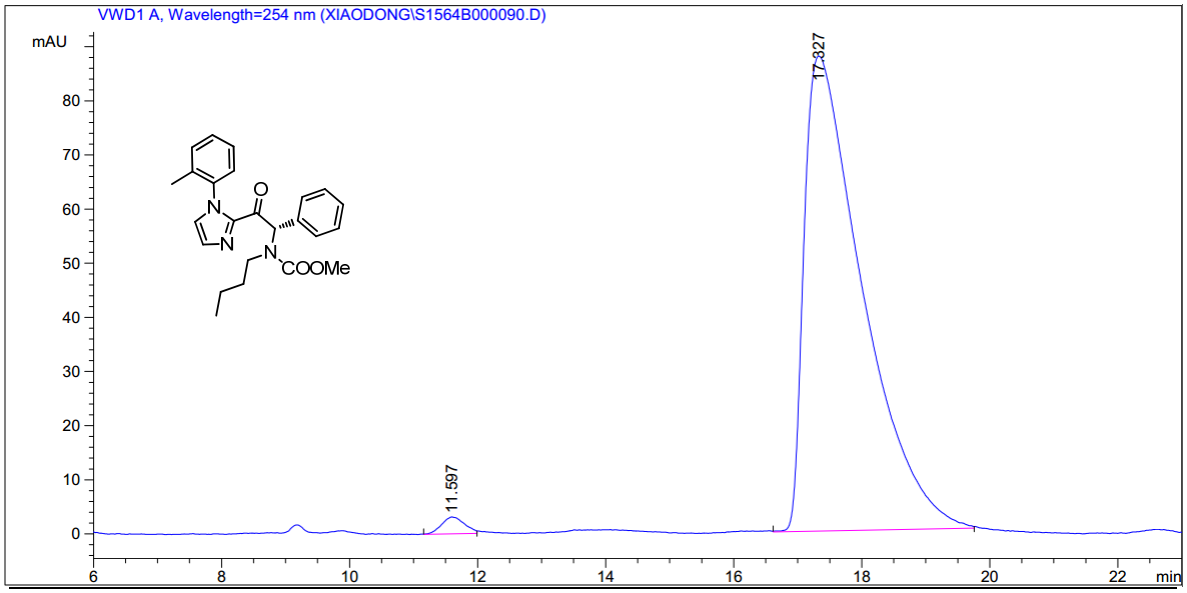


| Peak # | RetTime [min] | Type | Width [min] | Area [mAU*s] | Height [mAU] | Area % |
|---|---|---|---|---|---|---|
| 1 | 11.597 | VV | 0.3083 | 78.69935 | 3.14173 | 1.4027 |
| 2 | 17.327 | VB | 0.8753 | 5531.80273 | 87.74110 | 98.5973 |

**Figure 123** HPLC traces of compound **133**.

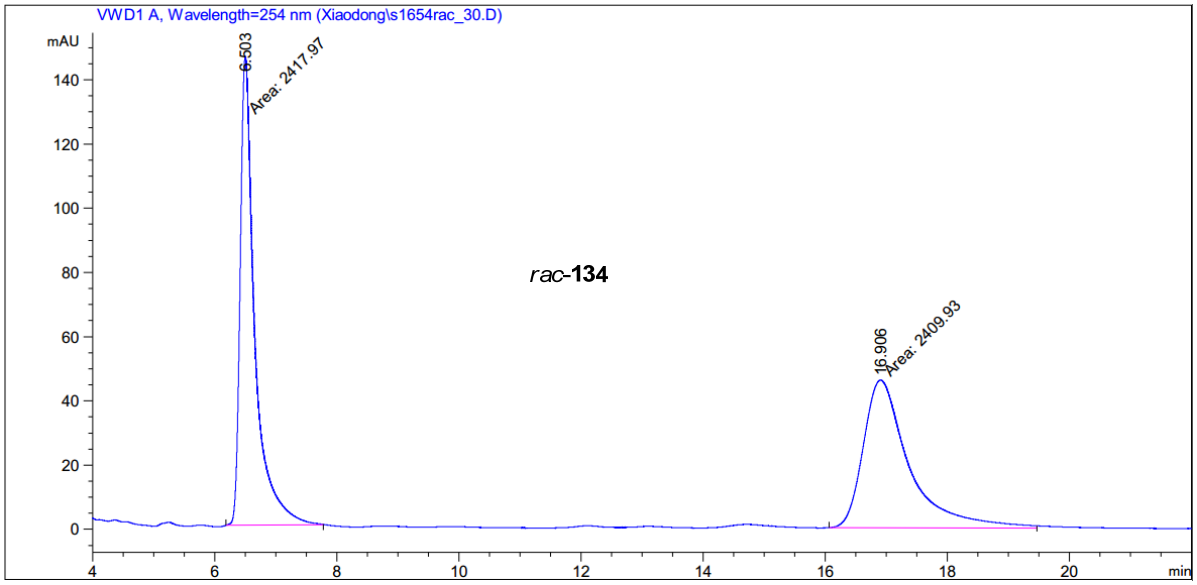


| Peak # | RetTime [min] | Type | Width [min] | Area [mAU*s] | Height [mAU] | Area % |
|---|---|---|---|---|---|---|
| 1 | 6.503 | MM | 0.2759 | 2417.96924 | 146.05011 | 50.0833 |
| 2 | 16.906 | MM | 0.8724 | 2409.93018 | 46.04045 | 49.9167 |

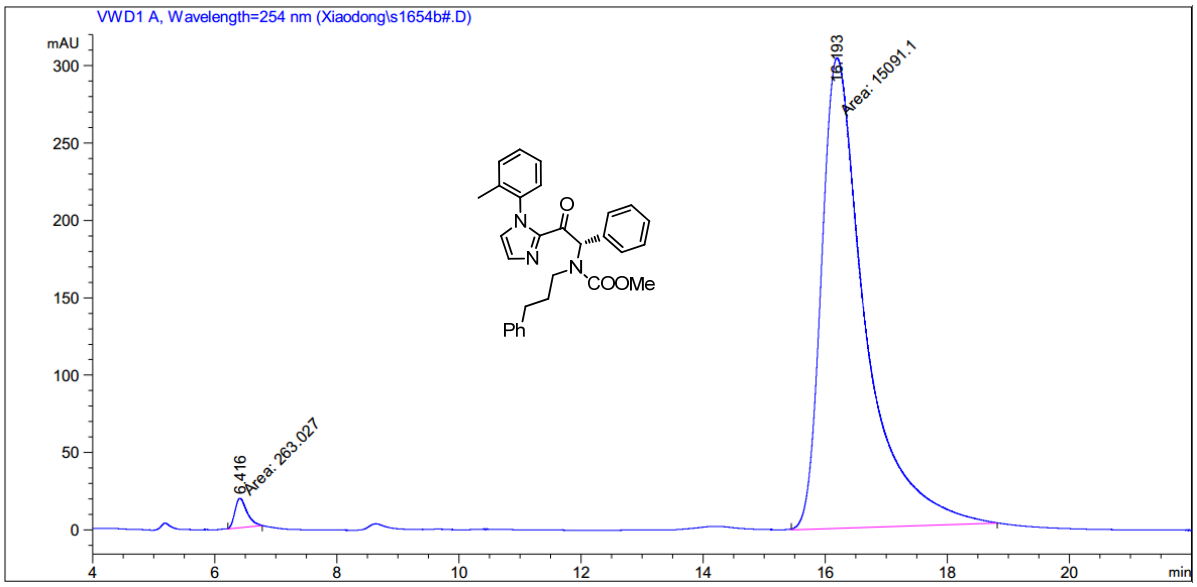


| Peak # | RetTime [min] | Type | Width [min] | Area [mAU*s] | Height [mAU] | Area % |
|---|---|---|---|---|---|---|
| 1 | 6.416 | MM | 0.2304 | 263.02747 | 19.02546 | 1.7131 |
| 2 | 16.193 | MM | 0.8279 | 1.50911e4 | 303.78659 | 98.2869 |

**Figure 124** HPLC traces of compound **134**.

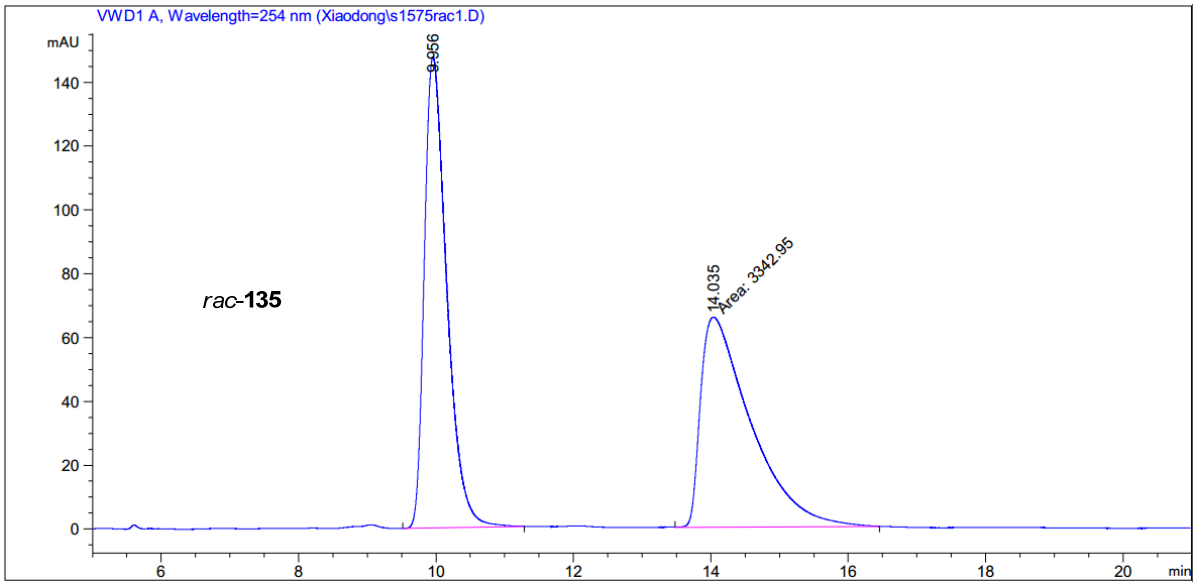


| Peak # | RetTime [min] | Type | Width [min] | Area [mAU*s] | Height [mAU] | Area % |
|---|---|---|---|---|---|---|
| 1 | 9.956 | BB | 0.3295 | 3339.85767 | 147.61003 | 49.9769 |
| 2 | 14.035 | MM | 0.8466 | 3342.94507 | 65.80769 | 50.0231 |

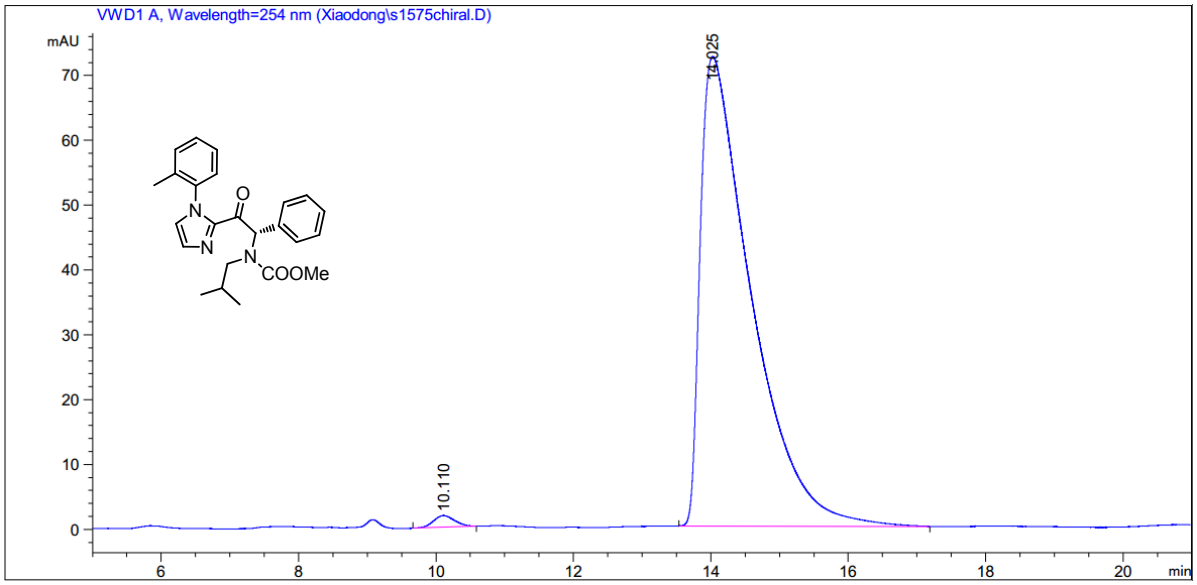


| Peak # | RetTime [min] | Type | Width [min] | Area [mAU*s] | Height [mAU] | Area % |
|---|---|---|---|---|---|---|
| 1 | 10.110 | VB R | 0.2542 | 38.96045 | 1.79869 | 1.0375 |
| 2 | 14.025 | BV R | 0.6250 | 3716.41553 | 72.38879 | 98.9625 |

**Figure 125** HPLC traces of compound **135**.

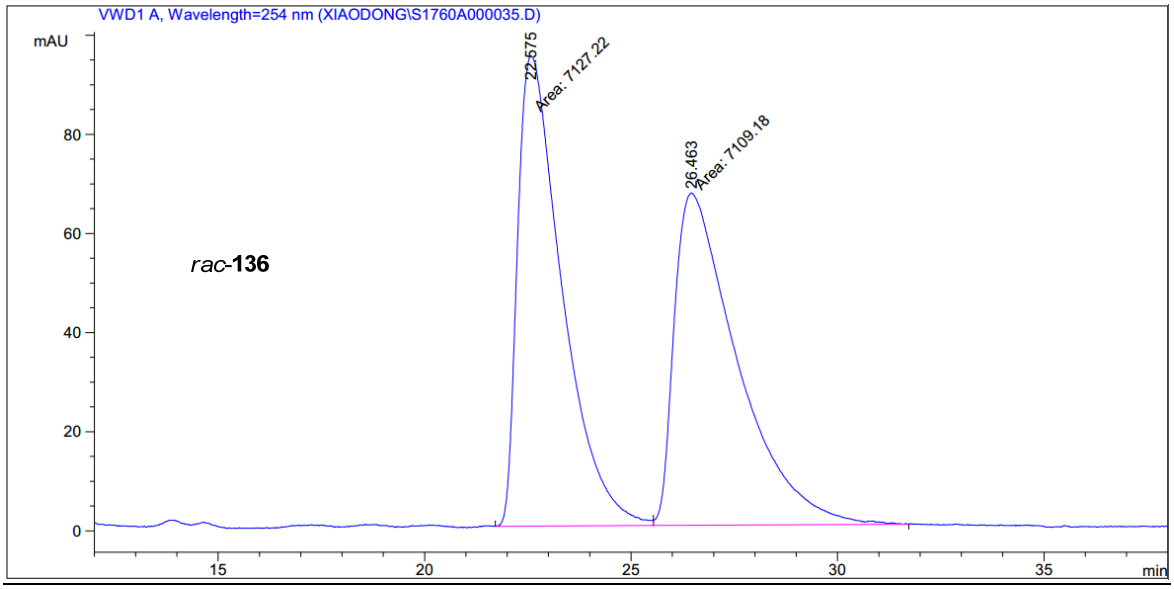


| Peak # | RetTime [min] | Type | Width [min] | Area [mAU*s] | Height [mAU] | Area % |
|---|---|---|---|---|---|---|
| 1 | 22.575 | MF | 1.2512 | 7127.22266 | 94.93864 | 50.0634 |
| 2 | 26.463 | FM | 1.7672 | 7109.17676 | 67.04777 | 49.9366 |

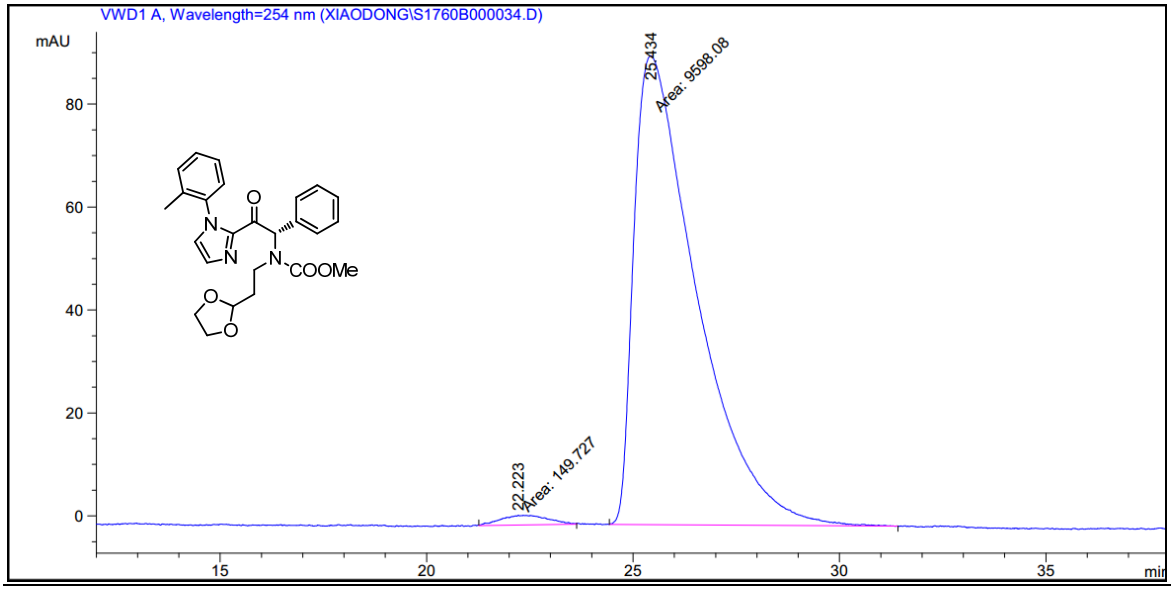


| Peak # | RetTime [min] | Type | Width [min] | Area [mAU*s] | Height [mAU] | Area % |
|---|---|---|---|---|---|---|
| 1 | 22.223 | MM | 1.3158 | 149.72749 | 1.89653 | 1.5360 |
| 2 | 25.434 | MM | 1.7561 | 9598.08105 | 91.09293 | 98.4640 |

**Figure 126** HPLC traces of compound **136**.

# Appendix 8. List of Crystal Structure Data

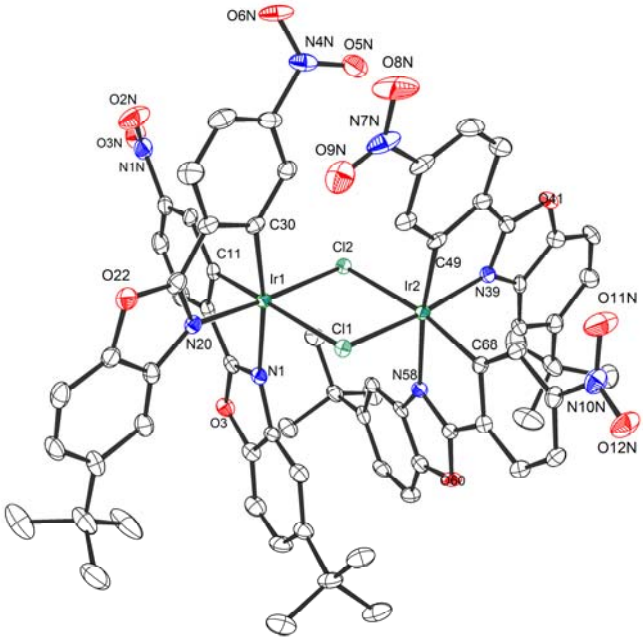


*rac*-**18**

**Table 16** Crystal Data and Structure Refinement for *rac*-**18** (*N,N*-cis-configuration)

**Crystal data:**

| | | |
|---|---|---|
| Identification code | s691_0m_sq | |
| Habitus, colour | plate, red | |
| Crystal size | 0.33 × 0.23 × 0.09 $mm^3$ | |
| Crystal system | Monoclinic | |
| Space group | P $2_1$/c | Z = 4 |
| Unit cell dimensions | a = 18.3305(7) Å | α = 90° |
| | b = 14.4543(6) Å | β = 94.3573(13)° |
| | c = 29.0787(12) Å | γ = 90° |
| Volume | 7682.3(5) $Å^3$ | |
| Cell determination | 9974 peaks with Theta 2.3 to 27.5°. | |
| Empirical formula | $C_{75}$ $H_{76}$ $Cl_4$ $Ir_2$ $N_8$ $O_{12}$ | |
| Formula weight | 1807.63 | |
| Density (calculated) | 1.563 $Mg/m^3$ | |
| Absorption coefficient | 3.664 $mm^{-1}$ | |
| F(000) | 3600 | |

**Data collection:**

| | |
|---|---|
| Diffractometer type | Bruker D8 QUEST area detector |
| Wavelength | 0.71073 Å |
| Temperature | 100(2) K |
| Theta range for data collection | 2.228 to 25.500°. |
| Index ranges | -22<=h<=22, -16<=k<=17, -35<=l<=32 |
| Data collection software | BRUKER APEX2 |
| Cell refinement software | SAINT V8.34A (Bruker AXS Inc., 2013) |
| Data reduction software | SAINT V8.34A (Bruker AXS Inc., 2013) |

**Solution and refinement:**

| | |
|---|---|
| Reflections collected | 40619 |
| Independent reflections | 14192 [R(int) = 0.0311] |
| Completeness to theta = 25.242° | 99.1 % |
| Observed reflections | 11853[II > 2(I)] |
| Reflections used for refinement | 14192 |
| Absorption correction | Numerical |
| Max. and min. transmission | 0.73 and 0.44 |
| Largest diff. peak and hole | 1.609 and -1.393 e.$Å^{-3}$ |
| Solution | Direct methods |
| Refinement | Full-matrix least-squares on $F^2$ |
| Treatment of hydrogen atoms | Calculated positions, constraint refinement |
| Programs used | SHELXS-97 (Sheldrick, 2008)<br>SHELXL-2013 (Sheldrick, 2013)<br>DIAMOND (Crystal Impact) |
| Data / restraints / parameters | 14192 / 106 / 982 |
| Goodness-of-fit on $F^2$ | 1.037 |
| R index (all data) | $wR_2$ = 0.0689 |
| R index conventional [I>2sigma(I)] | $R_1$ = 0.0304 |

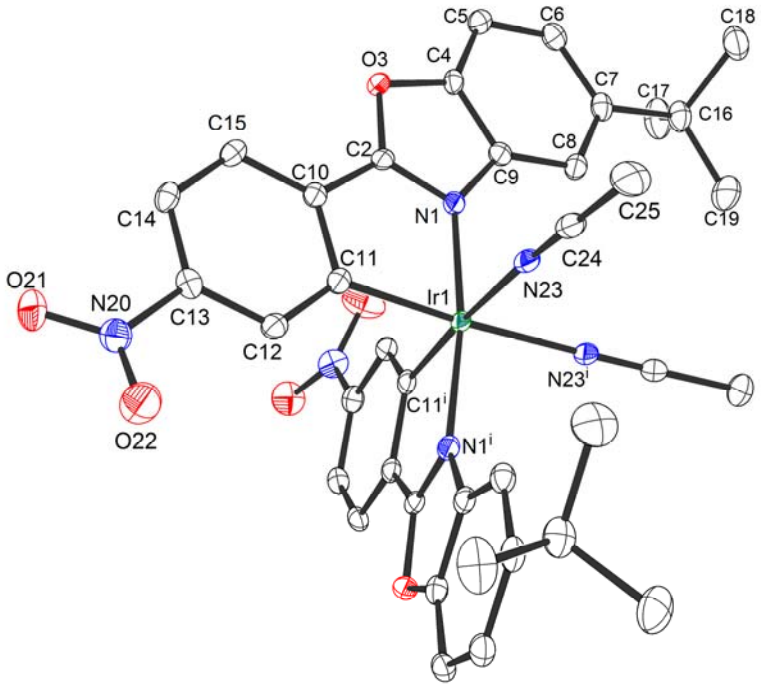


*rac*-**IrO(NO$_2$)**

**Table 17** Crystal Data and Structure Refinement for *rac*-**IrO(NO$_2$)**

**Crystal data:**

| | | |
|---|---|---|
| Identification code | s745_0m | |
| Habitus, colour | block, orange | |
| Crystal size | 0.360 × 0.080 × 0.080 mm$^3$ | |
| Crystal system | Monoclinic | |
| Space group | C 2/c | Z = 4 |
| Unit cell dimensions | a = 26.4047(8) Å | α = 90° |
| | b = 10.9883(3) Å | β = 112.9949(11)° |
| | c = 15.5720(6) Å | γ = 90° |
| Volume | 4159.1(2) Å$^3$ | |
| Cell determination | 214 peaks with Theta 5.7 to 26.8°. | |
| Empirical formula | $C_{39}$ $H_{38.40}$ $Cl_2$ $F_6$ Ir $N_6$ $O_{6.20}$ P | |
| Formula weight | 1098.42 | |
| Density (calculated) | 1.754 Mg/m$^3$ | |
| Absorption coefficient | 3.459 mm$^{-1}$ | |
| F(000) | 2176 | |

**Data collection:**

| | |
|---|---|
| Diffractometer type | Bruker D8 QUEST area detector |
| Wavelength | 0.71073 Å |
| Temperature | 100(2) K |
| Theta range for data collection | 2.662 to 27.555°. |
| Index ranges | -34<=h<=33, -14<=k<=14, -20<=l<=20 |
| Data collection software | BRUKER APEX2 |
| Cell refinement software | APEX2 v2014.1-1 (Bruker AXS) |
| Data reduction software | SAINT V8.34A (Bruker AXS Inc., 2013) |

**Solution and refinement:**

| | |
|---|---|
| Reflections collected | 38682 |
| Independent reflections | 4795 [R(int) = 0.0413] |
| Completeness to theta = 25.242° | 99.9 % |
| Observed reflections | 4547[II > 2(I)] |
| Reflections used for refinement | 4795 |
| Absorption correction | Numerical |
| Max. and min. transmission | 0.77 and 0.36 |
| Largest diff. peak and hole | 0.628 and -0.333 e.Å$^{-3}$ |
| Solution | Direct methods |
| Refinement | Full-matrix least-squares on $F^2$ |
| Treatment of hydrogen atoms | calculated positions, constr ref. |
| Programs used | SHELXS-97 (Sheldrick, 2008)<br>SHELXL-2013 (Sheldrick, 2013)<br>DIAMOND (Crystal Impact) |
| Data / restraints / parameters | 4795 / 10 / 332 |
| Goodness-of-fit on $F^2$ | 1.083 |
| R index (all data) | $wR_2$ = 0.0390 |
| R index conventional [I>2sigma(I)] | $R_1$ = 0.0165 |

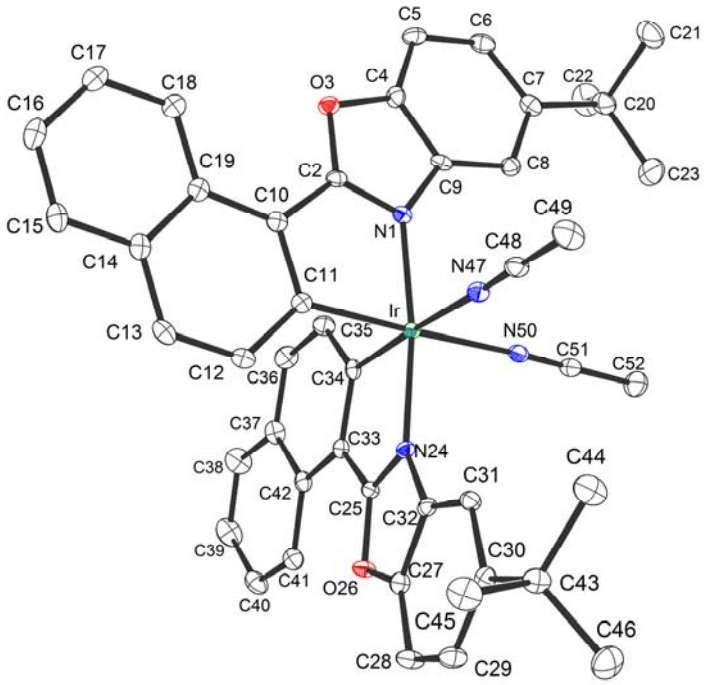


*rac*-**IrO(nap)**

**Table 18** Crystal Data and Structure Refinement for *rac*-**IrO(nap)**

**Crystal data:**

| | | |
|---|---|---|
| Identification code | s735_0m | |
| Habitus, colour | block, red | |
| Crystal size | 0.39 × 0.20 × 0.11 $mm^3$ | |
| Crystal system | Monoclinic | |
| Space group | P $2_1$/n | Z = 4 |
| Unit cell dimensions | a = 15.4823(6) Å | α = 90° |
| | b = 20.4836(7) Å | β = 104.5380(13)° |
| | c = 15.6035(5) Å | γ = 90° |
| Volume | 4789.9(3) $Å^3$ | |
| Cell determination | 9378 peaks with Theta 2.4 to 27.5°. | |
| Empirical formula | $C_{48}$ $H_{46}$ $Cl_4$ $F_6$ Ir $N_4$ $O_2$ P | |
| Formula weight | 1189.86 | |
| Density (calculated) | 1.650 $Mg/m^3$ | |
| Absorption coefficient | 3.111 $mm^{-1}$ | |
| F(000) | 2368 | |

**Data collection:**

| | |
|---|---|
| Diffractometer type | Bruker D8 QUEST area detector |
| Wavelength | 0.71073 Å |
| Temperature | 100(2) K |
| Theta range for data collection | 2.403 to 27.564°. |
| Index ranges | -20<=h<=19, -26<=k<=26, -20<=l<=20 |
| Data collection software | BRUKER APEX2 |
| Cell refinement software | SAINT V8.34A (Bruker AXS Inc., 2013) |
| Data reduction software | SAINT V8.34A (Bruker AXS Inc., 2013) |

**Solution and refinement:**

| | |
|---|---|
| Reflections collected | 164058 |
| Independent reflections | 11051 [R(int) = 0.0516] |
| Completeness to theta = 25.242° | 99.9 % |
| Observed reflections | 9800[II > 2(I)] |
| Reflections used for refinement | 11051 |
| Absorption correction | Numerical |
| Max. and min. transmission | 0.73 and 0.48 |
| Largest diff. peak and hole | 0.665 and -0.508 e.$Å^{-3}$ |
| Solution | Direct methods |
| Refinement | Full-matrix least-squares on $F^2$ |
| Treatment of hydrogen atoms | calc. positions, riding model |
| Programs used | SHELXS-97 (Sheldrick, 2008) |
| | SHELXL-2013 (Sheldrick, 2013) |
| | DIAMOND (Crystal Impact) |
| Data / restraints / parameters | 11051 / 14 / 636 |
| Goodness-of-fit on $F^2$ | 1.055 |
| R index (all data) | $wR_2$ = 0.0396 |
| R index conventional [I>2sigma(I)] | $R_1$ = 0.0185 |

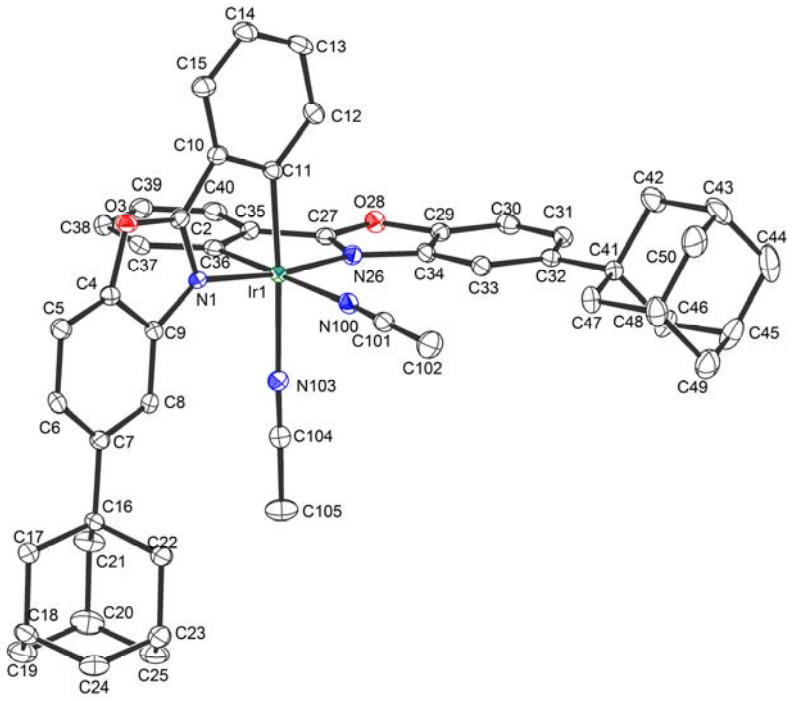


*rac*-**IrO(ada)**

**Table 19** Crystal Data and Structure Refinement for *rac*-**IrO(ada)**

**Crystal data:**

| | | |
|---|---|---|
| Identification code | s751_0m | |
| Habitus, colour | prism, yellow | |
| Crystal size | 0.400 × 0.280 × 0.150 $mm^3$ | |
| Crystal system | Triclinic | |
| Space group | P -1 | Z = 2 |
| Unit cell dimensions | a = 12.0272(8) Å | α = 97.856(2)° |
| | b = 20.2463(13) Å | β = 102.209(2)° |
| | c = 21.3725(15) Å | γ = 101.316(2)° |
| Volume | 4900.8(6) $Å^3$ | |
| Cell determination | 9526 peaks with Theta 2.6 to 27.5°. | |
| Empirical formula | $C_{103}$ $H_{106}$ $Cl_6$ $F_{12}$ $Ir_2$ $N_8$ $O_4$ $P_2$ | |
| Formula weight | 2406.99 | |
| Density (calculated) | 1.631 $Mg/m^3$ | |
| Absorption coefficient | 2.989 $mm^{-1}$ | |
| F(000) | 2412 | |

**Data collection:**

| | |
|---|---|
| Diffractometer type | Bruker D8 QUEST area detector |
| Wavelength | 0.71073 Å |
| Temperature | 100(2) K |
| Theta range for data collection | 1.975 to 27.550°. |
| Index ranges | -14<=h<=15, -26<=k<=26, -27<=l<=27 |
| Data collection software | BRUKER APEX2 |
| Cell refinement software | SAINT V8.34A (Bruker AXS Inc., 2013) |
| Data reduction software | SAINT V8.34A (Bruker AXS Inc., 2013) |

**Solution and refinement:**

| | |
|---|---|
| Reflections collected | 98229 |
| Independent reflections | 22587 [R(int) = 0.0437] |
| Completeness to theta = 25.242° | 99.9 % |
| Observed reflections | 18214[II > 2(I)] |
| Reflections used for refinement | 22587 |
| Absorption correction | Numerical |
| Max. and min. transmission | 0.66 and 0.38 |
| Largest diff. peak and hole | 1.751 and -1.401 e.$Å^{-3}$ |
| Solution | Direct methods |
| Refinement | Full-matrix least-squares on $F^2$ |
| Treatment of hydrogen atoms | Calc. positions, constr. Ref. |
| Programs used | SHELXS-97 (Sheldrick, 2008) |
| | SHELXL-2013 (Sheldrick, 2013) |
| | DIAMOND (Crystal Impact) |
| Data / restraints / parameters | 22587 / 348 / 1423 |
| Goodness-of-fit on $F^2$ | 1.042 |
| R index (all data) | $wR_2$ = 0.0632 |
| R index conventional [I>2sigma(I)] | $R_1$ = 0.0276 |

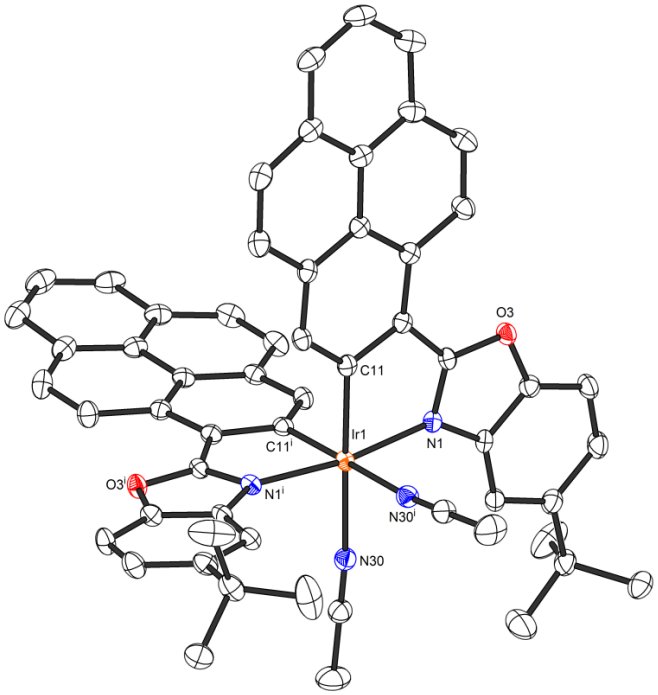


*rac*-**IrO(pyrene)**

**Table 20** Crystal Data and Structure Refinement for *rac*-**IrO(pyrene)**

**Crystal data**

| | | |
|---|---|---|
| Identification code | s1412_0m | |
| Habitus, colour | block, orange | |
| Crystal size | 0.34 × 0.20 × 0.17 $mm^3$ | |
| Crystal system | Monoclinic | |
| Space group | C2/c | Z = 4 |
| Unit cell dimensions | a = 18.6985(10) Å | α= 90°. |
| | b = 22.2223(11) Å | β= 114.850(2)°. |
| | c = 13.3462(7) Å | γ = 90°. |
| Volume | 5032.2(5) $Å^3$ | |
| Cell determination | 9913 peaks with Theta 2.5 to 26.4°. | |
| Empirical formula | $C_{59}$ $H_{48}$ $Cl_2$ $F_6$Ir $N_4$ $O_2$ P | |
| Moiety formula | $C_{58}$ $H_{46}$Ir $N_4$ $O_2$, $F_6$ P, C $H_2$ $Cl_2$ | |
| Formula weight | 1253.08 | |
| Density (calculated) | 1.654 $Mg/m^3$ | |
| Absorption coefficient | 2.864 $mm^{-1}$ | |
| F(000) | 2504 | |

**Data collection:**

| | |
|---|---|
| Diffractometer type | Bruker D8 QUEST area detector |
| Wavelength | 0.71073 Å |
| Temperature | 110(2) K |
| Theta range for data collection | 2.488 to 26.436°. |
| Index ranges | -23<=h<=23, -27<=k<=27, -15<=l<=16 |
| Data collection software | BRUKER APEX2 2014.9-0 |
| Cell refinement software | BRUKER SAINT |
| Data reduction software | SAINT V8.34A (Bruker AXS Inc., 2013) |

**Solution and refinement:**

| | |
|---|---|
| Reflections collected | 45331 |
| Independent reflections | 5184 [R(int) = 0.0271] |
| Completeness to theta = 25.242° | 99.8 % |
| Observed reflections | 5020[I>2sigma(I) ] |
| Reflections used for refinement | 5184 |
| Absorption correction | Numerical |
| Max. and min. transmission | 0.64 and 0.42 |
| Largest diff. peak and hole | 0.964 and -1.160 e.$Å^{-3}$ |
| Solution | Direct methods |
| Refinement | Full-matrix least-squares on $F^2$ |
| Treatment of hydrogen atoms | Calculated positions, constr. ref. |
| Programs used | XT V2014/1 (Bruker AXS Inc., 2014)<br>SHELXL-2014/7 (Sheldrick, 2014)<br>DIAMOND (Crystal Impact) |
| Data / restraints / parameters | 5184 / 63 / 375 |
| Goodness-of-fit on$F^2$ | 1.091 |
| R index (all data) | $wR_2$ = 0.0461 |
| R index conventional [I>2sigma(I)] | $R_1$ = 0.0184 |

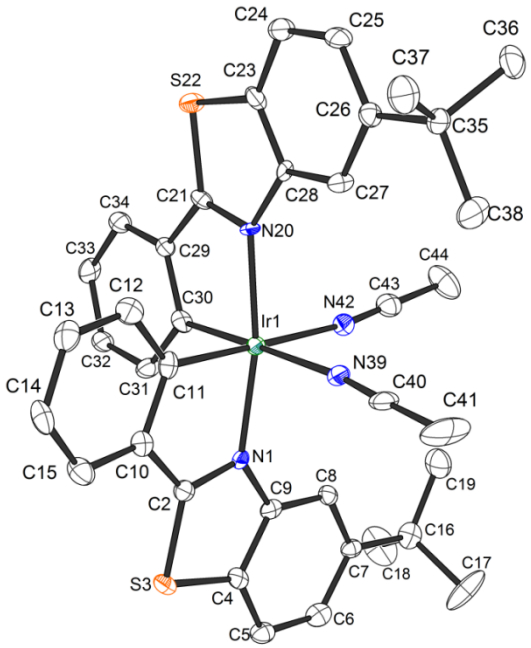


**Λ-IrS**

**Table 21** Crystal Data and Structure Refinement for Λ-**IrS**

**Crystal data:**

| | | |
|---|---|---|
| Identification code | s829_0m | |
| Habitus, colour | block, yellow | |
| Crystal size | 0.22 × 0.16 × 0.08 $mm^3$ | |
| Crystal system | Triclinic | |
| Space group | P 1 | Z = 2 |
| Unit cell dimensions | a = 12.4534(7) Å | α = 102.428(3)° |
| | b = 13.3039(7) Å | β = 103.411(2)° |
| | c = 14.0333(7) Å | γ = 91.556(3)° |
| Volume | 2201.3(2) $Å^3$ | |
| Cell determination | 9714 peaks with Theta 2.4 to 25.3°. | |
| Empirical formula | $C_{40}$ $H_{42}$ $Cl_4$ $F_6$ Ir $N_4$ P $S_2$ | |
| Moiety formula | $C_{38}$ $H_{38}$ Ir $N_4$ $S_2$, $F_6$ P, 2(C $H_2$ $Cl_2$) | |
| Formula weight | 1121.86 | |
| Density (calculated) | 1.693 $Mg/m^3$ | |
| Absorption coefficient | 3.467 $mm^{-1}$ | |
| F(000) | 1112 | |

**Data collection:**

| | |
|---|---|
| Diffractometer type | Bruker D8 QUEST area detector |
| Wavelength | 0.71073 Å |
| Temperature | 115(2) K |
| Theta range for data collection | 1.983 to 25.322°. |
| Index ranges | -14<=h<=14, -16<=k<=16, -16<=l<=16 |
| Data collection software | BRUKER APEX2 2014.1-1 |
| Cell refinement software | SAINT V8.34A (Bruker AXS Inc., 2013) |
| Data reduction software | SAINT V8.34A (Bruker AXS Inc., 2013) |

**Solution and refinement:**

| | |
|---|---|
| Reflections collected | 73320 |
| Independent reflections | 15699 [R(int) = 0.0283] |
| Completeness to theta = 25.242° | 99.9 % |
| Observed reflections | 15102[I> 2σ(I)] |
| Reflections used for refinement | 15699 |
| Absorption correction | Numerical |
| Max. and min. transmission | 0.77 and 0.54 |
| Flack parameter (absolute struct.) | 0.0136(19) |
| Largest diff. peak and hole | 1.223 and -0.865 e.Å$^{-3}$ |
| Solution | direct/ difmap |
| Refinement | Full-matrix least-squares on $F^2$ |
| Treatment of hydrogen atoms | geom, constr |
| Programs used | SHELXS-97 (Sheldrick, 2008)<br>SHELXL-2014 (Sheldrick, 2014)<br>DIAMOND (Crystal Impact) |
| Data / restraints / parameters | 15699 / 168 / 1061 |
| Goodness-of-fit on $F^2$ | 1.073 |
| R index (all data) | $wR_2$ = 0.0520 |
| R index conventional [I>2sigma(I)] | $R_1$ = 0.0204 |

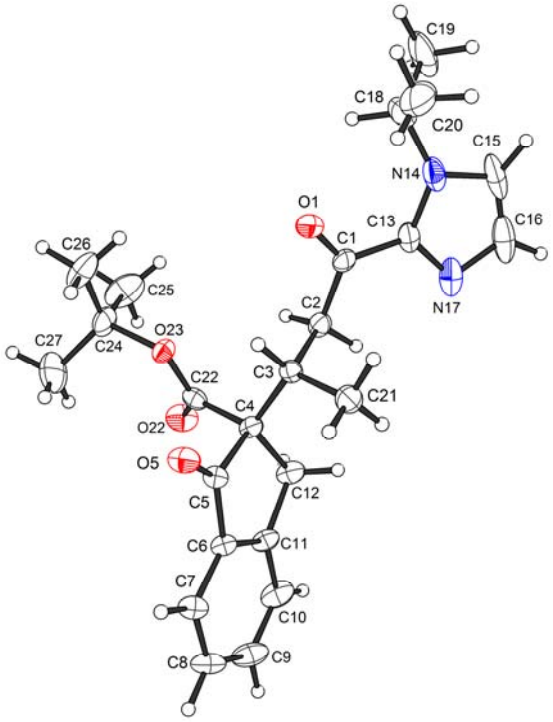


**51**

**Table 22** Crystal Data and Structure Refinement for **51**

**Crystal data**

| | | |
|---|---|---|
| Identification code | s838b_0m | |
| Habitus, colour | plate, colourless | |
| Crystal size | 0.29 × 0.25 × 0.05 $mm^3$ | |
| Crystal system | Orthorhombic | |
| Space group | P $2_1$ $2_1$ $2_1$ | Z = 4 |
| Unit cell dimensions | a = 7.1543(4) Å | α= 90°. |
| | b = 8.3654(5) Å | β= 90°. |
| | c = 37.755(2) Å | γ = 90°. |
| Volume | 2259.6(2) $Å^3$ | |
| Cell determination | 6629 peaks with Theta 2.5 to 27.5°. | |
| Empirical formula | $C_{24}H_{30}N_2O_4$ | |
| Formula weight | 410.50 | |
| Density (calculated) | 1.207 $Mg/m^3$ | |
| Absorption coefficient | 0.082 $mm^{-1}$ | |
| F(000) | 880 | |

**Data collection:**

| | |
|---|---|
| Diffractometer type | Bruker D8 QUEST area detector |
| Wavelength | 0.71073 Å |
| Temperature | 100(2) K |
| Theta range for data collection | 2.158 to 25.498°. |
| Index ranges | -8<=h<=8, -10<=k<=10, -45<=l<=45 |
| Data collection software | BRUKER APEX2 |
| Cell refinement software | SAINT V8.34A (Bruker AXS Inc., 2013) |
| Data reduction software | SAINT V8.34A (Bruker AXS Inc., 2013) |

**Solution and refinement:**

| | |
|---|---|
| Reflections collected | 17182 |
| Independent reflections | 4200 [R(int) = 0.0359] |
| Completeness to theta = 25.242° | 100.0 % |
| Observed reflections | 3419[II > 2(I)] |
| Reflections used for refinement | 4200 |
| Absorption correction | Numerical |
| Max. and min. transmission | 1.00 and 0.96 |
| Flack parameter (absolute struct.) | 0.5(4) |
| Largest diff. peak and hole | 0.265 and -0.241 e.Å$^{-3}$ |
| Solution | Direct methods |
| Refinement | Full-matrix least-squares on $F^2$ |
| Treatment of hydrogen atoms | Calculated positions, constr. ref. |
| Programs used | SHELXS-97 (Sheldrick, 2008) |
| | SHELXL-2013 (Sheldrick, 2013) |
| | DIAMOND (Crystal Impact) |
| Data / restraints / parameters | 4200 / 0 / 277 |
| Goodness-of-fit on $F^2$ | 1.046 |
| R index (all data) | $wR_2$ = 0.0932 |
| R index conventional [I>2sigma(I)] | $R_1$ = 0.0420 |

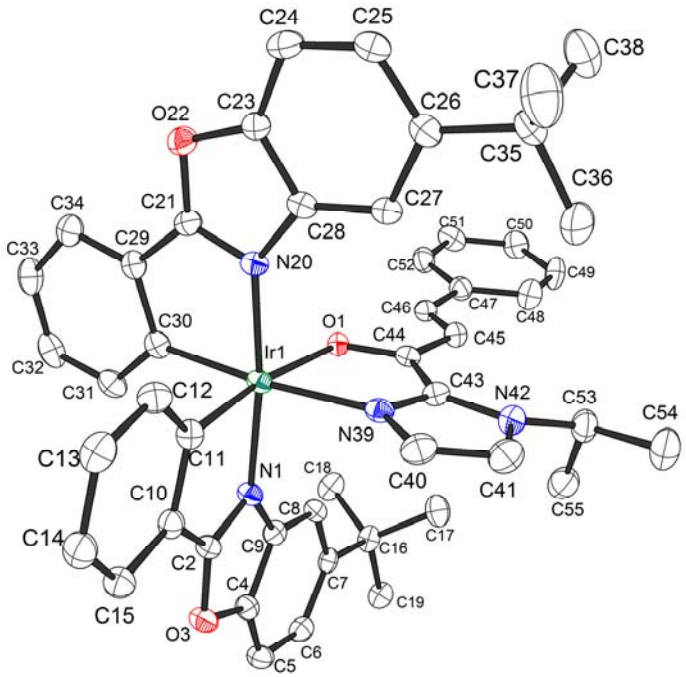


**Complex 79**

**Table 23** Crystal Data and Structure Refinement for **79**

**Crystal data:**

| | | |
|---|---|---|
| Identification code | s862_0m | |
| Habitus, colour | plate, yellow | |
| Crystal size | 0.35 × 0.26 × 0.07 $mm^3$ | |
| Crystal system | Monoclinic | |
| Space group | P $2_1$/c | Z = 4 |
| Unit cell dimensions | a = 15.9181(5) Å | α = 90° |
| | b = 24.5405(7) Å | β = 107.7885(12)° |
| | c = 13.2954(4) Å | γ = 90° |
| Volume | 4945.4(3) $Å^3$ | |
| Cell determination | 9203 peaks with Theta 2.4 to 27.5°. | |
| Empirical formula | $C_{51}$ $H_{50}$ $Cl_2$ $F_3$ Ir $N_4$ $O_6$ S | |
| Formula weight | 1167.11 | |
| Density (calculated) | 1.568 $Mg/m^3$ | |
| Absorption coefficient | 2.915 $mm^{-1}$ | |
| F(000) | 2344 | |

**Data collection:**

| | |
|---|---|
| Diffractometer type | Bruker D8 QUEST area detector |
| Wavelength | 0.71073 Å |
| Temperature | 100(2) K |
| Theta range for data collection | 2.135 to 26.000°. |
| Index ranges | -19<=h<=19, -30<=k<=30, -16<=l<=16 |
| Data collection software | BRUKER APEX2 |
| Cell refinement software | SAINT V8.34A (Bruker AXS Inc., 2013) |
| Data reduction software | SAINT V8.34A (Bruker AXS Inc., 2013) |

**Solution and refinement:**

| | |
|---|---|
| Reflections collected | 46884 |
| Independent reflections | 9723 [R(int) = 0.0336] |
| Completeness to theta = 25.242° | 99.9 % |
| Observed reflections | 8804[II > 2(I)] |
| Reflections used for refinement | 9723 |
| Absorption correction | Numerical |
| Max. and min. transmission | 0.81 and 0.53 |
| Largest diff. peak and hole | 2.048 and -1.402 e.$Å^{-3}$ |
| Solution | Direct methods |
| Refinement | Full-matrix least-squares on $F^2$ |
| Treatment of hydrogen atoms | Calculated positions, constr. ref. |
| Programs used | SHELXS-97 (Sheldrick, 2008)<br>SHELXL-2013 (Sheldrick, 2013)<br>DIAMOND (Crystal Impact) |
| Data / restraints / parameters | 9723 / 0 / 640 |
| Goodness-of-fit on $F^2$ | 1.074 |
| R index (all data) | $wR_2$ = 0.0574 |
| R index conventional [I>2sigma(I)] | $R_1$ = 0.0261 |

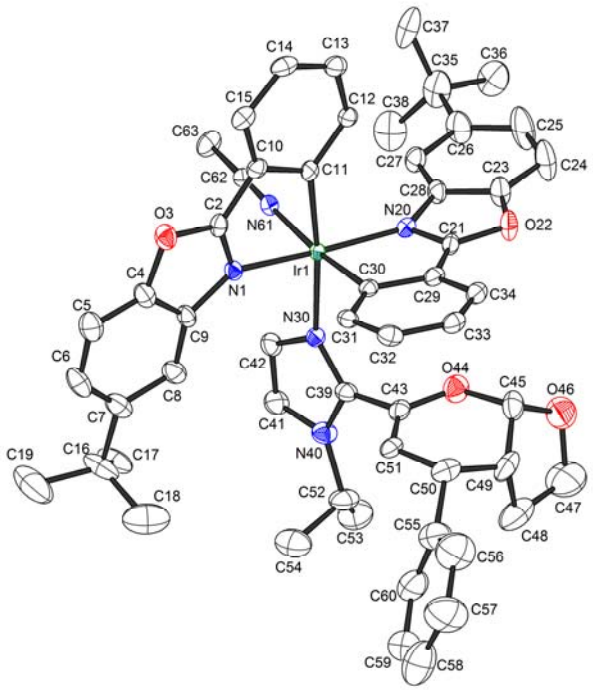


**Complex 80**

**Table 24** Crystal Data and Structure Refinement for **80**

**Crystal data:**

| | | |
|---|---|---|
| Identification code | s875_0m | |
| Habitus, colour | nugget, yellow | |
| Crystal size | 0.27 × 0.22 × 0.17 $mm^3$ | |
| Crystal system | Monoclinic | |
| Space group | P $2_1/n$ | Z = 4 |
| Unit cell dimensions | a = 17.6254(7) Å | α = 90° |
| | b = 14.9443(5) Å | β = 103.4033(14)° |
| | c = 22.3943(9) Å | γ = 90° |
| Volume | 5738.0(4) $Å^3$ | |
| Cell determination | 9737 peaks with Theta 2.7 to 25.3°. | |
| Empirical formula | $C_{58}\,H_{61}\,Cl_4\,F_3\,Ir\,N_5\,O_7\,S$ | |
| Moiety formula | $C_{55}\,H_{57}\,Ir\,N_5\,O_4$, C $F_3\,O_3\,S$, 2(C $H_2\,Cl_2$) | |
| Formula weight | 1363.17 | |
| Density (calculated) | 1.578 $Mg/m^3$ | |
| Absorption coefficient | 2.616 $mm^{-1}$ | |
| F(000) | 2752 | |

**Data collection:**

| | |
|---|---|
| Diffractometer type | Bruker D8 QUEST area detector |
| Wavelength | 0.71073 Å |
| Temperature | 100(2) K |
| Theta range for data collection | 2.395 to 25.335°. |
| Index ranges | -21<=h<=21, -17<=k<=17, -26<=l<=26 |
| Data collection software | BRUKER APEX2 2014.1-1 |
| Cell refinement software | SAINT V8.34A (Bruker AXS Inc., 2013) |
| Data reduction software | SAINT V8.34A (Bruker AXS Inc., 2013) |

**Solution and refinement:**

| | |
|---|---|
| Reflections collected | 132737 |
| Independent reflections | 10435 [R(int) = 0.0473] |
| Completeness to theta = 25.242° | 99.9 % |
| Observed reflections | 9261[II > 2(I)] |
| Reflections used for refinement | 10435 |
| Absorption correction | Numerical |
| Max. and min. transmission | 0.67 and 0.47 |
| Largest diff. peak and hole | 2.055 and -1.646 e.Å$^{-3}$ |
| Solution | Direct methods |
| Refinement | Full-matrix least-squares on $F^2$ |
| Treatment of hydrogen atoms | Calculated positions, constr. ref. |
| Programs used | SHELXS-97 (Sheldrick, 2008) |
| | SHELXL-2014 (Sheldrick, 2014) |
| | DIAMOND (Crystal Impact) |
| Data / restraints / parameters | 10435 / 81 / 783 |
| Goodness-of-fit on $F^2$ | 1.046 |
| R index (all data) | $wR_2$ = 0.1113 |
| R index conventional [I>2sigma(I)] | $R_1$ = 0.0403 |

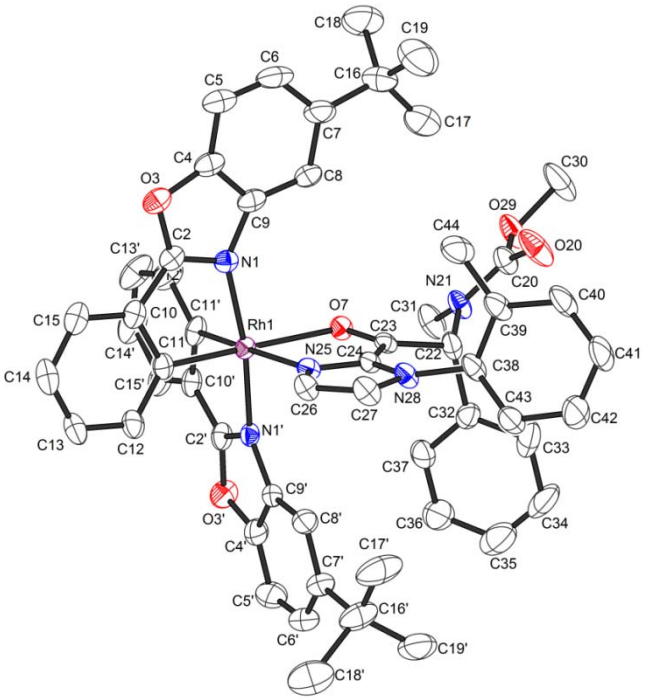


**Complex 138**

**Table 25** Crystal Data and Structure Refinement for **138**

**Crystal data:**

| | | |
|---|---|---|
| Identification code | s1789b_0m_sq | |
| Habitus, colour | prism, green | |
| Crystal size | 0.44 × 0.35 × 0.09 $mm^3$ | |
| Crystal system | Monoclinic | |
| Space group | $P2_1$ | Z = 2 |
| Unit cell dimensions | a = 9.5431(4) Å | α = 90°. |
| | b = 22.2792(10) Å | β = 97.985(2)°. |
| | c = 13.6884(6) Å | γ = 90°. |
| Volume | 2882.1(2) $Å^3$ | |
| Cell determination | 9906 peaks with Theta 2.4 to 26.4°. | |
| Empirical formula | $C_{55}$ $H_{53}$ $F_6$ $N_5$ $O_5$ P Rh | |
| Moiety formula | $C_{55}$ $H_{53}$ $N_5$ $O_5$ Rh, $F_6$ P | |
| Formula weight | 1111.90 | |
| Density (calculated) | 1.281 $Mg/m^3$ | |
| Absorption coefficient | 0.391 $mm^{-1}$ | |
| F(000) | 1144 | |

**Data collection:**

| | |
|---|---|
| Diffractometer type | Bruker D8 QUEST area detector |
| Wavelength | 0.71073 Å |
| Temperature | 110(2) K |
| Theta range for data collection | 2.155 to 26.436°. |
| Index ranges | -11<=h<=11, -27<=k<=27, -16<=l<=17 |
| Data collection software | APEX3 |
| Cell refinement software | SAINT V8.35A (Bruker AXS Inc., 2015) |
| Data reduction software | SAINT V8.35A (Bruker AXS Inc., 2015) |

**Solution and refinement:**

| | |
|---|---|
| Reflections collected | 47009 |
| Independent reflections | 11797 [R(int) = 0.0371] |
| Completeness to theta = 25.242° | 99.9 % |
| Observed reflections | 11015[I>2sigma(I) ] |
| Reflections used for refinement | 11797 |
| Absorption correction | Semi-empirical from equivalents |
| Max. and min. transmission | 0.7454 and 0.6942 |
| Flack parameter (absolute struct.) | -0.015(7) |
| Largest diff. peak and hole | 0.284 and -0.417 e.Å$^{-3}$ |
| Solution | Direct methods |
| Refinement | Full-matrix least-squares on $F^2$ |
| Treatment of hydrogen atoms | Calculated positions, constr. ref. |
| Programs used | XT V2014/1 (Bruker AXS Inc., 2014) |
| | SHELXL-2014/7 (Sheldrick, 2014) |
| | DIAMOND (Crystal Impact) |
| Data / restraints / parameters | 11797 / 454 / 817 |
| Goodness-of-fit on $F^2$ | 1.039 |
| R index (all data) | $wR_2$ = 0.0647 |
| R index conventional [I>2sigma(I)] | $R_1$ = 0.0276 |

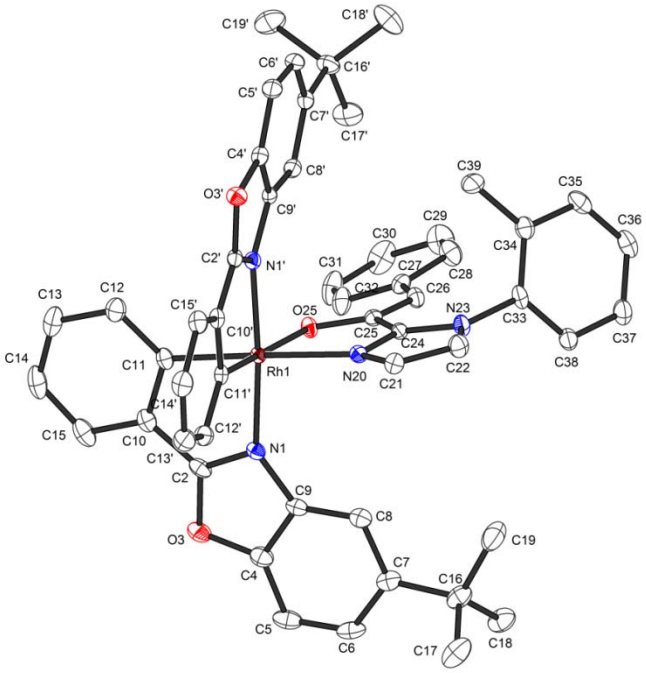


**Complex 139**

**Table 26** Crystal Data and Structure Refinement for **139**

**Crystal data:**

| | | |
|---|---|---|
| Identification code | s1604_0m | |
| Habitus, colour | prism, red | |
| Crystal size | 0.28 × 0.16 × 0.13 $mm^3$ | |
| Crystal system | Triclinic | |
| Space group | P-1 | Z = 2 |
| Unit cell dimensions | a = 12.1532(5) Å | α = 80.767(1)° |
| | b = 12.4927(5) Å | β = 86.511(1)° |
| | c = 16.5165(7) Å | γ = 67.404(1)° |
| Volume | 2285.15(16) $Å^3$ | |
| Cell determination | 9423 peaks with Theta 2.5 to 27.5°. | |
| Empirical formula | $C_{53}$ $H_{49}$ $Cl_2$ $N_4$ $O_3$ Rh | |
| Moiety formula | $C_{52}$ $H_{47}$ $N_4$ $O_3$ Rh, C $H_2$ $Cl_2$ | |
| Formula weight | 963.77 | |
| Density (calculated) | 1.401 $Mg/m^3$ | |
| Absorption coefficient | 0.539 $mm^{-1}$ | |
| F(000) | 996 | |

**Data collection:**

| | |
|---|---|
| Diffractometer type | Bruker D8 QUEST area detector |
| Wavelength | 0.71073 Å |
| Temperature | 100(2) K |
| Theta range for data collection | 2.203 to 27.579°. |
| Index ranges | -15<=h<=15, -16<=k<=16, -21<=l<=21 |
| Data collection software | BRUKER APEX2 2014.9-0 |
| Cell refinement software | BRUKER SAINT |
| Data reduction software | SAINT V8.34A (Bruker AXS Inc., 2013) |

**Solution and refinement:**

| | |
|---|---|
| Reflections collected | 45256 |
| Independent reflections | 10428 [R(int) = 0.0287] |
| Completeness to theta = 25.242° | 99.6 % |
| Observed reflections | 9372[I>2sigma(I) ] |
| Reflections used for refinement | 10428 |
| Absorption correction | Semi-empirical from equivalents |
| Max. and min. transmission | 0.93 and 0.89 |
| Largest diff. peak and hole | 0.451 and -0.502 e.Å$^{-3}$ |
| Solution | Direct methods |
| Refinement | Full-matrix least-squares on $F^2$ |
| Treatment of hydrogen atoms | Calculated positions, constr. ref. |
| Programs used | XT V2014/1 (Bruker AXS Inc., 2014)<br>SHELXL-2014/7 (Sheldrick, 2014)<br>DIAMOND (Crystal Impact) |
| Data / restraints / parameters | 10428 / 21 / 603 |
| Goodness-of-fit on $F^2$ | 1.041 |
| R index (all data) | $wR_2$ = 0.0603 |
| R index conventional [I>2sigma(I)] | $R_1$ = 0.0277 |

# Erklärung

gemäß § 10, Abs. 1 der Promotionsordnung der mathematisch-naturwissenschaftlichen Fachbereiche und des Medizinischen Fachbereichs für seine mathematisch-naturwissenschaftlichen Fächer der Philipps-Universität Marburg vom 15.07.2009

Ich erkläre, dass eine Promotion noch an keiner anderen Hochschule als der Philipps-Universität Marburg, Fachbereich Chemie, versucht wurde und versichere, dass ich meine vorgelegte Dissertation

**Octahedral Chiral-at-Metal Iridium and Rhodium Complexes as Versatile Asymmetric Catalysts**

selbst und ohne fremde Hilfe verfasst, nicht andere als die in ihr angegebenen Quellen oder Hilfsmittl benutz, alle vollständig oder sinngemäß übernommenen Zitate als solche gekennzeichnet sowie die Dissertation in der vorliegenden oder ähnlichen Form noch bei keiner anderen in- oder ausländischen Hochschule anlässlich eines Promotionsgesuchs oder zu anderen Prüfungszwecken eingereicht habe.

Xiaodong Shen
Marburg, den 15.04.2016

# Curriculum Vitae

**Name:** Xiaodong Shen
**Place of Birth:** Jiangsu, P. R. China
**Date of Birth:** 14-12-1986
**Email:** shenxiaodongsuda@163.com

## Education

- *University of Marburg (Germany)*

***PhD student*** of Organic Chemistry 2012.9-2016.2

**Subject:** Octahedral Chiral-at-Metal Iridium Catalysts: Versatile Chiral Lewis Acids for Asymmetric Conjugate Additions; Asymmetric photoredox transition-metal catalysis activated by visible light.

**Supervisor:** Prof. Dr. Eric Meggers

**Publications:**

(1) **X. Shen**, K. Harms, M. Marsch, E. Meggers, *Chem. Eur. J.,* **2016**, DOI: 10.1002/chem.201601572.
(2) J. Ma, **X. Shen**, K. Harms, E. Meggers, *Dalton Trans.,* **2016**, DOI: 10.1039/c6dt01063f.
(3) C. Wang, J. Qin, **X. Shen**, R.Riedel, K. Harms, E. Meggers, *Angew. Chem. Int. Edit.,* **2016**, 55, 685.
(4) H. Huo, X. Huang, **X. Shen**, K. Harms, E. Meggers, *Synlett*, **2016**, *27*, 749.
(5) **X. Shen**, H. Huo, C. Wang, B. Zhang, K. Harms, E. Meggers, *Chem. Eur. J.,* **2015**, *21*, 9720.
(6) C. Wang, L.-A. Chen, H. Huo, **X. Shen**, K. Harms, L. Gong, E.Meggers, *Chem. Sci.*, **2015**, *6*, 1094.
(7) H. Huo, **X. Shen**, C. Wang, L. Zhang, P. Röse, L.-A. Chen, K. Harms, M. Marsch, G. Hilt, E. Meggers, *Nature,* **2014**, *515*, 100.

- *Soochow University (China)*

***Master*** of Organic Chemistry (Organometallic) 2009.9-2012.6

**Subject:** Synthesis and Characterization of Bis-β-diketiminato Rare-Earth-Metals Complexes and their Catalytic Activity.

**Supervisor:** Prof. Dr. Qi Shen

**Publications:**

(1) Y. Zheng, R.Jiao, **X. Shen**, M. Xue, Y. Yao, Y. Zhang, Q. Shen, *Appl. Organomet. Chem.*, **2014**, *28*, 461.
(2) **X. Shen**, M. Xue, R. Jiao, Y. Ma, Y. Zhang, Q. Shen, *Organometallics*, **2012**, *31*, 6222.
(3) **X. Shen**, Y. Zhang, M. Xue, Q.Shen, *Dalton Trans.*, **2012**, *41*, 3668.
(4) R. Jiao, M. Xue, **X. Shen**, Y. Zhang, Y. Yao, Q. Shen, *Eur. J. Inorg. Chem.,* **2011**, 1448.
(5) R. Jiao, **X. Shen**, M. Xue, Y. Zhang, Y.Yao, Q. Shen, *Chem. Commun*., **2010**, *46*, 4118.
(6) R. Jiao, M. Xue, **X. Shen**, Y. Zhang, Y. Yao, Q. Shen, *Eur. J. Inorg. Chem.,* **2010**, 2523.

- *Soochow University (China)*

***Bachelor*** of Chemistry 2005.9-2009.6

**Subject:** The Catalytic Behavior of Tris-β-diketiminato Lanthanide Complexes (bachelor thesis, 2008.9-2009.6).

**Supervisor:** Prof. Dr. Qi Shen